Advances and Technical Standards in Neurosurgery 48
Series Editor: Concezio Di Rocco

Concezio Di Rocco *Editor*

Advances and Technical Standards in Neurosurgery

Volume 48

Springer

Advances and Technical Standards in Neurosurgery

Volume 48

This series, which has earned a reputation over the years and is considered a classic in the neurosurgical field, is now relaunched under the editorship of Professor Di Rocco, which relies on the collaboration of a renewed editorial board.

Both volumes focused on recent advances in neurosurgery and on technical standards, and monographs devoted to more specific subjects in the neurosurgical field will implement it. Written by key opinion leaders, the series volumes will be useful for young neurosurgeons in their postgraduate training but also for more experienced clinicians.

Concezio Di Rocco
Editor

Advances and Technical Standards in Neurosurgery

Volume 48

Springer

Editor
Concezio Di Rocco
International Neuroscience Institute
Hannover, Germany

ISSN 0095-4829 ISSN 1869-9189 (electronic)
Advances and Technical Standards in Neurosurgery
ISBN 978-3-031-36784-7 ISBN 978-3-031-36785-4 (eBook)
https://doi.org/10.1007/978-3-031-36785-4

This Springer imprint is published by the registered company Springer Nature Switzerland AG
The registered company address is: Gewerbestrasse 11, 6330 Cham, Switzerland

Preface

Advances and Technical Standards in Neurosurgery (ATSN) represents the successful achievement of the wish of Jean Brihaye, Bernard Pertuised, Fritz Loew, and Hugo Krayenbuhl to provide the European neurosurgeons in training with a high-level publication to accompany the teaching provided by the European postgraduate course. The project was conceived during the joint meeting of the German and Italian Neurosurgical Societies in Taormina in 1972, and the first volume was published in 1974. The English language was chosen to facilitate the international exchange of information and the circulation of scientific progress. Since then, the ATSN has hosted chapters by eminent European neurosurgeons and has become one of the most renowned educational tools on the continent for both young and experienced neurosurgeons. The successive editorial boards have maintained the ATSN's high scientific quality and ensured a good balance between contributions dealing with advances in neurosciences over the years and detailed descriptions of surgical techniques as well as analyses of clinical experiences. Additional appeal has been added by freedom granted by the editor and publisher in the length, style, and organization of the published papers.

The current series aims to preserve the original spirit of the publication and its high-level didactic function but intends to present itself not only as a historic European publication but as a truly international forum for most advanced clinical research and modern operating standards.

Hannover, Germany — Concezio Di Rocco

Contents

Chapter 1
The Greatest Healthcare Disparity: Addressing Inequities in the Treatment of Childhood Central Nervous System Tumors in Low- and Middle-Income Countries

Jordan T. Roach, Nathan A. Shlobin, Jared M. Andrews, Ronnie E. Baticulon, Danny A. Campos, Daniel C. Moreira, Ibrahim Qaddoumi, and Frederick A. Boop

1.1 Introduction

Each day, over 1000 children are diagnosed with cancer around the globe. The most common type of cancer among children is acute lymphoblastic leukemia (ALL). While once the leading cause of pediatric cancer-related death, with proper diagnosis and treatment, ALL now has a cure rate of approximately 90% due to the landmark implementation of multimodality treatment and combination chemotherapy [1]. As a result of this progress, central nervous system (CNS) malignancies have surpassed leukemia as the leading cause of cancer-related morbidity and mortality in children [2, 3]. Fortunately, advances in prognostic clinical and biological factors and optimized treatment regimens incorporating multidisciplinary care have improved survival rates for all childhood cancer types, including CNS tumors. Through steady, incremental improvements in care, the 5-year survival rate for children diagnosed with cancer in high-income countries (HICs) now exceeds 80% [4, 5].

The antithesis between childhood cancer survival rates in HICs and in low- and middle-income countries (LMICs) represents one of healthcare's most significant disparities. As a result of inaccessible or unaffordable contemporary treatment options and supportive care, the survival rate for childhood cancer in LMICs is roughly 20% [6]. Population dynamics further exacerbate inequitable survival rates as approximately 90% of the world's children, and therefore 80% of children with cancer reside in LMICs [7, 8]. Through an analysis of disability-adjusted life-years, a metric used to directly compare the lifelong implications of childhood cancer against other diseases, Force and colleagues have shown that childhood cancer represents a substantial disease burden in LMICs despite its low relative incidence [9].

C. Di Rocco (ed.), *Advances and Technical Standards in Neurosurgery*, Advances and Technical Standards in Neurosurgery 48,
https://doi.org/10.1007/978-3-031-36785-4_1

For the neurosurgical community, the most staggering illustration of disparate outcomes and disease burden is highlighted by the fact that the 5-year survival rate of a child with brain cancer is not determined by the complex biology of the tumor but rather the country in which the child receives care [10]. Epidemiological data suggests that in much of the world, children with brain tumors die without ever being diagnosed [11]. The major challenge for neurosurgeons moving forward will be to address inequities in the treatment of childhood CNS malignancies by aiding in timely diagnosis and ensuring that standard and innovative therapies are available and accessible, whether in HICs or LMICs [12–17].

In this chapter, we discuss the burden of childhood cancer with a particular focus on the treatment of pediatric low-grade glioma (LGG) across the globe. We provide an overview of the World Health Organization's (WHO) Global Initiative for Childhood Cancer and highlight a critical role for pediatric neurosurgery in addressing inequities in treating childhood CNS tumors. We further outline actions that the neurosurgical community should consider to improve survival outcomes for children in LMICs with CNS tumors.

1.2 The Burden of Childhood Cancer in Low- and Middle-Income Countries

Cancer diagnoses for children living in LMICs contrast starkly from those in HICs [8]. Moreover, the disease burden in LMICs can be challenging to quantify. Unlike HICs, LMICs often lack population-based cancer registries to evaluate disease incidence [8]. Insufficient cancer registries coupled with underdiagnosis in LMICs have led to inaccurate reporting of incidence rates for childhood cancers, such as ALL [18]. For pediatric brain tumors, underdiagnosis is particularly problematic. Moreover, there is limited published data on the epidemiology of pediatric CNS tumors in LMICs.

Unlike adults with cancer who can be diagnosed and treated at any hospital, children with cancer require highly specialized care often provided by a regional children's hospital. This suggests that incidence and outcome data for most children with cancer in a LMIC can be appropriately captured by implementing a children's hospital-based tumor registry, absent a nationwide cancer registry which is necessary to evaluate incidence and outcome trends in adult patients (Fig. 1.1).

Apart from lacking the necessary infrastructure to evaluate disease burden, LMICs frequently have insufficient medical resources which may include diagnostic imaging, life-saving medications, and radiation treatment modalities. Deficiencies within the healthcare system combined with delayed disease presentation, abandonment of treatment, and complexities involving social, economic, and cultural circumstances have significantly impeded pediatric cancer care in LMICs [8, 19]. Despite these challenges, implementing effective treatment protocols and international cooperation, institutional twinning programs, for example, have significantly

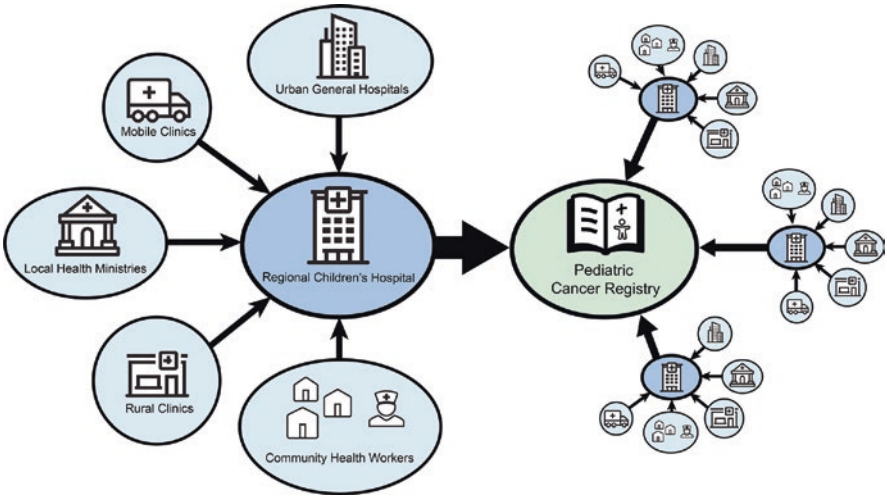

Fig. 1.1 Improving pediatric cancer registries. Diagram illustrating how regional children's hospitals in LMICs can collaborate with local and regional health partners to implement a children's hospital-based tumor registry and capture most children with cancer in LMICs until a national cancer registry becomes available

improved survival rates for children with Burkitt lymphoma in equatorial Africa and medulloblastoma in Jordan [20, 21]. With modern treatments and multidisciplinary care conferring enhanced survival rates for childhood cancer in HICs, the WHO, in collaboration with St. Jude Children's Research Hospital, seeks to address the burden of childhood cancer in LMICs and save the lives of upwards of one million additional children with cancer in the next decade [6].

1.3 An Overview of the World Health Organization Global Initiative for Childhood Cancer

To address the burden of childhood cancer globally, the WHO launched the Global Initiative for Childhood Cancer in 2018 with the ambitious goal of achieving a survival rate of at least 60% for pediatric cancer worldwide by the year 2030 [6]. To effectively monitor progress across variable healthcare systems, the WHO selected six index cancers: acute lymphoblastic leukemia, Burkitt lymphoma, Hodgkin lymphoma, retinoblastoma, Wilms' tumor, and low-grade glioma. These index cancers are highly curable with proven therapies, are prevalent in all LMICs, and comprise 50–60% of childhood cancers (Fig. 1.2) [6]. Pediatric LGGs represent a unique opportunity for the neurosurgical community to directly contribute to a paradigm shift in the survival outcomes of children in LMICs, as many LGGs can be managed with surgical resection alone [22].

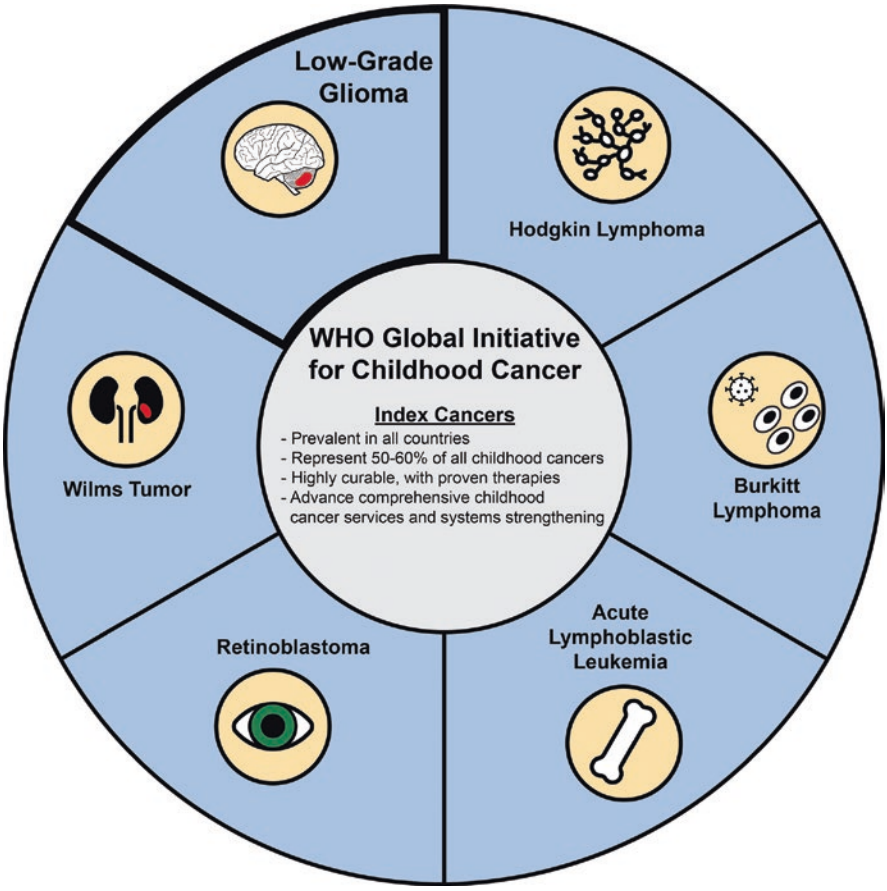

Fig. 1.2 An overview of the World Health Organization Global Initiative for Childhood Cancer. Diagram illustrating the WHO Global Initiative for Childhood Cancer index cancers

1.4 Pediatric Low-Grade Glioma: A Critical Role for Prompt Diagnosis and Neurosurgical Care

Pediatric LGGs comprise 45% of childhood CNS tumors and are classified as either WHO grade 1 or WHO grade 2 tumors [23]. Among pediatric LGGs, WHO grade 1 pilocytic astrocytomas account for 20% of brain neoplasms in children and adolescents under 20 years of age and often follow an indolent course [24]. In contrast, adults diagnosed with LGG, such as WHO grade 2 infiltrative astrocytoma, commonly exhibit malignant transformation to a higher-grade tumor [25]. Although exceedingly rare, a small proportion of WHO grade 1 pilocytic astrocytomas and WHO grade 2 astrocytomas in children have been reported to exhibit pathologic progression to tumors of higher grade [26, 27]. Typically, when this occurs, it is due

to the child harboring a genetic cancer predisposition syndrome or from the child receiving prior radiation therapy or other treatment for the low-grade tumor [28–30].

Despite most pediatric LGGs exhibiting excellent outcomes, delay in diagnosis remains a significant problem for LGGs and pediatric brain tumors, in general, relative to other childhood cancers [31–33]. When one considers that most brain tumors in children present with headaches, nausea, vomiting, and lethargy, it is perhaps unsurprising that families and caregivers may mistake these symptoms for a gastrointestinal illness. Moreover, diagnosis becomes increasingly nuanced in the setting of LGG as the typical triad of headache, vomiting, and papilledema is not often present in these tumors [34]. To aid physicians in promptly diagnosing children with brain tumors, particularly LGG, Arnautovic and colleagues coined the term LOW-OR-PAY, a mnemonic for "think low-grade glioma or the patient will pay the price." This mnemonic represents "local (focal) symptoms," "ongoing (long-term) symptoms," "worsening of existing symptoms," "other, associated signs/symptoms," "relapsing and remitting symptoms," "persistent symptoms," "alterations (change) of symptoms and adolescence," and "young (new) symptoms (Fig. 1.3) [33]. The lack of access to CT and/or MRI scanners contributes further to misdiagnoses and lead to increased delays in receiving appropriate treatment [35].

In children, LGGs display remarkable diversity in their histopathology and molecular alterations. Histopathological diagnoses of childhood LGG comprise both astrocytic and oligodendroglial histology and tumors of mixed glial-neuronal components [28]. While the 2021 WHO classification of central nervous system tumors provides enormous insight into present best practices for tumor classification, methylation profiling and molecular diagnostics are not feasible in most LMICs. In fact, many clinicians rely on basic histological staining techniques, such as H&E staining, for the classification of CNS tumors due to limited resources. There may also be a shortage of pathologists with adequate training and experience in neuropathology.

Fortunately, despite variability in genetic alterations and histopathology, pediatric LGGs are primarily regarded as a surgical disease, excluding rare exceptions of pathologic progression and tumors in brain regions not amenable to surgical resection (e.g., optic pathway, thalamus, hypothalamus, and brainstem) [22]. For WHO grade 1 pilocytic astrocytomas in brain regions in which complete surgical resection cannot be achieved, conformal radiation therapy has been shown to aid in long-term disease control for most children [36]. Unfortunately, the availability of equipment and high treatment costs remain significant barriers to accessible radiotherapy for children in LMICs. Moreover, young children are at enhanced risk for developing late effects from radiation treatment, including intellectual disabilities, hearing loss, endocrinopathies, and secondary neoplasms, for which long-term surveillance may be difficult in patients from geographically isolated and disadvantaged areas [36–38].

To manage tumors that are not amenable to surgical resection and recurrent or refractory LGGs, conventional chemotherapies, such as carboplatin and vincristine combination therapy and weekly vinblastine monotherapy, are viable treatment options in LMICs with limited resources. Although not usually curative, these

chemotherapy regimens have been shown to stabilize disease progression in up to 50% of patients and are well tolerated [39, 40]. While conventional chemotherapy offers an opportunity to treat recurrent or refractory LGGs and those tumors incapable of being surgically cured, this treatment approach is not without limitations. For instance, chemotherapy must be administered multiple times to achieve LGG disease stabilization [24]. Additionally, frequency and duration of treatment are important considerations as abandonment of therapy, defined as the "failure to start or complete (potentially) curative treatment," is the most common cause of treatment failure in pediatric cancer patients [15, 16, 41, 42]. Nonetheless, chemotherapy remains a feasible treatment option for LGG disease stabilization in LMICs in the setting of unresectable, recurrent, or diffusely infiltrative LGGs.

For pediatric LGGs in brain regions amenable to surgical resection**,** prospective and retrospective studies support a critical role for aggressive tumor excision (gross total resection) as a practical approach to achieve long-term event-free survival [22, 43]. In one of the most extensive, prospective pediatric brain tumor studies ever performed, for patients in whom a GTR was achieved, the 8-year overall survival and 8-year progression-free survival was 96% and 78%, respectively, without further adjuvant therapy [22]. These findings support a critical role for neurosurgical care as one measure to decrease the burden of pediatric cancer by curing most children with LGGs in LMICs. Therefore, approaching children with LGGs with curative intent should be the treatment goal regardless of the modality used (Fig. 1.3).

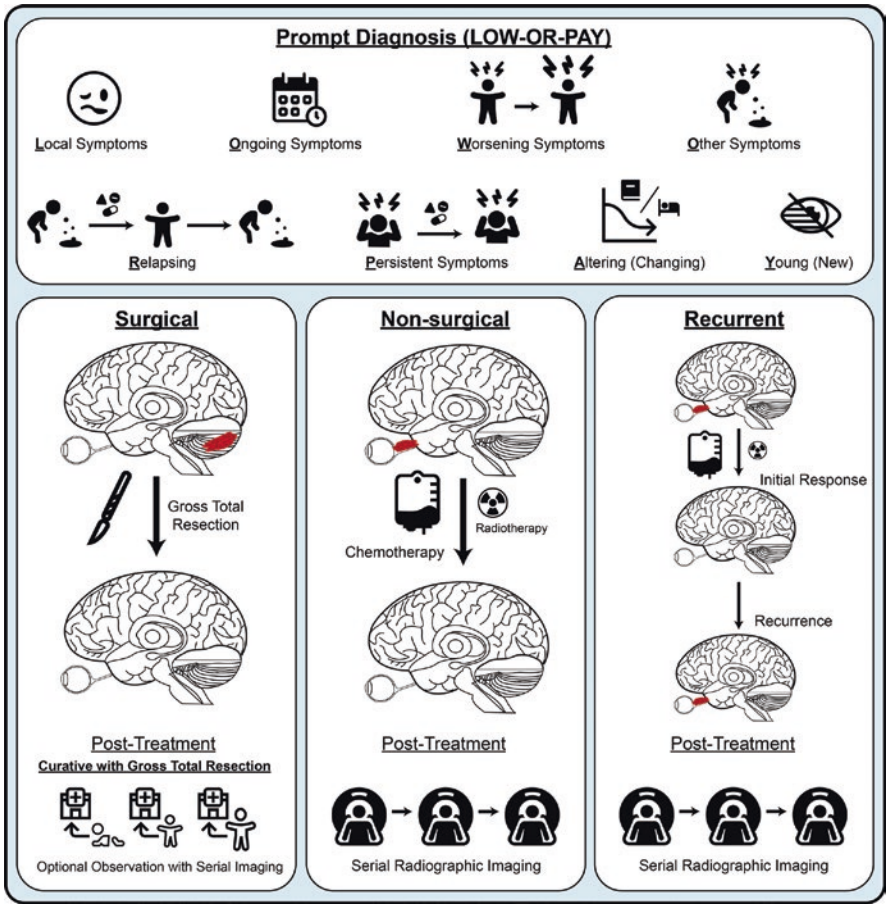

Fig. 1.3 The critical role for prompt diagnosis and neurosurgical care in children with low-grade gliomas in brain regions amenable to surgical resection. Diagram illustrating LOW-OR-PAY criteria for early diagnosis and treatment schema for surgical, nonsurgical, and recurrent low-grade gliomas

1.5 Our Capacity for Care: The Distribution of Pediatric Neurosurgeons Around the Globe

There are approximately 49,000 neurosurgeons worldwide with up to 44% living in HICs. Given that neurosurgical practice typically requires expensive surgical equipment, dedicated neuro-intensive care units capable of ventilatory support, and specialized ancillary team members, neurosurgeons often practice in urban locations; therefore, access to neurosurgical care is particularly limited in rural regions around the globe [44]. Fellowship-trained pediatric neurosurgeons generally practice in regional pediatric referral centers, typically found in larger cities [45]. Full-time

pediatric neurosurgery requires the availability of experts in pediatric emergency medicine, anesthesia, intensive care, neonatology, and nursing. For pediatric neuro-oncology, which requires additional pediatric subspecialists in hematology-oncology, radiology, radiation oncology, neuropathology, physical medicine, and rehabilitation, as well as administrative support, the coordination of care can be even more difficult. Thus, disparities in the distribution of the neurosurgical workforce are more pronounced in pediatric neuro-oncology.

Outside of HICs, most pediatric neurosurgical care is administered by general neurosurgeons and, in some instances, general surgeons, who provide the best care they can with limited resources. Despite neurosurgical conditions contributing to significant morbidity and mortality among children in LMICs, it is not feasible for fellowship-trained pediatric neurosurgeons to provide care to all children. Neither is it pragmatic given the present shortage and maldistribution of the global pediatric neurosurgery workforce. In Asia and Australasia, only about two-thirds of pediatric patients with brain tumors are seen and managed by pediatric neurosurgeons, the rest being cared for by general neurosurgeons [35, 44–47].

To quantify the geographic representation of pediatric neurosurgeons around the globe, Dewan and colleagues surveyed 459 surgeons across 76 countries. Their findings estimated a total of 2297 pediatric neurosurgical subspecialists worldwide, with nearly 86% of subspecialists practicing in HICs. In LMICs, access to pediatric neurosurgical care is severely limited. In fact, only 330 pediatric neurosurgeons are available to care for 1.2 billion children in LMICs [35].

In many African nations, there is roughly one pediatric neurosurgeon per every 30 million children. In such settings where the incidence of pediatric patients with trauma, hydrocephalus, spina bifida, and other congenital malformations is also high, neurosurgeons may face delays in providing surgical care due to a lack of ICU beds or operating theater time. Technologies that increase the chances of maximal safe resection (e.g., stereotactic navigation, 5-ALA, and intraoperative MRI) are often unavailable, and thus the management of complex brain tumors becomes tremendously challenging for neurosurgeons in LMICS.

In contrast, HICs exhibit ratios closer to one pediatric neurosurgeon for every 370,000 children, with lower ratios reported for some HICs [35]. It has been estimated that nearly 23,000 additional neurosurgeons, overall, need to be trained to address present treatment demands. This is almost 2.5 times the number being educated. As 13.4 million new neurosurgical cases arise each year, with greater than 80% occurring in LMICs, approximately 5 million patients will fail to undergo therapeutic intervention for a treatable neurosurgical condition [44]. Recognizing that it takes 5–7 years to train a neurosurgeon, political leaders and ministers of health in LMICs must be proactive in addressing present and future challenges facing neurosurgical care, especially for children. This can be especially challenging for countries with limited gross domestic product (GDP) healthcare expenditures where resources are often directed toward treating cardiovascular disease [48, 49]. To aid neurosurgical efforts, health institutions in HICs and organized neurosurgical groups must continue to prioritize developments in education, health, and research infrastructure while maintaining continued professional support for neurosurgical colleagues in LMICs.

1.6 Addressing Global Inequities in the Neurosurgical Treatment of Childhood Central Nervous System Tumors

To impact the global burden of childhood LGG, the neurosurgical community must respond to initiatives set forth by the WHO Global Initiative for Childhood Cancer and assume a critical role in providing children with brain tumors in LMICs both a timely diagnosis and a curative treatment option. Herein, we outline what neurosurgeons can do to improve care for children in LMICs with CNS cancer, particularly LGG. These approaches include supporting educational initiatives, increasing access to surgical tools and ancillary support, identifying centers of excellence for brain tumor treatment, establishing regional referral networks, recognizing socioeconomic and sociocultural barriers to care, understanding the importance of community support, and advocating for global neurosurgical initiatives.

1.7 Expanding Opportunities for Subspecialty Training in Pediatric Neurosurgery and Enhancing Neurosurgical Capacity in Low- and Middle-Income Countries

When Dewan and colleagues evaluated pediatric neurosurgical subspecialty training in HICs and LMICs, they found that 89.5% of respondents in HICs reported receiving subspecialty training compared to only 54.4% in LMICs [35]. Looking further at training inquiries, survey reports indicated that few respondents requested additional surgical training in shunt insertion to treat hydrocephalus or trauma-related neurosurgical procedures [35]. This is not surprising given the number of these procedures performed each year with nearly 400,000 children born with hydrocephalus and approximately three million children sustaining a traumatic brain injury annually around the globe [47, 50]. In contrast to hydrocephalus and traumatic brain injury, pediatric brain tumors are much less common, with incidence rates ranging from 1.12 to 5.14 cases per 100,000 persons and rates varying by country [51]. To provide neurosurgeons who are interested in dedicated pediatric brain tumor care enhanced exposure and protected time to operate on these complex cases, high-volume brain tumor centers in HICs and organized neurosurgery may consider increasing the number of subspecialty training fellowships. As the neurosurgical capacity for pediatric brain tumor treatment is expanded in LMICs through the formation of additional national or regional pediatric centers with robust referral networks, further subspecialty training opportunities within LMICs could be considered.

One example of subspecialty training in LMICs is the CURE Hydrocephalus and Spina Bifida (CHSB) fellowship supported by the CURE Children's Hospital of Uganda, which has had enormous success. Through 8 weeks of postgraduate training, fellows receive a unique operative experience that includes a high volume of endoscopic third ventriculostomies with choroid plexus cauterization,

myelomeningocele closures, and ventriculoperitoneal shunting procedures. Training through this fellowship opportunity has culminated in the graduation of 33 subspecialty-trained neurosurgeons from 20 different countries, who are performing thousands of hydrocephalus and spina bifida cases each year [52]. This model may be extended to pediatric brain tumors.

Apart from enhancing opportunities for subspecialty fellowship training, a priority should be given to strengthening neurosurgical capacity in LMICs. Dewan and colleagues found that many neurosurgeons in LMICs did not have access to the necessary technologies required to deliver care. These include electric drills, microscopes, headlights, endoscopes, and other microsurgical equipment [35]. Moreover, it is not uncommon for neurosurgeons in LMICs to lack access to a blood bank, anesthesia care with ventilatory support, and/or a dedicated neuro-intensive care unit. These resources are necessary to provide proper care for pediatric brain tumor patients. This benefit extends beyond neurosurgery to health systems overall, particularly in LMICs. For example, increasing the neurosurgical capacity in Uganda has positively impacted the overall delivery of healthcare as improvements in neurosurgical accessibility have led to better care within the emergency, general medical, and intensive care settings [53]. This supports the vital role that neurosurgery provides in advancing the overall functioning of healthcare systems, particularly in LMICs.

1.8 Identifying National Centers of Excellence and Establishing Regional Referral Networks for Children with Low-Grade Glioma

The diagnosis of a CNS malignancy is strongly correlated with the availability of resources such as health expenditure per capita, the ratio of neurosurgeons per 100,000 people, and access to diagnostic imaging, including magnetic resonance imaging (MRI) [5]. Pediatric brain tumors often go undiagnosed in countries with limited resources, and incidence data is scarce [13, 54, 55]. For children with brain tumors, treatment includes collaborative efforts among members of a multidisciplinary care team involving neurosurgeons, neuro-oncologists, neuroradiologists, radiation oncologists, and skilled nursing team members. Unfortunately, most LMICs lack specialized centers with the necessary equipment and experienced staff capable of providing a multidisciplinary treatment approach [56–58].

In Egypt and Jordan, successful efforts in the treatment of pediatric brain tumors have been achieved through the development of a large comprehensive charity cancer hospital dedicated to children in Cairo, Egypt, and the implementation of treatment protocols through an international collaboration between the King Hussein Cancer Center in Amman, Jordan, and the Hospital for Sick Children in Toronto, Canada [21, 59]. Concentrating expert pediatric neuro-oncology staff in a fully equipped regional facility for referral is a strategic approach to providing

specialized care and should be considered in other LMICs. Although specialized centers of care are expensive to construct, staff, and maintain, local philanthropy is often eager to help children, especially those diagnosed with cancer. In the long term, clinicians must advocate for robust health financing in pediatric neuro-oncology, compelling governments to provide universal health coverage for a disease with potential for cure and freedom from disability.

To establish effective and sustainable pediatric cancer care for children in LMICs, government leaders and ministries of health must view pediatric oncology as a public health priority. This was one impetus for launching the Global Initiative for Childhood Cancer, a combined effort between the WHO and St. Jude Children's Research Hospital. This initiative focuses on four pillars represented by the acronym, CURE. The first pillar, "centers of excellence," includes developing care models with referral pathways, strengthening the training of a multidisciplinary workforce, and ensuring facilities have the necessary infrastructure and technologies. The second pillar is denoted by "universal health coverage," which aims to expand coverage of cancer interventions to all children. The third pillar encompasses "regimens for management," aiming to develop national standards of care and ensure a reliable supply of quality-controlled medications for childhood cancer treatment. Finally, the fourth pillar is termed "evaluation and monitoring." This pillar aims to strengthen cancer registries, invest in research infrastructure, and monitor quality improvement [6].

To successfully treat children with LGGs and other forms of childhood brain tumors in LMICs, the neurosurgical community must assist in identifying and establishing centers of excellence with accompanying regional referral networks focusing on pediatric neuro-oncology. By working in liaison with neurosurgeons and other brain tumor specialists in LMICs, the greater neurosurgical body can identify regional representatives who have strong relationships with community leaders, an interest in caring for children, and knowledge of local health infrastructures, which may include the status of surgical referral networks, specialized equipment needs, and capacity for multidisciplinary care.

With institutions such as the Children's Cancer Hospital Egypt and the King Hussein Cancer Center being in large, metropolitan areas, establishing surgical referral networks in rural regions will be critical for providing timely access to specialized care as new centers are identified and developed. Historically, access to surgery and surgical referral networks has been insufficient or completely lacking for rural populations outside of city centers in LMICs. As globalization progresses, what was once considered a luxury health service is now being pursued in cities and rural regions within LMICs [60, 61]. The increased adoption of telemedicine in healthcare systems worldwide, brought about by the COVID-19 pandemic, can help facilitate prompt referrals and long-term follow-up, even among patients from distant geographic regions.

As our community takes steps toward assisting in the establishment of robust referral networks for childhood brain tumors, it is essential to be mindful of factors influencing referral capabilities. In a review of surgical referral systems in LMICs by Pittalis and colleagues, many LMICs lacked sufficient surgical infrastructure,

comprehensive protocols for surgical referrals, equipment, and personnel. Moreover, some clinicians demonstrated gaps in referral decision-making skills. These obstacles severely hamper appropriate surgical referrals. Interventions to improve this process include enhanced coordination and communication among tertiary facilities and incorporating a standard protocol [62]. As neurosurgeons begin to play leading roles in establishing referral networks for patients with LGG, we must pay particular attention to both systemic and cultural barriers and develop timely solutions. These steps will ensure that rural populations are appropriately cared for by specialists with the necessary expertise to treat patients with LGG, without neglecting the important role of primary care physicians, pediatricians, and neurosurgeons in their respective communities for long-term care.

1.9 Traversing Socioeconomic and Sociocultural Barriers to Pediatric Brain Tumor Care

Almost 46% of the world's population lives on less than $5.50 per day. While the number of individuals who live in extreme poverty, defined as living on less than $1.90 per day, continues to decrease, socioeconomic status remains a significant barrier to care for most individuals in LMICs [63]. For many families in LMICs, the lack of financial resources limits potential treatment for a child with a CNS tumor. The diagnosis of a pediatric brain tumor can create an enormous financial burden when considering the cost of diagnostic imaging, treatment, and supportive care. In rural regions across LMICs, it is not uncommon for community members to pool resources to support treatment. Unfortunately, this is not a practical approach to mitigate financial costs as one MRI scan can easily surpass the annual income of multiple families. So, how can we begin to address these challenges for children with LGG?

Neurosurgery is an inherently technology-driven surgical specialty [64]. As such, there is a great need for cost-effective neurosurgical innovation to address specialty-related socioeconomic barriers to care. With the Lancet Commission now placing surgical care at the forefront of global health initiatives, neurosurgeons must continue to establish a strong emphasis on cost-effective treatment approaches for low-income patient populations. We must continue to strive for affordable treatment options and pursue cost-effective technologies that provide a similar standard of care without a significant financial burden.

Historically, the treatment of neurosurgical diseases has failed to garnish priority attention from governmental and private health organizations [65]. However, the cost-benefit analysis for treating a condition such as infantile hydrocephalus in sub-Saharan Africa was shown to be more favorable than the surgical treatment of trauma, cleft palate repair, and elective orthopedic interventions [66]. Incorporating endoscopic third ventriculostomy with and without choroid plexus cauterization for children in Uganda with hydrocephalus has decreased many burdens associated

with shunt placement. These include access to reliable transportation, economic limitations, and lack of appropriate follow-up [67]. With respect to pediatric LGG, a one-time curative treatment option such as tumor removal would decrease morbidity and mortality while eliminating the economic and logistical challenges associated with chemotherapy and serial radiographic imaging.

In addition to socioeconomic challenges, sociocultural barriers also hinder access to neurosurgical care and other treatment modalities for pediatric brain tumor patients. In certain regions of sub-Saharan Africa, neurosurgical interventions are viewed as futile [56]. Moreover, in some cultures, a cancer diagnosis is plagued by negative perceptions of care. Families have been reported to abandon therapy or forego conventional therapeutic options for folklore medicine, such as tribal healers and indigenous herbalism [55, 56, 68]. Gender can also influence treatment. In one study, social workers captured nuances in discontinuing treatment between male and female patients whereby surgical disfigurement was presumed to impact marital status [69]. As clinicians, engaging in open communication with patients and their families is crucial to identifying misconceptions, understanding concerns, and alleviating doubts surrounding treatment options.

1.10 Advancing Neurosurgery on a Global Scale

As the Lancet Commission on Global Surgery 2030 continues to gain momentum in supporting universal access to safe and affordable surgical care, neurosurgeons must join international health experts and advocate for increased neurosurgical access in LMICs. By assuming leadership positions at the regional, national, and global levels, neurosurgeons will be poised to contribute their expertise in advocacy for policies that expand neurosurgical care to underserved populations in LMICs. Perhaps, most importantly, neurosurgical organizations and leaders in the field must make sure that LMIC neurosurgeons have presence and active roles at international health meetings to articulate regional needs on the global stage. As most evidence-based guidelines are developed in HICs, often without input from treating physicians in LMICs, these approaches may not be possible to implement in low-resource settings. Ensuring LMIC representation will provide an empirical stance on those components of neurosurgical care and delivery that require immediate attention.

In a review from Velin and colleagues, high travel costs, marginal acceptance rates of research abstracts, and receiving governmental visas were common barriers preventing representatives from LMICs from attending global health meetings [70]. To address these barriers, event organizers must be encouraged to provide travel grants specific to LMIC representatives. Neurosurgeons in HICs and LMICs must also forge new partnerships and collaborative networks to strengthen research infrastructure and enhance capacity building initiatives in LMICs. This will provide robust epidemiological data on the status of neurosurgical conditions in LMICs and support an avenue to explore innovative research questions focusing on underserved populations. Moreover, these measures will offer platforms wherein neurosurgeons

from LMICs can share how they overcome challenges to surgical care in their clinical practice and advocate for further capacity building initiatives.

Finally, international neurosurgical societies such as the International Society for Pediatric Neurosurgery (ISPN), the World Federation of Neurosurgical Societies (WFNS), the Foundation for International Education in Neurological Surgery (FIENS), and the Neurosurgical Atlas continue to provide high-quality surgical videos and online learning tools available at no cost to neurosurgeons [71–73]. These efforts coupled with annual pediatric neurosurgical short courses over the span of 3–4 days in Asia, Australasia, Europe, and Latin America play a significant role in pediatric neurosurgical education for neurosurgeons in LMICs, especially those who may not have the availability to participate in a full-time fellowship [74–76]. Nevertheless, virtual meeting formats resulting from the COVID-19 pandemic have substantially impacted neurosurgical education without the expense of travel or time away from practice and should continue to be heavily pursued.

1.11 Final Thoughts

The difference in survival rates of children with brain tumors in LMICs compared to HICs is a somber reminder of childhood cancer's global burden. By responding to the World Health Organization and St. Jude Children's Research Hospital's Global Initiative for Childhood Cancer, neurosurgeons are uniquely positioned to improve survival rates for pediatric LGG around the globe. The neurosurgical community can dramatically increase the number of pediatric neurosurgeons capable of treating surgically curable childhood brain tumors by supporting additional educational initiatives. Fellowship opportunities aimed at retaining surgeons in LMICs while providing them with the necessary resources to achieve maximally safe GTR will drastically improve survival rates for LGG in LMICs. Each country should aim to establish centers of excellence in pediatric neuro-oncology, where pediatric neurosurgeons are able to provide timely and safe neurosurgery, as part of comprehensive multidisciplinary care from trained specialists. These centers must be supported by robust regional referral networks and be sufficiently funded to cushion patients and their families from catastrophic health expenditure. As we embark on these global health initiatives to decrease the burden of childhood cancer and expand neurosurgical access to individuals in LMICs, we acknowledge that significant work lies ahead. Fortunately, our field continues to recruit some of the world's brightest minds who are eager to take on the global challenges impacting the neurosurgical care of vulnerable patient populations. By 2030, we hope to have made significant strides in decreasing the burden of childhood cancer worldwide and expanding access to neurosurgical care.

Acknowledgments The authors wish to thank Alexis N. Antonopoulos, DO (Arkansas Children's Hospital), and Susanna Downing, MS (Center for Pediatric Neurological Disease Research at St. Jude Children's Research Hospital), for their helpful comments and editing of this manuscript.

Compliance with Ethical Standards Funding: No sources of funding were received for this manuscript.
Conflicts of interest/competing interests: None of the authors have any financial conflicts of interests to disclose.
Ethics approval: Not applicable.
Consent to participate: Not applicable.
Consent for publication: All authors have approved the final version of this manuscript.
Availability of data and material: All references are cited.
Code availability: Not applicable.

Delineation of Author Duties Author contributions to the manuscript preparation include the following:

Conception and design: Jordan T. Roach and Frederick A. Boop.

Drafting the chapter: Jordan T. Roach.

Drafting figures for the chapter: Jordan T. Roach and Jared M. Andrews.

Critically revising the chapter: Nathan A. Shlobin, Jared M. Andrews, Ronnie E. Baticulon, Danny A. Campos, Daniel C. Moreira, Ibrahim Qaddoumi, and Frederick A. Boop.

Approved final version of the manuscript on behalf of all authors: Frederick A. Boop.

References

1. Pui CH, Evans WE. A 50-year journey to cure childhood acute lymphoblastic leukemia. Semin Hematol. 2013;50:185–96.
2. Ward E, DeSantis C, Robbins A, Kohler B, Jemal A. Childhood and adolescent cancer statistics, 2014. CA Cancer J Clin. 2014;64:83–103.
3. Curtin SC, Miniño AM, Anderson RN. Declines in cancer death rates among children and adolescents in the United States. 1999.
4. Hudson MM, Link MP, Simone J, v. Milestones in the curability of pediatric cancers. J Clin Oncol. 2014;32:2391–7.
5. Moreira D, Qaddoumi I, Bhakta N, Gajjar A, Rodriguez-Galindo C. EPID-07. A global perspective on the burden of pediatric central nervous system tumors. Neuro-Oncology. 2020;22:iii320.
6. World Health Organization. CureALL framework: WHO Global Initiative for Childhood Cancer: increasing access, advancing quality, saving lives. 2021.
7. World Bank staff estimates based on age/sex distributions of United Nations Population Division's world population prospects: 2019 revision. 2019.
8. Rodriguez-Galindo C, Friedrich P, Morrissey L, Frazier L. Global challenges in pediatric oncology. Curr Opin Pediatr. 2013;25:3–15.
9. Force LM, Abdollahpour I, Advani SM, et al. The global burden of childhood and adolescent cancer in 2017: an analysis of the global burden of disease study 2017. Lancet Oncol. 2019;20:1211–25.
10. Sullivan R, Kowalczyk JR, Agarwal B, et al. New policies to address the global burden of childhood cancers. Lancet Oncol. 2013;14:e125–35.
11. Allemani C, Matsuda T, di Carlo V, et al. Global surveillance of trends in cancer survival 2000–14 (CONCORD-3): analysis of individual records for 37 513 025 patients diag-

nosed with one of 18 cancers from 322 population-based registries in 71 countries. Lancet. 2018;391:1023–75.
12. Azad TD, Shrestha RK, Vaca S, Niyaf A, Pradhananga A, Sedain G, Sharma MR, Shilpakar SK, Grant GA. Pediatric central nervous system tumors in Nepal: retrospective analysis and literature review of low- and middle-income countries. World Neurosurg. 2015;84:1832–7.
13. Ezzat S, Kamal M, El-Khateeb N, El-Beltagy M, Taha H, Refaat A, Awad M, Abouelnaga S, Zaghloul MS. Pediatric brain tumors in a low/middle income country: does it differ from that in developed world? J Neurooncol. 2016;126:371–6.
14. Haizel-Cobbina J, Chen JW, Belete A, Dewan MC, Karekezi C. The landscape of neuro-oncology in East Africa: a review of published records. Childs Nerv Syst. 2021;37:2983–92.
15. Baskin JL, Lezcano E, Kim BS, et al. Management of children with brain tumors in Paraguay. Neuro-Oncology. 2013;15:235–41.
16. Suresh S, Srinivasan A, Scott J, Rao S, Chidambaram B, Chandrasekar S. Profile and outcome of pediatric brain tumors – experience from a tertiary care pediatric oncology unit in South India. J Pediatr Neurosci. 2017;12:237.
17. Oigman G, Osorio DS, Ferman S, Stanek JR, Aversa do Souto A, Christiani MMC, Magalhaes DMA, Finlay JL, Vianna DA. Epidemiological characteristics and survival outcomes of children with medulloblastoma treated at the National Cancer Institute (INCA) in Rio de Janeiro, Brazil. Pediatr Blood Cancer. 2022;69:e29274. https://doi.org/10.1002/pbc.29274.
18. Howard SC, Metzger ML, Wilimas JA, Quintana Y, Pui C-H, Robison LL, Ribeiro RC. Childhood cancer epidemiology in low-income countries. Cancer. 2008;112:461–72.
19. Rodriguez-Galindo C, Friedrich P, Alcasabas P, et al. Toward the cure of all children with cancer through collaborative efforts: pediatric oncology as a global challenge. J Clin Oncol. 2015;33:3065–73.
20. Hesseling P, Molyneux E, Kamiza S, Israels T, Broadhead R. Endemic Burkitt lymphoma: a 28-day treatment schedule with cyclophosphamide and intrathecal methotrexate. Ann Trop Paediatr. 2009;29:29–34.
21. Qaddoumi I, Musharbash A, Elayyan M, Mansour A, Al-Hussaini M, Drake J, Swaidan M, Bartels U, Bouffet E. Closing the survival gap: implementation of medulloblastoma protocols in a low-income country through a twinning program. Int J Cancer. 2008;122:1203–6.
22. Wisoff JH, Sanford RA, Heier LA, Sposto R, Burger PC, Yates AJ, Holmes EJ, Kun LE. Primary neurosurgery for pediatric low-grade gliomas: a prospective multi-institutional study from the Children's oncology group. Neurosurgery. 2011;68:1548–55.
23. Ostrom QT, Cioffi G, Gittleman H, Patil N, Waite K, Kruchko C, Barnholtz-Sloan JS. CBTRUS statistical report: primary brain and other central nervous system tumors diagnosed in the United States in 2012–2016. Neuro-Oncology. 2019;21:v1–v100.
24. Chalil A, Ramaswamy V. Low grade gliomas in children. J Child Neurol. 2016;31:517–22.
25. McCormack BM, Miller DC, Budzilovich GN, Voorhees GJ, Ransohoff J. Treatment and survival of low-grade astrocytoma in adults--1977–1988. Neurosurgery. 1992;31:636–42.
26. Krieger MD, Gonzalez-Gomez I, Levy ML, McComb G. Recurrence patterns and anaplastic change in a long-term study of pilocytic astrocytomas. Pediatr Neurosurg. 1997;27:1–11.
27. Broniscer A, Baker SJ, West AN, et al. Clinical and molecular characteristics of malignant transformation of low-grade glioma in children. J Clin Oncol. 2007;25:682–9.
28. Ryall S, Tabori U, Hawkins C. Pediatric low-grade glioma in the era of molecular diagnostics. Acta Neuropathol Commun. 2020;8:30.
29. Dirks P, Jay V, Becker L, Drake J, Humphreys R, Hoffman H, Rutka J. Development of anaplastic changes in low-grade astrocytomas of childhood. Neurosurgery. 1994;1:68–78.
30. Phuphanich S, Edwards MSB, Levin VA, Vestnys PS, Wara WM, Davis RL, Wilson CB. Supratentorial malignant gliomas of childhood. J Neurosurg. 1984;60:495–9.
31. Gajjar A, Sanford RA, Heideman R, Jenkins JJ, Walter A, Li Y, Langston JW, Muhlbauer M, Boyett JM, Kun LE. Low-grade astrocytoma: a decade of experience at St. Jude Children's Research Hospital. J Clin Oncol. 1997;15:2792–9.

32. Flores LE. Delay in the diagnosis of pediatric brain tumors. Arch Pediatr Adolesc Med. 1986;140:684.
33. Arnautovic A, Billups C, Broniscer A, Gajjar A, Boop F, Qaddoumi I. Delayed diagnosis of childhood low-grade glioma: causes, consequences, and potential solutions. Childs Nerv Syst. 2015;31:1067–77.
34. Edgeworth J, Bullock P, Bailey A, Gallagher A, Crouchman M. Why are brain tumours still being missed? Arch Dis Child. 1996;74:148–51.
35. Dewan MC, Baticulon RE, Rattani A, Johnston JM, Warf BC, Harkness W. Pediatric neurosurgical workforce, access to care, equipment and training needs worldwide. Neurosurg Focus. 2018;45:E13.
36. Merchant TE, Conklin HM, Wu S, Lustig RH, Xiong X. Late effects of conformal radiation therapy for pediatric patients with low-grade glioma: prospective evaluation of cognitive, endocrine, and hearing deficits. J Clin Oncol. 2009;27:3691–7.
37. Mulhern RK, Merchant TE, Gajjar A, Reddick WE, Kun LE. Late neurocognitive sequelae in survivors of brain tumours in childhood. Lancet Oncol. 2004;5:399–408.
38. Collett-Solberg PF, Sernyak H, Satin-Smith M, Katz LL, Sutton L, Molloy P, Moshang TJ. Endocrine outcome in long-term survivors of low-grade hypothalamic/chiasmatic glioma. Clin Endocrinol (Oxf). 1997;47:79–85.
39. Ater JL, Zhou T, Holmes E, et al. Randomized study of two chemotherapy regimens for treatment of low-grade glioma in young children: a report from the Children's oncology group. J Clin Oncol. 2012;30:2641–7.
40. Bouffet E, Jakacki R, Goldman S, et al. Phase II study of weekly vinblastine in recurrent or refractory pediatric low-grade glioma. J Clin Oncol. 2012;30:1358–63.
41. Friedrich P, Lam CG, Itriago E, Perez R, Ribeiro RC, Arora RS. Magnitude of treatment abandonment in childhood cancer. PLoS One. 2015;10:e0135230.
42. Mostert S, Arora RS, Arreola M, et al. Abandonment of treatment for childhood cancer: position statement of a SIOP PODC working group. Lancet Oncol. 2011;12:719–20.
43. Upadhyaya SA, Ghazwani Y, Wu S, Broniscer A, Boop FA, Gajjar A, Qaddoumi I. Mortality in children with low-grade glioma or glioneuronal tumors: a single-institution study. Pediatr Blood Cancer. 2018;65:e26717.
44. Dewan MC, Rattani A, Fieggen G, Arraez MA, Servadei F, Boop FA, Johnson WD, Warf BC, Park KB. Global neurosurgery: the current capacity and deficit in the provision of essential neurosurgical care. Executive summary of the global neurosurgery initiative at the program in global surgery and social change. J Neurosurg. 2019;130:1055–64.
45. Baticulon RE, Dewan MC, Wittayanakorn N, Aldana PR, Maixner WJ. Pediatric neurosurgery in Asia and Australasia: training and clinical practice. J Neurosurg Pediatr. 2021;27:93–101.
46. Park KB, Johnson WD, Dempsey RJ. Global neurosurgery: the unmet need. World Neurosurg. 2016;88:32–5.
47. Dewan MC, Rattani A, Mekary R, Glancz LJ, Yunusa I, Baticulon RE, Fieggen G, Wellons JC, Park KB, Warf BC. Global hydrocephalus epidemiology and incidence: systematic review and meta-analysis. J Neurosurg. 2019;130:1065–79.
48. Ezzati M, Pearson-Stuttard J, Bennett JE, Mathers CD. Acting on non-communicable diseases in low- and middle-income tropical countries. Nature. 2018;559:507–16.
49. Bennett JE, Stevens GA, Mathers CD, et al. NCD countdown 2030: worldwide trends in non-communicable disease mortality and progress towards sustainable development goal target 3.4. Lancet. 2018;392:1072–88.
50. Dewan MC, Mummareddy N, Wellons JC, Bonfield CM. Epidemiology of global pediatric traumatic brain injury: qualitative review. World Neurosurg. 2016;91:497–509.e1.
51. Johnson KJ, Cullen J, Barnholtz-Sloan JS, et al. Childhood brain tumor epidemiology: a brain tumor epidemiology consortium review. Cancer Epidemiol Biomark Prev. 2014;23:2716–36.
52. Dewan MC, Onen J, Bow H, Ssenyonga P, Howard C, Warf BC. Subspecialty pediatric neurosurgery training: a skill-based training model for neurosurgeons in low-resourced health systems. Neurosurg Focus. 2018;45:E2.

53. Fuller A, Tran T, Muhumuza M, Haglund MM. Building neurosurgical capacity in low and middle income countries. eNeurologicalSci. 2016;3:1–6.
54. El-Gaidi MA. Descriptive epidemiology of pediatric intracranial neoplasms in Egypt. Pediatr Neurosurg. 2011;47:385–95.
55. Zaghloul MS. Pediatric neuro-oncology in low-/middle-income countries. Neurooncology. 2016. https://doi.org/10.5772/63111.
56. El-Fiki M. African neurosurgery, the 21st-century challenge. World Neurosurg. 2010;73:254–8.
57. Ribeiro RC, Steliarova-Foucher E, Magrath I, et al. Baseline status of paediatric oncology care in ten low-income or mid-income countries receiving my child matters support: a descriptive study. Lancet Oncol. 2008;9:721–9.
58. Chan MH, Boop F, Qaddoumi I. Challenges and opportunities to advance pediatric neuro-oncology care in the developing world. Childs Nerv Syst. 2015;31:1227–37.
59. Zaghloul MS. Single pediatric neuro-oncology center may make difference in low/middle-income countries. Childs Nerv Syst. 2016;32:241–2.
60. Meara JG, Leather AJM, Hagander L, et al. Global surgery 2030: evidence and solutions for achieving health, welfare, and economic development. Lancet. 2015;386:569–624.
61. Oyemolade TA, Adeleye AO, Olusola AJ, Ehinola BA, Aikhomu EP, Iroko AA. Burden of pediatric neurosurgical disease in a rural developing country: perspectives from Southwest Nigeria. J Neurosurg Pediatr. 2022;29:162–7.
62. Pittalis C, Brugha R, Gajewski J. Surgical referral systems in low- and middle-income countries: a review of the evidence. PLoS One. 2019;14:e0223328.
63. Nearly half the world lives on less than $5.50 a day. 2018.
64. Marcus HJ, Hughes-Hallett A, Kwasnicki RM, Darzi A, Yang G-Z, Nandi D. Technological innovation in neurosurgery: a quantitative study. J Neurosurg. 2015;123:174–81.
65. Härtl R, Ellegala DB. Neurosurgery and Global Health: going far and fast, together. World Neurosurg. 2010;73:259–60.
66. Warf BC, Alkire BC, Bhai S, Hughes C, Schiff SJ, Vincent JR, Meara JG. Costs and benefits of neurosurgical intervention for infant hydrocephalus in sub-Saharan Africa. J Neurosurg Pediatr. 2011;8:509–21.
67. Warf BC. Hydrocephalus in Uganda: the predominance of infectious origin and primary management with endoscopic third ventriculostomy. J Neurosurg Pediatr. 2005;102:1–15.
68. Walubita M, Sikateyo B, Zulu JM. Challenges for health care providers, parents and patients who face a child hood cancer diagnosis in Zambia. BMC Health Serv Res. 2018;18:314.
69. Faruqui N, Bernays S, Martiniuk A, Abimbola S, Arora R, Lowe J, Denburg A, Joshi R. Access to care for childhood cancers in India: perspectives of health care providers and the implications for universal health coverage. BMC Public Health. 2020;20:1641.
70. Velin L, Lartigue J-W, Johnson SA, Zorigtbaatar A, Kanmounye US, Truche P, Joseph MN. Conference equity in global health: a systematic review of factors impacting LMIC representation at global health conferences. BMJ Glob Health. 2021;6:e003455.
71. Mosberg WH, Svien HJ, Tyrer AR, Mount L, Voris HC, Evans JP, Hayes GJ, Livingston KE, Thompson RK, Uihlein A. Foundation for International Education in neurological surgery, incorporated. J Neurosurg. 1970;33:481–4.
72. Blankstein U, Dakurah T, Bagan M, Hodaie M. Structured online neurosurgical education as a novel method of education delivery in the developing world. World Neurosurg. 2011;76:224–30.
73. Teton ZE, Freedman RS, Tomlinson SB, Linzey JR, Onyewuenyi A, Khahera AS, Hendricks BK, Cohen-Gadol AA. The neurosurgical atlas: advancing neurosurgical education in the digital age. Neurosurg Focus. 2020;48:E17.
74. Wang B, Han Y, Wang Q, Ma J. The establishment of Shanghai pediatric neurosurgical society and the 12th Asian Australasian advanced course in pediatric neurosurgery (12th AAACPN): adventure and opportunity for Chinese pediatric neurosurgeons. Childs Nerv Syst. 2018;34:793–5.

75. de Oliveira RS, Machado HR. Latin American course in pediatric neurosurgery: 10 years of history. Childs Nerv Syst. 2013;29:2321–2.
76. Choi J-U. The promotion of pediatric neurosurgery throughout the world. Childs Nerv Syst. 2007;23:929–36.

Chapter 2
Brainstem Surgery: Functional Surgical Anatomy with the Use of an Advanced Modern Intraoperative Neurophysiological Procedure

Nobuhito Morota and Vedran Deletis

2.1 Introduction: History of Brainstem Surgery and Intraoperative Neurophysiology

The brainstem, once called as "no man's land," has come to within reach of surgery by expertized hands [1–7]. Looking back at the history of brainstem surgery, the first surgical resection appeared in 1909 [8], followed by 1910 [9]. Cushing was one of those pioneers in brainstem surgery, whose first patient was operated on in 1910 with a dismal outcome [10]. Matson, one of the founders of modern pediatric neurosurgery in North America, mentioned the brainstem glioma in 1969 as "…the location of these tumors in itself obviates the possibility of surgical removal. Exploration for confirmation of the diagnosis should be avoided if possible." However, he did not completely exclude the possibility of surgery, which was indicated only if the clinical and radiological findings were atypical [11]. On the other hand, favorable long-term outcome following surgery was reported by Pool in 1968, though all three reported patients seemed to be atypical or low-grade brainstem tumors [12]. It was not until about the early 1980s that Epstein and Hoffman used the direct surgical approach. Both of them were leading pediatric neurosurgeons at that time, fearlessly challenging the brainstem tumors [3–5, 13]. They classified brainstem tumors, mainly gliomas, and discussed surgical indications based on the tumor location and extension to the surrounding structures [3, 4, 14].

The importance of intraoperative neurophysiology (ION) arose more as direct surgical approach to the brainstem became more common and the concept of

N. Morota (✉)
Department of Neurosurgery, Kitasato University Hospital, Sagamihara, Japan

V. Deletis
Department of Neurosurgery, University Hospital, Zagreb, Croatia

C. Di Rocco (ed.), *Advances and Technical Standards in Neurosurgery*,
Advances and Technical Standards in Neurosurgery 48,
https://doi.org/10.1007/978-3-031-36785-4_2

brainstem surgery shifted from “lifesaving” brainstem surgery to “functionally preserved” brainstem surgery in the 1990s. Advanced surgical technology with detailed information of microanatomy-based surgical approaches, together with the advanced magnetic resonance imaging (MRI), opened the door to the brainstem. However, it still remained a great challenge for neurosurgeons to operate lesions in and around the brainstem. Distortion of the brainstem by a brainstem lesion leads to shifting the brainstem’s anatomical architecture. Normal landmarks which guide neurosurgeons to identify safe entry zones into the brainstem would be lost [15–19]. Brainstem auditory evoked potentials (BAEPs) have been known to reflect part of the brainstem functional integrity. It was applied as a traditional ION methodology together with somatosensory evoked potentials (SSEPs) for brainstem surgeries [20]. However, it should be reminded that the pathway of BAEPs and SSEPs covers only 20% of the brainstem area [21]. Their role in terms of preserving the functional integrity of cranial nerve motor nuclei (CNMN) is limited. A new methodology of ION for the modern use of brainstem surgery had been expected.

The dawn of ION for brainstem surgery came in 1993 when neurophysiological localization of the facial nucleus on the floor of the fourth ventricle became available and was named brainstem mapping (BSM) [22, 23]. In this original BSM, the floor was electrically stimulated using a monopolar stimulator, and the muscle response (EMG) was recorded from the targeted muscle. The muscles monitored for BSM are mainly facial (cranial motor nuclei VII: CNMN VII) and hypoglossal (cranial motor nuclei XII: CNMN XII) nuclei. Other CNMNs, such as glossopharyngeal/vagus complex (CNMN IX/X) nuclei, can be mapped in selected cases [16]. Intraoperative neurophysiological procedures can help neurosurgeons to challenge tough lesions and are expected to play a critical role in performing those demanding surgeries safely [24, 25].

This paper aims to demonstrate comprehensive clinical application of neurophysiological procedures for brainstem surgeries, focusing mainly on BSM on the floor of the fourth ventricle and the CBT-MEP monitoring [24–29]. The authors explain the detail of the surgical perspective of BSM when approached through the floor of the fourth ventricle and that of the CBT-MEP monitoring. Modified application of BSM, when approached from other skull base routes to the brainstem, is also discussed [26, 30–32]. It should be reminded that safety of surgery in and around the brainstem can be maximized with the use of those cutting-edge neurophysiological procedures.

2.2 Role of Intraoperative Neurophysiology

In general, ION consists of two main modalities: mapping and monitoring. The mapping technique is defined as the functional identification of nervous tissue, usually by electrical stimulation. The monitoring technique is defined as continuous feedback on the functional integrity of the nervous tissue [33]. Neurophysiological mapping in the brainstem surgery corresponds to BSM. Monitoring the motor

function integrity of CNMN corresponds to the corticobulbar tract (CBT) motor evoked potential (MEP). Combination of both mapping and monitoring is expected to enable the preservation of the functional integrity of CMN during surgery of the brainstem.

The role of ION in the brainstem surgery would be counted in three points. The first is to locate CMN on the floor of the fourth ventricle when a brainstem lesion is approached through the fourth ventricle. BSM is the answer for this purpose. The detail of BSM with its methodology and neurophysiological background is to be described later. The second is to monitor the functional integrity of the cranial nerve motor pathways originating from the cerebral cortex. The solution is the corticobulbar tract (CBT) motor evoked potential (MEP) monitoring which is emerging as an indispensable tool for the brainstem surgery [24, 29]. Neurophysiological aspects of the CBT-MEP are also described. The last is to preserve a variety of vital reflex circuits derived from the brainstem. Several new methodologies which have been introduced in the last decade are described.

2.3 Normal Anatomy of the Floor of the Fourth Ventricle and Safe Entry Zones

Figure 2.1 demonstrates the normal anatomy of the floor of the fourth ventricle and its subependymal intrinsic brainstem structures relating to the BSM [34, 35]. The facial colliculus and the stria medullaris are two major landmarks on the floor of the fourth ventricle. CNMN VII is mapped at the facial colliculus. It is not exactly the facial nucleus that is electrically stimulated but the intramedullary root of the facial nerve at its closest point to the floor of the fourth ventricle [18]. The stria medullaris suggests the border between the pons and medulla on the floor of the fourth ventricle. However, its direction and number have a wide individual variation; thus, it is not regarded as a reliable surgical landmark. The lower CNMNs are located beneath the hypoglossal and vagus triangles, which are included in the area of the calamus scriptorius [1, 2, 36]. CNMN XII, which locates beneath the hypoglossal triangle, is usually mapped along the midline near the obex [37]. CNMN IX/X is, if mapped, localized at the area rostro-lateral to the point where CNMN IX/X was mapped [16].

Inside of the brainstem are many vital structures and other important functions, and it is very difficult to get into its inner space safely. The term “safe entry zone” to the brainstem was first advocated by Kyoshima in 1993 [15]. Using anatomical landmarks as guidance, he demonstrated supra- and infra-facial triangles as the safe entry zone to the brainstem through the floor of the fourth ventricle (Fig. 2.1).

Suprafacial triangle

Medial border: the medial longitudinal fascicle (MLF)
Caudal border: the facial nerve
Lateral border: the superior and inferior cerebellar peduncles

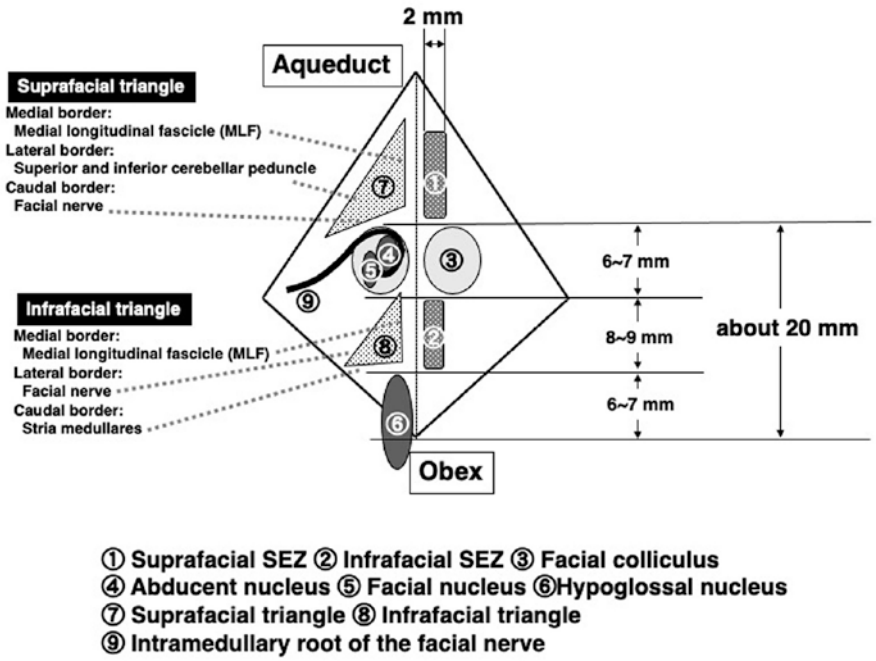

Fig. 2.1 Normal anatomy and morphometrical measurement of the floor of the fourth ventricle. Kyoshima's original safe entry zone on the floor of the fourth ventricle is shown in the left. The rostral end of the facial colliculus is located about 20 mm from the obex. CNMNs VI and VII locate under the facial colliculus. CNMN XII locates under the hypoglossal triangle. Note the actual SEZ is defined as more restricted area based on the morphometrical and cytoarchitectonic studies (SEZ: safe entry zone)

Infra-facial triangle

Medial border: the MLF
Caudal border: the stria medullaris
Lateral border: the facial nerve

A series of morphometric and cytoarchitectonic studies confirmed the safe entry zone and its exact location on the floor of the fourth ventricle [37Bogucki, 18Strauss97]. The structural distance shown in Fig. 2.1 is derived from Bogucki and Strauss's detailed morphometric anatomical study [18, 37].

The idea of "safe entry zone" to the brainstem spread and gained great applause. It ignited surgical challenge to the intrinsic brainstem lesion [1, 38]. Specific safe entry zones for other surgical approaches have been proposed since then. Bricolo added the area acustica as another safe entry zone on the floor of the fourth ventricle [2]. With the advent of skull base surgery, more than ten safe entry zones have been documented and acknowledged in the midbrain, pons, and medulla [34, 36, 38, 39].

2.4 Brainstem Mapping

2.4.1 Role of Brainstem Mapping

The original idea of BSM as an intraoperative neurophysiological procedure is to locate CNMN on the floor of the fourth ventricle (Fig. 2.2). It is the role of BSM. The original safe entry zone on the floor of the fourth ventricle under the normal anatomy does not necessarily assure safe entry to the brainstem. The brainstem is often distorted by the lesion, and the normal landmarks on the floor of the fourth ventricle would be obscure or lost [19, 22, 40, 41]. It is why BSM is required as an indispensable neurophysiological procedure to assist safe brainstem surgeries. BSM makes it possible to locate CMN on the distorted floor of the fourth ventricle and guides neurosurgeons to the area of safe entry zone to the brainstem [16, 22, 23, 27, 28].

The idea of BSM is changing as time goes on, and more surgical approaches are introduced as safe entries to the brainstem. Originally, BSM is the BSM performed on the floor of the fourth ventricle. This is a "narrow" definition. BSM on the other surface of the brainstem is relatively new [26, 30–32]. It is a contemporary application and includes more roles of the original BSM. As a "wide definition," both original and new BSMs are included.

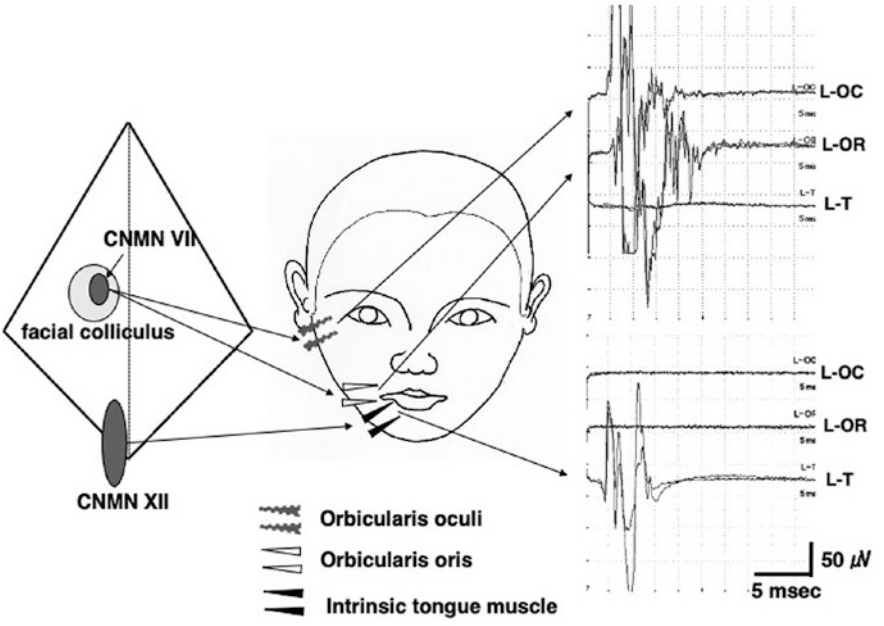

Fig. 2.2 Schema of BSM. Left: CNMN of the floor of the fourth ventricle is electrically stimulated by a handheld monopolar stimulator. Center: A pair of EMG needles are inserted into the targeted muscles. Right: Compound muscle action potentials are recorded following the BSM of each CNMN (*L-OC* left orbicularis oculi, *L-OR* left orbicularis oris, *L-T* left intrinsic tongue muscle)

BSM enables neurosurgeons to preserve CMNs before getting into the brainstem. Direct damage to the CMN would be avoided by BSM because it tells neurosurgeons where the safe entry zone is located and how it shifts [7, 19, 27, 28, 40, 41]. It should be reminded that BSM is a mapping technique to localize a CMN and its intramedullary root. It does not reflect the functional integrity of the whole motor pathway of a CMN, including the CBT. Functional preservation of the sensory pathway is also not assured by BSM. Nevertheless, BSM plays a critical role in brainstem surgeries since functional preservation of the CMN is the primary concern for neurosurgeons who challenge the lesion inside the brainstem.

2.4.2 Methodology of Brainstem Mapping

The technical aspect of BSM through the floor of the fourth ventricle has been published before, and its outline is briefly explained here [16, 28, 41].

2.4.2.1 Preparation for Recording

BSM is performed through the surgically exposed floor of the fourth ventricle. Following endotracheal anesthesia, EMG electrodes are inserted into the appropriate muscles to be mapped intraoperatively (Fig. 2.2). Standard BSM for the brainstem surgery is performed for CNMNs VII and XII. A pair of EMG needles are inserted into both sides of the orbicularis oculi and oris for BSM of the CNMN VII. In the same way, a pair of EMG needles are placed into the lateral aspect of the tongue (intrinsic tongue muscle) on both sides to record the response from the CNMN XII. The impedance of the recording EMG needles should be checked before and after placing the patient in a prone position before starting surgery [16, 28, 41]. Standard recording parameters for BSM are shown in Table 2.1.

2.4.2.2 The Technical Aspect of Stimulation

After surgical exposure of the floor of the fourth ventricle, electrical stimulation is delivered using a handheld monopolar stimulation probe as a cathode. The tip of the electrode is a round shape with a diameter of 0.75–1.0 mm for safety. A corkscrew electrode placed at Fz (10–20 international EEG system) or a needle electrode inserted in a muscle in the surgical field is used as a reference (anode). BSM initially starts with the stimulation intensity of 2.0 mA for searching the CNMNs. The stimulation probe on the floor of the fourth ventricle should stay at one point for a couple of seconds and move in each direction every 1 mm distance for mapping the CNMN. Once muscle responses are obtained, the stimulation intensity is gradually reduced to determine the threshold. The threshold intensity varies from 0.2 to 2.0 mA based on the relationship between the brainstem lesion and CNMNs [16, 28,

Table 2.1 Standard parameters for BSM and CBT-MEP monitoring

	BSM	CBT-MEP monitoring
Stimulation		
Cathode	Handheld monopolar probe	C3(+) - C4(−) or C4(+) - C3(−)
Anode	Fz or muscles in the surgical field	Alternatively or depending on laterality of the lesion
Stimulus form	Square wave	Square wave
Stimulus duration	0.2 ms	0.5 ms
Number of stimulation	Single	Train of 5 (max. 7)
Rate	1.0–4.0 Hz	Interstimulus interval for train: 2 ms
Average	×1	Maximum intensity: 200 mA
Intensity	2.0 mA for screening, threshold intensity for precise localization	Suprathreshold intensity for monitoring
Recording		
Epoch time	20 ms	100 ms
Filter	20–3000 Hz	20–3000 Hz
Amplification	10,000 times	10,000 times
Muscles for EMG recording	Orbicularis oculi and oris (CNMN VII)	Orbicularis oculi and oris (CNMN VII)
	Posterior pharyngeal wall or cricothyroideus (CNMN IX/X)	Posterior pharyngeal wall or cricothyroideus (CNMN IX/X)
	Intrinsic tongue muscle (CNMN XII)	Intrinsic tongue muscle (CNMN XII)
	Other muscles innervated by CMNs as needed	Other muscles innervated by CNMNs as needed
		Abductor pollicis brevis for standard (CST-) MEP monitoring
Others	Stimulation on one point less than 5 s	No muscle response following single stimulation

41]. Minimum stimulation intensity is essential to exactly locate the CNMN [42]. Standard stimulation parameters for BSM are shown in Table 2.1. The safety of BSM under those conditions seems to be secured based on Strauss's proposal which advocated safe margin of BSM as maximum stimulation intensity of 2 mA, stimulation duration up to 400 μs, and stimulation frequency limited to 10 Hz [19].

BSMs for CNMNs IX and X were once included as a standard BSM procedure [Morota95,96,20]. Because of the difficulty in placing electrodes, less reliability in EMG response, and obscure role in determining safe entry zone, it is no more a routine procedure in my practice. However, a new technique of recording the CNMN IX/X response from cricothyroid muscles reported by Deletis would change the clinical evaluation in the future [43]. Electrodes can also be safely inserted in the extraocular muscles for mapping CNMNs III, IV, and VI when a midbrain lesion is operated [44].

2.4.2.3 Anesthesia Regimen of BSM

Anesthetics used for general anesthesia have nearly no influence for BSM. Because BSM stimulates the CNMNs or the intramedullary roots, any type of anesthesia except a long-lasting muscle relaxant is compatible with BSM [16, 28, 32, 45]. However, since BSM is applied together with the CBT-MEP monitoring for the brainstem surgery, total intravenous anesthesia using propofol, fentanyl, a nitrous oxide, and oxygen mixture is the present standard anesthesia regimen. A short-acting muscle relaxant is used only before intubation.

2.4.3 Functional Surgical Anatomy and Its Implications in Brainstem Surgery

2.4.3.1 Functional Surgical Anatomy

Functional anatomy of the brainstem, when approached through the floor of the fourth ventricle, is revealed by BSM [19, 23, 27, 28, 40, 41]. Functional anatomy, in this situation, is nearly a synonym of surgical anatomy. Once CNMNs are mapped (positive mapping), the safe entry zone to the brainstem is identified as the silent neurophysiological area (negative mapping). The brainstem lesion is reached through the safe entry zone. BSM can be repeated from time to time on the floor of the fourth ventricle or through the lesion inside the brainstem. The advantage of BSM is that it avoids direct damage to the CNMN.

An example of functional surgical anatomy revealed by BSM is shown in the following case.

Case 1

This is an 11-year-old boy with diffuse intrinsic pontine glioma (DIPG). The boy showed sudden onset of consciousness disturbance with right facial weakness. Right abducens palsy and mild left hemiparesis were also presented. A CT and MRI revealed intratumoral hemorrhage of a brainstem tumor which is located in the midpons which predominantly shifted on the right side (Fig. 2.3). Emergency surgery for hematoma and tumor removal was carried out.

The fourth ventricle was opened through the suboccipital midline approach. The right side of the floor of the fourth ventricle was bulged by tumor and hematoma, and the median raphe shifted to the left side. BSM was performed with the stimulation intensity of 2.0 mA for a search of the CNMN (Fig. 2.3). After roughly locating the CNMNs, the stimulation intensity was squeezed to 1.0 mA for precise localization of the CNMNs. A map of functional surgical anatomy of the floor of the fourth ventricle was made (Fig. 2.4). A myelotomy was placed on the silent (negative mapping) area, compatible with the suprafacial triangle which was unrecognizable. During hematoma and tumor removal, the CBT-MEP and CST-MEP were continuously monitored. There was no change or deterioration of the MEP responses

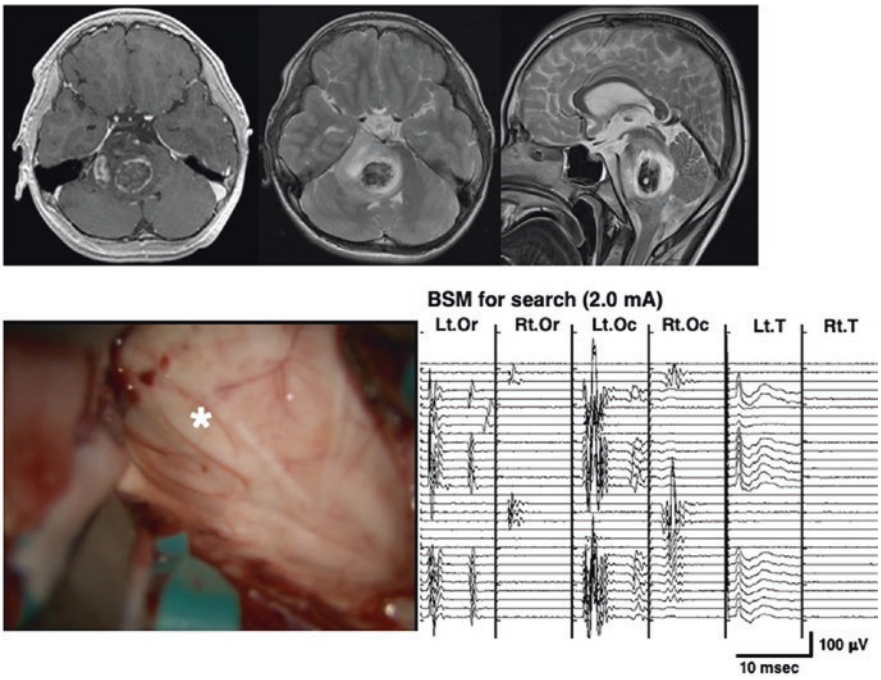

Fig. 2.3 An 11-year-old boy with a diffuse intrinsic pontine glioma and intratumoral hemorrhage. Upper: MRI showed a diffuse intrinsic pontine tumor predominantly located in the right mid-pons with intratumoral hemorrhage. Lower left: An intraoperative photograph of the floor of the fourth ventricle showed bulging of the right side of the floor (asterisk) with a midline shift to the left side. Lower right: BSM using the stimulation intensity of 2.0 mA for a search of the CNMN (*Or* orbicularis oris muscle, *Oc* orbicularis oculi muscle, *T* intrinsic tongue muscle)

(Fig. 2.5). At the end of the hematoma and tumor removal, BSM was repeated (Fig. 2.6). Postoperatively, the boy woke up without neurological deterioration. The pathological diagnosis of the tumor was anaplastic astrocytoma.

2.4.3.2 Deviation of CNMNs Caused by Brainstem Lesions

BSM demonstrated high variability in size and location of CNMN in those with brainstem pathologies [40, 41]. In our experience, BSM showed there was a repetitive pattern of the CNMN displacement depending on the location of the lesion [27, 28, 41, 45] (Fig. 2.7).

In pontine tumors, the CNMN VII is displaced around the edge of the tumor on the floor of the fourth ventricle. If a tumor is at the upper part of the pons, the CNMN VII is displaced caudally and laterally. A lower pontine tumor displaces CNMN VII rostrally and laterally. In selected cases, the orbicularis oculi and oris

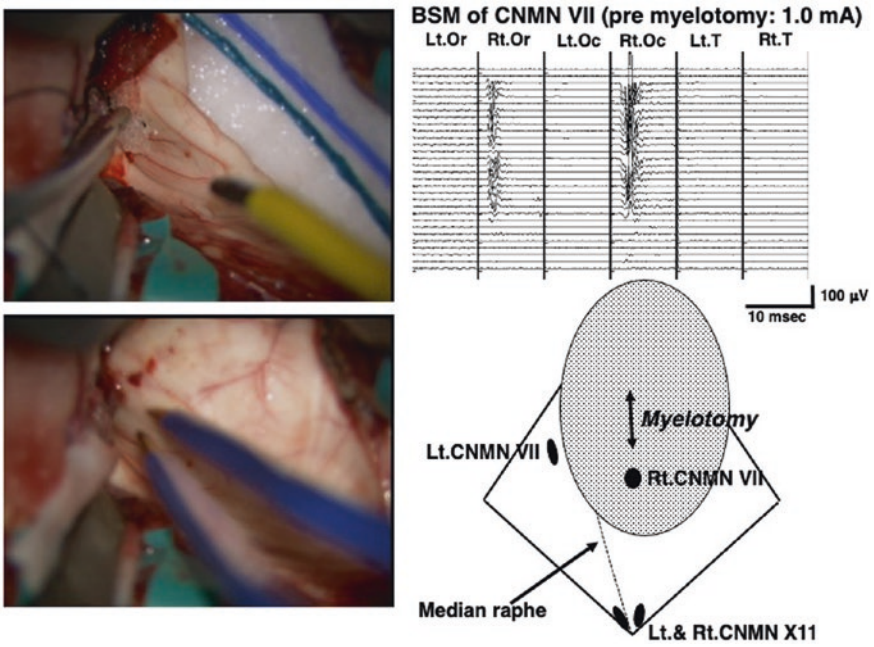

Fig. 2.4 Upper left: BSM on the floor of the fourth ventricle, locating the CNMN VII. Upper right: BSM with the stimulation intensity of 1.0 mA for precise localization of the right CNMN VII. Lower left: Coagulation at a safe entry zone (the suprafacial triangle) on the floor of the fourth ventricle before myelotomy. Lower right: A functional surgical map of the floor of the fourth ventricle based on the result of BSM. Myelotomy was placed rostral to the right CNMN VII (same patient in Fig. 2.3)

muscle responses are mapped at a different but adjacent area on the floor of the fourth ventricle [16, 41].

In case of medullary tumors, one or more lower CNMNs locate ventrally to the tumor. It means BSM of lower CNMN before tumor resection can result in negative mapping and be unable to identify the targeted CNMN. Mapping of lower CNMN in those cases is only possible near the end of tumor resection at the bottom of the tumor cavity. Therefore, unsuccessful BSM of lower CNMN suggests important information that the lower CNMNs are located ventral to the tumor.

Although cervicomedullary junction (CMJ) spinal cord tumors are not a part of a brainstem lesion, they usually displace lower CNMN rostrally if the tumor is not a malignant invasive one [41].

It should be reminded that the abovementioned specific displacement patterns were derived from the case with a brainstem tumor. The result can be different in the case of a hematoma, cavernous angioma, and other pathologies [27, 41].

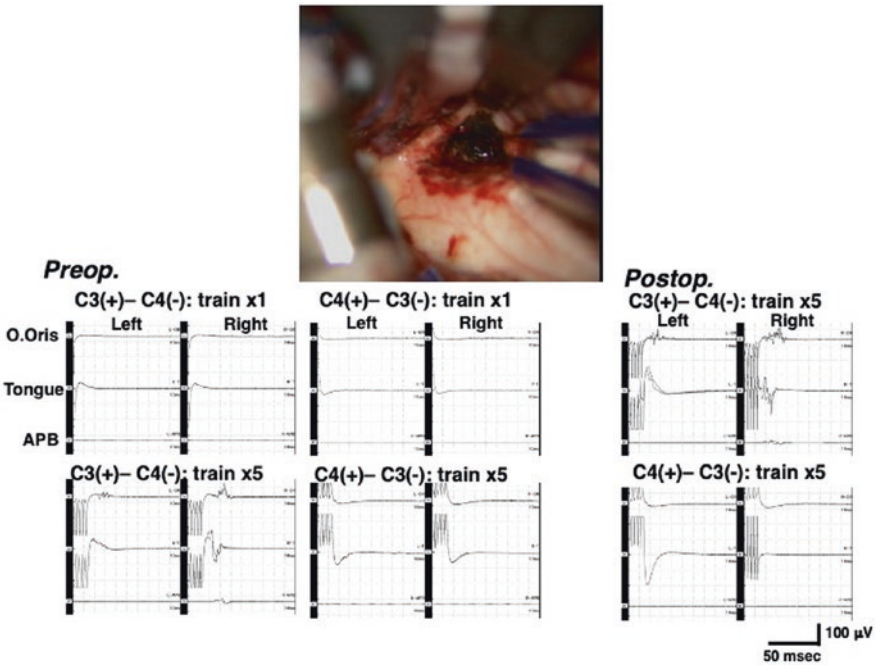

Fig. 2.5 Upper: Removal of tumor and hematoma through the myelotomy placed on the safe entry zone (the suprafacial triangle). Lower: Recording of pre- and postoperative CBT-MEPs (stimulation intensity: 80 mA). No CBT-MEP was recorded when a single transcranial stimulation was delivered. The CBT-MEP was recorded from the left orbicularis oris muscle (O oris) and the tongue intrinsic muscle (tongue) when anodal stimulation was delivered at the C3 with a train of five stimuli (interstimulus interval: 2 ms). Small amplitude of CST-MEP was also recorded from the right abductor pollicis brevis muscle (APB). No muscle activity was evoked when stimulated from the C4. The finding was approximately the same between pre- and postoperative recordings (same patient in Figs. 2.3 and 2.4)

2.4.3.3 The Surgical Implication of Brainstem Mapping

BSM results on the floor of the fourth ventricle suggest several important surgical implications in terms of safe brainstem surgery [27, 28, 41, 45]. First, the risk of damaging CNMN VII exists at the edge of the tumor (Fig. 2.7). The intrinsic pontine tumor usually pushes the CNMN VII around the tumor edge. It means precise localization of the CNMN VII before tumor resection is mandatory to avoid direct damage by retraction or myelotomy incision on the floor of the fourth ventricle. Once a shifted CNMN VII is mapped, one can estimate the approximate area of the safe entry zone. In general, the midline upper pontine tumor displaces the CNMN VII caudally; thus, the safe entry zone where myelotomy is placed locates rostral to the tumor. Myelotomy should be directed rostrally. On the contrary, the midline lower pontine tumor displaces the CNMN VII rostrally; thus, the safe entry zone locates caudal to the tumor. Myelotomy should be directed caudally (Fig. 2.8).

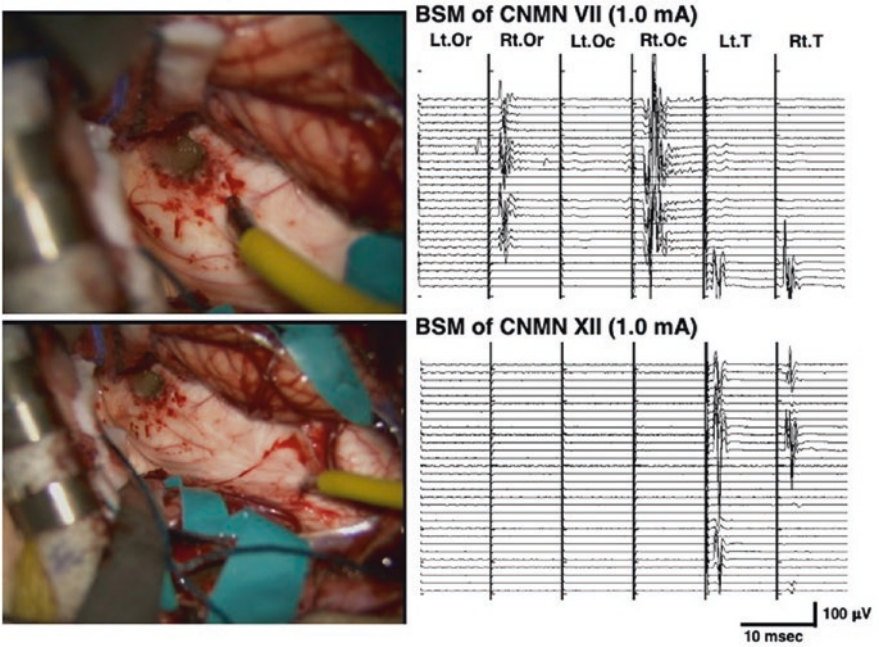

Fig. 2.6 BSM performed after the tumor and hematoma removal. Upper: BSM of the right CNMN VII, which was located caudal to the myelotomy. Lower: BSM of the CNMN XII, which was located near the obex of the fourth ventricle (same patient in Figs. 2.3, 2.4, and 2.5)

Second, in case of the medullary tumor, the risk of damaging lower CNMN exists at the bottom of the tumor cavity (Fig. 2.8). Most tumors grow exophytic while compressing some of the lower CNMN ventral to the tumor (Fig. 2.7). Ventrally displaced lower CNMN can be unmapped before tumor resection because the tumor is on the way of stimulating current. The EMG response can appear as the tumor resection progresses to the bottom of the tumor cavity. Initial negative mapping in BSM before tumor resection is an alarming signal that the lower CNMNs are pushed ventral to the tumor. Negative mapping can turn to positive mapping on the way of tumor resection. Repeating BSM from time to time is recommended as tumor resection comes close to the bottom of the cavity. Once the unmapped lower CNMN is detected, it would be recommended to leave the rest of the tumor untouched for functional preservation of the lower CNMN (Fig. 2.8).

In the case of the CMJ spinal cord tumor, if it is large and extends into the fourth ventricle, the displacement pattern is different. The tumor pushes the caudal part of the floor of the fourth ventricle including the lower CNMN rostrally [Morota96,06,20] (Fig. 2.7). Those lower CNMNs are at high risk of damage if approached from the rostral direction. It is strongly recommended to approach the rostral end of the tumor from the caudal side while undermining the floor of the fourth ventricle (Fig. 2.8).

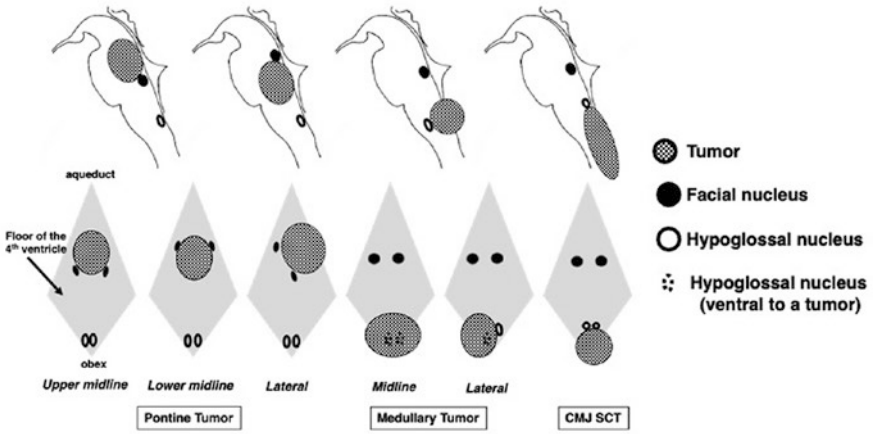

Fig. 2.7 Typical displacement pattern of CNMN by brainstem tumors in a different location. In pontine tumors, CNMN VII is displaced at around the edge of the tumor. Precise localization of CNMN VII by BSM before tumor resection is strongly recommended to avoid direct damage during surgery. Medullary tumors typically grow more exophytic fashion. Uni- or bilateral CNMN XII could be compressed ventral side of the tumor. Failed BSM of CNMN XII before tumor resection would suggest the CMN locates at the bottom of the tumor cavity. It is recommended to repeat BSM when the tumor resection approaches near the bottom of the tumor cavity. Cervicomedullary junction spinal cord tumors (CMJ SCT) displace the lower CNMN rostrally, while the tumor extends and undermines the floor of the fourth ventricle. Care should be paid to the rostral end of the tumor cavity

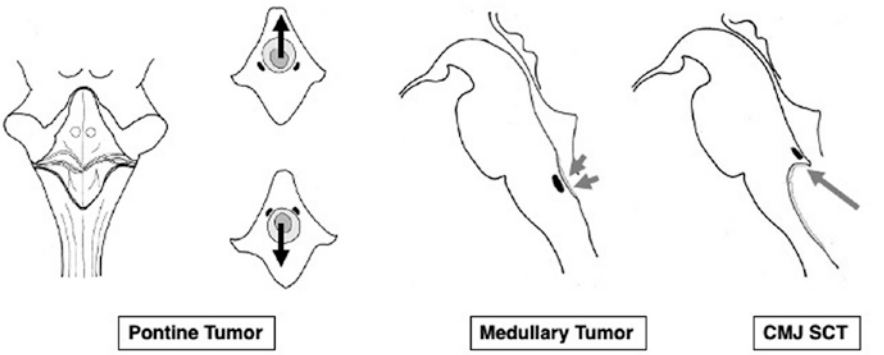

Fig. 2.8 Surgical implications derived from BSM. Left: The midline upper pontine tumor displaces the CNMN VII caudally. Myelotomy from the exposed tumor or the shortest distance from the tumor should be directed rostrally. The midline lower pontine tumor displaces the CNMN VII rostrally. Myelotomy should be directed caudally. Center: In the case of the medullary tumor, the risk of damaging lower CNMN exists at the bottom of the tumor cavity. It is recommended to repeat BSM as tumor resection comes close to the bottom of tumor resection. Right: In the case of the CMJ spinal cord tumor, the tumor pushes the caudal part of the floor of the fourth ventricle rostrally. The risk of damaging the lower CNMN exists at the rostral end of the tumor

2.4.4 Limitations of Brainstem Mapping

BSM has been recognized as an indispensable intraoperative neurophysiological procedure that protects the CNMN from direct damage during surgery of brainstem lesions. Distorted brainstem anatomy fails to indicate the exact location of displaced CNMN. Positive BSM outlines the dangerous area to enter the brainstem. Negative BSM suggests a relatively safe entry zone to the brainstem. Without BSM, a neurosurgeon would be at a loss to find safe entry zone to get into the brainstem lesion. However, BSM does have limitations.

First, BSM is a neurophysiological mapping technique, not a monitoring one. BSM is performed intermittently to localize the CNMN or confirm the functional integrity distal to the CNMN. It is not a continuous procedure to monitor the functional integrity of the CNMN throughout the surgery. When performed, surgery must be interrupted. In addition, repeating BSM frequently consumes time. Nevertheless, damage to the CNMN can develop during the tumor resection between BSMs. To overcome this limitation, combined use of BSM and the CBT-MEP monitoring is strongly required [24, 27, 29].

Second, BSM cannot detect or prevent direct damage to the CBT. Preserved EMG response evoked by BSM does not necessarily assure preserved CBT functional integrity. Chance of selective CBT injury seems unlikely when approached from the floor of the fourth ventricle since the CBTs generally approach the CNMN from a ventral to the dorsal direction [46]. However, the possibility of CBT injury cannot be excluded completely.

Third, positive results of BSM of the lower CNMN do not necessarily guarantee preserved lower brainstem function. Functional integrity of the lower CNMN involved in swallowing, coughing, and vocalization consists of both afferent (sensory) and efferent (motor) reflex circuits. Damage to the intramedullary afferent root or inter-nucleus connecting pathway is undetectable by BSM. It should be reminded that Pick's bundle, one of the medullary CBT branches, forms a loop to innervate lower CNMN (Figs. 2.9 and 2.10). One of its roles is supposed to be connection between the lower CNMNs [46, 47]. Theoretically, damage to Pick's bundle while having positive BSM still can lead to the functional deterioration of the lower CNMN postoperatively.

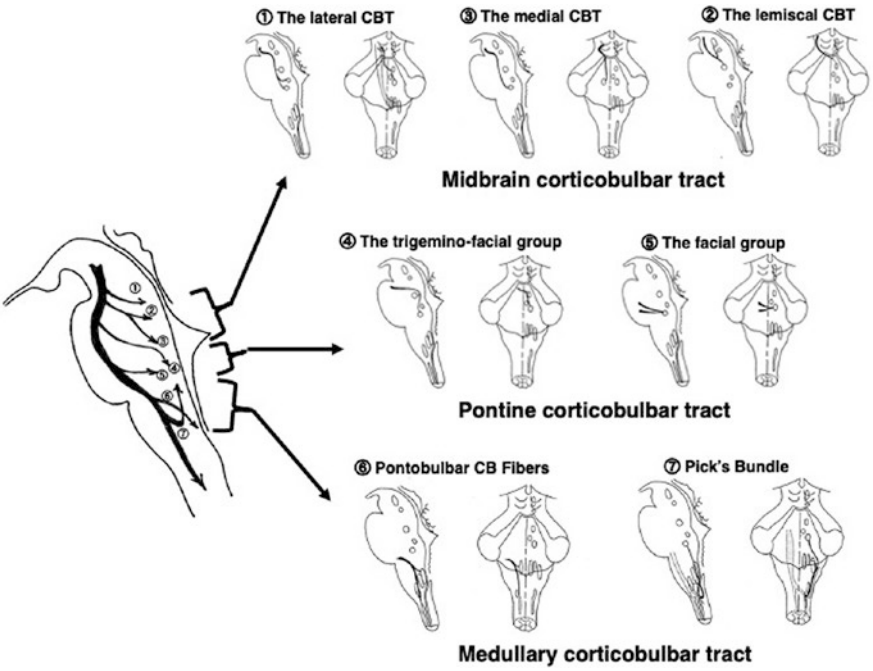

Fig. 2.9 Schematic drawing of the CBT and its branches. The branches are classified into three groups based on the anatomical location. Note that the CBT innervates CNMN in the ventrodorsal direction with multiple innervations to a CMN (from Morota et al., Intraoperative neurophysiology for surgery in and around the brainstem: role of brainstem mapping and corticobulbar tract motor-evoked potential monitoring. Child Nervous Sytem, 26, pages 513–521 (2010), with permission)

2.5 Corticobulbar Tract

2.5.1 Anatomy of CBT

There has been limited knowledge about the detailed anatomy of CBT innervating the CNMN in the brainstem. The CBT is derived from the precentral gyrus and run down aside the corticospinal tract (CST) [48]. It passes the genu of the internal capsule, medial-most region of the cerebrum peduncle, and then spreads into several branches as it goes down [49]. Several branching fibers to the CNMNs VII and XII have been depicted on recent MRI-based studies [47, 50–52].

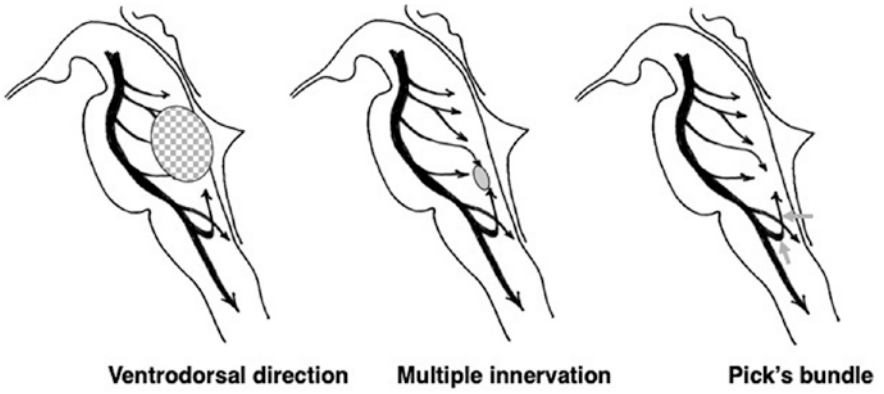

Fig. 2.10 Surgical implications based on the CBT anatomy. Left: The CBT runs ventral-to-dorsal direction to CNMNs. Direct damage to CNMNs seems less likely if the brainstem lesion was approached from the floor of the fourth ventricle. Center: The CNMN receives several branch fibers from the CBT. Multiple innervations of the CNMN by CBT branches mean that the permanent CNMN dysfunction is less when a single branch fiber was damaged. Right: Pick's bundle (gray arrows) forms a medullary loop. Its damage would result in serious lower cranial nerve dysfunction

Krieg is the first to reveal the minute anatomy of the CBT using what we call "fiber dissecting method" in the 1950s [46]. According to his study, the CBT diverges from the CST in the brainstem as several branch fibers. His description of the CBT origin was as follows: "Fibers for the cranial nerve nuclei are the most medial of the pyramidal fibers in the peduncle, but below this level they begin to leave the peduncle to reach their terminations in the brain stem" (Fig. 2.9).

Seven main branches were described, and their courses to the CNMN were shown in a three-dimensional figure in Krieg's book. These branch fibers were classified into three groups based on their locations and targets in the brainstem: midbrain CBT, pontine CBT, and medullary CBT (Fig. 2.9) [24]. Each branch included two to three groups of fibers that synapse directly to the CNMN or indirectly through interneurons. The following explanations are a summary of the original Krieg's description [46].

Midbrain CBT

1. The lateral CBT: It separates the dorsomedial face of the peduncle, directs dorsomedially into the tegmentum, then decussates, and descends to terminate the CNMN V.
2. The medial CBT: It separates from the peduncle, curves ventromedially, then runs dorsally between the medial lemniscus fibers (MLF), turns caudally along the medial of the MLF, decussates, and passes dorsolaterally to reach the CNMN VII and possibly to the CNMNs V and VI.
3. The lemniscal CBT: It courses much like that of the medial CBT, but it diverges laterally to pass into the CNMN V and it branches laterally to pass.

Pontine CBT

4. The trigemino-facial group: It leaves the pyramidal tract at dorsomedial aspect in the upper pons. It reaches the midline and courses directly dorsally just below the fourth ventricle, then decussates, goes laterally to the CNMN VI, and ends to the CNMNs V and VII.
5. The facial group: It leaves the dorsal aspect of the pyramidal tract in the middle and lower pons. After reaching the midline, it gradually decussates and runs dorsally and then runs directly to the CNMN VII.

Medullary CBT

6. The pontobulbar corticobulbar fibers: It leaves the pyramidal tract at the pontomedullary junction and runs dorsally to end in the CNMN X11 and spinal accessory nuclei.
7. Picks bundle: It leaves the pyramidal tract just after decussating, turns cranially, and runs upward just medial to the spinal ambiguous nucleus, while its highest fibers run up to the CNMN VII.

2.5.2 Surgical Implications of CBT Anatomy

Krieg's detailed description of the normal anatomy of the CBT gives us information when we face the brainstem surgery (Fig. 2.10). First, the CBT is not a single bundle like the CST. It is an assembly of a group of fibers. Second, after the CBT branches leave the CST, they run ventral-to-dorsal direction to the CNMN in the brainstem. It means that if the brainstem lesion is approached from the floor of the fourth ventricle, it seems less likely to damage the CBT directly. Third, the CNMN receives several branches from the CBT. There seems to be no one-to-one innervation between a CBT branch and a CNMN. Multiple innervations of the CNMN by CBT branches mean it behaves like a biological "safeguard system," less vulnerable to damage. A single injury to a CBT branch does not necessarily result in CNMN dysfunction. Mild to moderate motor dysfunction of the CNMN caused by direct damage to a CBT branch could possibly recover later. Fourth and finally, one branch of the CBT (Pick's bundle, in the medullary CBT) forms a medullary loop and turns to run caudal-to-rostral direction while innervating the pontomedullary cranial nuclei [47, 51–53]. This atypical, unusual route of the CBT branch could have some role in the complex reflex circuits formed among the lower cranial nerves [24, 27]. Damage to Pick's bundle would cause injury to those critical reflex circuits and result in serious lower cranial nerve dysfunction.

2.5.3 CBT-MEP Monitoring

The functional integrity of the entire CBT ending up to the CNMN is monitored by the CBT-MEP monitoring during the surgery in and around the brainstem [24, 25, 26, 29].

In Fig. 2.11, a 2-year-old boy with anaplastic ependymoma demonstrates the optimal indication for CBT-MEP monitoring. The tumor located at the right cerebellopontine angle to a pontomedullary junction and extended to the ventral side of the brainstem. The fourth ventricle was compressed and shifted to the left side. BSM was inapplicable since the floor of the fourth ventricle would be exposed at the last stage of tumor resection. Intramedullary and subarachnoid parts of the peripheral facial and lower cranial nerves, together with the CBT, seemed to be at high risk of damage by tumor resection. The CBT-MEP monitoring plays a critical role in performing the safe tumor removal by the feedback of real-time functional integrity of the CBT to surgeons [24].

The technical aspect of the CBT-MEP monitoring has the common background in terms of placing electrodes for recording (Fig. 2.2). Stimulation electrodes are placed at C3 and C4 (10–20 international electroencephalographic electrode system) (Fig. 2.12). Using C3 and C4 electrodes alternatively as anode for transcranial electrical stimulation (TcES), the CBT-MEP on each side is recorded from the same muscles used for BSM. The parameters of TcES for the CBT-MEP are the same as the standard CST-MEP monitoring. Train of five stimuli with the interstimulus interval of 2 ms (500 Hz) is delivered over the scalp to elicit the CBT-MEP. Before monitoring the CBT-MEP, a single transcranial electrical stimulation is delivered to

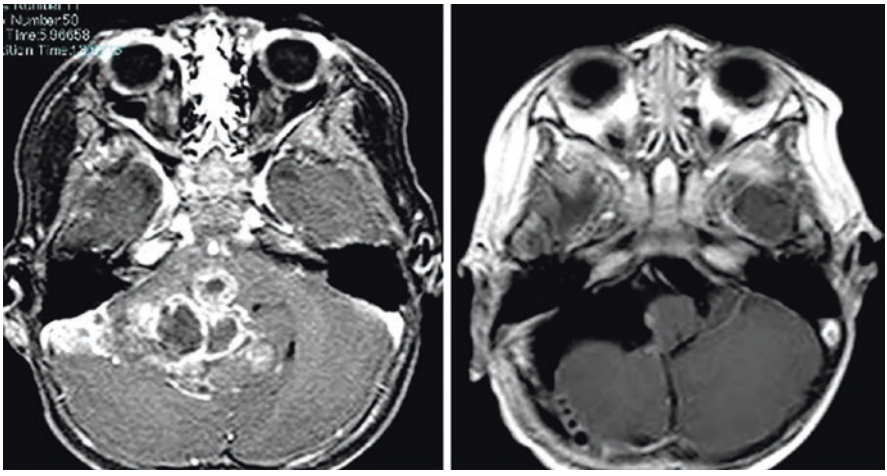

Fig. 2.11 A case of anaplastic ependymoma in a 2-year-old boy. Left: Preoperative Gd-enhanced MRI demonstrated the tumor extending from the right cerebellopontine angle to the ventral side of the brainstem. Right: Postoperative Gd-enhanced MRI showed gross total resection of the tumor. A small part of the tumor remained on the right lateral surface of the brainstem

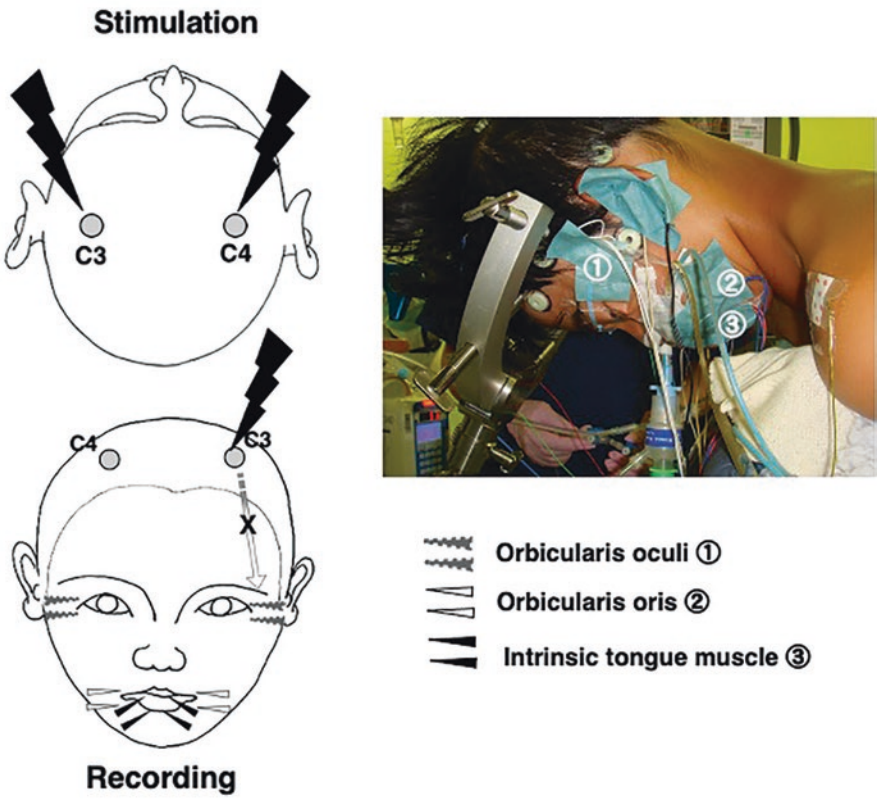

Fig. 2.12 Left: Position of electrodes placed for transcranial stimulation of the CBT-MEP and for recording from cranial nerve-innervated muscles. Recording from the orbicularis oculi muscle is excluded whenever surface conduction of the stimulation current is suspected. Right: Intraoperative photograph after turning the patient in a prone position. Electrodes for recording are fixed on the face with tapes

confirm that the response originated from the CBT, not by peripheral activation of the facial nerve induced by surface conduction from the stimulation electrode (Fig. 2.13). If any muscle contraction is recorded following a single stimulation, the stimulation intensity is reduced to avoid the muscle contraction evoked by surface conduction of the current (Fig. 2.1). Subthreshold stimulation intensity is the must-rule for eliciting reliable CBT-MEPs. The maximum stimulation intensity is restricted up to 200 mA for safety reasons, the same as the standard CST-MEP monitoring.

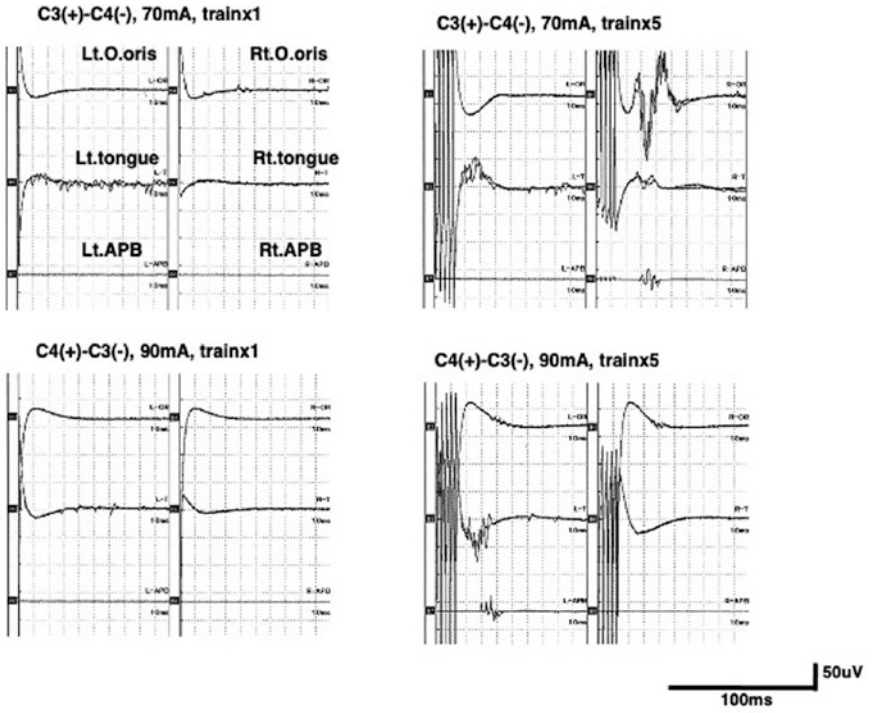

Fig. 2.13 Record of the CBT-MEPs. Left: Prior to monitoring the CBT-MEP, no response following a single transcranial electrical stimulation is confirmed to exclude the peripheral activation of the facial nerve. Right: Train of five stimuli with the interstimulus interval of 2 ms (500 Hz) is delivered to elicit the CBT-MEP (*O oris* orbicularis oris muscle, *tongue* intrinsic tongue muscle, *APB* abductor pollicis brevis muscle)

2.5.4 Advantages and Limitations of Monitoring the CBT-MEP

The advantages of the CBT-MEP monitoring are that it can be applied in all surgeries in and around the brainstem [24, 43, 54]. Its clinical use during surgery of acoustic neurinoma and other skull base surgeries has been reported [55–59]. In addition, the advantage of monitoring the CBT-MEP is that it enables to monitor the entire motor pathway from the motor cortex to the cranial motor nerve-innervated muscle. Unlike BSM, which interrupts surgery for the mapping, the CBT-MEP is monitored simultaneously with the surgical procedure [55].

Limitation in monitoring the CBT-MEP does exist. It has been pointed out that possibility of peripheral activation by surface conduction cannot be completely excluded entirely when monitoring the facial CBT-MEP [60]. It could lead to a false-negative result and should be avoided. Since the orbicularis oculi muscle is most vulnerable to peripheral activation caused by surface conduction, it would be excluded from the CBT-MEP monitoring in selected cases. Another limitation is its

lack of monitoring of the sensory part of the cranial nerves and their contribution to the sensory pathway. Reflex circuits of swallowing and coughing could be damaged without reflecting on the CBT-MEP monitoring. The lower cranial nerves are composed of sensory and motor parts. The CBT-MEP monitoring can monitor the functional integrity of the whole motor pathway to the CNMN but not the sensory pathways of cranial nerves. Considering the anatomical background of the CBT, it would be fair to say that the result of CBT-MEP monitoring innervating CNMNs VII and XII can correspond to functional preservation. This result may show some discrepancy for CNMN IX/X. The CBT-MEP monitoring cannot monitor sensory input through the afferent fibers. Lower cranial nerve dysfunction, such as dysphagia and dysarthria, can develop despite preserved CBT-MEP responses. Preserved CBT-MEPs do not necessarily assure the preserved lower cranial nerve function [57]. Finally, defined warning criteria for the CBT-MEP monitoring have not been established. Amplitude reduction of more than 50% has been reported, with the same warning criteria as the CST-MEP [58]. However, it should be carefully verified because it is not sure that the same criteria can be applied for pure motor function (CNMN VII, CNMN XII) and the lower CNMN included in the complex reflex circuit. Different criteria based on a different function of the CNMN could be required in the future.

2.6 Comprehensive ION Procedures in the Contemporary Brainstem Surgery

It should be emphasized again that the branches of CBT run ventrodorsal direction and the CMN is innervated by multiple CBT branches (Figs. 2.9 and 2.10) [17, 27, 46, 47, 50]. Those anatomical features of CBT suggest that permanent damage to the CBT is less likely when the lesion is approached from the fourth ventricle. Nevertheless, damage to the CNMN and its intra- or extramedullary root can develop during the surgery. The situation is the same when other various skull base approaches are used for the brainstem surgery [32]. It is the reason why the combined application of both BSM and the CBT-MEP monitoring is critical and indispensable for the safe surgery in and around the brainstem [24, 29, 61]. It is the role of ION procedures in contemporary brainstem surgeries.

Presently, newly recognized safe entry zones exist in almost all aspects of the brainstem surface [7, 34, 38, 39, 62]. Even if a brainstem lesion is approached other than through the floor of the fourth ventricle, the role of BSM still exists. Together with the CNMN, the CST and CBT can be mapped either positively or negatively (Fig. 2.14) [26]. Positive mapping on the brainstem surface warns that there is a critical brainstem structure present underneath the region. Negative mapping assures that the mapped site is safe to get into the brainstem.

BSM can be applied through inside of the brainstem to estimate how the mapped point is close to an intrinsic brainstem structure [63]. It is the brainstem version of

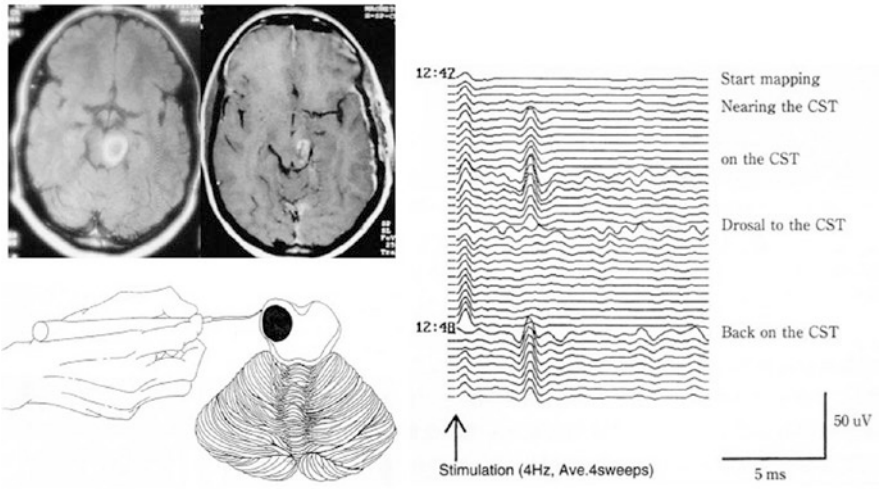

Fig. 2.14 Modified application of BSM for detecting the CST on the lateral surface of the brainstem. The CST was mapped on the lateral surface of the midbrain. Left upper: Pre- and postoperative MRI showing subtotal removal of the left midbrain tumor. Left lower: Schematic drawing of modified application of BSM. Right: BSM on the lateral surface of the midbrain demonstrated the D waves recorded from an electrode inserted in the spinal epidural space, when the stimulation is delivered on the left CST (positive mapping). No response was recorded when the stimulation moved dorsally from the tumor (negative mapping)

the subcortical white matter mapping [64]. It should be reminded that the relationship between stimulation intensity and the distance from the point of stimulation to the mapped structure demonstrated no linear correlation [65, 66]. Variability of the estimated distance would come from a heterogeneity of tissue, the condition of the surgical field, and different neurophysiological parameters [65, 67]. It would be especially true in the brainstem where CMNs and their intramedullary roots exist together with the CBT and CST. On the other hand, from the practical viewpoint, rough estimation "1 mA = 1 mm" (stimulation of 1 mA intensity penetrates 1 mm within the brainstem tissue) is derived according to Shiban's data [65]. This is an approximation and should be adjusted from patient to patient.

Representative cases of the brainstem surgery are presented.

Case 2

This is a 7-year-old girl with a long history of gait disturbance and slow progression. Mild hoarseness and swallowing also gradually developed. An MRI revealed a lesion with high signal intensity on T2-weighted image from the right pons to the cerebellar peduncle (Fig. 2.15). Open tumor biopsy through the fourth ventricle was performed.

After exposure to the floor of the fourth ventricle, BSM was performed. The initial stimulation intensity of 1.0 mA was delivered to search the location of the CNMNs. Then, the stimulation intensity was reduced to 0.4 mA for precise localization of the CNMNs (Fig. 2.15).

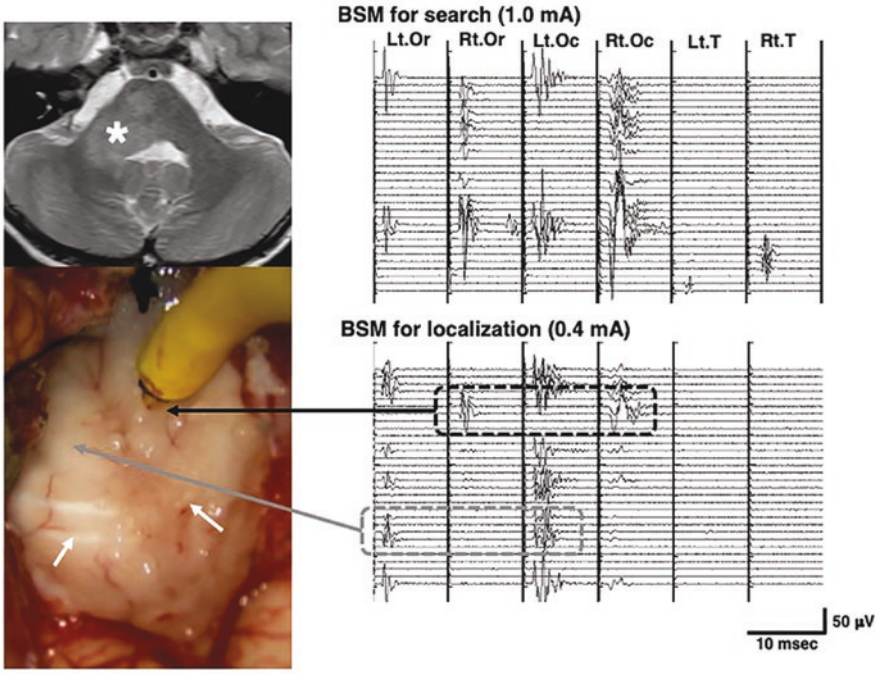

Fig. 2.15 A 7-year-old girl with a tumor extending from the cerebellar peduncle to the brainstem. The girl presented with ataxic gait, which gradually worsened over a few years. Hoarseness and occasional swallowing difficulty developed slowly. Upper left: An MRI revealed a high signal intensity from the right cerebellar peduncle to the brainstem on T2-weighted image (asterisk), and there was no enhancement after the gadolinium injection. Upper right: BSM for search of the CNMNs with the stimulation intensity of 1.0 mA. Lower: With the use of a stimulation intensity of 0.4 mA, precise localization of the CNMN VII was performed. The black arrow indicates the right CNMN VII, and the gray arrow is the left one (white arrows: stria medullaris)

The tumor biopsy was performed near the base of the right cerebellar peduncle, away from the right CNMN of the facial nerve. The CBT-MEP remained stable before and after the biopsy, though the responses from the CNMN VII were very small in amplitude (Fig. 2.16).

To the brainstem lesion located more ventrally, the lateral approach would be the choice of surgery [34, 38, 68, 69]. Bertalanffy strongly recommended the postero-lateral approach to the pons as it was safer to preserve CNMN VI and VII function than approaching through the floor of the fourth ventricle [7]. BSM can reveal the location of the CST or CNMN on the lateral surface of the pons (Fig. 2.14) [26]. The CBT-MEP monitoring is continuously carried out through the surgical approach and procedures inside the brainstem.

Case 3

This is an 11-year-old boy with a pontine cavernous angioma. The boy had a history of repeated hemorrhage from a pontine cavernous angioma. He underwent removal

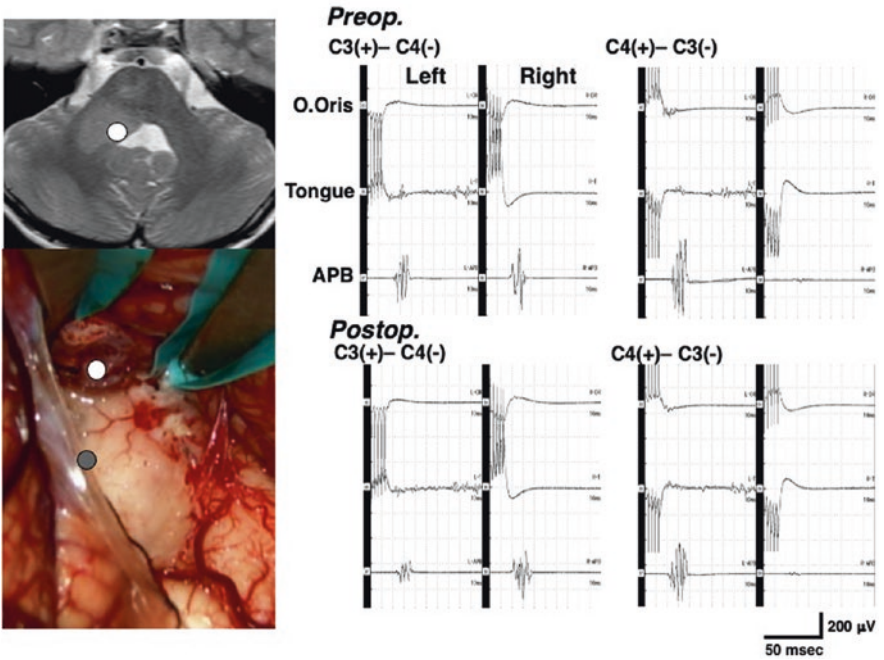

Fig. 2.16 Upper left: A white circle shows the lesion where biopsy specimens were sampled. Lower left: Intraoperative photograph shows the biopsy taken from the white circle. A dark circle shows the location of the right CNMN VII. Right: Pre- and postoperative CBT-MEPs (stimulation intensity: 80 mA). In this case, CBT-MEPs from the left CNMNs remained stable but were absent from the right CNMNs. Note CST-MEPs recorded from the APB remained stable (same patient in Fig. 2.15)

of the cavernous angioma through the supracondylar fossa (far lateral) approach 2 years before the second surgery. The rostral part of the angioma was tightly attached to the surrounding brainstem tissue and left untouched. This time, he noticed worsened right facial palsy and right hemiparesis. A CT and MRI revealed rebreeding from the residual angioma (Fig. 2.17). The second surgery was scheduled through the posterior trans-petrosal approach. During the surgery, the lateral surface of the pons was exposed after cutting the cerebral tentorium and opening the arachnoid membrane. BSM was carried out on the lateral surface of the pons between CNMNs V and VII (Fig. 2.18). The CNMN VII was located at the caudal end of the surgical field (positive mapping). Myelotomy of the pons was placed on the silent area of BSM (negative mapping), which was supposed to be a safe entry zone of the infratrigeminal lateral approach to the pons [7, 34, 39]. The hematoma and the angioma were gross totally removed. The CBT-MEP and the CST-MEP were continuously monitored during the procedure (Fig. 2.18). The CBT-MEP of the right CNMNs VII and XII remained approximately the same amplitude. In

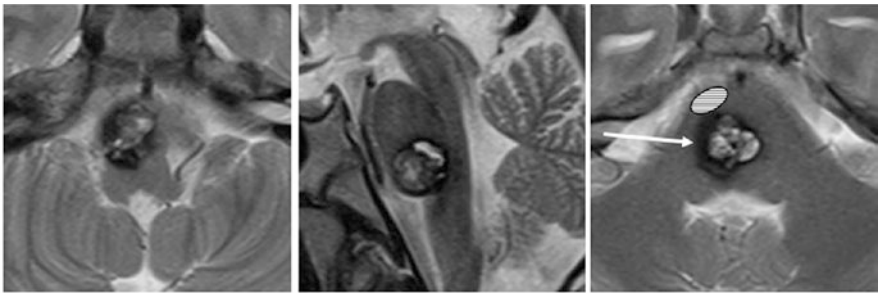

Fig. 2.17 An 11-year-old boy with recurrent hemorrhage from a brainstem cavernous angioma. Left and center: Recurrent hemorrhage from a cavernous angioma was observed in the right lower pons. Right: Surgical approach to the pons (arrow) and the location of CST (lined oblique oval) are shown

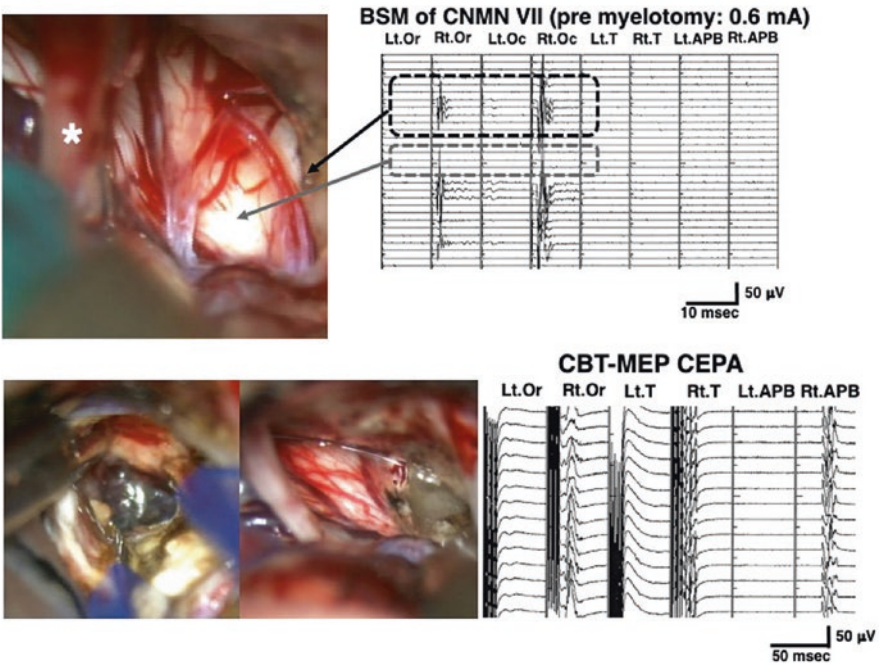

Fig. 2.18 Upper: Result of BSM on the lateral surface of the pons. When stimulated between the trigeminal (asterisk) and facial nerves, no response was recorded (negative mapping: dark arrow). Facial muscle contraction was recorded when stimulated near the exit zone of the facial nerve (positive mapping: black arrow). Lower left and center: Exposure of the cavernous angioma (left) and after removal of the cavernous angioma (center) was shown. Lower right: The CBT-MEP and the CST-MEP were continuously monitored during the surgical resection of the cavernous angioma (CEPA, continuous evoked potential array; Or, orbicularis oris muscle; Oc, orbicularis oculi muscle; T, intrinsic tongue muscle; APB, abductor pollicis brevis muscle) (same patient in Fig. 2.16)

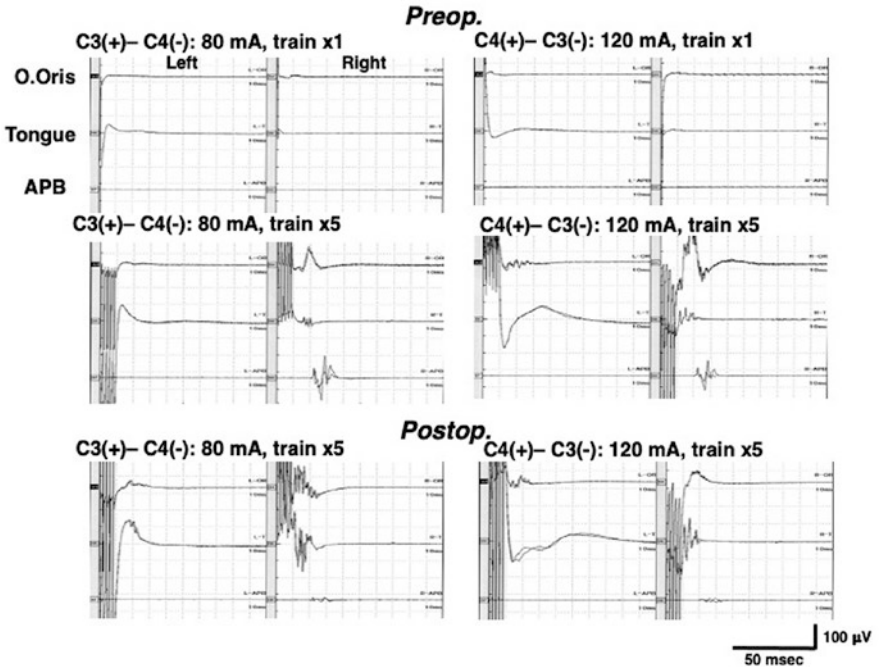

Fig. 2.19 Pre- and postoperative recordings of the CBT-MEP. Note there was no muscle contraction when transcranial electrical stimulation was delivered by single stimulation. By the end of surgery, the CBT-MEP was approximately preserved, but the CST-MEP from the right APB reduced its amplitude (*O oris* orbicularis oris muscle, *tongue* intrinsic tongue muscle, *APB* abductor pollicis brevis muscle) (same patient in Figs. 2.16 and 2.17)

contrast, the CST-MEP on the right side reduced its amplitude (Fig. 2.19). The boy woke up with mildly deteriorated right hemiparesis, but it improved within a month.

2.7 Future Perspective on the Role of ION Procedures in the Brainstem Surgery

Surgery to the brainstem has made remarkable advancements in the last two decades after the introduction of various skull base approaches [70, 71]. With the advent of surgery, so were the ION procedures applied for brainstem surgical interventions. Original BSM through the floor of the fourth ventricle is no more the sole procedure of BSM in the contemporary ION.

2.7.1 Advanced Brainstem Imaging and the Role of ION

Morphometrical visualization of the brainstem to support anatomical guidance to the brainstem structure was first attempted at the end of twentieth century [72]. Presently, diffusion tensor tractography (DTT) visualizes the pyramidal tract noninvasively in the brain and has been regarded as promising technique which enhances the capability of surgical approach, mainly for brain tumors [73, 74]. The accuracy of DTT in relationship with the brain lesion still remains controversial, and the combined use of ION has been discussed [75–77]. Nevertheless, DTTs of the CST and CBT have been opening a new field of the brainstem's functional anatomy and its surgery [52, 78, 79].

Recent advancements in MRI have brought great impact not only in diagnosis but also the selection of surgical approaches. Subnuclei in the basal ganglion can be visualized by using 7 T MRI [80]. Furthermore, the presently invisible internal architecture of the brainstem can be visualized using 11.7 T MRI [62]. An anatomical safe entry zone to an intrinsic brainstem lesion can be defined on an 11.7 T MRI before surgery.

It would be possible to reach the lesion with the use of a high-resolution MRI-guided navigation system. If DTT of the CBT has reached the clinical use, it would also be helpful for the surgeon to plan a surgical approach. It means an "on the image" safe entry zone can be visualized with high-resolution MRI and DTT. At the same time, the importance of BSM and the CBT-MEP monitoring looks unshakable in the real-world surgery because real-time feedback brought by ongoing ION procedures plays an indispensable role for the neurosurgeon. In addition, positive and negative BSM results can tell which direction the cortical myelotomy would be safely extended on the surface of the brainstem [81]. Combined application of the latest image-oriented neuronavigation and ION procedures seems indispensable, enabling safer than ever brainstem surgery in the future.

2.7.2 Monitoring of the Reflex Circuit of the Lower Cranial Nerve

Monitoring of the lower cranial nerve functional integrity is not straightforward. Most of the lower cranial nerve function is composed of reflex circuits, such as gag reflex. Injury to the sensory pathway would produce disturbed lower cranial nerve function.

The CBT-MEP of the laryngeal muscle closely relates to vocalization, which can be traced back to the end of the 1980s when Amassian first demonstrated it by transcranial magnetic stimulation [82]. Clinical application of the laryngeal muscle CBT-MEP monitoring has been reported since then, but non about the neurophysiological monitoring of the functional integrity of reflex circuits of the lower cranial nerves [43, 58]. Further evolution of ION in this field is awaited [83–85].

2.7.3 Stereotactic Biopsy of Brainstem Lesions and the Role of ION

The paradigm shift is going on in managing diffuse intrinsic pontine glioma (DIPG). The first impact came in the early 1990s when MRI was introduced to diagnose DIPG. Once diagnosed on MRI, DIPGs have been regarded as no surgical indication since then [86]. It should be reminded that Albright did not deny all biopsy surgery for brainstem gliomas. He mentioned the need for biopsy surgeries in 10–15% of brainstem gliomas with atypical MRI findings. Despite his detailed description, the treatment modality of the MRI diagnosis followed by radiation therapy stayed the mainstream of DIPG treatment, with a median survival of less than a year or so for the last two decades [86–88].

The second impact hits at around 2010 when the role of biopsy surgeries was reevaluated because inconsistency of MRI diagnosis of certain DIPGs appeared to be acknowledged [89]. As histopathological heterogenesis of DIPG became more recognized with the advancement of molecular diagnosis, a biopsy surgery has emerged again as an indispensable procedure for the subsequent management of DIPG [90–99]. Direct open biopsy with the use of BSM is desirable in selected cases [93, 96]. On the other hand, less invasive stereotactic biopsy has become a mainstream surgical procedure [100–102]. Presently, convection-enhanced delivery (CED) has appeared in the limelight as a promising new treatment to break through the dilemma of DIPG management [90, 103–106]. Again, stereotactic insertion of a drug-delivering catheter with or without tumor biopsy is required for CED.

Any complications in the brainstem surgery could be severe damage to the patient and should be avoided. The reliability and safety of stereotactic biopsy seem acceptable. Diagnostic success was around 96%, morbidity was 7–8%, with permanent morbidity accounting for 1–2%, and mortality rates less than 1% have been reported [107, 108]. The role of ION in stereotactic brainstem biopsy has not been established yet. However, the combined application of ION of BSM and the white matter mapping could be a useful adjunct for the safe stereotactic brainstem surgery [109, 110]. Figure 2.20 shows an example of a modified application of BSM (stereotactic BSM) for a 59-year-old patient with a brainstem tumor. A specially ordered stimulation electrode whose tip was uninsulated only 1/4 surface for the direction-guide was inserted into a target point of biopsy. Electrical stimulation was delivered to circumscribed structures in all directions at the target. Biopsy samples were obtained from the direction that demonstrated negative mapping. The patient awoke without neurological deterioration, and the pathology of the tumor was malignant lymphoma. A recent paper reported a similar application of BSM during stereotactic biopsy of brainstem lesions in nine patients [111]. The authors utilized a stimulating probe which was integrated into a biopsy needle. Before the biopsy the targeted site was electrically stimulated, and EMG response from CNMNs (VII, IX/X, XII) and the muscles from extremities were monitored. The result sounds intriguing because a targeted biopsy site was modified based on the evoked EMG potentials after electrical stimulation in two out of nine cases. No postoperative

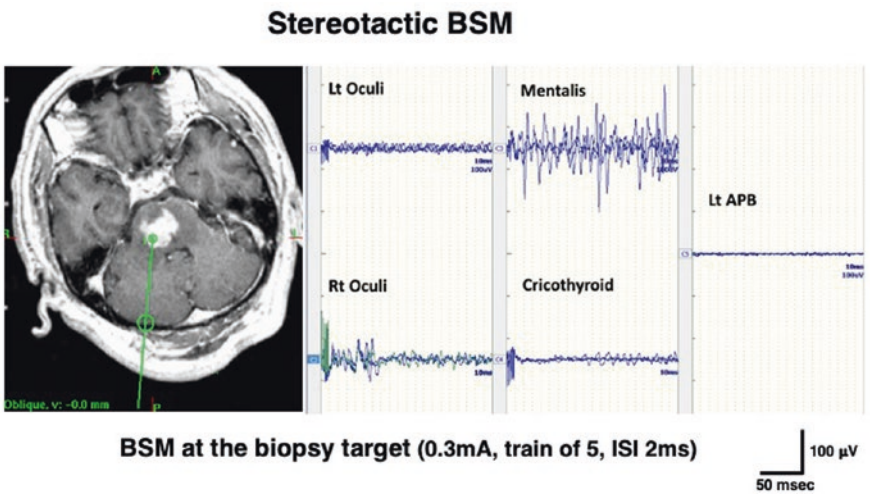

Fig. 2.20 BSM during a stereotactic brainstem biopsy (stereotactic BSM). Left: BSM was carried out at the target point in a pontine tumor. Right: Positive mapping from the right orbicularis oculi muscle was recorded when the stimulation of BSM was directed at a lateral side of the target point. Biopsy specimens were sampled from the medial side of the target point

complication developed in all patients. This new application of BSM for the stereotactic biopsy of brainstem lesions seems a promising future ION procedure. Less invasive surgery with more sophisticated ION procedures would bring safer than ever brainstem surgery possible.

2.8 Summary

The present status and recent advancement of ION in brainstem surgery were reviewed. Special attention was focused on BSM and the CBT-MEP monitoring. The original idea of BSM on the floor of the fourth ventricle was expanded to the wider definition of BSM on the surface of the brainstem. Negative mapping has a clinical role in that the mapped site suggested a safe entry zone to the brainstem. The modern ION procedure can reveal the brainstem's functional surgical anatomy and contribute to the safe brainstem surgery.

The evolution of ION procedures in brainstem surgery are still going on while surgery of the brainstem is advancing with the introduction of skull base approaches and the use of the latest MRI. However, surgery in and around the brainstem still remains a challenge to surgeons even in the era of modern neurosurgery. Image-guided neurosurgery can lead surgeons to reach the brainstem lesion very accurately. However, only ION procedures can reveal distorted functional surgical anatomy on the brainstem and enable monitoring of the functional integrity of CMNs and the motor pathway. Functionally guided brainstem surgery based on the

ION procedures is the critical armamentarium to perform such complex surgery safely. It seems clear that integrated intraoperative application of mapping and monitoring techniques provides the best chance of success in the brainstem surgery. Further development of ION in the stereotactic biopsy of intrinsic brainstem lesions is awaiting.

References

1. Bricolo A, Turazzi S. Surgery for gliomas and other mass lesions of the brainstem. Adv Tech Stand Neruosurg. 1995;22:261–341.
2. Bricolo A. Surgical management of intrinsic brain stem gliomas. Oper Tech Neurosurg. 2000;3:137–54.
3. Epstein F. A staging system for brain stem gliomas. Cancer. 1985;56:1804–6.
4. Epstein F, McCleary EL. Intrinsic brain-stem tumors of childhood: surgical indications. J Neurosurg. 1986;64:11–5.
5. Hoffman JH, Becker L, Craven MA. A clinically and pathologically distinct group of benign brain stem gliomas. Neurosurgery. 1980;7:243–8.
6. Bertalanffy H, Ichimura S, Kar S, Tsuji Y, Huang C. Optimal access route for pontine cavernous malformation resection with preservation of abducent and facial nerve function. J Neurosurg. 2021;135:683–92.
7. Jallo GI, Biser-Rohrbaugh A, Freed D. Brainstem gliomas. Childs Nerv Syst. 2004;20:143–53.
8. Weisenburg TH. Extensive gliomatous tumor involving the cerebellum and the posterior portions of the medulla, pons and cerebral peduncle and the posterior limb of one internal capsule. J Am Med Assoc. 1909;53(25):2086–91.
9. Zenner P. Two cases of tumor of the pons. J Nerv Ment Dis. 1910;37:27–36.
10. Dmetrichuk JM, Pendleton C, Jallo GI, Quiñones-Hinojosa A. Father of neurosurgery: Harvey Cushing's early experience with a pediatric brainstem glioma at the Johns Hopkins Hospital. J Neurosurg Pediatr. 2011;8:337–41.
11. Matson D. Gliomas of the brain stem. In: Matson D, editor. Neurosurgery of infancy and childhood. 2nd ed. Springfield, IL: Charles C Thomas; 1969. p. 469–77.
12. Pool JL. Gliomas in the resion of the brain stem. J Neurosurg. 1968;29:164–7.
13. Pollack IF, Hoffman HJ, Humphreys RP, Becker L. The long-term outcome after surgical treatment of dorsally exophytic brainstem gliomas. J Neurosurg. 1993;29:164–7.
14. Stroink AR, Hoffman HJ, Hendrick EB, Humphreys RP, Davidson G. Transependymal benign dorsally exophytic brain stem gliomas in childhood: diagnosis and treatment recommendations. Neurosurgery. 1987;20:439–44.
15. Kyoshima K, Kobayashi S, Gibo H, Kuroyanagi T. A study of safe entry zones via the floor of the fourth ventricle for brain-stem lesions: report of three cases. J Neurosurg. 1993;78:987–93.
16. Morota N, Deletis V, Epstein FJ, Kofler M, Abbott R, Lee M, Ruskin K. Brain stem mapping: neurophysiological localization of motor nuclei on the floor of the fourth ventricle. Neurosurgery. 1995;37:922–30.
17. Morota N, Deletis V, Epstein FJ. Brainstem mapping. In: Deletis V, Shils JL, editors. Neurophysiology in neurosurgery. Academic Press: London; 2002. p. 319–35.
18. Strauss C, Lutjen-Drecoll E, Fahlbusch R. Pericollicular surgical approaches to the rhomboid fossa. Part 1. Anatomical basis. J Neurosurg. 1997;87:893–9.
19. Strauss C, Romstock J, Fahlbusch R. Pericollicular approaches to the rhomboid fossa. Part II. Neurophysiological basis. J Neurosurg. 1999;91:768–75.
20. Wiedemayer H, Fauser B, Sandalciogle IE, Schàer H, Stolke D. The impact of neurophysiological intraoperative monitoring on surgical decisions: a critical analysis of 43 cases. J Neurosurg. 2002;96:255–62.

21. Fahlbusch R, Strauss C. The surgical significance of brainstem cavernous hemangiomas. Zentrabl Neurochi. 1991;52:25–32.
22. Katsuta T, Morioka T, Fujii K, Fului M. Physiological localization of the facial colliculus during direct surgery on an intrinsic brain stem lesion. Neurosurgery. 1993;32:861–3.
23. Strauss C, Romstock J, Nimsky C, Fahlbusch R. Intraoperative identification of motor areas of the rhomboid fossa using direct stimulation. J Neurosurg. 1993;79:393–9.
24. Morota N, Ihara S, Deletis V. Intraoperative neurophysiology for surgery in and around the brainstem: role of brainstem mapping and corticobulbar tract motor-evoked potential monitoring. Childs Nerv Syst. 2010;26:513–21.
25. Sala F, Coppola A, Tramontano V. Intraoperative neurophysiology in posterior fossa tumor in children. Childs Nerv Syst. 2015;31:1791–806.
26. Deletis V, Sala F, Morota N. Intraoperative neurophysiological monitoring and mapping during brainstem surgery. A modern approach. Oper Tech Neurosurg. 2000;3:109–13.
27. Morota N, Deletis V. The importance of brainstem mapping in brainstem surgical anatomy before the fourth ventricle and implication for intraoperative neurophysiological mapping. Acta Neurochir. 2006;148:499–509.
28. Morota N, Deletis V, Epstein F. Brain stem mapping. In: Deletis V, Shils JL, Sala F, Seidel K, editors. Neurophysiology in neurosurgery. London: Academic Press; 2020. p. 151–62.
29. Sala F, Manganotti P, Tramontano V, Bricolo A, Gerosa M. Monitoring of motor pathways during brain stem surgery: what we have achieved and what we still miss? Clin Neurophysiol. 2007;37:399–406.
30. Tanaka S, Kobayashi I, Utsuki S, Iwamoto K, Takanashi J. Biopsy of brain stem glioma using motor-evoked potential mapping by direct peduncular stimulation and individual adjuvant therapy. Neuro Med Chir (Tokyo). 2005;45:49–55.
31. Tanaka S, Takanashi J, Fujii K, Ujiie H, Hori T. Motor evoked potential mapping and monitoring by direct brainstem stimulation. J Neurosurg. 2007;107:1053–7.
32. Deletis V, Fernández-Conejero I. Intraoperative monitoring and mapping of the functional integrity of the brainstem. J Clin Neurol. 2016;12:262–73.
33. Deletis V. Evoked potential. In: Lake CL, editor. Clinical monitoring for anesthesia and critical care. 2nd ed. Philadelphia: W.B. Saunders Co.; 1994. p. 282–314.
34. Cavalheiro S, Yagmurlu K, Silva da Costa MD, Nicácio JM, Rodrigues TP, Chaddad-Neto F, Rhoton AL. Surgical approaches for brainstem tumors in pediatric patient. Childs Nerv Syst. 2015;31:1815–40.
35. Mussi AC, Matushita H, Andrade FG, Rhoton AL. Surgical approaches to IV ventricle – anatomical study. Childs Nerv Syst. 2015;31:1807–14.
36. Yagmurlu K, Rhoton AL, Tanriover N, Bennett JA. Three-dimensional microsurgical anatomy and the safe entry zones of the brainstem. Neurosurgery. 2014;10:602–20.
37. Bogucki J, Czernicki Z, Gielecki J. Cytoarchitectonic basis for safe entry into the brainstem. Acta Neurochir (Wien). 2000;142:383–7.
38. Cavalcanti DD, Preul MC, Kalani YS, Spetzler RF. Microsurgical anatomy of safe entry zones to the brainstem. J Neurosurg. 2016;124:1359–76.
39. Ferroli P, Schiariti M, Cordella R, Boffano C, Mava S, La Corte E, Cavallo C, Bauer D, Castiglione M, Broggi M, Acerbi F, Broggi G. The lateral infratrigeminal transpontine window to deep pontine lesions. J Neurosurg. 2015;123:699–710.
40. Bertalanffy H, Tissira N, Krayenbühl N, Bozinov O, Sarnthein J. Inter- and intrapatient variability of facial nerve response areas in the floor of the fourth ventricle. Neurosurgery. 2011;68(ONS Suppl 1):ons23–31.
41. Morota N, Deletis V, Lee M, Epstein FJ. Functional anatomic relationship between brain stem tumors and cranial motor nuclei. Neurosurgery. 1996;39:787–94.
42. Schmitt WR, Daube JR, Carlson ML, Mandrekar JN, Beatty CW, Neff B, Driscoll CL, Link MJ. Use of supramaximal stimulation to predict facial nerve outcomes following vestibular schwannoma microsurgery: results from a decade of experience. J Neurosurg. 2013;118:206–12.

43. Deletis V, Fernández-Conejero I, Ulkatan S, Rogić M, Carbó EL, Hiltzik D. Methodology for intra-operative recording of the corticobulbar motor evoked potentials from cricothyroid muscles. Clin Neurophysiol. 2011;122:1883–9.
44. Sekiya T, Hatayama T, Shimamura N, Suzuki S. Intraoperative electrophysiological monitoring of oculomotor nuclei and their intramedullary tracts during midbrain tumor surgery. Neurosurgery. 2000;47:1170–7.
45. Sala F, D'Amico A. Intraoperative neurophysiological monitoring during brainstem surgery. In: Jallo GI, Noureldine MHA, Shimony N, editors. Brainstem tumors. Cham: Springer; 2020. p. 109–30.
46. Krieg WJS. Brain mechanisms in diachrome. 2nd ed. Bloomington, IL: Brain Books; 1957. p. 287–90.
47. Urban PP, Wicht S, Vucorevic G, Fitzek S, Marx J, Thomke F, Mika-Gruttner A, Fitzek C, Stoeter P, Hopf HC. The course of corticofacial projection in the human brainstem. Brain. 2001;124:1866–76.
48. Liégeois FJ, Butler J, Morgan AT, Clayden JD, Clark CA. Anatomy and lateralization of the human corticobulbar tracts: an fMRI-guided tractography study. Brain Struct Funct. 2016;221:3337–45.
49. Yim SH, Kim JH, Han ZA, Jeon S, Cho JH, Kim GS, Choi SA, Lee JH. Distribution of the corticobulbar tract in the internal capsule. J Neurol Sci. 2013;334:63–8.
50. Terao S, Miura N, Takeda A, Takahashi A, Mitsuma T, Sobue G. Course and distribution of facial corticobulbar tract fibers in the lower brain stem. J Neuron Neurosurg Psychiatry. 2000;69:262–5.
51. Oswald AM, Urban NN. There and back again: the corticobulbar loop. Neuron. 2012;76:1045–7.
52. Jenabi M, Peck KK, Young RJ, Brennan YN, Holodny AI. Identification of the corticobulbar tracts of the tongue and face using deterministic and probabilistic DTI fiber tracking in patients with brain tumor. AJNR Am J Neuroradiol. 2015;36:2036–41.
53. Kanbayashi T, Sonoo M. The course of facial corticobulbar tract fibers in the dorsolateral medulla oblongata. BMC Neurol. 2021;21:214.
54. Deletis V, Fernandez-Conejero I, Ulkatan S, Costantino P. Methodology for intraoperatively elicited motor evoked potentials in the vocal muscles by electrical stimulation of the corticobulbar tract. Clin Neurophysiol. 2009;120:336–41.
55. Dong CCJ, MacDonald DB, Akagawa R, Westerberg B, Alkhani A, Kanaan I, Hassounah M. Intraoperative facial motor evoked potential monitoring with transcranial electrical stimulation during skull base surgery. Clin Neurophysiol. 2005;116:588–96.
56. Fukuda M, Oishi M, Takao T, Saito A, Fujii Y. Facial nerve motor-evoked potential monitoring during skull base surgery predicts facial nerve outcome. J Neurol Neurosurg Psychiatry. 2008;79:1066–70.
57. Fukuda M, Oishi M, Hiraishi T, Saito A, Fujii Y. Pharyngeal motor evoked potentials elicited by transcranial electrical stimulation for intraoperative monitoring during skull base surgery. J Neurosurg. 2012;116:605–10.
58. Ito E, Ichikawa M, Itakura T, Ando H, Matsumoto Y, Oda K, Sato T, Watanabe T, Sakuma J, Saito K. Motor evoked potential monitoring of the vagus nerve with transcranial electrical stimulation during skull base surgeries. J Neurosurg. 2013;118:195–201.
59. Zhang M, Zhou Q, Zhang L, Jiang Y. Facial corticobulbar motor-evoked potential monitoring during the clipping of large and giant aneurysms of the anterior circulation. J Clin Neurosci. 2013;20:873–8.
60. Téllez MJ, Ulkatan S, Urriza J, Arranz-Arranz B, Deletis V. Neurophysiological mechanism of possibly confounding peripheral activation of the facial nerve during corticobulbar tract monitoring. Clin Neurophysiol. 2016;127:1710–6.
61. Gläsker S, Pechstein U, Vougioukas VI, van Velthoven V. Monitoring motor function during resection of tumours in the lower brain stem and fourth ventricle. Childs Nerv Syst. 2006;22:1288–95.

62. Guberinic A, van den Elshout R, Kozicz T, ter Laan M, Hanssen D. Overview of the microanatomy of the human brainstem in relation to the safe entry zones. J Neurosurg. 2022; 1–11. https://doi.org/10.3171/2022.2.JNS211997.
63. Li Z, Wang M, Zhang L, Fan X, Tao X, Qi L, Ling M, Xiao X, Wu Y, Guo D, Qiao H. Neuronavigation-guided corticospinal tract mapping in brainstem tumor surgery: better preservation of motor function. World Neurosurg. 2018;116:e291–7.
64. Kamada K, Todo T, Ota T, Ino K, Matsutani Y, Aoki S, Takeuchi F, Kawai K, Saito N. The motor-evoked potential evaluation by tractography and electrical stimulation. J Neurosurg. 2009;111:785–95.
65. Shiban E, Krieg SM, Haller B, Buchmann N, Obermueller T, Boeckh-Behrens T, Wostrack M, Meyer B, Ringel F. Intraoperative subcortical motor evoked potential stimulation: how close is the corticospinal tract? J Neurosurg. 2015;123:711–20.
66. Nossek E, Korn A, Shahar T, Kanner AA, Yaffe H, Marcovici D, Ben-Harosh C, Ami HB, Weinstein M, Shapira-Lichter I, Constantini S, Hendler T, Ram Z. Intraoperative mapping and monitoring of the corticospinal tracts with neurophysiological assessment and 3 dimensional ultrasonography-based navigation. J Neurosurg. 2011;114:738–46.
67. Yamaguchi F, Ten H, Higuchi T, Omura T, Kojima T, Adachi K, Kitamura T, Kobayashi S, Takahashi H, Teramoto A, Morita A. An intraoperative motor tract positioning method in brain tumor surgery: technical note. J Neurosurg. 2018;129:576–82.
68. Deshmukh VR, Rangel-Castilla L, Spetzler RF. Lateral inferior cerebellar peduncle approach to dorsolateral medullary cavernous malformation. J Neurosurg. 2014;121:723–9.
69. Šteňo J, Bízik I, Šteňová J, Timárová G. Subtemporal transtentorial resection of cavernous malformations involving the pyramidal tract in the upper pons and mesencephalon. Acta Neurochir. 2011;153:1955–62.
70. Da L, Hao SY, Tang J, Xiao XR, Jia GJ, Wu Z, Zang LW, Zhang JT. Surgical management of pediatric brainstem cavernous malformations. J Neurosurg Pediatr. 2014;13:484–502.
71. Gross BA, Batjer HH, Awad IA, Bendok BR. Brainstem cavernous malformations. Neurosurgery. 2009;64:805–18.
72. Niemann K, van den Boom R, Haeselbarth K, Afshar F. A brainstem stereotactic atlas in a three-dimensional magnetic resonance imaging navigation system: first experiences with atlas-to-patient registration. J Neurosurg. 1999;90:891–901.
73. Berman JI, Berger MS, Chung SW, Nagarajan SS, Henry RG. Accuracy of diffusion tensor magnetic resonance imaging tractography assessed using intraoperative subcortical stimulation mapping and magnetic source imaging. J Neurosurg. 2007;107:488–94.
74. Ohue S, Kohno S, Inoue A, Yamashita D, Harada H, Kumon Y, Kikuchi K, Miki H, Ohnishi T. Accuracy of diffusion tensor magnetic resonance imaging-based tractography for surgery of gliomas near the pyramidal tract: a significant correlation between subcortical electrical stimulation and postoperative tractography. Neurosurgery. 2012;70:283–94.
75. Czernicki T, Maj E, Podgorska A, Kunert P, Prokopienko M, Nowak A, Cieszanowski A, Marchel A. Diffusion tensor tractography of pyramidal tracts in patients with brainstem and intramedullary spinal cord tumors: relationship with motor deficits and intraoperative MEP changes. J Magn Reson Imaging. 2017;46:715–23.
76. Ille S, Schroeder A, Wagner A, Negwer C, Kreiser K, Meyer B, Krieg SM. Intraoperative MRI–based elastic fusion for anatomically accurate tractography of the corticospinal tract: correlation with intraoperative neuromonitoring and clinical status. Neurosurg Focus. 2021;50(1):E9.
77. Mikuni N, Okada T, Nishida N, Taki J, Enatsu R, Ikeda A, Miki Y, Hanakawa T, Fukuyama H, Hashimoto N. Comparison between motor evoked potential recording and fiber tracking for estimating pyramidal tracts near brain tumors. J Neurosurg. 2007;106:128–33.
78. Flores BC, Whittemore AR, Samson DS, Barnett S. The utility of preoperative diffusion tensor imaging in the surgical management of brainstem cavernous malformation. J Neurosurg. 2015;122:653–62.

79. Xiao X, Kong L, Pan C, Zhang P, Chen X, Sun T, Wang M, Qiao H, Wu Z, Zhang J, Zhang L. The role of diffusion tensor imaging and tractography in the surgical management of brainstem gliomas. Neurosurg Focus. 2021;50(1):E10.
80. Rusheen AE, Goyal A, Owen RL, Berning EM, Bothun DT, Giblon RE, Blaha CD, Welker KM, Hustn J III, Bennet KE, Oh Y, Fagan AJ, Lee KH. The development of ultra-high field MRI guidance technology for neuronavigation. J Neurosurg. 2022; 1–13. https://doi.org/10.3171/2021.11.JNS211078.
81. Kalani MYS, Yagmurlu K, Martirosyan NL, Cavalcanti DD, Spetzler RF. Approach selection for intrinsic brainstem pathologies. J Neurosurg. 2016;125:1596–607.
82. Amassian VE, Anziska BJ, Cracco JB, Cracco RQ, Maccabee PJ. Focal magnetic excitation of frontal cortex activates laryngeal muscles in man. Proc Physiol Soc. 1987; 41.
83. Téllez MJ, Ulkatan S, Sinclair CF. Intraoperative monitoring of the vagus and laryngeal nerves with thelaryngeal adductor reflex. In: Deletis V, Shils JL, Sala F, Seidel K, editors. Neurophysiology in neurosurgery. A modern approach. 2nd ed. London: Academic press; 2020. p. 209–21.
84. Téllez MJ, Ulkatan S. Bringing the masseter reflex into the operating room. In: Deletis V, Shils JL, Sala F, Seidel K, editors. Neurophysiology in neurosurgery. A modern approach. 2nd ed. London: Academic press; 2020. p. 223–8.
85. Fernándes-Conejero I, Deletis V. Blink reflex. In: Deletis V, Shils JL, Sala F, Seidel K, editors. Neurophysiology in neurosurgery. A modern approach. 2nd ed. London: Academic press; 2020. p. 229–37.
86. Albright AL, Packer RJ, Zimmerman R, Rorke LB, Boyett J, Hammond GD. Magnetic resonance scans should replace biopsies for the diagnosis of diffuse brain stem gliomas: a report from the Children's Cancer Group. Neurosurgery. 1993;33:1026–9.
87. Farmer JP, Montes JL, Freeman CR, Meagher-Villemure K, Bond MC, O'Gorman AM. Brainstem gliomas: a 10-year institutional review. Pediatr Neurosurg. 2001;34:206–14.
88. Rechberger JS, Lu VM, Zhang L, Power EA, Daniels DJ. Clinical trials for diffuse intrinsic pontine glioma: the current state of affairs. Childs Nerv Syst. 2020;36:39–46.
89. Hankinson TC, Campagna EJ, Foreman NK, Handler MH. Interpretation of magnetic resonance images in diffuse intrinsic pontine glioma: a survey of pediatric neurosurgeons. J Neurosurg Pediatr. 2011;8:97–102.
90. Frazier JL, Lee J, Thomale UW, Noggle JC, Cohen K, Jallo GI. Treatment of diffuse intrinsic brainstem gliomas: failed approaches and future strategies. J Neurosurg Pediatr. 2009;3:259–69.
91. Hersh DS, Kumar R, Moore KA, Smith LGF, Tinkle CL, Chiang J, Patay Z, Gajjar A, Choudhri AF, Lee-Diaz J, Vaughn B, Klimo P. Safety and efficacy of brainstem biopsy in children and young adults. J Neurosurg Pedatr. 2020;26:552–62.
92. Dellaretti M, Touzet G, Reyns N, Dubois F, Gusmão S, Pereira JLB, Blond S. Correlation among magnetic resonance imaging findings, prognostic factors for survival, and histological diagnosis of intrinsic brainstem lesions in children. J Neurosurg Pediatr. 2011;8:539–43.
93. Sufit A, Donson AM, Birks DK, Knipstein JA, Fenton LZ, Jedlicka P, Hankinson TC, Handler MH, Foreman NK. Diffuse intrinsic pontine tumors: a study of primitive neuroectodermal tumors versus more common diffuse intrinsic pontine gliomas. J Neurosurg Pediatr. 2012;10:81–8.
94. Phi JH, Chung HT, Wang KC, Ryu SK, Kim SK. Transcerebellar biopsy of diffuse pontine gliomas in children: a technical note. Childs Nerv Syst. 2013;29:489–93.
95. Cage TA, Samagh SP, Mueller S, Nicolaides T, Haas-Kogan D, Prados M, Banerjee A, Auguste KI, Gupta N. Feasibility, safety, and indications for surgical biopsy of intrinsic brainstem tumors in children. Childs Nerv Syst. 2013;29:1313–9.
96. Ogiwara H, Morota N. The efficacy of a biopsy of intrinsic brainstem lesions for decision making of the treatments. Childs Nerv Syst. 2013;29:833–7.
97. Pincus DW, Richter EO, Yachnis AT, Bennett J, Bhatti T, Smith A. Brainstem stereotactic biopsy sampling in children. J Neurosurg. 2006;104(2 Suppl):108–14.

98. Rajshekhar V, Moorthy RK. Status of stereotactic biopsy in children with brain stem masses: insights from a series of 106 patients. Stereotact Funct Neurosurg. 2010;88:360–6.
99. Samadani U, Judy KD. Stereotactic brainstem biopsy is indicated for the diagnosis of a vast array of brainstem pathology. Stereotact Funct Neurosurg. 2003;81:5–9.
100. Puget S, Beccaria K, Blauwblomme T, Roujeau T, James S, Grill J, Zerah M, Varlet P, Sainte-Rose C. Biopsy in series of 130 pediatric diffuse intrinsic pontine gliomas. Childs Nerv Syst. 2015;31:1773–80.
101. Williams JR, Young CC, Vidtanza NA, McGrath M, Feroze AH, Browd SR, Hauptman JS. Progress in diffuse intrinsic pontine glioma: advocating for stereotactic biopsy in the standard of care. Neurosurg Focus. 2020;48(1):E4.
102. Jaradat A, Nowacki A, Fishtner J, Schlaeppi JA, Pollo C. Stereotactic biopsies of brainstem lesions: which approach? Acta Neurochir. 2021;163:1957–64.
103. Anderson RCE, Kennedy B, Yanes CL, Garvin J, Needle M, Canoll P, Feldstein NA, Bruce JN. Convection-enhanced delivery of topotecan into diffuse intrinsic brainstem tumors in children. J Neurosurg Pediatr. 2013;11:289–95.
104. Chittiboina P, Heiss JD, Warren KE, Lonser RR. Magnetic resonance imaging properties of convective delivery in diffuse intrinsic pontine gliomas. J Neurosurg Pediatr. 2014;13:276–82.
105. Kuzan-Fischer CM, Souweidane MM. The intersect of neurosurgery with diffuse intrinsic pontine glioma. J Neurosurg Pediatr. 2019;24:611–21.
106. Souweidane MM, Kramer K, Pandit-Taskar N, Zhou Z, Haque S, Zanzonico P, Carrasquillo JA, Lyashchenko SK, Thakur SB, Donzelli M, Turner RS, Lewis JS, Cheung NKV, Larson SM, Dunkel IJ. Convection-enhanced delivery for diffuse intrinsic pontine glioma: a single-center, dose-escalation, phase 1 trial. Lancet Oncol. 2018;19:1040–50.
107. Hamisch C, Kickingereder P, Fischer M, Simon T, Ruge MI. Update on the diagnostic value and safety of stereotactic biopsy for pediatric brainstem tumors: a systematic review and meta-analysis of 735 cases. J Neurosurg Pediatr. 2017;20:261–8.
108. Kickingereder P, Willet P, Simon T, Ruge MI. Diagnostic value and safety of stereotactic biopsy for brainstem tumors: a systematic review and meta-analysis of 1480 cases. Neurosurgery. 2013;72:873–82.
109. Iijima K, Hirato M, Miyagishima T, Horiguchi K, Sugawara K, Hirato J, Yokoo H, Yoshimoto Y. Microrecording and image-guided stereotactic biopsy of deep-seated brain tumors. J Neurosurg. 2015;123:978–88.
110. Ooba H, Abe T, Momii Y, Fujiki M. Stereotactic biopsy with electrical monitoring for deep-seated brain tumors. World Neurosurg. 2013;79(207):e1–201.e5.
111. Labuschagne J, Mutyaba D, Nel J, Casieri C. Use of intra-operative stimulation of brainstem lesion target sites for frameless stereotactic biopsies. Childs Nerv Syst. 2021;37:1515–23.

Chapter 3
MR Protocols for Paediatric Neurosurgical Common Conditions: An Update Guide for Neurosurgeons

Andrea De Vito, Ido Ben Zvi, and Felice D'Arco

3.1 Hydrocephalus

Even though computerised tomography (CT) is used in the acute assessment of hydrocephalus, magnetic resonance imaging (MRI) is the gold standard for evaluating it: it is the test of choice to visualise dilatation of the ventricular system, distinguish ventriculomegaly from obstructive hydrocephalus that needs surgical intervention and distinguish the underlying cause such as infection, obstruction, etc. [1, 2].

The MR approach for hydrocephalus must address many aspects of the disease: specific morphologic features, site(s) of obstruction, effects of hydrocephalus on the brain, recognition of the causal disease with its specific impact on the brain tissue and CSF dynamics (Fig. 3.1).

To address this, the imaging protocol should include [3–5] (Table 3.1):

- 3D-T1 (e.g. MPRAGE) with reformatting in multiple planes to evaluate the general brain morphology.
- Coronal T2-turbo spin echo (i.e. T2-TSE) demonstrates the contour of the lateral ventricles, especially the temporal horns with the medial compression of the hippocampus.

A. De Vito (✉)
Department of Neuroradiology, H. S. Gerardo Monza, Monza, Italy
e-mail: a.devito@campus.unimib.it

I. Ben Zvi
Paediatric Neurosurgery Department, Great Ormond Street Hospital, London, UK

F. D'Arco
Department of Radiology, Great Ormond Street Hospital, London, UK

C. Di Rocco (ed.), *Advances and Technical Standards in Neurosurgery*, Advances and Technical Standards in Neurosurgery 48,
https://doi.org/10.1007/978-3-031-36785-4_3

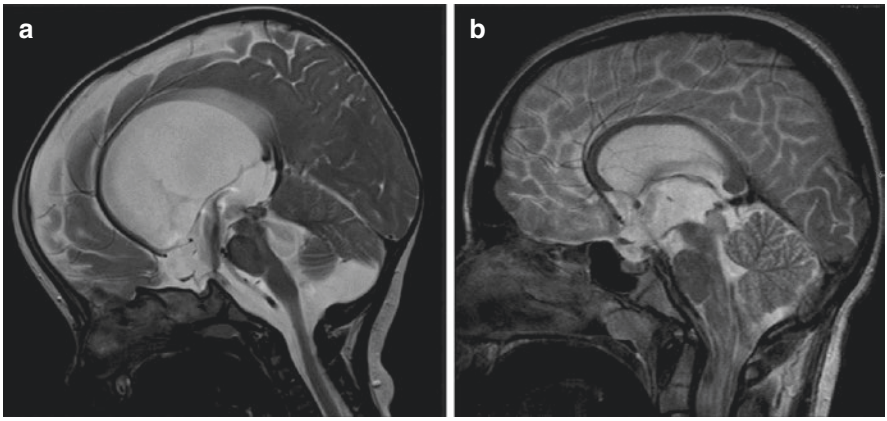

Fig. 3.1 Usefulness of T2WI on a sagittal plane to show the flow artefacts associated with a patent endoscopic third ventriculostomy in a patient with hydrocephalus due to a persistent Blake's pouch cyst (**a**) and in a patient with a low-grade tumour centred in the quadrigeminal plate and obstructing the cerebral aqueduct (**b**)

Table 3.1 Suggested basic MR protocol in children with suspected hydrocephalus

Coronal (or axial) T2- and sagittal T2-weighted images (WI)[a]	Shape of the ventricles and flow voids
3D sagittal high-resolution heavily weighted T2WI (CISS, FIESTA, etc.) on the midline	Integrity of the third ventricular shunt or presence of thin membranes which can create obstruction of the CSF flow
Axial or coronal FLAIR	Changes in the brain parenchyma and periventricular oedema
Axial DWI	Acute ischaemia and pus
3D T1WI MPRAGE	General brain anatomy
Optional: Post-contrast T1WI/CSF-flow studies	

[a]Sagittal thin slices (e.g. 2 mm) on midline to see the flow voids

- Thin sagittal T2 TSE assesses the main ventricular/cisternal CSF flow voids and the gross morphology of the midline structures.
- High-definition, submillimetric sagittal steady-state T2 imaging (FIESTA/CISS sequence) is of paramount importance in the analysis of hydrocephalus. Only this sequence provides clear images of the thin membranes, in the ventricles, aqueduct or cisterns; it is especially important in the pre-third ventriculostomy assessment to ascertain the patency of the interpeduncular cistern. After ventriculostomy, and together with sagittal T2 FSE, it demonstrates the anatomic (patent stoma) as well as the functional (transtuberal flow void) efficacy of the procedure.
- Axial FLAIR sequence shows the axial ventricular morphology and the parenchyma.

Besides these basic sequences, other sequences may contribute by illustrating specific features.

Nowadays, the CSF pathways from the ventricles to the cortical subarachnoid compartment and the CSF flow at various sites should be analysed in detail to better assess/evaluate the best treatment options (including endoscopic procedures and shunt insertion) and to guide surgical intervention [1, 2]. Although various MR cisternography and motion-sensitive MRI techniques have been employed, 3D-CISS or equivalent, TSE or FSE and cine phase contrast (PC) have gained wide acceptance in the assessment of CSF flow and/or cistern anatomy.

Three-dimensional sampling improvement by applying optimised contrast using different flip angle evolution (commercial names: 3D CISS, FIESTA, etc.) sequences is an advanced MRI technique. As of late, it is gaining popularity as a sensitive imaging modality in hydrocephalus, especially obstructive, because it permits more precise identification and localisation of very thin membranes and provides useful information regarding the level of obstruction [6] (Fig. 3.2). The 3D CISS sequence in hydrocephalus patients is very sensitive in distinguishing between obstructive and communicating hydrocephalus, thereby selecting more accurately patients as candidates for endoscopic fenestrations and reducing the need for and complications of shunt procedures. Another modality that has gained popularity is cardiac-gated cine phase-contrast imaging, which is another way of demonstrating flow, as it allows flow quantification in selected groups of subjects or patients [7].

Gradient echo (GRE) T2* or susceptibility-weighted imaging (SWI) easily detects previous bleeding in the ventricles and cisterns. In the case of marked susceptibility or blooming consistent with a severe previous haemorrhage superimposed on the basal cisterns and ventricles, shunt insertion may be the best alternative

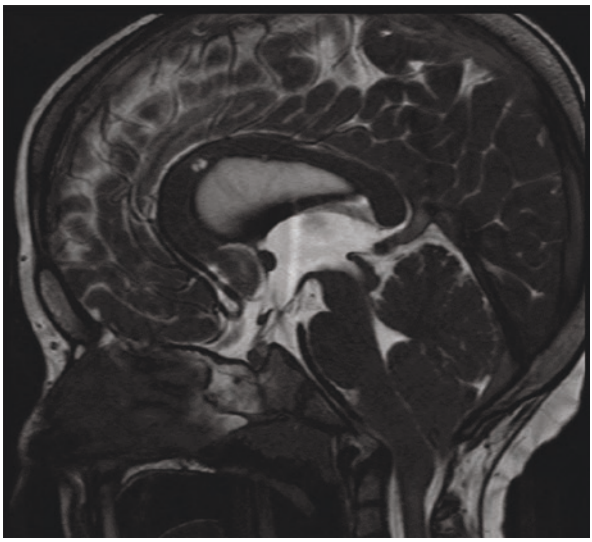

Fig. 3.2 3D heavily T2WI sequence (CISS, FIESTA, etc.) in a patient with hydrocephalus and Chiari malformation demonstrating the anatomy of the third ventricle with tuber cinereum and anterior recesses well seen due to the very high resolution of this sequence. While the T2WI shown in Fig. 3.1 (a spin-echo sequence) is more sensitive to the flow artefacts, this sequence is better for the pure anatomical visualisation

especially when there is no direct evidence of obstructive membranes in the cisterns, ventricles or both in the 3D CISS sequence [8].

Standard MR images have lengthy acquisition times and require sedation or general anaesthesia, especially in neonates and uncooperative children, which subjects them to risks of anaesthesia-related complications. For this reason, fast brain MRI protocols have been implemented to circumvent the need for sedation during image acquisition in paediatric hydrocephalus patients. Fast brain MRI uses short pulse sequences to acquire MR images in 23 s per slice, sufficient to make rapid clinical decisions in most paediatric hydrocephalus patients. Nevertheless, due to concerns of poor image quality and susceptibility to motion artefacts, indications for fast brain MRI in hydrocephalus have been limited to gross anatomical/structural and ventricular catheter placement assessments [9–11].

Post-contrast sequences and diffusion-weighted images (DWI) are critical to diagnose brain infections. In fact, meningitis and ependymitis are often associated with hydrocephalus, and DWI is sensitive in detection of pus in pyogenic infections [12].

3.2 Preterm Intraventricular Haemorrhage

Germinal matrix haemorrhage (GMH), intraventricular haemorrhage (IVH), periventricular haemorrhagic infarction (PHI) and its complication, posthaemorrhagic ventricular dilatation (PHVD), are the most common and most important neurologic injuries in preterm neonates. The brain of the premature infant lacks the ability to autoregulate cerebral blood pressure; thus, fluctuations in cerebral blood pressure and flow can rupture the primitive germinal matrix vessels or lead to infarction of the metabolically active germinal matrix. The damage can extend into the periventricular white matter, resulting in significant neurologic sequelae, including cerebral palsy, cognitive delay and seizures. Injury to the germinal matrix has substantial mortality and morbidity rates [13–15].

Ultrasonography (US) is the preferred screening and diagnostic tool for GMH [16, 17]. Preterm infants are often unstable during the first days of life, when GMH-IVH typically presents. US allows prompt diagnosis of GMH-IVH as well as assessment of its evolution [18]. In the most critical phase, US should be as "quick and gentle" as possible, in order to minimise stress for fragile neonates.

Moreover, US has several advantages over CT and MRI: it is safe (US has no ionising radiation, unlike CT), portable, easily repeated, usually readily available and economical and requires no special preparation. In preterm infants, obtaining views through anterior and mastoid fontanels permits good visualisation of the ventricular system, white matter and cerebellum. US is ideal for detecting GMH-IVH, large cerebellar bleeds, cysts and echogenic areas in white matter. One disadvantage is that US is operator-dependent, and subtle lesions may be missed in less experienced hands [19].

CT was previously used to assess for calcifications, haemorrhage, brain injury, oedema secondary to hypoxia-ischaemia, venous sinus thrombosis, masses and structural abnormalities. This modality however is now largely supplanted by MRI due to the ionising radiation required for imaging. Except for emergencies, CT

scans are now generally avoided for newborn imaging. A normal CT scan finding for GMH and IVH does not exclude abnormal neurodevelopment with a negative predictive value of 50–60% at the age of 2 years [19].

MRI offers the highest resolution for detecting and quantifying white matter injury (WMI), low-grade IVH, cerebral malformation and posterior fossa abnormalities, due to its greater neuroanatomical definition [20–22]. The standard MR protocol should include unenhanced sagittal and axial T1, axial gradient echo, axial FLAIR and T2 TSE, axial DWI and ADC.

WMI is the most common finding seen on MRI in preterm infants. Such injuries include cystic and punctate lesions, delayed myelination, volume loss, thinning of the corpus callosum and diffuse white matter oedema [23]. Among the disadvantages of MRI cost, both time and resources, it is not always available and may require sedation, although in infants a "feed-and-wrap" procedure may be used [24]. MRI before term-corrected age can be challenging to organise in critically ill infants.

The strongest predictors of abnormal neuromotor function on US include severe IVH (Papile grades 3 and 4), cystic PVL and PHVD [25]. For MRI imaging at term-equivalent age, moderate-to-severe WMI, cerebellar injury and abnormal myelination in the posterior limb of the internal capsule (PLIC) are the main predictors of motor impairments [23, 25, 26]. Any combination of these predictors increases the risk of motor deficiencies. As for neurocognitive and behavioural impairments, the predictive value of both US and MRI is limited [26].

The suggested protocol for suspected IVH is a standard brain MRI protocol (with fast sequences if the child is unstable[1]) but with gradient or SWI sequences which are sensitive to blood. An MRV may be added in case of suspected thrombosis (Fig. 3.3).

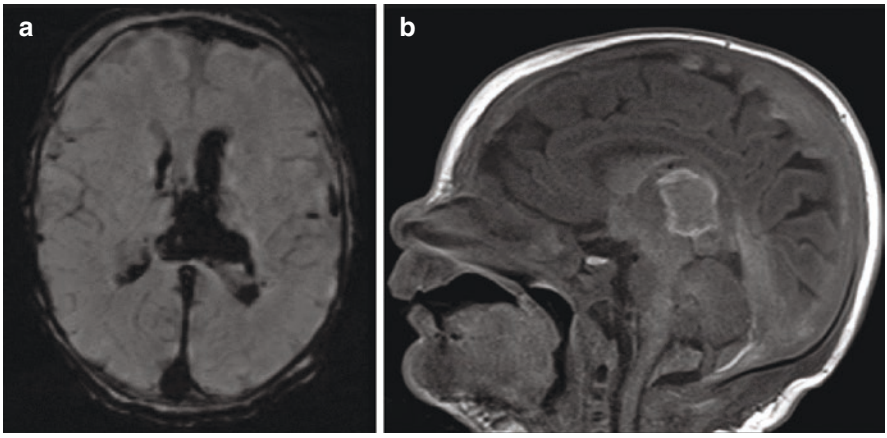

Fig. 3.3 A 6-day-old preterm infant with large intraventricular haemorrhage whose extension is clearly visible on SWI (**a**). There is also venous thrombosis involving the straight and sagittal sinus and associated thalamic haemorrhagic infarction (**b**)

[1] Standard and fast brain protocol changes depending on the institution and radiologist preferences; in our institution axial T2WI, axial DWI, coronal FLAIR and 3D T1WI are used.

3.3 Chiari 1 Malformation

Diagnostic neuroimaging has been an essential tool in elucidating the pathophysiology and treatment of Chiari 1 malformation. The advent of MR imaging transformed the way this controversial disorder is diagnosed and managed. The newer dynamic neuroimaging cine-MR imaging flow studies have furthered the understanding of CSF flow and pressure gradients, thus creating an in vivo way of measuring normal and abnormal physiologic processes and allowing more refined treatment protocols [27].

Frequently, Chiari 1 malformation is discovered incidentally on CT or MR imaging of the head or spine; it is important to remember that often a head CT scan represents the first step in the radiological approach of patients with clinical signs and symptoms such as headache, raised intracranial pressure or other symptoms that may coincide with tonsillar descent/Chiari 1 whether it is related or not. Furthermore, CT represents the investigation of choice for a correct characterisation of bony structures in skull base and craniocervical junction abnormalities such as platybasia, basilar invagination, assimilation of the arch of C1 and instability. It is also useful for preoperative planning [28, 29]. Routine CT scans done for headaches or in children with craniosynostosis should always be reviewed for evidence of cerebellar tonsillar crowding, as this is easily missed. 3D reconstruction and thin bone windows are fundamental for the assessment of sutures in children either considered for surgery or already operated. If Chiari 1 is suspected on a head CT scan, MR imaging of the brain and spinal axis (cervical, thoracic and lumbar) should be obtained [30].

MRI represents the "gold standard" for the radiological diagnosis and evaluation of Chiari 1 malformation and low cerebellar tonsils. Despite the limits of MRI in emergency settings, especially in children requiring sedation or general anaesthesia (GA), conventional T1- and T2-weighted image (WI) MRI sequences can provide the highest quality images regarding brain anatomy and its variation from the physiological range [31].

The goal of MRI is to evaluate the shape and position of the cerebellar tonsils. Moreover, it can assess the associated syrinx in the spinal cord, cranial vault, skull base and vertebral anomalies (Fig. 3.4).

The standard cervical spine MRI protocol for the study of CVJ in patients with Chiari 1 deformity/low cerebellar tonsils (Table 3.2) should include sagittal spin-echo T1WI (for the study of the anatomical position of the cerebellar tonsils and size of the foramen magnum), axial and sagittal spin-echo T2WI (for the study of the cord signal, i.e. diagnosis of associated myelomalacia), coronal T1 or T2WI in case of diastematomyelia, vertebral segmentation anomalies and scoliosis [32].

Post-gadolinium sequences in case of syrinx can be added on the first scan only to exclude an associated tumour. Sequences as a 3D steady-state T2 (i.e. DRIVE/CISS) to assess in more spatial detail the CVJ, posterior fossa cisterns and cranial nerves can be added [32].

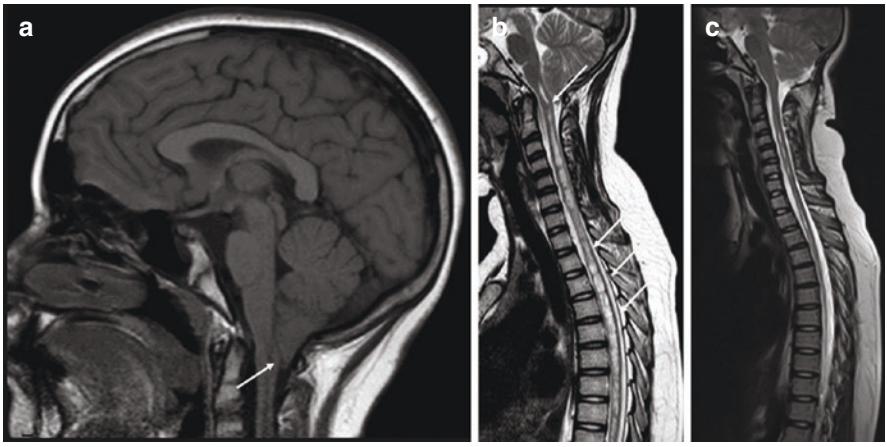

Fig. 3.4 Sagittal T1W of the brain shows low and pointed appearances of the cerebellar tonsils (white arrow in **a**) in keeping with Chiari 1. Spinal images show involvement of the cord at the cervico-medullary junction and large associated cord syrinx (white arrows in **b**). Sagittal T2WI post-occipital decompression (**c**) shows marked improvement of the position of the tonsils and of the spinal syrinx

Table 3.2 Suggested basic MR protocol in children with suspected Chiari 1

Standard brain protocol	As per previous protocol
Sagittal T1 and T2WI of the entire spine	Syrinx and vertebral morphology
Axial T2 of the CVJ	Myelomalacia
Optional: Coronal T2WI of the spine	Vertebral segmentation anomalies

Flow-sensitive MRI techniques and three-dimensional high-resolution sequences are useful modalities for the functional and anatomical assessment of CSF flow dynamics [33–35]. A cine phase-contrast sequence can demonstrate pulsatile CSF flow at the level of the CVJ: acquisitions are synchronised with the cardiac cycle, producing images with velocity information that provide the ability to calculate stroke volume, mean velocity and peak flow in systole and diastole [36]. Cine-MR imaging flow studies are used as a dynamic measure of the severity of compression within the posterior fossa.

Therefore, these sequences allow for qualitative (i.e. monitoring of CSF flow through the Sylvius aqueduct and the basal subarachnoid spaces such as prepontine premedullary cisterns) and quantitative (i.e. can estimate the volume and flow of CSF) in patients with Chiari 1. Moreover, axial T2WI may be acquired for better detection of intracranial haemorrhage as a cause of hydrocephalus with a possible secondary tonsillar descent.

Fast MRI (fsMRI) is derived from T2-weighted MRI with very short acquisition times, often aimed at answering very specific clinical questions [9]. While fast sequences have image contrast and resolution inferior to those of conventional T2-weighted MRI sequences, fsMRI has shown utility in the evaluation of ventricle

size and extra-axial CSF spaces. Conventional brain MRI has longer acquisition times and often requires sedation in young children or clinically unstable patients who are prone to movement or unable to tolerate lengthy exams [10, 37]. Therefore, fsMRI can be particularly beneficial in such patient populations. The main indication for fsMRI has traditionally been for evaluating ventricle size in hydrocephalus [38]. However, the use of fsMRI has been increasingly expanded to evaluate other neurosurgical conditions such as macrocephaly, intracranial cysts and select congenital abnormalities, as well as in postoperative settings. Unlike other known clinical indications for fsMRI, at present, the diagnostic performance of fsMRI for the CM-I population is unknown.

3.4 Craniosynostosis

Craniosynostosis is encountered in the paediatric population in isolated or syndromic forms. The resulting deformity depends on the number and type of sutures involved.

Radiologic evaluation has traditionally played an important role in the diagnosis and characterisation of craniosynostosis. Imaging techniques have also evolved rapidly from skull radiography to highly sophisticated CT scans with 3D reconstructions of the cranial vault [39–42]. Present imaging techniques are utilised for accurate diagnosis, surgical planning and posttreatment evaluation. Imaging is also important to identify coexistent anomalies and complications associated with these deformities.

Initial imaging evaluation after clinical assessment may include high-frequency ultrasound (US) of the sutures, plain films or low-dose (21 mAs) three-dimensional (3D) CT scans. Although CT is not essential for diagnosis, it may be used in equivocal cases or for preoperative planning. High-frequency postnatal US is reported as capable of evaluating suture width, bone thickness in the affected area, bone overlap in positional plagiocephaly and partial or complete synostosis [43]. Secondary signs of raised intracranial pressure including diastatic sutures and hydrocephalus can also be identified on US images [44, 45].

Historically, radiography has served as an initial imaging modality in children with abnormal head shapes, and it remains a cost-effective method in infants with low risk of craniosynostosis [46]. In children with low pre-test probability of craniosynostosis, skull radiography with its specificity of 95% is a rapid and low-radiation diagnostic tool [47]. Radiography, however, has poor sensitivity in detecting complex and minor sutural synostoses, and it should be avoided. The use of a low-dose CT is considered the gold standard [48].

MRI should be requested in case of suspicion of brain parenchymal involvement (Fig. 3.5). The suggested protocol is a standard MRI brain with MR venography (MRV).

In fact, MRI helps to detect cerebral and craniofacial soft tissue anomalies seen in association with craniosynostosis, especially of the syndromic variety. MR

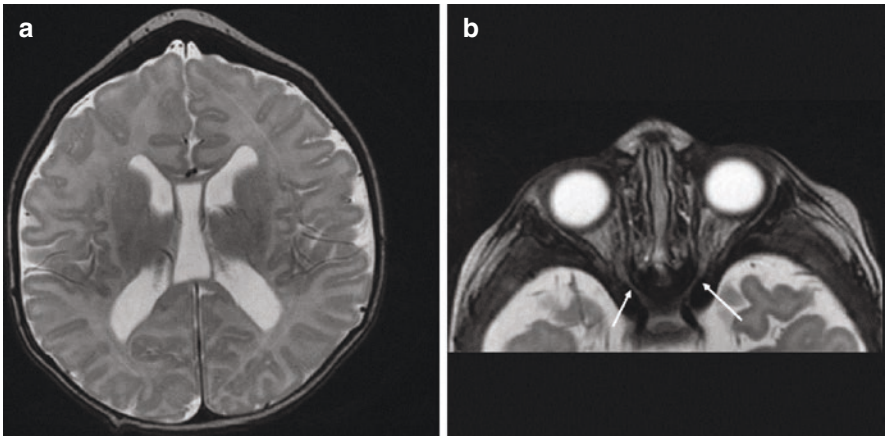

Fig. 3.5 Example of brain and cranial nerve complications associated with craniosynostosis in a child with genetic cause of craniosynostosis (i.e. Carpenter syndrome). The trigonocephaly due to metopic suture is evident in (**a**) with associated enlargement "ex vacuo" of the lateral ventricle due to loss of white matter bulk. There is stenosis of the optic foramina with optic nerve atrophy (arrows in **b**)

venography and cerebrospinal fluid studies at the craniocervical junction might reveal chronic venous hypertension, tonsillar herniation and cerebrospinal fluid (CSF) obstruction. Other associated anomalies can be evaluated with MRI such as cranial neuropathies caused by skull base hypoplasia and foraminal narrowing, vascular malformations, orbital abnormalities and optic nerve atrophy [49–51].

In preoperative syndromic cases, an MRI may also be performed with an MR venogram to allow assessment of any venous stenosis and emissary veins that may increase the risk of intraoperative blood loss.

CT with 3D surface-rendered image reconstruction is the investigation of choice in the management of craniosynostosis [47, 52]. Three-dimensional CT allows for complete assessment of the cranial vault, skull base, orbits and facial bones. Endocranial 3D images are especially helpful in evaluating skull base hypoplasia and minor suture synostoses. Axial, sagittal and coronal plane bone reconstruction algorithms are especially useful if the synostosis is not well characterised with 3D images.

3.5 Paediatric Nonaccidental Injury (NAI)

Abusive head trauma (AHT) is the leading cause of fatal head injuries in children under the age of 2 years. Because the aetiology of the injury is multifactorial (shake, shake and impact, impact, etc.), the present best and most inclusive term is AHT. There is no controversy over the medical validity of the presence of AHT with multiple components, including subdural hematoma, intracranial and spinal

changes, complex retinal haemorrhages and rib and other fractures inconsistent with the stated mechanism of trauma. The evaluation must rule out medical conditions that can mimic AHT [53].

Appropriate use of laboratory testing and imaging is critical for accurate diagnosis and treatment [53]. Recent papers discuss the assessment of bleeding and bone disease in cases of suspected abuse [54, 55]. All children with potential AHT, especially children under 2 years of age, should have a skeletal survey according to present guidelines [56]. In older children, long bone fractures can be more reliably suspected if the extremities are tender, swollen or unable to bear weight. For an acutely ill child with neurological impairments, an optimal imaging strategy includes first unenhanced CT with 3D reformatted images of the calvarium [57], followed by MRI of the brain and spine as soon as possible and with specific sequences. Multi-sequence MRI of the brain and spine is useful to characterise extra-axial haemorrhages and to define brain contusions, lacerations and other parenchymal injuries (Table 3.3).

Proper timing of intracranial injuries in abusive head trauma (AHT) is a crucial but challenging task, both to properly identify the individual who caused the injuries and to rule out those who did not. Intracranial haemorrhage, and particularly subdural haemorrhage (SDH), is the most commonly observed imaging feature in AHT, and timing decisions often focus on the initial onset and evolution of SDH in assessing the timing of the injury. In general, a broad time scale has been proposed to determine the approximate age of SDH. For example, based on CT attenuation, SDH has been classified as hyperacute (<3 h), acute (3 h to 7–10 days), subacute (2–3 weeks) and chronic (>3 weeks) [58]. However, previous studies have provided contradictory results for these time frames [59–62].

Spinal injury is common in AHT and predominantly involves the craniocervical junction in most children. The injury also mainly reflects a flexion-extension injury mechanism of the soft tissue structures, particularly involving the posterior suboccipital region. Because the spinal injury of AHT mostly involves ligamentous and soft tissues and only rarely involves bony fractures, more than 90% of the MRI injury findings are missed on CT or radiographs of the spine [63].

The most consistently identified imaging findings in AHT include posterior suboccipital muscle and ligamentous injuries [64, 65]. These include larger structures such as the nuchal ligament and smaller ligamentous structures such as the

Table 3.3 Suggested basic protocol in children with suspected AHT (Fig. 3.6)

Standard brain protocol	Acute or chronic brain damage
Axial SWI or gradient T2	To increase sensitivity to intracranial (particularly subdural) bleeds
Sagittal T1 and T2WI of the entire spine	
Sagittal T2 with fat saturation	Ligamentous injury
Axial T2 spinal cord	If areas of myelomalacia are suspected
Sagittal gradient T2 of the spine	To increase sensitivity to intraspinal blood

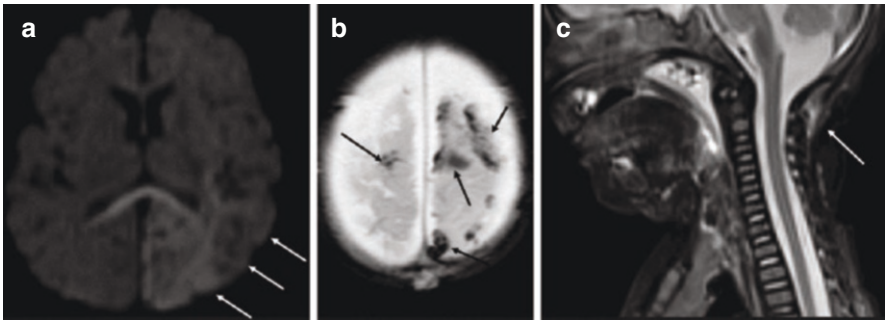

Fig. 3.6 Typical brain and spine findings in a case of abusive head trauma. DWI of the brain (**a**) shows areas of acute ischaemia in the left parietal hemisphere (white arrows) and corpus callosum. Axial T2 gradient shows multiple subdural haematomas (black arrows in **b**). Sagittal T2 of the cervical spine with fat saturation shows ligamentous injury (white arrow in **c**)

atlanto-axial and atlanto-occipital membranes, interspinous ligaments and capsular ligaments of occiput–C1 and C1–C2 articulations.

The nuchal ligament contains fat and on short tau inversion recovery (STIR) sequence should appear predominantly hypointense. If injury is present, T2 hyperintensity is evident in this region along with fatty stranding on T1 or T2 sequence. Similarly, T2 hyperintensity along the capsular ligaments of occiput–C1 and C1–C2 articulation is frequently identified, and this represents evidence of injury. Distraction injury is suspected when there is also an increase in joint space with an effusion. Mild distraction injury, rather than frank dissociation, is more commonly seen in AHT [53].

Outside the neonatal time period, abusive head trauma (AHT) is the most common cause of retinal haemorrhage in children, with an incidence ranging 51–100% [66–68]. The gold standard for diagnosing retinal haemorrhage is a dilated direct or indirect fundoscopy with photographic documentation. Dilated fundoscopic examination requires invasive pharmacological dilation and is not always possible because of the systemic or neurologic status of the patient. The timing of this exam is critical. If not performed within 2 days of the trauma, the retinal haemorrhage might be missed because of absorption of the blood [68]. Furthermore, studies have shown that non-ophthalmologists, such as emergency physicians and paediatricians, are more likely to miss retinal haemorrhages on routine clinical exam [69].

MRI plays an important role in diagnosing AHT. MRI of retinal haemorrhages, however, is challenging for many reasons. The timing of the imaging, the severity of the injury, differences in imaging equipment and technique and the field strength of the MRI all affect visualisation on MRI. Sequences such as T2* gradient-recalled echo (GRE) and SWI, which are more sensitive for blood products, have been used to try to diagnose retinal haemorrhages. More recently, orbit-optimised SWI has shown increased sensitivity in the detection of retinal haemorrhage. To that end, a focused MRI protocol for AHT that includes dedicated imaging of the orbits might aid in the diagnosis of retinal haemorrhage [70].

3.6 Spinal Dysraphism

Congenital malformations of the spine and spinal cord are generally described under the umbrella term spinal dysraphisms (SDs).

SDs are a group of developmental disorders with multifactorial aetiology, comprising genetic, environmental and nutritional components [71, 72].

Plain radiographs can be used as a screening modality for bony spinal anomalies. Ultrasound is a good modality for the evaluation of spinal anomalies in the antenatal period, but in young infants, it can be used only as a screening modality as it is sensitive to detect dysraphism with cystic component but is less sensitive to MRI in closed spinal dysraphism [73]. The quality of an ultrasound study also depends on the available acoustic window and operator's skill. Computed tomography (CT) scan with multiplanar reformations is an excellent modality to diagnose vertebral anomalies and bony septum in diastematomyelia, but it has less soft tissue contrast and requires an intrathecal injection of nonionic iodinated contrast to evaluate the thecal sac and its contents [74]. Ultrasound and CT scans cannot demonstrate small abnormalities of the spinal cord and nerves and do not have good soft tissue contrast as MRI, which makes MRI the initial investigation of choice [75]. MRI scan is the best modality to diagnose spinal dysraphism and is usually the only investigation required for diagnosis and pre-surgical planning for spinal dysraphism and associated syndromes.

A proper protocol is essential for a complex modality such as MRI; otherwise, the abnormality/lesion may not be detected [74]. MRI is time-consuming. Many paediatric patients require sedation or short general anaesthesia to obtain a good-quality MRI scan without motion artefacts.

The ideal MR protocol should aim to identify the subtle abnormalities and the interface between the neural placode and fat or meninges (depending on the malformations) and distinguish between fatty and nonfatty components of the malformations (Fig. 3.7). For these purposes, a sagittal high-resolution heavily weighted

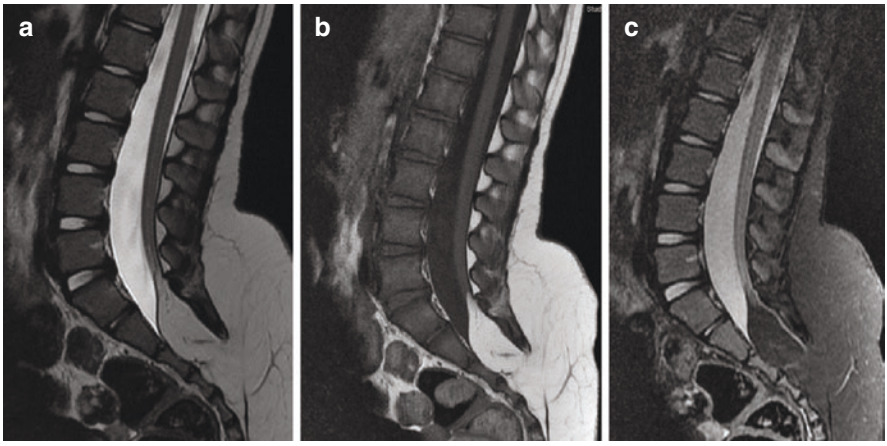

Fig. 3.7 A lipomyelocele with intraspinal lipoma shown in T2WI (**a**), T1WI (**b**) and fat-saturated T2WI (**c**) sagittal sequences of the spine. Note the disappearance of the bright (hyperintense) signal of the fat in (**c**)

sequence and axial T1 of the lower spine need to be added to the standard spine protocol; fat-saturated sequences can be used to confirm the presence of fat. Brain images should also be performed given the associated brain malformations in some of the spinal dysraphisms, such as Chiari 2.

3.7 Conclusion

In this chapter, we summarised the rationale for different approaches to MR protocols in some of the common, complex and acute paediatric neurosurgical diseases. This is intended as a guide to explain why specific sequences need to be added to the "standard" MRI protocol of the brain and spine in order to provide the neurosurgeon with as much information as possible for the pre- and postoperative planning and evaluation. A balance between fast and simple protocols and accurate clinical information is critical in daily practice, and knowledge of the indication of MRI scans is of the utmost importance for their proper clinical use.

References

1. Dinçer A, Yildiz E, Kohan S, Memet Özek M. Analysis of endoscopic third ventriculostomy patency by MRI: value of different pulse sequences, the sequence parameters, and the imaging planes for investigation of flow void. Childs Nerv Syst. 2011;27:127–35.
2. Dinçer A, Kohan S, Özek MM. Is all "communicating" hydrocephalus really communicating? Prospective study on the value of 3D-constructive interference in steady state sequence at 3T. AJNR Am J Neuroradiol. 2009;30:1898–906.
3. Citrin CM, Sherman JL, Gangarosa RE, Scanlon D. Physiology of the CSF flow-void sign: modification by cardiac gating. AJR Am J Roentgenol. 1987;148:205–8.
4. Del Bigio MR. Neuropathological changes caused by hydrocephalus. Acta Neuropathol. 1993;85:573–85.
5. Fletcher JM, McCauley SR, Brandt ME, Bohan TP, Kramer LA, Francis DJ, Thorstad K, Brookshire BL. Regional brain tissue composition in children with hydrocephalus. Relationships with cognitive development. Arch Neurol. 1996;53:549–57.
6. Doll A, Christmann D, Kehrli P, Abu Eid M, Gillis C, Bogorin A, Thiebaut A, Dietemann JL. Contribution of 3D CISS MRI for pre- and post-therapeutic monitoring of obstructive hydrocephalus. J Neuroradiol. 2000;27:218–25.
7. Laitt RD, Mallucci CL, Jaspan T, McConachie NS, Vloeberghs M, Punt J. Constructive interference in steady-state 3D Fourier-transform MRI in the management of hydrocephalus and third ventriculostomy. Neuroradiology. 1999;41:117–23.
8. Dinçer A, Özek MM. Radiologic evaluation of pediatric hydrocephalus. Childs Nerv Syst. 2011;27:1543–62.
9. Christy A, Murchison C, Wilson JL. Quick brain magnetic resonance imaging with diffusion-weighted imaging as a first imaging modality in pediatric stroke. Pediatr Neurol. 2018;78:55–60.
10. Malviya S, Voepel-Lewis T, Eldevik OP, Rockwell DT, Wong JH, Tait AR. Sedation and general anaesthesia in children undergoing MRI and CT: adverse events and outcomes. Br J Anaesth. 2000;84:743–8.

11. DiMaggio C, Sun LS, Li G. Early childhood exposure to anesthesia and risk of developmental and behavioral disorders in a sibling birth cohort. Anesth Analg. 2011;113:1143–51.
12. Muccio CF, Caranci F, D'Arco F, Cerase A, De Lipsis L, Esposito G, Tedeschi E, Andreula C. Magnetic resonance features of pyogenic brain abscesses and differential diagnosis using morphological and functional imaging studies: a pictorial essay. J Neuroradiol. 2014;41:153–67.
13. Luo J, Luo Y, Zeng H, Reis C, Chen S. Research advances of germinal matrix hemorrhage: an update review. Cell Mol Neurobiol. 2019;39:1–10.
14. Wu T, Wang Y, Xiong T, Huang S, Tian T, Tang J, Mu D. Risk factors for the deterioration of periventricular–intraventricular hemorrhage in preterm infants. Sci Rep. 2020;10:1–8.
15. Payne AH, Hintz SR, Hibbs AM, Walsh MC, Vohr BR, Bann CM, Wilson-Costello DE, Eunice Kennedy Shriver National Institute of Child Health and Human Development Neonatal Research Network. Neurodevelopmental outcomes of extremely low-gestational-age neonates with low-grade periventricular-intraventricular hemorrhage. JAMA Pediatr. 2013;167:451–9.
16. Parodi A, Morana G, Severino MS, Malova M, Natalizia AR, Sannia A, Rossi A, Ramenghi LA. Low-grade intraventricular hemorrhage: is ultrasound good enough? J Matern Fetal Neonatal Med. 2015;28(Suppl 1):2261–4.
17. Intrapiromkul J, Northington F, Huisman TAGM, Izbudak I, Meoded A, Tekes A. Accuracy of head ultrasound for the detection of intracranial hemorrhage in preterm neonates: comparison with brain MRI and susceptibility-weighted imaging. J Neuroradiol. 2013;40:81–8.
18. Parodi A, Govaert P, Horsch S, Bravo MC, Ramenghi LA, eurUS.brain group. Cranial ultrasound findings in preterm germinal matrix haemorrhage, sequelae and outcome. Pediatr Res. 2020;87:13–24.
19. Guillot M, Chau V, Lemyre B. Routine imaging of the preterm neonatal brain. Paediatr Child Health. 2020;25:249–62.
20. Leijser LM, de Vries LS. Preterm brain injury: germinal matrix-intraventricular hemorrhage and post-hemorrhagic ventricular dilatation. Handb Clin Neurol. 2019;162:173–99.
21. Plaisier A, Raets MMA, Ecury-Goossen GM, Govaert P, Feijen-Roon M, Reiss IKM, Smit LS, Lequin MH, Dudink J. Serial cranial ultrasonography or early MRI for detecting preterm brain injury? Arch Dis Child Fetal Neonatal Ed. 2015;100:F293–300.
22. Petropoulou C, Bouza H, Nikas I, Chrousos G, Anagnostakou M, Gouliamos A, Alexopoulou E. Magnetic resonance imaging versus ultrasound at early post-term age in brain imaging of preterm infants. J Neonatal Perinatal Med. 2012;5:363–71.
23. Anderson PJ, Cheong JLY, Thompson DK. The predictive validity of neonatal MRI for neurodevelopmental outcome in very preterm children. Semin Perinatol. 2015;39:147–58.
24. Horsch S, Skiöld B, Hallberg B, Nordell B, Nordell A, Mosskin M, Lagercrantz H, Adén U, Blennow M. Cranial ultrasound and MRI at term age in extremely preterm infants. Arch Dis Child Fetal Neonatal Ed. 2010;95:F310–4.
25. Nongena P, Ederies A, Azzopardi DV, Edwards AD. Confidence in the prediction of neurodevelopmental outcome by cranial ultrasound and MRI in preterm infants. Arch Dis Child Fetal Neonatal Ed. 2010;95:F388–90.
26. Ibrahim J, Mir I, Chalak L. Brain imaging in preterm infants <32 weeks gestation: a clinical review and algorithm for the use of cranial ultrasound and qualitative brain MRI. Pediatr Res. 2018;84:799–806.
27. McVige JW, Leonardo J. Imaging of Chiari type I malformation and syringohydromyelia. Neurol Clin. 2014;32:95–126.
28. Manara R, Concolino D, Rampazzo A, Zanetti A, Tomanin R, Faggin R, Scarpa M. Chiari 1 malformation and holocord syringomyelia in hunter syndrome. JIMD Rep. 2014;12:31–5.
29. Chirossel JP, Passagia JG, Gay E, Palombi O. Management of craniocervical junction dislocation. Childs Nerv Syst. 2000;16:697–701.
30. Massimi L, Novegno F, di Rocco C. Chiari type I malformation in children. Adv Tech Stand Neurosurg. 2011;37:143–211.
31. Hukki A, Koljonen V, Karppinen A, Valanne L, Leikola J. Brain anomalies in 121 children with non-syndromic single suture craniosynostosis by MR imaging. Eur J Paediatr Neurol. 2012;16:671–5.

32. D'Arco F, Ganau M. Which neuroimaging techniques are really needed in Chiari I? A short guide for radiologists and clinicians. Childs Nerv Syst. 2019;35:1801–8.
33. Battal B, Kocaoglu M, Bulakbasi N, Husmen G, Tuba Sanal H, Tayfun C. Cerebrospinal fluid flow imaging by using phase-contrast MR technique. Br J Radiol. 2011;84:758–65.
34. Yamada S, Tsuchiya K, Bradley WG, Law M, Winkler ML, Borzage MT, Miyazaki M, Kelly EJ, McComb JG. Current and emerging MR imaging techniques for the diagnosis and management of CSF flow disorders: a review of phase-contrast and time-spatial labeling inversion pulse. AJNR Am J Neuroradiol. 2015;36:623–30.
35. Mohammad SA, Osman NM, Khalil RM. Phase-contrast and three-dimensional driven equilibrium (3D-DRIVE) sequences in the assessment of paediatric obstructive hydrocephalus. Childs Nerv Syst. 2018;34:2223–31.
36. Shah S, Haughton V, del Río AM. CSF Flow through the Upper Cervical Spinal Canal in Chiari I Malformation. AJNR Am J Neuroradiol. 2011;32:1149–53.
37. Ramaiah R, Bhananker S. Pediatric procedural sedation and analgesia outside the operating room: anticipating, avoiding and managing complications. Expert Rev Neurother. 2011;11:755–63.
38. Patel DM, Tubbs RS, Pate G, Johnston JM Jr, Blount JP. Fast-sequence MRI studies for surveillance imaging in pediatric hydrocephalus. J Neurosurg Pediatr. 2014;13:440–7.
39. Benson ML, Oliverio PJ, Yue NC, Zinreich SJ. Primary craniosynostosis: imaging features. AJR Am J Roentgenol. 1996;166:697–703.
40. Kotrikova B, Krempien R, Freier K, Mühling J. Diagnostic imaging in the management of craniosynostoses. Eur Radiol. 2007;17:1968–78.
41. Kirmi O, Lo SJ, Johnson D, Anslow P. Craniosynostosis: a radiological and surgical perspective. Semin Ultrasound CT MR. 2009;30:492–512.
42. Khanna PC, Thapa MM, Iyer RS, Prasad SS. Pictorial essay: the many faces of craniosynostosis. Indian J Radiol Imaging. 2011;21:49–56.
43. Regelsberger J, Delling G, Tsokos M, Helmke K, Kammler G, Kränzlein H, Westphal M. High-frequency ultrasound confirmation of positional plagiocephaly. J Neurosurg. 2006;105:413–7.
44. Soboleski D, Mussari B, McCloskey D, Sauerbrei E, Espinosa F, Fletcher A. High-resolution sonography of the abnormal cranial suture. Pediatr Radiol. 1998;28:79–82.
45. Soboleski D, McCloskey D, Mussari B, Sauerbrei E, Clarke M, Fletcher A. Sonography of normal cranial sutures. AJR Am J Roentgenol. 1997;168:819–21.
46. Medina LS, Richardson RR, Crone K. Children with suspected craniosynostosis: a cost-effectiveness analysis of diagnostic strategies. AJR Am J Roentgenol. 2002;179:215–21.
47. Vannier MW, Hildebolt CF, Marsh JL, Pilgram TK, McAlister WH, Shackelford GD, Offutt CJ, Knapp RH. Craniosynostosis: diagnostic value of three-dimensional CT reconstruction. Radiology. 1989;173:669–73.
48. Blaser SI. Abnormal skull shape. Pediatr Radiol. 2008;38(Suppl 3):S488–96.
49. Rollins N, Booth T, Shapiro K. MR venography in children with complex craniosynostosis. Pediatr Neurosurg. 2000;32:308–15.
50. Cinalli G, Sainte-Rose C, Kollar EM, Zerah M, Brunelle F, Chumas P, Arnaud E, Marchac D, Pierre-Kahn A, Renier D. Hydrocephalus and craniosynostosis. J Neurosurg. 1998;88:209–14.
51. Collmann H, Sörensen N, Krauss J. Hydrocephalus in craniosynostosis: a review. Childs Nerv Syst. 2005;21:902–12.
52. Medina LS. Three-dimensional CT maximum intensity projections of the calvaria: a new approach for diagnosis of craniosynostosis and fractures. AJNR Am J Neuroradiol. 2000;21:1951–4.
53. Choudhary AK, Servaes S, Slovis TL, et al. Consensus statement on abusive head trauma in infants and young children. Pediatr Radiol. 2018;48:1048–65.
54. Servaes S, Brown SD, Choudhary AK, et al. The etiology and significance of fractures in infants and young children: a critical multidisciplinary review. Pediatr Radiol. 2016;46:591–600.
55. Anderst JD, Carpenter SL, Abshire TC, Section on Hematology/Oncology and Committee on Child Abuse and Neglect of the American Academy of Pediatrics. Evaluation for bleeding disorders in suspected child abuse. Pediatrics. 2013;131:e1314–22.

56. Meyer JS, Gunderman R, Coley BD, et al. ACR Appropriateness Criteria(®) on suspected physical abuse-child. J Am Coll Radiol. 2011;8:87–94.
57. Choudhary AK, Jha B, Boal DK, Dias M. Occipital sutures and its variations: the value of 3D-CT and how to differentiate it from fractures using 3D-CT? Surg Radiol Anat. 2010;32:807–16.
58. Vezina G. Assessment of the nature and age of subdural collections in nonaccidental head injury with CT and MRI. Pediatr Radiol. 2009;39:586–90.
59. Bradford R, Choudhary AK, Dias MS. Serial neuroimaging in infants with abusive head trauma: timing abusive injuries. J Neurosurg Pediatr. 2013;12:110–9.
60. Vinchon M, Noulé N, Tchofo PJ, Soto-Ares G, Fourier C, Dhellemmes P. Imaging of head injuries in infants: temporal correlates and forensic implications for the diagnosis of child abuse. J Neurosurg. 2004;101:44–52.
61. Adamsbaum C, Morel B, Ducot B, Antoni G, Rey-Salmon C. Dating the abusive head trauma episode and perpetrator statements: key points for imaging. Pediatr Radiol. 2014;44(Suppl 4):S578–88.
62. Sieswerda-Hoogendoorn T, Postema FAM, Verbaan D, Majoie CB, van Rijn RR. Age determination of subdural hematomas with CT and MRI: a systematic review. Eur J Radiol. 2014;83:1257–68.
63. Haq I, Jayappa S, Desai SK, Ramakrishnaiah R, Choudhary AK. Spinal ligamentous injury in abusive head trauma: a pictorial review. Pediatr Radiol. 2021;51:971–9.
64. Choudhary AK, Ishak R, Zacharia TT, Dias MS. Imaging of spinal injury in abusive head trauma: a retrospective study. Pediatr Radiol. 2014;44:1130–40.
65. Kadom N, Khademian Z, Vezina G, Shalaby-Rana E, Rice A, Hinds T. Usefulness of MRI detection of cervical spine and brain injuries in the evaluation of abusive head trauma. Pediatr Radiol. 2014;44:839–48.
66. Vinchon M, de Foort-Dhellemmes S, Desurmont M, Delestret I. Confessed abuse versus witnessed accidents in infants: comparison of clinical, radiological, and ophthalmological data in corroborated cases. Childs Nerv Syst. 2010;26:637–45.
67. Bhardwaj G, Chowdhury V, Jacobs MB, Moran KT, Martin FJ, Coroneo MT. A systematic review of the diagnostic accuracy of ocular signs in pediatric abusive head trauma. Ophthalmology. 2010;117:983–992.e17.
68. Levin AV. Retinal hemorrhage in abusive head trauma. Pediatrics. 2010;126:961–70.
69. Binenbaum G, Forbes BJ. The eye in child abuse: key points on retinal hemorrhages and abusive head trauma. Pediatr Radiol. 2014;44(Suppl 4):S571–7.
70. Bhatia A, Mirsky DM, Mankad K, Zuccoli G, Panigrahy A, Nischal KK. Neuroimaging of retinal hemorrhage utilizing adjunct orbital susceptibility-weighted imaging. Pediatr Radiol. 2021;51:991–6.
71. Aoulad Fares D, Schalekamp-Timmermans S, Nawrot TS, Steegers-Theunissen RPM. Preconception telomere length as a novel maternal biomarker to assess the risk of spina bifida in the offspring. Birth Defects Res. 2020;112:645–51.
72. Lei Y-P, Zhang T, Li H, Wu B-L, Jin L, Wang H-Y. VANGL2 mutations in human cranial neural-tube defects. N Engl J Med. 2010;362:2232–5.
73. Dhingani DD, Boruah DK, Dutta HK, Gogoi RK. Ultrasonography and magnetic resonance imaging evaluation of pediatric spinal anomalies. J Pediatr Neurosci. 2016;11:206–12.
74. Mehta DV. Magnetic resonance imaging in paediatric spinal dysraphism with comparative usefulness of various magnetic resonance sequences. J Clin Diagn Res. 2017;11:TC17–22.
75. Altman NR, Altman DH. MR imaging of spinal dysraphism. AJNR Am J Neuroradiol. 1987;8:533–8.

Chapter 4
Chiari Type 1 Malformation and Syringomyelia in Children: Classification and Treatment Options

Jehuda Soleman, Jonathan Roth, and Shlomi Constantini

4.1 Introduction

Hans Chiari (1851–1916) was the first to systematically describe Chiari malformation as a pathological ectopy of the cerebellar tonsils below the level of the foramen magnum (FM). He further distinguished four types of malformation dividing them into Chiari malformation types 1–4. Over the last decades, our understanding of these pathologies has grown, while some researches nowadays refer to Chiari type 1 malformation (CIM) as a syndrome (rather than a malformation), while types 2–4 are still defined as malformations, since in contrast to CIM, they are almost exclusively associated with embryonal defects of the neural tube [1]. CIM is defined as tonsillar ectopia of >5 mm. Around 1–3.6% of the children present with CIM; however, in approximately 90% of the cases, it is an incidental finding not requiring any treatment [2–5]. The range of age at diagnosis varies greatly and is estimated on average at 8 years [2]. No gender predilection is seen in CIM; however, girls seem to present more often with symptoms than boys [3].

Syringomyelia (SM) is defined as a cerebrospinal fluid (CSF)-filled cavity larger than 3 mm dissecting the spinal cord [6, 7]. CIM-associated syringomyelia typically involves the cervical and/or upper thoracic portion of the spinal cord, while

J. Soleman
Department of Pediatric Neurosurgery, Tel Aviv Medical Center, Tel Aviv, Israel

Department of Pediatric Neurosurgery, Children's University Hospital of Basel, Basel, Switzerland

Faculty of Medicine, University of Basel, Basel, Switzerland

J. Roth · S. Constantini (✉)
Department of Pediatric Neurosurgery, Tel Aviv Medical Center, Tel Aviv, Israel
e-mail: sconsts@netvision.net.il

C. Di Rocco (ed.), *Advances and Technical Standards in Neurosurgery*, Advances and Technical Standards in Neurosurgery 48,
https://doi.org/10.1007/978-3-031-36785-4_4

elongated forms affecting the entire length of the spinal cord (holocord syringomyelia) may occur [6, 8]. CIM-associated syringomyelia occurs in around 35–75% of CIM patients [6, 9–12].

The prevalence of Chiari malformation is estimated at 7.74:100'000, with an incidence of 3.08:100'000. Syringomyelia prevalence is estimated at 4.84:100'000 and the incidence at 0.82:100'000 [13].

Controversy emerges in every aspect of CIM and syringomyelia, including etiology, indication for treatment, timing of treatment, surgical technique, follow-up regime, and outcome.

4.2 Classification

4.2.1 Chiari Malformation Type I

4.2.1.1 Pathophysiological Classification

The pathophysiology of CIM is not fully understood, while it is described in general as a para-axial mesoderm disorder, where the posterior fossa is underdeveloped and an overcrowding of the hindbrain is apparent [14, 15]. Therefore, tonsillar herniation can be caused either by a congenitally too small posterior fossa, a defect of the skull base, or a malformation of the vertebra, which is known as the congenital CIM (or primary CIM, "true" CIM). On the other hand, any process increasing the size of the cerebellar content (without a congenital anomaly) leading to tonsillar ectopia is referred to as acquired CIM (or secondary CIM, "false" CIM) [14]. While the congenital CIM requires direct management of the posterior fossa and/or its associated structures, the acquired CIM requires management of the underlying condition.

The pathophysiological classification is however still controversially discussed within the literature. Buell classified the mechanisms of CMI into four groups: (1) overcrowding due to underdevelopment of the bony posterior fossa structures, (2) increased cranial pressure due to hemodynamic disturbance, (3) tumor leading to higher volume in the posterior fossa, and (4) downward herniation due to reduced intracranial pressure (e.g., due to lumboperitoneal shunt) [16]. A different classification by Poretti et al. described four groups as well: (1) structural skull base anomalies, (2) abnormal segmentation of cervical vertebral bodies, (3) small cranial vault or posterior fossa causing overcrowding, and (4) increased volume in the posterior fossa or entire cranial vault [17]. Raybaud et al. classified three groups: (1) classical (primary) CIM, including abnormal growth of the posterior fossa or abnormal segmentation of the vertebral bodies; (2) secondary CIM, including macrocerebellum/megalencephaly or basilar impression/platybasia or craniosynostosis; and (3) tonsillar herniation, including idiopathic intracranial hypertension or AVM with venous congestion, intracranial hypotension, and cranial/intracranial lesions [18]. Finally, Fiaschi et al. proposed a classification divided into two categories, summarizing all previous classifications (Table 4.1) [14].

Congenital ("true") CIM is caused by congenital causes of craniocervical junction, congenital overgrowth syndrome, or overcrowding of the posterior fossa. In

Table 4.1 Pathophysiological classification of CIM (adapted from Fiaschi et al.)

Congenital ("true") CIM	(a) Structural anomalies of the skull base and/or abnormal segmentation of the cervical vertebral bodies (b) Congenital overgrowth syndrome (i.e., Beckwith-Wiedemann, Sotos, fragile X, osteopetrosis, fibrous dysplasia) (c) Overcrowding of the posterior fossa caused by a congenital small skull/posterior fossa (i.e., craniostenosis)
Acquired ("false") CIM	(a) Excessive tissue in the posterior fossa or entire skull (b) Craniospinal pressure imbalance (c) Spinal malformation

Table 4.2 Pathologies causing acquired ("false") CIM

Excessive tissue in the posterior fossa	• Posterior fossa cysts
	• Isolated fourth ventricle
	• Tumor of the posterior fossa or supratentorial
	• Cerebellar hemorrhage
	• Cerebellar swelling (e.g., stroke)
	• Hydrocephalus
Craniospinal pressure imbalance	• Idiopathic intracranial hypertension
	• Gorham disease
	• Shunt overdrainage syndrome
	• Spontaneous intracranial hypotension
	• Spinal cerebrospinal fluid leak
Spinal malformations	• Tight filum terminale
	• Any form of tethered cord

50% of CIM patients, a discrepancy between the size of the posterior fossa and its contents is found, often associated with craniocervical anomalies such as Klippel-Feil deformity or atlanto-occipital assimilation [14]. Congenital overgrowth syndrome is a heterogeneous group of rare diseases leading to tissue hyperplasia in the brain (e.g., Beckwith-Wiedemann syndrome, megalencephaly-capillary malformation, polymicrogyria syndrome, Sotos syndrome) [17, 19, 20]. Pathological overgrowth of the calvarium is seen in rare diseases leading to osteoproduction such as osteopetrosis or fibrous dysplasia [21, 22]. CIM is usually apparent, but not exclusively, in syndromic multisuture craniosynostosis (e.g., Crouzon's or Pfeiffer syndrome). It has been also described in single suture craniosynostosis [23, 24]. In the literature, controversy exists whether in cases of craniosynostosis with tonsillar herniation posterior fossa decompression should be undertaken independent of craniosynostosis repair or only if symptoms persist after craniosynostosis surgery [14]. Our practice would be to first treat the craniosynostosis itself, and only if symptoms persist in a radiological persistent CIM would we treat the CIM surgically. Other syndromes that have been described as associated with CIM are neurofibromatosis type I, Noonan syndrome, Goldenhar syndrome, Williams syndrome, and Costello syndrome [14]. Acquired ("false") CIM includes multiple underlying diseases, summarized in Table 4.2.

4.2.1.2 Clinical Classification

In general, a clinical classification for CIM does not exist. Often CIM is classified into incidental and non-incidental CIM. Incidental CIM is defined when a tonsillar ectopia is seen on MRI (with or without syringomyelia), while no clinical symptoms are apparent. Non-incidental CIM is when tonsillar ectopia is seen and clinical symptoms are present. The first attempt to classify CIM in accordance to outcome after surgery was undertaken by Versari et al. in 1993 [25] (Table 4.3). By correlating the preoperative score and the postoperative clinical outcome, four grades were defined. Grades I and II showed significant better postoperative outcome than grades III and IV leading to the conclusion that foramen magnum decompression (FMD) is not recommended for grade IV patients [25]. An additional classification, the Chiari severity score, was described by Greenberg et al. in 2015 [26]. This grading consists of a clinical part, describing the type of headaches presented by the patients or the presence of myelopathic symptoms, and a radiological part, describing the presence

Table 4.3 Proposed score for CIM outcome prediction (adapted from Versari et al.)

Category	Variable	Score
Clinical evolution	0	1
	3–5 years	1
	6–10 years	2
	<10 years	3
Neurological impairment	Symptoms such as headache, cervical and nuchal pain, cervicobrachialgy, dizziness	0
	Impairment of cranial nerves and/or long tract dysfunction	1
	Symptoms such as sensory changes, amyotrophies, chronic pains, and fasciculations	2
Radiological features	Ectopia <5 mm	0
	Ectopia >5 mm	1
	“Small” syrinx	0
	“Extensive” syrinx	1
	Arachnoiditis	1
	Cranio-vertebral junction malformation	1
	Kyphoscoliosis	1
	Hydrocephalus	1
Range of severity		0–11
Grade I		0–2
Grade II		3–5
Grade III		6–8
Grade IV		9–11

Table 4.4 Chiari severity score (adapted from Greenberg et al.)

	Clinical grade		
Neuroimaging grade	1 (poorly localized/ classical CIM headaches)	2 (frontotemporal or no headaches)	3 (myelopathic symptoms
A (no syrinx, syrinx <6 mm)	Grade I	Grade II	
B (syrinx >6 mm)	Grade I	Grade III	

Table 4.5 Radiological classification of Chiari malformation types

Chiari malformation type	Description	Considered malformation
1	Tonsillar ectopia	No
0	Syringomyelia without tonsillar ectopia	No
1.5	Tonsillar ectopia with caudal displacement of the brainstem	No
2	Tonsillar ectopia/displacement of hindbrain structures below the foramen magnum in patients with myelomeningocele	Yes
3	Posterior fossa encephalocele containing brainstem and cerebellar tissue	Yes
4	Hypoplasia or aplasia of the cerebellum	Yes

or size of a syringomyelia (Table 4.4). The score consists of three grades: while grade I showed postoperative improvement in 86%, 69% improvement was seen in grade II, and 45% in grade III [26]. Thakar et al. developed a point-based algorithm to predict outcome after surgery in 2018 [27]. The score consists of the measurement of obex position (OP, in millimeter), the M-line–fourth ventricle vertex distance (M-line-FVV; in millimeters), and the presence of gait instability (score = 162- 10 x gait instability + OP + M-line-FVV), with a score > 128 predicting good clinical outcome [27].

However, based on recent studies, these published algorithms failed to provide prediction value for clinical improvement following CIM surgery [28, 29].

4.2.1.3 Radiological Classification

In his first classification of Chiari malformations, Hans Chiari distinguished four types of malformations, based on pathology specimens (Table 4.5). Some authors distinguish clearly CIM from the other Chiari malformation types, since as opposed to types 2–4, it is not considered to be based on a "true" malformation [1]. CIM is by far the most common type of Chiari malformation, while types 3 and 4 are extremely rare [2]. Due to the radiological advances and further research over the last decades, two additional types of Chiari malformations have been described and are considered subtypes of the classical CIM (Table 4.5) [30–32]. Chiari

malformation type 0 describes patients presenting with syringomyelia but no tonsillar ectopia. In these patients, after FMD and restoration of the CSF flow at the cervicomedullary junction (CVJ), the syringomyelia usually resolves [30]. Chiari malformation type 1.5 is considered to be a severe variant of CIM in which in addition to the tonsillar ectopia a caudal displacement of the brainstem below the FM occurs as well [32]. Finally, CIM is classified as CIM-syrinx complex if an associated syringomyelia is found.

4.2.2 Syringomyelia

4.2.2.1 Pathophysiological Classification

Syringomyelia (SM) describes the accumulation of fluid within the spinal cord caused by a variety of pathogenetic disorders. In CIM-associated SM, the pathophysiology is not fully understood, while over the years three main theories have been proposed [33].

The "communicating" theory introduced by Gardner et al. and followed by Williams et al. and du Boulay et al. claims that due to the narrowing and closed foramina at the level of the FM, the herniating structures create a systolic "water hammer" effect leading to a one-way pump and valve toward the central canal of the spinal cord, whereas CSF accumulates in the central canal creating the SM [33, 34]. While Gardner describes the driving force to be the systolic pressure, Williams believes it to be repetitive Valsalva maneuver (e.g., coughing or sneezing) leading to venous congestion resulting in spinal displacement of CSF [35]. Finally, du Boulay supports Gardner's theory on systolic pulse; however, he claims that two systolic pulse waves, namely, a ventricular one (Gardner's described pulse wave) and a cisternal one, which due to the obstruction at the level of the FM is not pushed into the spinal subarachnoid space but via the fourth ventricle into the central canal [33, 36].

The "transmedullary infiltration theory" evolved once further understanding of the complexity of SM grew, and it was noticed that only a very small percentage of CIM-associated SM shows actual communication between the SM and the fourth ventricle. Ball et al. proved the "water hammer" theory to be inadequate and proposed a theory of their own [37]. They claimed that the SM wall frequently exhibits a great number of small arteries and veins with a hyperplastic adventitia. In patients with FM obstruction, congestion of the epidural venous plexus during Valsalva maneuver leads to a rise in the spinal subarachnoid pressure forcing CSF into the spinal parenchyma via the Virchow-Robin space forming a SM [33, 37]. Oldfield et al. concur with the theory placed by Ball et al., while they claim the driving force is not venous congestion, but rather the systolic congestion of the brain leads to higher pressure that cannot be compensated due to obstruction of the FM, driving CSF into the Virchow-Robin space of the spinal cord [38].

The "parenchymal formation theory" resulted due to studies showing that the pressure within the SM is equal to that in the subarachnoid space, putting the

transmedullary theory into question. Therefore, Klekamp et al. suggest that syrinx forms due to exchange between CSF and the intramedullary extracellular fluid (ECF) [39]. Obstruction of the FM leads to a medullary flow of fluid and causes changes in spinal cord movements. This results in increased CSF flow resistance creating ECF accumulation in the parenchyma or the central canal (edema) and accumulates into a SM [33, 39]. Levine et al. placed a theory based on a disproportion, which is created through the blockage at the level of the FM, between the CSF pressure in the subarachnoid space and the venous system (two hydrostatic systems which are in equilibrium). The blockage at the level of the FM through CIM causes pressure dissociation between the two systems influencing the transmural pressure of the venous system, which is influenced by physical activity. Physical activity causes mechanical stress on the vessels, leading to leakage of blood products into the cord through destruction of the blood-spinal cord barrier, leading to the formation of SM [40]. Koyanagi et al. described posterior spinal veins lacking pial coverage located directly in the subarachnoid space. In CIM the subarachnoid compliance as well as the compliance of the pial veins is reduced. This results in vessel dilatation, impended return of blood to the heart, leading to edema and finally SM within the spinal cord [41].

4.2.2.2 Clinical Classification

In general, SM is classified into CIM-associated SM, accounting for over 70% of SM, and SM caused by other pathologies such as trauma, meningitis, bleeding, arachnoiditis, hydrocephalus, or tumor [33, 42]. Over the years, other classification attempts have been made classifying SM based on the association with other diseases (e.g., CIM, hydrocephalus, scoliosis tethered cord, spinal fistulas, etc.); the assumed pathogenesis (e.g., communicating, non-communicating, atrophic, neoplastic); the SM fluid composition; communication between the SM, the fourth ventricle, and the central canal; or the microanatomical localization of the SM [33, 35, 39, 43–45].

4.2.2.3 Radiological Classification

Radiologically, SM can be classified according to the affected segments: cervical SM, thoracic SM, holocord SM (affecting the whole spinal cord), bulbar SM (syringobulbia, affecting the brainstem), and terminal SM (affecting the lower part of the spinal cord). Recently, Guan et al. defined a novel classification for CIM-associated SM based on high-resolution MRI, dividing the patients into four groups:

Type A: classic communicating (clear communication between fourth ventricle and SM)

Type B: partial communicating (partial communication between fourth ventricle and SM)

Type C: non-communicating (no communication between fourth ventricle and SM)

Type D: atrophic (clear atrophic spinal cord leading to SM) [46]

They were able to show that in types A and B, the SM resolved in a significantly higher percentage after any surgical treatment than for type C and D SM. However, prospective studies are needed to underline these findings and validate this classification.

4.3 Clinical Workup of CIM and SM

4.3.1 Neurological/ENT/Ophthalmology/ Hematological Workup

Pediatric patients presenting with CIM with or without syringomyelia on imaging, even as an incidental finding, should undergo thorough neurological evaluation, ideally by a pediatric neurologist. A thorough neurological examination has shown to be crucial in achieving correct indication for surgery. Typical symptoms of CIM are considered transient suboccipital headache, which are commonly aggravated by the Valsalva maneuver and at times by head dependency, postural changes, and exertion [47]. With the help of an experienced pediatric neurologist, they can be distinguished from migraine-related headaches. Symptoms such as vertigo, nystagmus, and tinnitus can be present due to hindbrain descent; however, they are not specific for CIM. Vocal cord paralysis, hoarseness, palatal weakness, tongue atrophy, cricopharyngeal achalasia, sleep apnea, and nystagmus are due to bulbar and other brainstem dysfunction [48, 49]. They typically occur in CIM patients with associated skull base anomalies [47]. Careful neurological evaluation is also mandatory to rule out comorbidities and assess behavioral or cognitive disorders and their potential association with CIM. Neurophysiological evaluation (MEP, SSEP, AEP) for CIM and syringomyelia should not be used routinely but rather be driven by the presentation of each specific patient.

Workup by an ear-nose-throat specialist is advised at first presentation to rule out lower cranial nerve deficits or breathing disorders suggesting sleep apnea.

In case of ocular movement disorders or suspected intracranial pressure, ophthalmology workup should be sought by a pediatric neuro-ophthalmologist to rule out papillary edema, visual field deficits, or ocular paralysis.

In case of CIM, the typical clinical symptom of SM, namely, progressive dissociated sensory loss, caused by pressure on the spinothalamic pain and temperature pathways, should be ruled out as well. Other symptoms and signs of SM include burning dysesthesia, weakness, initially in the intrinsic hand muscles, spasticity, and autonomic dysfunction [47]. Motor deficits tend to be a late symptom. The most frequent syringobulbia-related symptoms are headache, limb weakness or

dysesthesia, lower cranial nerve dysfunction, gait balance disorders, persistent hiccup, nystagmus, Horner syndrome, and central hypoventilation syndrome [48].

Rarely CIM can be caused by growth hormone or vitamin D deficiency, which should be ruled out, since medical substitute of these can help avoid surgical treatment [50–54]. Although some authors describe a worsening of CIM and SM under growth hormone replacement, a recent large study did not confirm these statements [52, 53].

4.3.2 Radiological Workup

The gold standard imaging for diagnosis is cranial MRI. The tonsillar ectopia is best measured on T2 sequences, while simultaneously associated pathologies (e.g., hydrocephalus) or brain pathologies leading to secondary CIM (e.g., intracranial cysts, intracranial tumors) can be ruled out. Although tonsillar ectopia is often measured on midsagittal planes, some authors claim coronal plane measurements to be more accurate and lead to less overestimation of the degree of ectopia (Fig. 4.1) [55, 56]. In case the diagnosis of CIM is confirmed, whole spinal MRI should be completed as well, to rule out associated pathologies such as syringomyelia, basilar invagination/platybasia, and medullary kinking. In addition, tethered cord with low-lying conus should be ruled out in all patients, since this could affect the treating course of the patient. Further, scoliosis or other spinal deformities and spinal cord tumors can be ruled out as well. In symptomatic patients with signs of instability on MRI or with associated pathologies such as basilar invagination/platybasia, dynamic

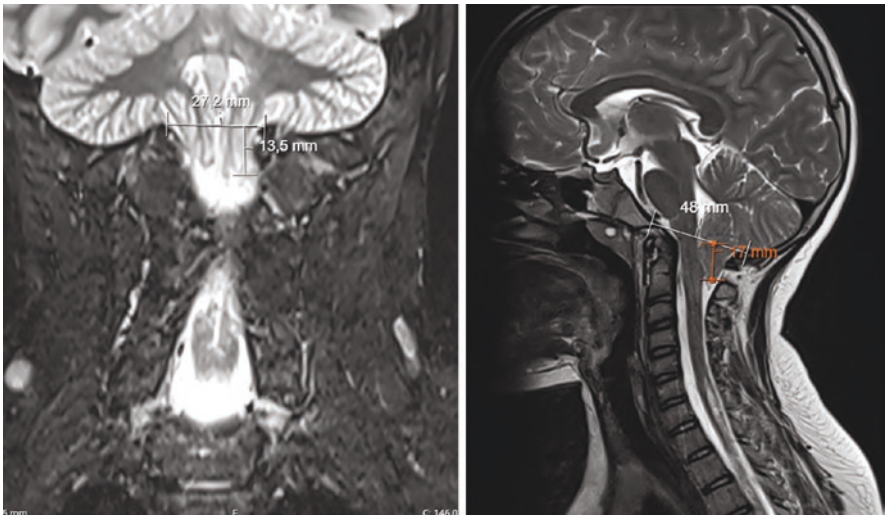

Fig. 4.1 MRI with T2 sagittal and coronal plane demonstrating the measurement of tonsillar ectopia in a Chiari type I malformation patient (13.5 mm on coronal plane, 17 mm on sagittal plane)

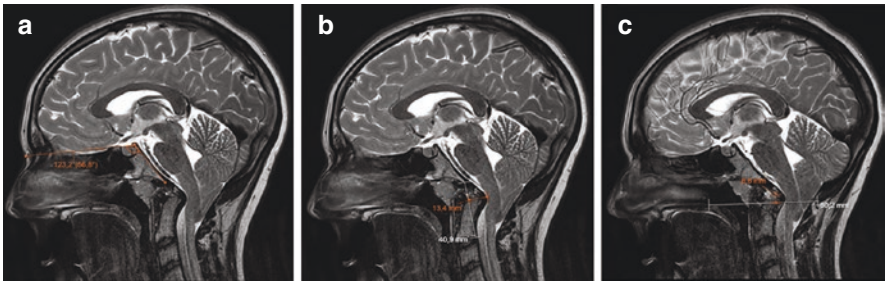

Fig. 4.2 MRI of Chiari type I malformation with basilar invagination, platybasia, and significant ventral brainstem compression with medullary kinking. (**a**) Pathological clivo-axial angle (CXA) of <125° indicating platybasia; (**b**) pB-C2 measurement of >9 mm indicating ventral brainstem compression; (**c**) chamberlain line with displacement of the odontoid of more than 3 mm toward the foramen magnum indicating basilar invagination

X-rays of the craniocervical junction should be considered to rule out instability potentially indicating fusion surgery. Figure 4.2 summarizes important radiological measurements of CIM and associated craniocervical junction (CVJ) anomalies. Further, dynamic studies such as phase contrast cine MRI have been used to assess the degree of obstruction at the craniocervical junction in CIM. Dynamic studies might be helpful in some borderline cases, where a more successful surgical outcome in case of obstructed flow can be predicted, and at times for following CIM patients. However, further studies are warranted before the real value of these studies is clear and becomes a tool which should be used on a routine basis [47].

Similar to CIM, MRI is the gold standard imaging diagnosis for SM, while syrinxes are best shown on T2-weighted images. Contrast-enhanced images in the context of CIM-associated SM are less useful and might be used if an underlying lesion in the spine is suspected [47]. SM appears most commonly at the C4 to C6 level and is more often seen in patients with greater tonsillar herniation and CSF flow obstruction. In case a terminal syrinx, located in the distal spinal cord, is detected, a tethered cord or spinal dysraphism should be excluded [47].

4.3.3 Polysomnography for CIM

Obstructive and central sleep apneas, with and without hypoventilation, have been described as CIM-associated symptoms with a prevalence of 24–70% [57]. Central sleep apnea most likely results from direct medullary compression, which is more common in neonates, typically leading to stridor. On the other hand, lower cranial nerve impairment leads to obstructive pattern causing weak pharyngeal muscles and impairing vocal cord function [57]. In case of suspected sleep apnea, a polysomnography should be undertaken. In children under the age of 6 years some advice to conclude in all patients a routine screening polysomnography, especially if the posterior fossa looks very crowded on MRI [48]. Some authors describe a

correlation between radiological severity and polysomnographic results in CIM patients [58].

4.3.4 Neurocognitive and Behavioral Assessment

In addition to its role in the control of movement, the cerebellum, especially its posterior regions, shows a widespread of cortical connections, influencing cognitive and behavioral processes [59]. Damage to brainstem fiber tracts, with or without cerebellar anomalies, seems to contribute to cognitive impairment as well [60]. Whether CIM patients suffer more frequently from cognitive, behavioral, or even psychiatric disorders remains to date controversial. Therefore, no guidelines exist on neurocognitive, behavioral, or psychiatric evaluation in these children [59, 61]. It seems that screening these patients for neurocognitive, behavioral, or psychiatric symptoms is not necessary; however, once these symptoms are suspected, further assessment should be initiated and treatment tailored accordingly, since some reports show improvement after surgical treatment, mainly in adult patients [62, 63].

4.4 Treatment of Chiari Type I Malformation

4.4.1 Conservative Treatment

4.4.1.1 Wait and Watch/Wait and Scan

It is mainly agreed upon that asymptomatic and mildly symptomatic patients with CIM (incidental CIM) can be managed conservatively but followed until the end of their growth period [48]. It is known that generally these patients follow a benign course and only around 5% will require surgical treatment for clinical (new or progressing symptoms) or radiological reasons (development of syringomyelia or ventriculomegaly) [64]. However, clear guidelines on the frequency of follow-up and if these should be done using routine MRI controls do not exist and remain controversial. Incidental CIM might progress radiologically, or develop syringomyelia over time, even though remaining neurologically silent [65, 66]. For this reason, some authors recommend repeat routine cranial and spine MRI. However, the question remains whether progressive but clinically silent CIM and/or syringomyelia indicates surgical treatment. If not, routine follow-up MRI can be spared since it does not lead to any clinical consequence [67]. The decision of how frequent to follow these patients should be tailored according to the individual patient, while the indication for MRI is best based on the individual neurological presentation at each follow-up.

4.4.1.2 Sports Participation

Studies evaluating the risk of athletes with incidental CIM suffering catastrophic injuries (death, coma, or paralysis) are sparse. Some case reports report on CIM patients deteriorating neurologically or even experiencing sudden death after head or neck trauma during sports activities [68]. However, two larger case series showed that the risk of catastrophic injuries in pediatric patients is minimal and therefore did not recommend any restriction for these patients concerning sports participation [69, 70]. The decision remains a case-by-case decision, since patients with signs of potential instability such as platybasia or basilar invagination were not included in the abovementioned studies, and therefore restrictions for these patients might apply.

4.4.2 Indication for Surgery

In general, surgery for CIM is indicated in patients presenting with typical symptoms (intractable Valsalva maneuver-associated headaches, neurological symptoms attributed to brainstem compression) and/or SM larger than 5–8 mm or progressing over time [48]. The severity of tonsillar ectopia, tonsillar morphology, and CSF flow at the foramen magnum on MRI should not affect the indication for surgical treatment, since none of these factors were shown to be predictive of headache, neurological symptoms, and the need for future surgery or postoperative improvement/resolution [64]. On the other hand, some clinical factors have been proven to predict progression of CIM. Older age at time of diagnosis shows an increased risk of developing headache and significant neurological symptoms [71]. The presence of Valsalva maneuver-associated headaches showed less spontaneous regression at follow-up as opposed to headaches not associated with Valsalva maneuver [72]. Lastly, patients with symptom duration of 2 years or less showed better outcomes after surgical treatment [73]. Overall, when carefully selected, surgically managed patients show high rates of clinical (75%) and radiological (87.5%) improvement [4].

4.4.3 Surgical Treatment Options

The surgical treatment for children with CIM remains controversial and challenging in every aspect. The lack of treatment guidelines is due to various reasons [74]. Clinical presentation is highly variable and very subjective, making the selection of ideal surgical candidates very difficult. The etiology and pathogenesis are still a matter of debate and subject to evolvement and change, which influences the evolvement of surgical techniques. Further, the underlying etiology is often influenced by coexisting pathologies (hydrocephalus, migraines, genetic disorders, etc.). The natural history and predictive factors of neurological progression remain uncertain.

The analyses of the efficacy of surgical techniques and their outcome are still not assessed within large, prospective, comparative, high-quality studies. To date, the surgical approach is not tailored specifically for each individual patient, since we are still not able to truly appreciate the underlying cause of tonsillar ectopia based on MRI.

4.4.3.1 Foramen Magnum Decompression

Forman magnum decompression (FMD) with C1 laminectomy still remains the preferred surgical method to treat CIM. However, the type of FMD surgery varies widely and remains controversial. No consensus exists concerning the ideal type of FMD surgery, with many different procedures described within the literature: extradural FMD (eFMD), eFMD with arachnoid scarring/outer leaf durotomy, intradural FMD (iFMD) with duraplasty alone, iFMD with opening of the arachnoid, iFMD with tonsillar coagulation, iFMD with tonsillar resection, iFMD with insertion of a fourth ventricular stent, and additional resection of C2 lamina in very low-lying tonsils. Adjacent tools are also discussed controversly such as intraoperative ultrasound to help tailor the approach (eFMD or iFMD) intraoperatively or usage of intraoperative neuromonitoring to enhance safety during positioning of the patient [74, 75].

For CIM patients, due to the heterogeneity in the underlying pathophysiology/etiology, the concept of a one-size-fits-all surgical treatment is probably not suitable. The approach is best tailored based on the assumed and probable cause for tonsillar herniation [74]. Patients with assumed small posterior fossa (often younger patients) are best treated with eFMD with or without dural scarring or removal of the outer dura leaf. Multiple studies show the benefit of eFMD in children with significant lower complication (12.5% vs. 57.1%) and revision surgery (0–0.7% in eFMD and 2–19% in iFMD) rates and similar neurological (eFMD improvement in 47–100%, iFMD improvement in 64–100%) and radiological outcome as iFMD, while the risk of repeat surgery seems higher in eFMD (2–19%) than after iFMD (0–0.7%) [48, 64, 74, 76, 77]. In case of CIM with associated SM, some reports show no benefit of iFMD over eFMD, while others show higher rates of SM resolution after iFMD [48, 64, 74, 78]. Further, iFMD showed shorter surgical time and length of hospital stay [64, 74]. Some authors argue that for each child presenting with CIM, iFMD should be concluded since arachnoid veils or scarring was found during approximately 8% of FMDs [73, 74]. In patients where arachnoid scarring (arachnoiditis) is presumed, or in patients with failed eFMD, iFMD with opening of arachnoid veils should be concluded, while some authors recommend the placement of a fourth ventricular stent [74]. In case of suspected craniocervical junction instability, a C1–C2 fixation should be discussed and offered as stand-alone treatment or adjacent to FMD surgery (see more details below) [79].

Controversies exist in the surgical technique of iFMD as well. While some advocate opening of the dura without arachnoidotomy to refrain from postoperative scarring [80, 81], others recommend durotomy with tonsillar manipulation, either

coagulation and shrinkage of the tonsils or tonsil resection [73, 82, 83]. When preforming iFMD, duraplasty is advised, while controversies regarding the technique and the material for performing the duraplasty exist as well. A recent study showed no advantage of autologous dura over non-autologous dura and of adding glue to the sutures concerning clinical and radiological outcome [84, 85], while another recent study showed that autologous graft led to lower rates of pseudomeningocele and complication rates, with similar clinical and radiological outcomes [86]. Note that these studies included adult as well as pediatric patients and might therefore not be representative for the pediatric population.

Intraoperative monitoring (IOM) for FMD is controversially discussed in the literature. Some show a benefit in outcome and safety and recommend its routine usage, while others show no benefit in outcome and morbidity, even if changes are seen on IOM intraoperatively [87–90].

In children overall, there is an increasing trend that if no holocord SM is apparent, eFMD approach is chosen as the first-line treatment, since in the majority of pediatric patients (>80% of the cases), this treatment leads to good clinical outcome and reduces complication rates significantly. Early treatment in symptomatic pediatric CIM patients is sought, since the outcome seems better when early surgery is undertaken [74]. If symptoms do not resolve after eFMD, iFMD should be undertaken. This of course needs to be discussed thoroughly with the patient and/or the parents as part of the informed consent prior to surgical treatment. Note that concerning radiological outcome, especially if SM is apparent, the decision of failed surgery should be made with great caution, since the radiological improvement often presents at a later stage than clinical improvement [11]. Clearly, further large, prospective, and randomized trials assessing the value of eFMD compared to iFMD are urgently needed.

4.4.3.2 Atlantoaxial Fixation

Most authors agree that atlantoaxial fixation (AAF) is indicated only in patients with “complex” CIM usually including CVJ anomalies such as basilar invagination, craniocervical instability, or brainstem compression [91–93]. Risk factors for the need of AAF either as adjunct to FMD or in a late fashion include basilar invagination, CIM 1.5, and clivo-axial angle (CXA) <125° [91]. However, Goel et al. have been advocating for decades that CIM is a neuronal alteration of the body due to atlantoaxial instability and therefore the surgery of choice should be upfront AAF for any kind of CIM [79, 94–96]. AAF includes the insertion of monoaxial screws directly into the facet of the atlas and via the pars/pedicle into the facet of axis. In addition, bone graft is placed in the midline over the bone of the arch of the atlas and lamina of the axis. Soft neck collar is placed for 3 months after surgery. With this technique, they describe over the years a patient satisfaction rate of over 95% in CIM patients with or without SM [79]. Vertebral artery injury is described in 1.8% of the cases, while 0.25% died (one patient) due to injury of the vertebral artery and ischemia. Postoperative neuropathic pain and lower cranial nerve weakness occurred

in 0.25% each [79]. Other authors validated the results of AAF in CIM patients, while the results were controversial, as some found similar results to Goel's, while others describe no advantage of AAF over FMD [97, 98].

4.5 Treatment Options of Chiari Type I Malformation-Associated Syringomyelia

4.5.1 Conservative Treatment

4.5.1.1 Wait and Watch/Wait and Scan

The decision-making of when to treat asymptomatic patients with CIM-associated SM is less clear than with CIM only. A survey undertaken in 2018 revealed that 70% of neurosurgeons would treat patient with a CIM-associated SM of 2 mm or less conservatively, while in a SM size of 8 mm, only 20% would not indicate surgery [99]. Since in most reports assessing the natural history of incidental CIM, patients with SM are excluded, the natural history in CIM-associated SM patients remains ambiguous. Similarly, reports on the natural history of CIM-associated SM in adults are rare, while Nishizawa et al. reported two decades ago that in adult patients long-term clinical courses of incidental CIM-associated SM are benign. In addition, they found that recommendation for interventional surgery could not be predicted by MRI parameters [100]. Spontaneous regression of incidental CIM-associated SM has been described as well. Therefore, a wait and watch regimen as a first-step treatment might be justified in incidentally detected CIM-associated SM patients. However, once progression or new neurological sequel is apparent, surgical treatment should be discussed with the patients/parents. Naturally, clear guidelines for the follow-up regimen of these patients do not exist. Further studies on the natural history of incidental CIM-associated SM and follow-up guidelines are urgently needed.

4.5.1.2 Sports Participation

Studies evaluating the risk of incidental CIM-associated syrinx suffering catastrophic injuries (death, coma, or paralysis) are sparse. Wan et al. assessed a series of 85 incidental CIM patients, of which 54 had an associated SM [101]. The incidence for presenting with new symptoms after head or neck injury for those patients with incidental CIM was 3.2% and 3.7% for those with incidental CIM-associated SM [68, 101]. Based on these limited reports, it seems that no restriction for these patients concerning sports participation should be recommended; however, decision-making should be done on a case-by-case basis, with rigorous informed consent, concerning the limited data available.

4.5.2 Surgical Treatment Options

The gold standard treatment of symptomatic CIM associated with SM is FMD with or without duraplasty, with the goal of treating both the CIM and SM. Some authors recommend primary atlantoaxial fusion or direct syrinx shunting alone or in combination with FMD [9, 11]. As mentioned above, some reports show no benefit of iFMD over eFMD when it comes to the resolution of SM, while others show higher rates of SM resolution after iFMD [48, 64, 74, 78, 102]. Studies on the natural history of CIM-associated SM after primary treatment (mostly FMD) are sparse [12, 103–105]. However, it has been shown that SM can persist, progress, recur, or newly appear as an expression of failed FMD, in 30–50% of cases, potentially requiring further treatment [9, 11]. The median time of SM regression of >50% was described at 8 months; therefore, sufficient follow-up is indicated before declaring the primary treatment as a failure [106]. Even in cases with persistent or worsened SM after FMD, as long as the patients are asymptomatic, one should not rush to declare failure of FMD, since spontaneous regression of the SM over time has been described in some reports [107]. The treatment options for failed FMD remain controversial and include clinical and radiological follow-up, redo-FMD, SM or CSF shunting procedures, terminal ventriculostomy, or atlantoaxial fusion [9, 11, 93, 105]. The question, which surgical treatment should be preferred after failed treatment, remains unanswered with multiple reports in favor of one or the other surgical technique. As in the primary treatment of CIM-associated SM, a one-size-fits-all approach is most probably not sufficient; therefore, the surgical technique needs to be matched to the suspected underlying pathophysiology leading to the failure of the initial treatment (e.g., instability, arachnoid scarring, hydrocephalus, etc.).

Notice that in cases of failed FMD with persisting, progressing, recurring, or newly appearing SM, similar to when the initial diagnosis is made, underlying causes other than CIM have to be taken into account and excluded. Especially in hydrocephalus, which has been described as a phenomenon appearing after FMD, a ventriculoperitoneal shunt (VPS) or endoscopic third ventriculostomy (ETV) should be done rather than a redo-FMD or SM shunting, since it has been shown to improve the SM in a vast majority of the cases [9, 11, 108].

4.5.2.1 Syrinx Shunting Procedures

To date, three SM shunting procedures have been described in the literature, namely, syringosubarachnoid shunt (SSS), syringopleural shunt (SPS), and syringoperitoneal shunt (SPRS) [10, 109–111]. The techniques consist of a one- to two-level laminectomy/laminoplasty, midline durotomy, and dorsal midline myelotomy or myelotomy at the dorsal root entry zone (DREZ) followed by drainage of the SM cavity and insertion of the drain into the SM cavity on one end and into the subarachnoid space (for SSS), the pleural space (SPS), or the peritoneal cavity (SPRS) on the other end [9, 10]. Overall, the majority of the studies analyzing these

procedures show good results in the short-term follow-up, while long-term follow-up results are greatly missing [11, 12, 103–105, 112–122]. Large homogenous cohorts analyzing specifically CMI patients undergoing SM shunt procedures are sparse. However, overall, mortality and permanent morbidity rates seem to be low independent of the surgical technique [12, 109, 111, 112, 121]. Studies directly comparing the different shunt techniques in CIM patients do not exist, and therefore the technique of choice should be the technique in which the treating pediatric neurosurgeon is mostly familiar with. SSS represents the technique mostly described in the literature, showing, in experienced hands, very good clinical and radiological outcome, and has the advantage that it does not involve a procedure in an additional cavity [9].

4.5.2.2 Redo-FMD

Some authors claim redo-FMD to be the first-line strategy after failed FMD, while none emphasized the technical aspects or the clinical and radiological outcomes of redo-FMD surgery [39, 103–105, 113, 123]. In patients with failed eFMD, an approach of redo using iFMD might be reasonable, although in some series the majority of patients with failed FMD initially underwent iFMD, underlying the theory that FMD may fail irrespective of the technique [9, 11, 124, 125]. As mentioned above, cine flow MRI is discussed controversially in the literature for the assessment of CSF obstruction in CIM after FMD and might at times be helpful to tailor the chosen procedure in failed FMD cases [126–128]. Since no high-quality studies exist, providing us with robust data, to date, redo-FMD does not seem to be superior to shunting procedures and vice versa. Therefore, as mentioned before, the chosen surgical approach is mainly based on the surgeon's preference and experience, as well as the suspected underlying pathophysiology leading to the FMD failure.

4.5.2.3 Other Techniques

Terminal ventriculostomy (sectioning of the filum terminale), fourth ventricular shunting, and atlantoaxial fixation have been described as further possible procedures in case of failed FMD. Terminal ventriculostomy, despite its theoretical appeal, is seldom described in the literature. Gardner et al. first proposed terminal ventriculostomy for the treatment of caudally located syringomyelia in 1977 [129]. Over the following years, some reports described the outcome of terminal ventriculostomy in CIM-associated SM [130–133]. However, this procedure is mostly reserved for patients with radiographic evidence of SM extending into the filum terminale and is not considered a first-line therapy of CIM-associated SM but may be a useful adjuvant therapy in SM refractory to standard treatment [133].

AAF is considered by some authors as the primary treatment of CIM and CIM-associated SM, while others refer to it as a second-tier treatment [93]. For

second-tier treatment, most reports describe the outcome in adult patients and only few in pediatric patients. It seems that in case of platybasia, basilar invagination, or clear instability, this technique should be discussed for failed FMD [134–136]. The available data in children is very sparse; therefore, the role and indication of these procedures after failed FMD remain unclear.

Reports exist on the benefit of the placement of fourth ventricular stents into the cervical subarachnoid space in patients with CIM-associated SM refractory to other procedures [137]. This treatment is not recommended as adjacent to FMD or as first-tier therapy of CIM-associated SM; however, for failed FMD, it can be considered. Even when fixing the catheter to the subarachnoid space, catheter migrations have been reported in the literature [137]. Still, this technique can be considered in challenging SM cases refractory to other treatments.

4.6 Chiari Type I Malformation and Syringomyelia-Associated Anomalies and Their Treatment

4.6.1 Tethered Cord

Tethered cord syndrome (TCS), in form of a low-lying conus with fatty or thickened filum terminale, has been described as a potentially associated disease with CIM (Fig. 4.3). Some authors suggest that TCS causes traction of the spinal cord leading to CMI herniation, and therefore release of the fatty or thickened filum [138] will lead to improvement of the tonsillar ectopia and occurring symptoms [139]. Others claim that associated cases of CIM and TCS are rather genetic, and not mechanical, since in their series no clear improvement of tonsillar ectopia was seen [140]. Occult

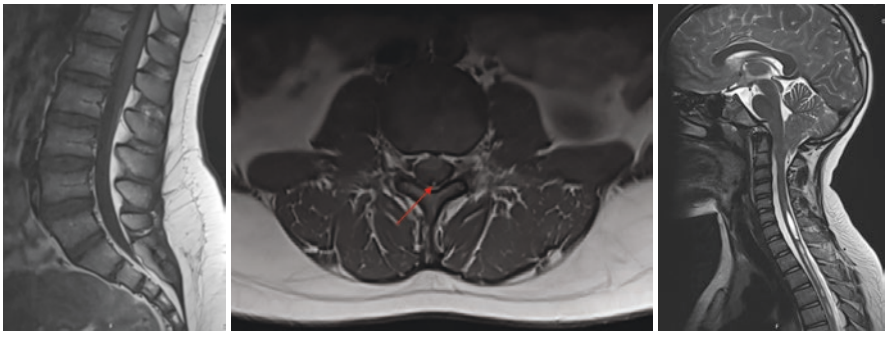

Fig. 4.3 MRI of 10-year-old Chiari type I malformation patient showing on sagittal T2 brain MRI (right image) tonsillar ectopia and cervico-thoracal syringomyelia. Simultaneously on sagittal (left image) and axial (middle image) T1 "fat sat" lumbar MRI signs of tethered cord syndrome with a low-lying conus and fatty filum (red arrow) at the level of L2/L3

tethered cord (without low-lying conus and/or fatty or thickened filum) is discussed as a potential cause of CIM. However, there is no scientific support that occult tethered cord leads to CIM, and therefore sectioning of the filum terminale (SFT) is not supported in CIM patients without evidence of TCS [141]. Whether in patients with typical CIM symptoms and incidentally diagnosed TCS one should first treat the CIM in form of FMD or the TCS in form of SFT remains a debate, and further studies are warranted. Note that SFT is a shorter procedure with potentially less complications than FMD (especially iFMD), and therefore in patients with clear TCS, SFT should be considered as the primary treatment, especially if the presenting symptoms are not typical for CIM [142].

4.6.2 Scoliosis

The prevalence of scoliosis (Cobb's angle >10°) among patients with isolated CIM is estimated between 13% and 36% and in patients with CIM with SM between 53% and 85% (Fig. 4.4) [143]. In patients under the age of 6 years CIM was present in 28%, while concomitant SM was found in the vast majority of the cases [143]. Scoliosis is rarely the presenting complaint in CM-I patients. It is usually associated with atypical scoliosis (as opposed to idiopathic scoliosis) features such as left apical or kyphotic curvature, neurological deficits, and early onset of the disease [144]. When scoliosis is suspected on physical examination, imaging studies are necessary. Spinal X-ray is the initial study of choice (Fig. 4.5), while MRI is concluded

Fig. 4.4 T2-weighted sagittal MRI presenting a Chiari type I malformation with concordant hydrocephalus and cervical syringomyelia. The patient presented with Chiari typical symptoms and mild papilledema

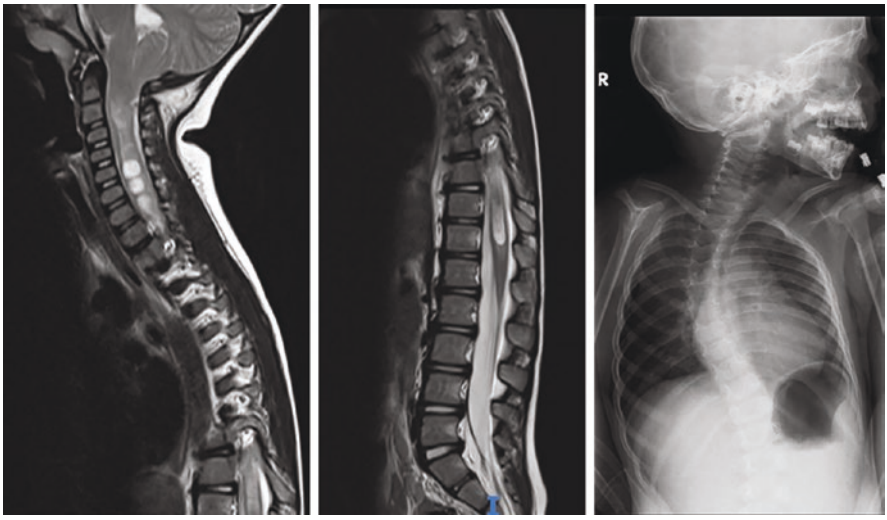

Fig. 4.5 T2-weighted sagittal cervico-thoracic (left image) and lumbar (middle image) MRI presenting a Chiari type I malformation with associated SM. In the anteroposterior X-ray, an associated scoliosis is clearly seen (right image)

as well. It is important to evaluate the disease severity and curve pattern, search for concurrent anomalies, and assess the degree of skeletal maturity. Since patients diagnosed with CIM require MRI of their whole neuro-axis at times, scoliosis may be diagnosed incidentally in these patients. The pathophysiology behind the instigation and progression of scoliosis in CIM patients remains unclear [143]. Some authors claim that the cerebellar tonsillar compression on the dorsal surface of the cervicomedullary junction affects the postural reflex and leads to difficulty in maintaining a proper posture and subsequent scoliosis [145, 146]. Other authors believe that SM is the leading pathology behind scoliosis, since in some cohorts the prevalence of scoliosis was not significantly increased in patients with CIM without SM as opposed to those with CIM-associated SM [147]. Since the SM cyst is often uneven within the spinal cord, an asymmetric dysfunction of the anterior horn cells supplying the paraspinal and deep back muscles may be present. The originating uneven denervation of these muscles leads to a subsequent scoliosis with a convex vertebral curvature on the less innervated side [148]. Patients with incidental mild scoliosis and CIM should be monitored for curve progression. CIM patients with factors such as refractory back pain, atypical curve patterns, Cobb's angle $>30°$, Cobb's angle between 20° and 29° in children aged 12–14 years, $\geq 5°$ progression of Cobb's angle from last examination scoliometer measurements, and $\geq 7°$ and $\geq 5°$ angle of trunk rotation in patients with body mass index $\geq$ 85th percentile are considered at a higher risk for progression/complications and should therefore be referred for discussion of scoliosis treatment either by bracing or fusion [143, 149]. Based on the limited literature available, no evidence exists to recommend

prophylactic FMD previous to correction of the spinal deformity in CIM patients with associated scoliosis; on the contrary, primary posterior spinal fusion might even lead to improvement of the CIM and SM [150, 151]. In addition, there is limited evidence to support FMD to improve scoliosis outcome in the absence of symptoms referable to CIM, although this remains a debate among authors in the literature, while CIM-associated SM seems to be a stronger indicator for scoliosis progression [73, 152–155]. However, whether prophylactic surgery of the SM within the context of scoliosis should be undertaken remains unclear [156].

4.6.3 Hydrocephalus

The association between CIM and hydrocephalus (HCP) is a well-known and described phenomenon [157]. In about 7–10% of the patients presenting with CIM, an associated HCP is apparent [157]. At times these patients present with a SM due to the CIM and/or HCP. The exact pathogenesis of HCP associated with CIM remains somewhat ambiguous, and therefore there still are controversies on how to treat these patients, while the treatment is tailored depending on the assumed pathogenesis. One hypothesis is the "pressure from above hypothesis," where it is assumed that the pressure caused by the HCP leads to a transient and reversible tonsillar caudal ectopia and at times aggravates an existing minor and asymptomatic CIM. In these cases, the preferred treatment would be to treat the HCP through ETV or placing a VPS [158–160]. Another hypothesis is the "blockage hypothesis," where the HCP appears secondarily due to the occlusion of the basal CSF pathways caused by the CIM, leading to an obstructive HCP [157]. In these cases, treatment of the blockage caused by the CIM at the level of the foramen magnum through a FMD would be the treatment of choice [157]. Due to these uncertainties, the debate which pathology, the CIM or the HCP, should be addressed first is still vivid. Hydrocephalus occurring after CIM treatment has been described in 5–7% of the cases and can occur also late after surgery (described up to 8 months) [108]. The pathophysiology of this phenomenon remains unclear, while CSF shunting seems to be the best treatment. In selected cases, temporary CSF drainage or acetazolamide as well as ETV can be successful [108].

4.6.4 Basilar Invagination

Basilar invagination (BI) is an occipito-cervical malformation characterized by odontoid displacement toward the foramen magnum and is generally a congenital pathology [161]. BI is defined as an odontoid breaching the chamberlain line more than 3 mm on sagittal MRI and/or CT imaging (Fig. 4.2) [162]. As opposed to BI, "basilar impression" refers to a secondarily acquired protrusion of the odontoid due to softening of the skull, while "cranial settling" occurs only within the context of

rheumatoid arthritis [163]. Platybasia is defined as flattening of the skull base determined by a clivo-axial angle (CXA) of under 125° (Fig. 4.2). Platybasia is often associated with BI and causes symptoms in general when basilar invagination is apparent. BI is associated with CIM in around 13% of the cases [164, 165]. BI is considered to be associated with atlantoaxial instability, while the definition of such remains controversial [163]. Most consider posterior displacements of the atlas over the axis and anterior displacements by more than 5 mm unstable and probably in need of surgical treatment. However, displacement of less than 5 mm or rotatory facetal subluxation is considered stable and should be treated conservatively, while surgery is reserved for selected cases only [163]. Goel et al. claim CIM to be generally unstable, independent of radiological features and associated craniocervical anomalies, such as BI; however, this theory remains controversial within the literature [94, 163]. Clinical manifestations of BI are rather unspecific and typically include all symptoms occurring in CIM. The treatment of BI associated with CIM remains controversial. However, it is fairly agreed upon that in asymptomatic cases follow-up is warranted. Further, in cases of CIM with BI without radiological evidence of atlantoaxial instability, FMD is the treatment of choice, while in case of instability craniocervical or atlantoaxial fixation is necessary with or without FMD (depending whether typical CIM symptoms are present) [161, 165]. In patients with an odontoid significantly compressing against the brainstem (pB-C2 line of more than 9 mm, Fig. 4.2) and bulbar symptoms, even without instability, transoral or transnasal (anterior) approach for odontoid removal is recommended [161].

4.7 Outcome

4.7.1 Morbidity and Mortality

The morbidity rates after the treatment of CIM or SM patients are not well described within the literature but seem to be rather low in most described reports. This is probably due to the fact that multiple variables, such as patient characteristics, radiological factors, operative technique applied, etc., have a significant effect on morbidity. Depending on the surgical procedure and on the CIM or SM severity, different complications occur. FMD has an estimated morbidity range of 1–3% with a large variety of potential complications, among others, failure of treatment with persisting symptoms and/or persisting or progressing SM, new onset of hydrocephalus, pseudomeningocele, CSF leaks, CSF infections, stroke, hemorrhage, anesthesia-related complications, and neurological sequel including breathing and swallowing disorders [166]. Pain is an often morbidity after FMD which should be managed in cooperation with an experienced neuro-anesthesiology team, while standardized pain management protocols (such as scheduled nonsteroidal anti-inflammatory drugs alternating with scheduled acetaminophen and diazepam) seem to reduce pain and reduce the need for opioids [167]. After spinal instrumentation

procedures (e.g., AAF), neurological sequel, including bulbar symptoms, screw dislocation or misplacement, superficial infections, CSF infections, and superficial or deep hematomas, as well as pain, may occur, but the rate of complications seems rather low [79, 98]. For SM shunt procedures apart from superficial or deep infections, complications such as hematoma, dissociative neurological symptoms, hypo- or dysesthesia, shunt migration or shunt malfunctions, and kyphosis can occur. The rate of complications varies within the literature but is overall low, lying within 5% in experienced hands [12, 104, 112]. The mortality rate of CIM patient with or without SM after surgery is under 1%, independent of the surgical technique applied.

4.7.2 Measurement of Outcome in CIM Patients

Some clinical outcome reporting systems for CIM exist, while no uniform outcome reporting system is used consecutively in studies evaluating CIM patients. This leads to heterogeneous reporting of outcome in CIM, making a comparison between the studies cumbersome. The Chicago Chiari Outcome Scale (CCOS) is a validated outcome reporting system, intended to provide an objective evaluation of outcomes for patients with CIM (Table 4.6) [26, 29, 168–170]. The Chiari Health Index for Pediatrics (CHIP) is an additional outcome reporting system for CIM patients described in the literature [171]. It includes a physical (pain frequency, pain severity, non-pain symptoms) and psychosocial domain, while the scores of these domains are combined to create an overall health-related quality-of-life (HRQOL) score [171]. A validation study has shown the effectiveness of CHIP to assess HRQOL and its usefulness in a clinical setting [172]. Others have implemented a validated patient-reported outcome information system (PROMIS), showing the importance of measuring subjective outcome among CIM patients [63, 173–175]. Generally, the number of reports on HRQOL and PROMIS in CIM patients is very scarce, while over the last years some authors highlight the importance of such

Table 4.6 The Chicago Chiari Outcome Scale (CCOS), adapted from Aliaga et al. Scores between 13 and 16 indicated improvement; scores between 9 and 12 indicated unchanged situation; scores between 4 and 8 indicated worsening

Pain	Non-pain	Functionality	Complications	Total score
1 – worse	1 – worse	1 – unable to attend	1 – persistent complication, poorly controlled	4 – incapacitated outcome
2 – unchanged and refractory to medication	2 – unchanged and refractory to medication	2 – moderate impairment (<50% attendance)	2 – persistent complication, well controlled	8 – impaired outcome
3 – improved or controlled with medication	3 – improved and unimpaired	3 – moderate impairment (>50% attendance)	2 – transient complication	12 – functional outcome
4 – resolved	4 – resolved	4 – fully functional	4 – uncomplicated course	16 – excellent outcome

measurement tools in addition to other clinical outcome measurement tools like the CCOS or CHIP. Radiological outcome measurements and potential radiological findings suggesting worst outcome mostly show controversial results making the validation of these factors difficult [46, 176–178]. For SM the Modified Japanese Orthopedic Association Scale (mJOAS) is often used for outcome measurement [12]. In the future, studies should implement standardized and validated clinical outcome measurement tools (e.g., CCOS) combined with standardized and validated PROMS assessing the subjective HRQOL of CIM patients, so that generality and comparison between the different studies will be possible. Especially (neuro-) psychological studies should be undertaken before and after surgical treatment, so the effect of these treatments on the (neuro-)psychological effect of HRQOL can be assessed and compared [62, 63, 179]. Only through standardized objective and subjective measurement of clinical and radiological outcome the treatment of CIM can be assessed and improved in an objective manner.

4.8 Conclusion

CIM is a rather frequent diagnosis in the pediatric age; however, in the vast majority, it represents an incidental finding not in need of surgical treatment. CIM-associated SM occurs in around half of all CIM patients, while the degree of SM is diverse and usually affects the clinical course of these patients. The pathophysiology of CIM and SM is still a matter of debate; therefore, the ideal treatment remains controversial. The gold standard treatment of CIM, to date, is FMD, with some authors advocating upfront AAF. EFMD as a first-step treatment in children is gaining more and more support within the literature, since surgical morbidity rates are lower than for iFMD. However, in around 20% of the patients, repeat surgery will be needed, a fact that needs to be discussed thoroughly with the family of the child. It seems that a one-size-fits-all surgical treatment for CIM patients does not apply, due to the heterogeneity of the disease itself and the underlying pathophysiology which differs from patient to patient. Due to the variety of the underlying pathophysiology in "idiopathic" CIM, and taking into account the variation of CIM-associated diseases, such as genetic diseases, connective tissue diseases, craniosynostosis, basilar invagination, atlantoaxial instability, tethered cord, scoliosis, and hydrocephalus, future treatment and research should be moving toward utilizing individual management plans taking these factors into account. Similarly, in CIM-associated SM, the ideal surgical treatment remains a matter of debate, while the primary treatment usually offered is FMD; however, once the SM persists, redo-FMD, SM shunting, or AAF are discussed as valid options within the literature. In general, pediatric CIM are best treated in a multidisciplinary setting including specialized pediatric neurosurgeons, pediatric neurologists, pediatric spine surgeons, pediatric geneticists, and pediatric anesthesiologists. Outcome measurements based on objective clinical, (neuro-) psychological, and radiological outcome combined with subjective HRQOL measurements based on PROMs are vital and should be concluded based

on standardized and validated test batteries in a standardized fashion throughout large, multicenter, prospective, clinical study so that we can better understand and improve our treatment for these patients.

References

1. Frič R, Eide PK. Chiari type 1-a malformation or a syndrome? A critical review. Acta Neurochir (Wien). 2020;162(7):1513–25. https://doi.org/10.1007/s00701-019-04100-2.
2. Albert GW. Chiari malformation in children. Pediatr Clin North Am. 2021;68(4):783–92. https://doi.org/10.1016/j.pcl.2021.04.015.
3. Tubbs RS, Oakes WJ, editors. The chiari malformations. New York: Springer; 2013. https://doi.org/10.1007/978-1-4614-6369-6.
4. Pomeraniec IJ, Ksendzovsky A, Awad AJ, Fezeu F, Jane JA Jr. Natural and surgical history of Chiari malformation Type I in the pediatric population. J Neurosurg Pediatr. 2016;17(3):343–52. https://doi.org/10.3171/2015.7.PEDS1594.
5. Novegno F, Caldarelli M, Massa A, et al. The natural history of the Chiari type I anomaly. J Neurosurg Pediatr. 2008;2(3):179–87. https://doi.org/10.3171/PED/2008/2/9/179.
6. Hiremath SB, Fitsiori A, Boto J, et al. The perplexity surrounding Chiari malformations - are we any wiser now? AJNR Am J Neuroradiol. 2020;41(11):1975–81. https://doi.org/10.3174/ajnr.A6743.
7. Petit-Lacour MC, Lasjaunias P, Iffenecker C, et al. Visibility of the central canal on MRI. Neuroradiology. 2000;42(10):756–61. https://doi.org/10.1007/s002340000373.
8. Menezes AH. Chiari I malformations and hydromyelia--complications. Pediatr Neurosurg. 1991;17(3):146–54. https://doi.org/10.1159/000120586.
9. Soleman J, Roth J, Constantini S. Direct syrinx drainage in patients with Chiari I malformation. Childs Nerv Syst. 2019;35(10):1863–8. https://doi.org/10.1007/s00381-019-04228-7.
10. Soleman J, Roth J, Constantini S. Syringo-subarachnoid shunt: how I do it. Acta Neurochir (Wien). 2019;161(2):367–70. https://doi.org/10.1007/s00701-019-03810-x.
11. Soleman J, Bartoli A, Korn A, Constantini S, Roth J. Treatment failure of syringomyelia associated with Chiari I malformation following foramen magnum decompression: how should we proceed? Neurosurg Rev. 2019;42(3):705–14. https://doi.org/10.1007/s10143-018-01066-0.
12. Soleman J, Roth J, Bartoli A, Rosenthal D, Korn A, Constantini S. Syringo-subarachnoid shunt for the treatment of persistent syringomyelia following decompression for Chiari type I malformation: surgical results. World Neurosurg. 2017;108:836–43. https://doi.org/10.1016/j.wneu.2017.08.002.
13. Ciaramitaro P, Massimi L, Bertuccio A, et al. Diagnosis and treatment of Chiari malformation and syringomyelia in adults: international consensus document. Neurol Sci. 2022;43(2):1327–42. https://doi.org/10.1007/s10072-021-05347-3.
14. Fiaschi P, Morana G, Anania P, et al. Tonsillar herniation spectrum: more than just Chiari I. Update and controversies on classification and management. Neurosurg Rev. 2020;43(6):1473–92. https://doi.org/10.1007/s10143-019-01198-x.
15. Elster AD, Chen MY. Chiari I malformations: clinical and radiologic reappraisal. Radiology. 1992;183(2):347–53. https://doi.org/10.1148/radiology.183.2.1561334.
16. Buell TJ, Heiss JD, Oldfield EH. Pathogenesis and cerebrospinal fluid hydrodynamics of the Chiari I malformation. Neurosurg Clin N Am. 2015;26(4):495–9. https://doi.org/10.1016/j.nec.2015.06.003.
17. Poretti A, Ashmawy R, Garzon-Muvdi T, Jallo GI, Huisman TAGM, Raybaud C. Chiari type 1 deformity in children: pathogenetic, clinical, neuroimaging, and management aspects. Neuropediatrics. 2016;47(5):293–307. https://doi.org/10.1055/s-0036-1584563.

18. Raybaud C, Jallo GI. Chiari 1 deformity in children: etiopathogenesis and radiologic diagnosis. Handb Clin Neurol. 2018;155:25–48. https://doi.org/10.1016/B978-0-444-64189-2.00002-0.
19. Tubbs RS, Oakes WJ. Beckwith—Wiedemann syndrome in a child with Chiari I malformation: Case report. J Neurosurg Pediatr. 2005;103(2):172–4. https://doi.org/10.3171/ped.2005.103.2.0172.
20. Garavelli L, Leask K, Zanacca C, et al. MRI and neurological findings in macrocephaly-cutis marmorata telangiectatica congenita syndrome: report of ten cases and review of the literature. Genet Couns. 2005;16(2):117–28.
21. Urgun K, Yılmaz B, Toktaş ZO, et al. Craniospinal polyostotic fibrous dysplasia, aneurysmal bone cysts, and Chiari type 1 malformation coexistence in a patient with McCune-Albright syndrome. Pediatr Neurosurg. 2016;51(5):253–6. https://doi.org/10.1159/000444937.
22. Dlouhy BJ, Menezes AH. Osteopetrosis with Chiari I malformation: presentation and surgical management. J Neurosurg Pediatr. 2011;7(4):369–74. https://doi.org/10.3171/2011.1.PEDS10353.
23. Tubbs RS, Elton S, Blount JP, Oakes WJ. Preliminary observations on the association between simple metopic ridging in children without trigonocephaly and the Chiari I malformation. Pediatr Neurosurg. 2001;35(3):136–9. https://doi.org/10.1159/000050407.
24. Leikola J, Koljonen V, Valanne L, Hukki J. The incidence of Chiari malformation in nonsyndromic, single suture craniosynostosis. Childs Nerv Syst. 2010;26(6):771–4. https://doi.org/10.1007/s00381-009-1044-y.
25. Versari PP, D'Aliberti G, Talamonti G, Collice M. Foraminal syringomyelia: suggestion for a grading system. Acta Neurochir (Wien). 1993;125(1-4):97–104. https://doi.org/10.1007/BF01401835.
26. Greenberg JK, Yarbrough CK, Radmanesh A, et al. The Chiari severity index: a preoperative grading system for Chiari malformation type 1. Neurosurgery. 2015;76(3):279–85. https://doi.org/10.1227/NEU.0000000000000608.
27. Thakar S, Sivaraju L, Jacob KS, et al. A points-based algorithm for prognosticating clinical outcome of Chiari malformation Type I with syringomyelia: results from a predictive model analysis of 82 surgically managed adult patients. J Neurosurg Spine. 2018;28(1):23–32. https://doi.org/10.3171/2017.5.SPINE17264.
28. Feghali J, Xie Y, Chen Y, Li S, Huang J. External validation of current prediction systems of improvement after decompression surgery in Chiari malformation type I patients: can we do better? J Neurosurg. 2020;134(5):1466–71. https://doi.org/10.3171/2020.2.JNS20181.
29. Ahluwalia R, Foster J, Brooks E, et al. Chiari type I malformation: role of the Chiari severity index and Chicago Chiari outcome scale. J Neurosurg Pediatr. 2020;26(3):262–8. https://doi.org/10.3171/2020.2.PEDS19770.
30. Chern JJ, Gordon AJ, Mortazavi MM, Tubbs RS, Oakes WJ. Pediatric Chiari malformation Type 0: a 12-year institutional experience: Clinical article. J Neurosurg Pediatr. 2011;8(1):1–5. https://doi.org/10.3171/2011.4.PEDS10528.
31. Iskandar BJ, Hedlund GL, Grabb PA, Oakes WJ. The resolution of syringohydromyelia without hindbrain herniation after posterior fossa decompression. J Neurosurg. 1998;89(2):212–6. https://doi.org/10.3171/jns.1998.89.2.0212.
32. Tubbs RS, Iskandar BJ, Bartolucci AA, Oakes WJ. A critical analysis of the Chiari 1.5 malformation. J Neurosurg Pediatrics. 2004;101(2):179–83. https://doi.org/10.3171/ped.2004.101.2.0179.
33. Blegvad C, Grotenhuis JA, Juhler M. Syringomyelia: a practical, clinical concept for classification. Acta Neurochir (Wien). 2014;156(11):2127–38. https://doi.org/10.1007/s00701-014-2229-z.
34. Gardner WJ, Angel J. The cause of syringomyelia and its surgical treatment. Cleve Clin Q. 1958;25(1):4–8. https://doi.org/10.3949/ccjm.25.1.4.
35. Williams B. The distending force in the production of "communicating syringomyelia". Lancet. 1969;2(7613):189–93. https://doi.org/10.1016/s0140-6736(69)91427-5.

36. du Boulay G, Shah SH, Currie JC, Logue V. The mechanism of hydromyelia in Chiari type 1 malformations. Br J Radiol. 1974;47(561):579–87. https://doi.org/10.1259/0007-1285-47-561-579.
37. Ball MJ, Dayan AD. Pathogenesis of syringomyelia. Lancet. 1972;2(7781):799–801. https://doi.org/10.1016/s0140-6736(72)92152-6.
38. Oldfield EH, Muraszko K, Shawker TH, Patronas NJ. Pathophysiology of syringomyelia associated with Chiari I malformation of the cerebellar tonsils. Implications for diagnosis and treatment. J Neurosurg. 1994;80(1):3–15. https://doi.org/10.3171/jns.1994.80.1.0003.
39. Klekamp J. The pathophysiology of syringomyelia – historical overview and current concept. Acta Neurochir (Wien). 2002;144(7):649–64. https://doi.org/10.1007/s00701-002-0944-3.
40. Levine DN. The pathogenesis of syringomyelia associated with lesions at the foramen magnum: a critical review of existing theories and proposal of a new hypothesis. J Neurol Sci. 2004;220(1-2):3–21. https://doi.org/10.1016/j.jns.2004.01.014.
41. Koyanagi I, Houkin K. Pathogenesis of syringomyelia associated with Chiari type 1 malformation: review of evidences and proposal of a new hypothesis. Neurosurg Rev. 2010;33(3):271–84; discussion 284-285. https://doi.org/10.1007/s10143-010-0266-5.
42. Apok V, Constantini S, Roth J. Microsurgical fenestration of retrocerebellar cysts as a treatment for syringomyelia. Childs Nerv Syst. 2012;28(4):653–6. https://doi.org/10.1007/s00381-011-1652-1.
43. Milhorat TH. Classification of syringomyelia. Neurosurg Focus. 2000;8(3):E1. https://doi.org/10.3171/foc.2000.8.3.1.
44. Kyoshima K, Kuroyanagi T, Oya F, Kamijo Y, El-Noamany H, Kobayashi S. Syringomyelia without hindbrain herniation: tight cisterna magna. Report of four cases and a review of the literature. J Neurosurg. 2002;96(2 Suppl):239–49. https://doi.org/10.3171/spi.2002.96.2.0239.
45. Milhorat TH, Capocelli AL, Anzil AP, Kotzen RM, Milhorat RH. Pathological basis of spinal cord cavitation in syringomyelia: analysis of 105 autopsy cases. J Neurosurg. 1995;82(5):802–12. https://doi.org/10.3171/jns.1995.82.5.0802.
46. Guan J, Yuan C, Zhang C, et al. A novel classification and its clinical significance in Chiari I malformation with syringomyelia based on high-resolution MRI. Eur Spine J. 2021;30(6):1623–34. https://doi.org/10.1007/s00586-021-06746-y.
47. Tam SKP, Chia J, Brodbelt A, Foroughi M. Assessment of patients with a Chiari malformation type I. Brain Spine. 2022;2:100850. https://doi.org/10.1016/j.bas.2021.100850.
48. Massimi L, Peretta P, Erbetta A, et al. Diagnosis and treatment of Chiari malformation type 1 in children: the international consensus document. Neurol Sci. 2022;43(2):1311–26. https://doi.org/10.1007/s10072-021-05317-9.
49. Bolognese PA, Brodbelt A, Bloom AB, Kula RW. Chiari I malformation: opinions on diagnostic trends and controversies from a panel of 63 international experts. World Neurosurg. 2019;130:e9–e16. https://doi.org/10.1016/j.wneu.2019.05.098.
50. Tubbs RS, Wellons JC, Smyth MD, et al. Children with growth hormone deficiency and Chiari I malformation: a morphometric analysis of the posterior cranial fossa. Pediatr Neurosurg. 2003;38(6):324–8. https://doi.org/10.1159/000070416.
51. Gupta A, Vitali AM, Rothstein R, Cochrane DD. Resolution of syringomyelia and Chiari malformation after growth hormone therapy. Childs Nerv Syst. 2008;24(11):1345–8. https://doi.org/10.1007/s00381-008-0675-8.
52. Ballard H, Fuell W, Elwy R, Lou XY, Albert GW. Effects of growth hormone therapy in pediatric patients with growth hormone deficiency and Chiari I malformation: a retrospective study. Childs Nerv Syst. 2020;36(4):835–9. https://doi.org/10.1007/s00381-019-04370-2.
53. Naftel RP, Tubbs RS, Menendez JY, Oakes WJ. Progression of Chiari I malformations while on growth hormone replacement: a report of two cases. Childs Nerv Syst. 2013;29(12):2291–4. https://doi.org/10.1007/s00381-013-2080-1.
54. Kuether TA, Piatt JH. Chiari malformation associated with vitamin D-resistant rickets: case report. Neurosurgery. 1998;42(5):1168–71. https://doi.org/10.1097/00006123-199805000-00134.

55. Tubbs RS, Yan H, Demerdash A, et al. Sagittal MRI often overestimates the degree of cerebellar tonsillar ectopia: a potential for misdiagnosis of the Chiari I malformation. Childs Nerv Syst. 2016;32(7):1245–8. https://doi.org/10.1007/s00381-016-3113-3.
56. Ebrahimzadeh SA, Loth F, Ibrahimy A, Nwotchouang BST, Bhadelia RA. Diagnostic utility of parasagittal measurements of tonsillar herniation in Chiari I malformation. Neuroradiol J. 2022;35(2):233–9. https://doi.org/10.1177/19714009211041524.
57. Abel F, Tahir MZ. Role of sleep study in children with Chiari malformation and sleep disordered breathing. Childs Nerv Syst. 2019;35(10):1763–8. https://doi.org/10.1007/s00381-019-04302-0.
58. Amin R, Sayal P, Sayal A, et al. The association between sleep-disordered breathing and magnetic resonance imaging findings in a pediatric cohort with Chiari 1 malformation. Can Respir J. 2015;22(1):31–6. https://doi.org/10.1155/2015/831569.
59. Rogers JM, Savage G, Stoodley MA. A systematic review of cognition in Chiari I malformation. Neuropsychol Rev. 2018;28(2):176–87. https://doi.org/10.1007/s11065-018-9368-6.
60. Allen PA, Houston JR, Pollock JW, et al. Task-specific and general cognitive effects in Chiari malformation type I. PLoS One. 2014;9(4):e94844. https://doi.org/10.1371/journal.pone.0094844.
61. Sari SA, Ozum U. The executive functions, intellectual capacity, and psychiatric disorders in adolescents with Chiari malformation type 1. Childs Nerv Syst. 2021;37(7):2269–77. https://doi.org/10.1007/s00381-021-05085-z.
62. Seaman SC, Deifelt Streese C, Manzel K, et al. Cognitive and psychological functioning in Chiari malformation type I before and after surgical decompression - a prospective cohort study. Neurosurgery. 2021;89(6):1087–96. https://doi.org/10.1093/neuros/nyab353.
63. Almotairi FS, Hellström P, Skoglund T, Nilsson ÅL, Tisell M. Chiari I malformation-neuropsychological functions and quality of life. Acta Neurochir (Wien). 2020;162(7):1575–82. https://doi.org/10.1007/s00701-019-03897-2.
64. Saletti V, Farinotti M, Peretta P, et al. The management of Chiari malformation type 1 and syringomyelia in children: a review of the literature. Neurol Sci. 2021;42(12):4965–95. https://doi.org/10.1007/s10072-021-05565-9.
65. Strahle J, Muraszko KM, Kapurch J, Bapuraj JR, Garton HJ, Maher CO. Natural history of Chiari malformation Type I following decision for conservative treatment. J Neurosurg Pediatr. 2011;8(2):214–21. https://doi.org/10.3171/2011.5.peds1122.
66. Benglis D Jr, Covington D, Bhatia R, et al. Outcomes in pediatric patients with Chiari malformation type I followed up without surgery. J Neurosurg Pediatr. 2011;7(4):375–9. https://doi.org/10.3171/2011.1.peds10341.
67. Whitson WJ, Lane JR, Bauer DF, Durham SR. A prospective natural history study of non-operatively managed Chiari I malformation: does follow-up MRI surveillance alter surgical decision making? J Neurosurg Pediatr. 2015;16(2):159–66. https://doi.org/10.3171/2014.12.PEDS14301.
68. Spencer R, Leach P. Asymptomatic Chiari Type I malformation: should patients be advised against participation in contact sports? Br J Neurosurg. 2017;31(4):415–21. https://doi.org/10.1080/02688697.2017.1297767.
69. Strahle J, Geh N, Selzer BJ, et al. Sports participation with Chiari I malformation. J Neurosurg Pediatr. 2016;17(4):403–9. https://doi.org/10.3171/2015.8.PEDS15188.
70. Meehan WP, Jordaan M, Prabhu SP, Carew L, Mannix RC, Proctor MR. Risk of athletes with Chiari malformations suffering catastrophic injuries during sports participation is low. Clin J Sport Med. 2015;25(2):133–7. https://doi.org/10.1097/JSM.0000000000000107.
71. Aitken LA, Lindan CE, Sidney S, et al. Chiari type I malformation in a pediatric population. Pediatr Neurol. 2009;40(6):449–54. https://doi.org/10.1016/j.pediatrneurol.2009.01.003.
72. Killeen A, Roguski M, Chavez A, Heilman C, Hwang S. Non-operative outcomes in Chiari I malformation patients. J Clin Neurosci. 2015;22(1):133–8. https://doi.org/10.1016/j.jocn.2014.06.008.

73. Tubbs RS, Beckman J, Naftel RP, et al. Institutional experience with 500 cases of surgically treated pediatric Chiari malformation Type I. J Neurosurg Pediatr. 2011;7(3):248–56. https://doi.org/10.3171/2010.12.PEDS10379.
74. Alexander H, Tsering D, Myseros JS, et al. Management of Chiari I malformations: a paradigm in evolution. Childs Nerv Syst. 2019;35(10):1809–26. https://doi.org/10.1007/s00381-019-04265-2.
75. Dherijha MSA, Waqar M, Palin MS, Bukhari S. Foramen magnum decompression in adults with Chiari type 1 malformation: use of intraoperative ultrasound to guide extent of surgery. Br J Neurosurg. 2021;1-4. https://doi.org/10.1080/02688697.2021.1981238.
76. Jiang E, Sha S, Yuan X, et al. Comparison of clinical and radiographic outcomes for posterior fossa decompression with and without duraplasty for treatment of pediatric Chiari I malformation: a prospective study. World Neurosurg. 2018;110:e465–72. https://doi.org/10.1016/j.wneu.2017.11.007.
77. Chenghua Y, Min W, Wei L, Xinyu W, Fengzeng J. Comparison of foramen magnum decompression with and without duraplasty in the treatment of adult Chiari malformation Type I: a meta-analysis and systematic review. Turk Neurosurg. 2022. https://doi.org/10.5137/1019-5149.JTN.35727-21.5.
78. Massimi L, Frassanito P, Chieffo D, Tamburrini G, Caldarelli M. Bony decompression for Chiari malformation type I: long-term follow-up. Acta Neurochir Suppl. 2019;125:119–24. https://doi.org/10.1007/978-3-319-62515-7_17.
79. Goel A, Jadhav D, Shah A, et al. Chiari 1 formation redefined-clinical and radiographic observations in 388 surgically treated patients. World Neurosurg. 2020;141:e921–34. https://doi.org/10.1016/j.wneu.2020.06.076.
80. Navarro R, Olavarria G, Seshadri R, Gonzales-Portillo G, McLone DG, Tomita T. Surgical results of posterior fossa decompression for patients with Chiari I malformation. Childs Nerv Syst. 2004;20(5):349–56. https://doi.org/10.1007/s00381-003-0883-1.
81. Zhao JL, Li MH, Wang CL, Meng W. A systematic review of Chiari I malformation: techniques and outcomes. World Neurosurg. 2016;88:7–14. https://doi.org/10.1016/j.wneu.2015.11.087.
82. Galarza M, Sood S, Ham S. Relevance of surgical strategies for the management of pediatric Chiari type I malformation. Childs Nerv Syst. 2007;23(6):691–6. https://doi.org/10.1007/s00381-007-0297-6.
83. Guyotat J, Bret P, Jouanneau E, Ricci AC, Lapras C. Syringomyelia associated with type I Chiari malformation. A 21-year retrospective study on 75 cases treated by foramen magnum decompression with a special emphasis on the value of tonsils resection. Acta Neurochir (Wien). 1998;140(8):745–54. https://doi.org/10.1007/s007010050175.
84. Balasa A, Kunert P, Dziedzic T, Bielecki M, Kujawski S, Marchel A. Comparison of dural grafts and methods of graft fixation in Chiari malformation type I decompression surgery. Sci Rep. 2021;11(1):14801. https://doi.org/10.1038/s41598-021-94179-4.
85. Hu Z, Liao G, Lu Y, Wang C, Mei J. Comparison of dural graft types and graft fixation methods in Chiari malformation type I decompression surgery. World Neurosurg. 2022;164:e458–62. https://doi.org/10.1016/j.wneu.2022.04.127.
86. Yahanda AT, Simon LE, Limbrick DD. Outcomes for various dural graft materials after posterior fossa decompression with duraplasty for Chiari malformation type I: a systematic review and meta-analysis. J Neurosurg. 2021;1–14. https://doi.org/10.3171/2020.9.JNS202641.
87. Barzilai O, Roth J, Korn A, Constantini S. The value of multimodality intraoperative neurophysiological monitoring in treating pediatric Chiari malformation type I. Acta Neurochir (Wien). 2016;158(2):335–40. https://doi.org/10.1007/s00701-015-2664-5.
88. Barzilai O, Roth J, Korn A, Constantini S. Letter to the Editor: Evoked potentials and Chiari malformation Type 1. J Neurosurg. 2017;126(2):654–7. https://doi.org/10.3171/2016.4.JNS161061.
89. Moncho D, Poca MA, Minoves T, Ferré A, Cañas V, Sahuquillo J. Are evoked potentials clinically useful in the study of patients with Chiari malformation Type 1? J Neurosurg. 2017;126(2):606–19. https://doi.org/10.3171/2015.11.JNS151764.

90. Rasul FT, Matloob SA, Haliasos N, Jankovic I, Boyd S, Thompson DNP. Intraoperative neurophysiological monitoring in paediatric Chiari surgery-help or hindrance? Childs Nerv Syst. 2019;35(10):1769–76. https://doi.org/10.1007/s00381-019-04312-y.
91. Bollo RJ, Riva-Cambrin J, Brockmeyer MM, Brockmeyer DL. Complex Chiari malformations in children: an analysis of preoperative risk factors for occipitocervical fusion. J Neurosurg Pediatr. 2012;10(2):134–41. https://doi.org/10.3171/2012.3.PEDS11340.
92. Jea A. Editorial: Chiari malformation I surgically treated with atlantoaxial fixation. J Neurosurg Spine. 2015;22(2):113–5. https://doi.org/10.3171/2014.9.SPINE14893.
93. İştemen İ, Harman F, Arslan A, et al. Is C1-C2 reduction and fixation a good choice in the treatment of recurrent Chiari-like symptoms with syringomyelia? World Neurosurg. 2021;146:e837–47. https://doi.org/10.1016/j.wneu.2020.11.023.
94. Goel A. Is atlantoaxial instability the cause of Chiari malformation? Outcome analysis of 65 patients treated by atlantoaxial fixation. J Neurosurg Spine. 2015;22(2):116–27. https://doi.org/10.3171/2014.10.SPINE14176.
95. Goel A, Gore S, Shah A, Dharurkar P, Vutha R, Patil A. Atlantoaxial fixation for Chiari 1 formation in pediatric age-group patients: report of treatment in 33 patients. World Neurosurg. 2018;111:e668–77. https://doi.org/10.1016/j.wneu.2017.12.137.
96. Goel A, Kaswa A, Shah A. Atlantoaxial fixation for treatment of Chiari formation and syringomyelia with no craniovertebral bone anomaly: report of an experience with 57 cases. Acta Neurochir Suppl. 2019;125:101–10. https://doi.org/10.1007/978-3-319-62515-7_15.
97. Salunke P, Karthigeyan M, Malik P, Panchal C. Changing perception but unaltered reality: how effective is C1-C2 fixation for Chiari malformations without instability? World Neurosurg. 2020;136:e234–44. https://doi.org/10.1016/j.wneu.2019.12.122.
98. Arslan A, Olguner SK, Acik V, et al. Surgical outcomes of C1-2 posterior stabilization in patients with Chiari malformation type 1. Global Spine J. 2022;12(1):37–44. https://doi.org/10.1177/2192568220945293.
99. Singhal A, Cheong A, Steinbok P. International survey on the management of Chiari 1 malformation and syringomyelia: evolving worldwide opinions. Childs Nerv Syst. 2018;34(6):1177–82. https://doi.org/10.1007/s00381-018-3741-x.
100. Nishizawa S, Yokoyama T, Yokota N, Tokuyama T, Ohta S. Incidentally identified syringomyelia associated with Chiari I malformations: is early interventional surgery necessary? Neurosurgery. 2001;49(3):637–40; discussion 640-1.
101. Wan MJ, Nomura H, Tator CH. Conversion to symptomatic Chiari I malformation after minor head or neck trauma. Neurosurgery. 2008;63(4):748–53; discussion 753. https://doi.org/10.1227/01.NEU.0000325498.04975.C0.
102. Mozaffari K, Davidson L, Chalif E, et al. Long-term outcomes of posterior fossa decompression for Chiari malformation type 1: which patients are most prone to failure? Childs Nerv Syst. 2021;37(9):2891–8. https://doi.org/10.1007/s00381-021-05280-y.
103. Sacco D, Scott RM. Reoperation for Chiari malformations. Pediatr Neurosurg. 2003;39(4):171–8. https://doi.org/10.1159/000072467.
104. Schuster JM, Zhang F, Norvell DC, Hermsmeyer JT. Persistent/Recurrent syringomyelia after Chiari decompression-natural history and management strategies: a systematic review. Evid Based Spine Care J. 2013;4(2):116–25. https://doi.org/10.1055/s-0033-1357362.
105. Knafo S, Malcoci M, Morar S, Parker F, Aghakhani N. Surgical management after Chiari decompression failure: craniovertebral junction revision versus shunting strategies. J Clin Med. 2022;11(12):3334. https://doi.org/10.3390/jcm11123334.
106. Chotai S, Chan EW, Ladner TR, et al. Timing of syrinx reduction and stabilization after posterior fossa decompression for pediatric Chiari malformation type I. J Neurosurg Pediatr. 2020;26(2):193–9. https://doi.org/10.3171/2020.2.PEDS19366.
107. Szuflita NS, Phan TN, Boulter JH, Keating RF, Myseros JS. Nonoperative management of enlarging syringomyelia in clinically stable patients after decompression of Chiari malformation type I. J Neurosurg Pediatr. 2021;1–6. https://doi.org/10.3171/2020.12.PEDS20621.

108. Bartoli A, Soleman J, Berger A, et al. Treatment options for hydrocephalus following foramen magnum decompression for Chiari I malformation: a multi-center study. Neurosurgery. 2020;86(4):500–8.
109. Isik N, Elmaci I, Isik N, et al. Long-term results and complications of the syringopleural shunting for treatment of syringomyelia: a clinical study. Br J Neurosurg. 2013;27(1):91–9. https://doi.org/10.3109/02688697.2012.703350.
110. Lesoin F, Petit H, Thomas CE, Viaud C, Baleriaux D, Jomin M. Use of the syringoperitoneal shunt in the treatment of syringomyelia. Surg Neurol. 1986;25(2):131–6.
111. Fan T, Zhao X, Zhao H, et al. Treatment of selected syringomyelias with syringo-pleural shunt: the experience with a consecutive 26 cases. Clin Neurol Neurosurg. 2015;137:50–6. https://doi.org/10.1016/j.clineuro.2015.06.012.
112. Vernet O, Farmer JP, Montes JL. Comparison of syringopleural and syringosubarachnoid shunting in the treatment of syringomyelia in children. J Neurosurg. 1996;84(4):624–8. https://doi.org/10.3171/jns.1996.84.4.0624.
113. Attenello FJ, McGirt MJ, Gathinji M, et al. Outcome of Chiari-associated syringomyelia after hindbrain decompression in children: analysis of 49 consecutive cases. Neurosurgery. 2008;62(6):1307–13.; discussion 1313. https://doi.org/10.1227/01.neu.0000333302.72307.3b.
114. Mazzola CA, Fried AH. Revision surgery for Chiari malformation decompression. Neurosurg Focus. 2003;15(3):E3.
115. Hida K, Iwasaki Y, Koyanagi I, Sawamura Y, Abe H. Surgical indication and results of foramen magnum decompression versus syringosubarachnoid shunting for syringomyelia associated with Chiari I malformation. Neurosurgery. 1995;37(4):673–8; discussion 678-9.
116. Sgouros S, Williams B. A critical appraisal of drainage in syringomyelia. J Neurosurg. 1995;82(1):1–10. https://doi.org/10.3171/jns.1995.82.1.0001.
117. Heiss JD, Suffredini G, Smith R, et al. Pathophysiology of persistent syringomyelia after decompressive craniocervical surgery. Clinical article. J Neurosurg Spine. 2010;13(6):729–42. https://doi.org/10.3171/2010.6.spine10200.
118. Tator CH, Briceno C. Treatment of syringomyelia with a syringosubarachnoid shunt. Can J Neurol Sci. 1988;15(1):48–57.
119. Tator CH, Meguro K, Rowed DW. Favorable results with syringosubarachnoid shunts for treatment of syringomyelia. J Neurosurg. 1982;56(4):517–23. https://doi.org/10.3171/jns.1982.56.4.0517.
120. Vaquero J, Martínez R, Salazar J, Santos H. Syringosubarachnoid shunt for treatment of syringomyelia. Acta Neurochir (Wien). 1987;84(3-4):105–9.
121. Davidson L, Krieger MD, McComb JG. Posterior interhemispheric retrocallosal approach to pineal region and posterior fossa lesions in a pediatric population. J Neurosurg Pediatr. 2011;7(5):527–33. https://doi.org/10.3171/2011.2.PEDS10123.
122. Cacciola F, Capozza M, Perrini P, Benedetto N, Di Lorenzo N. Syringopleural shunt as a rescue procedure in patients with syringomyelia refractory to restoration of cerebrospinal fluid flow. Neurosurgery. 2009;65(3):471–6; discussion 476. https://doi.org/10.1227/01.NEU.0000350871.47574.DE.
123. Tubbs RS, Webb DB, Oakes WJ. Persistent syringomyelia following pediatric Chiari I decompression: radiological and surgical findings. J Neurosurg. 2004;100(5 Suppl Pediatrics):460–4. https://doi.org/10.3171/ped.2004.100.5.0460.
124. Isu T, Sasaki H, Takamura H, Kobayashi N. Foramen magnum decompression with removal of the outer layer of the dura as treatment for syringomyelia occurring with Chiari I malformation. Neurosurgery. 1993;33(5):845–9; discussion 849-50.
125. Lu VM, Phan K, Crowley SP, Daniels DJ. The addition of duraplasty to posterior fossa decompression in the surgical treatment of pediatric Chiari malformation Type I: a systematic review and meta-analysis of surgical and performance outcomes. J Neurosurg Pediatr. 2017;20(5):439–49. https://doi.org/10.3171/2017.6.PEDS16367.

126. Fakhri A, Shah MN, Goyal MS. Advanced imaging of Chiari 1 malformations. Neurosurg Clin N Am. 2015;26(4):519–26. https://doi.org/10.1016/j.nec.2015.06.012.
127. Liu LL, Leung JM. Predicting adverse postoperative outcomes in patients aged 80 years or older. J Am Geriatr Soc. 2000;48(4):405–12. https://doi.org/10.1111/j.1532-5415.2000.tb04698.x.
128. Quon JL, Grant RA, DiLuna ML. Multimodal evaluation of CSF dynamics following extradural decompression for Chiari malformation type I. J Neurosurg Spine. 2015;22(6):622–30. https://doi.org/10.3171/2014.10.SPINE1433.
129. Gardner WJ, Bell HS, Poolos PN, Dohn DF, Steinberg M. Terminal ventriculostomy for syringomyelia. J Neurosurg. 1977;46(5):609–17. https://doi.org/10.3171/jns.1977.46.5.0609.
130. Blagodatsky MD, Larionov SN, Manohin PA, Shanturov VA, YuV G. Surgical treatment of "hindbrain related" syringomyelia: new data for pathogenesis. Acta Neurochir (Wien). 1993;124(2-4):82–5. https://doi.org/10.1007/BF01401127.
131. Ur-Rahman N, Jamjoom ZA. Surgical management of Chiari malformation and syringomyelia: experience in 14 cases. Ann Saudi Med. 1991;11(4):402–10. https://doi.org/10.5144/0256-4947.1991.402.
132. Filizzolo F, Versari P, D'Aliberti G, Arena O, Scotti G, Mariani C. Foramen magnum decompression versus terminal ventriculostomy for the treatment of syringomyelia. Acta Neurochir (Wien). 1988;93(3-4):96–9. https://doi.org/10.1007/BF01402888.
133. Wilson DA, Fusco DJ, Rekate HL. Terminal ventriculostomy as an adjuvant treatment of complex syringomyelia: a case report and review of the literature. Acta Neurochir (Wien). 2011;153(7):1449–53.; discussion 1453. https://doi.org/10.1007/s00701-011-1020-7.
134. Yq D, Gy Q, Yh Y, T L, Xg Y. Posterior atlantoaxial facet joint reduction, fixation and fusion as revision surgery for failed suboccipital decompression in patients with basilar invagination and atlantoaxial dislocation: operative nuances, challenges and outcomes. Clin Neurol Neurosurg. 2020:194. https://doi.org/10.1016/j.clineuro.2020.105793.
135. Shah A, Sathe P, Patil M, Goel A. Treatment of "idiopathic" syrinx by atlantoaxial fixation: Report of an experience with nine cases. J Craniovertebr Junction Spine. 2017;8(1) https://doi.org/10.4103/0974-8237.199878.
136. Hwang SW, Heilman CB, Riesenburger RI, Kryzanski J. C1-C2 arthrodesis after transoral odontoidectomy and suboccipital craniectomy for ventral brain stem compression in Chiari I patients. Eur Spine J. 2008;17(9):1211–7. https://doi.org/10.1007/s00586-008-0706-x.
137. Riordan CP, Scott RM. Fourth ventricle stent placement for treatment of recurrent syringomyelia in patients with type I Chiari malformations. J Neurosurg Pediatr. 2018;23(2):164–70. https://doi.org/10.3171/2018.7.PEDS18312.
138. Greuter L, Licci M, Terrier A, Guzman R, Soleman J. Minimal invasive interlaminar approach for untethering of fatty filum terminale in pediatric patients - how I do it. Acta Neurochir (Wien). 2022;164(6):1481–4. https://doi.org/10.1007/s00701-022-05204-y.
139. Milhorat TH, Bolognese PA, Nishikawa M, et al. Association of Chiari malformation type I and tethered cord syndrome: preliminary results of sectioning filum terminale. Surg Neurol. 2009;72(1):20–35. https://doi.org/10.1016/j.surneu.2009.03.008.
140. Valentini LG, Selvaggio G, Visintini S, Erbetta A, Scaioli V, Solero CL. Tethered cord: natural history, surgical outcome and risk for Chiari malformation 1 (CM1): a review of 110 detethering. Neurol Sci. 2011;32(Suppl 3):S353–6. https://doi.org/10.1007/s10072-011-0745-7.
141. Milano JB, Barcelos ACES, Onishi FJ, et al. The effect of filum terminale sectioning for Chiari 1 malformation treatment: systematic review. Neurol Sci. 2020;41(2):249–56. https://doi.org/10.1007/s10072-019-04056-2.
142. Glenn C, Cheema AA, Safavi-Abbasi S, Gross NL, Martin MD, Mapstone TB. Spinal cord detethering in children with tethered cord syndrome and Chiari type 1 malformations. J Clin Neurosci. 2015;22(11):1749–52. https://doi.org/10.1016/j.jocn.2015.05.023.
143. Noureldine MHA, Shimony N, Jallo GI, Groves ML. Scoliosis in patients with Chiari malformation type I. Childs Nerv Syst. 2019;35(10):1853–62. https://doi.org/10.1007/s00381-019-04309-7.

144. Saifuddin A, Tucker S, Taylor BA, Noordeen MH, Lehovsky J. Prevalence and clinical significance of superficial abdominal reflex abnormalities in idiopathic scoliosis. Eur Spine J. 2005;14(9):849–53. https://doi.org/10.1007/s00586-004-0850-x.
145. Brockmeyer DL. Editorial. Chiari malformation Type I and scoliosis: the complexity of curves. J Neurosurg Pediatr 2011;7(1):22-23; discussion 23-24. doi:https://doi.org/10.3171/2010.9.PEDS10383
146. Muhonen MG, Menezes AH, Sawin PD, Weinstein SL. Scoliosis in pediatric Chiari malformations without myelodysplasia. J Neurosurg. 1992;77(1):69–77. https://doi.org/10.3171/jns.1992.77.1.0069.
147. Strahle J, Smith BW, Martinez M, et al. The association between Chiari malformation type I, spinal syrinx, and scoliosis. J Neurosurg Pediatr. 2015;15(6):607–11. https://doi.org/10.3171/2014.11.PEDS14135.
148. Zhu Z, Wu T, Sha S, et al. Is curve direction correlated with the dominant side of tonsillar ectopia and side of syrinx deviation in patients with single thoracic scoliosis secondary to Chiari malformation and syringomyelia? Spine (Phila Pa 1976). 2013;38(8):671–7. https://doi.org/10.1097/BRS.0b013e3182796ec5.
149. Zhang T, Bao H, Zhang X, et al. Brace treatment for scoliosis secondary to chiari malformation type 1 or syringomyelia without neurosurgical intervention: A matched comparison with idiopathic scoliosis. Eur Spine J. 2021;30(12):3482–9. https://doi.org/10.1007/s00586-021-06958-2.
150. Rodriguez VV, Tello CA, Piantoni L, et al. Chiari 1: Is decompression always necessary previous to scoliosis surgery? Spine Deform. 2021;9(5):1253–8. https://doi.org/10.1007/s43390-021-00336-0.
151. Iwami T, Watanabe K, Suzuki S, et al. Spontaneous reduction of Chiari malformation and syringomyelia after posterior spinal fusion for scoliosis: a case report JBJS Case Connect. 2021;11(2). https://doi.org/10.2106/JBJS.CC.20.00779
152. Eule JM, Erickson MA, O'Brien MF, Handler M. Chiari I malformation associated with syringomyelia and scoliosis: a twenty-year review of surgical and nonsurgical treatment in a pediatric population. Spine (Phila Pa 1976). 2002;27(13):1451–5. https://doi.org/10.1097/00007632-200207010-00015.
153. Strahle JM, Taiwo R, Averill C, et al. Radiological and clinical associations with scoliosis outcomes after posterior fossa decompression in patients with Chiari malformation and syrinx from the Park-Reeves Syringomyelia Research Consortium. J Neurosurg Pediatr. 2020;26(1):53–9. https://doi.org/10.3171/2020.1.PEDS18755.
154. Shanmugasundaram S, Viswanathan VK, Shetty AP, et al. Type I Arnold Chiari malformation with syringomyelia and scoliosis: radiological correlations between tonsillar descent, syrinx morphology and curve characteristics: a retrospective study. Asian Spine J. 2022;17(1):156–65. https://doi.org/10.31616/asj.2021.0483.
155. Chotai S, Nadel JL, Holste KG, et al. Longitudinal scoliosis behavior in Chiari malformation with and without syringomyelia. J Neurosurg Pediatr. 2021;28(5):585–91. https://doi.org/10.3171/2021.5.PEDS20915.
156. Zhu C, Huang S, Song Y, et al. Surgical treatment of scoliosis-associated with syringomyelia: the role of syrinx size. Neurol India. 2020;68(2):299–304. https://doi.org/10.4103/0028-3886.280648.
157. Di Rocco C, Frassanito P, Massimi L, Peraio S. Hydrocephalus and Chiari type I malformation. Childs Nerv Syst. 2011;27(10):1653–64. https://doi.org/10.1007/s00381-011-1545-3.
158. Mathkour M, Keen JR, Huang B, et al. "Two-Birds-One-Stone" approach for treating an infant with Chiari I malformation and hydrocephalus: is cerebrospinal fluid diversion as sole treatment enough? World Neurosurg. 2020;137:174–7. https://doi.org/10.1016/j.wneu.2020.01.188.
159. Decq P, Le Guérinel C, Sol JC, Brugières P, Djindjian M, Nguyen JP. Chiari I malformation: a rare cause of noncommunicating hydrocephalus treated by third ventriculostomy. J Neurosurg. 2001;95(5):783–90. https://doi.org/10.3171/jns.2001.95.5.0783.

160. Massimi L, Pravatà E, Tamburrini G, et al. Endoscopic third ventriculostomy for the management of Chiari I and related hydrocephalus: outcome and pathogenetic implications. Neurosurgery. 2011;68(4):950–6. https://doi.org/10.1227/NEU.0b013e318208f1f3.
161. JNPO B, BAD S, Nascimento IF, Martins LA, Tavares CB. Basilar invagination associated with chiari malformation type I: a literature review. Clinics. 2019;74:e653. https://doi.org/10.6061/clinics/2019/e653.
162. Chamberlain WE. Basilar impression (Platybasia). Yale J Biol Med. 1939;11(5):487–96.
163. Wagner A, Grassner L, Kögl N, et al. Chiari malformation type I and basilar invagination originating from atlantoaxial instability: a literature review and critical analysis. Acta Neurochir (Wien). 2020;162(7):1553–63. https://doi.org/10.1007/s00701-020-04429-z.
164. Pinter NK, McVige J, Mechtler L. Basilar invagination, basilar impression, and platybasia: clinical and imaging aspects. Curr Pain Headache Rep. 2016;20(8):49. https://doi.org/10.1007/s11916-016-0580-x.
165. Klekamp J. Chiari I malformation with and without basilar invagination: a comparative study. Neurosurg Focus. 2015;38(4):E12. https://doi.org/10.3171/2015.1.FOCUS14783.
166. Fuentes AM, Chiu RG, Nie J, Mehta AI. Inpatient outcomes of posterior fossa decompression with or without duraplasty for Chiari malformation type I. Clin Neurol Neurosurg. 2021;207:106757. https://doi.org/10.1016/j.clineuro.2021.106757.
167. Shao B, Tariq AA, Goldstein HE, et al. Multimodal analgesia after posterior fossa decompression with and without duraplasty for children with Chiari type I. Hosp Pediatr. 2020;10(5):447–51. https://doi.org/10.1542/hpeds.2019-0298.
168. Yarbrough CK, Greenberg JK, Smyth MD, Leonard JR, Park TS, Limbrick DD. External validation of the Chicago Chiari outcome scale. J Neurosurg Pediatr. 2014;13(6):679–84. https://doi.org/10.3171/2014.3.PEDS13503.
169. Greenberg JK, Milner E, Yarbrough CK, et al. Outcome methods used in clinical studies of Chiari malformation type I: a systematic review. J Neurosurg. 2015;122(2):262–72. https://doi.org/10.3171/2014.9.JNS14406.
170. Yarbrough CK, Greenberg JK, Park TS. Clinical outcome measures in Chiari I malformation. Neurosurg Clin N Am. 2015;26(4):533–41. https://doi.org/10.1016/j.nec.2015.06.008.
171. Ladner TR, Westrick AC, Wellons JC, Shannon CN. Health-related quality of life in pediatric Chiari type I malformation: the Chiari health index for pediatrics. J Neurosurg Pediatr. 2016;17(1):76–85. https://doi.org/10.3171/2015.5.PEDS1513.
172. Sellyn GE, Tang AR, Zhao S, et al. Effectiveness of the Chiari health index for pediatrics instrument in measuring postoperative health-related quality of life in pediatric patients with Chiari malformation type I. J Neurosurg Pediatr. 2020;27(2):139–44. https://doi.org/10.3171/2020.7.PEDS20250.
173. Baygani S, Zieles K, Jea A. PedsQL for prediction of postoperative patient-reported outcomes following Chiari decompression surgery. J Neurosurg Pediatr. 2019;1–6. https://doi.org/10.3171/2019.9.PEDS19409.
174. De Vlieger J, Dejaegher J, Van Calenbergh F. Multidimensional, patient-reported outcome after posterior fossa decompression in 79 patients with Chiari malformation type I. Surg Neurol Int. 2019;10:242. https://doi.org/10.25259/SNI_377_2019.
175. Savchuk S, Jin MC, Choi S, et al. Incorporating patient-centered quality-of-life measures for outcome assessment after Chiari malformation type I decompression in a pediatric population: a pilot study. J Neurosurg Pediatr. 2021;1–8. https://doi.org/10.3171/2021.8.PEDS21228.
176. Atchley TJ, Alford EN, Rocque BG. Systematic review and meta-analysis of imaging characteristics in Chiari I malformation: does anything really matter? Childs Nerv Syst. 2020;36(3):525–34. https://doi.org/10.1007/s00381-019-04398-4.
177. Takeshima Y, Matsuda R, Nishimura F, et al. Sequential enlargement of posterior fossa after duraplasty for Chiari malformation type 1. World Neurosurg X. 2019;2:100004. https://doi.org/10.1016/j.wnsx.2018.100004.

178. Mantha S, Coulthard LG, Campbell R. CSF-space volumetric change following posterior fossa decompression in paediatric Chiari type-I malformation: a correlation with outcome. Childs Nerv Syst. 2021;37(12):3861–9. https://doi.org/10.1007/s00381-021-05307-4.
179. Soleman J, Guzman R. Neurocognitive complications after ventricular neuroendoscopy: a systematic review. Behav Neurol. 2020;2020:2536319. https://doi.org/10.1155/2020/2536319.

Chapter 5
The Supraorbital Eyebrow Approach in Pediatric Neurosurgery: Perspectives and Challenges of Frontal Keyhole Surgery

Aminaa Sanchin, Eckart Bertelmann, Pablo Hernáiz Driever, Anna Tietze, and Ulrich-Wilhelm Thomale

5.1 Introduction

The fronto-basal neuro-structures such as the optic pathway and orbital anatomy with oculomotor functions can be affected by a variety of orbital or fronto-basal pathologies and require careful planning to select the appropriate surgical approach due to anatomical complexity. The main priority is to preserve stable vision and oculomotor function. Regarding the choice of a specific approach, the following aspects are of utmost importance: exact localization of the lesion and definition of the optimal targeting trajectory, permitting a sufficient working corridor and exposure of the affected structures according to the surgeon's experience applying as little collateral damage to the orbital or the frontal lobe structures as possible.

A. Sanchin
Department of Neurosurgery, Charité – Universitätsmedizin Berlin, Berlin, Germany
e-mail: aminaa.sanchin@charite.de

E. Bertelmann
Department of Ophthalmology, Charité – Universitätsmedizin Berlin, Berlin, Germany
e-mail: eckart.bertelmann@charite.de

P. Hernáiz Driever
Department of Pediatric Oncology and Hematology, Charité – Universitätsmedizin Berlin, Berlin, Germany
e-mail: pablo.hernaiz@charite.de

A. Tietze
Institute of Neuroradiology, Charité – Universitätsmedizin Berlin, Berlin, Germany
e-mail: anna.tietze@charite.de

U.-W. Thomale (✉)
Pediatric Neurosurgery, Charité – Universitätsmedizin Berlin, Berlin, Germany
e-mail: ulrich-wilhelm.thomale@charite.de

C. Di Rocco (ed.), *Advances and Technical Standards in Neurosurgery*, Advances and Technical Standards in Neurosurgery 48,
https://doi.org/10.1007/978-3-031-36785-4_5

Supraorbital craniotomy has been described suitable to achieve both orbital and anterior cranial fossa lesions [1, 2] and can be applied through an eyebrow incision, which may lead to satisfactory cosmetic results [3, 4]. In adult patients, supraorbital craniotomy through an eyebrow incision is well established for vascular procedures such as aneurysm clipping as well as for surgery of tumorous lesions in anterior cranial fossa or parasellar regions [5–8]. However, only few case series are reported on supraorbital craniotomy via eyebrow incision in pediatric patients [9, 10]. We present our experience from a case series of supraorbital eyebrow approaches in a single academic pediatric neurosurgical institution and analyze patient characteristics, clinical course, and surgical outcome.

5.2 Patients and Methods

Between January 2013 and April 2022, 37 supraorbital eyebrow approaches were performed in 30 patients in Pediatric Neurosurgery of Charité - Universitätsmedizin Berlin.

The age range included infants and toddlers to adolescents. Cases were analyzed retrospectively according to the institutional digital patient charts. Included pathologies were localized either intracranially or intraorbitally as visualized on preoperative MRI and/or CT.

Patient items such as age, sex, time interval between diagnosis in radiological imaging and performed surgery, histological diagnosis, location of the lesion, and mean duration of hospital stay were collected. The pathologies were grouped in intracranial and orbital lesions, which in turn were classified into tumor and non-tumor diseases. It was recorded whether adjuvant therapy such as chemotherapy or radiotherapy took place following surgery and whether repeated surgeries became necessary. In tumor patients, the most recent available imaging was evaluated by a pediatric neuroradiology consultant to assess the status of disease 3 months after surgery and at most recent time of follow-up. Ophthalmologic examination of the affected side was usually performed at preoperative state, postoperatively at 2 months, and at last available follow-up time point. Findings were classified according to the International Statistical Classification of Diseases and Related Health Problems – tenth revision (ICD-10), WHO version 2016, ranging from 0 to 5, equivalent to no or mild vision impairment (0) and amaurosis (5), respectively, and observed over time.

5.2.1 Surgery Characteristics and Surgical Technique

Clinical parameters for surgery included mean duration of surgery, proportion of patients with postoperative monitoring in an intensive care unit, duration of intensive care unit stays, need for application of red blood cell concentrates, and

complication rate. Postoperative MRI was acquired in all tumor patients. In tumor patients, the extent of resection was categorized according to the postoperative radiological findings in gross total resection (no remnants), subtotal resection (rim-like residuals), partial resection (solid remnants visible), and biopsy (no change of lesion volume). All surgeries were performed by the senior author (UWT). Orbital pathologies were operated in an interdisciplinary team in collaboration with the orbital surgeon (EB).

During surgery, patients were positioned prone with slight extension and tilting of the head toward the contralateral side in order to place the eyebrow at the highest point. Skin disinfection was achieved by locally applying Braunol (Braun, Melsungen, Germany). In all intracranial and most intraorbital lesions, the head was fixed in a Mayfield clamp. Neuronavigation and/or intraoperative ultrasound was applied according to the surgeon's preference in all cases. The incision usually included the two lateral thirds of the eyebrow and was adapted in length laterally according to the necessary size of craniotomy. The straight incision included the orbicularis muscle and periosteum just above the orbital rim and spared the supra-orbital nerve medially. The periosteum was additionally incised vertically at each end of the medial and lateral edges in order to expose orbital rim and sufficient area of the supraorbital calvarium cranially. Retractors were placed to expose the area of supraorbital craniotomy as given in Fig. 5.1a/d. Laterally, the temporal muscle was retracted for better lateral exposure if relevant. The craniotomy was accomplished with piezosurgery ultrasonic bone incision (Mectron, Genova, Italy) which yielded minimal bone defect at the rims of craniotomy for better subsequent cranioplasty. With a chisel, the orbital roof was opened along the craniotomy to elevate the bone

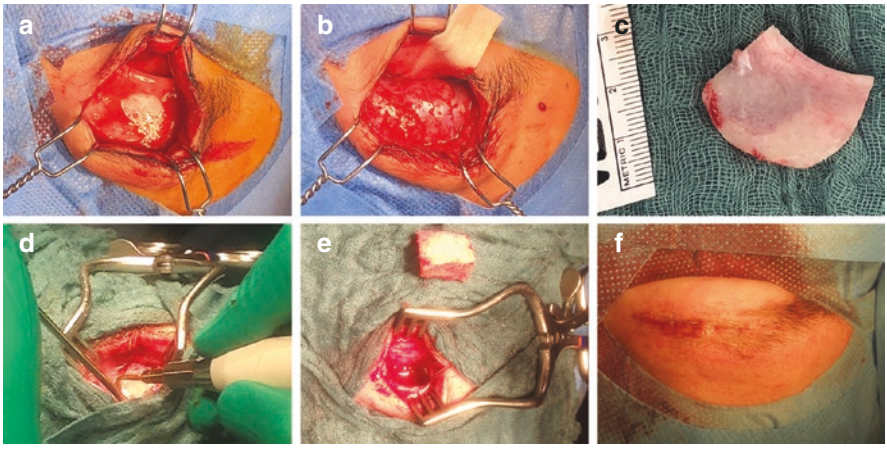

Fig. 5.1 The surgical technique includes a lateral two third eyebrow skin incision and soft tissue retraction (**a**). The craniotomy is performed using an ultrasonic bone incision device (Mectron, Genova, Italy) (**d**) to apply a supraorbital craniotomy with inclusion of the orbital rim to expose the dura and the periorbital layer (**b**, **c**, **e**). The skin closure is achieved by periosteum and muscle adaptation, subcutaneous sutures, and skin glue (**f**)

flap and expose the dura and periorbital layer, accordingly (Fig. 5.1b, c, e). For better exposure of either orbita or dura, additional bone was reduced of the orbital roof caudally by piezosurgical incision technique.

In microsurgical technique, either the dura for intracranial lesions or the periorbital layer was incised to approach the target lesion, accordingly. After the dural opening in intracranial lesions, an essential step was to open the basal cisterns for CSF to relieve and achieve enough space of access. Navigated microscopic view was useful to directly target the lesion with the help of augmented reality contour guidance [11, 12] (Fig. 5.2). In deep-seated intracranial lesions, the resection cavity may have been additionally inspected by assisted endoscopic technique which was well established parallel to modern neuromicroscopy (Qevo, Zeiss, Oberkochen, Germany).

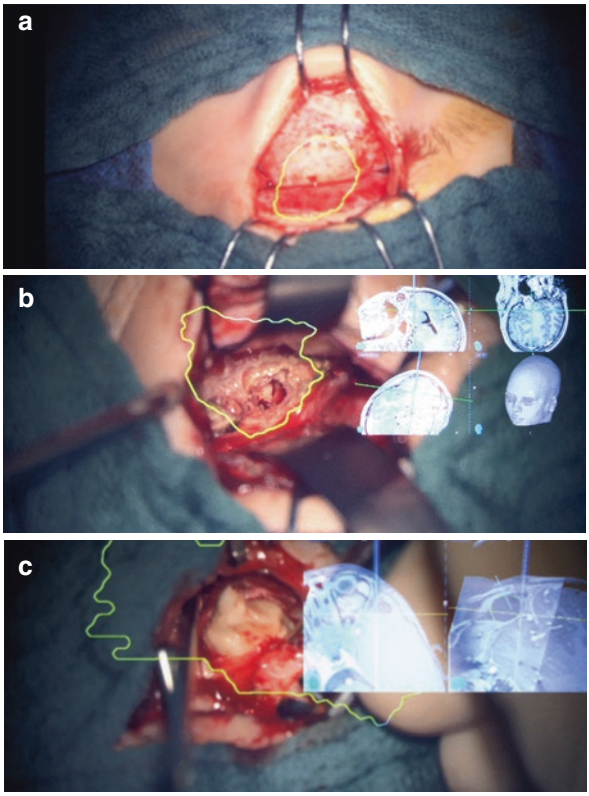

Fig. 5.2 Augmented reality function in the supraorbital keyhole approach. (**a**): optic nerve glioma. The contour of the tumor is projected on the surface of the dura and the periorbital layer. (**b**): fibrous osteoma. The focus point of the microscope is navigated and displayed in inline and perpendicular MRI sections along the viewing trajectory as shown in the upper right of the microscope field of view. (**c**): extensive dermoid lesion in the lateral and upper wall of the orbit. At the respective magnification the contour of the lesions extension is displayed to adapt the surgical perspective accordingly

For orbital lesions, the rectus muscles were secured, and a periorbital incision was performed from anterior to posterior at the exposed upper lateral quadrant in order to spare the oculomotor muscles and the levator palpebrae, accordingly. In cases of optic nerve glioma (patients were blind ipsilaterally), a complete resection of the optic nerve was accomplished from the anterior orbital portion to the chiasm, hence intraorbitally and intracranially. Therefore, the orbital portion was resected primarily followed by the intracranial prechiasmatic portion via a subfrontal approach, while the orbital canal was kept unaffected and shriveled over time, as described previously [13]. In the case of idiopathic intracranial hypertension, the orbital sheet was microsurgically incised in horizontal direction at multiple levels in order to allow continuous intralipomatous CSF relieve. Following target intervention, the dura and/or the periorbital layer were closed with a running 5–0 Vicryl suture. A layer of gel foam was placed intradurally, and the dural suture was additionally sealed with epidural TachoSil (Takeda, Tokyo, Japan) to prevent CSF leakage. The bony portion of the orbital roof was replaced between dura and periorbital layer, and the supraorbital bone flap was fixed in situ by using two titanium microplates (MatrixNEURO, Depuy Synthes, West Chester, USA). Muscle closure was performed by 4–0 Vicryl running sutures, and subcutaneous sutures were followed by gluing the skin (Dermabond, Ethicon, San Angelo, USA; Fig. 5.1d).

5.3 Results

Thirty-seven interventions in 30 patients were performed using a supraorbital eyebrow incision (28 male [60%] and 12 female [40%] patients). The mean age was 8 ± 6.5 years, and age range was 0.3 to 29.2 years (Table 5.1). Median time between diagnosis and surgery was 3 months (range from 0.1 to 19.1 months). Seventeen cases (45.9%) received surgery within 1 month and 16 cases (43.2%) within half a year of diagnosis. In three cases (8.1%), surgery was performed 6–12 months after diagnosis. One patient underwent surgical therapy after more than a year of wait-and-watch strategy. Mean follow-up time was 23.4 ± 24.1 months. Location included 11 intracranial (29.7%) and 26 orbital pathologies (70.3%; Fig. 5.3). Nine of the intracranial pathologies were tumor pathologies, whereas two were non-tumorous lesions. In orbital pathologies occurred 21 tumor diagnoses and five non-tumorous lesions (Figs. 5.4 and 5.5). Four cases with intracranial tumors and nine cases with orbital tumors received adjuvant therapy. The lesions were located as follows: orbit ($n = 26$), fronto-basal ($n = 7$), and sellar region ($n = 4$; Table 5.1). Supraorbital craniotomy was performed in 14 cases on the right side and in 23 cases on the left side.

The intracranial pathologies were epidermoid or dermoid ($n = 3$), arachnoid cyst, hypophysitis, hypothalamic hamartoma, Langerhans cell histiocytosis (LCH), low-grade glioma, neuroblastoma, osteosarcoma, and ossifying fibroma ($n = 1$), respectively. Orbital pathologies were ossifying fibroma ($n = 4$), low-grade glioma ($n = 4$), teratoma ($n = 3$), Langerhans cell histiocytosis (LCH, $n = 2$), lymphangioma ($n = 2$), refractory papilledema in idiopathic intracranial hypertension ($n = 2$), abscess,

Table 5.1 Patient characteristics

Affected side				
Right	14		37.8%	
Left	23		62.2%	
Age and sex	*Male*		*Female*	*Total*
Total patients	*18 (60%)*		*12 (40%)*	*30*
Mean age (years)	8 ± 6.5		*Range*: 0.3–29.2	
Location				
Orbit	26		70.2%	
Fronto-basal	7		18.9%	
Sellar region	4		10.8%	
Diagnosis	*Intracranial (n = 11)*		*Orbital (n = 26)*	
	Epidermoid cyst	2 (18.2%)	Ossifying fibroma	4 (20.0%)
	Arachnoid cyst	1 (9.1%)	Low-grade glioma	4 (16.0%)
	Dermoid	1 (9.1%)	Teratoma	3 (11.5%)
	Hypophysitis	1 (9.1%)	Langerhans cell histiocytosis	2 (7.7%)
	Ossifying fibroma	1 (9.1%)	Lymphangioma	2 (7.7%)
	Hypothalamic hamartoma	1 (9.1%)	Papilledema	2 (7.7%)
	Langerhans cell histiocytosis	1 (9.1%)	Abscess	1 (3.8%)
	Low-grade glioma	1 (9.1%)	Dermoid	1 (3.8%)
	Neuroblastoma	1 (9.1%)	Encephalocele	1 (3.8%)
	Osteosarcoma	1 (9.1%)	Foreign object	1 (3.8%)
			Malignant mesenchymal tumor	1 (3.8%)
			Meningioma	1 (3.8%)
			Neurofibroma	1 (3.8%)
			Osteosarcoma	1 (3.8%)
			Retinoblastoma	1 (3.8%)
Additional treatment, n = 30 (tumor cases only)				
Adjuvant therapy	13		43.3%	
Chemotherapy	13		100%	
Radiation	3		23.1%	
No adjuvant therapy	17		56.7%	
Outcome: tumor disease, n = 30 (tumor cases only)				
CR	13		43.3%	
SD	14		46.7%	
PD	1		3.3%	
Death	2		6.7%	

Table 5.1 (continued)

Affected side	
Outcome: non-tumor disease, n = 7	*Surgical goal achieved*
Foreign body (projectile from gunshot injury) (1)	Removal
Arachnoid cyst (frontotemporal) (1)	Fenestration with volume reduction
Orbital encephalocele (1)	Plastic reconstruction and tight dural closure
Orbital abscess (1)	Evacuation of abscess
Hypophysitis (1)	Histological confirmation
Idiopathic intracranial hypertension (2)	Fenestration of the optic sheet to sustain stable vision

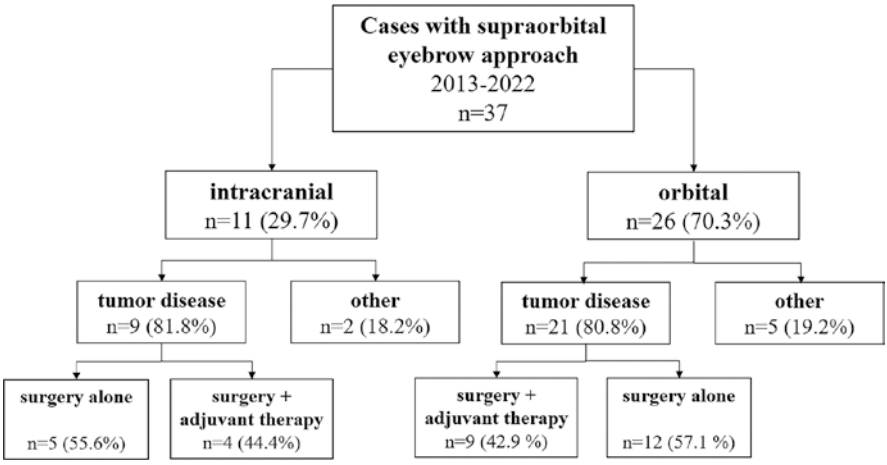

Fig. 5.3 Illustration of case enrolment and overview of intracranial and orbital pathologies

dermoid, encephalocele, foreign object, malignant mesenchymal tumor, meningioma, plexiform neurofibroma, osteosarcoma, and retinoblastoma (n = 1, respectively, Table 5.1).

The mean OR time was 163 ± 95 min. Postoperatively, approximately one third (n = 12) of cases were transferred to normal wards and the remainder (n = 25) to ICU. The mean ICU monitoring time was 1.44 days with a range of 1 to 6 days. In 32 cases, there was none or only one ICU overnight stay, three cases stayed for 2–3 days, and two cases stayed 4 days or longer due to the acute abscess formation for inflammatory and neurological observation and continuous intravenous antibiotic treatment and due to additional parallel extensive maxillofacial surgery. In three cases (ossifying fibroma and neuroblastoma pathology), the application of one red blood cell concentrate was necessary, respectively. Considering multiple surgeries,

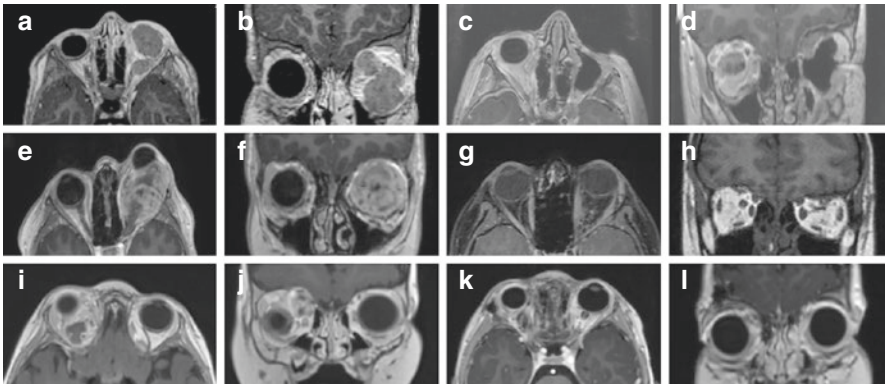

Fig. 5.4 Case illustrations – orbital pathologies. (**a**–**d**) Axial/coronal preoperative (**a**, **b**) and 6-month postoperative (**c**, **d**) T1-weighted Gd-enhanced MRI of a 3-year-old child with retinoblastoma in which the bulb excavation became necessary to achieve radical tumor resection. The patient developed tumor recurrence after radiation and chemotherapy and finally died. (**e**–**h**) Axial/coronal preoperative (**e**, **f**) and 1-year postoperative (**g**, **h**) T1-weighted Gd-enhanced MRI of an 11-year-old child with pilocytic astrocytoma grade 1 isolated to the optic nerve. A resection of the intraorbital as well as the prechiasmatic intracranial tumor portion was performed to achieve total resection and complete remission. (**i**–**l**) Axial/coronal preoperative (**i**, **j**) and 1-year postoperative (**k**, **l**) T1-weighted Gd-enhanced MRI of a 1-year-old child with ossifying fibroma of the orbital roof. After gross total resection, complete remission was achieved

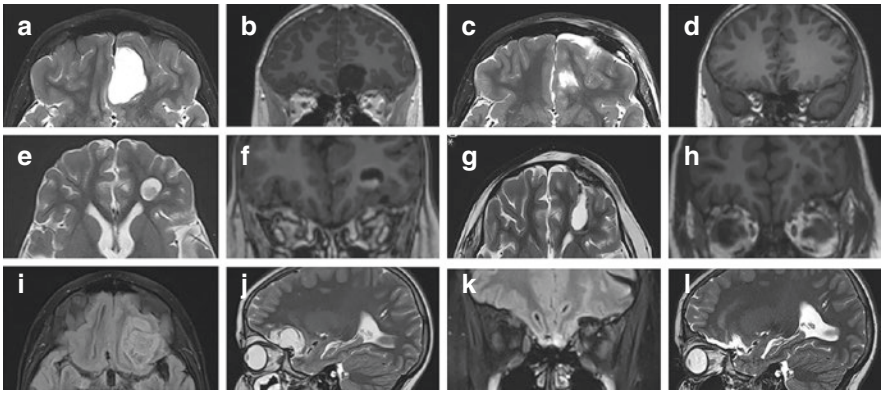

Fig. 5.5 Case illustrations – intracranial pathologies. (**a**–**d**) Axial/coronal preoperative (**a**, **b**) and early postoperative (**c**, **d**) T2-/T1-weighted MRI of an 11-year-old child with an epidermoid cyst. Complete resection was achieved and the cyst did not recur. (**e**–**h**) Axial/coronal preoperative (**e**, **f**) and early postoperative (**g**, **h**) T2-/T1-weighted Gd-enhanced MRI of a 6-year-old child with an intracerebral neuroblastoma who received complete tumor resection. After chemo- and radiation therapy, the patient died due to tumor recurrence. (**i**–**l**) Axial/sagittal preoperative (**i**, **j**) and coronal/sagittal 3-month postoperative (**k**, **l**) T2-FLAIR/T2-weighted MRI of a 12-year-old child with a disseminated low-grade glioma. The focal tumor mass could be resected completely, and LGG chemotherapy protocol was further applied

one 5-year-old patient was scheduled for surgery first on the left and then on the right side for papilledema in idiopathic intracranial hypertension. Five repeated surgeries on the same location were performed in four patients (Table 5.2). A 3-month-old patient with orbital teratoma received a biopsy at first, followed by a partial and eventually subtotal resection. Two patients with an ossifying fibroma underwent total resection after biopsy and subtotal resection, respectively. An orbital pilocytic astrocytoma in a 5-year-old patient was totally resected after initial tumor debulking when VEP potentials were still present at subjective state of amaurosis.

Postoperative imaging such as MRI or CT imaging in osseous lesions was used to determine the extent of resection: Total resection was successful in 20 cases, subtotal resection in six cases, and partial resection in one case. A biopsy was performed in three cases. In non-tumorous lesions, surgical goals were defined as follows: complete removal of an intraorbital projectile from a gunshot injury in a 29-year-old individual, volume reduction after fenestration of a frontotemporal arachnoid cyst in a 7-year-old patient, tight dural closure at fronto-basal level of an orbital encephalocele in a 4-year-old patient, evacuation of abscess, diagnostic yield in a biopsy, and maintaining stable vision in a 5-year-old patient with bilateral

Table 5.2 Treatment characteristics

	Mean ± SD/N	Range/percentage
Mean duration of hospital stay (d)	6.0 ± 1.9	2–28
Mean duration (min)	162.9 ± 94.8	
First day postoperative care		
Normal ward	12	32.4%
ICU	25	67.6%
Duration of ICU stay (days) mean: 1.44 ± 1.3, range: 1–6		
1	20	80.0%
2–3	3	16.0%
≥4	2	4.0%
Cases with need for RBC concentrate	3	8.6%
Extent of resection (tumor), $n = 30$		
Total	20	66.7%
Subtotal	6	20.0%
Partial	1	3.3%
Biopsy	3	10.0%
Complications		
No	35	94.6%
Yes	2	5.4%
Overview of further surgeries $n = 5$ cases	*First surgery*	*Further surgeries*
Teratoma	Biopsy	Partial resection, subtotal resection
Ossifying fibroma	Subtotal resection	Total resection
Ossifying fibroma	Biopsy	Total resection
Pilocytic astrocytoma	Biopsy	Total resection

papilledema in idiopathic intracranial hypertension. The surgical goals could be achieved in all patients, accordingly (Fig. 5.6).

Complications occurred in two individuals (5.4%). The first patient with a postoperative periorbital inflammation was treated by seroma puncture and successful targeted antibiotic treatment. The second patient involved one revision surgery due to loosening of osteosynthesis material. Cosmetic result as judged by the parents and the surgeons remained excellent during follow-up. No postoperative hemorrhage or cerebrospinal fluid leak was observed.

Ophthalmological findings were included in 28 cases according to the International Statistical Classification of Diseases and Related Health Problems. Eight patients suffered from amaurosis in the affected side from the beginning. Two

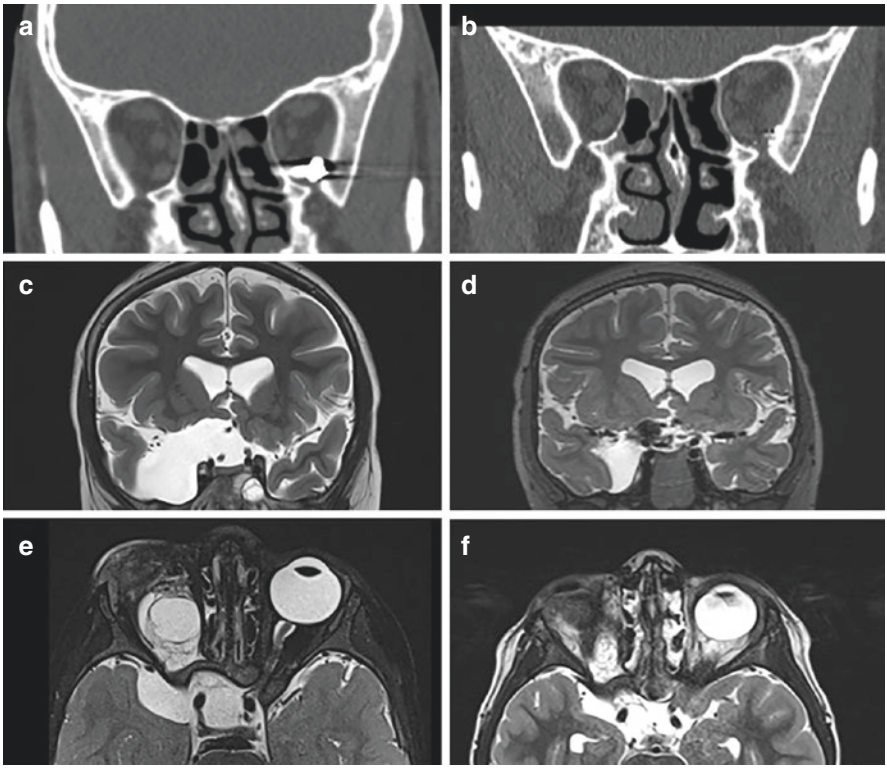

Fig. 5.6 Case illustrations – non-tumor pathologies. (**a**, **b**) Coronal preoperative (**a**) and early postoperative (**b**) CT scan of a 29-year-old patient with an intraorbital projectile after gunshot injury. The patient insisted on removal of the foreign body material, which could be achieved without complications. (**c**, **d**) Coronal preoperative (**c**) and 6-month postoperative (**d**) T2-weighted MRI of a 7-year-old child with a frontotemporal arachnoid cyst, which was endoscopically fenestrated through a supraorbital burr hole via eyebrow incision. The cysts significantly decreased in volume. (**e**, **f**) Axial preoperative (**e**) and 12-month postoperative (**f**) T2-weighted MRI of a 4-year-old child with an orbital encephalocele. There was a congenital malformation of the eye bulb. Surgery achieved dura reconstruction and resection of the meningoencephalocele

Table 5.3 Ophthalmologic evaluation of the affected eye (available findings from 28 individuals)

Category		<	≥	On admission	60 days after surgery	Last follow-up
0	Mild or no visual impairment		0.3	17 (60.7%)	19 (67.9%)	19 (67.9%)
1	Moderate visual impairment	0.3	0.1	2 (7.1%)	0 (0.0%)	0 (0.0%)
2	Severe visual impairment	0.1	0.05	1 (3.6%)	1 (3.6%)	1 (3.6%)
3	Amaurosis	0.05	0.02	0 (0.0%)	0 (0.0%)	0 (0.0%)
4	Amaurosis	0.02	Light perception	0 (0.0%)	0 (0.0%)	0 (0.0%)
5	Amaurosis	No light perception		8 (28.6%)	8 (28.6%)	8(28.6%)
			Total:	28 (100%)	28 (100%)	28 (100%)

According to International Classification of Diseases and Related Health Problems 10th Revision (ICD-10)-WHO-Version 2016

patients with moderate visual impairment improved to normal eye vision at 2-month follow-up. In all other patients, stable eye vision was maintained, and no visual impairment occurred (Table 5.3).

In the 30 tumor cases, the last available radiologic imaging was assessed for treatment response. The majority of cases (90%) displayed a favorable outcome with complete remission (CR, 43%) and stable disease (SD, 47%), respectively. Progressive disease (PD) was observed in one case with ossifying fibroma (3%), and two patients died during the observation period, both due to therapy refractory tumor malignancy (7%). One patient suffered from a retinoblastoma, while the other patient was diagnosed with a neuroblastoma (Fig. 5.4b).

5.4 Discussion

The purpose of keyhole neurosurgery is the optimal exposure of the affected anatomical structure at minimum opening or retraction and manipulation of non-targeted tissue. Pathologies involving the orbit or optic pathway are challenging for surgical resection due to their anatomical complexity. These interventions require careful planning and selection of an appropriate approach. Walter Dandy was the first neurosurgeon in the early twentieth century to report a transcranial subfrontal unilateral approach that provided access to the orbit as well as the optic canal and optic chiasm [14]. The supraorbital "keyhole" craniotomy via eyebrow incision was well described by Jane in 1982 [2] and adapted over the following decades, notably by Delashaw [15] and Perneczky [5]. However, this approach has been mostly used in adult patients, and evidence is scarce on its implementation in children. A case

series of 54 patients by Dlouhy from 2015 is of particular note [9]. Differences between their and our technical approach are, however, worth mentioning. They used a more medialized skin incision of the entire length of the eyebrow which might increase the likelihood of sensory disturbances due to affection of the supraorbital nerve. In addition, the craniotomy by Dlouhy et al. was applied with a craniotome and did not include the orbital rim. The bony gap between the bone flap and the surrounding calvarium thus increases which may result in uneven skin surface and possible bone dislocation. This issue was solved in their report by using CranioFix (BBraun-Aesculap, Tuttlingen, Germany) to keep the bone at its correct level. This might, however, be bulging through the skin and will cause problems in redo cases since the foreign material of titanium is difficult to remove at the inner cortical surface. Not including the orbital rim will restrict the access especially to the orbit. The study, however, presented similar favorable cosmetic results and represented a comparable heterogeneous group of histopathological indications.

5.4.1 Feasibility and Exposition of Targeted Structure

The supraorbital keyhole approach was shown to provide comparable insight into parasellar, suprasellar, and anterior fossa lesions compared to the standard pterional or supraorbital approach [16, 17]. This case series included intracranially located lesions consisting of fronto-basal and supra- and parasellar pathologies located in the optic pathway and fronto-temporally, and all showed decent intraoperative visualization of the lesion being excised via keyhole approach. It is important to mention that intraoperative navigation supported by augmented reality facilitates the approach toward intracranial lesion via a small craniotomy. Effective handling of two instruments together with the visual axis of the microscope requires experience and is a key for a minimally invasive surgical resection in those cases.

The orbital pathologies in this study (67.6%) could be well visualized by applying the supraorbital keyhole approach. The approach specifically fits the lesions located in the upper lateral or the central regions of the orbit accessible from the upper lateral quadrant in which the oculomotor musculature opens a natural window to intraorbital structures. The literature confirms that a transcranial approach is particularly suitable for orbital pathologies in this location, whereas an endoscopic transnasal approach should be chosen for processes located further medially toward the ethmoids [18]. In special cases, an interdisciplinary cooperation of ophthalmologists, maxillofacial physicians, and neurosurgeons becomes very helpful.

5.4.2 Surgical Outcome and Complications

Total resection of all lesions operated on in this study was achievable in 67% of cases, and subtotal resection was possible in 20% of cases. In patients with tumor disease, a favorable oncologic outcome in terms of CR or SD was achieved in 90%

of cases. The remaining cases needed either repeated surgery ($n = 1$) or were not curable by adjuvant therapy. The supraorbital eyebrow approach proved to be beneficial for maintaining a stable vision with a reasonable low complication rate. In only two cases, complications occurred which could be managed conservatively. Meningitis or CSF leaks did not occur.

Optimal patient positioning is crucial for achieving proper access toward the targeted structure, for example, the gravity moves the frontal lobe out of the field of access, thereby minimizing brain retraction and improving the trajectory for intraorbital lesions. In addition, neuronavigation in combination with augmented reality of target lesions and possible regions at risks is extremely helpful to optimally place the visual axis toward the lesion and anticipate spatial relationships and dimensions via a minimally invasive access without the need to implement a pointer in the surgical site or to recognize the navigation screen during surgery [11, 12, 19]. Furthermore, the most effective handling of instruments in relation to the optical axis of the microscope in small spaces is crucial. This requires experience and training. It depends on acquired skills in other approaches and has a non-negligible impact on the clinical and surgical outcome of patients. In some cases, assisted endoscopic inspection provides additional overview in the deep-seated cavities to better control completeness of resection, accordingly.

5.4.3 Conclusion

The supraorbital eyebrow approach is feasible and safe in well-selected pediatric neurosurgical cases and should be considered for intraorbital as well as fronto-basal pathologies especially extending toward the upper lateral quadrant as well as ipsilateral intracranial lesions adjacent to the skull base. Technical advances such as navigation and augmented reality as well as assisted endoscopic inspection offer advantages which supports the success of surgery. Surgical experience and interdisciplinary cooperation enable a broader spectrum of surgical options in complex, fronto-basal, skull base pathologies.

References

1. Delashaw JB Jr, Tedeschi H, Rhoton AL. Modified supraorbital craniotomy: technical note. Neurosurgery. 1992;30(6):954–6.
2. Jane JA, et al. The supraorbital approach: technical note. Neurosurgery. 1982;11(4):537–42.
3. Jho HD. Orbital roof craniotomy via an eyebrow incision: a simplified anterior skull base approach. Minim Invasive Neurosurg. 1997;40(3):91–7.
4. Reisch R, et al. Patients' cosmetic satisfaction, pain, and functional outcomes after supraorbital craniotomy through an eyebrow incision. J Neurosurg. 2014;121(3):730–4.
5. van Lindert E, et al. The supraorbital keyhole approach to supratentorial aneurysms: concept and technique. Surg Neurol. 1998;49(5):481–9; discussion 489–90.

6. Steiger HJ, et al. Transorbital keyhole approach to anterior communicating artery aneurysms. Neurosurgery. 2001;48(2):347–51; discussion 351–2.
7. Wilson DA, et al. The supraorbital endoscopic approach for tumors. World Neurosurg. 2014;82(1–2):e243–56.
8. Fatemi N, et al. Endonasal versus supraorbital keyhole removal of craniopharyngiomas and tuberculum sellae meningiomas. Neurosurgery. 2009;64(5 Suppl 2):269–84; discussion 284-6.
9. Dlouhy BJ, Chae MP, Teo C. The supraorbital eyebrow approach in children: clinical outcomes, cosmetic results, and complications. J Neurosurg Pediatr. 2015;15(1):12–9.
10. de Oliveira RS, et al. The supraorbital eyebrow approach for removal of craniopharyngioma in children: a case series. Childs Nerv Syst. 2018;34(3):547–53.
11. Pennacchietti V, et al. First experience with augmented reality neuronavigation in endoscopic assisted midline skull base pathologies in children. Childs Nerv Syst. 2021;37(5):1525–34.
12. Thomale UW, Stover JF, Unterberg AW. The use of neuronavigation in transnasal transsphenoidal pituitary surgery. Zentralbl Neurochir. 2005;66(3):126–32; discussion 132.
13. Zipfel J, et al. Surgical management of pre-chiasmatic intraorbital optic nerve gliomas in children after loss of visual function-resection from Bulbus to chiasm. Children (Basel). 2022;9(4):459.
14. Dandy WE. Prechiasmal intracranial tumors of the optic nerves. Am J Ophthalmol. 1922;5:169–88.
15. Delashaw JB Jr, et al. Supraorbital craniotomy by fracture of the anterior orbital roof. Technical note. J Neurosurg. 1993;79(4):615–8.
16. Cheng CM, et al. Quantitative verification of the keyhole concept: a comparison of area of exposure in the parasellar region via supraorbital keyhole, frontotemporal pterional, and supraorbital approaches. J Neurosurg. 2013;118(2):264–9.
17. Figueiredo EG, et al. An anatomical evaluation of the mini-supraorbital approach and comparison with standard craniotomies. Neurosurgery. 2006;59(4 Suppl 2):ONS212–20; discussion ONS220.
18. Abussuud Z, Ahmed S, Paluzzi A. Surgical approaches to the orbit: a neurosurgical perspective. J Neurol Surg B Skull Base. 2020;81(4):385–408.
19. Finger T, et al. Augmented reality in intraventricular neuroendoscopy. Acta Neurochir. 2017;159(6):1033–41.

Chapter 6
Optic Pathway Gliomas: The Trends of Basic Research to Reduce the Impact of the Disease on Visual Function

Federico Bianchi, Federico Maria Cocilovo, Antonio Ruggiero, and Gianpiero Tamburrini

6.1 Introduction

6.1.1 Epidemiology of OPG

Pediatric optic pathway gliomas (OPG) are low-grade brain tumors characterized by slow progression and invalidating visual loss. The most common histologies are WHO grade I juvenile pilocytic astrocytomas and pilomyxoid astrocytomas [1]. They represent approximately between 4% and 6% of all brain tumors in childhood, with 65% of the cases affecting children under the age of 5 years [2–4]. Neurofibromatosis type 1 (NF-1) is frequently documented in OPG patients being the evidence of bilateral OPG almost considered pathognomonic for the condition. In fact, such association is reported ranging from 10% to 70% [5, 6]. On the other hand, up to 15–20% of patients with NF-1 will have optic nerve glioma [5, 7]. OPGs can involve optic nerves, chiasm, or optic tracts and can extend posteriorly including optic radiations. It is interesting to underline how bilateral OPGs in NF-1 are often isolated to the optic nerve without intracranial extension in comparison with

F. Bianchi (✉)
Fondazione Policlinico Gemelli IRCCS, Rome, Italy
e-mail: federico.bianchi@policlinicogemelli.it

F. M. Cocilovo
Università Cattolica del Sacro Cuore, Milan, Italy

A. Ruggiero · G. Tamburrini
Fondazione Policlinico Gemelli IRCCS, Rome, Italy

Università Cattolica del Sacro Cuore, Milan, Italy
e-mail: Antonio.ruggero@policlinicogemelli.it; gianpiero.tamburrini@unicatt.it

C. Di Rocco (ed.), *Advances and Technical Standards in Neurosurgery*, Advances and Technical Standards in Neurosurgery 48,
https://doi.org/10.1007/978-3-031-36785-4_6

non-NF1 patients in which the lesion often involves the chiasm, posterior optic pathways, and the hypothalamus [5, 8].

6.1.2 OPG Management

OPG management in children remains controversial because of some specific features of these tumors. Such features are (a) the variable clinical course; (b) the absence of clinical, radiological, or even histologic criteria that allow differentiation between aggressive and indolent forms; and (c) the unpredictable response to various treatment modalities and the long life expectancy in several subjects, which is associated with significant functional deficits [9].

Untreated OPG physiological course is characterized by deterioration of visual acuity, progressive visual field deficits, and endocrine impairment; up to 30% of the patients may eventually die due to local tumor invasion and progression [7]. Therapeutic strategies include surgery, radiotherapy, chemotherapy, and combinations of these modalities. Tumor typical location usually precludes complete and radical surgical resection or optimum radiation dosing without an unacceptable neurological deficit. Thus, OPG management is highly individualized. Many children undergo a period observation with serial MRI unless there is a progressive growth or the beginning of visual symptoms.

The traditional management in the past has been represented by surgery, followed by radiotherapy in case of tumor progression [9, 10]. However, taking into account the possible disastrous sequelae of extensive treatment particularly in young children, most authors prefer to choose a more conservative approach. The diffusion of advanced neuroimaging techniques as well as the introduction in the clinical practice of new chemotherapeutic agents has contributed to the aforementioned change in the policy of treatment of the disease aimed at minimizing treatment-related morbidity in favor of the patient's quality of life [9].

The concept is even more valid in NF-1 patients, with OPG having a documented more benign and indolent course in these cases [4, 11–14].

In order to address the need for appropriate treatment strategies, the scientific community devised the Dodge classification in which OPGs are divided according to tumor extension (Table 6.1).

Both open craniotomic and endoscopic approaches have been considered for the surgical management.

Intraorbital Dodge type I optic nerve tumors or exophytic globular cystic tumors poorly infiltrating the neighboring structures are probably the only two conditions in which total tumor removal can be considered as a stand-alone treatment [9, 10, 15]. On a different note, gross total debulking is an option in the case of progressing tumors that do not respond to an integrated neoadjuvant treatment [9, 16]. In these cases, the main goal is to decompress the optic pathways preserving visual function [9, 17–19]. A further surgical indication regards the necessity to obtain rapid relief

Table 6.1 Dodge classification

Original dodge	PLAN classification	Description	Subcategories	(Description)
A	1a	Single optic nerve	1aL/R	Left/right
	1b	Bilateral optic nerve	1bL/R	Left>right/ right>left
	1c	Cisternal segment optic nerve	1cL/R/B	Left/right/ bilateral
			1cbL/R	Left>right/ right>left
B	2a	Central chiasmatic	2a	
	2b	Asymmetric chiasmatic	2bL/R	Left>right/ right>left
			2cL/R	Left only/right only
C	3	Optic tract	3 L/B/R	
	3b	Asymmetric tracts	3bL/R	Left>right/ right>left
	4	Diffuse posterior tracts	4L/B/R	Left/right/ bilateral
	4b	Asymmetric posterior tracts	4bL/R	Left>right/ right>left
	H+/−	Hypothalamic involvement		
	LM+/−	Leptomeningeal involvement		
	NF1+/−	Neurofibromatosis type 1		

of raised intracranial pressure in children with large tumors [9], which includes children with quickly enlarging tumoral cysts [9, 10, 20].

As for the neuroendoscopic management of OPG, transventricular marsupialization of neoplastic cysts into the ventricular system may offer the possibility to reduce the neoplastic mass effect [9, 20]. Tumor biopsy for molecular diagnostic purposes and the possibility to aid the treatment of the associated hydrocephalus are further purposes that may be reached with an endoscopic transventricular approach. The transsphenoidal route is a further option for endoscopy that may be considered in tumors whose prevalent growth is inside the sella with upward displacement of the optic chiasm.

Chemotherapy with primarily carboplatin-based regimens remains however the OPG predominant treatment modality. Most of them use a combination of carboplatin and vincristine, the still commonly followed one being the SIOP 2004 protocol. This regimen was initially used in children with low-grade gliomas and has been found to have a progression-free survival (PFS) of 75% at 2 years and 68% at 3 years [5, 21].

Some authors also suggested vinblastine monotherapy reporting a progression-free survival of 53.2% over 5 years associated with a 20% of patients with improved

visual acuity [5, 22]. Throughout the literature, there are plenty of alternative regimens with similar efficacy to the standard ones, the most common foreseeing the use of thioguanine, procarbazine, lomustine, and vincristine (TPCV) with or without dibromo-dulcitol [5, 23, 24]. However, these regimens represent a second-line treatment due to the increased risk of secondary neoplasms, particularly in patients with NF-1. For similar reasons, cisplatin and etoposide that demonstrated promising results are still not considered as first choice due to their ototoxicity [5, 25, 26].

In more recent years, monotherapies with temozolomide [27, 28], vinblastine [22, 27, 29], and vinorelbine [27, 30] have also been proposed for progressive or refractory disease with positive results and low toxicity.

Furthermore, MEK inhibitors such as selumetinib, refametinib, trametinib, and cobimetinib have recently been employed in the treatment of progressive and recurrent low-grade gliomas in children, with a 2-year PFS of up to 69% [27, 31].

Recently, bevacizumab has emerged as a promising treatment for OPGs expressing BRAF mutations [32], including those isolated to the optic nerve. Bevacizumab-based therapy has actually achieved objective responses and rapid improvement in visual symptoms in up to 86% of refractory cases [32]. Such good responses have been reported in monotherapy as well as in combination with irinotecan or other traditional agents [32–37].

Radiation therapy is an additional adjuvant treatment option. In the past, treatment with external beam radiation achieved up to 90% 10-year PFS [38]. However, this came at the expense of long-term endocrine abnormalities [38], cerebrovascular disease [39, 40], poor visual outcomes [38], secondary malignancies [40–42], and neurocognitive deficits, particularly in children lower than 5 years [43, 44]. The aforementioned complications depend on a lack of a defined optimal dose of RT in children with low-grade gliomas. The difficulty in defining it depends on various influencing factors, such as patient's age, tumor volume, and usual eloquent location.

Several studies on RT for OPGs defined optimal overall dose around 45–65 Gy administered in a fractionation scheme of 150–200 cGy per fraction [9]. One of the most common dosage schedules consists of administering an overall dose of 45–50 Gy for chiasmatic tumors and 50–55 Gy for prevalently hypothalamic tumors in fractions of 180 cGy each [9].

Regardless of NF1 status, RT is nowadays considered a last resort typically reserved to older patients or to those with no remaining chemotherapeutic options. Newer RT techniques such as conformal treatment [45], fractionated stereotactic radiation therapy [18, 46, 47], proton beam radiation therapy [48], and stereotactic radiosurgery [49, 50] have been pursued to minimize radiation dose to surrounding structures [51]. Although positive results have been reported, long-term outcomes and adverse events are pending.

6.2 The Influence of Available Treatments of OPG on Visual Function

In OPG patients, it is important to differ between PFS/OS and visual outcome, the two of them not being necessarily related. Visual outcome can be bad indeed even in the case of a stable tumoral condition.

Moreover, in most cases, available treatment strategies have limited possibilities to improve vision. Dodgshun and colleagues reported that 32% of children with chiasmatic/hypothalamic tumors experienced a long-term deterioration in vision and 45% were legally blind at the time of latest follow-up [11, 33], with a substantial lack of radiological prediction factors and visual deficit progression occurring in spite of a tumor response to oncological treatment [11].

The dissociation between PFS/OS and visual outcome is documented by what happens in NF1 patients.

In fact, in this specific category of children, in spite of a generally indolent course of the tumor, visual deficits tend to worsen over time. In the series of Campagna et al., visual deficit progression occurred in 56% of the cases in a mean follow-up of 6 years. A further factor that does not seem to be related with visual outcome is the rate of tumor resection; an independent progression not only of visual acuity but also of other associated ophthalmological parameters (VF, color, and contrast sensitivity) has been reported contributing to the compromise of the visual function [52].

In the attempt to define prognostic data on visual acuity, Tow et al. tried to connect Dodge grading with visual outcome failing in demonstrating an association between lower grade and better outcome [20].

Another debated issue is the role of RT on visual outcome. Acharya et al. carried out a study on 3D conformal photon therapy (total dose was 54 Gy in 1.8 Gy fractions over 6 weeks), intensity-modulated photon therapy, or intensity-modulated proton therapy (total dose of 52.2 GyRBE in 1.8 GyRBE fractions over 5.8 weeks in 41 patients with a median age at RT of 8 years). At a mean follow-up of 5 years, the cumulative incidence of visual acuity decline was approximately 15% in the worse eye and 10% in the better eye, with most of the visual acuity changes occurring within the first 2 years after the completion of RT. No correlation was found between visual acuity decline and radiographic progression of the tumor, highlighting the need to include VA as an independent outcome measure when evaluating the treatment of OPG.

An interesting observation from the author came from the evidence that 67% of tumors tested for BRAF alterations had a BRAF fusion and 13% had a BRAF V600E mutation. Even though no actual paper addresses the effect on visual acuity and BRAF antagonism, recent papers showed how MEK inhibitors (MEK-I) and BRAF inhibitors (BRAF-I) held promise in treating low-grade gliomas with BRAF alterations. Nonetheless, there is a lack of evidences in terms of whether the aforementioned new drugs might grant result in the preservation of vision [53, 54].

Radiosurgery has been considered as an alternative to radiotherapy and proton beam treatment in order to reduce radiation effects on visual function. El-Shehaby

et al. evaluated the effect of a single-session Gamma Knife radiosurgery in five children with optic nerve gliomas and 30 with hypothalamic/chiasmatic gliomas.

The visual field improved in seven (20%) cases, remained stable in 26 (74.3%), and became worse in two (5.7%) with a cumulative visual preservation rate of 94.3%. Visual improvement was observed at 3 to 12 months after treatment in three children and at 17 and 24 months in further two cases, in which an initial transient visual deterioration was documented. Vision was normal in eight cases before treatment; no worsening was found after treatment. Of the eight cases in which blindness was present before treatment, visual improvement was documented only in three. Finally, among 19 cases with pretreatment visual defects, four improved, 13 remained stable, and two worsened. Tumor progression was documented in the only patient with bilateral visual deterioration after treatment [49].

A systematic review of the effects of chemotherapy on visual outcome showed that less than 15% of cases had an improvement in vision, with deterioration occurring in 40% of the cases [55]. In patients with NF-1 treated with chemotherapy, visual acuity was found to remain stable or improved in 72% of patients and declined in 28% of patients. Many of these cases began treatment less than 5 months from the diagnosis, suggesting that earlier treatment may improve visual outcome [56].

6.3 Perspectives in the Medical Treatment of Visual Deficits in Children with OPGs

Retinal ganglion cells (RGCs), in particular retinal nerve fiber layer (RNFL), represent a major target of disease-induced visual damage in OPGs [12]. A reduction in RNFL thickness is in fact proportionally related to visual loss in children with optic pathway gliomas [57].

One of the most important receptors in RGC cells is the nerve growth factor one (NGF 1), which is extensively expressed, together with TrkA and $p75^{NTR}$, in the anterior ocular segment [58–63] in the cornea, iris, ciliary body, lens, and aqueous humor [13]. Furthermore, NGF plays an important role in ocular and vision homeostasis as highlighted from both in vitro and in vivo studies [61, 64].

The idea of using NGF to treat visual disturbances in OPGs came from coupling the described extensive ocular NGF involvement with multiple literature report on NGF treatment of CNS disorders [65–72]. In particular, Chiaretti et al. described the effect of intraventricular/intracerebral NGF administration in hypoxic–ischemic brain injury documenting how, after administration, there was a significant improvement in motor and cognitive functions, with good recovery of level of awareness, purposeful movements, and improvements in communicative skills [73]. The authors linked these results to the NGF-induced enhancement of cholinergic brain functions as well as to the improvement of cerebral perfusion and stimulation of the pathway of neurogenesis differentiation with the activation of doublecortin biosynthesis [69, 74]. Furthermore, in 2017, Chiaretti et al. also reported the intranasal use

of NGF in traumatic brain injury highlighting not only the potential use of this drug in neuroprotection but also showing how different administration routes are possible [66].

Pharmacodynamic studies in vitro have shown that the NGF administered as eye drops is able to reach not only the ocular surface but also the retina and the optic nerve [14, 58, 61, 75–79].

One of the major contributions in the understanding of NGF ocular administration comes from the work of Lambiase and colleagues. The author published several papers on the matter starting from 1998 when they described the effect of NGF administration on corneal neurotrophic ulcers. In this paper, the author reports the treatment of 12 patients, with severe corneal neurotrophic ulcers associated with corneal anesthesia, with topical nerve growth factor ten times daily for 2 days and then six times daily until the ulcers healed. The described treatment lasted for 2 weeks after ulcers healed with a mean follow-up of 15 months. During treatment and follow-up, slit-lamp examination, photography, fluorescein-dye testing, tests of corneal sensitivity, and best-corrected visual acuity were performed finding how all patients had complete healing of their corneal ulcers after 10 days to 6 weeks of treatment. Furthermore, corneal sensitivity improved in 13 eyes and returned to normal in two of them [61].

The 1998 results lead to a 2005 study that represents the most important contribution of the group. The authors aimed, in fact, to establish the bioavailability of topical NGF to the retina and optic nerve in rats. In doing so, they divided five groups of eight rats each performing autoradiography to evaluate whether exogenous 125I-labeled NGF reaches the retina and optic nerve when applied topically to the rat conjunctiva. ELISA testing was done to the retina, optic nerve, lens, sclera, and serum of rats at different time points after NGF administration (1–500 g/mL), while physiological activity of topically applied NGF was evaluated by determining retinal brain-derived neurotrophic factor (BDNF) protein and mRNA levels.

The five groups were so composed:

1. Not treated control group
2. Saline-treated group
3. 10 g/mL concentration
4. 200 g/ml concentration
5. 500 g/mL concentration

The first two groups were used to determine basal, physiologic expression of NGF mRNA and protein in the retina, optic nerve, lens, and sclera, while the remaining three groups were treated instilling NGF into the conjunctival fornix of one randomly selected eye. After 6 hours, the animals were sacrificed and the previously reported evaluation was carried on intraocular and serum NGF mRNA and protein levels were determined as described earlier.

From such analysis, it was determined how after 200 g/mL NGF administration there was a twofold increase in NGF levels in both the retina and optic nerve 6 hours after treatment (P 0.01). Not only it was possible to assess NGF arrival in the interested structures, but also it was feasible to determine increase in BDNF protein and

mRNA levels in rat retina showing the persistence of NGF vitality at target. In fact, NGF administration leads to an approximate threefold increase of basal BDNF protein levels, a significant increase compared with both basal and contralateral eyes (P 0.005). Finally, an interesting fact resides in the evidence of BDNF protein increase in both the treated and contralateral eyes [78].

Further interesting reports came from the work of Di Fausto et al. who tried to understand the mechanism responsible through which NGF reaches brain neurons includes anatomical connections between the eye and the brain. The author suggested that cholinergic neurons might represent the highway NGF travels to reach the forebrain. In order to better define the aforementioned route, Di Fausto et al. analyzed NGF application on eye surface of chemically injured BFCN through administration of ibotenic acid (IBO) to cause loss of neurons.

In doing so, an animal model was created subdividing mice into three groups:

1. 16 consecutive days of treatment with a solution containing 200 mcg/mL of NGF applied as collyrium to both eyes
2. 16 consecutive days of treatment with a collyrium solution containing 200 mcg/mL of cytochrome C, a compound with the physiochemical properties of NGF, but lacking its biologic activity
3. 16 consecutive days of treatment with a collyrium solution containing 200 mcg/mL of cytochrome

The authors describe how NGF eye administration, compared with the other group, leads to an increase in NGF cerebral availability. In particular, the normalization of the cholinergic pathway connecting the eye and the brain, as documented by the normalization in choline-acetyltransferase immunopositivity, indicates a restoration of NGF levels. Such a result may be related to an enhanced capacity of NGF-receptive cells to respond to the elevated NGF availability [76].

The last paper of interest is the one of Coassin and colleagues in which they sought to hinder retinal damage during experimental glaucoma with timely changes in NGF and its receptors, trkA^{NGFR} and p75^{NTR}. In the paper, a model of induced glaucoma in rat was constructed sacrificing the animal after 10, 20, and 35 days. Taking into account the linkage between RGC apoptosis and NGF retinal expression, an analysis of Bcl-2, Bax, trkA^{NGFR}, and p75^{NTR} transcript was performed.

In their work, Coassin et al. demonstrated RGC loss coupled by a timely increase in retinal NGF. In addition, the trkA^{NGFR}/p75^{NTR} mRNA ratio and the Bcl-2/Bax mRNA were decreased, indicating a p75^{NTR} and Bax overexpression. Those results suggest how NGF increase though present is unable to prevent RGC loss.

Even though some authors disagree with NGF efficacy in preventing RGC loss [80, 81], Coassin and colleagues argue that such a finding might be linked to a different relative expression of trkA^{NGFR} and p75^{NTR} by RGCs upon different circumstances. To demonstrate the aforementioned idea in this paper, the authors measured retinal expression of NGF, trkA^{NGFR}, and p75^{NTR} after 10, 20, and 35 days of elevated intraocular pressure correlating them with Bcl-2 and Bax expression. Intraocular hypertension was obtained through intraocular saline injection. The previously reported analysis showed how only at 35 days from saline injection, NGF increases

compared to controls ($p < 0.05$). Furthermore, injected retinas seem to undergo a progressive time-dependent NGFmRNA increase compared to controls. In order to understand such a finding, $trkA^{NGFR}$ levels were slightly decreased at 10 days, mildly increased at 20 days, and overexpressed at 35 days from injection, when compared to controls, while p75mRNA levels progressively increased during the experimental period. $TrkA^{NGFR}/p75^{NTR}$ mRNA ratio seems to decrease progressively depending on Bcl2/Bax mRNA ratio. Those results might explain the lack of sufficiently elevated NGF levels in association with a progressive upregulation of $p75^{NTR}$ in relation to $trkA^{NGFR}$ [14].

Starting from the work of Coassin et al., more recent papers highlighted how increasing NGF ocular levels through eye drop instillation, there might be a more extensive NGF link to TrkA with secondary Bcl-2 protein upregulation whose effects prevent caspase activation reducing RGC loss [75]. Furthermore, the long-lasting effect of the eye administration might suggest an ulterior protection mechanism related to new neural pathway formations [82, 83].

In order to further study the efficacy of NGF eye drop administration in improving visual outcome, in 2011 Falsini et al. devised a randomized, double-blind, placebo-controlled clinical study in patients with OPG-associated visual loss. NGF court received a total of 0.5 mg NGF diluted in 2.5 ml saline solution that was administered to the conjunctiva of both eyes (one drop each eye) three times a day, for 10 consecutive days. On the other hand, control group received a placebo. Both groups were assessed by physical examination and visual function tests, including physiological subjective and electrophysiological objective measures at baseline, 15, 30, 90, and 180 days posttreatment.

Main outcome variables were:

1. Best-corrected EDTRS visual acuity (BCVA)
2. Goldman perimeter visual field size (V/4 e Isoptera)
3. Amplitude and latency of the electroretinographic photopic negative response (PhNR)—a valuable tool for monitoring longitudinal change in RGC function in humans [84]
4. Amplitude and latency of the first and second harmonic components of the flicker VEP recording—a tool for monitoring visual cortical function, which has proved reliable in monitoring OPG progression [85]
5. RNFL thickness obtained from optical coherence tomography screening—a measure whose alteration has been shown to correlate with visual loss in a cross-sectional study of OPG in children [86]

Physiological measures of visual function were included as secondary outcome measures, while electrophysiological (VEP and electroretinogram) and anatomical (optical coherence tomography RNFL) ones were the main outcomes in the evaluation of potential drug efficacy.

Analyzing the results emerged how, despite the considerable degree of variability among OPG children, only placebo-treated patients presented major worsening, while the greatest improvements from baseline were in NGF-treated ones.

Multivariate analysis including all six electrophysiological experimental outcomes showed significant effects of the treatment on the PhNR and the VEP first harmonic amplitude. In particular, this model showed statistically significant mean differences between NGF-treated and placebo group of PhNR amplitude at 180 days (P 50.01) and of PhNR latency at 15 days (P 50.01) and at 180 days (P = 0.02) and of VEP first harmonic amplitude at 30 days (P50.01). There were no other statistically significant differences between the two study groups [87].

Clinically evaluating the patients treated with NGF, it was possible to assess how visual field improvement was more frequent compared with placebo-treated eyes (five versus one eyes, three versus one patients, respectively), while visual acuity did not show any significant change over the trial [87].

6.4 Conclusion

OPG treatment is a complex and multidisciplinary matter. Despite the histological benignity of the tumor, patients can carry significant disability primarily linked to visual loss. Nowadays, there is no effective treatment to prevent or to revert it; nonetheless, there are a crescent number of studies highlighting how NGF eye drop administration could improve visual campimetry and protect visual capability in such patients.

Further studies are warranted to promote and investigate such a potential treatment as a way to offer better treatment and better quality of life.

References

1. Binning MJ, Liu JK, Kestle JRW, Brockmeyer DL, Walker ML. Optic pathway gliomas: a review. Neurosurg Focus. 2007;23(5):E2.
2. Jahraus CD, Tarbell NJ. Optic pathway gliomas. Pediatr Blood Cancer. 2006;46(5):586–96.
3. Kelly JP, Leary S, Khanna P, Weiss AH. Longitudinal measures of visual function, tumor volume, and prediction of visual outcomes after treatment of optic pathway gliomas. Ophthalmology. 2012;119(6):1231–7.
4. Thiagalingam S, Flaherty M, Billson F, North K. Neurofibromatosis type 1 and optic pathway gliomas: follow-up of 54 patients. Ophthalmology. 2004;111(3):568–77.
5. Rasool N, Odel JG, Kazim M. Optic pathway glioma of childhood. Curr Opin Ophthalmol. 2017;28(3):289–95.
6. Sylvester CL, Drohan LA, Sergott RC. Optic-nerve gliomas, chiasmal gliomas and neurofibromatosis type 1. Curr Opin Ophthalmol. 2006;17(1):7–11.
7. Blazo MA, Lewis RA, Chintagumpala MM, Frazier M, McCluggage C, Plon SE. Outcomes of systematic screening for optic pathway tumors in children with Neurofibromatosis type 1. Am J Med Genet A. 2004;127A(3):224–9.
8. Kornreich L, Blaser S, Schwarz M, Shuper A, Vishne TH, Cohen IJ, et al. Optic pathway glioma: correlation of imaging findings with the presence of neurofibromatosis. AJNR Am J Neuroradiol. 2001;22(10):1963–9.

9. Massimi L, Tufo T, Di Rocco C. Management of optic-hypothalamic gliomas in children: still a challenging problem. Expert Rev Anticancer Ther. 2007;7(11):1591–610.
10. Caldarelli M, Pezzotta S. In: Pediatric neurosurgery. 1999.
11. Dodgshun AJ, Elder JE, Hansford JR, Sullivan MJ. Long-term visual outcome after chemotherapy for optic pathway glioma in children: site and age are strongly predictive. Cancer. 2015;121(23):4190–6.
12. Hegedus B, Hughes FW, Garbow JR, Gianino S, Banerjee D, Kim K, et al. Optic nerve dysfunction in a mouse model of neurofibromatosis-1 optic glioma. J Neuropathol Exp Neurol. 2009;68(5):542–51.
13. Lambiase A, Bonini S, Manni L, Ghinelli E, Tirassa P, Rama P, et al. Intraocular production and release of nerve growth factor after iridectomy. Invest Ophthalmol Vis Sci. 2002;43(7):2334–40.
14. Coassin M, Lambiase A, Sposato V, Micera A, Bonini S, Aloe L. Retinal p75 and bax overexpression is associated with retinal ganglion cells apoptosis in a rat model of glaucoma. Graefes Arch Clin Exp Ophthalmol. 2008;246(12):1743–9.
15. Ahn Y, Cho BK, Kim SK, Chung YN, Lee CS, Kim IH, et al. Optic pathway glioma: outcome and prognostic factors in a surgical series. Childs Nerv Syst. 2006;22(9):1136–42.
16. Liu GT. Visual loss in childhood. Surv Ophthalmol. 2001;46(1):35–42.
17. Osztie E, Várallyay P, Doolittle ND, Lacy C, Jones G, Nickolson HS, et al. Combined intraarterial carboplatin, intraarterial etoposide phosphate, and IV Cytoxan chemotherapy for progressive optic-hypothalamic gliomas in young children. AJNR Am J Neuroradiol. 2001;22(5):818–23.
18. Saran FH, Baumert BG, Khoo VS, Adams EJ, Garré ML, Warrington AP, et al. Stereotactically guided conformal radiotherapy for progressive low-grade gliomas of childhood. Int J Radiat Oncol Biol Phys. 2002;53(1):43–51.
19. Steinbok P, Hentschel S, Almqvist P, Cochrane DD, Poskitt K. Management of optic chiasmatic/hypothalamic astrocytomas in children. Can J Neurol Sci. 2002;29(2):132–8.
20. Garvey M, Packer RJ. An integrated approach to the treatment of chiasmatic-hypothalamic gliomas. J Neurooncol. 1996;28(2–3):167–83.
21. Packer RJ, Ater J, Allen J, Phillips P, Geyer R, Nicholson HS, et al. Carboplatin and vincristine chemotherapy for children with newly diagnosed progressive low-grade gliomas. J Neurosurg. 1997;86(5):747–54.
22. Lassaletta A, Scheinemann K, Zelcer SM, Hukin J, Wilson BA, Jabado N, et al. Phase II weekly Vinblastine for chemotherapy-naïve children with progressive low-grade glioma: a Canadian pediatric brain tumor consortium study. J Clin Oncol. 2016;34(29):3537–43.
23. Ater JL, Zhou T, Holmes E, Mazewski CM, Booth TN, Freyer DR, et al. Randomized study of two chemotherapy regimens for treatment of low-grade glioma in young children: a report from the Children's oncology group. J Clin Oncol. 2012;30(21):2641–7.
24. Prados MD, Edwards MS, Rabbitt J, Lamborn K, Davis RL, Levin VA. Treatment of pediatric low-grade gliomas with a nitrosourea-based multiagent chemotherapy regimen. J Neurooncol. 1997;32(3):235–41.
25. Massimino M, Spreafico F, Cefalo G, Riccardi R, Tesoro-Tess JD, Gandola L, et al. High response rate to cisplatin/etoposide regimen in childhood low-grade glioma. J Clin Oncol. 2002;20(20):4209–16.
26. Massimino M, Spreafico F, Riva D, Biassoni V, Poggi G, Solero C, et al. A lower-dose, lower-toxicity cisplatin-etoposide regimen for childhood progressive low-grade glioma. J Neurooncol. 2010;100(1):65–71.
27. Farazdaghi MK, Katowitz WR, Avery RA. Current treatment of optic nerve gliomas. Curr Opin Ophthalmol. 2019;30(5):356–63.
28. Gururangan S, Fisher MJ, Allen JC, Herndon JE, Quinn JA, Reardon DA, et al. Temozolomide in children with progressive low-grade glioma. Neuro Oncol. 2007;9(2):161–8.

29. Bouffet E, Jakacki R, Goldman S, Hargrave D, Hawkins C, Shroff M, et al. Phase II study of weekly vinblastine in recurrent or refractory pediatric low-grade glioma. J Clin Oncol. 2012;30(12):1358–63.
30. Cappellano AM, Petrilli AS, da Silva NS, Silva FA, Paiva PM, Cavalheiro S, et al. Single agent vinorelbine in pediatric patients with progressive optic pathway glioma. J Neurooncol. 2015;121(2):405–12.
31. Banerjee A, Jakacki RI, Onar-Thomas A, Wu S, Nicolaides T, Young Poussaint T, et al. A phase I trial of the MEK inhibitor selumetinib (AZD6244) in pediatric patients with recurrent or refractory low-grade glioma: a Pediatric Brain Tumor Consortium (PBTC) study. Neuro Oncol. 2017;19(8):1135–44.
32. Hwang EI, Jakacki RI, Fisher MJ, Kilburn LB, Horn M, Vezina G, et al. Long-term efficacy and toxicity of bevacizumab-based therapy in children with recurrent low-grade gliomas. Pediatr Blood Cancer. 2013;60(5):776–82.
33. Avery RA, Hardy KK. Vision specific quality of life in children with optic pathway gliomas. J Neurooncol. 2014;116(2):341–7.
34. Gorsi HS, Khanna PC, Tumblin M, Yeh-Nayre L, Milburn M, Elster JD, et al. Single-agent bevacizumab in the treatment of recurrent or refractory pediatric low-grade glioma: a single institutional experience. Pediatr Blood Cancer. 2018;65(9):e27234.
35. Gururangan S, Fangusaro J, Poussaint TY, McLendon RE, Onar-Thomas A, Wu S, et al. Efficacy of bevacizumab plus irinotecan in children with recurrent low-grade gliomas--a Pediatric Brain Tumor Consortium study. Neuro Oncol. 2014;16(2):310–7.
36. Packer RJ. Childhood brain tumors: accomplishments and ongoing challenges. J Child Neurol. 2008;23(10):1122–7.
37. Zhukova N, Rajagopal R, Lam A, Coleman L, Shipman P, Walwyn T, et al. Use of bevacizumab as a single agent or in adjunct with traditional chemotherapy regimens in children with unresectable or progressive low-grade glioma. Cancer Med. 2019;8(1):40–50.
38. Grabenbauer GG, Schuchardt U, Buchfelder M, Rödel CM, Gusek G, Marx M, et al. Radiation therapy of optico-hypothalamic gliomas (OHG)--radiographic response, vision and late toxicity. Radiother Oncol. 2000;54(3):239–45.
39. Grill J, Couanet D, Cappelli C, Habrand JL, Rodriguez D, Sainte-Rose C, et al. Radiation-induced cerebral vasculopathy in children with neurofibromatosis and optic pathway glioma. Ann Neurol. 1999;45(3):393–6.
40. Tsang DS, Murphy ES, Merchant TE. Radiation therapy for optic pathway and hypothalamic low-grade gliomas in children. Int J Radiat Oncol Biol Phys. 2017;99(3):642–51.
41. Evans DGR, Baser ME, McGaughran J, Sharif S, Howard E, Moran A. Malignant peripheral nerve sheath tumours in neurofibromatosis 1. J Med Genet. 2002;39(5):311–4.
42. Sharif S, Ferner R, Birch JM, Gillespie JE, Gattamaneni HR, Baser ME, et al. Second primary tumors in neurofibromatosis 1 patients treated for optic glioma: substantial risks after radiotherapy. J Clin Oncol. 2006;24(16):2570–5.
43. Lacaze E, Kieffer V, Streri A, Lorenzi C, Gentaz E, Habrand JL, et al. Neuropsychological outcome in children with optic pathway tumours when first-line treatment is chemotherapy. Br J Cancer. 2003;89(11):2038–44.
44. Sutton LN, Molloy PT, Sernyak H, Goldwein J, Phillips PL, Rorke LB, et al. Long-term outcome of hypothalamic/chiasmatic astrocytomas in children treated with conservative surgery. J Neurosurg. 1995;83(4):583–9.
45. Awdeh RM, Kiehna EN, Drewry RD, Kerr NC, Haik BG, Wu S, et al. Visual outcomes in pediatric optic pathway glioma after conformal radiation therapy. Int J Radiat Oncol Biol Phys. 2012;84(1):46–51.
46. Combs SE, Schulz-Ertner D, Moschos D, Thilmann C, Huber PE, Debus J. Fractionated stereotactic radiotherapy of optic pathway gliomas: tolerance and long-term outcome. Int J Radiat Oncol Biol Phys. 2005;62(3):814–9.

47. Marcus KJ, Goumnerova L, Billett AL, Lavally B, Scott RM, Bishop K, et al. Stereotactic radiotherapy for localized low-grade gliomas in children: final results of a prospective trial. Int J Radiat Oncol Biol Phys. 2005;61(2):374–9.
48. Hug EB, Muenter MW, Archambeau JO, DeVries A, Liwnicz B, Loredo LN, et al. Conformal proton radiation therapy for pediatric low-grade astrocytomas. Strahlenther Onkol. 2002;178(1):10–7.
49. El-Shehaby AMN, Reda WA, Abdel Karim KM, Emad Eldin RM, Nabeel AM. Single-session gamma knife radiosurgery for optic pathway/hypothalamic gliomas. J Neurosurg. 2016;125(Suppl 1):50–7.
50. Liang CL, Lu K, Liliang PC, Chen HJ. Gamma knife surgery for optic glioma. Report of 2 cases. J Neurosurg. 2010;113(Suppl):44–7.
51. Stieber VW. Radiation therapy for visual pathway tumors. J Neuroophthalmol. 2008;28(3):222–30.
52. Campagna M, Opocher E, Viscardi E, Calderone M, Severino SM, Cermakova I, et al. Optic pathway glioma: long-term visual outcome in children without neurofibromatosis type-1. Pediatr Blood Cancer. 2010;55(6):1083–8.
53. Acharya S, Quesada S, Coca K, Richardson C, Hoehn ME, Chiang J, et al. Long-term visual acuity outcomes after radiation therapy for sporadic optic pathway glioma. J Neurooncol. 2019;144(3):603–10.
54. Fangusaro J, Onar-Thomas A, Young Poussaint T, Wu S, Ligon AH, Lindeman N, et al. Selumetinib in paediatric patients with BRAF-aberrant or neurofibromatosis type 1-associated recurrent, refractory, or progressive low-grade glioma: a multicentre, phase 2 trial. Lancet Oncol. 2019;20(7):1011–22.
55. Moreno L, Bautista F, Ashley S, Duncan C, Zacharoulis S. Does chemotherapy affect the visual outcome in children with optic pathway glioma? A systematic review of the evidence. Eur J Cancer. 2010;46(12):2253–9.
56. Fisher MJ, Loguidice M, Gutmann DH, Listernick R, Ferner RE, Ullrich NJ, et al. Visual outcomes in children with neurofibromatosis type 1-associated optic pathway glioma following chemotherapy: a multicenter retrospective analysis. Neuro Oncol. 2012;14(6):790–7.
57. Gu S, Glaug N, Cnaan A, Packer RJ, Avery RA. Ganglion cell layer-inner plexiform layer thickness and vision loss in young children with optic pathway gliomas. Invest Ophthalmol Vis Sci. 2014;55(3):1402–8.
58. Bonini S, Aloe L, Bonini S, Rama P, Lamagna A, Lambiase A. Nerve growth factor (NGF): an important molecule for trophism and healing of the ocular surface. Adv Exp Med Biol. 2002;506(Pt A):531–7.
59. Caleo M, Menna E, Chierzi S, Cenni MC, Maffei L. Brain-derived neurotrophic factor is an anterograde survival factor in the rat visual system. Curr Biol. 2000;10(19):1155–61.
60. Di Girolamo N, Sarris M, Chui J, Cheema H, Coroneo MT, Wakefield D. Localization of the low-affinity nerve growth factor receptor p75 in human limbal epithelial cells. J Cell Mol Med. 2008;12(6B):2799–811.
61. Lambiase A, Rama P, Bonini S, Caprioglio G, Aloe L. Topical treatment with nerve growth factor for corneal neurotrophic ulcers. N Engl J Med. 1998;338(17):1174–80.
62. Rossi FM, Sala R, Maffei L. Expression of the nerve growth factor receptors TrkA and p75NTR in the visual cortex of the rat: development and regulation by the cholinergic input. J Neurosci. 2002;22(3):912–9.
63. Tropea D, Capsoni S, Covaceuszach S, Domenici L, Cattaneo A. Rat visual cortical neurones express TrkA NGF receptor. Neuroreport. 2002;13(10):1369–73.
64. Lambiase A, Mantelli F, Sacchetti M, Rossi S, Aloe L, Bonini S. Clinical applications of NGF in ocular diseases. Arch Ital Biol. 2011;149(2):283–92.
65. Alberch J, Pérez-Navarro E, Canals JM. Neurotrophic factors in Huntington's disease. Prog Brain Res. 2004;146:195–229.

66. Chiaretti A, Conti G, Falsini B, Buonsenso D, Crasti M, Manni L, et al. Intranasal nerve growth factor administration improves cerebral functions in a child with severe traumatic brain injury: a case report. Brain Inj. 2017;31(11):1538–47.
67. Chiaretti A, Eftimiadi G, Buonsenso D, Rendeli C, Staccioli S, Conti G. Intranasal nerve growth factor administration improves neurological outcome after GBS meningitis. Childs Nerv Syst. 2020;36(9):2083–8.
68. Chiaretti A, Falsini B, Aloe L, Pierri F, Fantacci C, Riccardi R. Neuroprotective role of nerve growth factor in hypoxicischemic injury. From brain to skin. Arch Ital Biol. 2011;149(2):275–82.
69. Fantacci C, Capozzi D, Ferrara P, Chiaretti A. Neuroprotective role of nerve growth factor in hypoxic-ischemic brain injury. Brain Sci. 2013;3(3):1013–22.
70. Hallbergson AF, Gnatenco C, Peterson DA. Neurogenesis and brain injury: managing a renewable resource for repair. J Clin Invest. 2003;112(8):1128–33.
71. Manni L, Conti G, Chiaretti A, Soligo M. Intranasal delivery of nerve growth factor in neurodegenerative diseases and Neurotrauma. Front Pharmacol. 2021;12:754502.
72. Sivilia S, Giuliani A, Fernández M, Turba ME, Forni M, Massella A, et al. Intravitreal NGF administration counteracts retina degeneration after permanent carotid artery occlusion in rat. BMC Neurosci. 2009;10:52.
73. Chiaretti A, Genovese O, Riccardi R, Di Rocco C, Di Giuda D, Mariotti P, et al. Intraventricular nerve growth factor infusion: a possible treatment for neurological deficits following hypoxic-ischemic brain injury in infants. Neurol Res. 2005;27(7):741–6.
74. Chiaretti A, Antonelli A, Genovese O, Fernandez E, Giuda D, Mariotti P, et al. Intraventricular nerve growth factor infusion improves cerebral blood flow and stimulates doublecortin expression in two infants with hypoxic-ischemic brain injury. Neurol Res. 2008;30(3):223–8.
75. Chiaretti A, Falsini B, Servidei S, Marangoni D, Pierri F, Riccardi R. Nerve growth factor eye drop administration improves visual function in a patient with optic glioma. Neurorehabil Neural Repair. 2011;25(4):386–90.
76. Di Fausto V, Fiore M, Tirassa P, Lambiase A, Aloe L. Eye drop NGF administration promotes the recovery of chemically injured cholinergic neurons of adult mouse forebrain. Eur J Neurosci. 2007;26(9):2473–80.
77. Lambiase A, Pagani L, Di Fausto V, Sposato V, Coassin M, Bonini S, et al. Nerve growth factor eye drop administrated on the ocular surface of rodents affects the nucleus basalis and septum: biochemical and structural evidence. Brain Res. 2007;1127(1):45–51.
78. Lambiase A, Tirassa P, Micera A, Aloe L, Bonini S. Pharmacokinetics of conjunctivally applied nerve growth factor in the retina and optic nerve of adult rats. Invest Ophthalmol Vis Sci. 2005;46(10):3800–6.
79. Sala R, Viegi A, Rossi FM, Pizzorusso T, Bonanno G, Raiteri M, et al. Nerve growth factor and brain-derived neurotrophic factor increase neurotransmitter release in the rat visual cortex. Eur J Neurosci. 1998;10(6):2185–91.
80. Cui Q, Lu Q, So KF, Yip HK. CNTF, not other trophic factors, promotes axonal regeneration of axotomized retinal ganglion cells in adult hamsters. Invest Ophthalmol Vis Sci. 1999;40(3):760–6.
81. Shi Z, Birman E, Saragovi HU. Neurotrophic rationale in glaucoma: a TrkA agonist, but not NGF or a p75 antagonist, protects retinal ganglion cells in vivo. Dev Neurobiol. 2007;67(7):884–94.
82. Lu B. Acute and long-term synaptic modulation by neurotrophins. Prog Brain Res. 2004;146:137–50.
83. Sofroniew MV, Howe CL, Mobley WC. Nerve growth factor signaling, neuroprotection, and neural repair. Annu Rev Neurosci. 2001;24:1217–81.
84. Abed E, Piccardi M, Rizzo D, Chiaretti A, Ambrosio L, Petroni S, et al. Functional loss of the inner retina in childhood optic gliomas detected by photopic negative response. Invest Ophthalmol Vis Sci. 2015;56(4):2469–74.

85. Falsini B, Ziccardi L, Lazzareschi I, Ruggiero A, Placentino L, Dickmann A, et al. Longitudinal assessment of childhood optic gliomas: relationship between flicker visual evoked potentials and magnetic resonance imaging findings. J Neurooncol. 2008;88(1):87–96.
86. Avery RA, Liu GT, Fisher MJ, Quinn GE, Belasco JB, Phillips PC, et al. Retinal nerve fiber layer thickness in children with optic pathway gliomas. Am J Ophthalmol. 2011;151(3):542–549.e2.
87. Falsini B, Chiaretti A, Rizzo D, Piccardi M, Ruggiero A, Manni L, et al. Nerve growth factor improves visual loss in childhood optic gliomas: a randomized, double-blind, phase II clinical trial. Brain. 2016;139(Pt 2):404–14.
88. Astrup J. Natural history and clinical management of optic pathway glioma. Br J Neurosurg. 2003;17(4):327–35.
89. Listernick R, Ferner RE, Liu GT, Gutmann DH. Optic pathway gliomas in neurofibromatosis-1: controversies and recommendations. Ann Neurol. 2007;61(3):189–98.
90. Miller NR. Primary tumours of the optic nerve and its sheath. Eye (Lond). 2004;18(11):1026–37.

Chapter 7
Endoscopic Endonasal Surgery for Uncommon Pathologies of the Sellar and Parasellar Regions

Waleed A. Azab, Tufail Khan, Marwan Alqunaee, Abdullah Al Bader, and Waleed Yousef

7.1 The Endoscope and Surgery for Sellar and Parasellar Lesions: A Perfect Match

The microscopic transsphenoidal approach has been the gold standard for pituitary tumor resection since the introduction of the surgical microscope into this type of surgery by Hardy in 1962 [1, 2].

After endoscopes became popularized in paranasal sinus surgery, interest increased in their usage for transsphenoidal pituitary surgery [3]. It was in 1992 when Jankowski et al. reported the first endoscopic endonasal resection of pituitary adenomas in three patients. The procedures were performed via mono- or bi-nostril techniques and included a routine middle turbinectomy [4].

In addition to its important advantage of obviating the need to transgress the critical neurovascular structures when approaching the majority of sellar lesions, further benefits of the endoscopic approach include panoramic visualization, improved illumination, angled views made available by angled lenses, and increased maneuverability of instruments [5]. The improved visualization entailed better identification of the anatomical structures at risk and enabled resection of adenomas with a supra- and parasellar extensions [1, 2].

W. A. Azab (✉) · T. Khan · W. Yousef
Neurosurgery Department, Ibn Sina Hospital, Kuwait City, Kuwait

M. Alqunaee
Rhinology - Endoscopic Sinus and Skull Base Surgery, Zain Hospital, Kuwait City, Kuwait

A. Al Bader
Rhinology - Endoscopic Sinus and Skull Base Surgery, Jaber Al Ahmad Hospital, Kuwait City, Kuwait

C. Di Rocco (ed.), *Advances and Technical Standards in Neurosurgery*, Advances and Technical Standards in Neurosurgery 48,
https://doi.org/10.1007/978-3-031-36785-4_7

From the optical point of view, the superior visualization within the relatively narrow nasal corridor is achieved because the endoscope brings the light and the viewing lens inside the surgical field resulting in a very highly illuminated area of interest. Furthermore, the close proximity of the light source to the structures being viewed eliminates shadows within the field, adding to the extreme clarity of the viewed images. The superiority of the endoscopic view (Fig. 7.1) is also contributed to by the high color fidelity and image definition capabilities of today's state-of-the-art rigid endoscopes. An additional advantage of the endoscopic view is the greater depth of focus in comparison to that of the microscope, which results in lesser need to adjust the focus of the endoscope during the procedure leading to a seamless operative workflow. The use of angled scopes also enables "looking around the corners" and therefore adds further to the efficacy and safety of the procedure specially when it comes to excision of suprasellar and parasellar tumors [6].

As a matter of fact, the demonstration of feasibility of endoscopic skull base surgery was followed by a period of validation and popularization with improved outcomes and newly developed treatment paradigms that incorporated the original and the emerging technologies and procedures [7]. For pituitary adenomas, the endoscopic transsphenoidal approach has subsequently been adopted worldwide as an alternative to the microscopic approach [1], and the extended endoscopic endonasal approaches to various skull base pathologies have exploded in popularity over the last two decades. Presently, the lesions treated can be located anywhere from the frontal sinus to the odontoid in the sagittal plane (Fig. 7.2) and from midline to the middle fossa in the coronal plane [8]. Examples of these pathologies include tuberculum sellae, planum sphenoidale, and olfactory groove meningiomas, craniopharyngiomas, clival tumors like chordomas and chondrosarcomas, petrous apex tumors, and lesions of the infratemporal fossa [9–17].

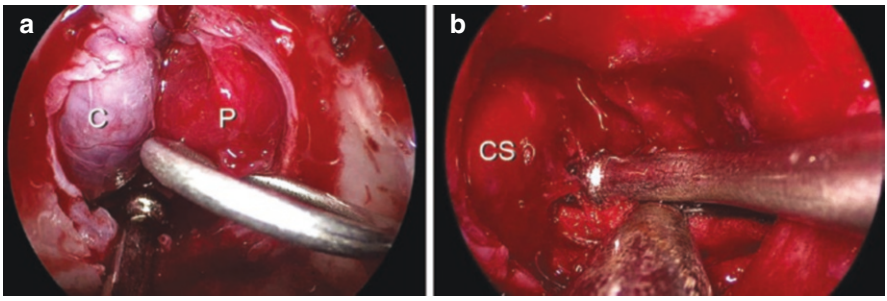

Fig. 7.1 The superiority of endoscopic view. An example from an endoscopic endonasal transsphenoidal approach for a giant pituitary adenoma after complete tumor excision. In (**a**), note the descending cistern, C, and the normal pituitary gland, P. In (**b**), a close-up view of the medial wall of the cavernous sinus; CS is seen

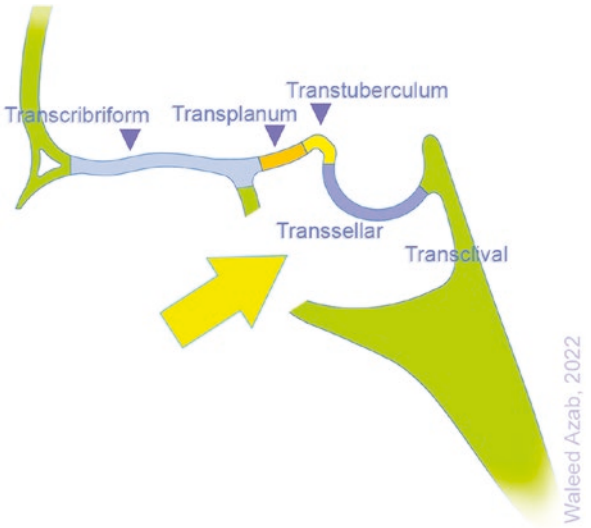

Fig. 7.2 The standard and extended endoscopic endonasal approaches to various skull base pathologies in the sagittal plane

7.2 Surgical Technique of Endoscopic Endonasal Transsphenoidal Approach

In our operating room setup, the operating surgeon stands on the right side of the patient, and the assistant stands on the left side facing the surgeon. The endoscope tower and monitor are positioned at the patient's head with a Mayo stand between the patient's head and the endoscope tower. The navigation monitor is positioned next to the endoscope tower and is facing the operating surgeon. The scrub nurse and instrument tables are on the left side of the operating table next to the assistant surgeon. Under general anesthesia, the patient is positioned supine, and the head is elevated 10–15 degrees above the level of the heart. On a MAYFIELD® Headrest, the head is neutrally positioned and then rotated 10 degrees toward the surgeon. Stereotactic image guidance is not a routine in all cases. We use navigation to identify the carotid arteries based on CTA images, to guide the extent of bone resection when extended approaches are performed, in patients with complex bony anatomy of the paranasal sinuses and in recurrent cases. In cases where neuronavigation is used, the patient's head is fixed by MAYFIELD® skull clamp. Flexion or extension of the patient's head is undertaken in transplanum-transtuberculum sellae and in transclival approaches, respectively. Cottonoids soaked in 0.5% adrenaline solution are packed into the nasal cavities immediately after the patient is anaesthetized and are later removed just before draping. The vasoconstriction induced by epinephrine reduces the thickness of the nasal mucosa and greatly helps developing a sufficiently wide surgical corridor. Furthermore, it decreases mucosal bleeding during the following steps of the procedure.

The procedure is carried out using a purely endoscopic approach primarily with the aid of a 0° 4-mm, 30-cm rigid endoscope (Karl Storz GmbH & Co. KG). The 0°

endoscope is to be held at the 12 o'clock position in the superior aspect of the nasal cavity. In this position, the endoscope shaft is pushed further superiorly against the elastic tissue of the nasal aperture, giving more room for instrument manipulation within the nasal cavity. Suction is usually positioned at 6 o'clock position. At the initial stages of the procedure when the two nasal cavities are still separated, in some patients with ample nasal cavity, another instrument can be inserted between the endoscope and the suction. No endoscopic holders or nasal specula are used.

The surgical technique of the endoscopic endonasal transsphenoidal approach basically consists of three stages, namely, *the nasal*, *the sphenoidal*, and *the sellar* steps.

7.2.1 The Nasal Step

The anatomical landmarks within the nasal cavity are identified and include the nasal floor, the inferior and middle turbinates, and the nasal septum. Adrenaline-soaked cottonoids are then inserted between the nasal septum and the middle turbinate. Lateralization of the middle turbinate is then performed using the shaft of a Freer elevator to develop the surgical corridor (Fig. 7.3a). At this stage, advancing the scope into the nasal cavity enables visualization of the choana, an important landmark based on which the approach proceeds further. Once the choana is reached, the endoscope is directed upward where the sphenoid face, sphenoethmoid recess, and the ostia of the sphenoid sinus are identified.

In cases where an extended endoscopic endonasal approach is performed, a middle turbinectomy is required to obtain sufficient space and angles during tumor resection. To spare the olfactory mucosa, the middle turbinate is cut parallel to the anterior skull base between its upper and lower two thirds using a septum scissors. Proceeding posteriorly, the blades of the scissors should be pushed inferiorly to complete the separation of the turbinate. The disconnected middle turbinate is then grasped using a Blakesley nasal forceps and removed.

7.2.2 The Sphenoidal Step

The sphenoidal step (Figs. 7.3b–f and 7.4) commences by coagulating the mucosa covering the face of sphenoid, the sphenoethmoid recess, and the posterior part of nasal septum using a suction monopolar. When harvesting a nasoseptal flap is planned, the posterior septal artery (supplying the pedicled flap) should be preserved. The nasal septum is then dislocated from its posterior attachment, and a posterior septectomy is performed using a backbiting forceps.

Drilling the whole sphenoid face and posterior vomer is subsequently undertaken using a 3- to 5-mm coarse diamond bit to widely open the sphenoid sinus. The sphenoid opening can be completed using a Kerrison rongeur if needed.

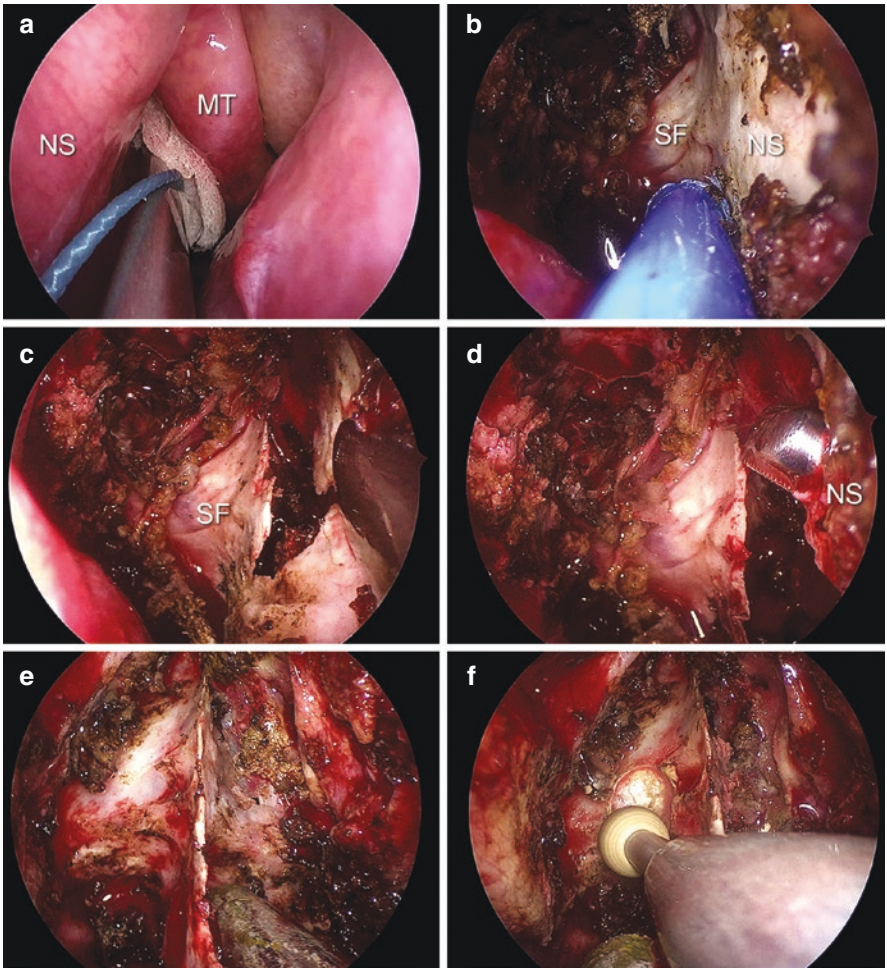

Fig. 7.3 The nasal and sphenoidal steps of the endoscopic endonasal transsphenoidal approach. In the nasal step (**a**), the operative corridor is developed by inserting an adrenaline-soaked cottonoid patty between the middle turbinate (MT) and the nasal septum (NS). The middle turbinate (MT) is then lateralized using a dissector. In the sphenoidal step (**b**–**f**), the mucosa covering the face of sphenoid face (SF) and the sphenoethmoid recess is coagulated and removed (**b**). The mucosa of the posterior nasal septum (NS) is then coagulated and removed bilaterally. The nasal septum (NS) is subsequently dislocated using a dissector (**c**), and a posterior septectomy is performed using a backbiting forceps (**d**). After the sphenoid face is completely exposed (**e**), its drilling is performed using a sharp or sharp diamond drill pit (**f**)

As the sphenoid sinus is entered, key anatomical landmarks within its cavity are visualized. These include the sellar face, optic canal, carotid protuberance, lateral and medial optico-carotid recesses, tuberculum sellae, planum sphenoidale, clival recess, and the paraclival carotids. Because of the variable pneumatization patterns

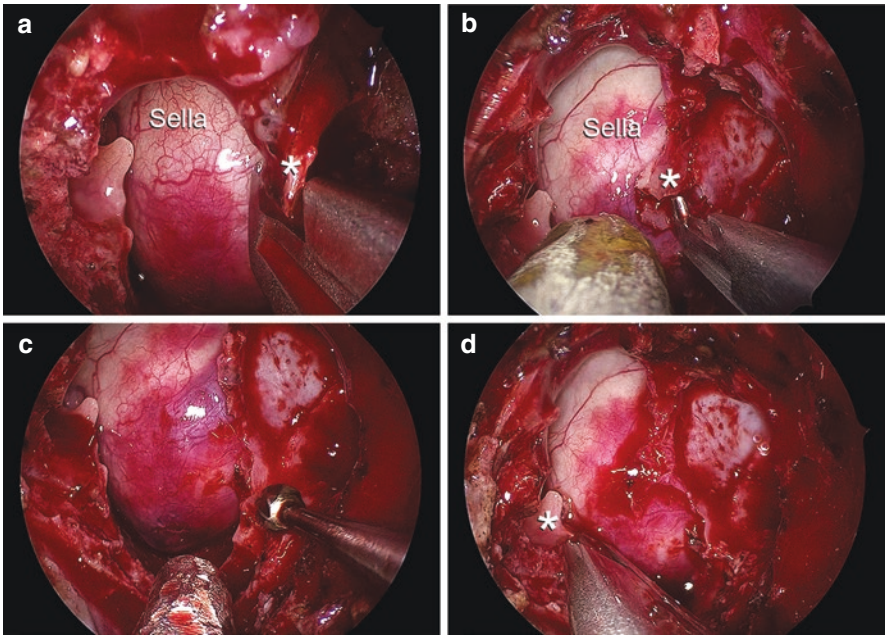

Fig. 7.4 During the sphenoidal step, the bony septa (asterisks) inside the sphenoid sinus should be drilled down to their attachment or carefully removed using a Kerrison rongeur as demonstrated in these serial operative views (**a**–**d**)

of the sphenoid sinus, some of the aforementioned anatomical landmarks may be not very clearly appreciable.

The sphenoid mucosa is then removed, and the bony septations within the sinus are carefully drilled down to their attachment. The bony septa within the sphenoid sinus usually lead to the internal carotid artery. Extreme care should therefore be practiced during their removal to avoid vascular injury.

7.2.3 The Sellar Step

The sellar step (Fig. 7.5) starts by drilling the sellar face down to the clival recess below and up to the tuberculum sellae in the standard transsellar approach. Bilaterally, it extends between the two carotid prominences. Removal of bone of the tuberculum sellae, planum sphenoidale, or the clival recess is undertaken when transtuberculum, transplanum, or transclival approaches are planned, respectively. Bone removal is performed using a 3- or 5-mm diamond burr, and the thin shell of bone remaining after drilling is removed using a fine microdissector. A 1-mm Kerrison rongeur is then used to complete the bone window.

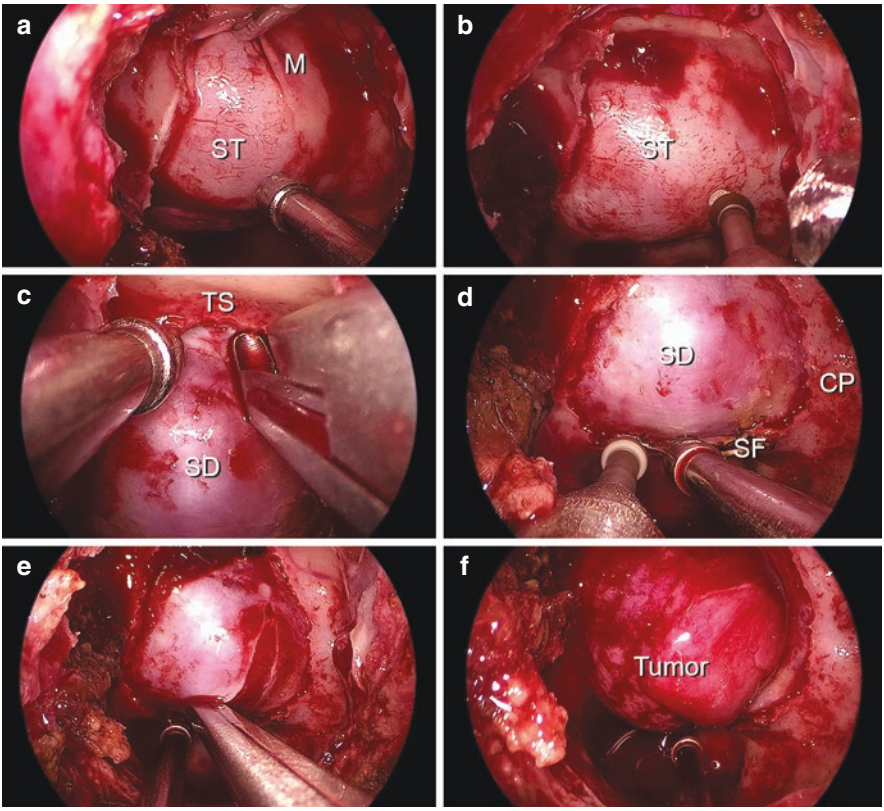

Fig. 7.5 The sphenoidal and sellar steps. (**a**) The sphenoidal step is completed by removing the sphenoid mucosa (M). (**b**) The sellar step then starts by drilling the bony face of the sella turcica (ST). The extent of sellar dura (SD) exposure in the basic transsellar approach extends from the tuberculum sellae (TS) above to the sellar floor (SF) below and between the carotid prominences (CP) bilaterally (**c**, **d**). The dural incision is then performed using a retractable knife and completed with an angled scissors (**e**) to gain access to the tumor (T) as seen in (**f**)

The dural incision is performed using a retractable knife and angled scissors. In cases of small sellar lesions, the incision can be cruciate or U-shaped and extends between the two cavernous sinuses bilaterally and between the superior and inferior intercavernous sinuses craniocaudally. In large pituitary adenomas, resecting a quadrangular dural flap greatly helps with tumor excision. In transtuberculum-transplanum approach, bipolar coagulation of the superior intercavernous sinus is performed before cutting through the sinus to avoid brisk venous bleeding.

For intrasellar pathologies, tissue biopsy is performed using a pituitary rongeur, and then tumor removal proceeds using mainly suction and pituitary ring curettes of variable angles. Piecemeal resection is sometimes needed when tumor is hard in consistency. In cases when the tumor is posterior to the pituitary gland, a vertical incision in the normal gland is made allowing access to the tumor. Thorough

endoscopic inspection of the sellar cavity is performed to make sure that no tumor tissue is left. Full descent of the suprasellar cistern is observed at this stage.

Tumor excision should start first from the inferior, posterior, and lateral parts of the sellar cavity, leaving the superior part of the tumor to the end in order to prevent an early descent of the suprasellar cistern which obstructs the view before tumor removal is completed. Should this occur, a cottonoid patty is used to elevate the bulging cistern and allow visualization of the remaining tumor tissue and its further resection. This maneuver can also be performed using a ring pituitary curette or a second suction tube to retract the redundant cistern and a suction tube to remove the tumor.

In the standard transsellar approach, angled 30° and 45° 4-mm scopes are used for visualization within the cavernous sinuses and the superior and superolateral corners near the end of tumor excision. In extended approaches, angled scopes are also very valuable for visualization of pathoanatomical structures and relationships. Bimanual technique of dissection and resection should be used.

In the transsellar approach, hemostasis and closure (Fig. 7.6) are performed using Floseal® and TISSEEL®, followed by layers of Surgicel®. Autologous fat is used in cases with minor CSF leaks and is reinforced with TISSEEL® and Surgicel®.

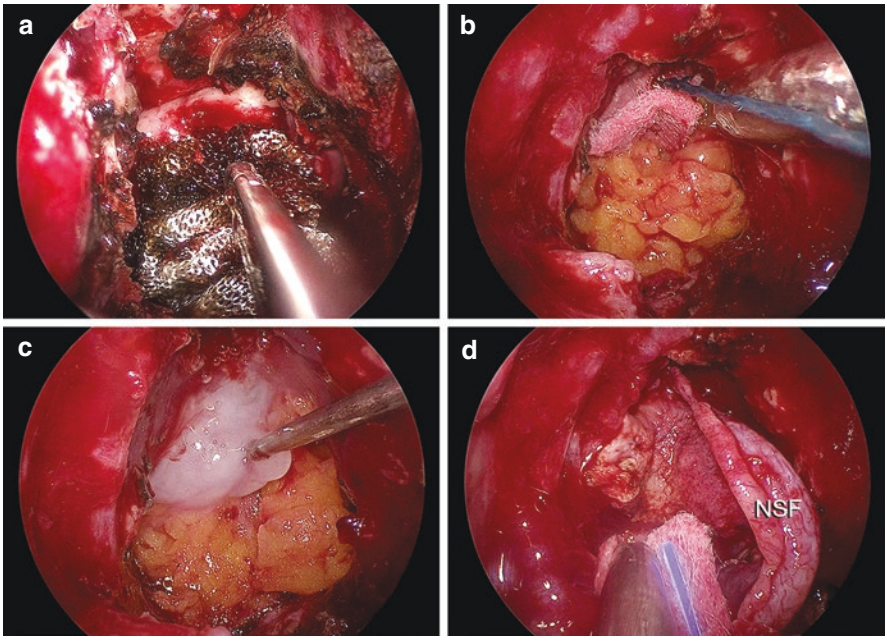

Fig. 7.6 The reconstruction after endoscopic endonasal transsphenoidal approach is performed by applying multiple layers of Surgicel® and applying TISSEEL® in cases without CSF leakage (**a**). In cases with minimal arachnoid breaches and CSF leaks, an autologous fat graft is used and reinforced with TISSEEL® and multiple layers of Surgicel® (**b**, **c**). A nasoseptal pedicled flap (NSF) is harvested and used over the fat graft in cases with large arachnoid defects and vigorous CSF leaks like extended approaches (**d**)

Surgicel® should not be packed in the sellar cavity and is to be left only in the sphenoid sinus. It functions as a scaffold to support the reconstruction and also enhances healing by lowering the local tissue pH. A free mucosal flap harvested from a resected middle turbinate can also be used when CSF leak takes place. In extended approaches, a vascularized nasoseptal flap based on the posterior septal branch of the sphenopalatine artery and autologous fat is used for skull base reconstruction. Before the procedure is concluded, the nasal cavity is inspected to control any bleeding points and to clear blood clots off the nasal passages. The lateralized middle turbinate is then medialized. Nasal packing is not needed in the majority of cases and is only routinely used when a free or nasoseptal flap is used [18].

7.3 The Uncommon Pathologies of the Sella

Apart from the common pathological entities, many other less frequent pathologies are encountered in the sellar and parasellar regions. As a matter of fact, classifying the rare and non-adenomatous lesions of the sellar area has been attempted by many research groups; however, no consensus presently exists in that regard.

The differential diagnosis of nonpituitary sellar masses is very broad [19]. In Table 7.1, many of these lesions are enlisted [20–66]. Differentiating among the potential etiologies may not always be straightforward because many of these rare sellar lesions mimic the clinical, endocrinologic, and radiographic presentations of pituitary adenomas [19, 67, 68]. Owing to the rarity of these lesions, the frequency and types of the encountered pathologies across the published series are quite variable [19, 67–70]. In one study combining cases from two centers, rare sellar pathologies comprised 78 patients out of 346 non-adenomatous sellar pathologies. Arachnoid cysts were the most frequently encountered (15%), followed by metastasis (14%), hypophysitis (10%), and oncocytoma and glioma (8% each). A standard endoscopic endonasal approach was performed in 56% and an extended approach was used in 44% of patients [67].

Extremely rare pathologies have also been reported in the sellar suprasellar area including diffuse large cell B cell lymphoma primary to the sellar/suprasellar region, primary fibrosarcoma of the sella, primary MPNST of the sella, GPA and NS with first presentation in CNS, CLL within a pituitary adenoma, and aberrant nerve fascicles within a pituitary adenoma [71]. An increased awareness of the unusual entities that may involve the sellar region is therefore needed [72]. It is of note that surgical endoscopic experience allows better interpretation of intraoperative features, orienting the diagnosis and subsequent management [67].

An exhaustive review of these pathological entities is beyond the scope of this chapter. In the following paragraphs, however, some of these lesions will be elaborated upon.

Table 7.1 Examples of uncommon sellar pathologies

1. *Neoplastic*	
(a) Uncommon pituitary adenomas (PitNET)	Honegger J, Nasi-Kordhishti I, Giese S. Hypophysenadenome [Pituitary adenomas]. Nervenarzt. 2019 Jun;90(6):568-577. German. doi: 10.1007/s00115-019-0708-4
(b) Posterior pituitary tumors	Kinoshita Y, Yamasaki F, Tominaga A, Usui S, Arita K, Sakoguchi T, Sugiyama K, Kurisu K. Transsphenoidal Posterior Pituitary Lobe Biopsy in Patients with Neurohypophysial Lesions. World Neurosurg. 2017 Mar;99:543-547. doi: 10.1016/j.wneu.2016.12.080. Epub 2016 Dec 27
(c) Pituitary blastoma	Chhuon Y, Weon YC, Park G, Kim M, Park JB, Park SK. Pituitary Blastoma in a 19-Year-Old Woman: A Case Report and Review of Literature. World Neurosurg. 2020 Jul;139:310-313. doi: 10.1016/j.wneu.2020.04.096
(d) Pituitary carcinoma	Sansur CA, Oldfield EH. Pituitary carcinoma. Semin Oncol. 2010 Dec;37(6):591-3. doi: 10.1053/j.seminoncol.2010.10.012
(e) Metastasis to the pituitary	Castle-Kirszbaum M, Goldschlager T, Ho B, Wang YY, King J. Twelve cases of pituitary metastasis: a case series and review of the literature. Pituitary. 2018 Oct;21(5):463-473. doi: 10.1007/s11102-018-0899-x
(f) Others:	
• Glial tumors	
Astrocytoma	Wang J, Liu Z, Du J, Cui Y, Fang J, Xu L, Li G. The clinicopathological features of pituicytoma and the differential diagnosis of sellar glioma. Neuropathology. 2016 Oct;36(5):432-440. doi: 10.1111/neup.12291
Glioblastoma	Mahta A, Buhl R, Huang H, Jansen O, Kesari S, Ulmer S. Sellar and supra-sellar glioblastoma masquerading as a pituitary macroadenoma. Neurol Sci. 2013 Apr;34(4):605-7. doi: 10.1007/s10072-012-1110-1
Pilocytic astrocytoma	Prashant Prasad G, Lang FF, Bruner JM, Ater JL, McCutcheon IE. Transsphenoidal removal of intrasellar pilocytic astrocytoma. J Clin Neurosci. 2014 Jun;21(6):1047-8. doi: 10.1016/j.jocn.2013.10.004
Pleomorphic xanthoastrocytoma	Arita K, Kurisu K, Tominaga A, Sugiyama K, Sumida M, Hirose T. Intrasellar pleomorphic xanthoastrocytoma: case report. Neurosurgery. 2002 Oct;51(4):1079-82; discussion 1082. doi: 10.1097/00006123-200210000-00042
• Glioneuronal and neuronal tumors	
Ganglioglioma	Matyja E, Maksymowicz M, Grajkowska W, Zieliński G, Kunicki J, Bonicki W, Witek P, Naganska E. Ganglion cell tumours in the sella turcica in close morphological connection with pituitary adenomas. Folia Neuropathol. 2015;53(3):203-18. doi: 10.5114/fn.2015.54421
Papillary glioneuronal tumor	Emanuelli E, Zanotti C, Munari S, Baldovin M, Schiavo G, Denaro L. Sellar and parasellar lesions: multidisciplinary management. Acta Otorhinolaryngol Ital. 2021 Apr;41(Suppl. 1):S30-S41. doi: 10.14639/0392-100X-suppl.1-41-2021-03

Table 7.1 (continued)

Gangliocytoma	Quiroga-Padilla PJ, González-Devia D, Andrade R, Escalante P, Jiménez-Hakim E. Sellar Gangliocytoma: Case Report and Review of an Extremely Rare Tumour. Case Rep Neurol. 2021 Jul 19;13(2):475-482. doi: 10.1159/000517368
Neurocytoma	Nery B, Bernardes Filho F, Costa RAF, Pereira LCT, Quaggio E, Queiroz RM, Abud LG, da Cunha Tirapelli DP. Neurocytoma mimicking macroadenoma. Surg Neurol Int. 2019 Jan 21;10:8. doi: 10.4103/sni.sni_387_18 Wang J, Song DL, Deng L, Sun SY, Liu C, Gong DS, Wang Y, Xu QW. Extraventricular neurocytoma of the sellar region: case report and literature review. Springerplus. 2016 Jul 7;5(1):987. doi: 10.1186/s40064-016-2650-2
• Ependymal tumors	
Ependymoma	Wang S, Zong W, Li Y, Wang B, Ke C, Guo D. Pituitary Ependymoma: A Case Report and Review of the Literature. World Neurosurg. 2018 Feb;110:43-54. doi: 10.1016/j.wneu.2017.10.134
• Choroid plexus tumors	
Choroid plexus papilloma	Kuo CH, Yen YS, Tu TH, Wu JC, Huang WC, Cheng H. Primary Choroid Plexus Papilloma over Sellar Region Mimicking with Craniopharyngioma: A Case Report and Literature Review. Cureus. 2018 Jun 20;10(6):e2849. doi: 10.7759/cureus.2849
• Embryonal tumors	
Atypical teratoid/rhabdoid tumor	Liu F, Fan S, Tang X, Fan S, Zhou L. Adult Sellar Region Atypical Teratoid/Rhabdoid Tumor: A Retrospective Study and Literature Review. Front Neurol. 2020 Dec 15;11:604612. doi: 10.3389/fneur.2020.604612
Neuroblastoma	Kalinin PL, Fomichev DV, Abdilatipov AA, Chernov IV, Astafieva LI, Kutin MA, Ryzhova MV, Panina TN, Shishkina LV, Nikitin PV, Kurnosov AB. Pervichnaya sellyarnaya neiroblastoma. Klinicheskoe nablyudenie i obzor literatury [Primary sellar neuroblastoma (clinical case and literature review)]. Zh Vopr Neirokhir Im N N Burdenko. 2020;84(2):83-92. Russian. doi: 10.17116/neiro20208402183
Primitive neuroectodermal tumor	Yakar F, Doğan İ, Meco C, Heper AO, Kahilogullari G. Sellar Embryonal Tumor: A Case Report and Review of the Literature. Asian J Neurosurg. 2018 Oct-Dec;13(4):1197-1201. doi: 10.4103/ajns.AJNS_30_17
• Cranial and paraspinal nerve tumors	

(continued)

Table 7.1 (continued)

Schwannoma	Kong X, Wu H, Ma W, Li Y, Yang Y, Xing B, Wei J, Yao Y, Gao J, Lian W, Xu Z, Dou W, Ren Z, Su C, Wang R. Schwannoma in Sellar Region Mimics Invasive Pituitary Macroadenoma: Literature Review With One Case Report. Medicine (Baltimore). 2016 Mar;95(9):e2931. doi: 10.1097/MD.0000000000002931 Zhang J, Xu S, Liu Q, Li X, Jia D, Li G. Intrasellar and Suprasellar Schwannoma Misdiagnosed as Pituitary Macroadenoma: A Case Report and Review of the Literature. World Neurosurg. 2016 Dec;96:612.e1-612.e7. doi: 10.1016/j.wneu.2016.08.128
Paraganglioma	Lyne SB, Polster SP, Fidai S, Pytel P, Yamini B. Primary Sellar Paraganglioma: Case Report with Literature Review and Immunohistochemistry Resource. World Neurosurg. 2019 May;125:32-36. doi: 10.1016/j.wneu.2019.01.094
• Meningiomas	
Meningioma (pure intrasellar)	Bang M, Suh JH, Park JB, Weon YC. Pure Intrasellar Meningioma Mimicking Pituitary Macroadenoma: Magnetic Resonance Imaging and Review of the Literature. World Neurosurg. 2016 Jul;91:675.e1-4. doi: 10.1016/j.wneu.2016.04.063
• Mesenchymal, non-meningothelial tumors	
Solitary fibrous tumor	Zhong Q, Yuan S. Total resection of a solitary fibrous tumor of the sellar diaphragm: A case report. Oncol Lett. 2013 Jun;5(6):1783-1786. doi: 10.3892/ol.2013.1293
Hemangioma	Singh U, Kalavakonda C, Venkitachalam S, Patil S, Chinnusamy R. Intraosseous Hemangioma of Sella: Case Report and Review of Literature. World Neurosurg X. 2019 Mar 9;3:100030. doi: 10.1016/j.wnsx.2019.100030
Hemangioblastoma	Ajler P, Goldschmidt E, Bendersky D, Hem S, Landriel F, Campero A, Ajler G. Sellar hemangioblastoma mimicking a macroadenoma. Acta Neurol Taiwan. 2012 Dec;21(4):176-9
Sarcoma	Guerrero-Pérez F, Vidal N, López-Vázquez M, Sánchez-Barrera R, Sánchez-Fernández JJ, Torres-Díaz A, Vilarrasa N, Villabona C. Sarcomas of the sellar region: a systematic review. Pituitary. 2021 Feb;24(1):117-129. doi: 10.1007/s11102-020-01073-9
Rhabdomyosarcoma	Arita K, Sugiyama K, Tominaga A, Yamasaki F. Intrasellar rhabdomyosarcoma: case report. Neurosurgery. 2001 Mar;48(3):677-80. doi: 10.1097/00006123-200103000-00048
Ewing sarcoma	Mattogno PP, Nasi D, Iaccarino C, Oretti G, Santoro L, Romano A. First Case of Primary Sellar/Suprasellar-Intraventricular Ewing Sarcoma: Case Report and Review of the Literature. World Neurosurg. 2017 Feb;98:869.e1-869.e5. doi: 10.1016/j.wneu.2016.12.045
Mesenchymal chondrosarcoma	Inenaga C, Morii K, Tamura T, Tanaka R, Takahashi H. Mesenchymal chondrosarcoma of the sellar region. Acta Neurochir (Wien). 2003 Jul;145(7):593-7; discussion 597. doi: 10.1007/s00701-003-0059-5

Table 7.1 (continued)

Chondrosarcoma	Zhang Y, Huang J, Zhang C, Jiang C, Ding C, Lin Y, Wu X, Wang C, Kang D, Lin Z. An Extended Endoscopic Endonasal Approach for Sellar Area Chondrosarcoma: A Case Report and Literature Review. World Neurosurg. 2019 Jul;127:469-477. doi: 10.1016/j.wneu.2019.04.075
• Notochordal tumors	
Sellar chordoma	Kikuchi K, Watanabe K. Huge sellar chordoma: CT demonstration. Comput Med Imaging Graph. 1994 Sep-Oct;18(5):385-90. doi: 10.1016/0895-6111(94)90010-8
• Melanocytic tumors	
Meningeal melanocytoma	Wang F, Ling S. Primary Meningeal Melanocytoma in Sellar Region, Simulating a Nonfunctioning Pituitary Adenoma: Case Report and Literature Review. World Neurosurg. 2018 Apr;112:209-213. doi: 10.1016/j.wneu.2018.01.145
• Hematolymphoid tumors	
– Lymphomas	
Lymphoma	Tarabay A, Cossu G, Berhouma M, Levivier M, Daniel RT, Messerer M. Primary pituitary lymphoma: an update of the literature. J Neurooncol. 2016 Dec;130(3):383-395. doi: 10.1007/s11060-016-2249-z
Primary diffuse large B-cell lymphoma of the CNS	Ravindra VM, Raheja A, Corn H, Driscoll M, Welt C, Simmons DL, Couldwell WT. Primary pituitary diffuse large B-cell lymphoma with somatotroph hyperplasia and acromegaly: case report. J Neurosurg. 2017 May;126(5):1725-1730. doi: 10.3171/2016.5.JNS16828
– Histiocytic tumors	
Erdheim-Chester disease	Oweity T, Scheithauer BW, Ching HS, Lei C, Wong KP. Multiple system Erdheim-Chester disease with massive hypothalamic-sellar involvement and hypopituitarism. J Neurosurg. 2002 Feb;96(2):344-51. doi: 10.3171/jns.2002.96.2.0344
Rosai-Dorfman disease	Zhang Y, Liu J, Zhu J, Zhou X, Zhang K, Wang S, Ma W, Pan H, Wang R, Zhu H, Yao Y. Case Report: Rosai-Dorfman Disease Involving Sellar Region in a Pediatric Patient: A Case Report and Systematic Review of Literature. Front Med (Lausanne). 2020 Nov 30;7:613756. doi: 10.3389/fmed.2020.613756
Langerhans cell histiocytosis	Tan H, Yu K, Yu Y, An Z, Li J. Isolated hypothalamic-pituitary langerhans' cell histiocytosis in female adult: A case report. Medicine (Baltimore). 2019 Jan;98(2):e13853. doi: 10.1097/MD.0000000000013853
• Germ cell tumors	
Teratoma	Saeger W, Ebrahimi A, Beschorner R, Spital H, Honegger J, Wilczak W. Teratoma of the Sellar Region: a Case Report. Endocr Pathol. 2017 Dec;28(4):315-319. doi: 10.1007/s12022-016-9465-0

(continued)

Table 7.1 (continued)

Germinoma	Li CS. Intrasellar germinoma treated with low-dose radiation. Acta Neurochir (Wien). 2006 Jul;148(7):795-9; discussion 799. doi: 10.1007/s00701-006-0776-7
Choriocarcinoma	Musiani P, Mancuso S. Coriocarcinoma primitivo intracranico originato da tumore germinale sellare in una bambina in età prepubere [Intracranial primary choriocarcinoma originating from a sellar germinal tumor in a girl of prepuberal age]. Arch Ital Anat Istol Patol. 1969 Dec;43(1):61-75. Italian. PMID: 5393121
Mixed germ cell tumor	Wildemberg LE, Vieira Neto L, Taboada GF, Moraes AB, Marcondes J, Conceição FL, Chimelli L, Gadelha MR. Sellar and suprasellar mixed germ cell tumor mimicking a pituitary adenoma. Pituitary. 2011 Dec;14(4):345-50. doi: 10.1007/s11102-008-0161-z
• Salivary gland-like lesions	*See text*
2. *Granulomatous, infectious, and inflammatory lesions*	
Xanthogranuloma	Cheng D, Yang F, Li Z, Qv F, Liu W. Juvenile Xanthogranuloma of the Sellar Region with a 5-Year Medical History: Case Report and Literature Review. Pediatr Neurosurg. 2021;56(5):440-447. doi: 10.1159/000515517
Granulomatosis with polyangiitis (GPA) (formerly Wegener granulomatosis)	*See text*
Hypophysitis	*See text*
Pituitary abscess	*See text*
3. *CSF-containing cysts*	
PEIR	*See text*
Intrasellar arachnoid cyst	Mangussi-Gomes J, Gentil AF, Filippi RZ, Momesso RA, Handfas BW, Radvany J, Balsalobre L, Stamm AC. Sellar and suprasellar arachnoid cyst. Einstein (Sao Paulo). 2019 Jan 31;17(1):eAI4269. doi: 10.31744/einstein_journal/2019AI4269
4. *Cell rest lesions*	
Colloid cysts	Guduk M, Sun HI, Sav MA, Berkman Z. Pituitary Colloid Cyst. J Craniofac Surg. 2017 Mar;28(2):e166-e168. doi: 10.1097/SCS.0000000000003142
Dermoid	Pan YB, Sun ZL, Feng DF. Intrasellar dermoid cyst mimicking pituitary apoplexy: A case report and review of the literature. J Clin Neurosci. 2017 Nov;45:125-128. doi: 10.1016/j.jocn.2017.05.023
Epidermoid	Vellutini EAS, Pahl FH, Stamm AEC, Teles Gomes MQ, de Oliveira MF, Martins HO, Ruschel LG. Endoscopic resection of sellar and suprasellar epidermoid cyst: report of two cases and review of literature. Br J Neurosurg. 2021 Feb 1:1-6. doi: 10.1080/02688697.2021.1877610

7.3.1 CSF-Containing Cysts

7.3.1.1 Intrasellar Arachnoid Cysts

Intrasellar arachnoid cysts (Fig. 7.7) are relatively rare, with only few reports available in the literature [73, 74].

Large intrasellar arachnoid cysts often result in compression of the neighboring anatomical structures and therefore produce a clinical picture that is similar to a non-secreting pituitary adenoma. They mainly manifest with visual disturbances and hypopituitarism [75, 76], requiring surgical intervention.

Immunohistochemical evaluation is helpful in differentiating arachnoid cysts from epithelial cysts, a distinction that is sometimes difficult to achieve using routine histopathological examination [74]. Arachnoid cysts are positive for EMA but are negative for cytokeratins, GFAP, S-100 protein, transthyretin, and CEA [77].

The advantages of endoscopic transsphenoidal approach in these lesions include precise identification of the cyst wall and the normal pituitary tissue that is usually adherent and thinned out over the arachnoid cyst wall. This contributes to proper opening of the capsular wall to communicate with the subarachnoid space and to preservation of pituitary function [75].

Communicating the cyst with the subarachnoid space has evidently a downside of higher CSF leakage. Endoscopic endonasal obliteration of the cyst cavity with fat graft has been described with good results [76].

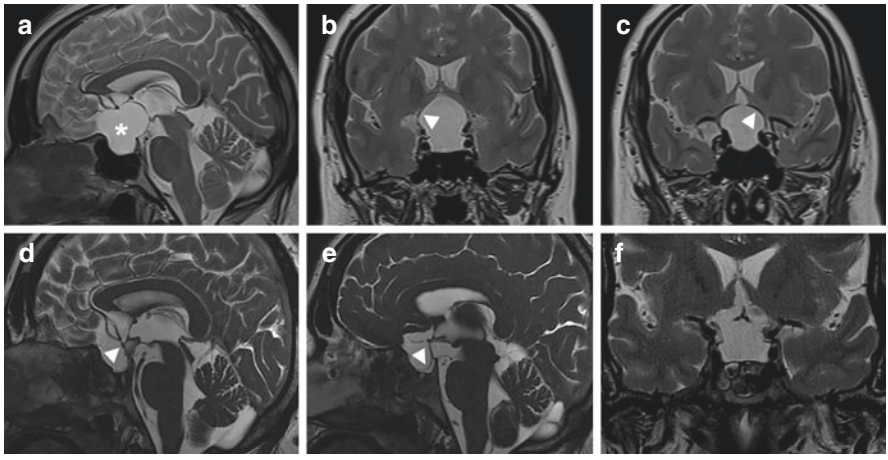

Fig. 7.7 Intrasellar arachnoid cyst. Preoperative T2-weighted MRI (**a**–**c**) revealing an intrasellar arachnoid cyst with suprasellar extension. (**a**) The lesion (asterisk) expands the sella turcica and causes compression of the floor of the third ventricle. (**b**) Coronal image demonstrating the stretched optic chiasm (arrowhead) on the superior aspect of the cyst wall. (**c**) Coronal image demonstrating the stretched A1 segment (arrowhead) on the superior aspect of the cyst wall. Postoperative T2-weighted MRI (**d**–**f**) revealed a full decompression of the cyst with notable descent of the anterior cerebral complex vessels (**d**; arrowhead) and superior cyst wall (**e**; arrowhead and **f**)

McLaughlin et al. described a fully endoscopic technique in which simple cyst fenestration is followed by obliteration of the cyst cavity using an autologous fat graft. A simplified skull base reconstruction is then performed and consists of multilayer repair and intrasellar extradural titanium micromesh reinforcement without pedicled flaps. In this technique, communicating the cyst with the subarachnoid space is avoided, and absence of diaphragmatic defects or arachnoid diverticula is confirmed under close-up endoscopic view [73].

7.3.1.2 Persisting Embryonal Infundibular Recess (PEIR) and TSE

Persisting embryonal infundibular recess (PEIR) is a very rare anomaly of the floor of the third ventricle [78] in which the embryonic morphology of the infundibular recess (IR) persists (Fig. 7.8) [79]. Rather than the normal postnatal configuration in which the IR is seen as a small funnel-shaped extension of the third ventricle within the pituitary stalk, PEIR is characterized by a tubular cavity that outpouches from the third ventricle and continues downward to terminate as dilated inferior end within the sella turcica. The tubular cavity is surrounded by a dilated pituitary stalk and displays the same signal intensity of cerebrospinal fluid (CSF) on magnetic resonance imaging (MRI) (Figs. 7.9 and 7.10) [79–81].

To the best of our knowledge, only 11 cases of PEIR have been reported so far in the English literature [82]. The main findings are generally those of a dilated pituitary stalk within which a tubular cavity that has the same signal intensity of CSF is

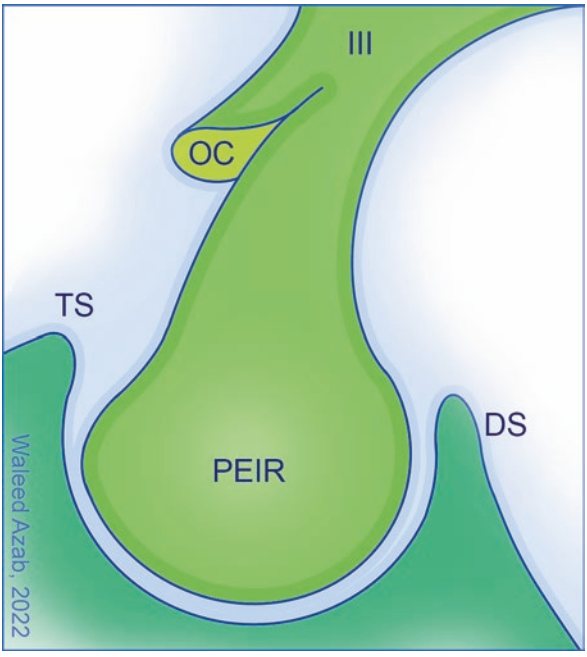

Fig. 7.8 PEIR is characterized by a tubular cavity that outpouches from the third ventricle and continues downward to terminate as dilated inferior end within the sella turcica

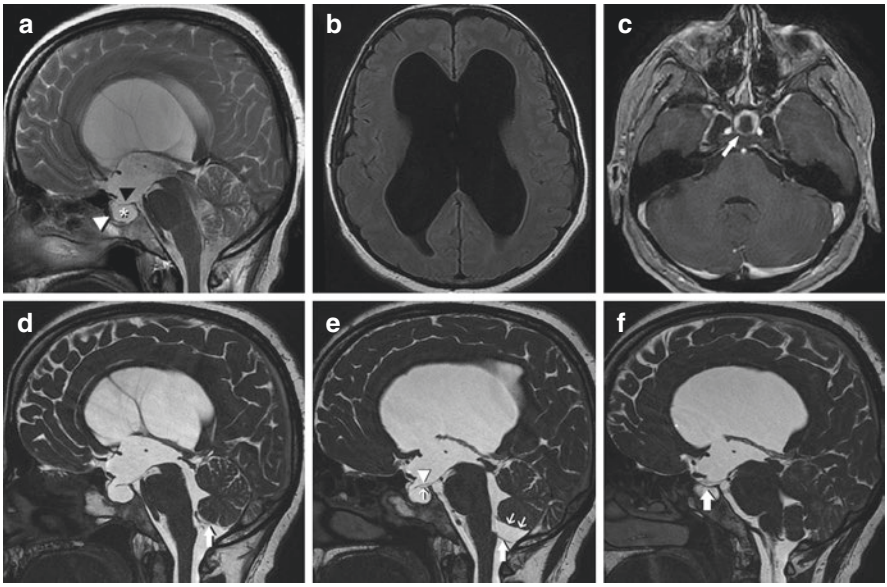

Fig. 7.9 PEIR with tetraventricular hydrocephalus in a patient who underwent ETV. Preoperative sagittal T2-wighted image (**a**) demonstrating an enlarged sella with a picture simulating that of an empty sella (asterisk) but suggestive of PEIR. The pituitary gland is probably seen at the sellar floor (white arrowhead). The diaphragma sellae (black arrowhead) is clearly seen. Note the enlarged third ventricle and patent aqueduct with CSF flow signal. Enlargement of the lateral and fourth ventricles is seen in the axial T2-Flair (**b**) and T1-wighted with contrast (**c**) MR images. Postoperative MRI 3D FIESTA-C (three-dimensional fast imaging employing steady-state acquisition cycled phases) (**d**–**f**) reveal the PEIR as a tubular downward extension of the third ventricular floor into a cystic expansion within the sella. A clear distinction is evident between the diaphragma sellae (**e**, small arrow and, **f**, arrow) and the membranous third ventricular floor with PEIR (**e**, arrowhead)

seen. The tubular cavity is in continuity with the third ventricle superiorly and extends downward into an inferior end within the sella turcica. The intrasellar end is often dilated, with variable morphological descriptions among the reported cases including a round pocket [83], a round cystic formation [78, 81, 84], a multicystic dilatation [85], or a diverticulum of the anterior third ventricle [86].

Recently, Kelsch et al. pointed out that PEIR should perhaps belong to the spectrum of abnormalities of midline encephaloceles [87]. In a recently published work, our group in collaboration with Naples group suggested that PEIR and TSE do actually represent the two extremes of one continuum of malformations [82]. This was based on (1) the very close morphological similarity between the third ventricle's floor and its IR in cases of TSE and those in the published cases of PEIR, (2) the intersecting spectra of associated anomalies in PEIR and TSE, (3) the frequent impossibility to identify the pituitary gland on imaging studies in both PEIR and TSE, (4) the associated pituitary dysfunction in PEIR and TSE, and (5) the possible

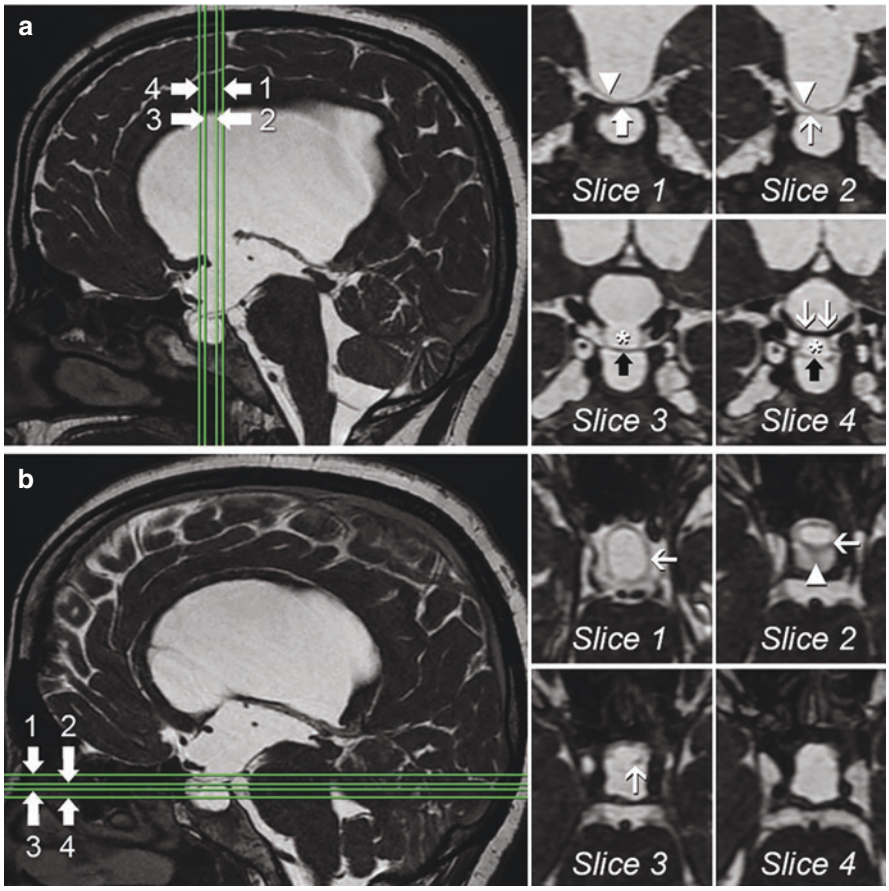

Fig. 7.10 Detailed imaging in PEIR. In (**a**), coronal reformatted images of the 3D FIESTA-C sequence are shown. At the level of the dorsum sellae (Slice 1), the dorsum sellae (arrow) and the third ventricle's floor (arrowhead) are seen. Through the diaphragma sellae (Slice 2), the diaphragma sellae (arrow) and the third ventricle's floor (arrowhead) can be distinguished. Through the plane of PEIR (Slice 3), the posterior wall (arrow) of the tubular-shaped PEIR (asterisk) is seen. Through the plane of PEIR and optic chiasm (Slice 4), the posterior wall (arrow) of the tubular-shaped PEIR (asterisk) is seen, while the anterior wall of the PEIR is attached to the optic chiasm (double arrows). In (**b**), axial reformatted images of the 3D FIESTA-C sequence are shown. At levels above (Slice 1), at (Slice 2), and just below (Slice 3) the level of the diaphragma sellae (arrowhead), the wall of the tubular PEIR (arrows) is seen. The cystic expansion within the sella is seen at a lower level within the sella (Slice 4)

embryogenetic role of the craniopharyngeal canal (CPC) in the pathogenesis of both conditions.

Accurate imaging diagnosis of PEIR and TSE is essential to avoid unnecessary treatment and complications. The condition can be confused with other cystic sellar lesions. While an endoscopic endonasal repair is obviously necessary in case of TSE, attempting remove a PEIR via a transsphenoidal approach is not only

contraindicated but also will result in postoperative CSF leak and risk of meningitis. Surgical treatment should target the associated disease that is per se indicated for surgery [82].

7.3.2 Granulomatous, Infectious, and Inflammatory Lesions

7.3.2.1 Rare Types of Hypophysitis

Hypophysitis is the collective diagnosis for inflammatory disorders of the pituitary gland and infundibulum. Most forms of hypophysitis are mediated by autoimmune reactions. However, some disorders classically considered hypophysitis are infections, e.g., with granulomatous infiltration, or neoplastic, e.g., Langerhans cell histiocytosis [88].

The diagnosis of hypophysitis is challenging and can be made on clinical and laboratory basis of unexplained hypopituitarism in addition to characteristic MRI findings including diffuse pituitary gland enlargement or thickening of the pituitary stalk or both. Pituitary stalk thickening, however, is only present in a subset of patients with hypophysitis [89].

Although scoring systems have been suggested to aid in distinguishing hypophysitis from pituitary adenomas [90], distinguishing hypophysitis from other pituitary lesions based on imaging alone is still at times very difficult [88].

Only in a minority of patients with presumed hypophysitis, a pituitary biopsy may be warranted to confirm the diagnosis if MRI findings are not completely convincing [89].

From the histopathological standpoint, primary hypophysitis falls into five subtypes including lymphocytic (LHP), granulomatous (GHP), xanthomatous (XHP), IgG4-related (IgG4rHP), and necrotizing (NHP) HP [89, 91–94]. On the other hand, secondary hypophysitis is an inflammatory condition of the pituitary gland, related to systemic pathologies, such as sarcoidosis (Fig. 7.11), Wegener granulomatosis, Langerhans cell histiocytosis, tuberculosis (Fig. 7.12), and connective tissue disorders [87].

7.3.2.2 Xanthogranuloma

Xanthomatous lesions of the sellar region have traditionally been divided into two separate categories: xanthomatous hypophysitis (XH) and xanthogranuloma (XG) of the sellar region [95]. Recent evidence suggests that xanthomatous lesions of the sella may represent a continuum and that both XH and XG in most cases can be linked to RCC leakage, rupture, or hemorrhage [95, 96]. Xanthogranulomas (Fig. 7.13) are granulomatous lesions that consist of an accumulation of foamy macrophages, multinucleated foreign body giant cells, cholesterol clefts, hemosiderin deposits, necrotic debris, lymphocytic infiltrates, and fibrous proliferation [97,

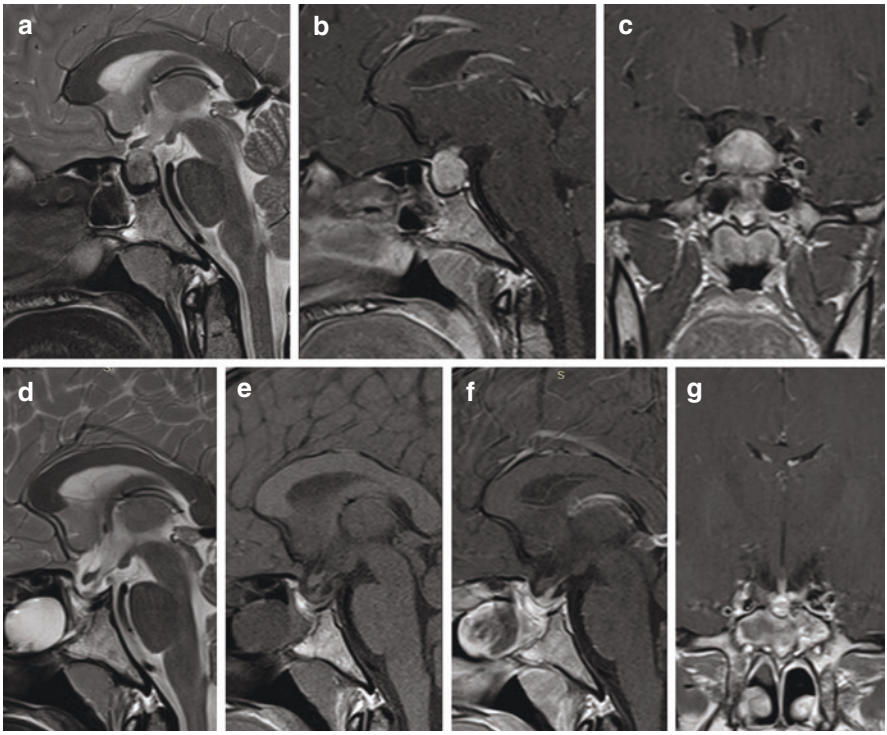

Fig. 7.11 Sarcoidosis of the pituitary gland. Pre- (**a**–**c**) and postoperative (**d**–**g**) MR images after endoscopic endonasal transsphenoidal resection of the lesion

98]. They present clinically with headache, weight loss, anorexia, nausea, fatigue, visual disturbances, and varying degrees of anterior pituitary hormonal deficiencies or panhypopituitarism. They may also lead to diabetes insipidus of central origin and obstructive hydrocephalus [99].

Paulus et al. were the first to suggest these lesions to be a separate entity from adamantinomatous craniopharyngiomas and reported their occurrence in adolescents and young adults, predominant intrasellar location, smaller lesion sizes, more severe endocrinological deficits, longer preoperative history, lower frequency of calcification and visual disturbances, and better resectability [98].

These lesions are difficult to diagnose on the basis of clinical or radiological presentations. There are no typical radiological characteristics or patterns for xanthogranuloma [99]. They present with variable MR signal intensities due to the intralesional inconsistent patterns of hemorrhage and calcification [100, 101]. Surgical resection is the present treatment for sellar xanthogranuloma, and gross total resection is considered as a gold standard treatment for this lesion. The endoscopic endonasal approach is favored over other approaches [102]. The endoscopic endonasal approach (Fig. 7.14) lends itself to the management of these lesions because the exposure and visualization of the supra- and parasellar areas are

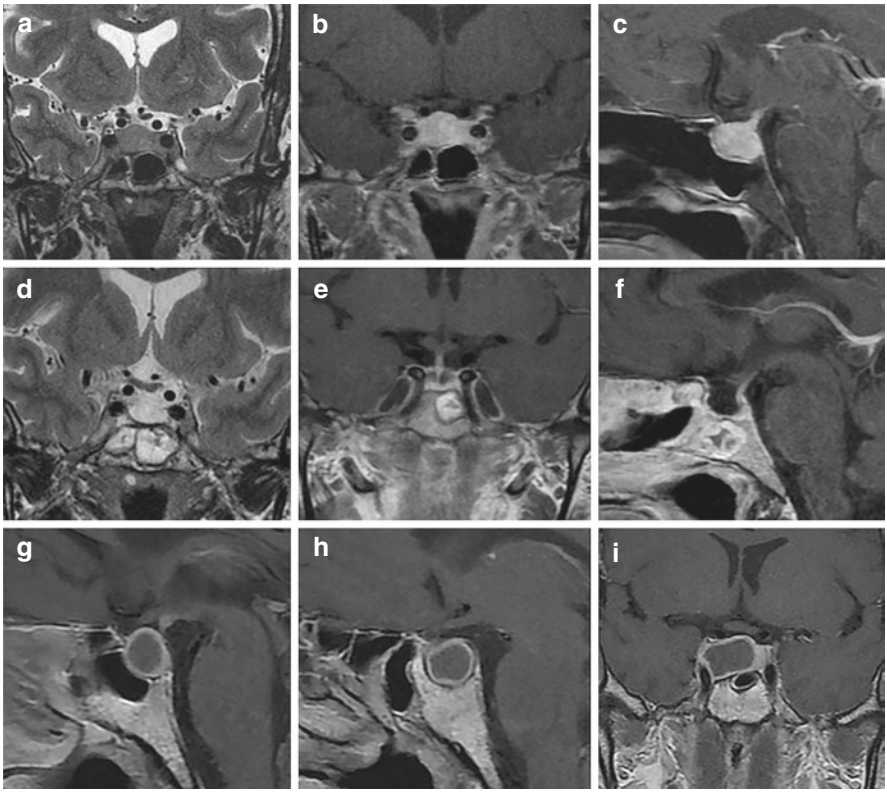

Fig. 7.12 Tuberculous hypophysitis and tuberculous pituitary abscess. Pre- (**a**–**c**) and postoperative (**d**–**f**) MR images in one case of tuberculous hypophysitis that was treated by endoscopic endonasal transsellar approach. (**g**–**i**) Preoperative MR images in another patient with pituitary tuberculous abscess

superior to a microscopic transsphenoidal approach and are less invasive than craniotomy [97].

7.3.2.3 Pituitary Abscess (PA)

Pituitary abscess (PA) is a rare disease that accounts for about 1% of operated sellar lesions [103, 104]. A secondary pituitary abscess may develop after surgery or on top of another pathology or sepsis [103–108]. On the other hand, a primary pituitary abscess occurs in previously healthy normal glands [103]. In these cases, the presentation is similar to other pituitary disorders making the diagnosis of pituitary abscess difficult and is usually made during or after drainage and evacuation of purulent contents of the lesion [104]. On MRI, pituitary abscess is very difficult to distinguish from other sellar cystic lesions and pituitary adenomas. Gadolinium injection is helpful as the absence of central enhancement suggests a fluid or necrotic

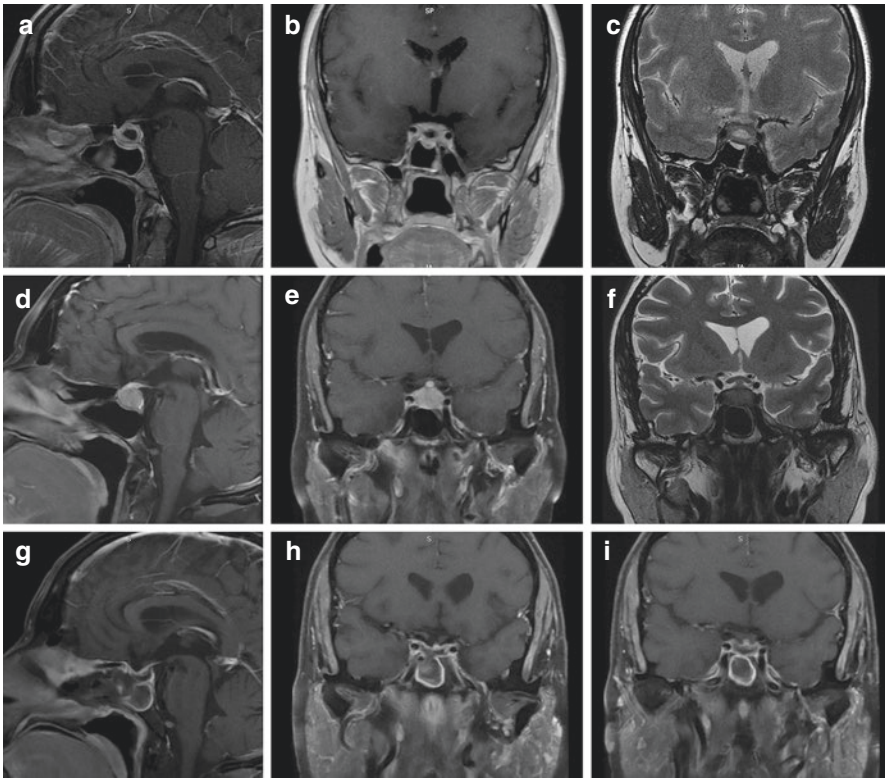

Fig. 7.13 Pituitary xanthogranuloma. First set of MR images (**a**–**c**) with a picture suggestive of hypophysitis. Repeat imaging (**d**–**f**) after medical treatment. (**g**–**i**) Postoperative MR images after endoscopic endonasal transsphenoidal approach

center [104]. Wang et al. described the majority of pituitary abscesses to be cystic or partially cystic, hypointense or isointense on T1-weighted imagine, and hyper- or isointense on T2-weighted imaging, with ring enhancement on post-gadolinium imaging [107]. Central hypo- or iso-intensity with internal heterogeneity and a surrounding hyperintense rim that enhances after contrast administration has also been described [107]. Diffusion restriction has also been demonstrated in pituitary abscesses [109, 110]. The aforementioned MR imaging findings are, however, also seen in sellar tumors undergoing central necrosis. Evidently, surgical evacuation via endoscopic transsphenoidal surgery and subsequent antibiotic therapy should immediately be undertaken.

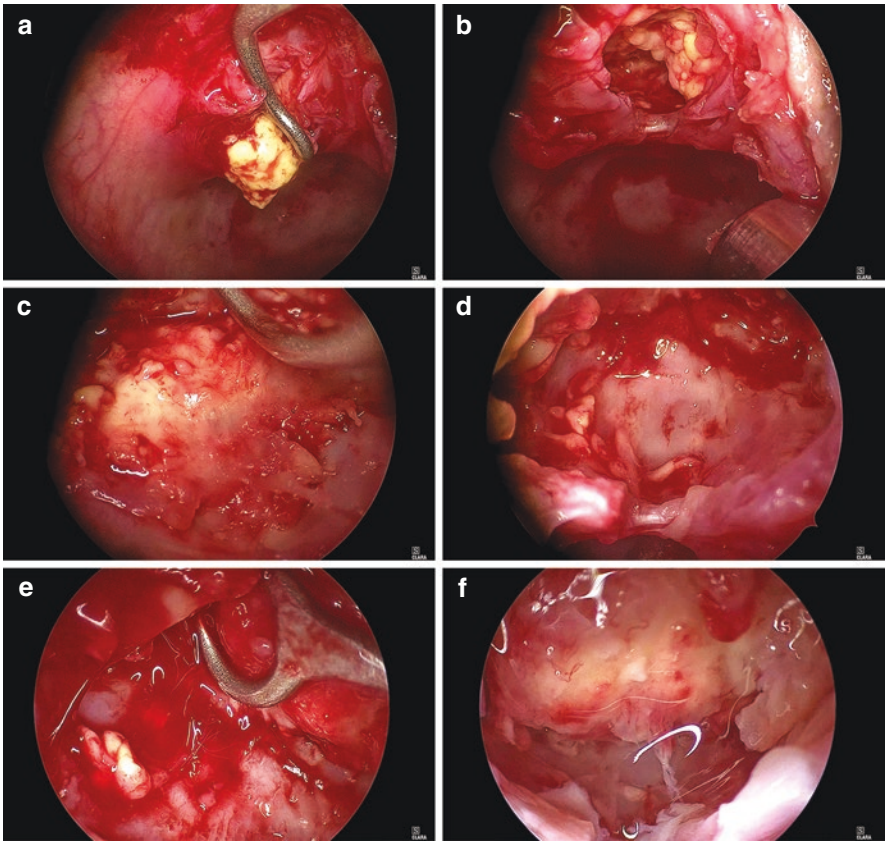

Fig. 7.14 Pituitary xanthogranuloma. Operative views (**a**–**f**) during endoscopic endonasal transsphenoidal approach

7.3.3 Neoplastic Lesions

7.3.3.1 Pituitary Blastoma

Pituitary blastoma is a distinctive and rare type of malignant neoplasms of the anterior hypophysis in infants described first by Scheithauer in 2008 [111, 112]. It appears to be an embryonal tumor originating in utero and is considered to be a pathognomonic feature of germline DICER1 mutation [22].

It presents in infants under 24 months of age and most frequently with Cushing's disease and elevated adrenocorticotropic hormone (ACTH) and occasionally with ophthalmoplegia, signs of increased intracranial pressure, diabetes insipidus, and thyrotropin deficit; Cushing's disease presenting in an infant suggests pituitary blastoma. The levels of other pituitary hormones can be variably affected. Excess serum cortisol causes severe and often lethal Cushing's disease [113–116].

Most cases have varying degrees of ACTH and growth hormone immunoreactivity which is an unusual combination of hormonal secretions in pituitary tumors. Immunohistochemical staining for other pituitary hormones are typically negative. The immunoprofile of pituitary blastoma includes keratins, galectin-3, annexin-1, scant GFAP and S100 expression in folliculostellate cells, and synaptophysin and chromogranin expression in secretory cells [113].

Pituitary blastoma is rare and has no specific imaging findings on MRI [20]. The tumor often appears as a large solid or partially cystic mass arising from the sella with extension into the hypothalamus. They may encompass the optic chiasm and/or cavernous sinuses [115].

Pituitary blastoma should be included in the differential diagnosis when an enhanced sellar and suprasellar mass with peripherally located cysts in the suprasellar portion is found in children; pituitary blastoma size usually ranges from 2 to 4 cm. They rarely calcify [22]. Radiological differential diagnosis includes pituitary adenoma, massive pituitary hyperplasia, hamartoma, and teratoma [111, 115].

The pathologic features include epithelial glands with rosette-like formations resembling immature Rathke's epithelium, small primitive-appearing cells with a blastoma-like appearance, and large secretory epithelial cells resembling adenohypophyseal cells expressing neuroendocrine markers such as ACTH in most cases and rarely GH [114, 115].

Germline *DICER1* mutation is the major and possibly sole predisposing genetic contributor for the development of a pituitary blastoma [111, 116, 117].

The diagnostic criteria of pituitary blastoma include (a) occurrence in infancy, (b) frequent endocrine hyperfunction (ACTH secretion with or without Cushing's disease), and (c) composition of Rathke's epithelium, folliculostellate cells, and secretory cells featuring ACTH and minor GH immunoexpression [112].

Total surgical resection of tumor cannot be achieved; however, gross total or near total resection is associated with better survival, and intensive focal radiotherapy is associated with some complication, particularly vasculopathy. Prognosis is unfavorable with almost half of these children dying shortly after the diagnosis [115, 116].

7.3.3.2 Uncommon Pituitary Adenomas (PitNETs)

Although a pituitary adenoma represents the most common pathology in the sellar region, some adenomas are quite rare. These subtypes include plurihormonal PIT-1-positive adenoma, acidophilic stem cell adenoma (ASCA), Crooke's cell adenoma, and COVID-19-induced pituitary adenoma apoplexy.

Plurihormonal PIT-1-positive adenoma (Fig. 7.15) is newly defined rare entity characterized by a monomorphous population of cells that express variable levels of GH, PRL, β-TSH, and α-SU. These adenomas have been previously called silent adenoma subtype 3 [118, 119]. Most plurihormonal PIT-1-positive adenomas are clinically silent, although some patients may present with acromegaly, hyperprolactinemia, or hyperthyroidism. Their recognition is of significance due to their

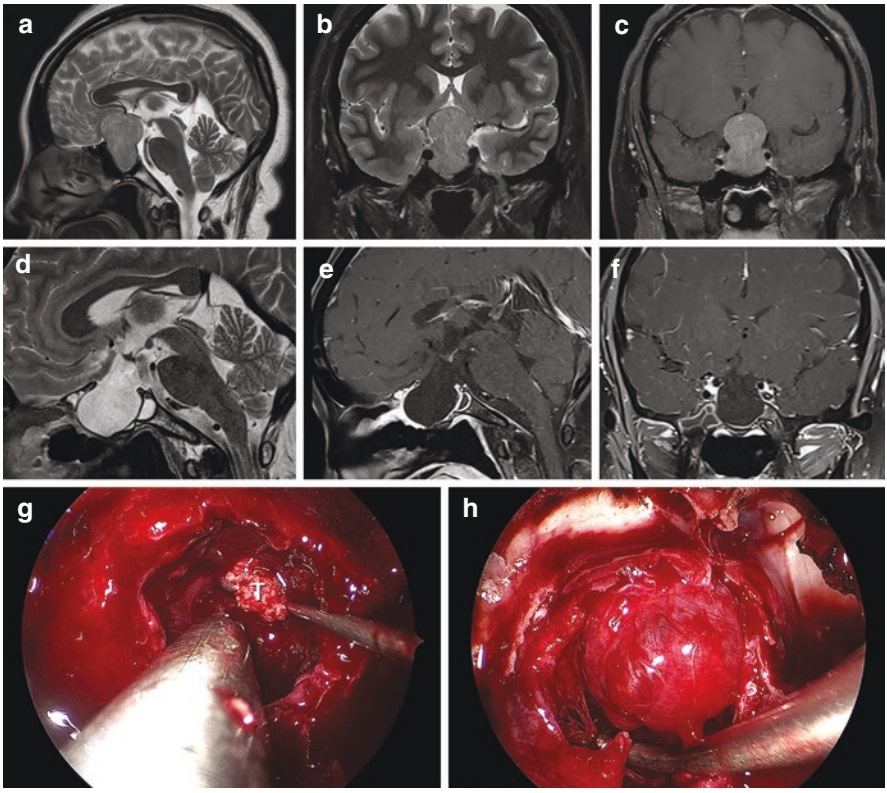

Fig. 7.15 Plurihormonal PIT-1-positive adenoma. Pre- (**a–c**) and postoperative (**d–f**) MR images. Intraoperative views demonstrating the tumor gross appearance (**g**) and its complete resection with full descent of the cistern (**h**)

intrinsic aggressive behavior with high degree of invasiveness, low rates of disease-free survival, and high tendency for recurrence [118].

Acidophilic stem cell adenoma (ASCA) is a rare subtype of lactotroph adenoma accounting for the minority of clinically diagnosed prolactin-secreting adenomas. These tumors are clinically characterized by variable degrees of hyperprolactinemia, with or without elevatation of growth hormone (GH) and insulin growth factor I (IGF-1) levels [118, 120]. The majority are rapidly growing macroadenomas with invasive features and more aggressive behavior than other lactotroph adenomas and a lower surgical cure rate [12]. The tumors are characterized by cells with acidophilic cytoplasm with focal oncocytic changes. Unlike lactotroph adenomas, ASCA display perinuclear, dot-like fibrous bodies confirmed by cytokeratin staining. A characteristic feature of ASCA is accumulation of mitochondria with sometimes dilated giant forms [118].

Crooke's cell adenoma (Fig. 7.16) is a very rare subtype of corticotroph pituitary adenomas that is known to be potentially aggressive [121, 122]. They contain Crooke's hyaline material in the cytoplasm of more than 50% of the tumor cells,

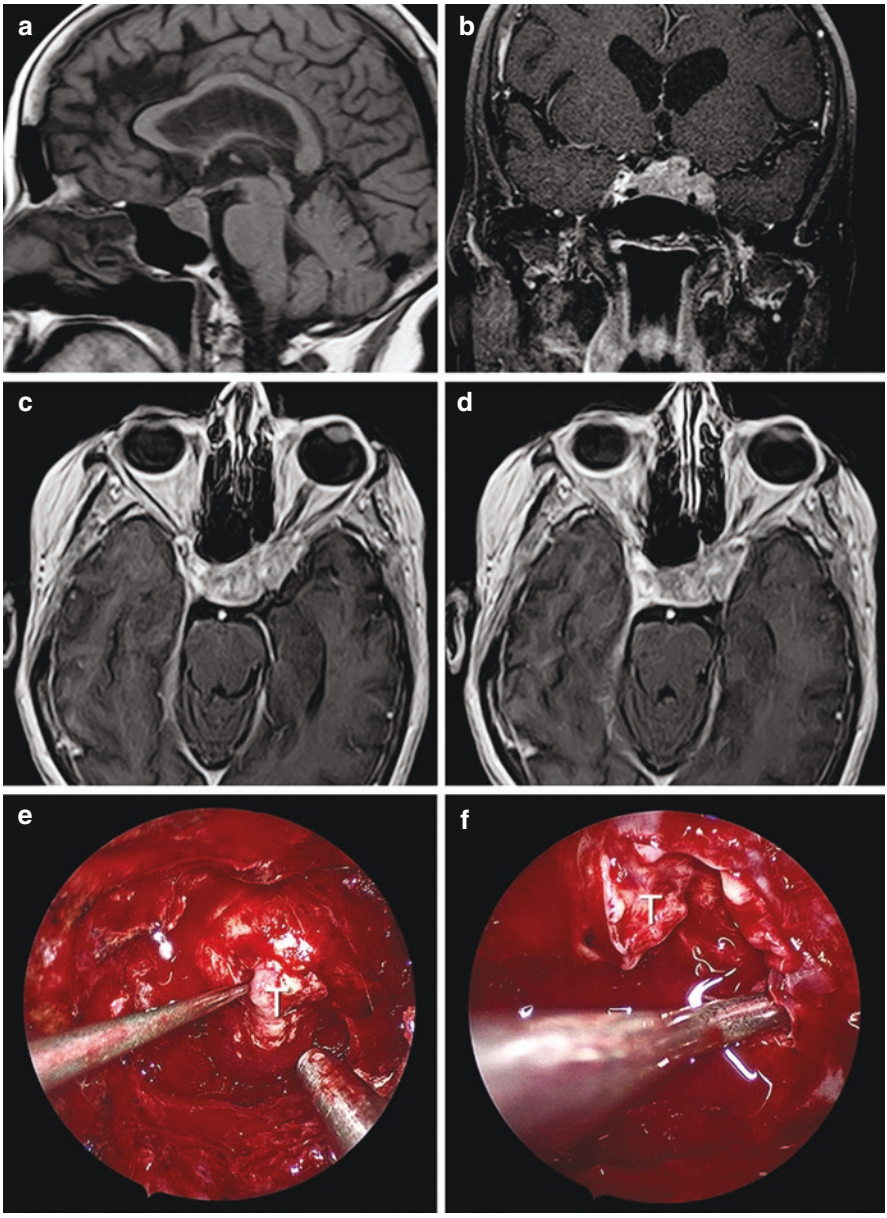

Fig. 7.16 Crooke's cell adenoma. Preoperative MR images (**a**–**d**) and intraoperative views during endoscopic endonasal transsphenoidal resection of the tumor (T), (**e**, **f**)

stain positively for adrenocorticotropic hormone (ACTH), and have variable degrees of clinical expression of Cushing's disease. The majority of Crooke's cell adenomas are macroadenomas with cavernous sinus invasion and suprasellar extension. They

tend to behave aggressively after surgical removal with more than 60% recurrence rate [123]. Endoscopic endonasal transsphenoidal excision is the first line of treatment. Other treatment modalities include fractionated radiation [121], GKRS [122], and temozolomide [124].

COVID-19-induced pituitary adenoma apoplexy is another rare pathology with few cases reported so far. Our group reported the fifth case of this entity (Fig. 7.17) [125]. We postulated that some pathophysiological mechanisms induced by COVID-19 can possibly lead to the development of pituitary apoplexy. In other words, the association between both conditions was not just a mere coincidence. Although the histopathological features of pituitary apoplexy associated with COVID-19 are similar to PA induced by other etiologies, future research may disclose unique pathological fingerprints of COVID-19 virus that explain its capability of inducing pituitary apoplexy [125].

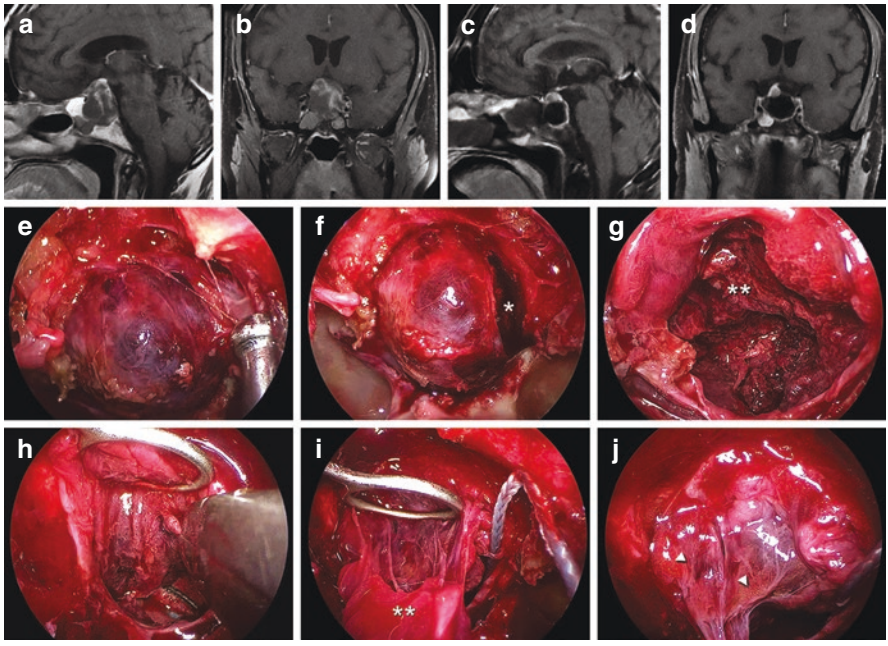

Fig. 7.17 MRI images in a case of COVID-19-associated pituitary apoplexy (**a**–**d**). Preoperative T1-weighted images reveal a large recurrent pituitary macroadenoma with minimal patchy enhancement after gadolinium injection (**a**, **b**). Postoperative T1-weighted images with contrast revealed near total excision of the adenoma (**c**, **d**). Intraoperative views during endoscopic endonasal transsphenoidal tumor excision (**e**–**j**). (**e**) Bluish discoloration of the dura caused by apoplexy of the underlying tumor is evident at the initial exposure. (**f**) Dark blood (asterisk) is seen upon initial dural opening. (**g**) View of the necrotic purple adenoma tissue being resected from within the sella. (**h**) A pituitary ring curette elevates the downward bulging cistern, and a pituitary rongeur is used to excise the superior part of the tumor. (**i**) The uppermost tumor components (double asterisks) have been separated from the arachnoid of the suprasellar cistern. (**j**) Final view after tumor resection. Note the fat from previous surgery (arrowheads) (Images and caption from Kamel et al. 2021 [125], reprinted with permission from Surgical Neurology International©, ScientificScholar)

7.3.3.3 Pituitary Carcinoma

Pituitary carcinomas are rare malignant neoplasms of adenohypophyseal cell origin and account for approximately 0.12% of adenohypophyseal tumors [126]. Pituitary carcinomas are defined by demonstration of craniospinal dissemination and/or systemic metastases [118]. They can be functioning or nonfunctioning. PCs more often are lactotroph or corticotroph tumors, producing prolactin (PRL) or adrenocorticotropic hormone (ACTH), respectively [126, 127]. They metastasize through postoperative drop metastasis, CSF spreading, or blood-borne sellar dura infiltration. They can disseminate to other organs like liver, bone, heart, ovaries, and lymph nodes [126]. The treatment of PCs remains multimodal and includes surgical resection, linear accelerator (LINAC)- and proton-beam-based fractionated radiotherapy, single-dose GKRS, chemotherapy, immunotherapy, and the use of other pharmacological agents targeting hormone production [126].

7.3.3.4 Pituitary Gland Metastasis

The pituitary fossa is an uncommon site for metastatic lesions; they occur in 1% of all pituitary lesions. The most common lesions that metastasize to the sellar region are from the breast and lung. Other primary sites include renal, prostate, and colon. Metastatic lesions to the pituitary fossa involve the neurohypophysis and posterior lobe more commonly than anterior lobe of the pituitary gland. More than 50% of the cases present with diabetes insipidus which rarely occurs with pituitary adenomas. Panhypopituitarism may also be present [128–131].

Metastasis to the pituitary gland should be in the differential diagnosis in a new sellar lesion in patients with known oncological history [132]. Imaging findings may offer some clues to whether a lesion is benign or metastatic, though a significant overlap exists making radiological examination nonspecific [133]. There is no standardized treatment for pituitary metastasis. Generally, surgery plays an important role for improving symptoms caused by the lesion, such as visual abnormalities. Total resection tends to be difficult to achieve due to high tumor vascularization and local invasiveness. EET seems very safe to achieve biopsy and symptomatic relief [134].

7.3.3.5 Ganglioglioma

Gangliogliomas of the sellar region are extremely rare and easily misdiagnosed lesions. Very few cases have been reported to originate from the pituitary [135], neurohypophysis [136, 137], and adenohypophysis [138]. Histologically, ganglioglioma is characterized by a mixture of atypical ganglion cells and neoplastic glial cells. Immunostaining of specific neural marker such as synaptophysin, chromogranin A, NFP, and GFAP can help with the diagnosis; GFAP is critical to diagnose glial component of ganglioglioma [135, 138].

The pathogenesis of ganglioglioma is still unclear. They possibly take origin from pluripotent progenitor cells or as a malformative neuronal lesion with glial component representing a transformed hamartomatous element [138]. In the case reported by Omofoye et al., an endoscopic endonasal transtuberculum sellae approach was used to expose the pituitary stalk. The tumor was 4 mm in diameter, firm, white, and integral to the right side of the enlarged pituitary stalk. The authors concluded that endoscopic endonasal approach for stalk gangliogliomas is a safe surgical approach to establish a tissue diagnosis [135]. In the case reported by Hong et al., the endoscopic endonasal transsphenoidal surgery revealed a dark red mass with firm texture and rich blood supply that was adherent to the diaphragma sellae. Subtotal resection was conducted because of the highly vascular nature of the tumor [138].

7.3.3.6 Gangliocytoma

The pituitary gangliocytoma is extremely rare benign brain tumor representing <1% sellar tumors. Ganglion cell tumors in sellar location are usually associated with functioning or nonfunctioning pituitary adenomas or pituitary cell hyperplasia. They are WHO grade I tumors [139–143]. The most frequent endocrine syndrome associated with gangliocytoma is acromegaly, followed by hyperprolactinemia, and less frequently Cushing's disease; around 85% of gangliocytoma cases are associated with a pituitary adenoma and are more prevalent in female patients [139, 140]. The diagnosis of these tumors is only possible after surgery as radiologically they are indistinguishable of sellar/suprasellar masses; the definitive diagnosis is determined by the histological and/or immunohistochemistry studies. They are well-differentiated slow-growing neuroepithelial tumors. The most common finding is the coexistence of neural tissue and GH-secreting pituitary adenoma [139, 140]. Three main theories have been proposed for the histogenesis of gangliocytoma: (1) primary gangliocytoma inducing an adenoma by paracrine secretion of hypothalamic hormonal stimulation, (2) transdifferentiation of adenomatous cells into neuronal/gangliocytic cells, and (3) a common progenitor/stem cell capable of transformation in the two cellular components [143].

Despite the rarity of mixed adenoma-gangliocytoma, this entity should be considered in the differential diagnosis of sellar masses. Complete tumor resection is considered curative [141, 143].

7.3.3.7 Neurocytoma

Sellar neurocytoma is an extremely rare form of extraventricular neurocytoma that originates from the hypothalamic-pituitary area. Very few cases have been reported in the literature [144].

Magnetic resonance imaging (MRI) remains the imaging modality of choice although no single feature is pathognomonic of extraventricular neurocytoma.

Speckled calcification may also be seen on CT scan. MRI may reveal an expanded sella with erosion of the sellar floor, sphenoid sinus invasion, and cavernous sinus involvement. The tumor may extend into the middle cranial fossa. The main radiological differential diagnosis includes pituitary adenoma, craniopharyngioma, sellar meningioma, and hypothalamic glioma [144].

Central neurocytomas generally have a favorable clinical prognosis, with surgical resection being the mainstay of treatment [144, 145].

Given the sellar and suprasellar location of the tumor, endoscopic transsphenoidal approach is considered safe for tumor resection and biopsy. In case of partial resection of tumor, adjuvant radiotherapy is important and essential because of the possibility of multiple remote disseminations in the spinal cord and drop metastasis in the initial route of surgery [144].

7.3.3.8 Sellar Ependymoma

Ependymomas are glial neoplasms that arise from the ependyma of cerebral ventricles, the spinal cord central canal, or cells of the terminal ventricle in the terminal filum. They may appear in the sellar region due to the presence of ependymal cells in the pituitary infundibulum [146]. It is thought that ependymomas that occur in the sella may be due to neoplastic transformation of either heterotopic ependymal cells or embryological remnants of the ependymal lining in the infundibular process [147].

Clinically, sellar ependymomas present with panhypopituitarism, headaches, and bitemporal hemianopia. Radiologically, both in CT and MRI, they resemble pituitary adenomas, where they have homogeneous enhancement. Parish et al. described the intraoperative findings to consist of yellowish-clear fluid from the suprasellar cyst and a grayish orange neoplasm, which was somewhat firmer than a typical pituitary tumor [147]. Surgery is the mainstay of treatment with the goal being gross total resection when feasible. EET is an excellent choice for ependymomas occurring in the sellar region.

7.3.3.9 Choroid Plexus Papilloma

Rare neuroectodermal tumors that develop from the choroid plexus epithelial cells tend to be in the ventricles. They account for less than 1% of all primary brain tumors. They frequently occur in the ventricular atrium and fourth ventricle. In adults, they generally occur in the fourth ventricle and very rarely do occur in extraventricular sites including the sellar region [148].

Radiologically, they vary from hypointense to hyperintense on both T1 and T2. They enhance after contrast. They resemble pituitary adenomas, and it is difficult to differentiate them based on neuroimaging alone [149]. They may show a cystic component where they appear similar to a craniopharyngioma. Clinically, they show symptoms of compression, with headaches and visual field defects being the most common. EET is an excellent approach for the resection of CPP [35].

7.3.3.10 Atypical Teratoid Rhabdoid Tumor

ATRTs are rare aggressive pediatric malignant tumors that generally occur in the cerebellum (60%). These tumors are extremely rare to occur in adults. When they do occur in adults, they are most common in the cerebral hemisphere followed by the sellar region [150]. Sellar ATRT occurs more frequently in females and presents with visual disturbances and headaches [151]. Radiologically, they are isointense on T1 and enhance with contrast. The diagnosis of AT/RT is based on tumor morphology and immunohistochemical features. They are characterized by rhabdoid cells and loss of INI-1/hSNF5 gene. Treatment requires surgery for which EET is adequate for diagnosis which is followed by chemotherapy and radiotherapy [152].

7.3.3.11 Neuroblastoma

Primary sellar neuroblastoma is an extremely rare tumor. They are easily misdiagnosed as non-secreting pituitary adenomas or other sellar masses. They mostly occur in women in the 4th decade of life [153–155]. They commonly present with visual field defects associated with hyperprolactinemia and gonadotrophin insufficiency [153]. No definite conclusion can be made by neuroimaging studies because of nonspecific CT and MRI characteristics. MRI brain shows a compressive sellar mass lesion with possible suprasellar or parasellar extension, sometimes calcified and tend to be fairly large. On MRI it is usually a differential diagnosis of non-secreting pituitary adenoma, tuberculum sellae, or diaphragma sellae meningiomas [153, 154].

Diagnosis is based on histopathological examination where immunohistochemical examination confirms the neuronal origin. These tumors are positive for neurofilaments, chromogranin, synaptophysin, and S100 protein and are negative for anterior pituitary hormones. Negative staining for EMA, GFAP, or TTF-1 is also present and excludes the possibility of posterior pituitary tumors [153–155].

The first line of treatment is surgical resection of the tumor. After diagnosis of primary sellar neuroblastomas is established, additional intra- and extracranial localizations should be sought, with particular attention to the nasal cavity. Adjuvant treatment to surgical resection might be proposed according to patient conditions and aggressive histopathological characteristics. Close endocrine follow-up and sellar MRI are required to assess for hypothalamo-pituitary dysfunction or tumor recurrence, and whole body imaging ^{123}I-MIBG scintigraphy might be useful as it is 90 to 95% sensitive for neuroblastomas [153–155].

7.3.3.12 Paraganglioma

Paragangliomas are neuroendocrine tumors the are extremely rare to occur in the sellar region. The pathogenesis is poorly understood but has been suggested that they may be derived from intrapituitary embryonic remnants of paraganglion cells

or may result from aberrant migration of the glossopharyngeal nerve to the pituitary [156]. A few cases have been documented in the literature [156–159].

The clinical features are attributed to mass effect and include headaches, visual disturbances, and endocrine abnormalities. They mimic pituitary adenomas and sellar meningiomas. They can be differentiated from adenomas on preoperative MR scan by their vascular flow voids and intense enhancement. SPECT is beneficial in differentiating paraganglioma and pituitary adenoma [158, 159].

Subtotal resections were often reported and followed by radiotherapy. Intraoperatively, these tumors are highly vascularized [41]. Chiasm decompression followed by adjuvant treatment or additional open surgery for further resection was the most common treatment course [160].

7.3.3.13 Purely Intrasellar Meningioma

Purely intrasellar meningiomas that arise from the dura covering the sella turcica are extremely rare [161]. The dura covering the sella turcica has an average surface area of about 6 cm^2 [162]. Preoperatively, they resemble a nonfunctioning pituitary macroadenoma both clinically and radiologically. Very few cases of pure intrasellar meningiomas arising from the floor of the sella turcica have also been published in the literature [163]. Purely intrasellar meningiomas present with symptoms of headaches, visual disturbances, and hormonal abnormalities due to the compression of the optic nerves and pituitary gland [164]. Generally, symptoms develop gradually. On MR scans, meningiomas enhance vividly after the administration of contrast. Hyperostosis of sella floor has been seen; however, it is difficult to identify the dural tail that is seen with meningiomas [165]. They can be approached via endoscopic endonasal transsphenoidal approach [166].

7.3.3.14 Chondrosarcoma

Chondrosarcomas are the most common intracranial malignant cartilage tumor. The occurrence of chondrosarcoma in the pituitary fossa is rare. There have been only a few cases in the literature. They typically present with symptoms attributed to mass effect. CT shows a calcified sella with destruction of the sellar bone. They are heterogeneously enhancing postcontrast administration [50]. The main differential diagnosis of chondrosarcomas is chordomas. They can be differentiated based on histopathology and immunohistochemistry with the prognosis of chondrosarcomas being more favorable than chordomas. Both chondrosarcomas and chordomas are positive for S-100 protein, though chondrosarcomas are negative for cytokeratin markers (CAM 5-2) and epithelial membrane antigens. Chondrosarcomas are divided into three histological grades: grade I (well differentiated), grade II (moderately differentiated), and grade III (poorly differentiated) [167].

Endoscopic endonasal transsphenoidal approach represents a good surgical option. The most important predictor of prognosis is the extent of resection. Since

they are relatively radioresistant, proton beam therapy is preferred over other adjuvant radiation modalities [50].

7.3.3.15 Lymphomas

Primary pituitary lymphoma may be indistinguishable from other sellar lesions as clinical and radiological features are typically nonspecific. At imaging one should consider lymphoma when evaluating an invasive sellar mass that is iso- to hypointense on T2-weighted images. The typical MR findings in primary CNS lymphoma are mass lesions that are iso- to hypointense on T1- and T2-weighted images; typically, contrast enhancement is intense and homogeneous in immunocompetent patients, but it is more likely to be inhomogeneous or ringlike in immunocompromised patients. Pituitary stalk thickening and perineural spread, however, are more distinctive for primary pituitary lymphoma. Pituitary lymphoma should be considered in the differential diagnosis of atypical masses of the sellar region in patients with hormonal dysfunction. Surgical biopsy, however, may prove invaluable in making a diagnosis in challenging cases [54, 168, 169].

7.3.3.16 Salivary Gland-Like Lesions

Microscopic aggregates of a few well-formed salivary acini, lined by low cuboidal epithelium, were first recognized to occur in the normal pituitary gland by Jakob Erdheim in 1940 and were subsequently referred to as "Erdheim rests" [170–172]. Schochet et al. demonstrated the presence of salivary gland tissue fragments in the posterior lobe of the pituitary in approximately 3% of 2300 examined human glands [173]. The presence of salivary gland rests in the sellar region that may probably be explained by the persistence of preexisting seromucous glands from the primitive oral cavity out of which the Rathke's pouch evaginates and migrates to fuse with an extension of the floor of the third ventricle, ultimately giving rise to the pituitary gland. Another explanation may be that during embryogenesis, mesenchymal components accompanying Rathke's pouch into the sella induce primitive pituitary epithelium to differentiate into salivary gland tissue [171]. Typically, these intrasellar ectopic salivary gland rests are localized in the vicinity of the neurohypophysis [174] or in the pars tuberalis and often communicate with the Rathke's cleft [175–177]. In very rare instances, they enlarge and become clinically significant because of mass effect with or without pituitary hormonal dysfunction [178, 179]. Symptomatic enlargement of ectopic SG rests may be in the form of (1) nonneoplastic enlarged ectopic salivary glands (NNESG) or (2) benign or malignant salivary tumors (ST) when neoplastic transformation takes place.

The NNSEGs mimic pituitary adenomas in clinical and radiological manifestations, making them difficult to diagnose before surgery [177]. In a recent systematic review by Feola et al. [174], 15 cases of NNESG have so far been reported. Most patients were younger than 30 years and were females (80%). The most frequent

complaints were headache, bitemporal hemianopia, blurred vision, decreased visual acuity, galactorrhea, and menstrual irregularities. Endocrine dysfunction was found in about 50% of cases and included mild elevation of serum PRL, GH deficiency, panhypopituitarism, and central hypothyroidism. Preoperative diabetes insipidus (DI) was present in 20% of cases [174]. The lesions may be intrasellar, may be typically localized in the posterior pituitary, or may display suprasellar extension [172]. On MR imaging, the lesions are characterized by variable signal intensities on T1- and T2-weighted images with inconstant contrast enhancement patterns and by frequent cystic components [174].

Benign or malignant salivary tumors (ST) mimic other nonfunctioning sellar lesions. One important consideration is that malignant salivary tumors derived from major or minor eutopic salivary glands may reach the sella through local invasion or blood spread; an extra-sellar origin should be excluded before diagnosing a primary malignancy originating from an intrasellar ectopic salivary gland rests [174, 180, 181]. Liu et al. [177] reported on 11 cases operated via a transsphenoidal approach. Intraoperatively, the 11 lesions were all cystic and filled with gelatinous fluid, which can be white, yellow, or gray material. Although intrasellar masses originating from ectopic salivary gland rests are rarely symptomatic, surgery is the preferred method to make a diagnosis and relieve symptoms.

7.3.3.17 Plasmacytoma of Sellar and Parasellar Region

Plasmacytoma or plasma cell tumor of sellar region is a neoplasm arising from monoclonal plasma cells present in the sella or surrounding bone, mucosa within the petrous or sphenoid bone or clivus. The most common plasma cell neoplasia is multiple myeloma; intrasellar plasmacytoma is a rare pituitary tumor, which originates from monoclonal plasma cells. Solitary sellar plasmacytomas are exceedingly rare, and their diagnosis is difficult because clinically and radiologically they mimic benign pituitary tumors [182–185].

The clinical manifestations reported in cases of intrasellar plasmacytoma include headache in 70% of patients. Many present with cranial nerve palsies, mainly involving nerves II–VI with symptoms of diplopia, visual loss, eye pain, ptosis, photophobia, facial numbness, and craniofacial pain. Some of the symptoms result from compression of the cranial nerves in the cavernous sinus (III, IV, V), whereas the anterior pituitary function is mostly intact [182, 183]. Hormonal abnormalities may, however, be present, among which hyperprolactinemia and sex hormone imbalance are the most frequent.

MRI typically reveals sellar mass with expansion into the sphenoid sinuses and suprasellar and parasellar areas, with features similar to other tumors of the region, especially pituitary adenomas and chordomas [185].

On MRI, differential diagnosis of sellar mass lesions such as pituitary adenomas and meningiomas and juxta-sellar mass lesions including craniopharyngioma, chordomas, germ cell tumors, and granulomatous lesions and metastases should be kept in mind [182, 183]. The definitive diagnosis of intrasellar plasmacytoma is made by

histopathological and immunohistochemical analysis of the sellar mass. In patients with diagnosis of intrasellar plasmacytoma, radiotherapy is the treatment of choice [182, 183]. Rapid tumor growth during follow-up and/or compression of the optic chiasm constitutes an indication for surgical decompression and exploration [183].

Endoscopic endonasal transsphenoidal surgical resection combined with postoperative RT might be the optimal initial treatment for the relief of mass effect and control of local recurrence. Long-term follow-up is essential because approximately 50% of cases of plasmacytoma without evidence of multiple myeloma at the diagnosis progress to overt multiple myeloma within 10 years, and 10% of them recur with a plasmacytoma, thereby underlining the importance of a correct and timely diagnosis in the management of these patients. The high-risk period for the development of disseminated disease has been suggested to be the first 3 years [182, 184].

7.4 The Uncommon Pathologies of the Clivus

There is a great variability of diseases involving the clivus; although not as vast as the sellar lesions, the list of these lesions is long. In Table 7.2 [186–210], the majority of these pathologies are enlisted. Such heterogeneity makes management of these lesions at times very challenging [211]. Managing clival lesions using a minimally invasive approach presents numerous therapeutic challenges because of the close proximity of surrounding critical structures, including the basilar artery, internal carotid artery, brain stem structures, and the cranial nerves [212]. Surgical management of clival lesions has evolved considerably over the last 2 decades, and endoscopic endonasal approaches are presently the standard of care for the vast majority of these lesions [212–215].

In the past, options for access included extended middle cranial approaches and transmaxillary, trans-oral, or even transcervical approaches; this was associated with significant morbidity and unnecessary resection of normal tissue. Even when access is achieved, the visibility often remained poor resulting in inadequate resection [216, 217]. The endoscopic endonasal transsphenoidal approach offers a direct route to the clivus. Detailed anatomical knowledge is required to appreciate the exact location and dimensions of surrounding vital structures. It is imperative to identify the internal carotid arteries, the cavernous sinus, and surrounding neurological structures before proceeding to tumor resection. The endoscope gives a clear visualization of these structures and therefore prevents potential complications and ensures optimal surgical results [218]. In the following paragraphs, a short overview of some of these rare lesions is presented.

Table 7.2 Examples of uncommon pathologies of the clivus

Amyloidoma	Schneider JR, Kwan K, Kulason KO, Faltings LJ, Colantonio S, Safir S, Loven T, Li JY, Black KS, Schaeffer BT, Eisenberg MB. Primary solitary retro-clival amyloidoma. Surg Neurol Int. 2018 May 15;9:100. doi: 10.4103/sni.sni_483_17
BNCT	Golden LD, Small JE. Benign notochordal lesions of the posterior clivus: retrospective review of prevalence and imaging characteristics. J Neuroimaging. 2014 May-Jun;24(3):245-9. doi: 10.1111/jon.12013
Brown tumor	Alwani MM, Monaco GN, Harmon SM, Nwosu OI, Vortmeyer AO, Payner TD, Ting J. A Systematic Review of Sellar and Parasellar Brown Tumors: An Analysis of Clinical, Diagnostic, and Management Profiles. World Neurosurg. 2019 Dec;132:e423-e429. doi: 10.1016/j.wneu.2019.08.126
Chondroblastoma	Liu J, Ahmadpour A, Bewley AF, Lechpammer M, Bobinski M, Shahlaie K. Chondroblastoma of the Clivus: Case Report and Review. J Neurol Surg Rep. 2015 Nov;76(2):e258-64. doi: 10.1055/s-0035-1564601
Ecchordosis physaliphora	Park HH, Lee KS, Ahn SJ, Suh SH, Hong CK. Ecchordosis physaliphora: typical and atypical radiologic features. Neurosurg Rev. 2017 Jan;40(1):87-94. doi: 10.1007/s10143-016-0753-4
Ectopic pituitary adenoma	Altafulla JJ, Prickett JT, Dupont G, Tubbs RS, Litvack Z. Ectopic Pituitary Adenoma Presenting as a Clival Mass. Cureus. 2019 Feb 28;11(2):e4158. doi: 10.7759/cureus.4158
Enchondroma	Velagapudi S, Alshammari SM, Velagapudi S. Maffucci Syndrome with Clival Enchondroma in Nasopharynx: A Case Report. Indian J Otolaryngol Head Neck Surg. 2019 Oct;71(Suppl 1):652-656. doi: 10.1007/s12070-018-1463-8
Fibromatosis	Zhang T, Xu L, Gu L, Chen W, Pandey G, Wang J, Wu Y. Calcifying fibrous tumor of the clivus presenting in an adult. Radiol Case Rep. 2019 Apr 10;14(6):771-774. doi: 10.1016/j.radcr.2019.03.028
Fibrous dysplasia	Heman-Ackah SE, Boyer H, Odland R. Clival fibrous dysplasia: Case series and review of the literature. Ear Nose Throat J. 2014 Dec;93(12):E4-9. doi: 10.1177/014556131409301202
Fungal mucocele	Zhang H, Jiang N, Lin X, Wanggou S, Olson JJ, Li X. Invasive sphenoid sinus aspergillosis mimicking sellar tumor: a report of 4 cases and systematic literature review. Chin Neurosurg J. 2020 Apr 9;6:10. doi: 10.1186/s41016-020-00187-0
Giant cell reparative granuloma	Nakamura H, Morisako H, Ohata H, Kuwae Y, Teranishi Y, Goto T. Pediatric giant cell reparative granuloma of the lower clivus: A case report and review of the literature. J Craniovertebr Junction Spine. 2021 Jan-Mar;12(1):86-90. doi: 10.4103/jcvjs.JCVJS_182_20
Giant cell tumor	Patibandla MR, Thotakura AK, Rao MN, Addagada GC, Nukavarapu MC, Panigrahi MK, Uppin S, Challa S, Dandamudi S. Clival giant cell tumor - A rare case report and review of literature with respect to current line of management. Asian J Neurosurg. 2017 Jan-Mar;12(1):78-81. doi: 10.4103/1793-5482.145112

Table 7.2 (continued)

Inflammatory	Tang H, Ding G, Xiong J, Zhu H, Hua L, Xie Q, Gong Y. Clivus Inflammatory Pseudotumor Associated with Immunoglobulin G4-Related Disease. World Neurosurg. 2018 Oct;118:71-74. doi: 10.1016/j.wneu.2018.06.174
Infrasellar craniopharyngioma	Yu X, Liu R, Wang Y, Wang H, Zhao H, Wu Z. Infrasellar craniopharyngioma. Clin Neurol Neurosurg. 2012 Feb;114(2):112-9. doi: 10.1016/j.clineuro.2011.09.010
Lipoma	Caranci F, Cirillo M, Piccolo D, Briganti G, Cicala D, Leone G, Briganti F. A rare case of intraosseous lipoma involving the sphenoclival region. Neuroradiol J. 2012 Dec 20;25(6):680-3. doi: 10.1177/197140091202500607
Lymphoma	Tsai VW, Rybak L, Espinosa J, Kuhn MJ, Kamel OW, Mathews F, Glatz FR. Primary B-cell lymphoma of the clivus: case report. Surg Neurol. 2002 Sep-Oct;58(3-4):246-50. doi: 10.1016/s0090-3019(02)00845-5
Meningioma	Kawaguchi A, Shin M, Hasegawa H, Shinya Y, Shojima M, Kondo K. Endoscopic extended transclival approach for lower clival meningioma. World Neurosurg. 2022 May 2:S1878-8750(22)00568-X. doi: 10.1016/j.wneu.2022.04.115
Metastasis	Mani A, Yadav P, Paliwal VK, Lal H. Isolated clival metastasis: a rare presentation of renal cell carcinoma. BMJ Case Rep. 2017 Aug 11;2017:bcr2017221570. doi: 10.1136/bcr-2017-221570
Osseous hemangioma	Moravan MJ, Petraglia AL, Almast J, Yeaney GA, Miller MC, Edward Vates G. Intraosseous hemangioma of the clivus: a case report and review of the literature. J Neurosurg Sci. 2012 Sep;56(3):255-9
Osteosarcoma	Mathkour M, Garces J, Beard B, Bartholomew A, Sulaiman OA, Ware ML. Primary High-Grade Osteosarcoma of the Clivus: A Case Report and Literature Review. World Neurosurg. 2016 May;89:730.e9-730.e13. doi: 10.1016/j.wneu.2016.01.054
Plasmacytoma	Goyal R, Gupta R, Radotra BD. Plasmacytoma of the clivus: a case report. Indian J Pathol Microbiol. 2006 Oct;49(4):568-70
PNET	Gupta S, Kumar A, Rangari KV, Mehrotra A, Pal L, Kumar R. Intracranial Peripheral Primitive Neuroectodermal Tumor Arising from the Clivus with Intracranial Metastasis in an Elderly Woman: Case Report and Review of the Literature. World Neurosurg. 2018 Nov;119:331-334. doi: 10.1016/j.wneu.2018.08.066
Rhabdomyosarcoma	Seiz M, Radek M, Buslei R, Kreutzer J, Hofmann B, Kottler U, Doerfler A, Nimsky C, Fahlbusch R. Alveolar rhabdomyosarcoma of the clivus with intrasellar expansion: Case report. Zentralbl Neurochir. 2006 Nov;67(4):219-22. doi: 10.1055/s-2006-942118
Sphenoid mucocele	Stavrakas M, Khalil HS, Tsetsos N, Muquit S. Clival Mucocele: A Rare Yet not Forgotten Pathology. Ear Nose Throat J. 2021 Jun 10:1455613211021176. doi: 10.1177/01455613211021176
Xanthoma	González-García L, Asenjo-García B, Bautista-Ojeda MD, Domínguez-Páez M, Romero-Moreno L, Martín-Gallego Á, Arráez-Sánchez MÁ. Endoscopic endonasal resection of clival xanthoma: case report and literature review. Neurosurg Rev. 2015 Oct;38(4):765-9. doi: 10.1007/s10143-015-0630-6

7.4.1 Isolated Sphenoid Fungal Mucocele

Isolated fungal granulomas originating within the sphenoid sinus are extremely rare in immunocompetent patients (Figs. 7.18, 7.19, 7.20, and 7.21) [219]. Its incidence ranges between 1% and 3% among patients with rhinosinusitis [219, 220]. The condition may be underdiagnosed because of its subtle onset, typically presenting with nonspecific facial pain or headaches. They may initially present when complications have already taken place [221, 222]. Complications in isolated fungal sphenoiditis occur because of the anatomical characteristics of the sphenoid sinus where important nearby structures including the pituitary gland, cavernous sinuses, internal carotids, and several cranial nerves are involved [222]. The combined presence of a fungal ball and mucocele together is rarely reported [223]. Once diagnosed, endoscopic endonasal surgery should be undertaken to prevent further compromise of neurological or ophthalmological function.

7.4.2 Giant Cell Tumor of the Clivus

Giant cell tumor of the clivus (Figs. 7.22, 7.23, and 7.24) is a rare entity. In an analysis of the 104 published reports of skull base GCTs, only 12 cases of clival giant cell tumor were encountered [224]. Given its critical location and the aggressive and locally destructive nature of the lesion, clival GCTs often present with significant neurological sequelae. As the disease progresses, more cranial nerves are involved.

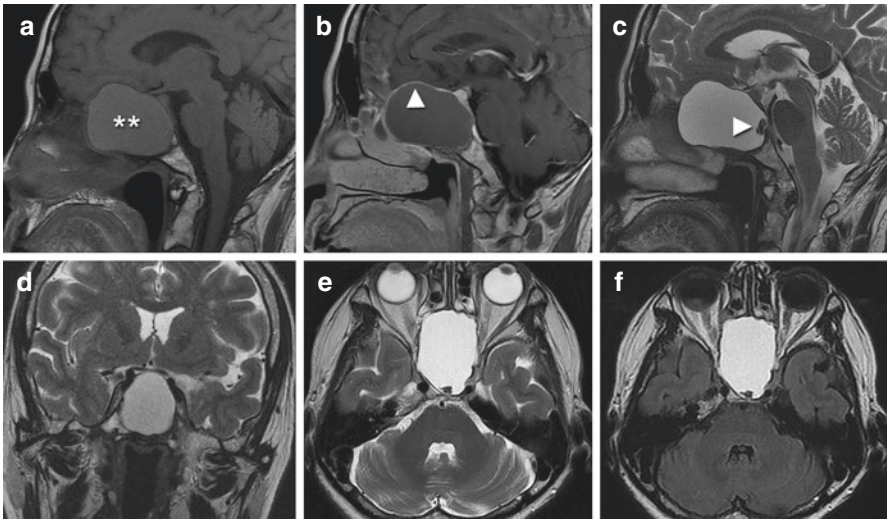

Fig. 7.18 Isolated giant fungal mucocele of the sphenoid sinus. Preoperative MR images (**a**–**f**)

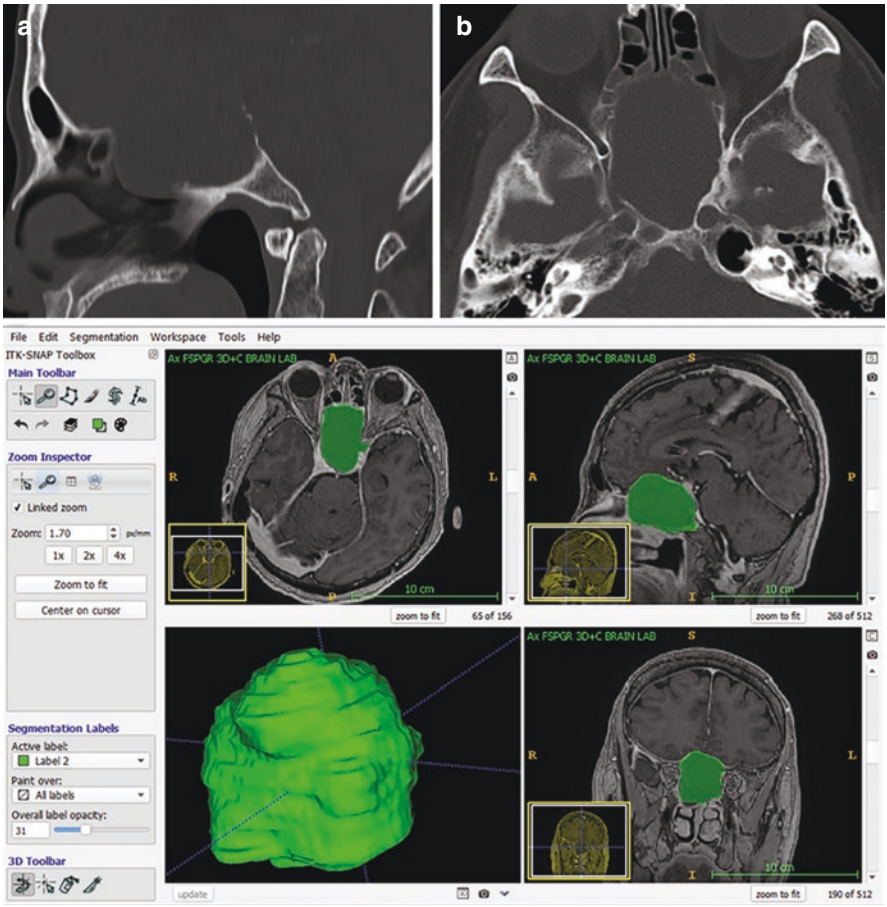

Fig. 7.19 Isolated giant fungal mucocele of the sphenoid sinus. Preoperative CT images (**a**, **b**) and preoperative volumetric analysis using ITK-Snap software

Patients present with headaches, visual field defects, diplopia, ophthalmoplegia, and deafness [225].

Radiologically, these tumors can be difficult to diagnose [226]. CT features usually show destructive and lytic lesions of the bony region involved. The nature of GCTs might vary significantly ranging from expansile to lytic lesions, and the majority show high vascularity. In general, GCTs appear to be isointense on T1-weighted MRI and hypointense on T2- and diffusion-weighted MRI [227].

Histopathological evaluation of GCTs demonstrates osteoclast-like giant cells scattered through the lesion with ovoid or spindle mononuclear stromal cells [228]. The osteolytic activity of the osteoclast-like cells makes the tumor locally destructive to the surrounding bone even though it is classified as a benign tumor [229, 230].

Histone 3.3 mutations of the *H3F3A* gene were recently described in GCT of bone and may prove useful in clarifying diagnosis in challenging cases [231].

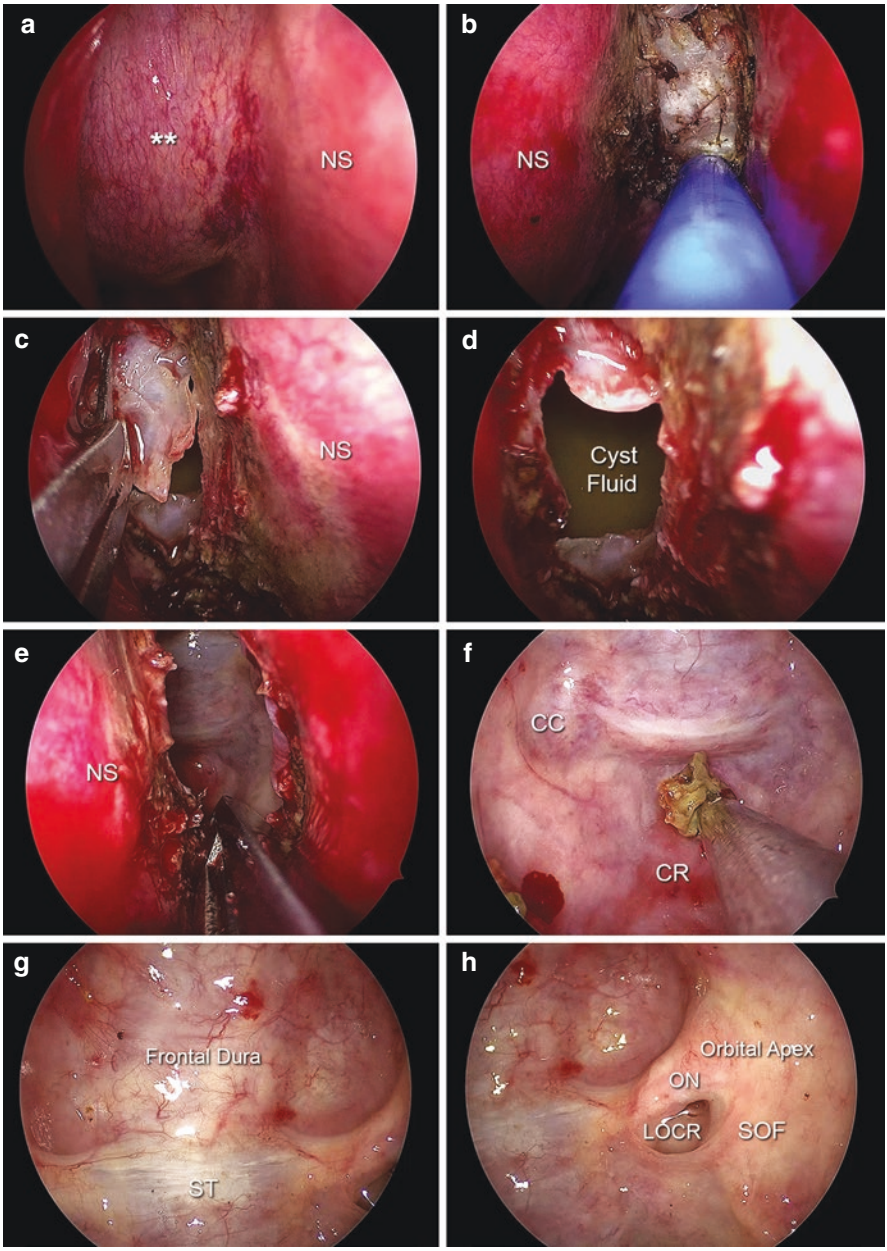

Fig. 7.20 Isolated giant fungal mucocele of the sphenoid sinus. Operative views (**a**–**h**) during cyst drainage via an endoscopic endonasal transsphenoidal approach. Note the fungus ball seen and removed after cyst fluid drainage (**f**). NS, nasal septum; double asterisks, cyst bulge into the nasal cavity; arrowheads, infiltrated clival bone; CC, cavernous carotids; CR, clival recess. ON, optic nerve; SOF, superior orbital fissure; LOCR, lateral optico-carotid recess; ST, sella turcica

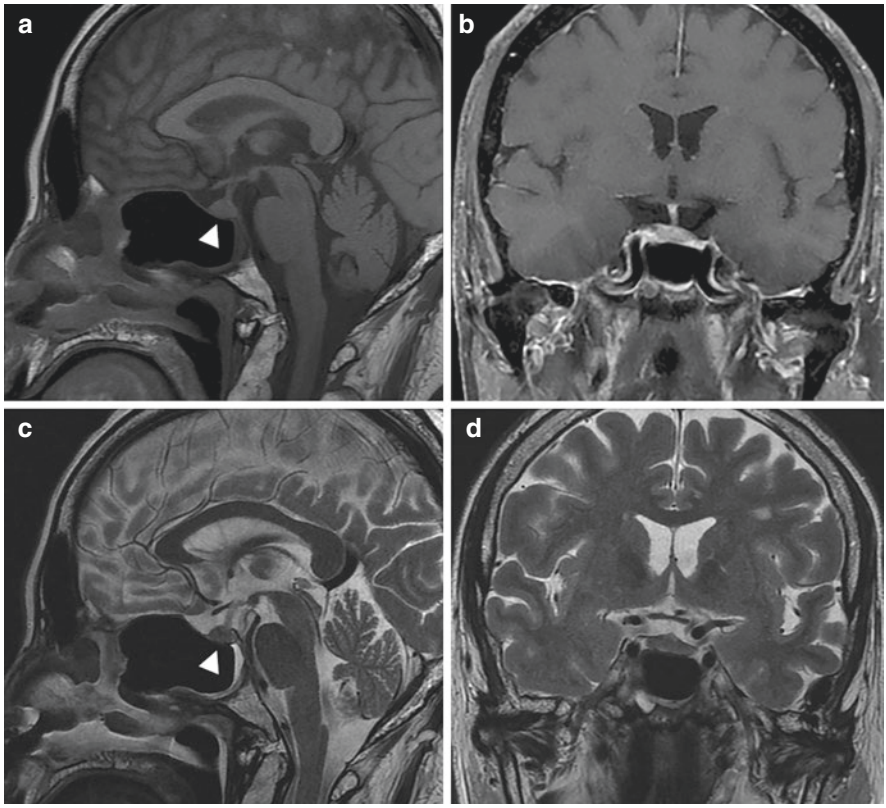

Fig. 7.21 Isolated giant fungal mucocele of the sphenoid sinus. Postoperative MRI images (**a**–**d**). Note the decompressed pituitary gland (**a**, **c**; arrowheads) and the decompressed optic chiasm in (**d**)

Although the giant cells are a significant part of this tumor, the stromal cells constitute the actual neoplastic component [224]. Neoplastic stromal cells of GCT overexpress RANKL (receptor activator of nuclear factor kappa-B ligand) and activate osteoclast-like giant cells [230]. The high expression of RANKL by the stromal cells within clival GCT offers an explanation as of why denosumab, a monoclonal antibody directed against RANKL, is effective in treating these lesions [224, 232, 233].

The aim of treatment of clival GCTs is total resection; unfortunately, this is rarely achieved due to the nature of the disease and its close proximity to vital structures. Endoscopic endonasal transclival approach allows better visualization of the clivus and tumor [234, 235]. Adjuvant radiotherapy is considered as a standard of care in the management of GCTs in most institutions nowadays although the concern that radiation may initiate sarcomatous transformation of the GCTs still remains [234].

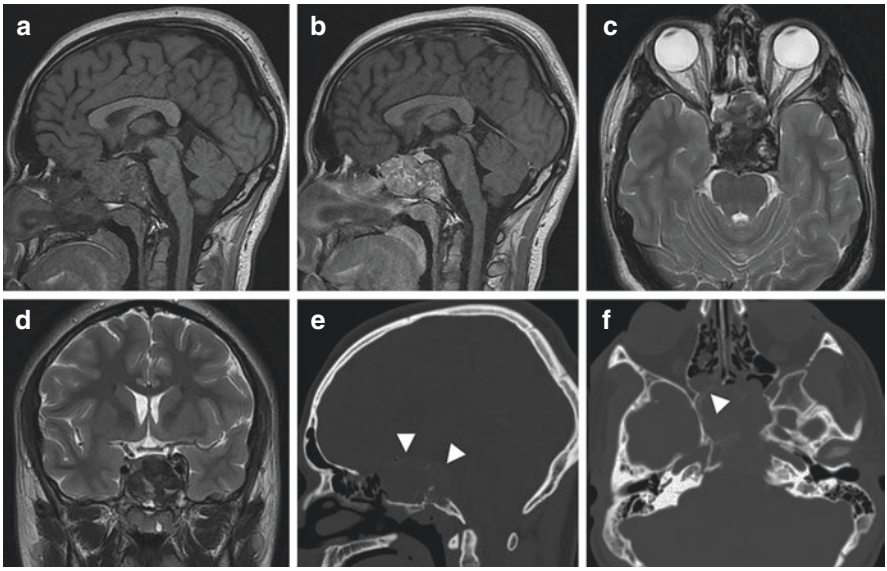

Fig. 7.22 Clival fibrous dysplasia. MR images (**a**–**d**) demonstrating a large clival mass. Note the bony expansion in the CT images (**e**, **f**; arrowheads)

7.4.3 Clival Fibrous Dysplasia

Fibrous dysplasia is a developmental disorder caused by abnormal proliferation of fibroblasts resulting in replacement of normal cancellous bone by structurally weak, immature osseous tissue. It is extremely rare to have fibrous dysplasia in the clivus (Fig. 7.25); only a few cases of fibrous dysplasia have been reported in the literature [236].

Postzygotic activating mutations in *GNAS* are the driving force behind the pathophysiology of fibrous dysplasia. *GNAS* encodes the α-subunit of the G_s stimulatory protein, and two potential mutations can occur resulting in interruption of the intrinsic GTPase activity of $G_s\alpha$. This leads to receptor activation and consequent inappropriate cyclic AMP-mediated signaling. The ultimate result is replacement of the normal cancellous bone and its marrow by proliferating bone marrow stromal cells, which form structurally weak discrete fibro-osseous lesions [237].

Fibrous dysplasia is a benign lesion, which progression usually halts after adolescence. In some instances, it continues to grow into adulthood, with males being more affected than females [238].

Although usually detected incidentally, clinical symptoms and signs may occur due to progressive bone deformation and depend on the location and extension of the abnormality. In the clival region, the symptoms are usually due to cranial nerve deficits (visual, auditory, olfactory, facial) caused by compression of the nerves in the narrow bony canals and skull base foramina. CT and MRI both offer valuable information for clival FD [239].

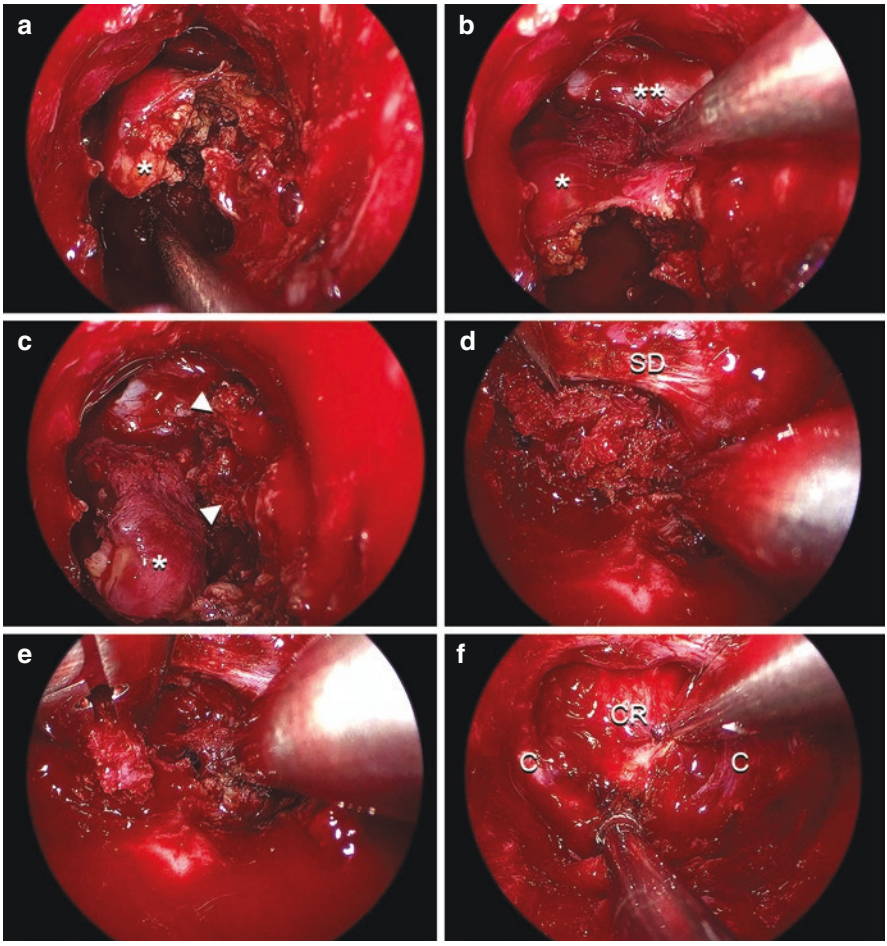

Fig. 7.23 Giant cell tumor of the clivus. Operative views (**a**–**f**) during tumor resection via an endoscopic endonasal transclival approach. SD, sellar dura; double asterisks, posterior fossa dura; arrowheads, infiltrated clival bone; C, paraclival carotids; asterisk, tumor; CR, clival recess

Fibrous dysplasia of clivus should be considered in any isolated clival lesion. Its diagnosis relies on imaging and histopathology. High-resolution CT is of significant importance in the evaluation [240]. A ground glass opacity, ballooning and expansion of the affected bone, and thinning of the cortex are the hallmark of fibrous dysplasia [241]. MR imaging of the clivus tends to show hypointensity in both T1 and T2 [194]. The signal intensity in T1-weighted images is directly related to the ratio of the fibrous tissue versus mineralized matrix, a lower signal intensity in highly mineralized matrix, whereas high fibrous content displays intermediate signal intensity. T2-weighted images show variable intensity depending on the metabolic activity of the lesions [239].

In asymptomatic patients, observation with serial CT scans is performed. In symptomatic patients, a standard endonasal endoscopic approach should be performed.

7.4.4 Metastatic Clival Lesions

Isolated metastatic lesions to the clivus are very rare (Figs. 7.26, 7.27, and 7.28), with less than 60 cases reported in the literature. The most common primary tumors are from prostate and renal cancer [242]. The most common symptom seen in patients with clival metastasis is diplopia due to sixth nerve palsy [243]. Regarding imaging, MR scanning remains the most sensitive in detecting clival lesions. Most metastatic lesions to the clivus are treated via surgery followed by radiotherapy or radiotherapy alone [242].

7.4.5 Benign Notochordal Cell Tumors (BNCTs) of the Clivus

Benign notochordal cell tumors (BNCTs) of the clivus are intraosseous benign lesions of notochordal cell origin [244, 245]. They represent notochordal rests that are most frequently found in the retroclival prepontine cistern [243]. A diagnosis of BNCT is favored over chordomas if the lesion has low proliferation index of Mib-1 antibody to Ki-67, less than 2 cm in size, and a gelatinous consistency with no bony invasion [187]. On imaging, BNCTs show no cortical or soft tissue invasion; they do not enhance with contrast and show low intensity on T1, with intermediate to high intensity on T2 [246].

BNCT contains cells with abundant vacuolated clear to eosinophilic cytoplasm, and the immunoprofile is identical to chordoma. BNCT has well-delineated borders and is confined to the bone without cortical permeation. They lack a lobular architecture, necrosis, conspicuous mitoses, and high-grade nuclei. Additionally, BNCT lacks extracellular myxoid matrix [247, 248]. BNCTs were identified in chordomas resected in the sacrococcygeal region, suggesting that they may represent a precursor lesion [249].

Although most cases are asymptomatic and treated with observation, one recent report documented two cases with histological features of BNCT and concomitant chordoma involving the clivus. In both cases, the clival lesions were incidentally

Fig. 7.24 Giant cell tumor of the clivus. Postoperative MRI with contrast in coronal (**a**) and sagittal (**b**) planes revealed near total resection of the tumor. Histopathological examination reveals a relatively well-circumscribed tumor rimmed by a shell of bone (**c**). Higher magnification (**d**) demonstrates a hypercellular tumor composed of giant multinucleated osteoclast-like cells (arrowheads) growing in sheets and mononuclear cells in a richly vascular background. There is no evidence of mitosis or necrosis

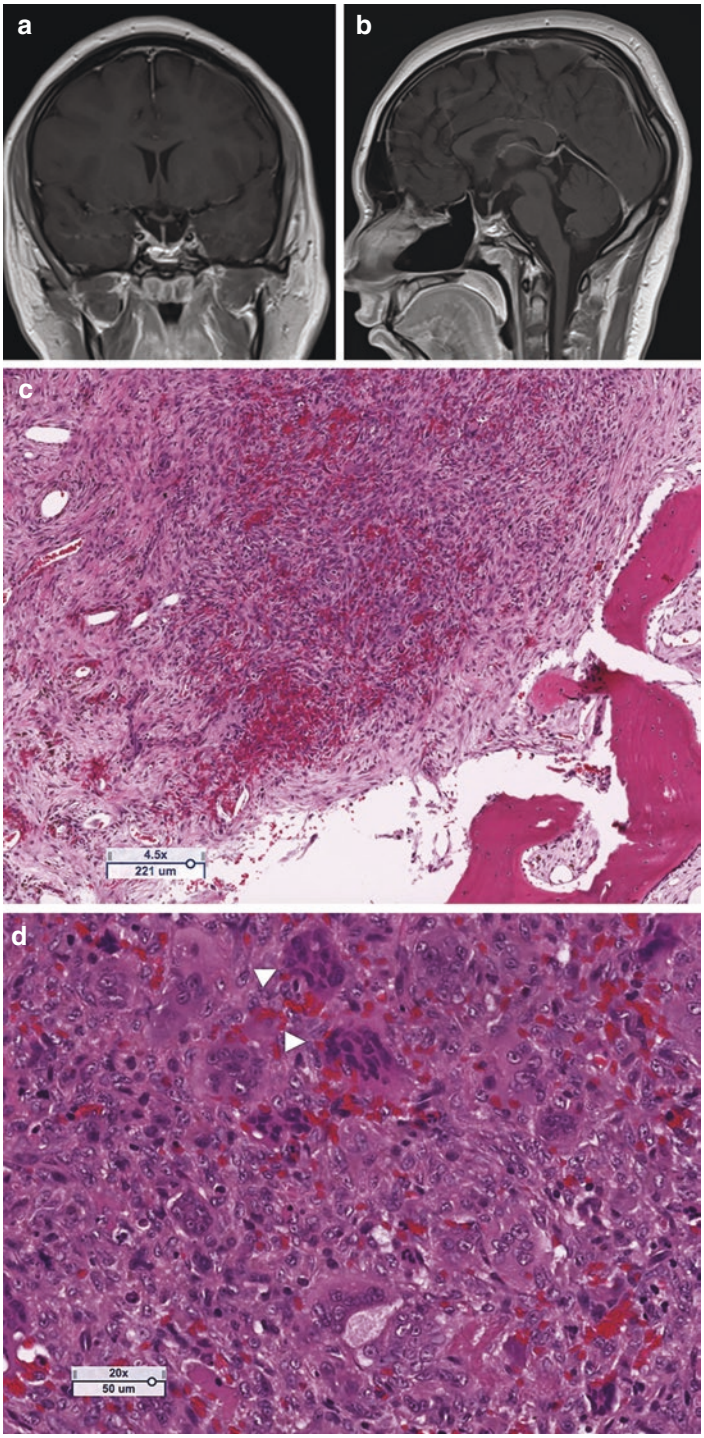
a
b
c
4.5x
221 um
d
20x
50 um

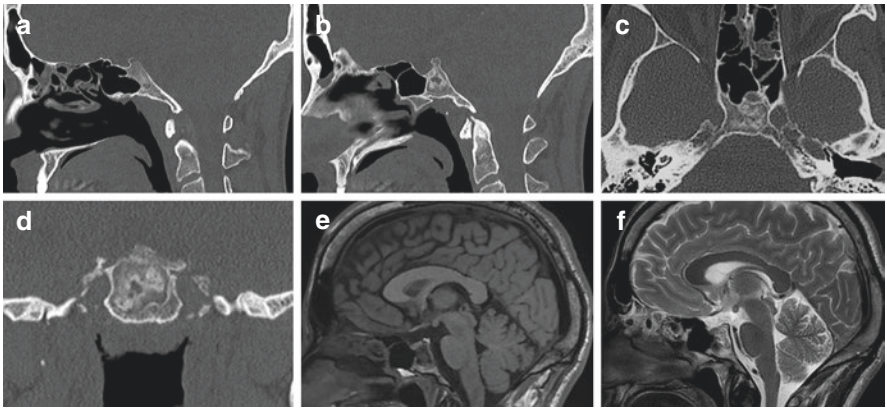

Fig. 7.25 Clival fibrous dysplasia. CT (**a**–**d**) and MR (**e**–**f**)

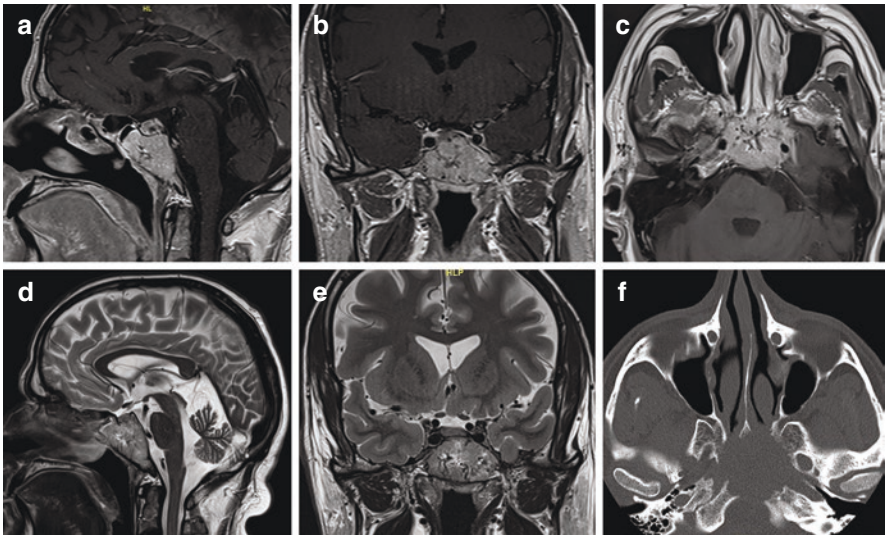

Fig. 7.26 Clival metastasis from a renal clear cell carcinoma. Preoperative T1-weighted MRI with contrast (**a**–**c**) and T2-weighted images (**d**, **e**) reveal a large clival tumor with notable vascular voids. Significant bone erosion is seen on CT (**f**)

discovered. They were both T2 hyperintense and T1 hypointense and non-enhancing in postcontrast imaging. Histologically, the tumor demonstrated areas of classic chordoma and a distinct intraosseous BNCT component. Surgical removal of the

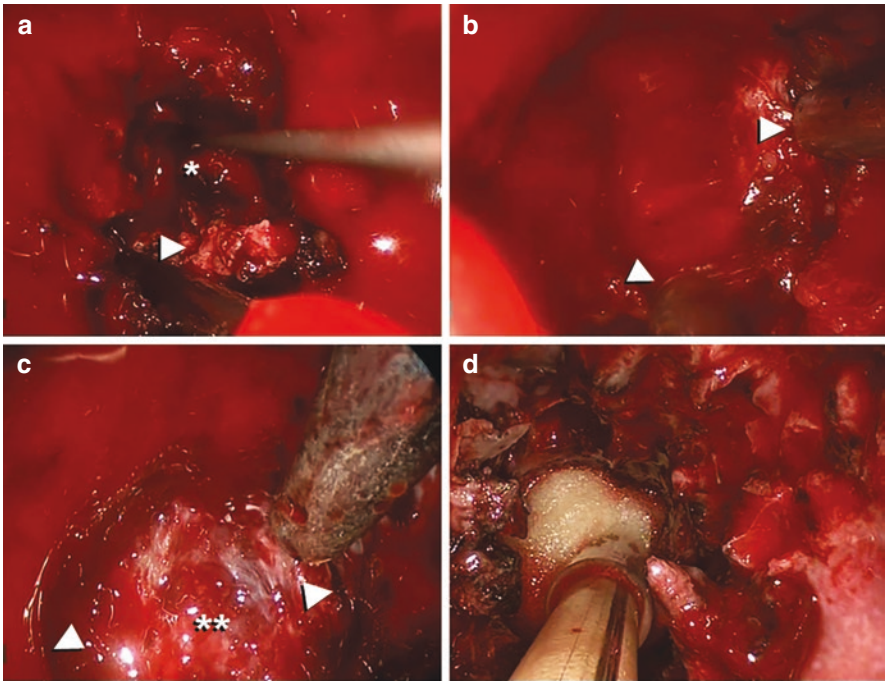

Fig. 7.27 Intraoperative views during endoscopic endonasal transclival approach for resection of a clival metastasis from a renal clear cell carcinoma. (**a**) The tumor is centrally debulked within the clival recess (asterisk), and peripheral parts of the tumor are seen and taken out (arrowhead). (**b**) The high vascularity and significant bleeding required two suction techniques (arrowheads) for visualization of the tumor and normal structures. (**c**) View after tumor resection was completed. Note the cleared posterior fossa dura (double asterisks) seen between the two paraclival carotid arteries (arrowheads). (**d**) Final hemostasis in the tumor bed using Floseal®

lesion was performed through an endoscopic transsphenoidal approach. Histological analysis revealed areas of BNCT with typical features of chordoma. These cases document histologically concomitant BNCT and chordoma involving the clivus, suggesting that the BNCT component may be a precursor of chordoma [250].

Our group had a similar experience in one case that we treated recently (Figs. 7.29, 7.30, and 7.31). It is however still unclear whether these cases are truly different from chordomas with typical features (Fig. 7.32).

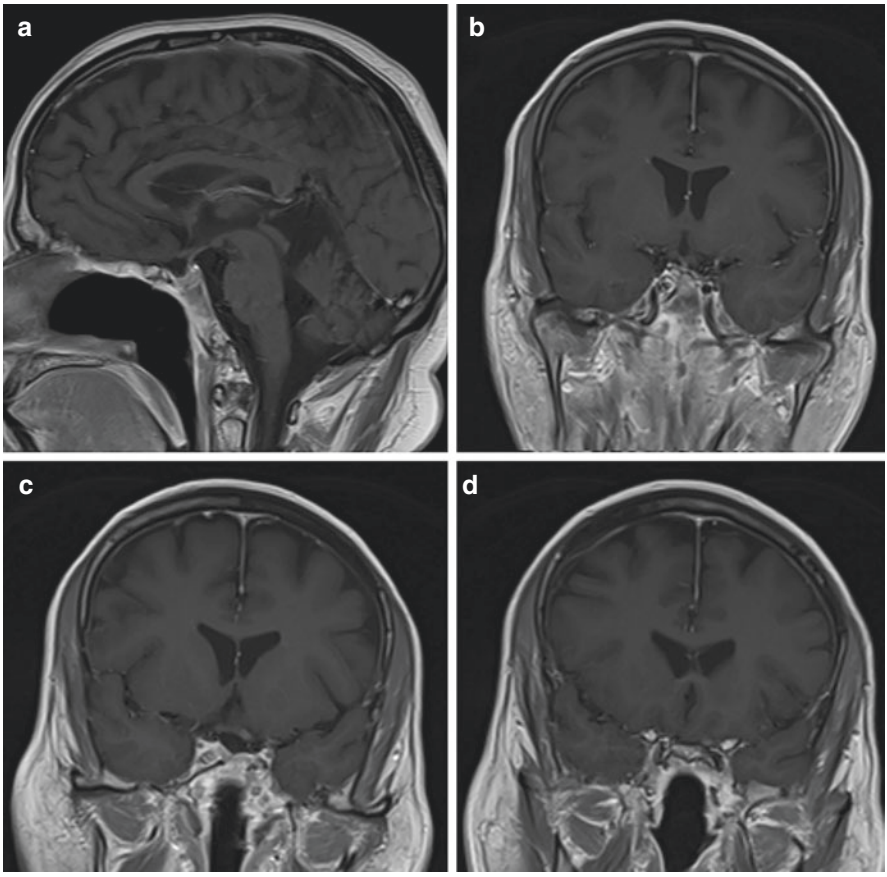

Fig. 7.28 Clival metastasis from a renal clear cell carcinoma. Postoperative T1-weighted MRI with contrast in sagittal (**a**) serial coronal (**b–d**) images demonstrating near total resection of the tumor

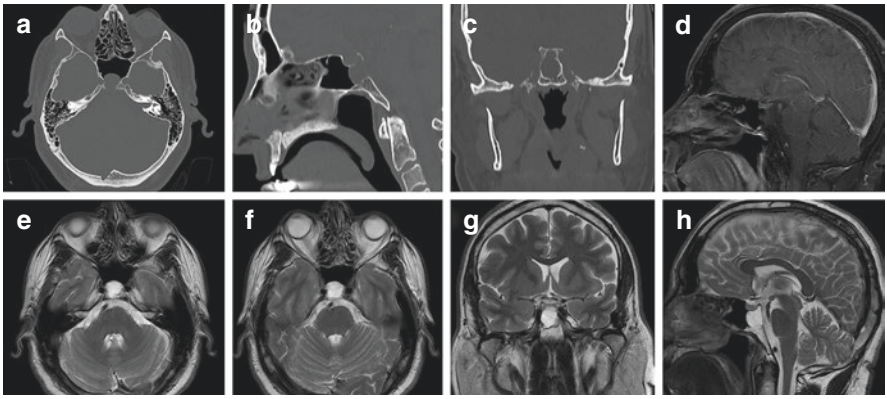

Fig. 7.29 Clival chordoma with BNCT. Preoperative CT images (**a**–**c**) demonstrating the lesion. Preoperative sagittal T1-weighted MRI with contrast revealed no enhancement of the lesion (**d**). Hyperintense signal of the lesion is seen on T2-weighted images (**e**–**h**)

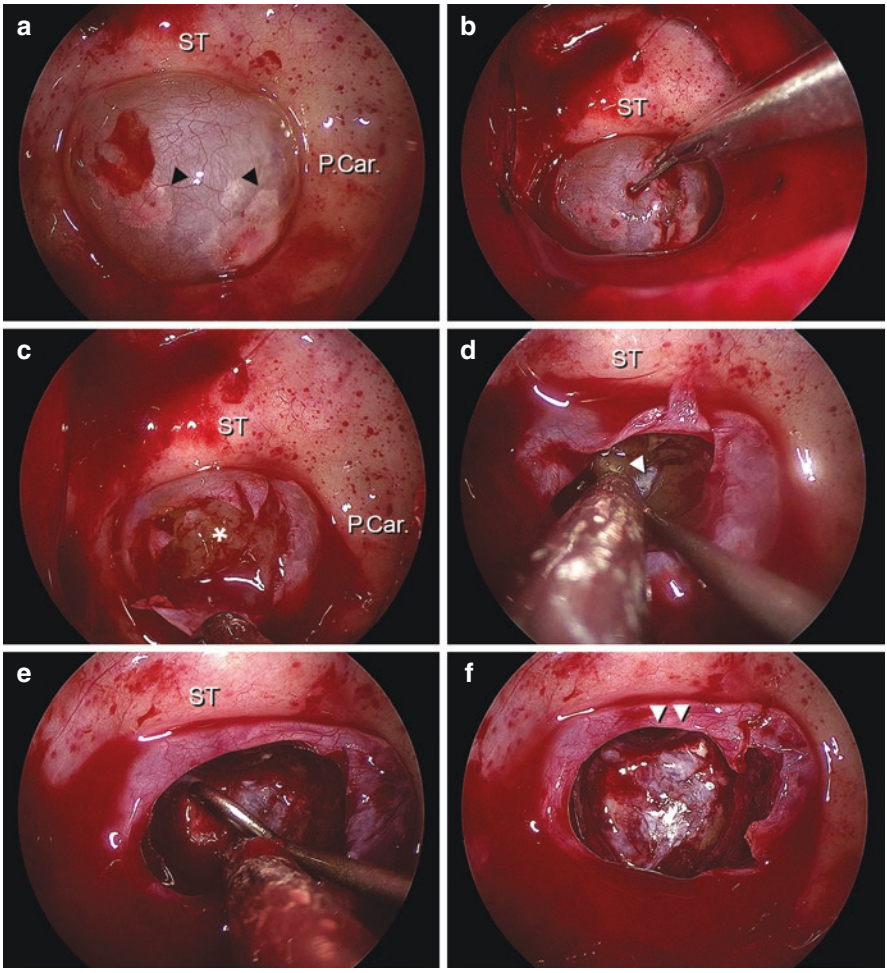

Fig. 7.30 Clival chordoma with BNCT. Operative views (**a**–**f**) during endoscopic endonasal transclival approach. ST, sella turcica; black arrowheads, cortical clival bone; P. Car., paraclival carotids; asterisk, tumor; white arrowhead, posterior fossa dura; double arrowhead, sphenoid sinus mucosa

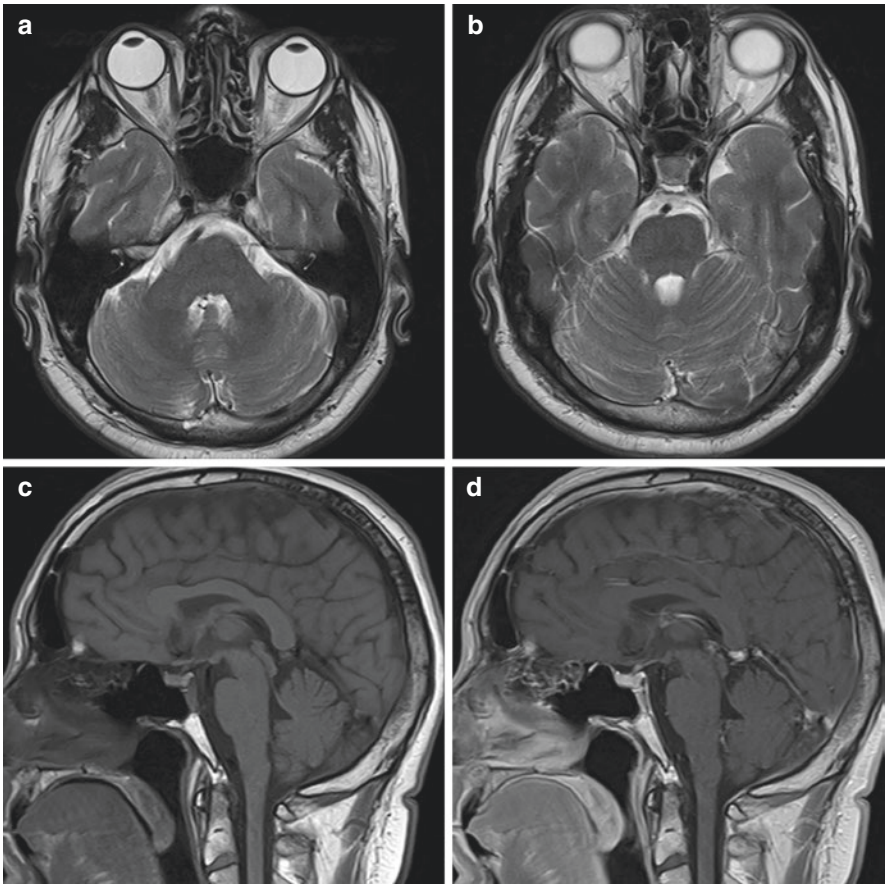

Fig. 7.31 Clival chordoma with BNCT. Postoperative axial T2 weighted (**a**, **b**) and sagittal T1 without (**c**) and with (**d**) contrast

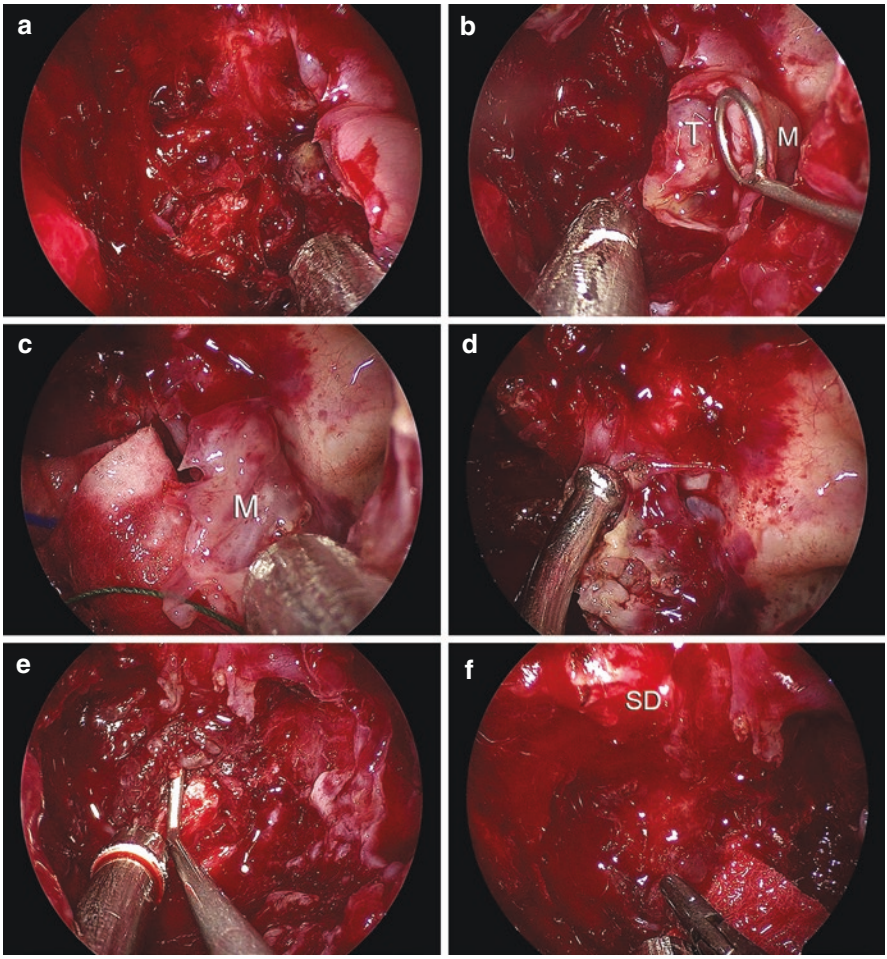

Fig. 7.32 Classic clival chordoma. Operative views (**a**–**f**) during tumor resection via an endoscopic endonasal transclival approach. SD, sellar dura; M, sphenoid sinus mucosa; T, tumor

7.5 The Uncommon Pathologies of the Suprasellar Area and the Cavernous Sinus

Indeed, many of the rare and uncommon pathologies in the suprasellar represent extensions from those originating from the sella or other anatomical structures in its vicinity. These lesions are very well suited to endoscopic endonasal transsphenoidal approach and its variations (Fig. 7.33). A dedicated review of these lesions as well as those purely originating from the cavernous sinuses is beyond the scope of this chapter.

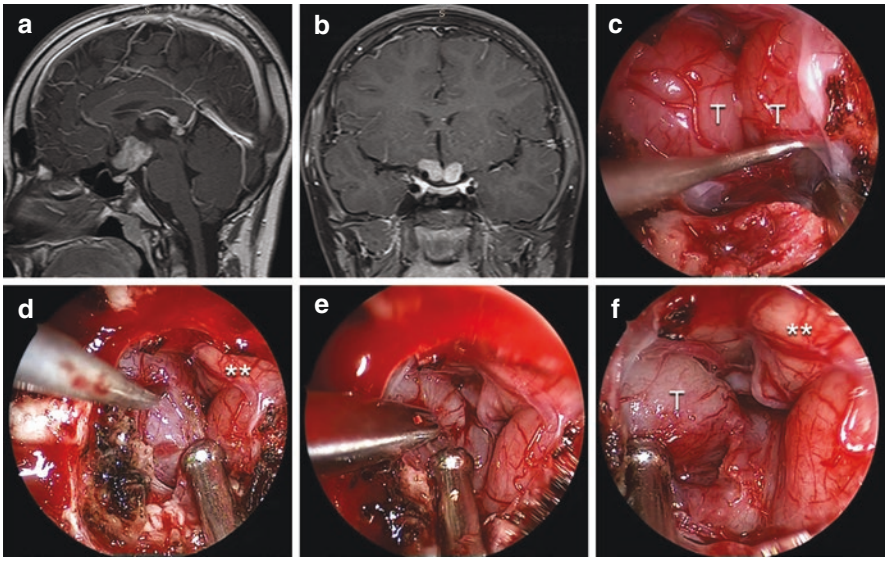

Fig. 7.33 Suprasellar GCT. Preoperative MR images (**a**, **b**). Operative views (**c**–**f**) during tumor biopsy via an endoscopic endonasal transtuberculum sellae approach. T, tumor; double asterisks, optic chiasm

References

1. Møller MW, Andersen MS, Glintborg D, et al. Endoscopic vs. microscopic transsphenoidal pituitary surgery: a single centre study. Sci Rep. 2020;10:21942. https://doi.org/10.1038/s41598-020-78823-z9.
2. Hardy J. Excision of pituitary adenomas by trans-sphenoidal approach. Union Med Can. 1962;91:933–45.
3. Jho HD, Carrau RL, Ko Y, Daly MA. Endoscopic pituitary surgery: an early experience. Surg Neurol. 1997;47(3):213–22; discussion 222-3. https://doi.org/10.1016/s0090-3019(96)00452-1.
4. Jankowski R, Auque J, Simon C, Marchal JC, Hepner H, Wayoff M. How i do it: head and neck and plastic surgery: endoscopic pituitary tumor surgery. Laryngoscope. 1992;102:198–202. https://doi.org/10.1288/00005537-199202000-00016.
5. Barkhoudarian G, Zada G, Laws ER. Endoscopic endonasal surgery for nonadenomatous sellar/parasellar lesions. World Neurosurg. 2014;82(6 Suppl):S138–46. https://doi.org/10.1016/j.wneu.2014.07.017.
6. Azab WA, Elmaghraby MA, Zaidan SN, Mostafa KH. Endoscope-assisted transcranial surgery for anterior skull base meningiomas. Mini-invasive Surg. 2020;4:88. https://doi.org/10.20517/2574-1225.2020.75.
7. Kassam AB. Endoscopic techniques in skull base surgery. Neurosurgical Focus FOC. 2005;19(1):1–1.
8. Hardesty DA, Prevedello DM. What are the limits of endoscopic endonasal approaches to the skull base? J Neurosurg Sci. 2018;62(3):285–6. https://doi.org/10.23736/S0390-5616.18.04401-6.

9. de Divitiis E, Cavallo LM, Esposito F, Stella L, Messina A. Extended endoscopic transsphenoidal approach for tuberculum sellae meningiomas. Neurosurgery. 2007;61:229–37. https://doi.org/10.1227/01.neu.0000303221.63016.f2.
10. Algattas HN, Wang EW, Zenonos GA, Snyderman CH, Gardner PA. Endoscopic endonasal surgery for anterior cranial fossa meningiomas. J Neurosurg Sci. 2021;65(2):118–32. https://doi.org/10.23736/S0390-5616.20.05085-7.
11. Youngerman BE, Banu MA, Gerges MM, Odigie E, Tabaee A, Kacker A, Anand VK, Schwartz TH. Endoscopic endonasal approach for suprasellar meningiomas: introduction of a new scoring system to predict extent of resection and assist in case selection with long-term outcome data. J Neurosurg. 2020;1–13. https://doi.org/10.3171/2020.4.JNS20475.
12. Roethlisberger M, Jayapalan RR, Hostettler IC, Bin Abd Kadir KA, Mun KS, Brand Y, Mariani L, Prepageran N, Waran V. Evolving strategies for resection of sellar/parasellar synchronous tumors via endoscopic endonasal approach: a technical case report and systematic review of the literature. World Neurosurg. 2020;133:381–391.e2. https://doi.org/10.1016/j.wneu.2019.08.102.
13. Solari D, Mastantuoni C, Cavallo LM, Esposito F, Cappabianca P. Endoscopic endonasal treatment of craniopharyngiomas: current management strategies and future perspectives. J Neurosurg Sci. 2023;67(1):26–35. https://doi.org/10.23736/S0390-5616.21.05507-7.
14. Ganz JC. Craniopharyngiomas. Prog Brain Res. 2022;268(1):217–27. https://doi.org/10.1016/bs.pbr.2021.10.033.
15. Ceylan S, Emengen A, Caklili M, Ergen A, Yılmaz E, Uzuner A, Icli D, Cabuk B, Anik I. Operative nuances and surgical limits of the endoscopic approach to clival chordomas and chondrosarcomas: a single-center experience of 72 patients. Clin Neurol Neurosurg. 2021;208:106875. https://doi.org/10.1016/j.clineuro.2021.106875.
16. Lee WJ, Hong SD, Woo KI, Seol HJ, Choi JW, Lee JI, Nam DH, Kong DS. Endoscopic endonasal and transorbital approaches to petrous apex lesions. J Neurosurg. 2021;136(2):431–40. https://doi.org/10.3171/2021.2.JNS203867.
17. Li L, London NR Jr, Prevedello DM, Carrau RL. Endoscopic endonasal approach to the pterygopalatine fossa and infratemporal fossa: comparison of the prelacrimal and Denker's corridors. Am J Rhinol Allergy. 2022;36(5):599–606. https://doi.org/10.1177/19458924221097159.
18. Azab WA. Endoscopic endonasal transsphenoidal approach for pituitary adenomas. In: Deopujari C, Quoreshi M, editors. WFNS guide for neuroendoscopy. 1st ed. Salubris Medical Publishers; 2022. p. 83–90.
19. Freda PU, Post KD. Differential diagnosis of sellar masses. Endocrinol Metab Clin North Am. 1999;28(1):81–117, vi. https://doi.org/10.1016/s0889-8529(05)70058-x.
20. Honegger J, Nasi-Kordhishti I, Giese S. Hypophysenadenome pituitary adenomas. Nervenarzt. 2019;90(6):568–77; German. https://doi.org/10.1007/s00115-019-0708-4.
21. Kinoshita Y, Yamasaki F, Tominaga A, Usui S, Arita K, Sakoguchi T, Sugiyama K, Kurisu K. Transsphenoidal posterior pituitary lobe biopsy in patients with neurohypophysial lesions. World Neurosurg. 2017;99:543–7. https://doi.org/10.1016/j.wneu.2016.12.080.
22. Chhuon Y, Weon YC, Park G, Kim M, Park JB, Park SK. Pituitary blastoma in a 19-year-old woman: a case report and review of literature. World Neurosurg. 2020;139:310–3. https://doi.org/10.1016/j.wneu.2020.04.096.
23. Sansur CA, Oldfield EH. Pituitary carcinoma. Semin Oncol. 2010;37(6):591–3. https://doi.org/10.1053/j.seminoncol.2010.10.012.
24. Castle-Kirszbaum M, Goldschlager T, Ho B, Wang YY, King J. Twelve cases of pituitary metastasis: a case series and review of the literature. Pituitary. 2018;21(5):463–73. https://doi.org/10.1007/s11102-018-0899-x.
25. Wang J, Liu Z, Du J, Cui Y, Fang J, Xu L, Li G. The clinicopathological features of pituicytoma and the differential diagnosis of sellar glioma. Neuropathology. 2016;36(5):432–40. https://doi.org/10.1111/neup.12291.

26. Mahta A, Buhl R, Huang H, Jansen O, Kesari S, Ulmer S. Sellar and supra-sellar glioblastoma masquerading as a pituitary macroadenoma. Neurol Sci. 2013;34(4):605–7. https://doi.org/10.1007/s10072-012-1110-1.
27. Prashant Prasad G, Lang FF, Bruner JM, Ater JL, McCutcheon IE. Transsphenoidal removal of intrasellar pilocytic astrocytoma. J Clin Neurosci. 2014;21(6):1047–8. https://doi.org/10.1016/j.jocn.2013.10.004.
28. Arita K, Kurisu K, Tominaga A, Sugiyama K, Sumida M, Hirose T. Intrasellar pleomorphic xanthoastrocytoma: case report. Neurosurgery. 2002;51(4):1079–82; discussion 1082. https://doi.org/10.1097/00006123-200210000-00042.
29. Matyja E, Maksymowicz M, Grajkowska W, Zieliński G, Kunicki J, Bonicki W, Witek P, Naganska E. Ganglion cell tumours in the sella turcica in close morphological connection with pituitary adenomas. Folia Neuropathol. 2015;53(3):203–18. https://doi.org/10.5114/fn.2015.54421.
30. Emanuelli E, Zanotti C, Munari S, Baldovin M, Schiavo G, Denaro L. Sellar and parasellar lesions: multidisciplinary management. Acta Otorhinolaryngol Ital. 2021;41(Suppl. 1):S30–41. https://doi.org/10.14639/0392-100X-suppl.1-41-2021-03.
31. Quiroga-Padilla PJ, González-Devia D, Andrade R, Escalante P, Jiménez-Hakim E. Sellar Gangliocytoma: Case Report and Review of an Extremely Rare Tumour. Case Rep Neurol. 2021;13(2):475–82. https://doi.org/10.1159/000517368.
32. Nery B, Bernardes Filho F, Costa RAF, Pereira LCT, Quaggio E, Queiroz RM, Abud LG, da Cunha Tirapelli DP. Neurocytoma mimicking macroadenoma. Surg Neurol Int. 2019;10:8. https://doi.org/10.4103/sni.sni_387_18.
33. Wang J, Song DL, Deng L, Sun SY, Liu C, Gong DS, Wang Y, Xu QW. Extraventricular neurocytoma of the sellar region: case report and literature review. Springerplus. 2016;5(1):987. https://doi.org/10.1186/s40064-016-2650-2.
34. Wang S, Zong W, Li Y, Wang B, Ke C, Guo D. Pituitary ependymoma: a case report and review of the literature. World Neurosurg. 2018;110:43–54. https://doi.org/10.1016/j.wneu.2017.10.134.
35. Kuo CH, Yen YS, Tu TH, Wu JC, Huang WC, Cheng H. Primary choroid plexus papilloma over sellar region mimicking with craniopharyngioma: a case report and literature review. Cureus. 2018;10(6):e2849. https://doi.org/10.7759/cureus.2849.
36. Liu F, Fan S, Tang X, Fan S, Zhou L. Adult sellar region atypical teratoid/rhabdoid tumor: a retrospective study and literature review. Front Neurol. 2020;11:604612. https://doi.org/10.3389/fneur.2020.604612.
37. Kalinin PL, Fomichev DV, Abdilatipov AA, Chernov IV, Astafieva LI, Kutin MA, Ryzhova MV, Panina TN, Shishkina LV, Nikitin PV, Kurnosov AB. Pervichnaya sellyarnaya neiroblastoma. Klinicheskoe nablyudenie i obzor literatury Primary sellar neuroblastoma (clinical case and literature review). Zh Vopr Neirokhir Im N N Burdenko. 2020;84(2):83–92; Russian. https://doi.org/10.17116/neiro20208402183.
38. Yakar F, Doğan İ, Meco C, Heper AO, Kahilogullari G. Sellar embryonal tumor: a case report and review of the literature. Asian J Neurosurg. 2018;13(4):1197–201. https://doi.org/10.4103/ajns.AJNS_30_17.
39. Kong X, Wu H, Ma W, Li Y, Yang Y, Xing B, Wei J, Yao Y, Gao J, Lian W, Xu Z, Dou W, Ren Z, Su C, Wang R. Schwannoma in sellar region mimics invasive pituitary macroadenoma: literature review with one case report. Medicine (Baltimore). 2016;95(9):e2931. https://doi.org/10.1097/MD.0000000000002931.
40. Zhang J, Xu S, Liu Q, Li X, Jia D, Li G. Intrasellar and suprasellar Schwannoma misdiagnosed as pituitary macroadenoma: a case report and review of the literature. World Neurosurg. 2016;96:612.e1–7. https://doi.org/10.1016/j.wneu.2016.08.128.
41. Lyne SB, Polster SP, Fidai S, Pytel P, Yamini B. Primary sellar paraganglioma: case report with literature review and immunohistochemistry resource. World Neurosurg. 2019;125:32–6. https://doi.org/10.1016/j.wneu.2019.01.094.

42. Bang M, Suh JH, Park JB, Weon YC. Pure intrasellar meningioma mimicking pituitary macroadenoma: magnetic resonance imaging and review of the literature. World Neurosurg. 2016;91(675):e1–4. https://doi.org/10.1016/j.wneu.2016.04.063.
43. Zhong Q, Yuan S. Total resection of a solitary fibrous tumor of the sellar diaphragm: a case report. Oncol Lett. 2013;5(6):1783–6. https://doi.org/10.3892/ol.2013.1293.
44. Singh U, Kalavakonda C, Venkitachalam S, Patil S, Chinnusamy R. Intraosseous hemangioma of sella: case report and review of literature. World Neurosurg X. 2019;3:100030. https://doi.org/10.1016/j.wnsx.2019.100030.
45. Ajler P, Goldschmidt E, Bendersky D, Hem S, Landriel F, Campero A, Ajler G. Sellar hemangioblastoma mimicking a macroadenoma. Acta Neurol Taiwan. 2012;21(4):176–9.
46. Guerrero-Pérez F, Vidal N, López-Vázquez M, Sánchez-Barrera R, Sánchez-Fernández JJ, Torres-Díaz A, Vilarrasa N, Villabona C. Sarcomas of the sellar region: a systematic review. Pituitary. 2021;24(1):117–29. https://doi.org/10.1007/s11102-020-01073-9.
47. Arita K, Sugiyama K, Tominaga A, Yamasaki F. Intrasellar rhabdomyosarcoma: case report. Neurosurgery. 2001;48(3):677–80. https://doi.org/10.1097/00006123-200103000-00048.
48. Mattogno PP, Nasi D, Iaccarino C, Oretti G, Santoro L, Romano A. First case of primary sellar/suprasellar-intraventricular ewing sarcoma: case report and review of the literature. World Neurosurg. 2017;98:869.e1–5. https://doi.org/10.1016/j.wneu.2016.12.045.
49. Inenaga C, Morii K, Tamura T, Tanaka R, Takahashi H. Mesenchymal chondrosarcoma of the sellar region. Acta Neurochir (Wien). 2003;145(7):593–7; discussion 597. https://doi.org/10.1007/s00701-003-0059-5.
50. Zhang Y, Huang J, Zhang C, Jiang C, Ding C, Lin Y, Wu X, Wang C, Kang D, Lin Z. An extended endoscopic endonasal approach for sellar area chondrosarcoma: a case report and literature review. World Neurosurg. 2019;127:469–77. https://doi.org/10.1016/j.wneu.2019.04.075.
51. Kikuchi K, Watanabe K. Huge sellar chordoma: CT demonstration. Comput Med Imaging Graph. 1994;18(5):385–90. https://doi.org/10.1016/0895-6111(94)90010-8.
52. Wang F, Ling S. Primary meningeal melanocytoma in sellar region, simulating a nonfunctioning pituitary adenoma: case report and literature review. World Neurosurg. 2018;112:209–13. https://doi.org/10.1016/j.wneu.2018.01.145.
53. Tarabay A, Cossu G, Berhouma M, Levivier M, Daniel RT, Messerer M. Primary pituitary lymphoma: an update of the literature. J Neurooncol. 2016;130(3):383–95. https://doi.org/10.1007/s11060-016-2249-z.
54. Ravindra VM, Raheja A, Corn H, Driscoll M, Welt C, Simmons DL, Couldwell WT. Primary pituitary diffuse large B-cell lymphoma with somatotroph hyperplasia and acromegaly: case report. J Neurosurg. 2017;126(5):1725–30. https://doi.org/10.3171/2016.5.JNS16828.
55. Oweity T, Scheithauer BW, Ching HS, Lei C, Wong KP. Multiple system Erdheim-Chester disease with massive hypothalamic-sellar involvement and hypopituitarism. J Neurosurg. 2002;96(2):344–51. https://doi.org/10.3171/jns.2002.96.2.0344.
56. Zhang Y, Liu J, Zhu J, Zhou X, Zhang K, Wang S, Ma W, Pan H, Wang R, Zhu H, Yao Y. Case report: Rosai-Dorfman disease involving sellar region in a pediatric patient: a case report and systematic review of literature. Front Med (Lausanne). 2020;7:613756. https://doi.org/10.3389/fmed.2020.613756.
57. Tan H, Yu K, Yu Y, An Z, Li J. Isolated hypothalamic-pituitary langerhans' cell histiocytosis in female adult: a case report. Medicine (Baltimore). 2019;98(2):e13853. https://doi.org/10.1097/MD.0000000000013853.
58. Saeger W, Ebrahimi A, Beschorner R, Spital H, Honegger J, Wilczak W. Teratoma of the sellar region: a case report. Endocr Pathol. 2017;28(4):315–9. https://doi.org/10.1007/s12022-016-9465-0.
59. Li CS. Intrasellar germinoma treated with low-dose radiation. Acta Neurochir (Wien). 2006;148(7):795–9; discussion 799. https://doi.org/10.1007/s00701-006-0776-7.
60. Musiani P, Mancuso S. Coriocarcinoma primitivo intracranico originato da tumore germinale sellare in una bambina in età prepubere Intracranial primary choriocarcinoma origi-

nating from a sellar germinal tumor in a girl of prepuberal age. Arch Ital Anat Istol Patol. 1969;43(1):61–75; Italian.
61. Wildemberg LE, Vieira Neto L, Taboada GF, Moraes AB, Marcondes J, Conceição FL, Chimelli L, Gadelha MR. Sellar and suprasellar mixed germ cell tumor mimicking a pituitary adenoma. Pituitary. 2011;14(4):345–50. https://doi.org/10.1007/s11102-008-0161-z.
62. Cheng D, Yang F, Li Z, Qv F, Liu W. Juvenile xanthogranuloma of the sellar region with a 5-year medical history: case report and literature review. Pediatr Neurosurg. 2021;56(5):440–7. https://doi.org/10.1159/000515517.
63. Mangussi-Gomes J, Gentil AF, Filippi RZ, Momesso RA, Handfas BW, Radvany J, Balsalobre L, Stamm AC. Sellar and suprasellar arachnoid cyst. Einstein (Sao Paulo). 2019;17(1):eAI4269. https://doi.org/10.31744/einstein_journal/2019AI4269.
64. Guduk M, Sun HI, Sav MA, Berkman Z. Pituitary colloid cyst. J Craniofac Surg. 2017;28(2):e166–8. https://doi.org/10.1097/SCS.0000000000003142.
65. Pan YB, Sun ZL, Feng DF. Intrasellar dermoid cyst mimicking pituitary apoplexy: a case report and review of the literature. J Clin Neurosci. 2017;45:125–8. https://doi.org/10.1016/j.jocn.2017.05.023.
66. Vellutini EAS, Pahl FH, Stamm AEC, Teles Gomes MQ, de Oliveira MF, Martins HO, Ruschel LG. Endoscopic resection of sellar and suprasellar epidermoid cyst: report of two cases and review of literature. Br J Neurosurg. 2021 Feb;1:1–6. https://doi.org/10.1080/02688697.2021.1877610.
67. Somma T, Solari D, Beer-Furlan A, Guida L, Otto B, Prevedello D, Cavallo LM, Carrau R, Cappabianca P. Endoscopic endonasal management of rare sellar lesions: clinical and surgical experience of 78 cases and review of the literature. World Neurosurg. 2017;100:369–80. https://doi.org/10.1016/j.wneu.2016.11.057.
68. Glezer A, Paraiba DB, Bronstein MD. Rare sellar lesions. Endocrinol Metab Clin North Am. 2008;37(1):195–211, x. https://doi.org/10.1016/j.ecl.2007.10.003.
69. Gong L, Chen H, Zhang W, Liu X, Wang Y, Mu X, Zhang F, Li Q, Heng L, Zhang W. Primary collision tumors of the sellar region: Experience from a single center. J Clin Neurosci. 2022;100:204–11. https://doi.org/10.1016/j.jocn.2022.04.024.
70. Koutourousiou M, Kontogeorgos G, Seretis A. Non-adenomatous sellar lesions: experience of a single centre and review of the literature. Neurosurg Rev. 2010;33(4):465–76. https://doi.org/10.1007/s10143-010-0263-8.
71. Abushamat LA, Kerr JM, Lopes MBS, Kleinschmidt-DeMasters BK. Very unusual sellar/suprasellar region masses: a review. J Neuropathol Exp Neurol. 2019;nlz044. https://doi.org/10.1093/jnen/nlz044.
72. Tan CL, Pang YH, Lim KHC, Sein L, Codd PJ, McLendon RE. Two extraordinary sellar neuronal tumors: literature review and comparison of clinicopathologic features. Am J Clin Pathol. 2019;151(3):241–54. https://doi.org/10.1093/ajcp/aqy155.
73. McLaughlin N, Vandergrift A, Ditzel Filho LF, Shahlaie K, Eisenberg AA, Carrau RL, Cohan P, Kelly DF. Endonasal management of sellar arachnoid cysts: simple cyst obliteration technique. J Neurosurg. 2012;116(4):728–40. https://doi.org/10.3171/2011.12.JNS11399.
74. Güdük M, HamitAytar M, Sav A, Berkman Z. Intrasellar arachnoid cyst: a case report and review of the literature. Int J Surg Case Rep. 2016;23:105–8. https://doi.org/10.1016/j.ijscr.2016.03.033.
75. Chen B, Miao Y, Hu Y, Liao Y, Tu M, Yang X, Qiu Y. Rare intrasellar arachnoid cyst distinguishing from other benign cystic lesions and its surgical strategies. J Craniofac Surg. 2019;30(5):e400–2. https://doi.org/10.1097/SCS.0000000000005315.
76. d'Artigues J, Graillon T, Boissonneau S, Farah K, Amodru V, Brue T, Fuentes S, Dufour H. Fully endoscopic endonasal approach for the treatment of intrasellar arachnoid cysts. Pituitary. 2022;25(1):191–200. https://doi.org/10.1007/s11102-021-01187-8.
77. Fuller GN, Perry A. In: Gregory Fuller N, Perry A, editors. Practical surgical neuropathology: a diagnostic approach. Philadelphia: Churchill Livingstone/Elsevier; 2010. p. 287–313.

78. Siow TY, Chuang CC, Toh CH, Castillo M. Persisting embryonal infundibular recess: case report and imaging findings. World Neurosurg. 2018;117:11–4. https://doi.org/10.1016/j.wneu.2018.05.228.
79. Belotti F, Lupi I, Cosottini M, Ambrosi C, Gasparotti R, Bogazzi F, Fontanella MM, Doglietto F. Persisting embryonal infundibular recess (PEIR): two case reports and systematic literature review. J Clin Endocrinol Metab. 2018;103(7):2424–9. https://doi.org/10.1210/jc.2018-00437.
80. Kuroiwa M, Kusano Y, Ogiwara T, Tanaka Y, Takemae T, Hongo K. A case of presumably Rathke's cleft cyst associated with postoperative cerebrospinal fluid leakage through persisting embryonal infundibular recess. Neurol Med Chir (Tokyo). 2014;54(7):578–81. https://doi.org/10.2176/nmc.cr2013-0014.
81. Šteňo A, Popp AJ, Wolfsberger S, Belan V, Šteňo J. Persisting embryonal infundibular recess. J Neurosurg. 2009;110(2):359–62. https://doi.org/10.3171/2008.7.JNS08287.
82. Azab WA, Cavallo LM, Yousef W, Khan T, Solari D, Cappabianca P. Persisting embryonal infundibular recess (PEIR) and transsphenoidal-transsellar encephaloceles: distinct entities or constituents of one continuum? Childs Nerv Syst. 2022;38(6):1059–67. https://doi.org/10.1007/s00381-022-05467-x.
83. Kühne D, Schwartz RB. Persisting intrapituitary recessus infundibuli. Neuroradiology. 1975;10(3):177–8. https://doi.org/10.1007/BF00341823.
84. Vallee B, Besson G, Person H, Mimassi N. Persisting recessus infundibuli and empty sella. Case report. J Neurosurg. 1982;57(3):410–2. https://doi.org/10.3171/jns.1982.57.3.0410.
85. Schumacher M, Gilsbach J. A new variety of "empty sella" with cystic intrasellar dilatation of the recessus infundibuli. Br J Radiol. 1979;52:862–4. https://doi.org/10.1259/0007-1285-52-623-862.
86. Cabanes J. Asymptomatic persistence of infundibularis recessus. Case report. J Neurosurg. 1978;49(5):769–72. https://doi.org/10.3171/jns.1978.49.5.0769.
87. Kelsch RD, Tarhuni MA, Saon M, Fischbein NJ, Khan A-M. The transsphenoidal encephalocele: associations and elusive origins. Neurographics. 2020;10(4):236–40. https://doi.org/10.3174/ng.2000007.
88. de Vries F, van Furth WR, Biermasz NR, Pereira AM. Hypophysitis: a comprehensive overview. Presse Med. 2021;50(4):104076. https://doi.org/10.1016/j.lpm.2021.104076.
89. Caranci F, Leone G, Ponsiglione A, Muto M, Tortora F, Muto M, Cirillo S, Brunese L, Cerase A. Imaging findings in hypophysitis: a review. Radiol Med. 2020;125(3):319–28. https://doi.org/10.1007/s11547-019-01120-x.
90. Gutenberg A, Larsen J, Lupi I, et al. A radiologic score to distinguish autoimmune hypophysitis from nonsecreting pituitary adenoma preoperatively. AJNR Am J Neuroradiol. 2009;30(9):1766–72.
91. Wang S, Wang L, Yao Y, et al. Primary lymphocytic hypophysitis: clinical characteristics and treatment of 50 cases in a single centre in China over 18 years. Clin Endocrinol (Oxf). 2017;87:177–84.
92. Bhansali A, Velayutham P, Radotra BD, et al. Idiopathic granulomatous hypophysitis presenting as non-functioning pituitary adenoma: description of six cases and review of literature. Br J Neurosurg. 2004;18:489–94.
93. Çavuşoğlu M, Elverici E, Duran S, et al. Idiopathic granulomatous hypophysitis: a rare cystic lesion of the pituitary. Intern Med. 2015;54(11):1407–10.
94. Su SB, Zhang DJ, Yue SY, et al. Primary granulomatous hypophysitis: a case report and literature review. Endocr J. 2011;58:467–73.
95. Kleinschmidt-DeMasters BK, Lillehei KO, Hankinson TC. Review of xanthomatous lesions of the sella. Brain Pathol. 2017;27(3):377–95. https://doi.org/10.1111/bpa.12498.
96. Burt MG, Morey AL, Turner JJ, Pell M, Sheehy JP, Ho KK. Xanthomatous pituitary lesions: a report of two cases and review of the literature. Pituitary. 2003;6(3):161–8.

97. Rahmani R, Sukumaran M, Donaldson AM, Akselrod O, Lavi E, Schwartz TH. Parasellar xanthogranulomas. J Neurosurg. 2015;122(4):812–7. https://doi.org/10.3171/2014.12.JNS14542.
98. Paulus W, Honegger J, Keyvani K, Fahlbusch R. Xanthogranuloma of the sellar region: a clinicopathological entity different from adamantinomatous craniopharyngioma. Acta Neuropathol. 1999;97(4):377–82. https://doi.org/10.1007/s004010051001.
99. Céspedes MT, Vargas JP, Yañez FA, León LS, Arancibia PÁ, Putz TS. Remarkable diagnostic magnetic resonance imaging findings in sellar xanthogranuloma: report of three first cases in Latin America. J Neurol Surg Rep. 2017;78(1):e26–33. https://doi.org/10.1055/s-0037-1598203.
100. Amano K, Kubo O, Komori T, Tanaka M, Kawamata HT, et al. Clinicopathological features of sellar region xanthogranuloma: correlation with Rathke's cleft cyst. Brain Tumor Pathol. 2013;30:233–41.
101. Jung CS, Schänzer A, Hattingen E, Plate KH, Seifert V. Xanthogranuloma of the sellar region. Acta Neurochir (Wien). 2006;148:473–7.
102. Shao X, Wang C, Min J. Xanthogranuloma of the sellar region: a case report. Medicine (Baltimore). 2020;99(40):e22619. https://doi.org/10.1097/MD.0000000000022619.
103. Cabuk B, Caklılı M, Anık I, Ceylan S, Celik O, Ustün C. Primary pituitary abscess case series and a review of the literature. Neuro Endocrinol Lett. 2019;40(2):99–104.
104. Agyei JO, Lipinski LJ, Leonardo J. Case report of a primary pituitary abscess and systematic literature review of pituitary abscess with a focus on patient outcomes. World Neurosurg. 2017;101:76–92. https://doi.org/10.1016/j.wneu.2017.01.077.
105. Dutta P, Bhansali A, Singh P, Kotwal N, Pathak A, Kumar Y. Pituitary abscess: report of four cases and review of literature. Pituitary. 2006;9:267–73.
106. Vates GE, Berger MS, Wilson CB. Diagnosis and management of pituitary abscess: a review of twenty-four cases. J Neurosurg. 2001;95:233–41.
107. Wang L, Yao Y, Feng F, Deng K, Lian W, Li G, Wang R, Xing B. Pituitary abscess following transsphenoidal surgery: the experience of 12 cases from a single institution. Clin Neurol Neurosurg. 2014;124:66–71.
108. Dalan R, Leow MK. Pituitary abscess: our experience with a case and a review of the literature. Pituitary. 2008;11:299–306.
109. Shuster A, Gunnarsson T, Sommer D, Miller E. Pituitary abscess: an unexpected diagnosis. Pediatr Radiol. 2010;40:219–22.
110. Taguchi Y, Yoshida K, Takashima S, Tanaka K. Diffusion-weighted MRI findings in a patient with pituitary abscess. Intern Med. 2012;51:683.
111. Scheithauer BW, Kovacs K, Horvath E, Kim DS, Osamura RY, Ketterling RP, Lloyd RV, Kim OL. Pituitary blastoma. Acta Neuropathol. 2008;116(6):657–66. https://doi.org/10.1007/s00401-008-0388-9.
112. Scheithauer BW, Horvath E, Abel TW, Robital Y, Park SH, Osamura RY, Deal C, Lloyd RV, Kovacs K. Pituitary blastoma: a unique embryonal tumor. Pituitary. 2012;15(3):365–73. https://doi.org/10.1007/s11102-011-0328-x.
113. de Kock L, Priest JR, Foulkes WD, Alexandrescu S. An update on the central nervous system manifestations of DICER1 syndrome. Acta Neuropathol. 2020;139(4):689–701. https://doi.org/10.1007/s00401-019-01997-y.
114. de Kock L, Sabbaghian N, Plourde F, Srivastava A, Weber E, Bouron-Dal Soglio D, Hamel N, Choi JH, Park SH, Deal CL, Kelsey MM, Dishop MK, Esbenshade A, Kuttesch JF, Jacques TS, Perry A, Leichter H, Maeder P, Brundler MA, Warner J, Neal J, Zacharin M, Korbonits M, Cole T, Traunecker H, McLean TW, Rotondo F, Lepage P, Albrecht S, Horvath E, Kovacs K, Priest JR, Foulkes WD. Pituitary blastoma: a pathognomonic feature of germline DICER1 mutations. Acta Neuropathol. 2014;128(1):111–22. https://doi.org/10.1007/s00401-014-1285-z.
115. Liu APY, Kelsey MM, Sabbaghian N, Park SH, Deal CL, Esbenshade AJ, Ploner O, Peet A, Traunecker H, Ahmed YHE, Zacharin M, Tiulpakov A, Lapshina AM, Walter AW, Dutta P,

Rai A, Korbonits M, de Kock L, Nichols KE, Foulkes WD, Priest JR. Clinical outcomes and complications of pituitary blastoma. J Clin Endocrinol Metab. 2021;106(2):351–63. https://doi.org/10.1210/clinem/dgaa857.
116. Sahakitrungruang T, Srichomthong C, Pornkunwilai S, Amornfa J, Shuangshoti S, Kulawonganunchai S, Suphapeetiporn K, Shotelersuk V. Germline and somatic DICER1 mutations in a pituitary blastoma causing infantile-onset Cushing's disease. J Clin Endocrinol Metab. 2014;99(8):E1487–92. https://doi.org/10.1210/jc.2014-1016.
117. Foulkes WD, Priest JR, Duchaine TF. DICER1: mutations, microRNAs and mechanisms. Nat Rev Cancer. 2014;14(10):662–72. https://doi.org/10.1038/nrc3802.
118. Lopes MBS. World Health Organization 2017 Classification of Pituitary Tumors. Endocrinol Metab Clin North Am. 2020;49(3):375–86. https://doi.org/10.1016/j.ecl.2020.05.001.
119. Mete O, Gomez-Hernandez K, Kucharczyk W, et al. Silent subtype 3 pituitary adenomas are not always silent and represent poorly differentiated monomorphous plurihormonal pit-1 lineage adenomas. Mod Pathol. 2016;29:131–42.
120. Rasul FT, Jaunmuktane Z, Khan AA, et al. Plurihormonal pituitary adenoma with concomitant adrenocorticotropic hormone (ACTH) and growth hormone (GH) secretion: a report of two cases and review of the literature. Acta Neurochir(Wien). 2014;156:141–6.
121. Giraldi EA, Neill SG, Mendoza P, Saindane A, Oyesiku NM, Ioachimescu AG. Functioning Crooke cell adenomas: case series and literature review. World Neurosurg. 2021;158:e754–65. https://doi.org/10.1016/j.wneu.2021.11.049.
122. Snyder MH, Shabo L, Lopes MB, Xu Z, Schlesinger D, Sheehan JP. Gamma knife radiosurgery in patients with Crooke cell adenoma. World Neurosurg. 2020;138:e898–904. https://doi.org/10.1016/j.wneu.2020.03.152.
123. de Silva NL, Somasundaram N, Constantine R, Kularatna H. Apoplexy of Crooke cell tumour leading to the diagnosis of severe Cushing disease; a case report. BMC Endocr Disord. 2021;21(1):93. https://doi.org/10.1186/s12902-021-00761-2.
124. Tanaka S, Yamamoto M, Morita M, Takeno A, Kanazawa I, Yamaguchi T, Yamada S, Inoshita N, Oki Y, Kurosaki M, Sugimoto T. Successful reduction of ACTH secretion in a case of intractable Cushing's disease with pituitary Crooke's cell adenoma by combined modality therapy including temozolomide. Endocr J. 2019;66(8):701–8. https://doi.org/10.1507/endocrj.EJ18-0547.
125. Kamel WA, Najibullah M, Saleh MS, Azab WA. Coronavirus disease 2019 infection and pituitary apoplexy: a causal relation or just a coincidence? A case report and review of the literature. Surg Neurol Int. 2021;12:317. https://doi.org/10.25259/SNI_401_2021.
126. Sinclair G, Olsson M, Benmakhlouf H, Al-Saffar Y, Johnstone P, Hatiboglu MA, Shamikh A. Pituitary carcinomas: rare and challenging. Surg Neurol Int. 2019;10:161. https://doi.org/10.25259/SNI_112_2019.
127. Majd N, Waguespack SG, Janku F, Fu S, Penas-Prado M, Xu M, Alshawa A, Kamiya-Matsuoka C, Raza SM, McCutcheon IE, Naing A. Efficacy of pembrolizumab in patients with pituitary carcinoma: report of four cases from a phase II study. J Immunother Cancer. 2020;8(2):e001532. https://doi.org/10.1136/jitc-2020-001532.
128. Sioutos P, Yen V, Arbit E. Pituitary gland metastases. Ann Surg Oncol. 1996;3(1):94–9. https://doi.org/10.1007/BF02409058.
129. Branch CL Jr, Laws ER Jr. Metastatic tumors of the sella turcica masquerading as primary pituitary tumors. J Clin Endocrinol Metab. 1987;65(3):469–74. https://doi.org/10.1210/jcem-65-3-469.
130. Javanbakht A, D'Apuzzo M, Badie B, Salehian B. Pituitary metastasis: a rare condition. Endocr Connect. 2018;7(10):1049–57. https://doi.org/10.1530/EC-18-0338.
131. Gopan T, Toms SA, Prayson RA, et al. Symptomatic pituitary metastases from renal cell carcinoma. Pituitary. 2007;10:251–9.
132. Komninos J, Vlassopoulou V, Protopapa D, Korfias S, Kontogeorgos G, Sakas DE, Thalassinos NC. Tumors metastatic to the pituitary gland: case report and literature review. J Clin Endocrinol Metab. 2004;89(2):574–80. https://doi.org/10.1210/jc.2003-030395.

133. Bailey D, Mau C, Zacharia B. Pituitary metastasis from urothelial carcinoma: a case report and review of the diagnosis and treatment of pituitary metastases. Cureus. 2021;13(8):e17574. https://doi.org/10.7759/cureus.17574.
134. Wendel C, Campitiello M, Plastino F, et al. Pituitary metastasis from renal cell carcinoma: description of a case report. Am J Case Rep. 2017;18:7–11. https://doi.org/10.12659/ajcr.901032.
135. Omofoye OA, Lechpammer M, Steele TO, Harsh GR. Pituitary stalk gangliogliomas: case report and literature review. Clin Neurol Neurosurg. 2020. https://doi.org/10.1016/j.clineuro.2020.106405.
136. Fehn M, Lohmann F, Ludecke DK, et al. Ganglioglioma of the neurohypophysis with secretion of vasopressin. Exp Clin Endocrinol Diabetes. 1998;106:425–30.
137. Scheithauer BW, Silva AI, Parisi JE, et al. Ganglioglioma of the neurohypophysis. Endocr Pathol. 2008;19:112–6.
138. Hong Y, Fang Y, Wu Q, Zhang J, Wang Y. Ganglioglioma of the adenohypophysis mimicking pituitary adenoma: a case report and review of literature. Medicine (Baltimore). 2018;97(30):e11583. https://doi.org/10.1097/MD.0000000000011583.
139. Tavares ABW, Tomaz GA, Leao LMCSM, Tabet A, Kraemer-Aguiar LG. Mixed somatotroph adenomagangliocytoma AND A rare sellar combined tumor. Int J Case Rep Images. 2020;11:101154Z01AT2020. https://doi.org/10.5348/101154Z01AT2020CR.
140. Cossu G, Daniel RT, Messerer M. Gangliocytomas of the sellar region: a challenging diagnosis. Clin Neurol Neurosurg. 2016;149:122–35. https://doi.org/10.1016/j.clineuro.2016.08.002.
141. Kissiedu JO, Prayson RA. Sellar gangliocytoma with adrenocorticotropic and prolactin adenoma. J Clin Neurosci. 2016;24:141–2. https://doi.org/10.1016/j.jocn.2015.07.006; Epub 2015 Aug 24.
142. Novello M, Gessi M, Doglietto F, Anile C, Lauriola L, Coli A. Characteristics of ganglion cells in pituitary gangliocytomas. Neuropathology. 2017;37(1):64–8. https://doi.org/10.1111/neup.12322.
143. Lopes MB, Sloan E, Polder J. Mixed gangliocytoma-pituitary adenoma: insights on the pathogenesis of a rare sellar tumor. Am J Surg Pathol. 2017;41(5):586–95. https://doi.org/10.1097/PAS.0000000000000806.
144. Wang YY, Kearney T, du Plessis D, Gnanalingham KK. Extraventricular neurocytoma of the sellar region. Br J Neurosurg. 2012;26(3):420–2. https://doi.org/10.3109/02688697.2011.633635.
145. Kawaji H, Saito O, Amano S, Kasahara M, Baba S, Namba H. Extraventricular neurocytoma of the sellar region with spinal dissemination. Brain Tumor Pathol. 2014;31(1):51–6. https://doi.org/10.1007/s10014-012-0128-7.
146. Mukhida K, Asa S, Gentili F, Shannon P. Ependymoma of the pituitary fossa. Case report and review of the literature. J Neurosurg. 2006;105(4):616–20. https://doi.org/10.3171/jns.2006.105.4.616.).
147. Parish JM, Bonnin JM, Goodman JM, Cohen-Gadol AA. Intrasellar ependymoma: clinical, imaging, pathological, and surgical findings. J Clin Neurosci. 2015;22(4):638–41. https://doi.org/10.1016/j.jocn.2014.10.026.).
148. Keskin F, Erdi F, Kaya B, Toy H. Sellar-suprasellar extraventricular choroid plexus papilloma: a case report and review of the literature. J Korean Neurosurg Soc. 2016;59(1):58–61. https://doi.org/10.3340/jkns.2016.59.1.58.).
149. Bian LG, Sun QF, Wu HC, Jiang H, Sun YH, Shen JK. Primary choroid plexus papilloma in the pituitary fossa: case report and literature review. Acta Neurochir (Wien). 2011;153(4):851–7. https://doi.org/10.1007/s00701-010-0884-2.
150. Ostrom QT, Chen Y, MdB P, Ondracek A, Farah P, Gittleman H, Wolinsky Y, et al. The descriptive epidemiology of atypical teratoid/rhabdoid tumors in the United States, 2001-2010. Neuro Oncol. 2014;16(10):1392–9.

151. Buscariollo DL, Park HS, Roberts KB, Yu JB. Survival outcomes in atypical teratoid rhabdoid tumor for patients undergoing radiotherapy in a surveillance, epidemiology, and end results analysis. Cancer. 2012;118(17):4212–9.
152. Park HG, Yoon JH, Kim SH, Cho KH, Park HJ, Kim SH, Kim EH. Adult-onset sellar and suprasellar atypical teratoid rhabdoid tumor treated with a multimodal approach: a case report. Brain Tumor Res Treat. 2014;2(2):108–13. https://doi.org/10.14791/btrt.2014.2.2.108.
153. Dupuy M, Bonneville F, Grunenwald S, Breibach F, Delisle MB, Chaynes P, Sol JC, Caron P, Primary sellar neuroblastoma. A new case and review of literature. Ann Endocrinol (Paris). 2012;73(3):216–21. https://doi.org/10.1016/j.ando.2012.02.001.
154. Schmalisch K, Psaras T, Beschorner R, Honegger J. Sellar neuroblastoma mimicking a pituitary tumour: case report and review of the literature. Clin Neurol Neurosurg. 2009;111(9):774–8. https://doi.org/10.1016/j.clineuro.2009.06.011.
155. Kamil M, Higa N, Yonezawa H, Fujio S, Sugata J, Takajo T, Hiraki T, Hirato J, Arita K, Yoshimoto K. A sellar neuroblastoma showing rapid growth and causing syndrome of inappropriate secretion of antidiuretic hormone: a case report. Surg Neurol Int. 2020;11:165. https://doi.org/10.25259/SNI_97_2020.
156. Bilbao JM, Horvath E, Kovacs K, et al. Intrasellar paraganglioma associated with hypopituitarism. Arch Pathol Lab Med. 1978;102:95–8.
157. Haresh KP, Prabhakar R, Anand Rajan KD, Sharma DN, Julka PK, Rath GK. A rare case of paraganglioma of the sella with bone metastases. Pituitary. 2009;12:276–9.
158. Salame K, Ouaknine GER, Yossipov J, et al. Paraganglioma of the pituitary fossa: diagnosis and management. J Neurooncol. 2001;54:49–52.
159. Sinha S, Sharma MC, Sharma BS. Malignant paraganglioma of the sellar region mimicking a pituitary macroadenoma. J Clin Neurosci. 2008;15:937–9.
160. Zorlu F, Selek U, Ulger S, Donmez T, Erden E. Paraganglioma in sella. J Neurooncol. 2005;73(3):265–7.
161. Huang BY, Castillo M. Nonadenomatous tumors of the pituitary and sella turcica. Top Magn Reson Imaging. 2005;16:289–99.
162. Kudo H, Takaishi Y, Minami H, Takamoto T, Kitazawa S, Maeda S, et al. Intrasellar meningioma mimicking pituitary apoplexy: case report. Surg Neurol. 1997;48:374–81.
163. Chen A, Xiang R, Zhou R. Pure intrasellar meningioma mimicking pituitary adenoma: a novel neuroradiologic finding. World Neurosurg. 2022;160:1–3. https://doi.org/10.1016/j.wneu.2021.11.075.
164. Orakdogeny M, Karadereler S, Berkman Z, Ersahin M, Ozdoğan C, Aker F, et al. Intrasuprasellar meningioma mimicking pituitary apoplexy. Acta Neurochir. 2004;146:511–5.
165. Sakamoto Y, Takahashi M, Korogi Y, Bussaka H, Ushio Y. Normal and abnormal pituitary glands: gadopentetate dimeglumine-enhanced MR imaging. Radiology. 1991;178:441–5.
166. Cappabianca P, Cirillo S, Alfieri A, D'Amico A, Maiuri F, Mariniello G, et al. Pituitary macroadenoma and diaphragma sellae meningioma: differential diagnosis on MRI. Neuroradiology. 1999;41:22–6.
167. Sharma M, Madan M, Manjari M, Kaur H. Pituitary Chondrosarcoma presenting as a sellar and suprasellar mass with parasellar extension: An Unusual presentation. Iran J Pathol. 2016;11(2):161–6.
168. Kaufmann TJ, Lopes MB, Laws ER Jr, Lipper MH. Primary sellar lymphoma: radiologic and pathologic findings in two patients. AJNR Am J Neuroradiol. 2002;23(3):364–7.
169. Wilkie MD, Al-Mahfoudh R, Javadpour M. A rare case of primary sellar lymphoma presenting a diagnostic challenge. Br J Neurosurg. 2012;26(5):782–3. https://doi.org/10.3109/02688697.2012.674578.
170. Romeis B, von Möllendorff W, Bargmann W. Handbuch der mikroskopischen Anatomie des Menschen. Bd. 6, Blutgefäß-und Lymphgefäßapparat, innersekretorische Drüsen: Teil 3, Innersektorische Drüsen: 2. Hypophyse. Berlin: Springer Verlag; 1940.
171. Ranucci V, Coli A, Marrucci E, Paolo MP, Della Pepa G, Anile C, Mangiola A. Ectopic salivary gland tissue in a Rathke's cleft cyst. Int J Clin Exp Pathol. 2013;6:1437–40.

172. Kleinschmidt-DeMasters BK, Rosenblum MK, Kerr JM, Lillehei KO. Cystic sellar salivary gland-like lesions. Clin Neuropathol. 2020;39(05):115–25. https://doi.org/10.5414/np301235.
173. Schochet SS Jr, McCormick WF, Halmi NS. Salivary gland rests in the human pituitary. Light and electron microscopical study. Arch Pathol. 1974;98:193–200.
174. Feola T, Gianno F, De Angelis M, Colonnese C, Esposito V, Giangaspero F, Jaffrain-Rea ML. Salivary gland tissues and derived primary and metastatic neoplasms: unusual pitfalls in the work-up of sellar lesions. A systematic review. J Endocrinol Invest. 2021;44(10):2103–22. https://doi.org/10.1007/s40618-021-01577-6.
175. Rittierodt M, Hori A. Pre-morbid morphological conditions of the human pituitary. Neuropathology. 2007;27:43–8.
176. Chimelli L, Gadelha MR, Une K, et al. Intra-sellar salivary gland-like pleomorphic adenoma arising within the wall of a Rathke's cleft cyst. Pituitary. 2000;3:257–61.
177. Liu Z, Zhang Y, Feng R, Tian Z, Rao Y, Lu Y, Xu J. Intrasellar symptomatic salivary gland: case series and literature review. Pituitary. 2019;22(6):640–6. https://doi.org/10.1007/s11102-019-01002-5.
178. Chen CH, Hsu SS, Lai PH, Lo YS. Intrasellar symptomatic salivary gland rest. J Chin Med Assoc. 2007;70(5):215–7. https://doi.org/10.1016/S1726-4901(09)70361-2.
179. Hwang JH. Pituitary symptomatic salivary gland rest cyst: case report. Brain Tumor Res Treat. 2013;1(1):54–6. https://doi.org/10.14791/btrt.2013.1.1.54.
180. Lavin V, Callipo F, Donofrio CA, Ellwood-Thompson R, Metcalf R, Djoukhadar I, Higham CE, Kearney T, Colaco R, Gnanalingham K, Roncaroli F. Primary epithelial–myoepithelial carcinoma of the pituitary gland. Neuropathology. 2020;40(3):261–7. https://doi.org/10.1111/neup.12628.
181. Giridhar P, Mallick S, Laviraj MA, Bhasker S. Adenoid cystic carcinoma sphenoid sinus with intracranial extension treated by radical radiotherapy: a rare case. Eur Arch Otorhinolaryngol. 2015;272(4):1037–40. https://doi.org/10.1007/s00405-014-3441-4.
182. Pujia R, Russo D, Guadagno E, Bartone L, Trapasso R, Piro E, Foti D, Brunetti A. Non-functional pituitary tumors: a misleading presentation of an intrasellar plasmacytoma. Acta Endocrinol (Buchar). 2019;15(4):518–21. https://doi.org/10.4183/Aeb.2019.518.
183. Soejbjerg A, Dyve S, Baerentzen S, Thorsell G, Poulsen PL, Jorgensen JO, Kampmann U. The solitary sellar plasmacytoma: a diagnostic challenge. Endocrinol Diabetes Metab Case Rep. 2016;2016:160031. https://doi.org/10.1530/EDM-16-0031.
184. Jin L, Gui S, Li C, Bai J, Cao L, Liu C, Wang X, Zhang Y. Differential diagnosis and treatment modality of parasellar plasmacytoma: clinical series and literature review. World Neurosurg. 2019;122:e978–88. https://doi.org/10.1016/j.wneu.2018.10.183.
185. Lee J, Kulubya E, Pressman BD, Mamelak A, Bannykh S, Zada G, Cooper O. Sellar and clival plasmacytomas: case series of 5 patients with systematic review of 65 published cases. Pituitary. 2017;20(3):381–92. https://doi.org/10.1007/s11102-017-0799-5.
186. Schneider JR, Kwan K, Kulason KO, Faltings LJ, Colantonio S, Safir S, Loven T, Li JY, Black KS, Schaeffer BT, Eisenberg MB. Primary solitary retro-clival amyloidoma. Surg Neurol Int. 2018;9:100. https://doi.org/10.4103/sni.sni_483_17.
187. Golden LD, Small JE. Benign notochordal lesions of the posterior clivus: retrospective review of prevalence and imaging characteristics. J Neuroimaging. 2014;24(3):245–9. https://doi.org/10.1111/jon.12013.
188. Alwani MM, Monaco GN, Harmon SM, Nwosu OI, Vortmeyer AO, Payner TD, Ting J. A systematic review of sellar and parasellar brown tumors: an analysis of clinical, diagnostic, and management profiles. World Neurosurg. 2019;132:e423–9. https://doi.org/10.1016/j.wneu.2019.08.126.
189. Liu J, Ahmadpour A, Bewley AF, Lechpammer M, Bobinski M, Shahlaie K. Chondroblastoma of the clivus: case report and review. J Neurol Surg Rep. 2015;76(2):e258–64. https://doi.org/10.1055/s-0035-1564601.

190. Park HH, Lee KS, Ahn SJ, Suh SH, Hong CK. Ecchordosis physaliphora: typical and atypical radiologic features. Neurosurg Rev. 2017;40(1):87–94. https://doi.org/10.1007/s10143-016-0753-4.
191. Altafulla JJ, Prickett JT, Dupont G, Tubbs RS, Litvack Z. Ectopic pituitary adenoma presenting as a clival mass. Cureus. 2019;11(2):e4158. https://doi.org/10.7759/cureus.4158.
192. Velagapudi S, Alshammari SM, Velagapudi S. Maffucci syndrome with clival enchondroma in nasopharynx: a case report. Indian J Otolaryngol Head Neck Surg. 2019;71(Suppl 1):652–6. https://doi.org/10.1007/s12070-018-1463-8.
193. Zhang T, Xu L, Gu L, Chen W, Pandey G, Wang J, Wu Y. Calcifying fibrous tumor of the clivus presenting in an adult. Radiol Case Rep. 2019;14(6):771–4. https://doi.org/10.1016/j.radcr.2019.03.028.
194. Heman-Ackah SE, Boyer H, Odland R. Clival fibrous dysplasia: case series and review of the literature. Ear Nose Throat J. 2014;93(12):E4–9. https://doi.org/10.1177/014556131409301202.
195. Zhang H, Jiang N, Lin X, Wanggou S, Olson JJ, Li X. Invasive sphenoid sinus aspergillosis mimicking sellar tumor: a report of 4 cases and systematic literature review. Chin Neurosurg J. 2020;6:10. https://doi.org/10.1186/s41016-020-00187-0.
196. Nakamura H, Morisako H, Ohata H, Kuwae Y, Teranishi Y, Goto T. Pediatric giant cell reparative granuloma of the lower clivus: a case report and review of the literature. J Craniovertebr Junction Spine. 2021;12(1):86–90. https://doi.org/10.4103/jcvjs.JCVJS_182_20.
197. Patibandla MR, Thotakura AK, Rao MN, Addagada GC, Nukavarapu MC, Panigrahi MK, Uppin S, Challa S, Dandamudi S. Clival giant cell tumor - a rare case report and review of literature with respect to current line of management. Asian J Neurosurg. 2017;12(1):78–81. https://doi.org/10.4103/1793-5482.145112.
198. Tang H, Ding G, Xiong J, Zhu H, Hua L, Xie Q, Gong Y. Clivus inflammatory pseudotumor associated with immunoglobulin G4-related disease. World Neurosurg. 2018;118:71–4. https://doi.org/10.1016/j.wneu.2018.06.174.
199. Yu X, Liu R, Wang Y, Wang H, Zhao H, Wu Z. Infrasellar craniopharyngioma. Clin Neurol Neurosurg. 2012;114(2):112–9. https://doi.org/10.1016/j.clineuro.2011.09.010.
200. Caranci F, Cirillo M, Piccolo D, Briganti G, Cicala D, Leone G, Briganti F. A rare case of intraosseous lipoma involving the sphenoclival region. Neuroradiol J. 2012;25(6):680–3. https://doi.org/10.1177/197140091202500607.
201. Tsai VW, Rybak L, Espinosa J, Kuhn MJ, Kamel OW, Mathews F, Glatz FR. Primary B-cell lymphoma of the clivus: case report. Surg Neurol. 2002;58(3-4):246–50. https://doi.org/10.1016/s0090-3019(02)00845-5.
202. Kawaguchi A, Shin M, Hasegawa H, Shinya Y, Shojima M, Kondo K. Endoscopic extended transclival approach for lower clival meningioma. World Neurosurg. 2022;164:117. https://doi.org/10.1016/j.wneu.2022.04.115.
203. Mani A, Yadav P, Paliwal VK, Lal H. Isolated clival metastasis: a rare presentation of renal cell carcinoma. BMJ Case Rep. 2017;2017:bcr2017221570. https://doi.org/10.1136/bcr-2017-221570.
204. Moravan MJ, Petraglia AL, Almast J, Yeaney GA, Miller MC, Edward Vates G. Intraosseous hemangioma of the clivus: a case report and review of the literature. J Neurosurg Sci. 2012;56(3):255–9.
205. Mathkour M, Garces J, Beard B, Bartholomew A, Sulaiman OA, Ware ML. Primary high-grade osteosarcoma of the clivus: a case report and literature review. World Neurosurg. 2016;89:730.e9–730.e13. https://doi.org/10.1016/j.wneu.2016.01.054.
206. Goyal R, Gupta R, Radotra BD. Plasmacytoma of the clivus: a case report. Indian J Pathol Microbiol. 2006;49(4):568–70.
207. Gupta S, Kumar A, Rangari KV, Mehrotra A, Pal L, Kumar R. Intracranial peripheral primitive neuroectodermal tumor arising from the clivus with intracranial metastasis in an elderly woman: case report and review of the literature. World Neurosurg. 2018;119:331–4. https://doi.org/10.1016/j.wneu.2018.08.066.

208. Seiz M, Radek M, Buslei R, Kreutzer J, Hofmann B, Kottler U, Doerfler A, Nimsky C, Fahlbusch R. Alveolar rhabdomyosarcoma of the clivus with intrasellar expansion: case report. Zentralbl Neurochir. 2006;67(4):219–22. https://doi.org/10.1055/s-2006-942118.
209. Stavrakas M, Khalil HS, Tsetsos N, Muquit S. Clival mucocele: a rare yet not forgotten pathology. Ear Nose Throat J. 2021;1455613211021176. https://doi.org/10.1177/01455613211021176.
210. González-García L, Asenjo-García B, Bautista-Ojeda MD, Domínguez-Páez M, Romero-Moreno L, Martín-Gallego Á, Arráez-Sánchez MÁ. Endoscopic endonasal resection of clival xanthoma: case report and literature review. Neurosurg Rev. 2015;38(4):765–9. https://doi.org/10.1007/s10143-015-0630-6.
211. Pagella F, Ugolini S, Zoia C, Matti E, Carena P, Lizzio R, Benazzo M. Clivus pathologies from diagnosis to surgical multidisciplinary treatment. Review of the literature. Acta Otorhinolaryngol Ital. 2021;41(Suppl. 1):S42–50. https://doi.org/10.14639/0392-100X-suppl.1-41-2021-04.
212. Folbe AJ, Svider PF, Liu JK, Eloy JA. Endoscopic Resection of Clival Malignancies. Otolaryngol Clin North Am. 2017;50(2):315–29. https://doi.org/10.1016/j.otc.2016.12.008.
213. Eloy JA, Vazquez A, Marchiano E, et al. Variations of mucosal-sparing septectomy for endonasal approach to the craniocervical junction. Laryngoscope. 2016;126:2220–5.
214. Moussazadeh N, Kulwin C, Anand VK, et al. Endoscopic endonasal resection of skull base chondrosarcomas: technique and early results. J Neurosurg. 2015;122:735–42.
215. Stamm AC, Pignatari SS, Vellutini E. Transnasal endoscopic surgical approaches to the clivus. Otolaryngol Clin North Am. 2006;39:639–56, xi.
216. Lanzino G, Dumont AS, Lopez MBS, Laws E. Skull base chordomas: overview of disease, management options, and outcome. Neurosurg Focus. 2001;10:E12.
217. Demonte F, Diaz E, Callender D, Suk I. Transmandibular, circumglossal, retropharyngeal approach for chordomas of the clivus and upper cervical spine. Technical note. Neurosurg Focus. 2001;10:E10.
218. Solares CA, Fakhri S, Batra P, Lee J, Lanza DC. Transnasal endoscopic resection of lesions of the clivus: a preliminary report. Laryngoscope. 2005;115:1917–22.
219. Lew D, Southwick FS, Montgomery WW, Weber AL, Baker AS, Sphenoid sinusitis. A review of 30 cases. N Engl J Med. 1983;309(19):1149–54.
220. Wang ZM, Kanoh N, Dai CF, Kutler DI, Xu R, Chi FL, et al. Isolated sphenoid sinus disease: an analysis of 122 cases. Ann Otol Rhinol Laryngol. 2002;111(4):323–7.
221. Ada M, Kaytaz A, Tuskan K, Güvenç MG, Selçuk H. Isolated sphenoid sinusitis presenting with unilateral VIth nerve palsy. Int J Pediatr Otorhinolaryngol. 2004;68(4):507–10. https://doi.org/10.1016/j.ijporl.2003.11.011.
222. Promsopa C, Polwiang P, Chinpairoj S, Kirtsreesakul V. Complications of isolated fungal sphenoiditis: patient clinical characteristics. ORL J Otorhinolaryngol Relat Spec. 2020;82(1):15–24. https://doi.org/10.1159/000503902.
223. Kim JS, Lee EJ. Endoscopic findings of fungal ball in the mucocele after endonasal transsphenoidal surgery. Ear Nose Throat J. 2021;100(3):NP169–70. https://doi.org/10.1177/0145561319867669.
224. Scotto di Carlo F, Divisato G, Iacoangeli M, Esposito T, Gianfrancesco F. The identification of H3F3A mutation in giant cell tumour of the clivus and the histological diagnostic algorithm of other clival lesions permit the differential diagnosis in this location. BMC Cancer. 2018;18(1):358. https://doi.org/10.1186/s12885-018-4291-z.
225. Zhao J, Qian T, Zhi Z, Li Q, Kang L, Wang J, et al. Giant cell tumour of the clivus: a case report and review of the literature. Oncol Lett. 2014;8:2782–6.
226. Singh S, Mankotia DS, Shankar KB, Siraj F. A rare tumor of clivus masquerading as pituitary adenoma. Asian J Neurosurg. 2020;154:1091–5. https://doi.org/10.4103/ajns.AJNS_188_20.
227. Akyigit A, Karlidag T, Sakallioglu Ö, Polat C, Keles E. Giant cell tumor of bone involving the temporomandibular joint and temporal bone. J Craniofac Surg. 2014;25:1397–9.

228. Campanacci M, Baldini N, Boriani S, Sudanese A. Giant-cell tumour of bone. J Bone Joint Surg Am. 1987;69:106–14.
229. Morgan T, Atkins GJ, Trivett MK, Johnson SA, Kansara M, Schlicht SL, et al. Molecular profiling of giant cell tumour of bone and the osteoclastic localization of ligand for receptor activator of nuclear factor kappaB. Am J Pathol. 2005;167:117–28.
230. Thomas DM. RANKL, denosumab, and giant cell tumor of bone. Curr Opin Oncol. 2012;24(4):397–403. https://doi.org/10.1097/CCO.0b013e328354c129.
231. Gaston CL, Grimer RJ, Parry M, Stacchiotti S, Dei Tos AP, Gelderblom H, Ferrari S, Baldi GG, Jones RL, Chawla S, Casali P, LeCesne A, Blay JY, Dijkstra SP, Thomas DM, Rutkowski P. Current status and unanswered questions on the use of Denosumab in giant cell tumor of bone. Clin Sarcoma Res. 2016;6(1):15. https://doi.org/10.1186/s13569-016-0056-0.
232. Goto Y, Furuno Y, Kawabe T, Ohwada K, Tatsuzawa K, Sasajima H, Hashimoto N. Treatment of a skull-base giant cell tumor with endoscopic endonasal resection and denosumab: case report. J Neurosurg. 2017;126(2):431–4. https://doi.org/10.3171/2016.3.JNS152802.
233. Singh VA, Puri A. The current standing on the use of denosumab in giant cell tumour of the bone. J Orthop Surg (Hong Kong). 2020;28(3):2309499020979750. https://doi.org/10.1177/2309499020979750.
234. Inoue A, Ohnishi T, Kohno S, Nishikawa M, Nishida N, Ohue S. Role of denosumab in endoscopic endonasal treatment for juvenile clival giant cell tumor: a case report and review of the literature. World Neurosurg. 2016;91(674):e1–6.
235. Iacoangeli M, Di Rienzo A, Re M, Alvaro L, Nocchi N, Gladi M, et al. Endoscopic endonasal approach for the treatment of a large clival giant cell tumor complicated by an intraoperative internal carotid artery rupture. Cancer Manag Res. 2013;5:21–4.
236. Contratti F, Menniti A, Fraioli MF, Fraioli B. Fibrous dysplasia of the clivus with a second T8 bone lesion: case report. Surg Neurol. 2006;65(2):202–5; discussion 205-6. doi: 10.1016/j.surneu.2005.05.025. Erratum in: Surg Neurol. 2006 May;65(5):528. Contratt, Filiberto corrected to Contratti, Filiberto.
237. Butt A, Patel K, Agrawal K, Arya A, Singh J. Fibrous dysplasia of the clivus - a case study and literature review. Radiol Case Rep. 2020;16(2):230–6. https://doi.org/10.1016/j.radcr.2020.11.019.
238. Adada B, Al-Mefty O. Fibrous dysplasia of the clivus. Neurosurgery. 2003;52(2):318–22; discussion 323. https://doi.org/10.1227/01.neu.0000043694.77162.6e.
239. Atalar M, Ozum U. Monostotic fibrous dysplasia of the clivus: imaging findings. Turk Neurosurg. 2010;20(1):77–81.
240. Sato K, Kubota T, Kaneko M, Kawano H, Kobayashi H. Fibrous dysplasia of the clivus. Surg Neurol. 1993;40(6):522–5. https://doi.org/10.1016/0090-3019(93)90059-a.
241. Levy ML, Chen TC, Weiss MH. Monostotic fibrous dysplasia of the clivus. Case report. J Neurosurg. 1991;75(5):800–3. https://doi.org/10.3171/jns.1991.75.5.0800.
242. Dekker SE, Wasman J, Yoo KK, Alonso F, Tarr RW, Bambakidis NC, Rodriguez K. Clival metastasis of a duodenal adenocarcinoma: a case report and literature review. World Neurosurg. 2017;100:62–8. https://doi.org/10.1016/j.wneu.2016.12.078.
243. Lee A, Chang KH, Hong H, Kim H. Sixth cranial nerve palsy caused by gastric adenocarcinoma metastasis to the clivus. J Korean Neurosurg Soc. 2015;57(3):208–10. https://doi.org/10.3340/jkns.2015.57.3.208.
244. Nishiguchi T, Mochizuki K, Ohsawa M, Inoue T, Kageyama K, Suzuki A, Takami T, Miki Y. Differentiating benign notochordal cell tumors from chordomas: radiographic features on MRI, CT, and tomography. AJR Am J Roentgenol. 2011;196(3):644–50. https://doi.org/10.2214/AJR.10.4460.
245. Ulich TR, Mirra JM. Ecchordosis physaliphora vertebralis. Clin Orthop Relat Res. 1982;(163):282-289.
246. George B, Bresson D, Herman P, Froelich S. Chordomas: a review. Neurosurg Clin N Am. 2015;26(3):437–52. https://doi.org/10.1016/j.nec.2015.03.012.

247. Ulici V, Hart J. Chordoma. Arch Pathol Lab Med. 2022;146(3):386–95. https://doi.org/10.5858/arpa.2020-0258-RA.
248. Lagman C, Varshneya K, Sarmiento JM, Turtz AR, Chitale RV. Proposed diagnostic criteria, classification schema, and review of literature of notochordderived ecchordosis physaliphora. Cureus. 2016;8(3):e547.
249. Fletcher CDM, Bridge JA, Hogendoorn P, Mertens F, editors. WHO classification of tumours of soft tissue and bone, World Health Organization classification of tumours, vol. 3. 5th ed. Lyon: International Agency for Research on Cancer; 2020.
250. Peris-Celda M, Salgado-Lopez L, Inwards CY, Raghunathan A, Carr CM, Janus JR, Stokken JK, Van Gompel JJ. Benign notochordal cell tumor of the clivus with chordoma component: report of 2 cases. J Neurosurg. 2019;1–5. https://doi.org/10.3171/2019.6.JNS19529.

Chapter 8
Surgical Approaches to the Third Ventricle: An Update

Nicola Onorini, Pietro Spennato, Giuseppe Mirone, Francesca Vitulli, Domenico Solari, Luigi Maria Cavallo, and Giuseppe Cinalli

8.1 Introduction

Since Dandy and Cushing's pioneering surgical approaches in the early twentieth century [1, 2], along with the gradual advancement of microsurgery and then neuroendoscopy, the perception of surgical inaccessibility to the third ventricle has gradually diminished. However, despite tremendous advances in surgical technique, anatomical knowledge, and understanding of diseases, even today, surgery of the third ventricle constitutes a formidable challenge for the neurosurgeon [3–5].

Approaching the third ventricle means dealing with vital neurovascular structures, involved in a wide spectrum of diseases with different prognosis and behavior, in patients of variable ages, and with a surgical goal that can vary from radical debulking to biopsy.

In addition, during third ventricle surgery, the site of the lesion plays a key role in guiding the choice of surgical route: for example, operating on a lesion involving the anterior third ventricle has different surgical implications than approaching a lesion of the posterior or middle third ventricle.

Surgical approaches to the third ventricle will be described here, following an anatomical criterion of presentation, from anterior to posterior, with particular emphasis on microsurgical technique and advances in neuroendoscopy. The main indications and implications will also be discussed.

N. Onorini · P. Spennato · G. Mirone · F. Vitulli · G. Cinalli (✉)
Department of Pediatric Neurosurgery, Santobono-Pausilipon Children's Hospital, AORN, Naples, Italy

D. Solari · L. M. Cavallo
Division of Neurosurgery, Department of Neurosciences and Reproductive and Odontostomatological Sciences, "Federico II" University, Naples, Italy

C. Di Rocco (ed.), *Advances and Technical Standards in Neurosurgery*, Advances and Technical Standards in Neurosurgery 48,
https://doi.org/10.1007/978-3-031-36785-4_8

8.2 Extended Endoscopic Trans-Sphenoidal Approach

The endonasal/transnasal transsphenoidal corridor in neurosurgery represented a real revolution since its introduction, providing direct exposure of midline skull base areas, via a short and direct route without any brain retraction.

Following the Italian pioneer surgeon Davide Giordano, Schloffer completed in 1907 the first successful transsphenoidal removal of a pituitary adenoma [6, 7]; this technique developed throughout ideas, decline and renaissance periods, thanks to the contributions of true giants of the worldwide neurosurgery.

Guiot first [8] used the endoscope in the 1960s for the inspection of the sellar cavity at the end of a transsphenoidal procedure, and in 1977, Michael Apuzzo [9] started to apply the concept of "adjunctive endoscopy" during the conventional transsphenoidal procedures.

The first reports of endoscopic removal of pituitary adenoma were made by an interdisciplinary team of ENT and neurosurgeons [10, 11], among whom Hae-Dong Jho and Ricardo Carrau, started to apply the "pure" endoscopic endonasal approach for the removal of pituitary adenomas in 1996 [12] and fixed the guidelines of the skull base fully endoscopic procedures.

The endoscopic endonasal surgery spread around the world, with different neurosurgical schools contributing to the development and diffusion, among them the group of Cappabianca and de Divitiis [13, 14], Frank and Pasquini [15], and Castelnuovo and Locatelli [16] together with the Pittsburgh team lead by Amin Kassam [17, 18].

The multiangled and close-up view provided by the endoscope, along with the advancements of the techniques and the technological progress, has pushed thereafter definition of a variety of modifications of the approach [19–23], embracing the "extended" approach concept brought in by Weiss [24]. The extended endoscopic transsphenoidal approach (EEA) revolutionized the treatment of selected midline cranial base lesions and expanded boundaries of accessibility the third ventricle cavity [25] and boosted the shift of surgical indications for the lesions involving this area [26–30].

Several different types of intracranial tumors can develop inside the third ventricle: primary intraventricular tumors include colloid cysts, choroid plexus papilloma, ependymoma, purely intraventricular craniopharyngioma, and subependymal glioma. Skull base tumors can secondarily expand into the third ventricle, mostly craniopharyngioma, pituitary adenoma, optic nerve, and hypothalamic glioma.

These lesions comprise 10–15% of all primary brain tumors, accounting for approximatively 5% of all intracranial tumors in pediatric population, in which the most common are craniopharyngiomas [31–33]. According to the growth axis of these latter lesions, a ventral corridor, that is, the so-called transtuberculum transplanum approach can be considered favorable, allowing appropriate and effective exposure of the third ventricle, particularly the anterior parts (the infundibular and foraminal areas) [25].

The EEA in children seldom is not preferred because of the smaller size of nasal cavity corridor and poor pneumatization of the sphenoid sinuses; this latter starts between the third and the fourth month of prenatal life and usually reaches its adult size only by the 12th years of age [34].

The advantages of the EEA include direct access to ventral midline structures with minimal associated neurovascular manipulation and/or brain retraction. Additionally, the ability to deliver the endoscopic camera and light source to the region of tumor involvement allows for enhanced visualization of the tumor-hypothalamic interface [35].

Despite these advantages, it has to be said that EEA offers limited vision over the utmost superior and superior-posterior areas in the third ventricle. The lateral extension and a higher risk of postoperative CSF leak have been claimed as limits of the endoscopic approach for the surgical management of these lesions as well as the limited maneuverability and inability to perform direct microvascular repair in the event of vessel injury.

However, recent improvements in reconstruction techniques and the increased anatomical and surgical experience have made the endoscopic approach a viable and safe approach for the management of selected third ventricle lesions.

8.2.1 Surgical Technique

The transtuberculum transplanum approach to the third ventricle lesions is performed using a rigid 0-degree endoscope, 18 cm in length 4 mm in diameter (Karl Storz Endoscopy-Europe, Tuttlingen, Germany). The endoscope is employed as the sole visualizing instrument of the surgical field, and sometimes angled scope is used to further explore the suprasellar area after the lesion removal. Dedicated surgical instruments with different angled tips are needed in order to permit movements in all the visible corners of the surgical field. The endoscopic endonasal approach is a two-surgeon, three- or four-handed technique procedure, according to the "microsurgical principles" [13, 36]. The patient, under general anesthesia, is placed supine or in slight Trendelenburg position, with the head turned 5–10 degrees toward the surgeon (the patient's right) regardless he/she is right or left-handed. The head can be slightly extended for about 10–15 degrees in order to achieve a more anterior trajectory, avoiding conflicts between instruments and patient's chest.

Before entering the endoscope, the nose is decongested with cotton pledgets soaked in a solution of 2 ml of adrenaline, 5 ml of 20% diluted lidocaine, and 4 ml of saline solution. The nose and the periumbilical area are prepped and draped, and a third- or fourth-generation cephalosporin antibiotic is administered for perioperative prophylaxis.

As any skull base procedure, the EEA is run in three moments: definition of an adequate corridor, tumor resection, and reconstruction.

The nasal corridor is created according to the surgeon's preferences and patient's anatomy [37]: middle turbinate removal according on the surgeon dominant hand

and lateralization of middle turbinate in the contralateral nostril along with removal of the posterior portion of the nasal septum, and superior ethmoid air cells are required.

The sphenoid anterior wall and the sphenoid septa are removed to achieve a wide exposure of the surgical field. Once the sphenoid sinus has been accessed, all septae are removed along with bony spiculae, and mucosa is ripped off to consent to lay down the flap during reconstruction phase. Bone removal starts with the drilling of the upper half of the sella and the removal of the tuberculum sellae, named as the suprasellar notch [38], which corresponds to the angle formed by the planum sphenoidale and the sellar floor. The lateral margin of bone removal spans from both medial opticocarotid recess. Bone removal can be extended anteriorly up to the falciform ligament, or more, according to the anterior extension of the lesion.

The dura is opened above and below the superior intercavernous sinus, which is isolated, coagulated, and incised with microscissors. The arachnoid is subsequently opened sharply with microscissors, revealing the suprasellar neurovascular structures.

The dissection and removal maneuvers in the endoscopic endonasal approach for third ventricle lesions follow the concept that the lesion itself paves the path for the surgeon and must be tailored to each case. The principles followed and goal pursued are the same of transcranial microsurgery: internal debulking of the solid part and/or cystic evacuation, followed by dissection from the main surrounding neurovascular structures: the tumor has to be debulked up to mobilizing its capsule, so that extracapsular sharp dissection can be performed [39]. After being isolated from the surrounding structures, the lesion can be sharply dissected [20]: it is crucial to respect the arachnoid representing a natural cleavage plane and thereby protect the micro perforating vessels and the hypothalamus and pituitary stalk [40, 41].

Our policy is to adapt the resection on both the relationships between the tumor and the stalk-infundibulum and the position of the ventricular floor [27, 29]. Whether the tumor grows inside and enlarges the stalk-infundibulum complex, its removal starts where it gets in the surface, while in case infundibulum has been compressed and moved anteromedially or anterolaterally by the tumor, access to the lesion will be provided through the floor of the third ventricle protruding into the subchiasmatic area. Tumor is debulked up to the cleavage plane off the ventricular wall is identified. The dissection should start from the superior wall and then extended to the lateral and inferior aspects. It is mandatory not to force the resection if any tumor adhesion is suspected on the floor of the third ventricle at the level or beyond the mammillary bodies, in order to avoid brain stem injury: indeed, we prefer not to remove fragments of tumor on the posterior mesencephalic segment of the third ventricular floor.

As compared to transcranial route, the transsphenoidal pathway offers the great advantage of approaching the tumor from its ventral aspects, while the critical neurovascular structures lie on its dorsum and/or perimeter. Furthermore, the endoscope offers the possibility of moving from a close-up to a wider panoramic view especially at the boundary between tumor and diencephalic structures, where great care is taken to complete safe dissection maneuvers [13].

After tumor removal, diluted papaverine is injected in the surgical field. An effective and watertight closure of osteodural defect is mandatory to prevent postoperative CSF leakage and related adverse event, including meningitis, brain herniation, and tension pneumocephalus. Along with the development of the endonasal approaches, various techniques and materials have been adopted in an effort of providing a resilient and reliable method of closure [42–46], with a slight preference toward to the use of autologous tissues, mostly pedicled mucosal flap [42, 47–53].

Accordingly, the 3F technique [54] has been introduced, with each F addressing for a critical moment of the reconstruction strategy; the first F stands for autologous *fat*, the second refers for naso-septal *flap,* and the third refers to our idea of *flash*, or early patient mobilization after surgery.

The first step is the positioning of a large piece of autologous periumbilical *fat* graft as a "cork" across the osteodural defect with and a thin layer of fibrin glue sprayed over to secure these tissues; thereafter, Hadad-Bassagasteguy naso-septal *flap* (HBF) is reflected and set over the skull base defect, and the sphenoid sinus is filled with oxidized cellulose sponges (Surgicel, Ethicon). Anterior nasal tamponade (Merocel standard dressing, Medtronic Inc., Minneapolis, Minesota, USA) is placed in the nostril where the flap has been raised and left in place for 3 days. A postoperative CT scan is performed on postoperative day (POD) 1, to evaluate the degree of pneumocephalus and the baseline positioning of fat cork. Patients are mobilized, encouraged to stand and walk as much as possible (*Fast* mobilization), and asked to lie in a semi-sitting position up to POD 10 (Fig. 8.1).

8.3 Subfrontal Approach

As described by Rhoton et al. in 1981 [5], subfrontal approach can be used for lesions involving the anterior-inferior part of the third ventricle that cannot be managed by trans-sphenoid surgery. Basal midline tumors with suprasellar extension may be readily approached by this approach either unilaterally or bilaterally. This approach may be undertaken along midline or oblique frontal corridor [55]. For midline tumors, alternative to subfrontal approach is frontobasal interhemispheric approach [56].

Even if in the last years indications for transphenoidal surgery are enlarged, original description of Rhoton should be kept in mind in the decision-making process between transsphenoidal and subfrontal approaches [5]. Subfrontal approach should be favored in case of tumors that do not extend inside the sella turcica, tumors separated from the sella by a layer of normal tissue, tumors entirely located inside the third ventricle, or tumors located above a non-pneumatized sphenoid bone (as in case of young children).

The subfrontal approach offers different routes to reach the third ventricle [5, 55–57]: subchiasmatic, translamina terminalis, and optico-carotid triangle (optic nerve medially, carotid artery laterally and anterior cerebral artery posteriorly). Craniopharyngiomas are the most common tumors removed via this approach [56].

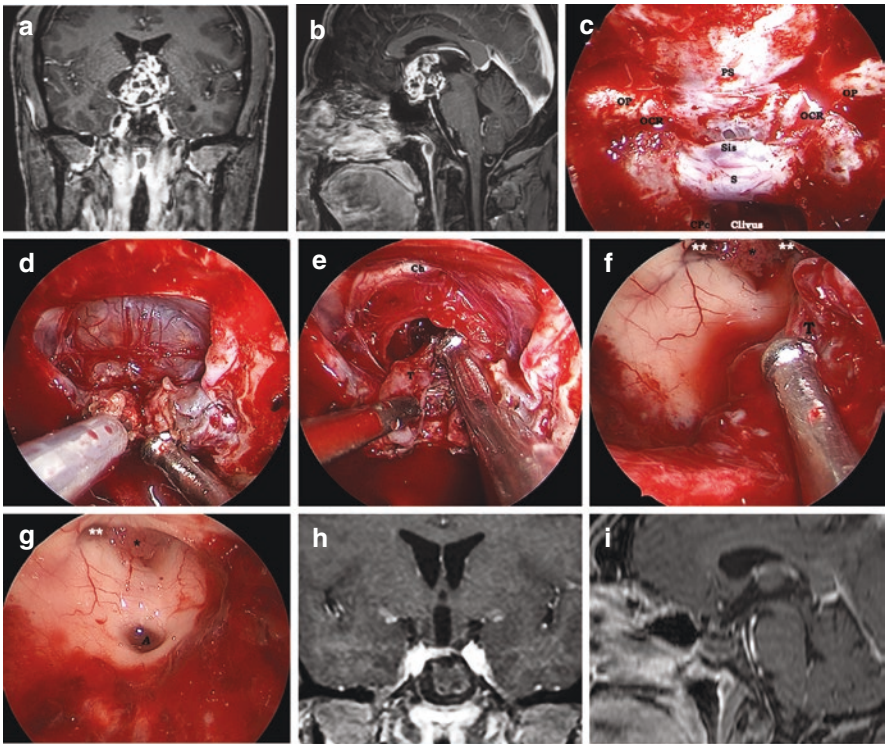

Fig. 8.1 Resection of intraventricular craniopharyngioma through an endoscopic trans-sphenoidal approach: Preoperative coronal (**a**) and sagittal (**b**) MRI scan showing an intraventricular craniopharyngioma. Bone opening (**c**) defining the transtuberculum-transplanum approach; after the opening of the dura, internal debulking of the tumor (**d**) is achieved with the aid of an ultrasonic surgical aspirator (CUSA). A cleavage plane ensures the dissection of the tumor from the optic chiasm (**e**) and the integrity of adjacent third ventricle wall (**f**). View into third ventricle demonstrating removal of tumor and the foramina of Monroe with choroid plexus (**g**). Third ventricle appears clear of residual tumor. Postoperative T1 coronal (**h**) and sagittal (**i**) MRI scan imaging performed at 6 months after surgery revealing the gross total resection of the tumor and the residual amount of autologous fat and the pedicled nasoseptal flap used to reconstruct the osteodural breach according to the 3F technique. *S* sella turcica, *Sis* superior intercavernous sinus, *OP* optic protuberance, *OCR* optic carotid recess, *CPc* paraclival internal carotid artery, *PS* planum sphenoidale, *Ch* optic chiasm, *T* tumor, * choroid plexus, ** Monro foramen, *A* aqueduct

The pathway of growth of craniopharyngiomas is the essential factor in selecting among operative approaches. The vertical tumor extension was classified into five grades by Oi and Sami [56]. Grade I tumors are located purely in the intrasellar or infradiaphragmatic region. Grade II tumors are in the cistern with or without intrasellar component. Grade III tumors extend into the lower half of the third ventricle. Grade IV tumors expand to the upper half of the third ventricle. Grade V tumors reaches the septum pellucidum or the lateral ventricle(s). Tumor growth in the horizontal plane may be associated with lateral and sagittal extensions in several

locations: sellar, lateral extension, anterior, and posterior. The presence of this additional tumor extension outside the third ventricle is useful in selecting the surgical approach. Another important factor is the position of the optic chiasm, which has an intimate relationship with the anterior communicating artery (that can be easily recognized on preoperative imaging). Most craniopharyngiomas have retrochiasmatic extension occupying the entire third ventricle and can be operated via subfrontal, translaminar terminalis approach.

8.3.1 Surgical Technique

To ensure adequate brain relaxation, a lumbar drain can be placed before final positioning, especially if the patient has not been already treated for hydrocephalus. Alternatively, an external ventricular drain can also be used in cases of untreated hydrocephalus. Electromagnetic (in young children) or optical neuronavigation is systematically used. Intraoperative monitoring of motor and somatosensory evoked potentials, and cranial nerves are used if needed.

The patients are placed in a supine position with the heads secured to a horseshaped headrest for younger children (in alternative to a special designed pediatric headrest with pediatric pins and gel pads) and in three-pin headrest for children older than 8 years.

The neck is extended approximately 30–45 degrees, so that frontal lobe will tend to fall back by gravity from the roof of the orbit. This maneuver minimizes the amount of retraction on frontal lobe.

According to the size of the tumor, the surgeon can choose a unilateral or bilateral approach. In case of unilateral approach, an emi-coronal scalp incision can be sufficient. Skin incision extends from the zygoma, 1 cm in front of the tragus, to the midpupillary line on contralateral side at the level of the hairline.

After making the incision, a soft tissue flap consisting of scalp and temporal muscle is turned down, far enough to expose the supraorbital ridge. It should be preferable to elevate the scalp in 2 layers: the galeocutaneous layer and a vascularized pedicled pericranial flap, which can be used at the moment of the closure. Craniotomy starts at key-point in the fronto-temporal region and medially reaches the paramedian region. In case of bilateral approach, craniotomy is extended to the contralateral keyhole. Usually, we avoid making burr holes just above sagittal sinuses, preferring two symmetric paramedian holes. Craniotomy should be as low as possible on the orbital ridge. To remove tumors of the anterior third ventricle, we strongly advise to remove the orbital bandeau, to reduce the need to retract the frontal lobe(s). Piezoelectric surgery (Mectron Medical Technology, Genoa, Italy) may be useful to reduce the amount of bone loss during osteotomies and to preserve soft tissues (dura, periorbita). Often, the frontal sinuses are entered; therefore, mucosa should be removed and the sinuses cranialized. Special attention should be given to an adequate watertight closure at the end of the procedure, which should be refined with the aid of pericranium and fibrin glue. At time of closure a pericranial flap is

rotated over the obliterated frontal sinuses to provide a vascularized barrier between the intra- and extracranial contents. The redundant distal portion of the pericranial flap is rotated over the dural closure.

Some authors suggest a modified one-piece extended transbasal approach [58]. This is essentially a bifrontal bone flap that incorporates the anterior wall of the frontal sinus so that the inferior osteotomy is flush with the contour of the anterior skull base. The frontal sinus is then exenterated, cranialized, and sealed off with betadine-soaked Gelfoam pledgets. The orbital roofs are then flattened with a high-speed drill.

After the bone flap is removed, the spinal drainage is opened, and the dura mater is opened in a cruciate fashion (on both sides of the sagittal sinus in case of bilateral exposure). Alternatively, the dura is opened transversely along the frontal base. Opening started laterally to avoid any bridging veins draining from the cerebrum into the sagittal sinus. In case of bilateral approach, the superior sagittal sinus is ligated and divided near the crista galli. The falx cerebri is then incised to expose the interhemispheric fissure. The procedure is continued under microscopic magnification microscope. Recently, three-dimensional (3D) exoscope has emerged as an alternative to microsurgery; however, at this moment, it does not appear to offer substantial advantages over traditional optical microscopes. We use self-retaining brain retractor that attaches to the head holder. At this point, in case of unilateral approach, the procedure continues through a subfrontal route. In case of bilateral approach, either an interhemispheric route or a subfrontal route can be chosen.

For the unilateral approach, retraction of the brain is begun laterally over the roof of the orbit, and the olfactory tract followed to the region of the optic chiasm. The arachnoid of the chiasmatic cistern is opened, so to expose both optic nerves and the optic chiasm. If necessary, only one olfactory nerve can be coagulated and divided. Positioning of the retractor near the falx offers a straighter approach to the optic chiasm.

In the rare cases of bilateral subfrontal approach, it is important to preserve the olfactory tracts retracting and dissecting the frontal lobe from them. It is important to dissect the arachnoid from both olfactory tracts so that they are not avulsed from the cribriform plate during frontal lobe elevation. Otherwise, permanent anosmia may result.

The lamina terminalis is a soft, thin, white matter structure located in the inferior part of the anterior ventricular wall, between the optic tracts, proceeding from the anterior commissure to the posterior limit of the chiasm. The supraoptic nuclei of the hypothalamus and the columns of the fornix lie in the anterior wall of the hypothalamus just dorsal to the optic chiasm and just lateral to the lamina terminalis.

The lamina is sometimes difficult to distinguish from the optic tracts and chiasm, but it has a faint reddish blush that identifies it [3].

If the chiasm is prefixed, the lamina terminalis (often distended by the mass) may be incised on the midline, to offer access to the tumor. Lamina terminalis entry is indicated in case of masses located above the sella turcica but below the foramen of Monro, especially if there is a prefixed chiasm blocking the subchiasmatic approach. Craniopharyngioma is the tumor removed more frequently through this approach.

To expose the lamina terminalis, the anterior cerebral artery complex can be retracted. Care should be taken to preserve all the perforating branches. The lamina terminalis is opened sharply at the level of her thinned portion. Tumors that have invaded into the third ventricle or are purely intraventricular are visible after the lamina terminalis is opened. During opening of the lamina terminalis, attention should be made to avoid damage to anterior commissure and rostrum of the corpus callosum above, the optic chiasm below and optic tracts, and columns of fornix and hypothalamic walls laterally [4, 5]. If craniopharyngiomas have elevated the floor of the third ventricle superiorly, the floor is incised to expose tumors in the retrochiasmatic space. Therefore, intratumoral debulking with an ultrasonic aspirator is alternated to extracapsular dissection to remove the tumor from the ependymal walls of the third ventricle and hypothalamus. In a more advanced phase of dissection, the mammillary bodies are encountered, and the tumor can be dissected away from the membrane of Liliequist. It is preferable to preserve the integrity of the membrane of Liliequist to protect of the basilar artery, posterior cerebral arteries, and P1 perforators. Limit of this approach is that the undersurface of the optic chiasm and nerves cannot be visualized directly. Although angled endoscopes and mirrors may aid in visualization, blind dissection can increase the risk of injury the perforating vessels feeding the optic apparatus. Moreover, the translamina terminalis approach may offer a limited working corridor. Therefore, it is important to sequentially debulk the tumor so that it can be safely delivered through this approach.

More often, the chiasm is postfixed, and the tumor can be approached between the optic nerves in the subchiasmatic region. The arachnoid of the anterior wall of the chiasmatic cistern is incised, so that it falls backward over the nerves and chiasm and provides a protective layer for them [6]. Pituitary stalk, which can be identified by the vertical striations of the portal system, can be identified and preserved. Already stretched optic nerves and chiasm should not be retracted; otherwise the risk of further visual loss increases. The capsule of the tumor should be incised and the cystic portion (if present) aspirated. Otherwise, tissue should be fragmented and removed inside the capsule, until the capsule collapses away from the optic apparatus. Therefore, the capsule is removed [5]. Tumors with paramedian extension can be approached through the optico-carotid triangle or the retrocarotid space. This is the reason for a wide craniotomy, extending to the pterion [58]. The optico-carotid approach can be used if the tumor widens the interval between the carotid artery and the optic nerve. Any attempts should be done to preserve the perforating branches of the carotid artery that cross the interval between the artery and the optic nerve [5].

In some cases, the tumor under the chiasm is difficult to reach or to manipulate because its hard consistency. Removing the tuberculum sellae may be an option [16]. Bone instruments or a high-speed drill can be used to remove the bone in front of the sella between the optic nerves.

Closure of the dura mater is accomplished with 4-0 absorbable Vicryl suture (polygalactin; Ethicon, Inc., Somerville, New Jersey) with the aid of a pericranial graft if necessary. The bone flap is than positioned and fixed with sutures. The temporalis muscle and fascia are closed with 2–0 absorbable Vicryl interrupted sutures.

The galea is closed with interrupted 3-0 absorbable Vicryl sutures with buried knots. The skin is closed with a running, continuous 3-0 rapid absorbable Vicryl.

8.4 Anterior Interhemispheric Approaches: Frontobasal and Subrostral

8.4.1 Fronto-Basal Approach (Fig. 8.2)

Interhemispheric trans-lamina terminalis approach can be used for lesions located in the anterior part of the third ventricle, especially for those that develop anteriorly from the line joining the anterior ridge of the foramen of Monro and the cerebral aqueduct [59]. The huge advantage of this approach is that it follows a pure interhemispheric corridor and does not require elevation of the frontal lobes, thus preserving olfactory tracts and allowing to work in a very large surgical corridor requiring little or no retraction.

Positioning and incision are like those used for subfrontal approach. In this case, a lumbar drainage is useful to obtain adequate brain relaxation. A bifrontal craniotomy is performed as low as possible on the orbital roofs. If the frontal sinus is opened, the mucosa is removed, as well as the internal bone lamina of the sinus. Removal of the midline orbital bandeau is strongly advised in case of tumors expanding in the upper part of the third ventricle. This can be performed only by removing a 4-cm midline part of the bandeau, medial to both supraorbital foramen, thus avoiding manipulation and possible damage of supraorbital nerves. The dura is then incised bilaterally, and the anterior sagittal sinus is fully identified and dominated bilaterally, clamped with two small curved Klemmer, separated and ligated. After the removal of both Klemmer and verifications of complete closure without oozing, the falx is followed and cut until the lower edge. At this level, there is no inferior sagittal sinus, so no precautions should be taken before cutting the lower edge of the falx. During fronto-basal interhemispheric exposure, the arachnoidal cistern surrounding the olfactory structures on the inferior face of the frontal lobes gives a microsurgical plane of cleavage. With an adequate surgical trajectory, there is no need to manipulate or dissect the olfactory tracts that barely come into vision during the approach. With a sharp basal interhemispheric dissection, the chiasmatic cistern and the lamina terminalis cistern are exposed [59] .

Dehdashti and De Tribolet [59] accurately described this approach, underlining advantages and disadvantages. Advantage are: width of the operative field is wide, which allows visualization of both optic nerves, the chiasm, arterial communicating artery, the lamina terminalis, both A2 segments, both internal carotid arteries, the posterior communicating arteries, their perforating branches, and the pituitary stalk. No damage is done to the brain tissue except to the lamina terminalis itself, which, depending on the nature of the lesion, is often widened and thinned. Disadvantages are: opening of the frontal sinuses and division of the sagittal sinus, which require

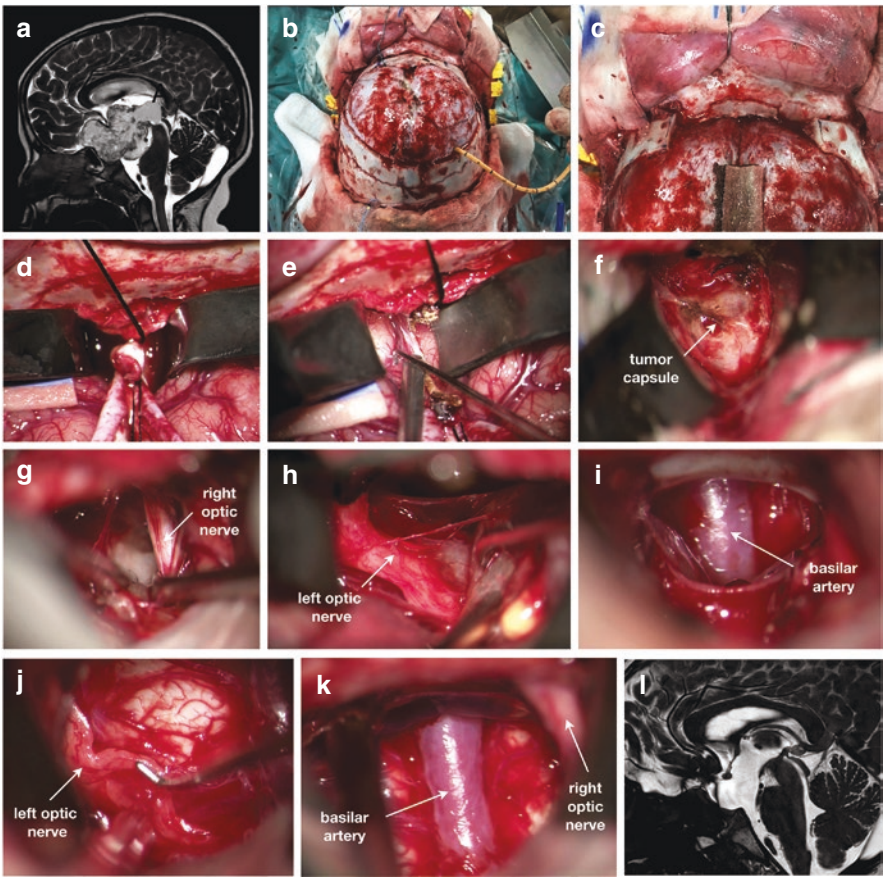

Fig. 8.2 Seven-year old boy admitted for diplopia and decreased visual acuity. MRI shows a large craniopharyngioma filling the suprasellar space and the third ventricle (**a**). Bifrontal craniotomy (**b**), removal of the orbital bar on the midline (**c**). Bilateral dural opening, dissection of the interhemispheric fissure bilaterally followed by ligation of the superior sagittal sinus (**d**). After section of the sinus, the falx is followed in the depth and separated (**e**). The anterior pole of the tumor is visible in the depth of interhemispheric fissure (**f**). Right (**g**) and left (**h**) are identified, dissected and protected during tumor debulking. Basilar artery is identified after complete tumor removal (**i**) as well as both optic nerves with the chiasm (**j**, **k**). Postoperative MRI confirms complete tumor removal

additional attention to avoid infections or hemorrhages. Moreover, removal of the orbital bandeau on the midline requires attention and carries the risk of bilateral rupture of the periorbita with possible damage to intraorbital content.

8.4.2 *Subrostral Approach (Fig. 8.3)*

In some circumstances, when the anterior communicating artery is pushed down by the tumor, frontobasal approaches may be hazardous for possible damage to branches of the anterior cerebral artery, particularly the hypothalamic and subcallosal branches. The interehemispheric dissection may be performed more superiorly, so to expose the anterior communicating artery and the subcallosal (subrostral) area, without dissection the frontal lobes from the anterior cranial fossa [60]. Surgical steps of the procedure are similar to those described above: bilateral craniotomy, bilateral opening of the dura, section of the sagittal sinus, section of the falx, anterior interhemispheric dissection, starting at the level of the frontal poles, until reaching the anterior communicating artery and the A2 complex, gentle lateral

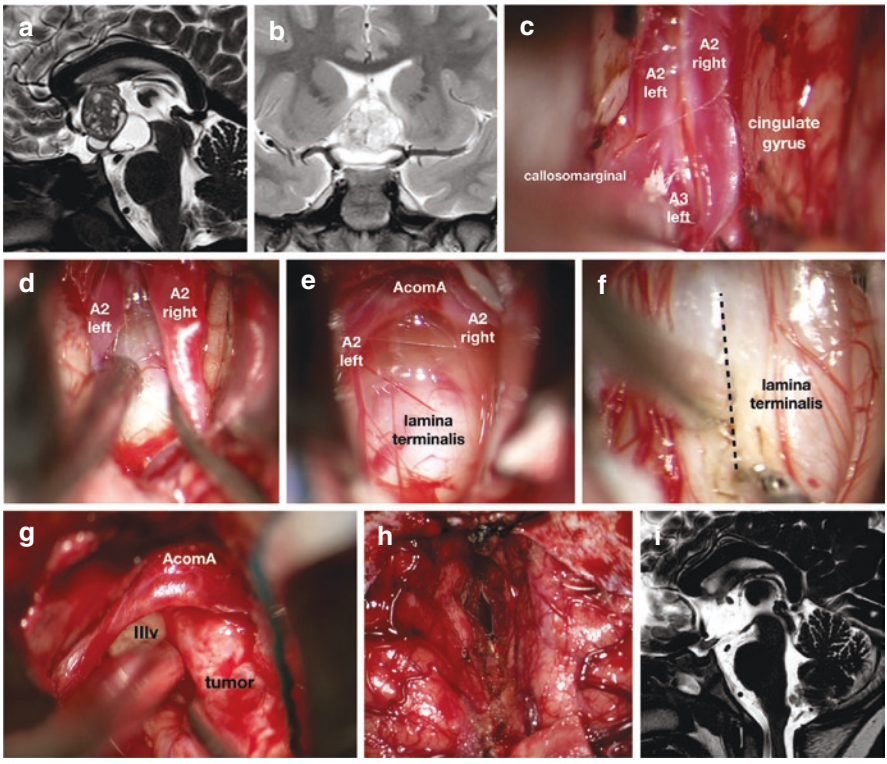

Fig. 8.3 Interhemispheric subrostral trans-lamina terminalis approach: Five-year-old girl with clinical onset of central diabetes insipidus and anterior third ventricle (**a**, **b**) lesion. Endoscopic biopsy revealed an immature teratoma that showed resistance to chemotherapy. The lesion was approached through the anterior subrostral trans-lamina terminalis interhemispheric route. The interhemispheric dissection proceeds between A2 (**c**, **d**) to expose lamina terminalis, above the AcomA, in the subcallosal area. Following the opening of the lamina terminalis (**e**, **f**), we proceed into the third ventricle with progressive debulking of the tumor (**g**), until complete resection (**h**, **i**) is achieved

retraction of both A2 tracts to reveal the lamina terminalis, incision and opening of the lamina terminalis, dissection, debulking and removal of the tumor from the anterior third ventricle.

8.5 Antero-Lateral Approaches

8.5.1 Pterional (Fronto-Temporal) Approach

Rhoton et al. in 1981 first indicated the frontotemporal approach as an option to treat lesions inside the third ventricle [5]. They recommended this approach if the tumor was centered lateral to the sella or extended into the middle cranial fossa.

From an anatomical point of view, suprasellar and parasellar lesions that can be adequately reached through a pterional approach are in an area from the planum sphenoidale anteriorly to the basilar artery caudally and vertically from within the sella to a point approximately 1.5 to 2.0 cm directly above the diaphragma sellae [3]. There is no limit to the lateral tumor extension if it is ipsilateral to the surgical flap. According with Cikla et al. [57], the pterional approach can provide a narrow working channel toward the anterior third ventricle after a wide dissection of the Sylvian fissure. Lamina terminalis can be opened also through this approach, and it expands the exposure.

Different types of lesions can be found in this area; the most common are craniopharyngiomas, pituitary adenomas, and aneurysms [3, 56].

If the lesion has significant lateral extension into the frontal or middle fossa, it should be approached from the side of maximal lateral extension; otherwise, the lesion should be approached from the side of maximal visual loss. If the lesion is strictly on the midline, perhaps it is better handled by alternative exposures; otherwise, it is preferable to operate from the side of the nondominant hemisphere. For multicompartmental tumors, the combination of pterional approach with a transventricular approach may be an option.

8.5.1.1 Surgical Technique

The patient is placed supine with a soft roll under the ipsilateral shoulder. In case of short, nonflexible neck, also a lateral decubitus position can be used. To ensure adequate brain relaxation, a lumbar drain can be placed before final positioning in case of large lesions, significant peritumoral edema, or in the presence of some other reason to believe that brain retraction will be difficult. In case of hydrocephalus, it should be managed before operation. When possible, three-point skull fixation clamp is preferable, at least in in older children, to prevent any unwanted head movement throughout the procedure. The position of the head is tilted a bit backward and turned 30 degree away from the side of operation. The usual incision

begins 1 cm anterior to the tragus and is extended up just behind the hairline to the midsagittal plane. The scalp incision may be varied to permit more frontal exposure or to permit more temporal exposure by gently curving it further back above the ear and then proceeding in a frontal direction. To avoid injuring the frontalis branch of the facial nerve, the temporalis fascia and muscle are incised immediately beneath the scalp incision, and all layers are turned forward as a unit. The standard flap is usually fashioned with four burr holes, one at the orbitofrontal angle, one over the middle of the coronal suture, one in the midtemporal region, and one low in the temporal fossa. The size of the flap is dictated by the amount of retraction necessary for appropriate exposure of the lesion. Once the flap is elevated, the lateral aspect of the sphenoid ridge is drilled away flush with the frontal fossa. This maneuver is combined with a small subtemporal craniectomy. The initial opening is curvilinear, 1.5–2 cm back from the sphenoid ridge, and the small dural flap is tacked back over the ridge. Several cruciate incisions are made in the dura mater overlying the frontal and temporal lobes. These dural flaps can be left in place for a modest amount of brain protection during the remainder of the procedure. Two retractors, a frontal and a temporal, are generally used. Strips of moist cottonoid can be used between the brain and the retractors. The frontal blade is carefully placed beneath the frontal lobe and gently advanced, exposing first the ipsilateral olfactory nerve and then the optic nerve at the anterior clinoid process. The temporal blade is used for gentle retraction of the anterior-superior temporal lobe. As this retractor is advanced, one needs to visualize, coagulate, and incise any bridging veins from the surface of the temporal lobe.

Microsurgical anatomy of this region can be described in terms of three triangles. The frontal triangle is that area bounded by the two anterior limbs of the optic chiasm and the tuberculum sellae. The middle triangle is bordered by the posterolateral aspect of the ipsilateral optic nerve, the anterolateral aspect of the ipsilateral internal carotid artery, and the A1 segment of the anterior cerebral artery. The posterior triangle is defined by the posterolateral aspect of the ipsilateral internal carotid artery, the tentorial edge, and the retracted temporal lobe. Working over the frontal retractor the surgeon first exposes the ipsilateral optic nerve and the infrachiasmatic cistern by gentle dissection of the surrounding arachnoid. Entry into the interchiasmatic region, or the frontal triangle, frequently results in a substantial egress of spinal fluid, which facilitates brain relaxation. Moving the frontal retractor posteriorly and after more arachnoidal dissection in the middle triangle, the internal carotid artery comes into view lateral and posterior to the optic nerve. With the addition of temporal retraction, the tentorial edge, third cranial nerve, posterior communicating artery, and interpeduncular cistern can be explored in the posterior triangle. With slightly more retraction with the frontal retractor, the anterior choroidal artery and the A1 segment of the anterior cerebral artery can be exposed. Working between and around these structures, it is possible to visualize adequately the anteromedial portion of the contralateral optic nerve, the diaphragma sellae, the infundibulum, the contralateral internal carotid artery, the ipsilateral posterior clinoid process, the superior portion of the clivus, and the basilar artery. The tumor can be removed with standard neurosurgical technique as described above. Also, from the pterional

approach, as well as subfrontal approaches, the inferior surface of the ipsilateral optic nerve and the hypothalamic recesses in the floor of the third ventricle are blind to view. Micromirrors or angled endoscopes may be of some help.

Tolerance to surgical manipulation of the normal anatomical structures encountered in these approaches is a concern: optic nerves or chiasm already stretched and distorted by adjacent tumor is extremely sensitive to any type of manipulation, as well as third cranial nerve. Usually, the large vessels tolerate better manipulation than the adjacent neural structures. The closure is similar to that described for subfrontal approaches.

8.5.2 Orbitozygomatic Approach

Besides pterional approach, other anterolateral corridors to the infero-anterior third ventricle have been described. Often, the use of these alternative approaches is established more on the base of the preference of the surgeon than on the characteristic of the lesions. These include orbitozygomatic and lateral supraorbital (frontolateral) approaches.

Supraorbital approaches can be achieved through a classic curvilinear incision behind the hairline but also through smaller eyebrow or eyelid incisions. In these cases, operative microscope can be replaced by an endoscopy.

Liu et al. [58] described a modified one-piece orbitozygomatic approach to manage tumors of the infero-lateral part of the third ventricle that expand toward the sylvian fissure. Its advantages over the classic pterional approach are that it offers a more basal (inferior-to-superior) surgical trajectory, increases the corridor of exposure, shortens the distance to the target, and improves surgical freedom (maneuverability of instruments) while minimizing brain retraction [58].

8.5.2.1 Surgical Technique

Positioning and skin incision of orbitozygomatic approach is similar to those used for pterional craniotomy. Interfascial dissection of the temporal muscle is advocated in order to protect the frontotemporal branch of the facial nerve, while the temporalis muscle is mobilized inferiorly toward the zygomatic arch. The one-piece orbitozygomatic craniotomy involves a frontotemporal pterional bone flap that incorporates the orbital rim and a small portion of the zygoma. A keyhole that exposes the frontal lobe dura, orbital roof, and periorbita should be drilled [61]. The orbital rim is then disarticulated with the frontotemporal bone flap as one piece. An orbital osteotomy is made just lateral to the supraorbital notch, inferior to the frontozygomatic suture, and across the orbital roof through the keyhole. The sphenoid wing is drilled down to the superior and lateral walls of the orbit toward the orbital apex at the level of the meningo-orbital band. After opening the dura, the sylvian fissure is opened, together with optic and chiasmatic cisterns so to relax the brain and expose the optic nerves,

chiasm, internal carotid artery, oculomotor nerve, and tumor. Tumor removal can be performed through the same surgical corridors described above: between nerves, trans-lamina terminalis, optic-carotid, and carotid-oculomotor windows.

The limits of this approach are similar to the limits of the other antero-lateral approaches: poor visualization of the undersurface of the chiasm where critical perforators supply the visual apparatus and poor visualization of the plane between the tumor capsule and the hypothalamus [58].

8.6 Lateral Approaches

8.6.1 Subtemporal Approach

The subtemporal approach is the main lateral corridor to the third ventricle, and it is mainly indicated if the tumor is located lateral to the sella turcica and extends into the middle cranial fossa [57].

In the subtemporal approach, the third ventricle is exposed through a corridor between the carotid artery and the oculomotor nerve. The third ventricle can be entered through the floor [6].

This approach is virtually reserved to lateral extending, retrochiasmatic tumors (usually craniopharyngiomas) [62]. Zielinski et al. [62] used this approach to manage all retrochiasmatic craniopharyngiomas, even if they do not have extension into the middle cranial fossa. According with these authors, subtemporal approach offers exposure of the lesion via a caudal-to-cranial direction, as well as endonasal approaches. This perspective limits manipulation of the hypothalamus and of the optic apparatus (that are deeper in the operative field) that is usually unavoidable in anterior and antero-lateral approaches.

Petrosal approaches, as discussed later, also offer an excellent caudal-to-cranial course; however, it requires a time-consuming bony exposure by a highly skilled cranial base surgeon and carries the risk of facial nerve injury and/or hearing impairment [62, 63].

8.6.1.1 Surgical Technique

The patient is placed in a supine position, with a shoulder roll placed under the right shoulder and the head turned contralaterally and fixed with a Mayfield head clamp. Lumbar drainage can be used to obtain brain relaxation indicated. The zygomatic arch is almost parallel to the floor, and the head is tilted downward to take advantage of gravity for temporal lobe retraction.

A question mark incision is made beginning 1 cm in front of the tragus, curving posteriorly above the ear, and then turning forward and stopping behind the temporal line. The temporal muscle is cut and reflected anteriorly. The superior edge of the

zygomatic arch is clearly visualized. A fronto-temporal craniotomy is then performed. The squamous temporal bone is drilled until it was flush with the floor of the middle fossa. The dura is then incised in a cruciate fashion. The vein of Labbé is identified and protected. The base of the temporal lobe is protected by cottonoids and slowly retracted with a spatula. Usually, the tumor is found in the middle cranial fossa; otherwise, the dissection continues until the tentorial incisure is identified. The trochlear nerve is identified at its entrance into the tentorial edge. The tentorium is coagulated and opened by the aid of bipolar diathermy and Tullium-LASER (RevoLix Jr., LISA Laser, Katlenburg-Lindau, Germany). Neuronavigation is helpful in planning the correct tentorial incision in front of the tumor.

The arachnoid of the ambient cistern is incised to allow for cerebrospinal fluid drainage. After careful dissection of arachnoid adhesions, the oculomotor nerve, posterior communicating artery with its perforators, and posterior cerebral artery come into view. The tumor capsule is normally incised below the posterior communicating artery and oculomotor nerve, and the tumor mass is internally debulked with an ultrasonic aspirator. The basilar artery bifurcation, ipsilateral internal carotid artery, optic nerve, optic chiasm, and then the contralateral internal carotid artery and optic nerve come into view. Behind the optic chiasm and pituitary stalk, the tumor capsule is separated from the bottom of the third ventricle. The intraventricular portion of the tumor is removed, opening the floor of the third ventricle into the interpeduncular fossa. When necessary, angled endoscope with 30 degree optics can be used, when possible, in association with angled instruments, for simple inspection at the end of the procedure, or for endoscope-controlled resection of the most peripheral parts of the tumor out of the visual field allowed by the microscope.

After hemostasis, the temporal lobe is released, the dura is sutured in watertight fashion, the bone flap is replaced and fixed with absorbable sutures, and the muscle, galea, and skin are closed in a standard fashion. Lumbar drain is removed.

8.6.2 Petrosal Approach

Petrosal approach is very rarely used to manage third ventricular lesions. It was first described by Hakuba et al. [64] to remove large retrochiasmatic craniopharyngiomas with extension into the third ventricle. More recently, Al Mefty [63] used this approach and discussed indications and operative nuances: trans petrosal approach may be considered for those large lesions (above all giant craniopharyngiomas), extending downward toward the posterior fossa and upward into the third ventricle, displacing the midbrain posteriorly and the optic chiasm anteriorly.

8.6.2.1 Surgical Technique

The patient is placed supine with the head turned on the contralateral side. The skin incision extends from the zygoma anterior to the tragus, turning 2–3 cm above the ear. It then descends medial to the mastoid process. A craniotomic flap extending above and under the transverse sinus is elevated. A complete mastoidectomy is performed, and the sigmoid sinus is skeletonized down to the jugular bulb, exposing the dura on both sides of the sinus. Attention should be given to preserve semicircular canals. The temporal dura is opened along the floor of the middle fossa and the dura of the presigmoid posterior fossa parallel to the sigmoid sinus. The superior petrosal sinus (that enters the sinus anteriorly at the angle between transverse and sigmoid sinuses) is coagulated and divided, preserving the vein of Labbé. The tentorium is coagulated and sectioned until incisura. At this point, the sigmoid sinus can be mobilized caudally, increasing exposure to the middle and posterior cranial fossae. The arachnoid membrane of the crural and ambient cistern is opened to identify the third and fourth cranial nerves, the posterior cerebral artery, and the superior cerebellar artery at the incisura. Therefore, the tumor is exposed in front of the midbrain. Tumor removal and dissection continue as for subtemporal approach. The third ventricle is entered superior to the pituitary stalk and anterior to the mamillary bodies.

At time of closure, the temporal and presigmoid dura are closed in a watertight fashion. The mastoid cavity should be filled with fat harvested from the patient's abdomen. The temporal muscle is rotated over the defect and sutured to the sternomastoid muscle. Soft tissue and skin are closed in standard fashion [63].

8.7 Endoscopic Transventricular Approaches

One of the safest, fastest, and easiest ways to reach the third ventricle is through the foramen of Monro, by an endoscope. The most common indication for neuroendoscopic surgery is ETV for obstructive hydrocephalus. Other common indications are biopsy of intraventricular tumors, drainage of tumoral or not tumoral cyst, aqueductoplasty, and stenting of the aqueduct (in case of isolated fourth ventricle). In the last years with advances of the neuroendoscopic armamentarium, also more complex procedures are possible through this minimally invasive approach, such as tumor removal [27, 28]. Moreover, optic and electromagnetic neuronavigation may obviate the necessity of ventricular enlargement that in the past was considered a prerequisite for ventricular neuro-endoscopy.

Two main approaches are used: a coronal burr hole allows access to the anterior third ventricle, while a more anterior burr hole allows access to the posterior third ventricle, in particular to the aqueductal and pineal regions.

8.7.1 *Endoscopic Pre-Coronal Approach (Fig. 8.4)*

The procedure is performed under general anesthesia. Through a burr hole placed usually just in front of the coronal suture and 2.5 cm away from the midline, the lateral ventricle is penetrated with the sheath of the endoscope. Neuronavigation is very useful in ventricular entry and highly recommended, whatever the ventricular

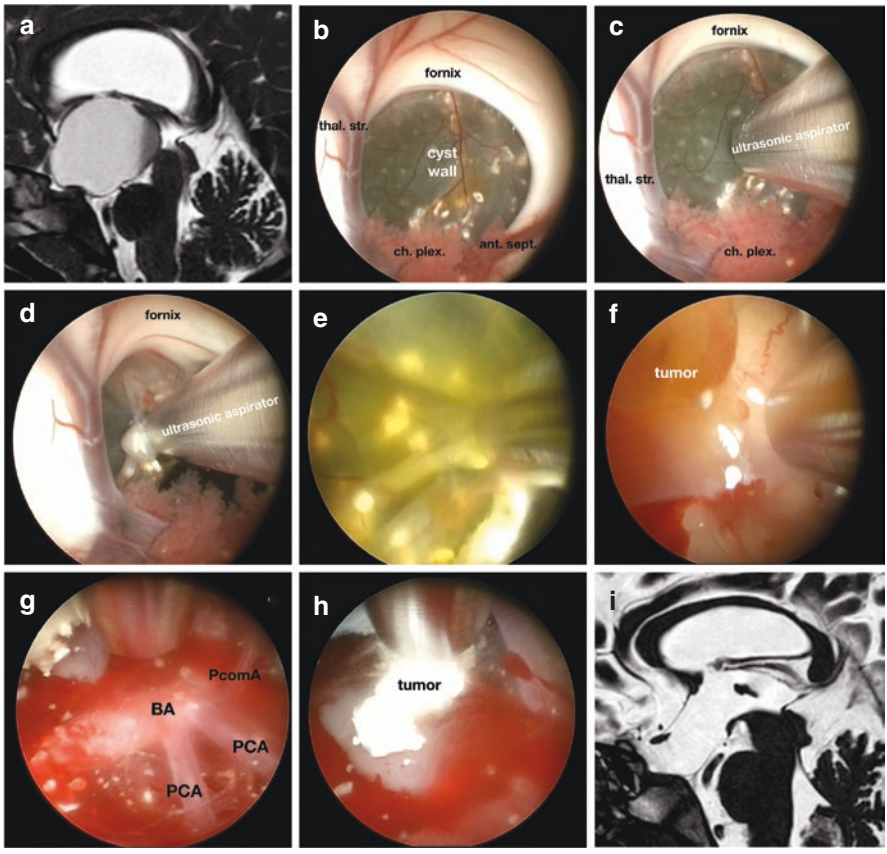

Fig. 8.4 Transforaminal endoscopic pre-coronal approach: Five-year-old boy with headache and papilledema. MRI shows a voluminous lesion with large intrasuprasellar cystic component, involving the third ventricle and causing foraminal obstruction with obstructive hydrocephalus (**a**). The lesion is approached via left pre-coronal pure endoscopic approach. Within the frontal horn of the left lateral ventricle the foramen of Monro, the left thalamostriate and anterior septal veins, the choroid plexus, and the fornix are identified (**b**). The third ventricle is completely occupied by a cystic lesion with calcific walls. With the help of endoscopic ultrasonic aspirator (**c**, **d**), the cystic wall is perforated and motor oil-like fluid is observed to leak out (**e**). Total excision of the tumor cyst and solid components (**f**, **h**) is performed until the posterior arterial circulation is visualized (**g**). Postoperative MRI shows complete excision of the lesion, which was found to be an adamantinomatous craniopharyngioma (**i**)

size, in order to eliminate all possible risks of thalamic, capsular, or dentate track. Neuronavigation is strictly mandatory in case of small ventricle. The correct entry point can be traced with neuronavigation prolonged to the skin a line that joins the target (the floor of the third ventricle in case of ETV) and the center of the foramen of Monro. The endoscope is then inserted into the sheath after stylet removal. The anatomic landmarks of the lateral ventricle (choroid plexus, thalamostriate, and septal veins and foramen of Monro) are identified. Through the foramen of Monro, the third ventricle is entered with the endoscope, and the anatomic landmarks of the floor, in particular the mammillary bodies and the infundibular recess, are carefully visualized. In case of obstructive hydrocephalus, the floor is usually visible as a translucent membrane. It can be perforated between the infundibular recess in front and the mammillary bodies behind. Many tumors can be biopsied or removed with this approach, above all intraventricular craniopharyngiomas, optic pathways gliomas, choroid plexus tumors, and gliomas. Historically, only small tumors (<2 cm) with moderate to low vascularity and soft consistency were considered for endoscopic resection. The possibility to use an ultrasonic aspirator inside the working channel of the endoscope has increased indication to much larger tumors, offering the possibility to achieve in optic pathways gliomas extent of removal that are comparable to microsurgical techniques. The dry field technique is promising because its application to tumor surgery allows to avoid the main limitation of endoscopic tumor surgery that is the blurring of vision induced by tumor bleeding [65, 66]. Once good visualization is achieved, the outside of the tumor is coagulated with either monopolar electrocautery or a laser. Microforceps, microscissors, and ultrasonic aspirator are used to debulk the lesion. If there is a cyst, it is opened and drained.

8.7.2 Endoscopic Approach to the Posterior Third Ventricle

This approach is used to manage pineal region tumor (biopsy or attempt of removal), fenestrate cyst (especially arachnoid cyst of the quadrigeminal cistern), and incannulate the aqueduct (in patients with isolated fourth ventricle) [29, 30]. If a steerable, flexible endoscope is available (that is no longer manufactured in many countries), standard pre-coronal burr hole can be used. When using a rigid endoscope, it is necessary to move more anteriorly the entry point. In pre-navigation era, the burr hole was generally placed at the level of the hairline. Nowadays, the aid of an electromagnetic neuronavigation system has become mandatory (Medtronic StealthStation™ surgical navigation system, Minneapolis, Minnesota, USA). Target point is placed at the level of the aqueductal inlet/pineal tumor/cyst. Intermediate entry point is placed in the middle of the foramen of Monro of the most dilated lateral ventricle. Real entry point is identified by projecting the so-identified trajectory to the skin of the frontal region. If this point is more anterior than the hairline, a curvilinear incision, just behind the hairline can be traced to avoid scar in the forehead. The lateral ventricle is cannulated with the endoscope. A careful inspection of

the frontal horn usually allows identification of the foramen of Monro. The endoscope is advanced through the foramen of Monro into the third ventricle. Interthalamic adhesion may obscure large part of the posterior third ventricle. Directing the endoscope inferiorly to the adhesion, the inlet of the aqueduct comes in view; directing the endoscope superiorly to the adhesion, the posterior commissure and suprapineal recess also come into view. The aqueduct should not be confused with the suprapineal recess, which is located above the aqueduct and behind the posterior commissure.

8.8 Anterior Interhemispheric Transcallosal

In the early twentieth century, since Dandy [1] described a transcortical-transventricular approach, partially resecting the frontal lobe, to access the third ventricle, many neurosurgeons have used this surgical route, with the addition of a cortical incision. The lateral ventricle used to be approached through an incision in the right middle frontal gyrus, easily exposing the ipsilateral foramen of Monro. The main obvious disadvantages of this approach included the excessive cerebral excision and retraction, especially with non-dilated ventricles, and poor visualization of the contralateral foramen of Monro [67]. In 1949, Greenwood [68] described an anterior transcallosal route to the third ventricle to remove a colloid cyst. Along with the implementation of microsurgical technique in the 1970s, the anterior interhemispheric transcallosal approach became widely used for the removal of third ventricle lesions. The transcallosal interhemispheric approach is a versatile approach to access the lateral intraventricular and third ventricular space. Besides avoiding violation of the cerebral cortex, the advantages of the transcallosal approach over the transcortical approach include a direct midline orientation with symmetric access to both lateral ventricles and both walls of the third ventricle. Complications may result from damage to venous (superior sagittal sinus, large bridging veins running into the sinus) or arterial (callosomarginal or pericallosal arteries) vascular structures during interhemispheric dissection. Aggressive retraction of both cingulate gyri may cause akinetic mutism [69]. The most common cognitive deficits after anterior callosotomy are related to long-term memory impairment, executive dysfunction, and information exchange between the cerebral hemispheres [70]. Clark and Geffen [71] reported that persistent short-term memory disturbances tended to occur in patients in whom extra-callosal injury had been inflicted. Woiciechowsky et al. [72] showed that a callosotomy length of less than 22 mm does not lead to persistent signs of interhemispheric disconnection in the late postoperative period. Recently, Ciavarro et al. [73] have shown that structural reorganization of intra- and inter-hemispheric connective fibers and structural network topology are observed after resection of the genu of the corpus callosum. It could be suggested that resection of the anterior corpus callosum does not preclude neural plasticity and may contribute to long-term postoperative cognitive recovery [73].

8.8.1 Surgical Technique

The patient's position is supine, with the head in a neutral position and the neck flexed (15 degrees) in a 3-pin Mayfield cranial frame. Alternatively, the lateral position can be used, taking advantage of spontaneous cerebral relaxation by gravity [74]. A standard bicoronal skin incision is performed. The craniotomy for the anterior interhemispheric approach extends approximately 2 cm behind the coronal suture and 5–6 cm anteriorly. The coronal suture is the bony reference for locating the craniotomy. However, several indications for performing a craniotomy for this approach have been reported: half anterior and half posterior to the suture or 4 cm anterior and 2 cm posterior to the suture or 2/3 anterior and 1/3 posterior or 3–6 cm anterior and 1 cm posterior [75].

Recently, Aldea et al. [75] analyzed 100 selective brain angiographies, trying to determine where to place the craniotomy in order to expose the most probable vein-free area. Analysis of bridging veins anatomy revealed that a 1-cm posterior extension is unusable in 62.5% of cases and a 2-cm posterior extension in 87.5%. On the other hand, the probability of encountering a bridging vein in the 4 cm anterior to the coronal is low (8.6%) and acceptable within 6 cm (22.5%). These results led to the suggestion of performing a purely precoronal craniotomy, measuring 5 cm, for the anterior interhemispheric approach [75].

The dura is opened in the U- or X-shape. While the brain is carefully separated from the fissure, a flexible self-retracting retractor can be positioned to mobilize the frontal lobe laterally, obtaining a better view along the fissure. The release of cerebrospinal fluid from the dissection of the arachnoid spaces results in progressive brain relaxation. During dissection of the interhemispheric fissure, some small bridging veins can be sacrificed with impunity. Dissection of interhemispheric fissures proceeds with gradual and deeper adjustments of the position of retractors, if used. During dissection, callosomarginal arteries, pericallosal arteries, and cingulate gyri are identified. In patients with chronic hydrocephalus, very often the two cingulate gyri are very adherent, and careful dissection is crucial to avoid injury to the cingulate gyri and to vascular structures. Considering the anatomic variability of the callosomarginal and pericallosal arteries, careful preoperative radiologic evaluation is necessary to avoid mistaking the corpus callosum for the cingulate gyri, especially when the gyri are extremely adherent to each other. When the ivory white of the corpus callosum is identified, callosotomy is performed. The interhemispheric fissure should be dissected to adequately separate the two cingulate gyri in order to avoid injury from excessive retraction during surgery and possible damage to surrounding structures during surgical maneuvers in the depth of the surgical corridor.

The callosomarginal and pericallosal arteries are gently retracted to the right and left, and the corpus callosum is exposed sufficiently to allow a standard callosotomy (approximately 2 cm) according to the neuronavigation.

Once inside the ventricular system, the third ventricle may be approached through the foramen of Monro, the fornix, or through the choroidal fissure. The above variants of approach are outlined below.

8.8.2 *Transforaminal Approach (Fig. 8.5)*

The foramen of Monro is the natural entry route leading from the lateral ventricle to the third ventricle, particularly useful when the foramen is enlarged by the mass itself or by the presence of obstructive hydrocephalus. When the foramen of Monro is not enlarged by the tumor, access to the mid-upper portion of the third ventricle is limited.

Historically, several methods of expanding the foraminal space have been reported. Shucart and Stein [76] described expanding the foramen of Monro with "gentle pressure with a small blunt dissector in all directions except medially." Dandy [1] introduced the technique of unilateral incision of the columna fornicis to expand the foramen of Monro anteriorly. Hirsch et al. [77] described the sacrifice of the talamostriate vein to increase the opening of the foramen posteriorly.

All of these methods are burdened with unacceptable neurologic sequelae, considering that expansion of the surgical foraminal corridor can be accomplished through operative pathways that respect neurovascular structures.

In 1997, Türe et al. [67] described a variation of the classic transforaminal exposure that allows access to the mid-superior portion of the third ventricle without significant damage to the surrounding eloquent structures. Identifying the location of the anterior septal vein-internal cerebral vein (ASV-ICV) junction is the key step for this exposure. When the ASV-ICV junction is located posteriorly, beyond the foramen of Monro, the transforaminal exposure can be adapted by widening the foramen itself along the choroidal fissure, preferably along the taenia fornicis, as far as the junction. Patel et al. [78] have more recently described an "expanded transforaminal" approach to enlarge the operative corridor through the foramen of Monro. In brief, the three main surgical steps include (1) coagulation of the choroid plexus, (2) coagulation and disconnection of the anterior septal vein, and (3) opening of the ependyma (choroidal fissure) at the posterior margin of the foramen and medial to the ipsilateral internal cerebral vein. In contrast to Türe et al. [67], in this case, it is necessary to sacrifice the anterior septal vein, with no need to dissect through the tela choroidea into the vessel-rich velum interpositum. However, if a larger exposure is needed, the tela choroidea must be dissected transchoroidally or subchoroidally (see later).

Moreover, as described earlier (see: "Endoscopic trans-ventricular approach" section), the neuroendoscopic technique has revolutionized the approach to the third ventricle through the foramen of Monro, going so far as to substitute, in selected cases, the microsurgical technique.

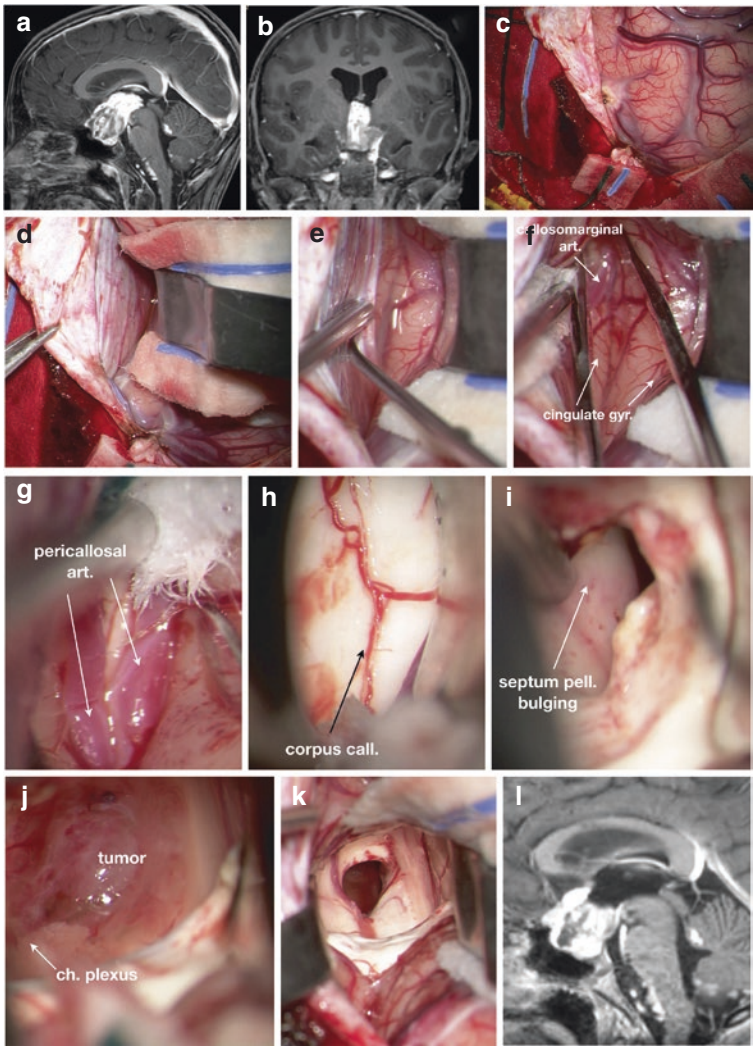

Fig. 8.5 Anterior interhemispheric transcallosal transforaminal approach: 11-year old boy with a month history pf headache and vomiting. Fundoscopy revealed bilateral optic atrophy. MRI (**a**, **b**) showed hypotalamo-chiasmatic mass invading the anterior two-thirds of the third ventricle. Secondary lesions are evident in the roof of the fourth ventricle and prebulbar subarachnioid spaces. Intraoperative views showing coagulation of a small bridging vein (**c**), gentle retraction of the right hemisphere to expose the falx and interhemispheric fissure (**d**), and adhesions between the two cingulate gyri are evident below the free edge of the falx (**e**). Left callosomarginal artery is identified above the left cingulate gyrus (**f**). Both pericallosal arteries must be identified after dissection of the two cingulate gyri and opening of the pericallosal cistern (**g**). The white ivory lucent surface of the corpus callosum is identified after retraction and protection of both pericallosal arteries (**h**). Callosotomy allows access to the right lateral ventricle; vision is obscured by the bulging of septum pellucidum that needs to be fenestrated (**i**). Identification of the tumor filling the foramen of Monro that is easily recognized due to the choroid plexus (**j**). At the end of the debulking (**k**) allowing decompression of the chiasm and resolution of hydrocephalus (**l**). Due to pilomixoid histology, the patient was sent to chemotherapy

8.8.3 *Interforniceal Approach (Fig. 8.6)*

The anterior interhemispheric transcallosal interforniceal approach is one of the operative variants to access the third ventricle after callosotomy, once the anterior interhemispheric fissure has been dissected. The key surgical step is dissection of the interforniceal raphe, creating a median working space between the two columna fornicis toward the third ventricle.

Originally, in 1944, Busch [79] described a technique for approaching the third ventricle via the transcortical interforniceal route. Apuzzo et al. modified this method of interforniceal exposure by substituting the anterior transcallosal approach

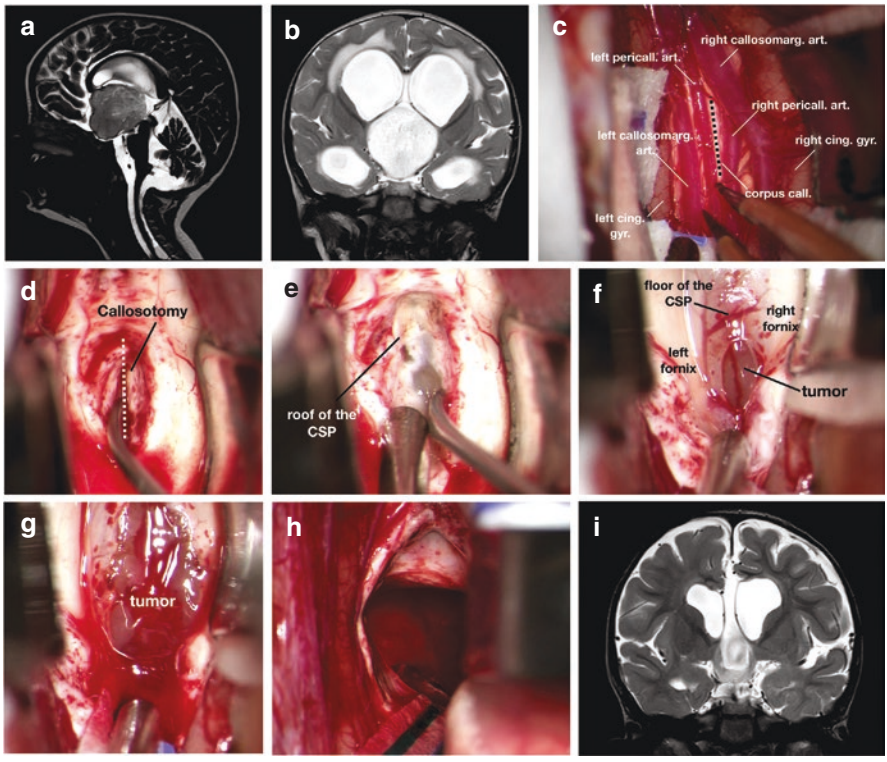

Fig. 8.6 Transcallosal-transeptal-interforniceal approach: 17-month-old child with gait disturbance and torticollis. MRI (**a**) reveals the presence of a large mass in the optic chiasm and hypothalamic area, with postero-superior extension into the third ventricle, occluding both foramina of Monro and causing supratentorial hydrocephalus, treated with VPS implantation. A large cavum septi pellucidi (CSP) (**b**) can be seen, which contributed to the choice of the transcallosal-transeptal-interforniceal approach. The interhemispheric fissure is dissected, identifying the anatomic landmarks (**c**), then proceeding to callosotomy (**d**), identification of the roof of the CSP (**e**), continuing the interforniceal dissection until reaching the floor of the CSP (**f**), and consequently the tumor (**g**). Tumor debulking is performed (**h**) until adequate resection of the tumor, which histology revealed to be a pilomyxoid astrocytoma, is achieved, with residual component above the plane of the optic pathways (**i**)

[80]. The interforniceal route may provide access to the portion of the third ventricle behind the foramen of Monro [81] without the dependence on hydrocephalus or mass effect to increase the operative exposure [82]. Potentially, this purely median approach avoids blind working areas around midline lesions within the third ventricle. It can also be useful for lesions located in the posterior aspect of the third ventricle [83]. However, the risk of disconnecting and damaging the normally fused fornices is significant [80]. Therefore, in our practice, we restrict the use of this approach in cases where (1) forniceal separation is due to the presence of a cavum septi pellucidi or (2) a mass separating the forniceal bodies [84].

8.8.3.1 Surgical Technique

Microsurgery

The patient is positioned with head in a neutral, slightly flexed position or by taking advantage of gravity resection in a lateral position, with the midsagittal plan parallel to the floor [74]. It is necessary to carefully plan callosotomy in the preoperatory setting using the interforniceal raphe as a projective target; we recommend the use of the intraoperative neuronavigation for this surgical step. At this point, once inside the lateral ventricle, two types of scenarios may occur: (1) the two septal leaflets are fused into the median raphe, which therefore needs to be carefully dissected and then divided, (2) the interforniceal raphe is naturally expanded by the tumor itself or by the presence of the cavum septi pellucidi. In the first case, it is necessary to coagulate the septum pellucidum by shrinking it to the forniceal bodies, allowing to dissect the columna fornicis along their raphe. The landmark for the raphe is the junction of the septum pellucidum and fornices. Sometimes, it can be very difficult to separate the two fused septal leaflets and find a clear dissection plane. It is necessary to remember that interforniceal dissection and separation of the raphe should be done no more than 1.5–2 cm posterior to the foramen of Monro in order to avoid damage to the hippocampal commissures, which must be identified and secured. The second scenario is the ideal situation: the natural separation of the columna fornicis provides access to the third ventricle through a safer surgical corridor, particularly when the forniceal spread is due to the cavum itself. It is reported that a cavum septi pellucidi is present in more than 85% of children at 3–6 months of age and in less than 20% of adults [85].

Short-term memory impairment is frequently reported in the immediate postoperative period; however, most patients recovered completely or improved significantly [83, 86]. Minimal manipulation of the fornices is essential to preserve short-term memory.

The most severe complications of this surgical route include (1) disconnection syndrome due to damage to the corpus callosum, (2) memory disturbances due to bilateral damage to the fornix, and (3) vascular damage to the deep venous system during interforniceal/tumoral dissection [82].

Therefore, it would be desirable to (1) limit the callosotomy to approximately 1.5–2.0 cm by targeting it at the interforniceal raphe with the support of intraoperative neuronavigation, (2) preserve the anterior commissure (avoiding to dissect too far anteriorly) and hippocampal commissures (avoiding extension beyond 1.5–2 cm posterior to the foramen of Monro), and (3) perform careful pre-surgical planning with special attention to the deep venous anatomy and its relationship to normal and tumoral structures.

Endoscopy

Some reports have described that trans-cavum septum pellucidum route to the third ventricle can be carried out by pure neuroendoscopic technique and has been found to be safe and effective [87, 88].

8.8.4 Transchoroidal and Subchoroidal Approaches (Fig. 8.7)

Within the lateral ventricle, an additional surgical route to access the third ventricle is the natural corridor of the choroidal fissure. The body portion of the choroidal fissure may be approached through the middle frontal gyrus or, usually, through an anterior transcallosal incision. Unlike the interforniceal route, going through the choroidal fissure does not require the sacrifice of eloquent structures.

The choroidal fissure is a natural cleft between the thalamus inferiorly and the body of the fornix medially, within the lateral ventricle, and it can be easily identified by following the choroid plexus from the foramen of Monro to the temporal horn [4, 89–91].

The choroidal fissure is usually divided into three portions: (1) a body portion, in the body of the lateral ventricle between the body of the fornix and the thalamus; (2) an atrial portion, in the atrium of the lateral ventricle between the crux fornicis and the pulvinar; and (3) a temporal portion, in the temporal horn between the fimbria fornicis and the inferior aspect of the thalamus [4, 89–91].

When the body portion of the choroidal fissure is opened, it is possible to expose, from the lateral ventricle, the velum interpositum, and the third ventricle [91].

It is necessary to be confident with the choroidal fissure anatomy in order to understand the two distinct variants of its approach: transchoroidal and subchoroidal.

The two membranes of the tela choroidea of the third ventricle proceed through the choroidal fissure to form the choroid plexus [89, 90]. The choroid plexus attaches medially to the fornix with the taenia fornicis and laterally to the thalamus with the taenia choroidea, which are, in fact, continuations of the ependyma leading from the ventricular cavity to the choroid plexus itself [90, 91].

The transchoroidal approach, whose first description is found in Nagata et al. [89], consists of dissecting the taenia fornicis, retracting the body of the fornix

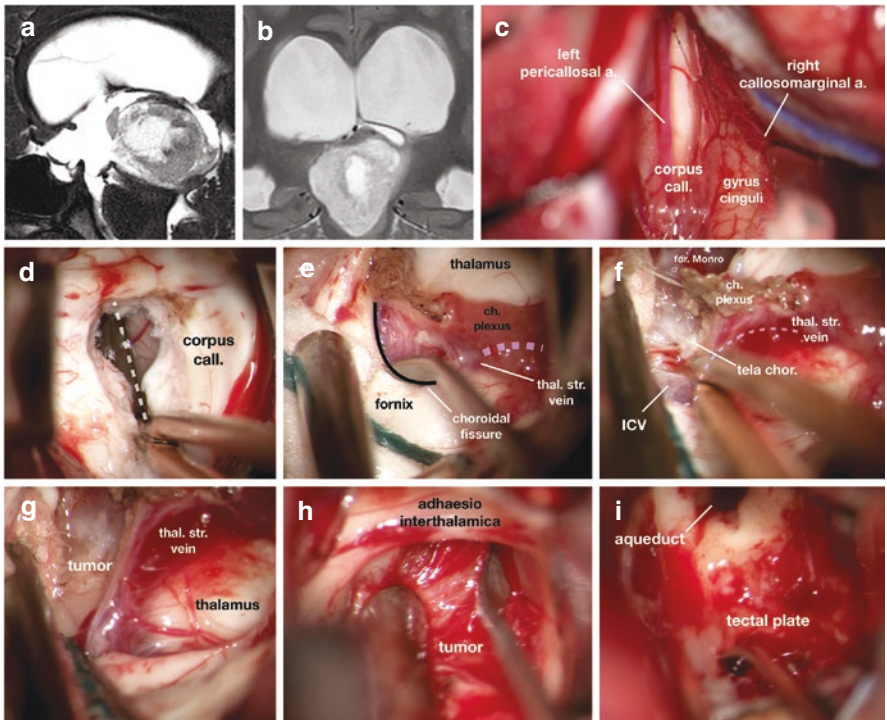

Fig. 8.7 Anterior interhemispheric transcallosal transchoroidal approach: Ten-year-old girl with signs of intracranial hypertension. MRI (**a**, **b**) shows a voluminous lesion of the posterior third ventricle obstructing the aqueduct and resulting in triventricular hydrocephalus, treated with urgent ETV. Contextual endoscopic biopsy failed because of excessive tumor bleeding. It was therefore decided to proceed with anterior interhemispheric transcallosal trans-choroidal surgery. The interhemispheric fissure, here extremely adherent for chronic hydrocephalus, is dissected by identifying major anatomic landmarks (**c**), and then callosotomy is performed (**d**). Within the right frontal horn (**e**), the choroidal fissure is identified by dissecting the taenia fornicis, after partially coagulating the choroid plexus (**e**, **f**). The fornix is medialized and the plexus lateralized. Choroidal fissure dissection proceeds until the confluence of the thalamostriate vein with the ipsilateral internal cerebral vein (ICV) is identified (**f**). The tela choroidea is dissected proceeding between the two ICVs, and then the tumor is identified (**g**). Debulking of the lesion (**h**) is performed until complete excision is achieved. At the end of the procedure, the aqueduct, pervious, and tumor-free tectal plate are recognized. Histopathological examination revealed a pilocytic astrocytoma

medially and lateralizing the choroid plexus [90]. Once the teania fornicis is opened, the upper membrane of the tela choroidea is exposed, and thus the contents of the velum interpositum come into view: the internal cerebral vein and the branches of the ipsilateral medial posterior choroidal artery [90, 91]. In order to open the inferior membrane of the tela choroidea and access the third ventricle, it is also necessary to proceed between the internal cerebral veins: at this point, dissection must occur medially to the ipsilateral internal cerebral vein [90].

The subchoroidal approach, first reported by Viale et al. [92] and Cossu et al. [93], consists of dissecting the ependyma laterally to the choroid plexus (taenia choroidea), medializing the choroid plexus and the body of the fornix and lateralizing the thalamus [90] in order to open the velum interpositum between the thalamus and the ipsilateral internal cerebral vein [67].

Bozkurt et al. [94] have compared the transcallosal-tranchoroidal and transcallosal-subchoroidal approaches. In this quantitative anatomic study, the transchoroidal route provides greater surgical freedom than the subchoroidal to access the ipsilateral and contralateral landmarks located in the middle third ventricle. When approaching the anterior and posterior regions of the third ventricle, neither approach is found to be superior in each plane. In addition, the surgical freedom for all contralateral landmarks is greater than for ipsilateral landmarks, both in the transchoroidal and subchoroidal. The transchoroidal approach provides also a greater surgical angle of attack (maximum approach angle allowed) in the horizontal plane to both ipsilateral and contralateral median landmarks on the floor of the third ventricle.

Dissecting the taenia choroidea during the subchoroidal route places at risk of injury the branches of the medial posterior choroidal artery and the superior superficial thalamic veins [89–91].

In addition, the risk of damaging the thalamostriate vein during this approach is greater than in the transchoroidal approach [95]. Some early reports considered the sacrifice of the thalamostriate vein to be without significant consequences [77, 96]. However, most of the evidence agrees that these consequences are clinically unacceptable [67].

We believe that opening the choroidal fissure on the thalamic side places major draining veins at an unnecessary risk. Opening the taenia choroidea does not improve third ventricular exposure compared with opening the taenia fornicis.

Ulm et al. identified three main anatomical limitations of the transcallosal transchoroidal approach: (1) the expanding width of the fornix limits the dissection and opening of the choroidal fissure to approximately 1.5 cm from the posterior border of the foramen of Monro, (2) the columna fornicis limit direct access to the anterior region of the third ventricle, and (3) following a posterior-to anterior-direction trajectory, the cortical veins are limiting when approaching the anterior third ventricle [97].

Therefore, the transcallosal transchoroidal approach provides an ideal route to access pathologies of the middle third ventricle and can be easily adapted for lesions involving the posterior third ventricle, by extending the opening of the choroidal fissure more posteriorly [98, 99]. However, due to the previously mentioned anatomical limitations, this approach may be sometimes unsuitable for lesions involving the anterior region of the third ventricle.

In any case, when choosing the transcallosal approach, it is crucial to plan craniotomies and callosotomies by considering the relationship between the lesion within the third ventricle and the surrounding anatomic and vascular structures [98–102].

8.8.4.1 Surgical Technique (Transchoroidal)

Microsurgery

The patient's position is supine [100] with the head in neutral position with 15 degrees of flexion in a 3-pin Mayfield skull clamp or in lateral position [74]. A standard bicoronal incision and bone flap is made for the transcallosal approach, exposing the midline and controlling the superior sagittal sinus. The dura can be U- or X-opened. The side of entry into the lateral ventricle through the callosotomy (ipsilateral to the craniotomy or contralateral) is planned in relation to the location of the lesion and ventricular size. Once the interhemispheric dissection and callosotomy have been performed, we proceed intraventricularly.

Careful and meticulous coagulation of the choroid plexus is then performed to expose the attachment of the plexus to the taenia fornicis. It is also necessary to expose the attachment of the taenia fornicis to the thalamostriate vein. The anterior septal vein can be sacrificed, coagulating it very carefully in order to avoid thermal damage to the fornix, to allow more posterior expansion of the foramen of Monro.

At this point, you can clearly recognize the course of the choroidal fissure, which is identified by the attachment of the taenia fornicis.

The dissection of the taenia fornicis continues going deeper into the choroidal fissure, exposing the tela choroidea and separating the taenia fornicis from the thalamostriate vein. Depending on the surgical target and the necessary working space, the dissection of the taenia fornicis may be extended more posteriorly.

Then the tela choroidea is coagulated and dissected up to the point where the thalamostriate vein passes through and becomes the internal cerebral vein. During this phase of dissection, it may be necessary to coagulate minor vessels that can bleed, but normally, after careful separation of the taenia fornicis, opening the tela choroidea is relatively easy. Identification of the ipsilateral internal cerebral vein from the contralateral and inter-venous proceeding is required at this time. This can also be done very posteriorly if the two veins are not very close together. The tela choroidea can be opened more or less widely and more or less easily, with a more or less recognizable plane of separation between the tela itself and the pathology. Identification and separation of the lesion from the internal cerebral veins to access the entire volume of the mass may be more or less easy.

Dissection of the choroidal fissure should always be very careful. Direct suction should not be applied to the veins, to avoid the risk of vascular injury [98, 99, 101].

Neurologic sequelae that may result from this approach are related to over manipulation of the fornix, resulting in mnestic disturbances and direct damage to the thalamostriate and internal cerebral veins.

Endoscopy

As neuroendoscopy has evolved, the well-standardized technique of transventricular transforaminal purely endoscopic resection of third ventricular colloid cysts has shown a surgical evolution in terms of extension through the choroidal fissure. Once

the choroidal fissure is opened, better exposure of the roof of the third ventricle and more posterior access to the colloid cyst can be achieved.

Iacoangeli et al. described this technique for purely endoscopic resection of colloid cysts of the third ventricle that were firmly adherent to the tela choroidea or located at the level of the middle/posterior roof of the third ventricle, which made the pure transforaminal endoscopic route unable to achieve full surgical control of the attachment site [103]. Recently, also with the usefulness of the endoscopic ultrasonic aspirator [104], some authors have extended the use of this technique to other neoplastic pathologic entities within the third ventricle, other than colloidal cysts, with safe and effective results [105].

The patient is positioned supine with the head fixed in a rigid support with 15–30 degrees of flexion.

The endoscope is navigated at all times. The entry point on the skin is planned as a line of projection of the lesion through the foramen of Monro. A 2–3 cm skin incision is made, and the burr hole is planned at the exact point where a line drawn from the lesion and passing through the center of the foramen of Monro projects to intersect the skull. The use of this method allows only one burr hole to be used. The anatomy of the cortical veins is carefully evaluated with preoperative imaging.

Within the lateral ventricle, the choroid plexus over the posterior aspect of the foramen of Monro is coagulated and resected in order to expose the venous confluence between the anterior septal and thalamostriate veins. Partial coagulation of the choroid plexus is often enough to provide adequate exposure of the choroidal fissure. In the event that further opening is needed, the anterior septal vein can be coagulated and sacrificed. Choroidal fissure dissection can be carried out by simultaneously utilizing both working channels of the endoscope, using scissors, bipolar coagulator, or the tip of a deflated Fogarty catheter as a dissector [103]. The opening of the choroidal fissure may be extended posteriorly to a variable extent depending on the pathology and surgical target [105].

8.9 Posterior Approaches

Surgery of the posterior part of the third ventricle and the pineal region is very demanding and needs accuracy and great knowledge of the specific anatomy of this area. Various operative approaches have been described (see Table 8.1), each with its advantages and disadvantages: Krause's midline infratentorial supracerebellar approach [106], Jamieson's [107] and Poppen's [108] occipital transtentorial approach, Van Wagenen's posterior transventricular approach [109], and Dandy's posterior transcallosal approach [110, 111] with different variants [112].

Selection of the surgical approach is carefully decided by many considerations, aside from the surgeon's preferences, such as the volume and the location of the lesion, its relationship with the deep venous system, the steepness of the tentorial angle, and the goal of surgery (biopsy, complete removal, restoration of CSF circulation) [3, 5, 113, 114]. Considering the complexity of anatomical measurement

Table 8.1 Posterior approaches to the third ventricle: advantages, disadvantages and indications

	Infratentorial supracerebellar	Occipital interhemispheric transtentorial	Posterior interhemispheric transcallosal
Advantages	• Easy orientation • Cerebellum falls inferiorly • Superior displacement of deep venous system (no need of manipulation)	• Bridging vein between occipital pole and transverse sinus are often absent	• The splenium is spared only a small section of the posterior aspect of the corpus callosum is transected
Disadvantages	• Sitting position: risk of air embolism, discomfort for the surgeon • Sacrifice of midline bridging vermian veins • Limited lateral or inferior visualization caused by the angle of the tentorium and the obstructive apex of the culmen	• Can be restricted by Vein of Galen and its tributaries • Disorientation	• Injury to the posterior corpus callosum fibers • Parasagittal veins (venous infarction)
Indications	• Small midline lesion in the posterior third ventricle and pineal region	• Wide exposure of the quadrigeminal plate: particularly useful for large pineal region tumors that extend laterally and inferiorly	• Effective for exposing large pineal region masses with infra and supratentorial extension

available in the literature and the scarcity of objective cutoff values that can help the surgeon to predict which approach to choose, Herophilus-Galen line has been recently proposed as a possible predictor of extent of resection in the occipital interhemispheric transtentorial approach to pineal tumors in children [115]. In recent years, endoscope-assisted or pure endoscopic variants of all these approaches have been proposed to expand the angle of vision of the classical surgical corridors [116–118].

Because of the highly relevant anatomy of the region, careful planning is mandatory. On the preoperative, MRI must be identified the location of the internal cerebral and Rosenthal veins and Galen vein in relation to the tumor but also the location of the dominant parasagittal veins in an interhemispheric approach is chosen. The long working distance and the narrow surgical corridors together with the need for maximal accuracy justify the use of MRI-based neuronavigation in order to decrease the possibility of complications. The use of a CSF derivation allows easier dissection and minimizes the need for brain retraction.

8.9.1 Supracerebellar Infratentorial Approach

The supracerebellar infratentorial approach is a midline approach with a direct view of the tumor via an infero-superior corridor through which dissection proceeds without transgressing the Galenic system located superior to the tumor [114]. Although the midline route is frequently selected, there is the potential for several off-midline routes between the torcula medially and the asterion at the junction of the transverse and sigmoid sinuses laterally [116]. This approach guarantees a good exposure with minimal neural damage, but lesions with a major lateral extension are difficult to remove completely.

The sacrifice of the bridging veins above the cerebellar surface, required to obtain the same effect, carries an implicit risk of venous cerebellar infarction [115]. Hemorrhagic venous infarction may also occur due to coagulation of even a limited number of tentorial bridging veins. There are no clear and reliable principles to determine which veins should be preserved and which can be safely sacrificed: the goal is to limit the sacrifice of bridging veins to the smallest number and to veins of the smallest size. Furthermore, Parinaud's syndrome can result from injury to the quadrigeminal plate during the approach.

8.9.1.1 Surgical Technique

The semi-sitting position is usually preferred for an infratentorial supracerebellar approach. The main advantages are gravity-assisted cerebellar retraction away from the tentorium, easier dissection of adherent veins off the tumor surface, and decreased pooling of blood and cerebrospinal fluid (CSF) in the surgical field [119], but there is the need of constant communication with the anesthesiologist because of the high risk of air embolism. To avoid systemic complications associated with the sitting position, the Concorde position has been proposed as it combines elements of both the prone and sitting positions.

A midline vertical incision extending from the C3 spinous process to about 2.5 cm above the inion is utilized. The muscles of the suboccipital and posterior cervical region are retracted after dividing the avascular ligamentum nuchae in the midline. Ligamentum nuchae can be also harvested for dural reconstruction [120].

The suboccipital craniotomy must expose the rim of the torcula and the transverse sinus superiorly until the foramen magnum inferiorly.

A "V-" or a "Y-"shaped dural incision, with the base up to the inferior margin of the transverse sinus near the midline, allows the midline dura to be reflected upward. After the dura mater is opened, the bridging veins crossing the infratentorial space between the tentorial surface of the cerebellum and the tentorial sinuses usually come into view. In case the surgical field of view is not adequate, the bridging veins (usually the midline precentral cerebellar vein) from the dorsal cerebellar surface to the tentorium may be sacrificed.

This exposure may be further enlarged beyond the tentorial notch by sectioning the tentorial edge or by gentle retraction of the vermis with self-retaining retractors.

Opening the arachnoid over the quadrigeminal cistern allows to visualize the deep venous system and the tumor. Once the tumor is encountered, internal decompression is done followed by careful dissection from the surrounding structures: the deep venous system superiorly, the pulvinar of the thalamus, the medial posterior choroidal and posterior cerebral arteries, antero-laterally, and the quadrigeminal plate, trochlear nerves, and superior cerebellar arteries inferiorly.

Following tumor decompression, the third ventricular cavity is well visualized right until the foramen of Monro.

Endoscopic supracerebellar infratentorial approaches require less cerebellar retraction and may aid in accessing pineal lesions without sacrificing bridging veins [118].

8.9.2 Occipital Interhemispheric Transtentorial Approach (Fig. 8.8)

Occipital interhemispheric transtentorial approach gives ample exposure of both the superior and inferior surfaces of the tentorial notch and therefore is excellent for tumors extending supra- and infratentorial [115]. It is also useful for lesions located in the posterior part of the third ventricle and pineal region above the deep venous system and extending laterally into the trigone of the lateral ventricle. Homonymous hemianopia can result because of damage to the occipital lobe [121] and posterior disconnection syndrome because of damage to the splenium of corpus callosum during the approach.

8.9.2.1 Surgical Technique

Surgical positions used for the approach include sitting, prone, Concorde, and three-quarter prone positions [122, 123]. In the latter, the table is slightly (15°) tilted to the ipsilateral side to enable gravity-dependent retraction of the occipital lobe from the falx cerebri. Occipital lobe retraction has been linked to postoperative transient or permanent homonymous hemianopia that is commonly encountered after an occipital transtentorial approach is performed in the semi-sitting position [121]. Anatomy off the sagittal sinus should be carefully evaluated due to possible asymmetry, and the side that offers the best possible straight trajectory should be chosen in order to optimize the line of sight of the microscope. If possible, surgery is performed from the nondominant side, and a preoperative lumbar drainage is mandatory due to the natural tendency of the occipital pole to erniate after dural opening. A U-shaped scalp flap with the vertical limb being just lateral to the midline and extending from just below the external occipital protuberance to 6–8 cm superior to

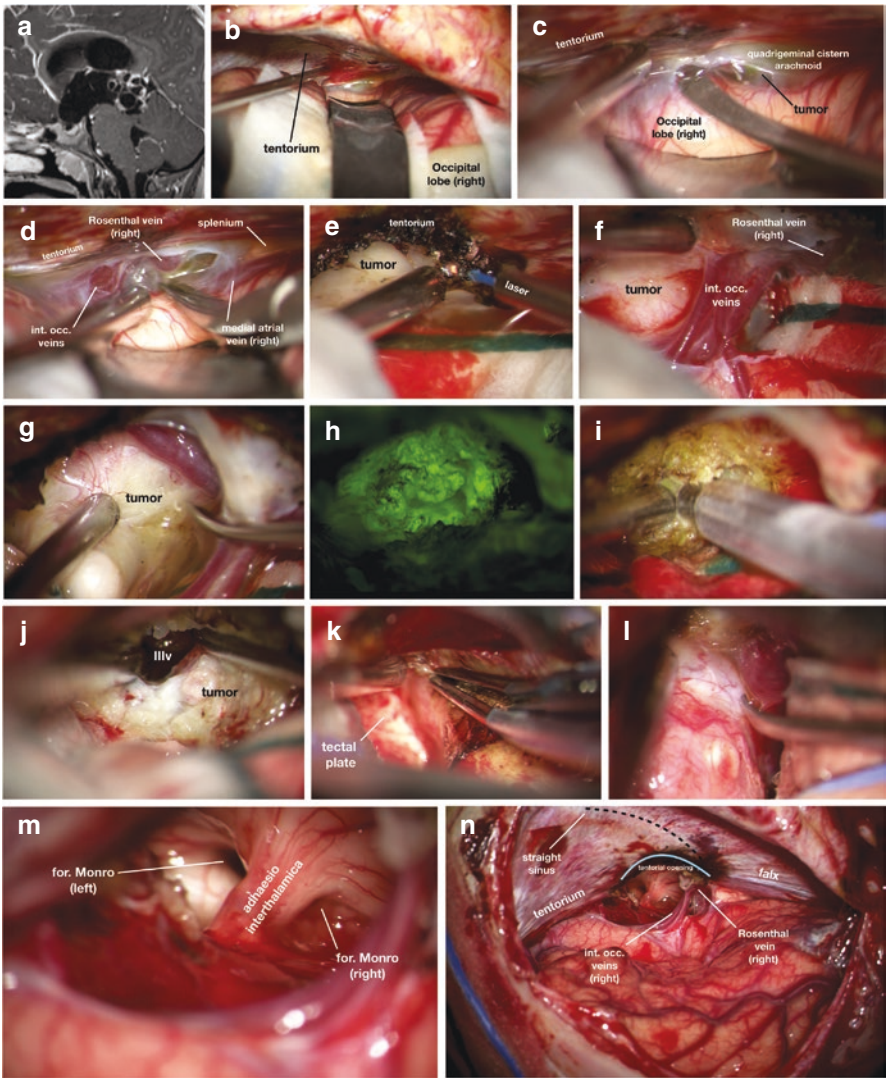

Fig. 8.8 Occipital interhemispheric transtentorial approach: seven-year-old boy. Gait disorder and Parinaud's syndrome. MRI (**a**) reveals a solid-microcystic lesion of the pineal region associated with triventricular hydrocephalus, treated with ETV. Endoscopic biopsy was inconclusive, but elevated CSF ß-HCG levels were found. Chemotherapy was performed, but tumor progressed at 2 months. Therefore, it was decided to proceed to surgery via interhemispheric occipital transtentorial approach. The occipital lobe is gently retracted along its inferomedial aspect (**b**). Interhemispheric dissection proceeds to identify the tentorium and arachnoid of the quadrigeminal cistern covering the tumor (**c**). Interhemispheric dissection proceeds to identify the inferior occipital vein complex, Rosenthal vein, medial atrial vein, and splenium (**d**). The tentorium is extensively coagulated parallel and lateral to the straight sinus with the aid of the laser (**e**). Dissection of the tumor from the venous complexes begins (**f**, **g**). The tumor area is confirmed using intraoperative fluorescein (**h**). Internal tumor debulking is performed (**i**). The third ventricle (**j**) and tectal plate (**k**) are exposed. Dissection of the tumor from the deep venous system (**l**) is performed as long as complete removal of the tumor is achieved. Final operative view (**m**, **n**)

this point and curving laterally and downward is used. A sigmoid incision can be also used, allowing easier midline dissection in the cervical region and larger occipitoparietal craniotomy. A parieto-occipital craniotomy (of about 5 cm × 5 cm) is fashioned to expose the transverse sinus inferiorly and the superior sagittal sinus medially. The dura is open in C-shaped fashion or as a pair of triangular leaves based on the superior sagittal and transverse sinuses. The surgical corridor is between the occipital lobe and falx cerebri because bridging veins entering the superior sagittal sinus for a distance of 4–5 cm proximal to the torcula are small and few. Some authors reported that additional gentle elevation of the occipital lobe off the tentorial surface is safe because of the peculiar venous drainage of the occipital lobe. Occipital lobe elevation allows a wider angle for maneuverability in the lateral to medial direction, thus enabling a better visualization of tumor parts extending contralaterally [119]. After opening of the lumbar drainage, the occipital lobe is gently retracted along the inferomedial aspect. Careful interhemispheric dissection allows identification of the tentorium and quadrigeminal cistern. The falx cerebri, the tentorium, and the dural covering of the straight sinus are encountered. After opening of the quadrigeminal cistern and further release of CSF, the tentorium is extensively coagulated parallel and lateral to the straight sinus by bipolar or laser. The divided leaflets of the tentorium are reflected using sutures, or the tentorium is simply rapidly and easily vaporized using the contact laser, thus creating very large and customized windows that improve the visibility of the area. Splitting the tentorium offers a panoramic supra and infratentorial view of the tumor, the surrounding deep venous structures, and the collicular plate of the midbrain. The arachnoid of the quadrigeminal cistern is exposed and further opened using a Rhoton dissector or a sharp dissector. In some cases, especially after chemotherapy, the arachnoid can be very thick, so sharp dissection is necessary at least to open the outer layer of arachnoid that covers both the tumor and the deep vein complex. In general, at this point, the outer layer of the tumor is then coagulated and opened, and biopsy followed by internal debulking can be carried out with the ultrasonic surgical aspirator until visualization of the third ventricular space. After the initial debulking, it is possible to continue the dissection looking for the vein of Galen, the internal cerebral veins, the basal veins of Rosenthal, and the superior vermian vein. Following tumor removal, the brain stem, the collicular plate, and the posterior thalamic regions are well visualized [124].

8.9.3 Posterior Interhemispheric Transcallosal Approach

The interhemispheric transcallosal route was originally described by Dandy [110, 111]. This approach has been the most widely used for many years and is useful for lesions located in the posterior portion of the third ventricle and pineal region, especially when a superior tumor extension is encountered, involving the splenium of the corpus callosum [3, 5, 57, 125]. We prefer to avoid this approach due to higher risk of disconnection syndrome or injury to the posterior part of the fornix.

8.9.3.1 Surgical Technique

This approach can be performed with the patient in either the lateral or supine position. An S-shaped incision allows greater scalp mobilization. A parasagittal craniotomy is created on the right side for midline lesions or on the ipsilateral side for paramedian lesions. The bone flap should be at least 5 cm anterior to posterior, with the anterior edge posterior to the coronal suture. Superior sagittal sinus must be exposed and the dura opened in a semilunar fashion, with the base located along the superior sagittal sinus. It may be necessary to sacrifice one or more bridging cortical veins to gain access to the interhemispheric fissure.

8.9.3.2 Intervenous-Interforniceal Variant for Midline Pathology

The anterior and posterior boundaries of the tumor determine the extent of the callosotomy; it is necessary to spare as much of the splenium as possible, in order to prevent disconnection syndrome. Callosotomy must be done directly in the midline to expose the avascular membrane separating the internal cerebral veins. Separation of the internal cerebral veins should start posteriorly just proximal to their confluence with the vein of Galen and then continue anteriorly. It is mandatory to prevent iatrogenic injury to keep moist the internal cerebral veins. After visualizing the tumor, by alternating between extracapsular dissection and internal debulking, the surgeon should be able to visualize the third ventricle. The tectal plate and the upper part of the cerebellum are then carefully dissected until the fourth ventricle is visible. Despite the goal to preserve the splenium, injury to the posterior corpus callosum fibers and the related risk of auditory deficits, amnesia, mutism, and dyslexia still exists [125].

8.9.3.3 Paravenous-Interforniceal Variant for Paramedian Pathology

If the pathology arises from the posterior thalamus, a different operative corridor could be used. In this case, the corpus callosum should be opened off midline and directly over the most superior extent of the tumor that extends into the lateral ventricle. The ideal entry point is between the two internal cerebral veins medially and ipsilateral forniceal crura laterally. Neuronavigation is crucial to assess the position of the internal cerebral veins during surgery. The tumor may or may not be covered by normal ependyma, depending on whether it is purely intrinsic or has an exophytic component. Intratumoral debulking is then carried out, progressing from a lateral to medial direction. The internal cerebral veins either will be displaced to the contralateral side, staying in an extracapsular location with respect to the tumor, or will course through the tumor. If the precise location of the ICVs is difficult to identify accurately without injuring the vein(s), the potential consequences of sacrificing one or both of the ICVs are not worth the potential benefit gained by greater resection [125].

References

1. Dandy WE. Benign tumors in the third ventricle of the brain: diagnosis and treatment. Springfield, IL: C.C. Thomas; 1933.
2. Cohen-Gadol AA, Geryk B, Binder DK, Tubbs RS. Conquering the third ventricular chamber. J Neurosurg. 2009;111:590–9.
3. Apuzzo ML. Surgery of the third ventricle. 1st ed. Baltimore: Williams & Wilkins; 1987.
4. Yamamoto I, Rhoton AL, Peace DA. Microsurgery of the third ventricle: part I. Microsurgical anatomy. Neurosurgery. 1981;8:334–56.
5. Rhoton AL, Yamamoto I, Peace DA. Microsurgery of the third ventricle: part 2. Operative approaches. Neurosurgery. 1981;8:357–73.
6. Artico M, Pastore FS, Fraioli B, Giuffrè R. The contribution of Davide Giordano (1864-1954) to pituitary surgery: the transglabellar-nasal approach. Neurosurgery. 1998;42:909–11; discussion 911–912.
7. Kanter AS, Dumont AS, Asthagiri AR, Oskouian RJ, Jane JA, Laws ER. The transsphenoidal approach. A historical perspective. Neurosurg Focus. 2005;18:e6.
8. Guiot J, Rougerie J, Fourestier M, Fournier A, Comoy C, Vulmiere J, et al. Intracranial endoscopic explorations. Presse Med. 1893;1963(71):1225–8.
9. Apuzzo ML, Heifetz MD, Weiss MH, Kurze T. Neurosurgical endoscopy using the side-viewing telescope. J Neurosurg. 1977;46:398–400.
10. Jankowski R, Auque J, Simon C, Marchal JC, Hepner H, Wayoff M. Endoscopic pituitary tumor surgery. Laryngoscope. 1992;102:198–202.
11. Sethi DS, Pillay PK. Endoscopic management of lesions of the sella turcica. J Laryngol Otol. 1995;109:956–62.
12. Jho HD, Carrau RL, Ko Y. Endoscopic pituitary surgery. In: Wilkins H, Rengachary S, editors. Neurosurgical operative atlas, vol. 5. Park Ridge, IL: American Association of Neurological Surgeons; 1996. p. 1–12.
13. Cappabianca P, Alfieri A, de Divitiis E. Endoscopic endonasal transsphenoidal approach to the sella: towards functional endoscopic pituitary surgery (FEPS). Minim Invasive Neurosurg. 1998;41:66–73.
14. Cappabianca P, Cavallo LM, Esposito F, de Divitiis O, Messina A, de Divitiis E. Extended endoscopic endonasal approach to the midline skull base: the evolving role of transsphenoidal surgery. In: Pickard JD, Akalan N, Di Rocco C, et al., editors. Advances and technical standards in neurosurgery. Wien: Springer; 2008. p. 152–99.
15. Frank G, Pasquini E, Mazzatenta D. Extended transsphenoidal approach. J Neurosurg. 2001;95:917–8.
16. Castelnuovo P, Locatelli D, Mauri S. Extended endoscopic approaches to the skull base. Anterior cranial base CSF leaks. In: de Divitiis E, Cappabianca P, editors. Endoscopic endonasal transsphenoidal surgery. Wien: Springer; 2003. p. 137–58.
17. Kassam A, Snyderman CH, Mintz A, Gardner P, Carrau RL. Expanded endonasal approach: the rostrocaudal axis. Part I. Crista galli to the sella turcica. Neurosurg Focus. 2005;19:E3.
18. Kassam A, Snyderman CH, Mintz A, Gardner P, Carrau RL. Expanded endonasal approach: the rostrocaudal axis. Part II. Posterior clinoids to the foramen magnum. Neurosurg Focus. 2005;19:E4.
19. de Divitiis E, Cappabianca P, Cavallo LM. Endoscopic transsphenoidal approach: adaptability of the procedure to different sellar lesions. Neurosurgery. 2002;51:699–705; discussion 705–707.
20. Kassam AB, Gardner PA, Snyderman CH, Carrau RL, Mintz AH, Prevedello DM. Expanded endonasal approach, a fully endoscopic transnasal approach for the resection of midline suprasellar craniopharyngiomas: a new classification based on the infundibulum. J Neurosurg. 2008;108:715–28.

21. Laufer I, Anand VK, Schwartz TH. Endoscopic, endonasal extended transsphenoidal, transplanum transtuberculum approach for resection of suprasellar lesions. J Neurosurg. 2007;106:400–6.
22. Cavallo LM, Messina A, Cappabianca P, Esposito F, de Divitiis E, Gardner P, et al. Endoscopic endonasal surgery of the midline skull base: anatomical study and clinical considerations. Neurosurg Focus. 2005;19:E2.
23. Cavallo LM, de Divitiis O, Aydin S, Messina A, Esposito F, Iaconetta G, et al. Extended endoscopic endonasal transsphenoidal approach to the suprasellar area: anatomic considerations--part 1. Neurosurgery. 2007;61:24–33; discussion 33–34.
24. Weiss MH. The transnasal transsphenoidal approach. In: Apuzzo MLJ, editor. Surgery of the third ventricle. Baltimore: Williams & Wilkins; 1987. p. 476–94.
25. Cavallo LM, Di Somma A, de Notaris M, Prats-Galino A, Aydin S, Catapano G, et al. Extended endoscopic Endonasal approach to the third ventricle: multimodal anatomical study with surgical implications. World Neurosurg. 2015;84:267–78.
26. Gardner PA, Prevedello DM, Kassam AB, Snyderman CH, Carrau RL, Mintz AH. The evolution of the endonasal approach for craniopharyngiomas. J Neurosurg. 2008;108:1043–7.
27. Cavallo LM, Solari D, Esposito F, Cappabianca P. The endoscopic endonasal approach for the management of craniopharyngiomas involving the third ventricle. Neurosurg Rev. 2013;36:27–37; discussion 38.
28. de Lara D, Ditzel Filho LFS, Muto J, Otto BA, Carrau RL, Prevedello DM. Surgical management of craniopharyngioma with third ventricle involvement. Neurosurg Focus. 2013;34:Video 5.
29. Cavallo LM, Frank G, Cappabianca P, Solari D, Mazzatenta D, Villa A, et al. The endoscopic endonasal approach for the management of craniopharyngiomas: a series of 103 patients. J Neurosurg. 2014;121:100–13.
30. Karavitaki N. Management of craniopharyngiomas. J Endocrinol Investig. 2014;37:219–28.
31. Zada G, Laws ER. Surgical management of craniopharyngiomas in the pediatric population. Horm Res Paediatr. 2010;74:62–6.
32. Elliott RE, Jane JA, Wisoff JH. Surgical management of craniopharyngiomas in children: meta-analysis and comparison of transcranial and transsphenoidal approaches. Neurosurgery. 2011;69:630–43; discussion 643.
33. Jane JA, Prevedello DM, Alden TD, Laws ER. The transsphenoidal resection of pediatric craniopharyngiomas: a case series. J Neurosurg Pediatr. 2010;5:49–60.
34. Gallieni M, Zaed I, Fahlbusch R, Giordano M. Transsphenoidal approach in children with partially or minimally developed sphenoid sinus. Childs Nerv Syst. 2021;37:131–6.
35. Forbes JA, Ordóñez-Rubiano EG, Tomasiewicz HC, Banu MA, Younus I, Dobri GA, et al. Endonasal endoscopic transsphenoidal resection of intrinsic third ventricular craniopharyngioma: surgical results. J Neurosurg. 2018;1–11.
36. Castelnuovo P, Pistochini A, Locatelli D. Different surgical approaches to the sellar region: focusing on the "two nostrils four hands technique". Rhinology. 2006;44:2–7.
37. Prevedello DM, Kassam AB, Snyderman C, Carrau RL, Mintz AH, Thomas A, et al. Endoscopic cranial base surgery: ready for prime time? Clin Neurosurg. 2007;54:48–57.
38. de Notaris M, Solari D, Cavallo LM, D'Enza AI, Enseñat J, Berenguer J, et al. The "suprasellar notch," or the tuberculum sellae as seen from below: definition, features, and clinical implications from an endoscopic endonasal perspective. J Neurosurg. 2012;116:622–9.
39. Laws ER. Transsphenoidal microsurgery in the management of craniopharyngioma. J Neurosurg. 1980;52:661–6.
40. Ferrareze Nunes C, Beer-Furlan A, Doglietto F, Carrau RL, Prevedello DM-S. The McConnell's capsular arteries and their relevance in endoscopic endonasal approach to the sellar region. Oper Neurosurg (Hagerstown). 2018;14:171–7.
41. Fernandez-Miranda JC, Pinheiro-Neto CD, Gardner PA, Snyderman CH. Endoscopic endonasal approach for a tuberculum sellae meningioma. Neurosurg Focus. 2012;32(Suppl 1):E8.

42. Hadad G, Bassagasteguy L, Carrau RL, Mataza JC, Kassam A, Snyderman CH, et al. A novel reconstructive technique after endoscopic expanded endonasal approaches: vascular pedicle nasoseptal flap. Laryngoscope. 2006;116:1882–6.
43. Cavallo LM, Messina A, Esposito F, de Divitiis O, Dal Fabbro M, de Divitiis E, et al. Skull base reconstruction in the extended endoscopic transsphenoidal approach for suprasellar lesions. J Neurosurg. 2007;107:713–20.
44. Leng LZ, Brown S, Anand VK, Schwartz TH. "Gasket-seal" watertight closure in minimal-access endoscopic cranial base surgery. Neurosurgery. 2008;62:ONSE342–3; discussion ONSE343.
45. Kassam AB, Thomas A, Carrau RL, Snyderman CH, Vescan A, Prevedello D, et al. Endoscopic reconstruction of the cranial base using a pedicled nasoseptal flap. Neurosurgery. 2008;63:ONS44–52; discussion ONS52–53.
46. Esposito F, Dusick JR, Fatemi N, Kelly DF. Graded repair of cranial base defects and cerebrospinal fluid leaks in transsphenoidal surgery. Oper Neurosurg (Hagerstown). 2007;60:295–303; discussion 303–304.
47. Zanation AM, Snyderman CH, Carrau RL, Kassam AB, Gardner PA, Prevedello DM. Minimally invasive endoscopic pericranial flap: a new method for endonasal skull base reconstruction. Laryngoscope. 2009;119:13–8.
48. Oliver CL, Hackman TG, Carrau RL, Snyderman CH, Kassam AB, Prevedello DM, et al. Palatal flap modifications allow pedicled reconstruction of the skull base. Laryngoscope. 2008;118:2102–6.
49. Fortes FSG, Carrau RL, Snyderman CH, Prevedello D, Vescan A, Mintz A, et al. The posterior pedicle inferior turbinate flap: a new vascularized flap for skull base reconstruction. Laryngoscope. 2007;117:1329–32.
50. Fortes FSG, Carrau RL, Snyderman CH, Kassam A, Prevedello D, Vescan A, et al. Transpterygoid transposition of a temporoparietal fascia flap: a new method for skull base reconstruction after endoscopic expanded endonasal approaches. Laryngoscope. 2007;117:970–6.
51. Hadad G, Rivera-Serrano CM, Bassagaisteguy LH, Carrau RL, Fernandez-Miranda J, Prevedello DM, et al. Anterior pedicle lateral nasal wall flap: a novel technique for the reconstruction of anterior skull base defects. Laryngoscope. 2011;121:1606–10.
52. Rivera-Serrano CM, Bassagaisteguy LH, Hadad G, Carrau RL, Kelly D, Prevedello DM, et al. Posterior pedicle lateral nasal wall flap: new reconstructive technique for large defects of the skull base. Am J Rhinol Allergy. 2011;25:e212–6.
53. Rivera-Serrano CM, Snyderman CH, Gardner P, Prevedello D, Wheless S, Kassam AB, et al. Nasoseptal "rescue" flap: a novel modification of the nasoseptal flap technique for pituitary surgery. Laryngoscope. 2011;121:990–3.
54. Cavallo LM, Solari D, Somma T, Cappabianca P. The 3F (fat, flap, and flash) technique for skull base reconstruction after endoscopic endonasal suprasellar approach. World Neurosurg. 2019;126:439–46.
55. Konovalov AN, Gorelyshev SK. Surgical treatment of anterior third ventricle tumours. Acta Neurochir. 1992;118:33–9.
56. Oi S, Samii A, Samii M. Operative techniques for tumors in the third ventricle. Oper Tech Neurosurg. 2003;6:205–14.
57. Cikla U, Swanson KI, Tumturk A, Keser N, Uluc K, Cohen-Gadol A, et al. Microsurgical resection of tumors of the lateral and third ventricles: operative corridors for difficult-to-reach lesions. J Neuro-Oncol. 2016;130:331–40.
58. Liu JK, Sevak IA, Carmel PW, Eloy JA. Microscopic versus endoscopic approaches for craniopharyngiomas: choosing the optimal surgical corridor for maximizing extent of resection and complication avoidance using a personalized, tailored approach. Neurosurg Focus. 2016;41:E5.
59. Dehdashti AR, de Tribolet N. Frontobasal interhemispheric trans-lamina terminalis approach for suprasellar lesions. Neurosurgery. 2005;56:418–24; discussion 418–424

60. Cinalli G, Onorini N. Interhemispheric subrostral translamina terminalis approach to a teratoma of the anterior third ventricle. Cham: Springer Nature; 2021.
61. Aziz KMA, Froelich SC, Cohen PL, Sanan A, Keller JT, van Loveren HR. The one-piece orbitozygomatic approach: the MacCarty burr hole and the inferior orbital fissure as keys to technique and application. Acta Neurochir. 2002;144:15–24.
62. Zieliński G, Sajjad EA, Robak Ł, Koziarski A. Subtemporal approach for gross Total resection of Retrochiasmatic Craniopharyngiomas: our experience on 30 cases. World Neurosurg. 2018;109:e265–73.
63. Al-Mefty O, Ayoubi S, Kadri PAS. The petrosal approach for the total removal of giant retrochiasmatic craniopharyngiomas in children. J Neurosurg. 2007;106:87–92.
64. Hakuba A, Nishimura S, Inoue Y. Transpetrosal-transtentorial approach and its application in the therapy of retrochiasmatic craniopharyngiomas. Surg Neurol. 1985;24:405–15.
65. Spennato P, De Rosa A, Meccariello G, Quaglietta L, Imperato A, Scala MR, et al. Endoscopic ultrasonic aspiration as alternative to more invasive surgery in initial management of optic pathway gliomas in children. Childs Nerv Syst. 2022;38:1281–7.
66. Cinalli G, Scala MR. Resection of a craniopharyngioma with endoscopic ultrasonic surgical aspirator. Cham: Springer. 2021. https://doi.org/10.1007/978-3-030-94362-2.
67. Türe U, Yaşargil MG, Al-Mefty O. The transcallosal—transforaminal approach to the third ventricle with regard to the venous variations in this region. J Neurosurg. 1997;87:706–15.
68. Greenwood J. Paraphysial cysts of the third ventricle; with report of eight cases. J Neurosurg. 1949;6:153–9.
69. Vogt B, Gabriel M. Neurobiology of cingulate cortex and limbic thalamus: a comprehensive handbook. Boston, MA: Birkhäuser; 1993.
70. Peltier J, Roussel M, Gerard Y, Lassonde M, Deramond H, Le Gars D, et al. Functional consequences of a section of the anterior part of the body of the corpus callosum: evidence from an interhemispheric transcallosal approach. J Neurol. 2012;259:1860–7.
71. Clark CR, Geffen GM. Corpus callosum surgery and recent memory. A review. Brain. 1989;112(Pt 1):165–75.
72. Woiciechowsky C, Vogel S, Lehmann R, Staudt J. Transcallosal removal of lesions affecting the third ventricle: an anatomic and clinical study. Neurosurgery. 1995;36:117–22; discussion 122–123.
73. Ciavarro M, Grande E, Bevacqua G, Morace R, Ambrosini E, Pavone L, et al. Structural brain network reorganization following anterior Callosotomy for colloid cysts: Connectometry and graph analysis results. Front Neurol. 2022;13:894157. https://doi.org/10.3389/fneur.2022.894157.
74. Lawton MT, Golfinos JG, Spetzler RF. The contralateral transcallosal approach: experience with 32 patients. Neurosurgery. 1996;39:729–34; discussion 734–735.
75. Aldea S, Apra C, Chauvet D, Le Guérinel C, Bourdillon P. Interhemispheric transcallosal approach: going further based on the vascular anatomy. Neurosurg Rev. 2021;44:2831–5.
76. Shucart WA, Stein BM. Transcallosal approach to the anterior ventricular system. Neurosurgery. 1978;3:339–43.
77. Hirsch JF, Zouaoui A, Renier D, Pierre-Kahn A. A new surgical approach to the third ventricle with interruption of the striothalamic vein. Acta Neurochir. 1979;47:135–47.
78. Patel P, Cohen-Gadol AA, Boop F, Klimo P. Technical strategies for the transcallosal transforaminal approach to third ventricle tumors: expanding the operative corridor: clinical article. J Neurosurg Pediatr. 2014;14:365–71.
79. Busch E. A new approach for the removal of tumors of the third ventricle. Acta Psychiatr Scand. 1944;19:57–60.
80. Apuzzo ML, Chikovani OK, Gott PS, Teng EL, Zee CS, Giannotta SL, et al. Transcallosal, interfornicial approaches for lesions affecting the third ventricle: surgical considerations and consequences. Neurosurgery. 1982;10:547–54.

81. Winkler PA, Weis S, Büttner A, Raabe A, Amiridze N, Reulen HJ. The transcallosal interforniceal approach to the third ventricle: anatomic and microsurgical aspects. Neurosurgery. 1997;40:973–81; discussion 981–982.
82. Liu W, Liu R, Ma Z, Li C. Transcallosal anterior interforniceal approach for removal of superior midbrain cavernous malformations in children: a retrospective series of 10 cases in a single center. World Neurosurg. 2018;118:e188–94.
83. Jia W, Ma Z, Liu IY, Zhang Y, Jia G, Wan W. Transcallosal interforniceal approach to pineal region tumors in 150 children. J Neurosurg Pediatr. 2011;7:98–103.
84. Cinalli G, Mirone G. Transcallosal-transseptal-interfornicial approach to a tumor of the third ventricle. New York, NY: Springer; 2019.
85. Tubbs RS, Krishnamurthy S, Verma K, Shoja MM, Loukas M, Mortazavi MM, et al. Cavum velum interpositum, cavum septum pellucidum, and cavum vergae: a review. Childs Nerv Syst. 2011;27:1927–30.
86. Graziano F, Ganau M, Meccio F, Iacopino DG, Ulm AJ. The transcallosal anterior Interfoniceal approach: a microsurgical anatomy study. J Neurol Surg B Skull Base. 2015;76:183–8.
87. Roth J, Berger A, Constantini S. Endoscopic transseptal transcaval interforniceal approach to the posterior third ventricle in the presence of cavum septum pellucidum. World Neurosurg. 2017;103:768–71.
88. Souweidane MM, Hoffman CE, Schwartz TH. Transcavum interforniceal endoscopic surgery of the third ventricle. J Neurosurg Pediatr. 2008;2:231–6.
89. Nagata S, Rhoton AL, Barry M. Microsurgical anatomy of the choroidal fissure. Surg Neurol. 1988;30:3–59.
90. Wen HT, Rhoton AL, de Oliveira E. Transchoroidal approach to the third ventricle: an anatomic study of the choroidal fissure and its clinical application. Neurosurgery. 1998;42:1205–17; discussion 1217–1219.
91. Rhoton AL. The lateral and third ventricles. Neurosurgery. 2002;51:S207–71.
92. Viale GL, Turtas S. The subchoroid approach to the third ventricle. Surg Neurol. 1980;14:71–4.
93. Cossu M, Lubinu F, Orunesu G, Pau A, Sehrbundt Viale E, Sini MG, et al. Subchoroidal approach to the third ventricle. Microsurgical anatomy. Surg Neurol. 1984;21:325–31.
94. Bozkurt B, Yağmurlu K, Belykh E, Tayebi Meybodi A, Staren MS, Aklinski JL, et al. Quantitative anatomic analysis of the transcallosal-transchoroidal approach and the transcallosal-subchoroidal approach to the floor of the third ventricle: an anatomic study. World Neurosurg. 2018;118:219–29.
95. Deopujari CE, Mohanty CB. Anatomic variations of the fornix and its clinical implications. Neurol India. 2016;64:947–9.
96. Delandsheer JM, Guyot JF, Jomin M, Scherpereel B, Laine E. Inter thalamo-trigonal approach to the third ventricle (author's transl). Neurochirurgie. 1978;24:419–22.
97. Ulm AJ, Russo A, Albanese E, Tanriover N, Martins C, Mericle RM, et al. Limitations of the transcallosal transchoroidal approach to the third ventricle: technical note. J Neurosurg. 2009;111:600–9.
98. Cinalli G, Onorini N. Transchoroidal approach to tumors of the posterior third ventricle. New York, NY: Springer; 2019.
99. Cinalli G, Scala MR, Marini A, Imperato A, Mirone G, Spennato P. Interhemispheric transcallosal transchoroidal approach to a pineal teratoma in a 15-year-old boy. Neurosurg Focus Video. 2021;5:V5.
100. Kasowski HJ, Nahed BV, Piepmeier JM. Transcallosal transchoroidal approach to tumors of the third ventricle. Oper Neurosurg. 2005;57:ONS-361–6.
101. Cinalli G, Onorini N. Combined staged telo-velar and trans-choroidaI approach to a tumor of the sylvian aqueduct. New York, NY: Springer; 2019.
102. Cinalli G, Spennato P. Removal of midbrain tumor via interhemispheric transcallosal-transchoroidal approach [internet]. Cham: Springer; 2022. https://link.springer.com/10.1007/978-3-030-95506-9

103. Iacoangeli M, di Somma LGM, Di Rienzo A, Alvaro L, Nasi D, Scerrati M. Combined endoscopic transforaminal-transchoroidal approach for the treatment of third ventricle colloid cysts: technical note. J Neurosurg. 2014;120:1471–6.
104. Cinalli G, Imperato A, Mirone G, Di Martino G, Nicosia G, Ruggiero C, et al. Initial experience with endoscopic ultrasonic aspirator in purely neuroendoscopic removal of intraventricular tumors. J Neurosurg Pediatr. 2017;19:325–32.
105. Tawk RG, Akinduro OO, Grewal SS, Brasiliense L, Grand W, Grotenhuis A. Endoscopic transforaminal transchoroidal approach to the third ventricle for cystic and solid tumors. World Neurosurg. 2020;134:e453–9.
106. Krause F. Operative Freilegung der Vierhugel nebst Beobachtungen uber Hirndruck and Dekompression. Zbl Chir. 1926;53:2812–9.
107. Jamieson KG. Excision of pineal tumors. J Neurosurg. 1971;35:550–3.
108. Poppen JL. The right occipital approach to a pinealoma. J Neurosurg. 1966;25:706–10.
109. Van Wagenen WP. A surgical approach for the removal of certain pineal tumors. Surg Gynecol Obstet. 1931;53:216–20.
110. Dandy WE. An operation for the removal of pineal tumors. Surg Gynecol Obstet. 1921;33:113–9.
111. Dandy WE. Operative experience in cases of pineal tumor. Arch Surg. 1936;33:19–46.
112. Moshel YA, Parker EC, Kelly PJ. Occipital transtentorial approach to the precentral cerebellar fissure and posterior incisural space. Neurosurgery. 2009;65:554–64.
113. Zaidi HA, Elhadi AM, Lei T, Preul MC, Little AS, Nakaji P. Minimally invasive endoscopic supracerebellar-infratentorial surgery of the pineal region: anatomical comparison of four variant approaches. World Neurosurg. 2015;84:257–66.
114. Hernesniemi J, Romani R, Albayrak BS, Lehto H, Dashti R, Ramsey C, et al. Microsurgical management of pineal region lesions: personal experience with 119 patients. Surg Neurol. 2008;70:576–83.
115. Cinalli G, Marini A, Russo C, Spennato P, Mirone G, Ruggiero C, et al. Herophilus-Galen line as a predictor of extent of resection in the occipital interhemispheric transtentorial approach to pineal tumors in children. J Neurosurg Pediatr. 2022;1–9.
116. Matsuo S, Baydin S, Güngör A, Miki K, Komune N, Kurogi R, et al. Midline and off-midline infratentorial supracerebellar approaches to the pineal gland. J Neurosurg. 2017;126:1984–94.
117. Joaquim A, Santos M, Silva E, Tedeschi H. Interhemispheric occipital transtentorial approach to the pineal region and dorsal midbrain – anatomy and surgical technique. Jornal Brasileiro de Neurocirurgia. 2009;20:22.
118. Shahrestani S, Ravi V, Strickland B, Rutkowski M, Zada G. Pure endoscopic supracerebellar infratentorial approach to the pineal region: a case series. World Neurosurg. 2020;137:e603–9.
119. Azab WA, Nasim K, Salaheddin W. An overview of the current surgical options for pineal region tumors. Surg Neurol Int. 2014;5:39.
120. Cools MJ, Quinsey CS, Elton SW. Chiari decompression outcomes using ligamentum nuchae harvest and duraplasty in pediatric patients with Chiari malformation type I. J Neurosurg Pediatr. 2018;22:47–51.
121. Nazzaro JM, Shults WT, Neuwelt EA. Neuro-ophthalmological function of patients with pineal region tumors approached transtentorially in the semisitting position. J Neurosurg. 1992;76:746–51.
122. Sano K. Pineal region masses: general considerations. Brain Surg. 1993;1:463–73.
123. Lozier AP, Bruce JN. Surgical approaches to posterior third ventricular tumors. Neurosurg Clin N Am. 2003;14:527–45.
124. Cinalli G, Barbato M. Interhemispheric transtentorial approach to a teratoma of the pineal region [internet]. Cham: Springer; 2022. https://link.springer.com/10.1007/978-3-030-95496-3
125. Patel PG, Cohen-Gadol AA, Mercier P, Boop FA, Klimo P. The posterior transcallosal approach to the pineal region and posterior third ventricle: intervenous and paravenous variants. Oper Neurosurg (Hagerstown). 2017;13:77–88.

Chapter 9
Treatment Strategies and Current Results of Petroclival Meningiomas

Sanjeev Pattankar and Basant K. Misra

9.1 Introduction

Petroclival meningiomas (PCMs) are those skull-base meningiomas that originate from the upper two-thirds of the clivus, lateral to the midline, from the petroclival synchondroses junction, remaining medial to the trigeminal nerve [1]. Though accounting for only 2% of all the intracranial meningiomas, PCMs still continue to pose a formidable surgical challenge to neurosurgeons worldwide [2]. This is due to their deep-seated location, intimate relationship with the brain stem and adjoining important neurovascular structures, and factors that have not been entirely possible to circumvent by the technical advances alone in the skull-base approaches [3]. Nevertheless, over the past three decades, these technical advances have resulted in a consistent improvement in surgical outcomes of PCMs.

Up to 1970, PCMs were considered inoperable, as only 10 of the 26 patients reported in the literature had survived surgery [4]. Parallel advances in microneurosurgery and the introduction of innovative lateral skull-base approaches in the late 1980s led to a renewed enthusiasm for radical excision of PCMs, and several successful series were published [5–9]. Back then, most practicing skull-base neurosurgeons accepted the accompanying morbidity as inevitable and went on with the approach of "total excision" lest they be frowned upon as incompetent. Only a few brave souls dared to question this approach [10]. Additionally, the successful reports of meningiomas being treated through gamma knife radiosurgery (GKRS) further dampened enthusiasm for the high-risk radical surgery of PCMs [11, 12]. There remains, however, a minority of brilliant neurosurgeons who have constantly

S. Pattankar · B. K. Misra (✉)
Department of Neurosurgery and Gamma Knife Radiosurgery, P D Hinduja Hospital and MRC, Mumbai, India
e-mail: dr_bmisra@hindujahospital.com

C. Di Rocco (ed.), *Advances and Technical Standards in Neurosurgery*, Advances and Technical Standards in Neurosurgery 48,
https://doi.org/10.1007/978-3-031-36785-4_9

strived to technically advance/modify the skull-base approaches and achieve gross total resection (GTR) in most patients with these tumors [1].

Despite the increased understanding of PCMs, via the increased volume of scientific literature available, many controversies remain regarding their "optimal management" [2, 13]. The advent of stereotactic radiosurgery (SRS), along with the shifting of management goals from complete radiological cure to maximal preservation of the patient's quality of life (QOL), has further cluttered the topic. Hence, proper addressing is required to establish algorithms for the choice of appropriate surgical approach, the timing of surgical intervention, and the role of SRS (adjuvant/primary). The purpose of this chapter is to summarize the scientific evidence pertaining to the management of PCMs, particularly those regarding the available treatment strategies and current outcomes, and discuss the decision-making process to formulate an "optimal management" plan for individual PCMs.

9.2 Treatment Strategies in PCMs

Differentiating PCMs from the other posterior fossa skull-base meningiomas is of paramount importance [1]. Pure clival meningiomas originate in the midline, from the dura over the upper two-thirds of the clivus, displacing the brain stem posteriorly. Although arising from the same upper two-thirds of the clivus, the true PCMs have their dural attachment centered on the petroclival junction, remaining medial to Vth cranial nerve, and displacing the brain stem/basilar artery posteriorly and contralaterally. Large PCMs commonly have extensions to the posterior cavernous sinus, parasellar region, tentorium, or the foramen magnum. On the other hand, meningiomas purely arising from the lower third of the clivus are called foramen magnum meningiomas. And the subgroup of posterior fossa meningiomas arising lateral to the Vth cranial nerve is grouped together as petrosal meningiomas, called either anterior or posterior type depending on the relation with the internal auditory meatus (IAM). Finally, the sphenopetroclival meningiomas, having bilateral extensions to cavernous sinuses and an en-plaque involvement of the ventral posterior fossa dura and/or tentorium, represent the most extensive and surgically incurable variety of the posterior fossa meningiomas. From the very definitions of the above-mentioned skull-base meningiomas, it is evident that their individual surgical challenges and achievable outcomes differ considerably, hence, the significance [1]. True PCMs with favorable consistencies and intact arachnoid plane all-around (particularly in relation to the brainstem) are often completely resectable [14].

The commonest age of presentation in PCMs is 40–50 years. The constellation of clinical symptoms/signs seen in these patients can be secondary to the following reasons: (1) cranial nerves involvement, (2) cerebellar involvement, (3) brain stem involvement, or (4) increased intracranial pressure (either due to tumor mass or obstructive hydrocephalus). Headache is the most frequent symptom. PCMs are commonly associated with multiple cranial neuropathies, with the fifth and eighth cranial nerves being the most frequent. Nearly half and one-third of these patients

have seventh cranial nerve and lower cranial nerve involvement, respectively. Despite the anatomical proximity of cranial nerves III, IV, and VI to the PCMs, their involvement is relatively infrequent. In addition, several cases of contralateral trigeminal neuralgia have also been reported in cases of posterior fossa skull-base meningiomas. Seen in approximately 70% of cases, cerebellar signs are among the commonest signs seen in PCMs. The signs of brain stem involvement, that is, long tract signs and somatosensory deficits, are quite inconsistent.

Once the diagnosis of PCM is established based on a thorough clinico-radiological evaluation, these patients can be managed in any of the following ways.

9.2.1 "Watchful Waiting" in PCMs

The understanding of the natural history of untreated PCMs has multiple lacunae [15]. Table 9.1 summarizes the dedicated studies reporting the temporal course (radiological and clinical) of untreated PCMs. Both Van Havenberg et al. [16] and Terasaka et al. [17] concluded from their observations that "watchful waiting" can be considered for small PCMs without symptoms. Additionally, Van Havenberg et al. [16] also reported that a change in growth rate predicted clinical deterioration in at least 50% of cases, in turn warranting an active treatment. A meta-analysis published by Sughrue et al. [18], including data from 22 studies and 675 patients of small untreated meningiomas, found that lesions <2 cm rarely developed new symptoms within 5 years of follow-up (despite radiological progression in a few). While some authors [19] have reported a relatively benign growth pattern in PCMs compared to other skull-base meningiomas, it is not supported by other publications [20].

Table 9.1 Summary of studies reporting the temporal course (radiological and clinical) of untreated PCMs

Authors	Group size (*N*)	Median Follow-up period (months)	Rate of radiological tumor growth (%)	Rate of clinical deterioration (%)	Conclusion
Van Havenberg et al. [16]	21	85	76	63	• PCMs are slow-growing tumors, but with highly variable growth rates • Change in growth rate predicted clinical deterioration in at least 50% of cases
Terasaka et al. [17] (Observation cohort)	15	40	60	47	• Observation for asymptomatic and microsurgery for symptomatic PCMs is a reasonable strategy

A recent study by Romani et al. [21], retrospectively analyzing 136 conservatively managed incidental meningiomas, reported that peritumoral edema and T2-weighted/FLAIR hyperintensity predicted tumor progression. Contrarily, calcifications indicated an indolent tumor. Hence, a close imaging follow-up in the early identification of aggressive behavior in meningiomas is warranted. This "watchful waiting" or "wait-and-scan" policy for small (<2 cm) asymptomatic meningiomas in general is supported by many study groups [2, 7, 22], although the schedule for radiological follow-up is not uniform among various study groups, as confirmed by a recent systematic review [23]. The justification for withholding even the noninvasive SRS in such cases is to avoid the potential risk of radiation-induced side effects, though marginal, of late cranial neuropathies or radiation-induced tumors, or possible de-differentiation of meningiomas into a more aggressive variety [11].

Considerable controversy exists in the "watchful waiting" policy in small asymptomatic PCMs. Ramina et al. [24] put forth a strong counterargument by achieving 100% GTR in their small asymptomatic/minimally symptomatic PCMs, with just 11.1% transient cranial neuropathies and no major morbidity. The authors substantiated their proactive intervention by enumerating the probable fallacies of the "watchful waiting" policy in PCMs, which are as follows: (1) minimal tumor growth can preclude a GTR by the invasion of either the cavernous sinus and/or vital neurovascular structures, and (2) smaller PCMs do not necessarily need extensive skull-base approaches, thereby avoiding approach-related complications. A well-planned randomized clinical trial is needed to clarify this dilemma of "watchful waiting" versus proactive intervention in small asymptomatic PCMs.

9.2.2 Surgical Strategies in PCMs

Microsurgical strategies, with their many skull-base approaches to choose from, remain the primary line of management for moderate/large-sized (>2 cm) PCMs [1, 3, 25]. Routine preoperative evaluation includes an accurate assessment of the neuroradiological characteristics (MRI brain plain, contrast with MR venogram; CT brain contrast with temporal bone thin cuts) of the tumor by the operating surgeon, to facilitate a safe tumoral resection [14]. Special emphasis should be laid on the analysis of the petrous temporal bone characteristics, venous architecture, neurovascular structures' displacement/encasement, brainstem edema/pial breach, and markers of tumor consistency [26]. Conventional angiogram and preoperative embolization may have selected roles in some large PCMs and practiced by some neurosurgeons. The authors do not routinely advise DSA and rarely ever employ preoperative embolization.

The presence of a T1 hypointense and T2 hyperintense rim around the tumor, signaling a good arachnoid cleavage plane, was shown to relate well with the resectability of the PCMs [27]. Contrarily, the presence of pial breach or brain stem edema reduced the tumor's resectability and increased long-term complications. This has been confirmed by various study groups like Sekhar et al. [28], Pirayesh et al. [27],

Al-mefty et al. [1], Seifert et al. [22], etc. Regarding the tumor consistency, both Maurer et al. [29] and Yao et al. [30] have cowenfirmed that a high T2-weighted signal intensity regularly correlated to a soft tumoral consistency. However, this soft tumoral consistency has not been found to correspond to either better resectability [1] or to better functional outcomes [31].

Various skull-base approaches that can be used for PCMs are Retrosigmoid and its modifications (postero-lateral corridor), transpetrosal and its modifications (lateral corridor), fronto-temporo-orbito-zygomatic (FTOZ, antero-lateral corridor) and its modifications, and extended endonasal approaches (EEA). For every patient with PCM, the appropriate surgical approach should be tailored according to the characteristics related to the tumor (epicenter, neurovascular relations, hearing status), patient (age, comorbidities, informed consent), and surgeon (experience, expertise).

9.2.2.1 Retrosigmoid Approach and Its Modifications

The last two decades have seen a shift toward the increasing employment of conservative surgical approaches like retrosigmoid or its modifications, with the use of adjuvant SRS on a need basis [32–35]. The retrosigmoid approach is best suited for PCMs with major posterior fossa extensions. It is a simpler and faster approach, and the time saved in the exposure is better utilized in the dissection and excision of the tumor. Moreover, the approach-related morbidities seen in transpetrous approaches are avoided. Procedural modifications like tentorial splitting [36] or supra-meatal drilling [32] provide modest access to the middle fossa and Meckel's cave as well. The use of the supra/paracerebellar corridor in a semi-sitting position facilitated better tumor removal, by facilitating an early recognition of the tumor-brain stem interface and better brain relaxation with reduced venous congestion [26]. Majority of cases in the author's practice are currently operated through the retrosigmoid route. The major disadvantage of this approach is pertaining to its deep surgical field and the risk of injuring the VII-VIII complex. Unlike transpetrosal approaches, the retrosigmoid approach provides a narrow trajectory for tumor decompression and separation from surrounding critical structures (reduced possibility of devascularization before tumor decompression), which might become technically demanding. Nevertheless, the recent addition of endoscopic assistance in the conventional retrosigmoid approach has led to circumventing the poor visualization of some of the blind spots (Meckel's cave/inferior clival depression/middle fossa) [37].

9.2.2.2 Transpetrosal Approach and Its Modifications

Transpetrosal approaches can be divided into three groups—anterior petrosectomy (Fig. 9.1), posterior petrosectomy (Fig. 9.2), or their combination (Fig. 9.3). The anterior petrosectomy was first developed by Bochenek and Kukwa and later modified by Kawase and colleagues [38]. It is indicated as an option in PCMs centered

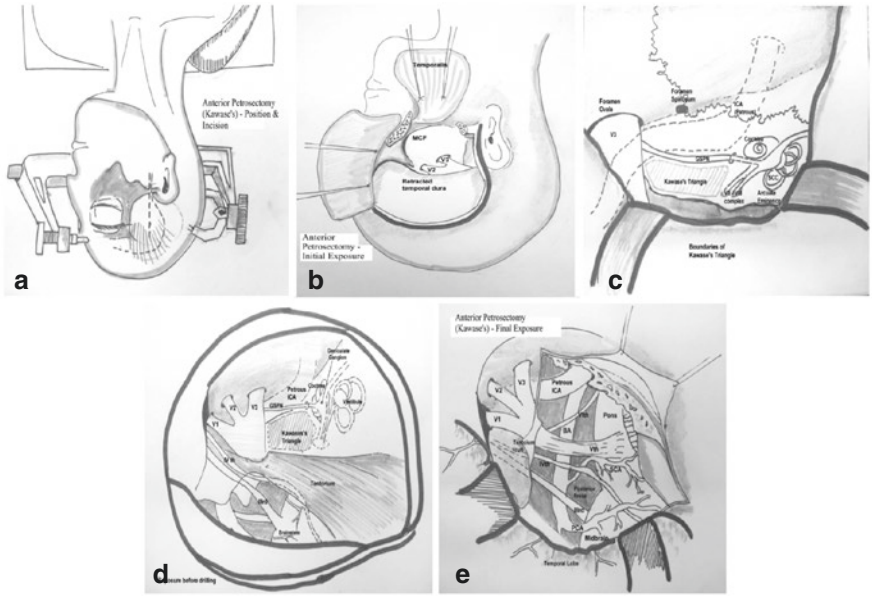

Fig. 9.1 Diagrammatic illustration of the anterior petrosectomy (Kawase's procedure) showing the position of the patient (**a**), the position of the skin flap with extent of craniotomy and exposure of middle cranial fossa (MCF) (**b**), the anatomical landmarks of the Kawase's triangle (**c**), the extent of drilling of the Kawase's triangle (**d**), and the final exposure of the posterior fossa after incising the dura and splitting the tentorium (**e**). *GSPN* greater superficial petrosal nerve, *ICA* internal carotid artery, *BA* basilar artery, *SCA* superior cerebellar artery, *PCA* posterior cerebral artery. (with permission from Misra BK & Purandare H. Petroclival Meningioma: Current Treatment Strategy. In Misra BK, Laws ER & Kaye AH, editors. Current Progress in Neurosurgery 1, Mumbai: Tree Life Media; 2014. p. 338–60)

superiorly and medially to the IAM. This approach builds on the basic middle fossa approach used for exposing the IAM with the removal of additional medial petrous bone lying within the Kawase's triangle (rhomboid), bounded by the greater superficial petrosal nerve (GSPN) laterally, the petrous ridge medially, the internal auditory canal axis posteriorly, and V3 division anteriorly. The medial petrous bone is resected to the level of the horizontal segment of the petrous internal carotid artery (ICA). The cochlea is at the posterolateral corner of the rhomboid. The limits of the extended middle fossa exposure are the inferior petrosal sinus inferiorly, the middle ear ossicles laterally, the Gasserian ganglion anteriorly, and the superior semicircular canal posteriorly. Technically, Kawase's approach differs minimally from the extended middle fossa approach with the addition of transverse division of the tentorium to the incisura, allowing full communication between the intradural middle and posterior fossa [38]. The anterior petrosal approach has the added benefit of allowing improved visualization of the clivus across the midline. Additionally, drilling of the post-meatal triangle (between internal auditory canal and superior semicircular canal) can help to manipulate the VII-VIII complex via endoscope. In

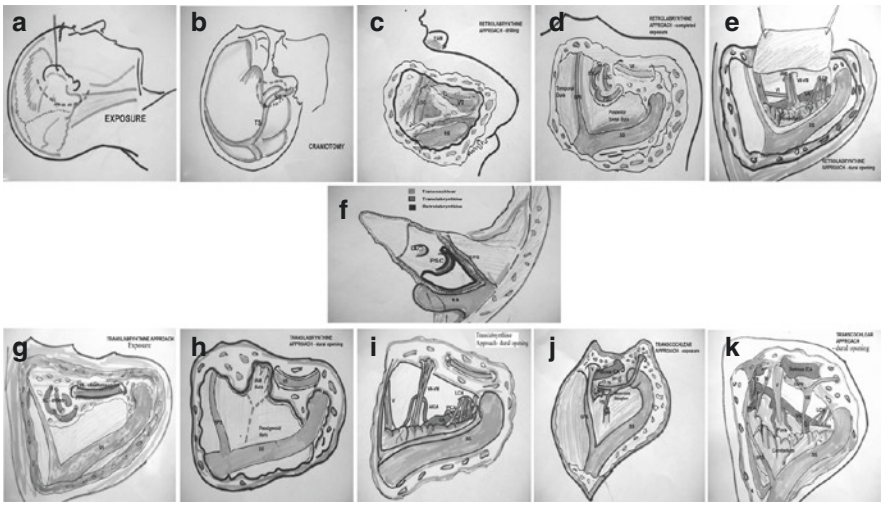

Fig. 9.2 Diagrammatic illustration of the posterior petrosectomy variants. The position of the skin incision (**a**) and the extent of mastoidectomy (**b**) is shown. (**f**) shows the relative extent of drilling the petrous bone in the retrolabyrinthine (**c**–**e**), translabyrinthine (**g**–**i**), and the transcochlear (**j**, **k**) approaches. In the retrolabyrinthine approach, the drilling landmarks (**c**) include the sigmoid sinus (SS) posteriorly, the lateral semicircular canal (LSC) medially, and the vertical segment of the facial nerve (VII). Complete exposure (**d**) showing skeletonization of the labyrinth, visualization of the sinodural angle, and the posterior fossa dura. The view of the posterior fossa contents after opening the dura (**e**). In translabyrinthine approach, (**g**) shows the bony exposure showing the mastoidectomy with removal of the labyrinth, exposure of the dura and fundus of the internal auditory meatus with subsequent dural opening (**h**, **i**). In the transcochlear approach, the bony exposure with drilling of the labyrinth and the cochlea and transposition of the VII nerve (**j**) provides maximum exposure of the posterior fossa and the midclival area with minimal cerebellar retraction (**k**). *TS* transverse sinus *SPS* superior petrosal sinus, *SSC* superior semicircular canal, *PSC* posterior semicircular canal, *IAM* internal auditory meatus, *VA* vertebral artery, *AICA* anterior inferior cerebellar artery, *PICA* posterior inferior cerebellar artery, *LCN* lower cranial nerves, *GSPN* greater superficial petrosal nerve, *ICA* internal carotid artery. (With permission from Misra BK & Purandare H. Petroclival Meningioma: Current Treatment Strategy. In Misra BK, Laws ER & Kaye AH, editors. Current Progress in Neurosurgery 1, Mumbai: Tree Life Media; 2014. p. 338–360)

comparison to the posterior transpetrosal approaches, here there is less risk of VII palsy, hearing loss, and CSF leak. However, the risk of GSPN injury or damage to the geniculate ganglion, along with temporal lobe edema secondary to prolonged retraction are common [39].

The posterior petrosal approaches involve the removal of a variable amount of temporal bone to increase the extent of exposure. Though nomenclatures vary within the neurosurgical and neurotologic literature, these posterior petrosal approaches can be divided into three varieties: retro-labyrinthine, trans-labyrinthine, and trans-cochlear approaches [39]. Al-Mefty's group pointed out that the key concept of posterior petrosectomy is "mobilization of the transverse-sigmoid junction to create surgical corridors inferior to the temporal bone, towards the basal cisterns"

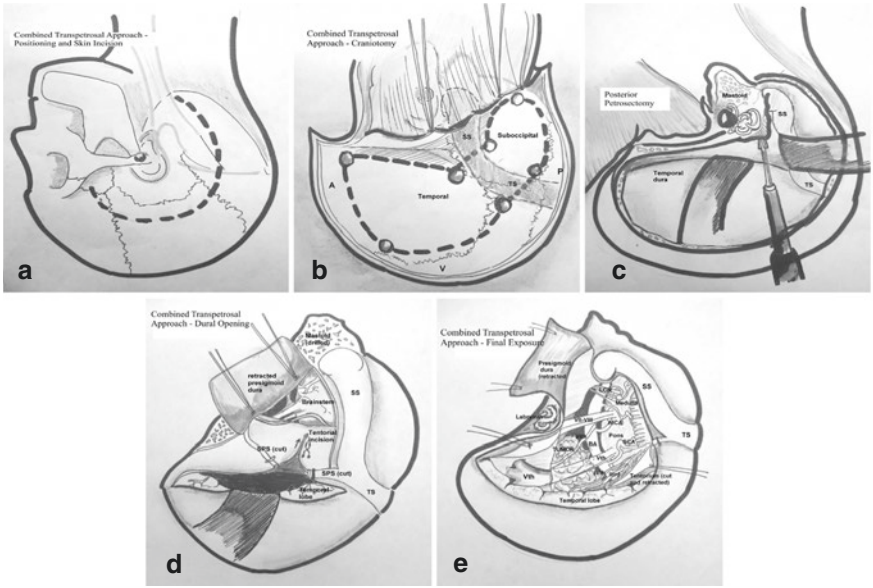

Fig. 9.3 Diagrammatic illustration of the combined petrosal approaches to petroclival meningiomas: skin incision (**a**) and craniotomy (**b**) flap tailored as per the requirement of exposure with drilling of bone across the transverse-sigmoid junction. Retrolabyrinthine exposure with petrous drilling is an invariable component of combined approaches (**c**). Technique of incision of presigmoid dura (posterior fossa) and middle fossa along the temporal base, and their connection across the sacrificed superior petrosal sinus (SPS). Further sectioning of the tentorium to the level of the incisura anterior to the IV cranial nerve (**d**) provides a comprehensive and unobstructed exposure of the anterolateral brainstem along with III to XII cranial nerves and the entire vertebrobasilar vascular tree (**e**). *SS* sigmoid sinus, *TS* transverse sinus, *LCN* lower cranial nerves, *BA* basilar artery, *AICA* anterior inferior cerebellar artery, *SCA* superior cerebellar artery. (With permission from Misra BK & Purandare H. Petroclival Meningioma: Current Treatment Strategy. In Misra BK, Laws ER & Kaye AH, editors. Current Progress in Neurosurgery 1, Mumbai: Tree Life Media; 2014. p. 338–360)

[6]. Extending the dural incision above the transverse sinus, and anterior to the sigmoid sinus, with sectioning of the superior petrosal sinus and tentorium, results in the sinus unlocking.

For large PCMs, a combination of posterior petrosal and anterior petrosal approaches is used, a combined petrosal approach [40]. The main advantage of using such a combination is early devascularization of tumor and establishing multiple trajectories to the tumor/neurovascular structures aiding meticulous dissection. In general, the transpetrosal approaches result in a shorter working distance, reduced need for brain retraction, early devascularization of the tumor, and the advantage of multiple trajectories/angles of attack for tumor resection [14]. On the downside, these extensive skull-base approaches are technically demanding and time-consuming and come with an elevated risk of approach-related complications (CSF leak, hearing loss, venous injury/thrombosis, etc.).

9.2.2.3 Fronto-Temporo-Orbito-Zygomatic Approach and its Modifications

The FTOZ approach utilizes the traditional fronto-temporal corridor with added removal of the lateral orbital rim and the zygoma, either in one or two pieces (Fig. 9.4). Next, the temporal lobe is extradurally mobilized by creating a plane between the temporal and cavernous dura [26]. It is ideal for a spheno-petroclival meningioma. The pros of using this approach are avoiding an intradural temporal retraction and related complications, with early devascularization of the middle meningeal artery feeders. The cons are the significant risks of III and IV cranial neuropathy and difficult access to the tumor's posterior fossa component.

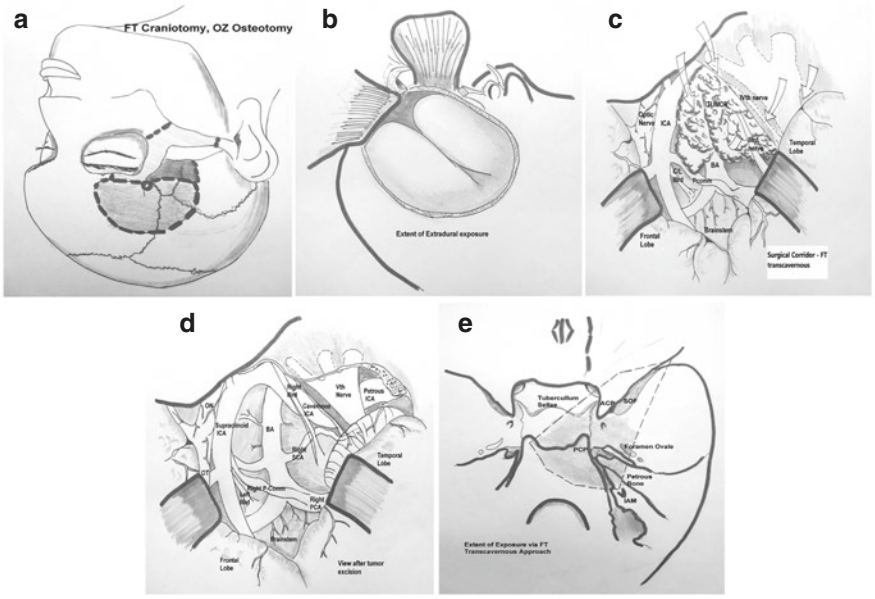

Fig. 9.4 Diagrammatic representation of the Fronto-temporo-orbito-zygomatic (FTOZ) approach to petroclival meningiomas. The extent of craniotomy (**a**) and the skull base exposure (**b**) are depicted. The complete exposure before the tumor resection (**c**) and after resection (**d**) shows the multiple corridors in between the neurovascular structures. (**e**) demonstrates the surgical corridor available in this approach. *ICA* internal carotid artery, *BA* basilar artery, *PCA* posterior cerebral artery, *SCA* superior cerebellar artery, *ACP* anterior clinoid process, *PCP* posterior clinoid process, *SOF* superior orbital fissure, *IAM* internal auditory meatus). (With permission from Misra BK & Purandare H. Petroclival Meningioma: Current Treatment Strategy. In Misra BK, Laws ER & Kaye AH, editors. Current Progress in Neurosurgery 1, Mumbai: Tree Life Media; 2014. p. 338–360)

9.2.2.4 Extended Endonasal Approaches

Although many anatomical studies on the utility of EEA as an access corridor to the petroclival region have been published, none present a satisfactory case [41, 42]. The rationale for such scientific endeavors was to test if EEA can provide better access to this delicate region by avoiding brain retraction and cranial nerve handling. A cadaveric study by Van Gompel et al. [43] showed that open anterior petrosectomy provides 50% more volumetric exposure than the endoscopic variant. Based on their observations, they proposed to rename the open anterior petrosectomy as "superior anterior petrosectomy" and the endoscopic variant as the "inferior anterior petrosectomy," the latter being indicated for only small dural lesions. Few other studies have pointed out that EEA is unsuitable for true PCMs, which tend to displace VI nerve medially, while better suited for mid-clival lesions displacing both V and VI nerves laterally [44]. Very limited clinical experience available with EEA has reported a high complication rate (CSF leak) and low GTR, further questioning its credibility in PCMs.

9.2.2.5 Staged Surgical Approaches

Due to the patient's frailty or tumor's unsurmountable character (giant size/sphenopetroclival variant), if a single extensive surgical approach to skull-base is deemed to fail, then a set of staged surgical approaches (interval of 3–6 months) is resorted to [45]. It is usually required in giant posterior fossa meningiomas of mixed anatomical variety (PCM invading lateral cavernous sinus/lower clivus). Commonly used combinations in staged surgical strategies for PCM variants are as follows (1): In sphenopetroclival variants, a retrosigmoid approach (posterior fossa decompression) followed by an FTOZ/its modification (middle fossa decompression), and [2] in PCMs extending to lower clivus, first an anterior transpetrosal approach followed by a retrosigmoid/far lateral approach. Always, the first stage is planned to achieve brain stem decompression, which is the critical part of preventing worsening neurological deficits. If the residual tumor does not cause symptoms, especially in frail old patients, the second stage can be withheld as a part of "watchful waiting." It is also argued that staged surgeries are better tolerated by patients in the case of giant PCMs. A staged combined petrosal approach (extradural phase followed by intradural phase) has also been described to mitigate duration-related surgical complications (including surgeon's fatigue) [46]. Additionally, the extradural phase can partially devascularize the PCMs, resulting in tumor softening/partial necrosis, subsequently aiding better resection rates. However, the dedicated literature comparing staged approaches to single approaches, in terms of complications and tumor control, is lacking. The authors currently favor a staged approach in giant tumors and in tumors requiring many hours of delicate dissection rather than operating a case for more than 10–12 h.

9.2.2.6 Algorithms for Deciding Surgical Approach

An appropriate surgical approach to any particular PCM is selected based on the following factors: (1) tumor epicenter and extensions (posterior fossa or posterior and middle cranial fossa); (2) preoperative neurological deficits, especially hearing status; (3) patient's general fitness for supra-major surgery; and (4) surgeon's expertise with the proposed surgical approach. Excellent results can be achieved with any appropriately selected surgical approach. There are no proven absolutes (superiors/inferiors) among the armamentarium of surgical approaches available for PCMs.

At our center, we follow a simple time-tested algorithm in selecting the appropriate surgical approaches (Fig. 9.5). It is based on two variables, tumor location, and preoperative hearing status [3]. We prefer the retrosigmoid approach and its modifications (tentorial incision, suprameatal drilling, etc.) wherever feasible, as a safe alternative to the more extensive lateral skull-base approaches [26]. In PCMs with favorable characteristics like T2-weighted hyperintensity and preserved arachnoidal plane, a classic retrosigmoid approach is adequate. Transpetrosal approaches are valuable in PCMs with posterior and middle fossa components, in the firm tumors with a breach in the arachnoidal plane and in smaller central tumors.

9.2.3 Radiosurgical Strategies in PCMs

Radiosurgery has become an acceptable treatment modality for PCMs, both in an adjunctive and primary role. Starke et al. [47] published the results of the largest and the only multicentric cohort receiving GKRS for PCMs. They reported 5-year progression-free survival (PFS) of 93%, with the following as predictors of tumor progression: (1) prolonged duration of symptoms, (2) prior radiotherapy, (3) larger tumor volume (< or >10 cm^3), and (4) reduced maximal dose. Additionally, the

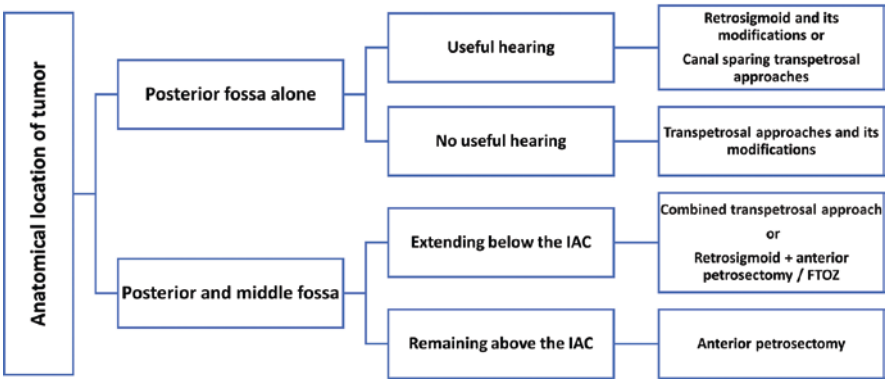

Fig. 9.5 Algorithm showcasing key considerations in deciding surgical approaches to PCMs. *IAC* Internal auditory canal, *FTOZ* Fronto-temporo-orbito zygomatic

female sex was associated with better outcomes after GKRS, confirming the role of gender in the decision-making process. Table 9.2 enlists the details of studies reporting the GKRS outcome in PCMs [11, 47–50]. There is enough evidence available to conclude that radiosurgery provides acceptable tumor control with very low morbidity rates in small PCMs.

The literature dedicated to GKRS outcomes in medium−/large-sized PCMs is very limited. A systematic review by Fatima et al. [51], studying the outcomes of SRS in large intracranial meningiomas (>8.1 cm^3; 77.6% skull-base), showed excellent PFS in the range of 84–100% but at the cost of 23% radiation-induced side effects. Iwai et al. [52] proposed staged GKRS in large meningiomas with modest 5-year tumor control of 76%. Hence, prudent use of GKRS is recommended in PCMs with volumes >8 cm^3. The theoretical advantage of using a hypofractionated SRS, like CyberKnife, in treating larger meningiomas (>10 cm^3) efficaciously was tested by recently Oh et al. [53]. With the median treated volume being 18.9 cm^3 in 31 skull-base meningiomas (6 PCMs) and a median cumulative radiation dose of 27.8 Gy delivered from three to five fractions, he reported a tumor control of 90.3% at 57 months median follow-up. Though further evidence is awaited, CyberKnife may be used safely in selected cases of large PCMs. Likewise, proton beam therapy is also emerging as a SRS modality for larger PCMs [2, 54]. In conclusion, with the current evidence available in large PCMs, SRS may be justified only in patients with advanced age and comorbidities that rules out surgical intervention.

Table 9.2 Summary of important studies reporting the GammaKnife Radiosurgery (GKRS) outcome in petroclival meningiomas (PCMs)

Authors	Group size (*N*)	Radiosurgery role (adjunctive/primary)	Median tumor volume (cm^3)	Median margin radiation dose (Gy)	Median follow-up period (months)	Progression-free survival (PFS)	Complications	Conclusions
Subach et al. (1998) [48] (Pittsburg group)	62	39/23	13.7[a]	15[a]	37	8-year PFS = 92.3%[b]	Permanent cranial neuropathy—5%	• GKRS is suitable especially for patients with tumors ≤30 mm in diameter • No statistically significant difference between adjunctive and primary cohorts
Roche et al. (2003) [11] (Marseille group)	32	8/24	2.28[a]	13[a]	48	5-year PFS = 100%	New cranial neuropathy—6.25% Permanent brainstem dysfunction—6.25%	• GKRS provides effective tumor control of small−/medium-sized PCMs and is an alternative to microsurgery
Flannery et al. (2010) [49] (Pittsburg group)	168	71/97	6.1	13	72	5-year PFS = 91%	Permanent cranial neuropathy—2%. Overall complications—8%	• Tumors >8 cm^3 and male sex were significantly associated with clinical and tumor progression after treatment

(continued)

Table 9.2 (continued)

Authors	Group size (*N*)	Radiosurgery role (adjunctive/ primary)	Median tumor volume (cm^3)	Median margin radiation dose (Gy)	Median follow-up period (months)	Progression-free survival (PFS)	Complications	Conclusions
Starke et al. (2014) [47] (North American GammaKnife Consortium)	254	114/140	7.8[a]	13	71.1[a]	5-year PFS = 93% 10-year PFS = 84%	No major radiation side effects	• Smaller PCMs with no prior radiation therapy are most likely to have favorable outcomes • Significant clinical neurological dysfunction likely poses a greater risk for an unfavorable outcome
Sadik et al. (2018) [50] (Netherlands group)	53	0/53	3.1	13	59	5-year PFS = 98%	Overall complication =5%	• GKRS yields significant volumetric tumor decrease in the first years of follow-up

[a]Mean values

[b]Tumor control rate at 8 years, after excluding patients with failed external beam radiotherapy previously and those with malignant meningiomas

9.3 Current Surgical Outcomes in PCMs

The chronological analysis of surgical outcomes in PCMs, reported from various advanced neurosurgical centers throughout the world, clearly demonstrates the progressive inclination toward less radical surgery (both in terms of surgical approaches and extent of resection) with a stronger emphasis on the functional outcome (Table 9.3) [1, 3, 7, 12, 13, 22, 24, 28, 33, 38, 55–64, 66–69]. The GTR rates have dropped over the years, from a high of 70–80% in the 2000s to the current lows of 40%. For example, Sekhar et al.'s [12, 28] GTR rates dropped from 78% to 32% between 1990 and 2007. Similarly, the group from Barrow Neurological Institute reported a GTR rate of 43% in 2007, down from 91% back in 1992 [9, 57]. The changing trend toward a less radical approach in almost all the recent series is aimed at a better functional outcome. That this attempt is succeeding is confirmed by the fact that the permanent morbidity rates are reducing in the recent series [3, 62–64].

Excellent results with SRS in PCMs, in terms of tumor control and safety, have made it the adjuvant therapy of choice in STR or recurrences in GTR [2]. Kim et al. [67] concluded that both GTR and STR + SRS groups had similar rates of PFS and that STR + SRS had a better functional outcome. Likewise, many recent series have substantiated the usefulness of SRS in non-GTR patients. The debate of upfront versus delayed SRS in non-GTR patients is yet to arrive at a meaningful conclusion based on scientific evidence. The support for upfront SRS is based on favorable results of a similar strategy in other skull-base meningiomas, while the counter to upfront SRS are the facts like PCMs have benign natural history, SRS comes with radiation side effects, and the irradiated tumors pose a surgical challenge if recurred [2].

The senior authors' experience of managing (surgery and SRS) over 124 PCMs since 1988 is a testament to these changing treatment goals [3, 4, 70]. A comparison of the postoperative function of patients in our series, between those operated on before 2001 (radical approach) and those after 2001 (safe excision), demonstrated significantly lower morbidity in the latter group (Fig. 9.6). Though ensuring better recurrence-free rates, the GTR comes at the cost of higher morbidity. We recommend upfront GKRS in patients with residual tumors, especially when the preoperative temporal course showed a rapid progression (either clinical or radiological). Our experiences with the flexible approach to individualizing the treatment protocol for a given patient have gone a long way toward an optimal outcome.

Table 9.3 Summary of studies (with group size >40) reporting the surgical outcomes in petroclival meningiomas (PCMs)

Authors	Group size (*N*)	Surgical approaches	Cranial nerve deficits (%)	Gross total resection (%)	Mortality (%)	Adjuvant therapy (SRS/RT)	Follow-up (months)	Recurrence (%)
Kawase et al. [38]	42	AP-100%	36	76	0	RT-1 patient	–	7
Tatagiba et al. [55]	54	PS + ST 44%; RS-35%; NS 21%	37	70	2	–	–	–
Couldwell et al. [7]	108	RS-53%; CP-19.2%; Transtemporal-10.4%; ST-9.7%; FT transcavernous-7.7%	33	69	3.7	–	52	13
Sekhar et al. [28]	75	CP-100%	60	–	–	SRS for residual (no specifics)	–	–
Little et al. [56]	137	CP-39.4%; RS-21.8%; FT-18.9%; AP-16.7%; TP-3.6%; Translab 2.9%	23	40	0.7	SRS for Intracavernous tumor (no specifics)	29.8	17.6
Park et al. [13]	49	PP-51%; CP-24%; AP-10.4%; RS-10.4%; OZ- 4.2%	28.6	20	2	SRS-7.7%; RT-20.5%	86	22.4; 2 (with SRS/RT)
Natarajan et al. [12]	150	Transpetrosal-80%; FTOZ-40%; RS-12%; transcondylar-2%; NS-1% (Total surgeries −207)	20.3	32	0	SRS-26%; RT-4.6%	102	5
Bambakidis et al. [57]	46	CP-15%; RS + degree of petrosectomy-59%; FTOZ-19%	30	43	0	RT-30.4%	42	15.5
Ramina et al. [24]	67	FTOZ/RS/transpetrosal (no specifics)	33	55	3	–	–	–
Seifert et al. [22]	93	RS-52%; CP-29%; FTOZ-14%; petrosal+far lateral-5%	23.6 (early); 17.2 (late)	37	0	SRS-15%	4–242	6 (GTR); 26 (STR); 12 (STR + SRS)

Li et al. [58]	57	RS-40.3%; CP-21%; FTOZ-19.4%; ST + RS-14%; Transpetrosal-5.3%	67	58	1.7	SRS-50% (in STR)	42	12.2 (GTR)
Yang et al. [59]	41	AP-41.4%; PS-21.9%; RS-14.7%; supra/ Infratentorial-7.4%; RS + far lateral-12.2%; Retromastoid-2.4%	65.9	61	0	SRS-15%	35	15
Chen et al. [33]	82	RS-51.2%; ST-28.2%; PS-14.6%; FT-6%	39	56	2.4	–	51	7
Nanda et al. [60]	50	Transpetrous-32%; FTOZ-26%; NS-42%	44	28	6	36%	22.1	12
Li et al. [61]	259	PS Retrolab-50.2%; AP-25.9%; NS-23.9%	II-9.5; III-21.2; IV-10.8; V-28.2; VI-12.4; VII-14.7; VIII-11.9; IX/X/ XI-2.3; XII-0.4	52.5	1.2	13.5%	55.3	4.2
Tao et al. [62]	66	PS-48.4%; RS-22.7%; ST-16.6%, NS-12.9%	15.1	43.9	2.7	–	–	12.1
Al-Mefty et al. [1]	64	PP-42.3%; AP-17.2%; CP-23.4%; TP-6.2%; RS-10.9%	III-9.3; IV-15.6; V-14; VI-35.9; VII-42; VIII-15.6; IX-6.2; X-7.8; XI-4.6; XII-4.6	64	1.56	–	71.5	20
Panigrahi et al. [63]	76	RS-90%; Transpetrosal-10%	9.2	77.6	2.6	31.5%	72	9.6

(continued)

Table 9.3 (continued)

Authors	Group size (*N*)	Surgical approaches	Cranial nerve deficits (%)	Gross total resection (%)	Mortality (%)	Adjuvant therapy (SRS/RT)	Follow-up (months)	Recurrence (%)
Sassun et al. [64]	51	PS Retrolab-61%; RS-22%; FTOZ-9.8%; PS + FTOZ-5.8%; Transcochlear-2%	44 (12 at last follow-up)	63	1.9	–	–	–
Bernard et al. [65]	154	AP-42%; RS-23.4%; CP-10.4%; NS-24%	78.4	26	3.9	22.1%	76	26
Qiao et al. [66]	176	AP-36.9%; RS-29%; PS-15.9%; NS-18%	III-41.8;VI-26.1;VII-30.7	34.7	3.9	27.8%	–	6.9 (GTR); 16.3 (STR)
Kim et al. [67]	92	PP-48%; RS-32%; NS-20%	44.6	14	2.2	61%	121	7.7 (GTR); 30.4 (STR); 12.5 (STR + SRS)
Zhao et al. [68]	162	RS-41.7%; RS Transtent-22.6%; NS-35.7%	40.5	70.8	1.2	20.8%	86.5	25.7
Our series [3]	72	RS-68.1%; Transpetrosal-12.5%; RS + Transpetrosal-7%; FTOZ-9.7%; RS + farlateral-2.7%	19.4	42.8	0	SRS-30.5%	66.65	10 (GTR); 33 (NTR); 50 (STR); 18.2 (with SRS)

AP anterior petrosectomy, *PS* presigmoid, *ST* subtemporal, *RS* retrosigmoid, *NS* non specified, *CP* combined petrosectomy, *FT* frontotemporal, *TP* total petrosectomy; PP posterior petrosectomy, OZ orbitozygomatic, *SRS* stereotactic radiosurgery, *RT* conventional radiotherapy, *GTR* gross total resection, *STR* subtotal resection, *NTR* near total resection

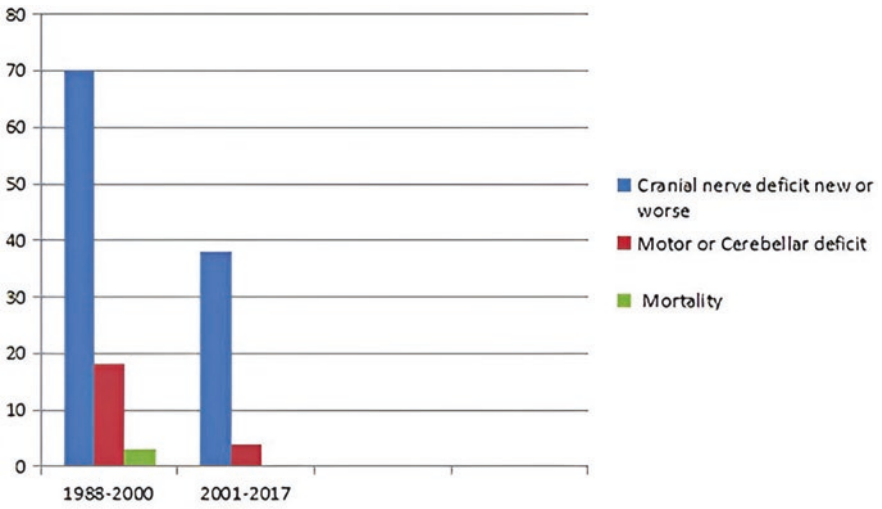

Fig. 9.6 Trends in complications after microsurgery in the senior authors' series, before and after 2001

9.4 Aim for GTR or STR + SRS?

Based on the evidence available (Table 9.3), GTR's role in achieving better PFS is an established fact. Additionally, STR + SRS is increasingly being reported to have comparable PFS to that of GTR but with better functional outcomes. Hence, it is prudent to say that, with persistent efforts to achieve GTR everywhere possible, the extent of resection should be balanced with the preservation of patient's functional status [2]. Figure 9.7 represents the senior author's algorithm for deciding "optimal management" strategy in PCMs [3]. A moderate-sized PCM with a good plane of cleavage from the adjacent neurovascular structures and without a wide attachment can and should undergo GTR. A planned STR is the way to go when the imaging findings suggest an excessive adhesiveness of neurovascular structures, a pial breach, brain stem edema, or a wide en plaque attachment of the tumor involving the exit foramina of multiple cranial nerves. Similarly, the senior author recommends leaving an intra-cavernous extension of the tumor. Patients with STRs can be planned for upfront SRS depending on the temporal course (clinical and radiological) in the preoperative period. Despite all the recent advances in imaging, surprises during surgery are not uncommon, and a seemingly difficult meningioma can occasionally be totally excised.

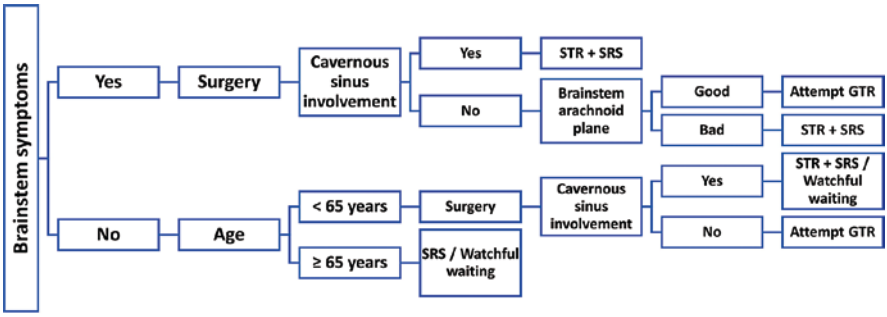

Fig. 9.7 Algorithm for management strategy in PCMs. *STR* subtotal resection, *SRS* stereotactic radiosurgery, *GTR* gross total resection

9.5 Patient Counseling and Decision-Making in PCMs

The management of PCMs is a significant enterprise, with a strong likelihood of permanent disability in a patient's life. It is an absolute necessity that the neurosurgeon spends enough time with the patient and/or relatives, explaining in length the diagnosis and possible therapeutic strategies and their implications. Usually, the benign temporal course of the disease provides sufficient time for multiple sessions of doctor-patient consultations and counseling, prior to scheduling an intervention. An ideal patient for surgical intervention is the one who is driven toward surgery by their tumor's progression (clinical/radiological) and not just by a neurosurgeon's advice. It is of paramount importance to discuss every complication possible, without being harsh, as well as the possible rehabilitation steps that can be taken (e.g., facial palsy can be rehabilitated with reanimation procedures). Discussions should encompass topics of probable cranial nerve palsies, brain stem dysfunction, prolonged hospital stay, tracheostomy/gastrostomy, etc. Though very rare, the mortality risk must be mentioned as well. The practice of omitting hard facts to avoid unpleasant conversations is strictly forbidden for neurosurgeons in PCM surgeries. Active involvement of the patient and/or relatives in the decision-making process will help bridge the gap between expectations and realities in PCM management.

9.6 Conclusion

PCMs are complex skull-base tumors, with variable natural history, and with the potential risk of life changing complications after surgical management. Hence, the process of decision-making—when and whether to intervene, what modality—microsurgery/SRS/combined, if microsurgery what goals- GTR or STR, through which surgical approach, and so on, is critical yet not easy. Not all patients with PCM need treatment. However, many who reach the neurosurgeons, with a symptomatic disease need surgery. The aim of the surgery in PCMs is always a GTR, yet

this can be achieved in less than half of the patients with acceptable morbidity. The remainder of the patients are better treated by STR followed by SRS for residual tumor control. A subset of patients with PCM may be best treated by primary SRS. A flexible approach to individualizing the "optimal management" strategy for a given patient is the only way forward. Unfortunately, decision-making comes with experience, and experience does not come without a price—the painful price of complications.

Conflict of Interest Statement The authors have no conflict of interest concerning reported materials or methods.

References

1. Almefty R, Dunn IF, Pravdenkova S, Abolfotoh M, Al-Mefty O. True petroclival meningiomas: results of surgical management. Clinical article. J Neurosurg. 2014;120(1):40–51.
2. Giammattei L, di Russo P, Starnoni D, Passeri T, Bruneau M, Meling TR, et al. Petroclival meningiomas: update of current treatment and consensus by the EANS skull base section. Acta Neurochir. 2021;163(6):1639–63.
3. Kankane V, Misra B. Petroclival meningioma: management strategy and results in 21st century. Asian J Neurosurg. 2021;16(1):89.
4. Misra B. Intracranial meningioma. In: Ramamurthi B, Tandon P, editors. Textbook of neurosurgery. 2nd ed. New Delhi: Churchill Livingstone; 1996. p. 1077–110.
5. Misra B, Rout D, Rao V, Rout A. Petroclival meningioma: surgical experience with 11 cases. In: In: 40th annual conference, neurological Society of India. Manipal; 1991. p. 25.
6. al-Mefty O, Ayoubi S, Smith RR. The petrosal approach: indications, technique, and results. In: Acta neurochirurgica Supplementum [Internet]. 1991. p. 166–70. Available from: http://link.springer.com/10.1007/978-3-7091-9183-5_27.
7. Couldwell WT, Fukushima T, Giannotta SL, Weiss MH. Petroclival meningiomas: surgical experience in 109 cases. J Neurosurg. 1996;84(1):20–8.
8. Samii M, Ammirati M, Mahran A, Bini W, Sepehrnia A. Surgery of petroclival meningiomas: report of 24 cases. Neurosurgery [Internet]. 1989;24(1):12–7. Available from: https://academic.oup.com/neurosurgery/article/24/1/12/2745939.
9. Spetzler RF, Daspit CP, Pappas CTE. The combined supra- and infratentorial approach for lesions of the petrous and clival regions; experience with 46 cases. J Neurosurg [Internet]. 1992;76(4):588–99. Available from: https://thejns.org/view/journals/j-neurosurg/76/4/article-p588.xml.
10. Ojemann RG. Skull-base surgery: a perspective. J Neurosurg [Internet]. 1992;76(4):569–70. Available from: https://thejns.org/view/journals/j-neurosurg/76/4/article-p569.xml.
11. Roche P-H, Pellet W, Fuentes S, Thomassin J-M, Régis J. Gamma knife radiosurgical management of petroclival meningiomas results and indications. Acta Neurochir (Wien) [Internet]. 2003;145(10):883–8. Available from: http://link.springer.com/10.1007/s00701-003-0123-1.
12. Natarajan SK, Sekhar LN, Schessel D, Morita A. Petroclival meningiomas: multimodality treatment and outcomes at long-term follow-up. Neurosurgery. 2007;60(6):965–79.
13. Park C-K, Jung H-W, Kim JE, Paek SH, Kim DG. The selection of the optimal therapeutic strategy for petroclival meningiomas. Surg Neurol [Internet]. 2006;66(2):160–5. Available from: https://linkinghub.elsevier.com/retrieve/pii/S009030190600067X.
14. Misra B. Management of central skull base tumors. In: Sindou M, editor. Practical handbook of neurosurgery: from leading neurosurgeons. 2nd ed. New York: Springer; 2009. p. 115–28.

15. Bindal R, Goodman JM, Kawasaki A, Purvin V, Kuzma B. The natural history of untreated skull base meningiomas. Surg Neurol [Internet]. 2003;59(2):87–92. Available from: https://linkinghub.elsevier.com/retrieve/pii/S0090301902009953.
16. Van Havenbergh T, Carvalho G, Tatagiba M, Plets C, Samii M. Natural history of Petroclival Meningiomas. Neurosurgery [Internet]. 2003;52(1):55–64. Available from: http://content.wkhealth.com/linkback/openurl?sid=WKPTLP:landingpage&an=00006123-200301000-00006.
17. Terasaka S, Asaoka K, Kobayashi H, Yamaguchi S, Sawamura Y. Natural history and surgical results of petroclival meningiomas. No Shinkei Geka [Internet]. 2010;38(9):817–24. Available from: http://www.ncbi.nlm.nih.gov/pubmed/20864770.
18. Sughrue ME, Rutkowski MJ, Aranda D, Barani IJ, McDermott MW, Parsa AT. Treatment decision making based on the published natural history and growth rate of small meningiomas. J Neurosurg [Internet]. 2010;113(5):1036–42. Available from: https://thejns.org/view/journals/j-neurosurg/113/5/article-p1036.xml.
19. Hashimoto N, Rabo CS, Okita Y, Kinoshita M, Kagawa N, Fujimoto Y, et al. Slower growth of skull base meningiomas compared with non–skull base meningiomas based on volumetric and biological studies. J Neurosurg [Internet]. 2012;116(3):574–80. Available from: https://thejns.org/view/journals/j-neurosurg/116/3/article-p574.xml.
20. Hunter JB, Weaver KD, Thompson RC, Wanna GB. Petroclival Meningiomas. Otolaryngol Clin North Am [Internet]. 2015;48(3):477–90. Available from: https://linkinghub.elsevier.com/retrieve/pii/S0030666515000213.
21. Romani R, Ryan G, Benner C, Pollock J. Non-operative meningiomas: long-term follow-up of 136 patients. Acta Neurochir (Wien) [Internet]. 2018;160(8):1547–53. Available from: http://link.springer.com/10.1007/s00701-018-3554-4.
22. Seifert V. Clinical management of petroclival meningiomas and the eternal quest for preservation of quality of life. Acta Neurochir (Wien) [Internet]. 2010;152(7):1099–116. Available from: http://link.springer.com/10.1007/s00701-010-0633-6.
23. Islim AI, Mohan M, Moon RDC, Srikandarajah N, Mills SJ, Brodbelt AR, et al. Incidental intracranial meningiomas: a systematic review and meta-analysis of prognostic factors and outcomes. J Neurooncol [Internet]. 2019;142(2):211–21. Available from: http://link.springer.com/10.1007/s11060-019-03104-3.
24. Ramina R, Neto MC, Fernandes YB, Silva EB, Mattei TA, Aguiar PHP. Surgical removal of small petroclival meningiomas. Acta Neurochir (Wien) [Internet]. 2008;150(5):431–9. Available from: http://link.springer.com/10.1007/s00701-007-1403-y.
25. Xu F, Karampelas I, Megerian CA, Selman WR, Bambakidis NC. Petroclival meningiomas: an update on surgical approaches, decision making, and treatment results. Neurosurg Focus. 2013;35(6):1–10.
26. Misra B. Surgical approaches to petroclival region. In: Prog Clin Neurosci. 14th ed. 1999. p. 183–92.
27. Pirayesh A, Petrakakis I, Raab P, Polemikos M, Krauss JK, Nakamura M. Petroclival meningiomas: magnetic resonance imaging factors predict tumor resectability and clinical outcome. Clin Neurol Neurosurg [Internet]. 2016;147:90–7. https://doi.org/10.1016/j.clineuro.2016.06.002.
28. Sekhar LN, Wright DC, Richardson R, Monacci W. Petroclival and foramen magnum meningiomas: surgical approaches and pitfalls. J Neurooncol [Internet]. 1996;29(3):249–59. Available from: http://link.springer.com/10.1007/BF00165655.
29. Maurer A, Safavi-Abbasi S, Cheema A, Glenn C, Sughrue M. Management of Petroclival Meningiomas: a review of the development of current therapy. J Neurol Surg Part B Skull Base [Internet]. 2014;75(05):358–67. Available from: http://www.thieme-connect.de/DOI/DOI?10.1055/s-0034-1373657.
30. Yao A, Pain M, Balchandani P, Shrivastava RK. Can MRI predict meningioma consistency?: a correlation with tumor pathology and systematic review. Neurosurg Rev [Internet]. 2018;41(3):745–53. Available from: http://link.springer.com/10.1007/s10143-016-0801-0.

31. Nicosia L, Di PS, Catapano M, Spadarella G, Sammut L, Cannataci C, et al. Petroclival meningiomas: radiological features essential for surgeons. Ecancermedicalscience [Internet]. 2019:13. Available from: https://ecancer.org/journal/13/full/907-petroclival-meningiomas-radiological-features-essential-for-surgeons.php.
32. Samii M, Tatagiba M, Carvalho GA. Retrosigmoid intradural suprameatal approach to Meckel's cave and the middle fossa: surgical technique and outcome. J Neurosurg [Internet]. 2000;92(2):235–41. Available from: https://thejns.org/view/journals/j-neurosurg/92/2/article-p235.xml.
33. Chen L, Yu X, Bu B, Xu B, Zhou D. The retrosigmoid approach to petroclival meningioma surgery. J Clin Neurosci [Internet]. 2011;18(12):1656–61. Available from: https://linkinghub.elsevier.com/retrieve/pii/S0967586811003080.
34. Singh N, Singh D, Ahmad F, Kumar R. The retrosigmoid approach: workhorse for petroclival meningioma surgery. Asian J Neurosurg [Internet]. 2019;14(1):188. Available from: http://www.asianjns.org/text.asp?2019/14/1/188/250005.
35. Siwanuwatn R, Deshmukh P, Figueiredo EG, Crawford NR, Spetzler RF, Preul MC. Quantitative analysis of the working area and angle of attack for the retrosigmoid, combined petrosal, and transcochlear approaches to the petroclival region. J Neurosurg [Internet]. 2006;104(1):137–42. Available from: https://thejns.org/view/journals/j-neurosurg/104/1/article-p137.xml.
36. Yamahata H, Tokimura H, Hirahara K, Ishii T, Mori M, Hanaya R, et al. Lateral suboccipital retrosigmoid approach with tentorial incision for petroclival meningiomas: technical note. J Neurol Surg B Skull Base [Internet]. 2014;75(4):221–4. Available from: http://www.ncbi.nlm.nih.gov/pubmed/25093143.
37. Qing-jiu Z, Bo L, Dangmuren-jiafu G, Qiang F, Xiao-jiang C, Kaheerman K, et al. Microsurgery with or without neuroendoscopy in 24 petroclival meningiomas. Turk Neurosurg [Internet]. 2013; Available from: http://www.turkishneurosurgery.org.tr/summary_en_doi.php3?doi=10.5137/1019-5149.JTN.8670-13.1.
38. Kawase T, Shiobara R, Toya S. Middle fossa transpetrosal-transtentorial approaches for petroclival meningiomas selective pyramid resection and radicality. Acta Neurochir (Wien) [Internet]. 1994;129(3–4):113–20. Available from: http://link.springer.com/10.1007/BF01406489
39. Bambakidis NC, Kakarla UK, Kim LJ, Nakaji P, Porter RW, Daspit CP, et al. Evolution of surgical approaches in the treatment of petroclival meningiomas. Neurosurgery [Internet]. 2008;62(suppl_3):ONS202–11. Available from: https://academic.oup.com/neurosurgery/article/62/suppl_3/ONS202/2607525.
40. Grossi PM, Nonaka Y, Watanabe K, Fukushima T. The history of the combined supra- and infratentorial approach to the petroclival region. Neurosurg Focus [Internet]. 2012;33(2):E8. Available from: https://thejns.org/view/journals/neurosurg-focus/33/2/2012.6.focus12141.xml.
41. Borghei-Razavi H, Truong HQ, Fernandes Cabral DT, Sun X, Celtikci E, Wang E, et al. Endoscopic endonasal petrosectomy: anatomical investigation, limitations, and surgical relevance. Oper Neurosurg [Internet]. 2019;16(5):557–70. Available from: https://journals.lww.com/01787389-201905000-00004.
42. Beer-Furlan A, Abi-Hachem R, Jamshidi AO, Carrau RL, Prevedello DM. Endoscopic trans-sphenoidal surgery for petroclival and clival meningiomas. J Neurosurg Sci [Internet]. 2016;60(4):495–502. Available from: http://www.ncbi.nlm.nih.gov/pubmed/27280545.
43. Van Gompel JJ, Alikhani P, Tabor MH, van Loveren HR, Agazzi S, Froelich S, et al. Anterior inferior petrosectomy: defining the role of endonasal endoscopic techniques for petrous apex approaches. J Neurosurg [Internet]. 2014;120(6):1321–5. Available from: https://thejns.org/view/journals/j-neurosurg/120/6/article-p1321.xml.
44. Beer-Furlan A, Vellutini EA, Gomes MQT, Cardoso AC, Prevedello LM, Todeschini AB, et al. Approach selection and surgical planning in posterior cranial fossa Meningiomas: how I do it. J Neurol Surg Part B Skull Base [Internet]. 2019;80(04):380–91. Available from: http://www.thieme-connect.de/DOI/DOI?10.1055/s-0038-1675589.

45. Samii M, Gerganov V, Giordano M, Samii A. Two step approach for surgical removal of petroclival meningiomas with large supratentorial extension. Neurosurg Rev [Internet]. 2011;34(2):173–9. Available from: http://link.springer.com/10.1007/s10143-010-0299-9.
46. Arnaout O, Al-Mefty O. Combined petrosal approach for petroclival meningioma. Neurosurg Focus [Internet]. 2017;43(videosuppl2):V6. Available from: https://thejns.org/view/journals/neurosurg-focus/43/videosuppl2/2017.10.FocusVid.17343.xml.
47. Starke R, Kano H, Ding D, Nakaji P, Barnett GH, Mathieu D, et al. Stereotactic radiosurgery of petroclival meningiomas: a multicenter study. J Neurooncol [Internet]. 2014;119(1):169–76. Available from: http://link.springer.com/10.1007/s11060-014-1470-x.
48. Brian RS, Lunsford LD, Douglas K, Ann HM, John CF. Management of petroclival meningiomas by stereotactic radiosurgery. Neurosurgery [Internet]. 1998;42(3):437–45. Available from: https://academic.oup.com/neurosurgery/article/42/3/437/2843300.
49. Flannery TJ, Kano H, Lunsford LD, Sirin S, Tormenti M, Niranjan A, et al. Long-term control of petroclival meningiomas through radiosurgery: clinical article. J Neurosurg. 2010;112(5):957–64.
50. Sadik ZHA, Te LS, Leenstra S, Hanssens PEJ. Volumetric changes and clinical outcome for petroclival meningiomas after primary treatment with Gamma Knife radiosurgery. J Neurosurg [Internet]. 2018;129(6):1623–9. Available from: https://thejns.org/view/journals/j--neurosurg/129/6/article-p1623.xml.
51. Fatima N, Meola A, Pollom E, Chaudhary N, Soltys S, Chang SD. Stereotactic radiosurgery in large intracranial Meningiomas: a systematic review. World Neurosurg [Internet]. 2019;129:269–75. Available from: https://linkinghub.elsevier.com/retrieve/pii/S1878875019316067.
52. Iwai Y, Yamanaka K, Shimohonji W, Ishibashi K. Staged gamma knife radiosurgery for large skull base meningiomas. Cureus. 2019;11(10):1–9.
53. Oh H-J, Cho YH, Kim JH, Kim CJ, Kwon DH, Lee D, et al. Hypofractionated stereotactic radiosurgery for large-sized skull base meningiomas. J Neurooncol [Internet]. 2020;149(1):87–93. Available from: https://link.springer.com/10.1007/s11060-020-03575-9.
54. Adeberg S, Harrabi SB, Verma V, Bernhardt D, Grau N, Debus J, et al. Treatment of meningioma and glioma with protons and carbon ions. Radiat Oncol [Internet]. 2017;12(1):193. Available from: http://www.ncbi.nlm.nih.gov/pubmed/29195506.
55. Tatagiba M, Samii M, Matthies C, Vorkapic P. Management of petroclival meningiomas: a critical analysis of surgical treatment. In: Modern neurosurgery of meningiomas and pituitary adenomas [internet]. Vienna: Springer; 1996. p. 92–4. Available from: http://link.springer.com/10.1007/978-3-7091-9450-8_25.
56. Little KM, Friedman AH, Sampson JH, Wanibuchi M, Fukushima T. Surgical management of petroclival meningiomas: defining resection goals based on risk of neurological morbidity and tumor recurrence rates in 137 patients. Neurosurgery. 2005;56(3):546–58.
57. Bambakidis NC, Kakarla UK, Kim LJ, Nakaji P, Porter RW, Daspit CP, et al. Evolution of surgical approaches in the treatment of Petroclival Meningiomas: a retrospective review. Oper Neurosurg [Internet]. 2007;61(suppl_5):ONS202–11. Available from: https://academic.oup.com/ons/article/61/suppl_5/ONS202/2408362.
58. Li P, Mao Y, Zhu W, Zhao N, Zhao Y, Chen L. Surgical strategies for petroclival meningioma in 57 patients. Chin Med J (Engl) [Internet]. 2010;123(20):2865–73. Available from: http://www.ncbi.nlm.nih.gov/pubmed/21034598.
59. Yang J, Fang T, Ma S, Yang S, Qi J, Qi Z, et al. Large and giant petroclival meningiomas: therapeutic strategy and the choice of microsurgical approaches – report of the experience with 41 cases. Br J Neurosurg [Internet]. 2011;25(1):78–85. Available from: http://www.tandfonline.com/doi/full/10.3109/02688697.2010.539716.
60. Nanda A, Javalkar V, Banerjee AD. Petroclival meningiomas: study on outcomes, complications and recurrence rates - clinical article. J Neurosurg. 2011;114(5):1268–77.
61. Li D, Hao S-Y, Wang L, Tang J, Xiao X-R, Zhou H, et al. Surgical management and outcomes of petroclival meningiomas: a single-center case series of 259 patients. Acta Neurochir

(Wien) [Internet]. 2013;155(8):1367–83. Available from: http://link.springer.com/10.1007/s00701-013-1795-9.
62. Tao J, Wang Y, Qiu B, Ou S, Wang Y, Wu P. Selection of surgical approaches based on semi-quantifying the skull-base invasion by petroclival meningiomas: a review of 66 cases. Acta Neurochir (Wien) [Internet]. 2014;156(6):1085–97. Available from: http://link.springer.com/10.1007/s00701-014-2084-y.
63. Panigrahi M, Vooturi S, Patibandla M, Kulkarni D. Novel classification for surgical approach of petroclival meningiomas: a single-surgeon experience. Neurol India [Internet]. 2015;63(5):718. Available from: http://www.neurologyindia.com/text.asp?2015/63/5/718/166551.
64. Sassun TE, Ruggeri AG, Delfini R. True petroclival meningiomas: proposal of classification and role of the combined supra-Infratentorial Presigmoid Retrolabyrinthine approach. World Neurosurg [Internet]. 2016;96:111–23. https://doi.org/10.1016/j.wneu.2016.08.023.
65. Bernard F, Troude L, Isnard S, Lemée JM, Terrier LM, François P, et al. Long term surgical results of 154 petroclival meningiomas: a retrospective multicenter study. Neurochirurgie. 2019;65(2–3):55–62.
66. Qiao L, Yu C, Zhang H, Zhang M, Qu Y, Ren M, et al. Clinical outcomes and survival analysis for petroclival meningioma patients receiving surgical resection: an analysis of 176 cases. Cancer Manag Res [Internet]. 2019;11:5949–59. Available from: https://www.dovepress.com/clinical-outcomes-and-survival-analysis-for-petroclival-meningioma-pat-peer-reviewed-article-CMAR.
67. Kim JW, Jung H-W, Kim YH, Park C-K, Chung H-T, Paek SH, et al. Petroclival meningiomas: long-term outcomes of multimodal treatments and management strategies based on 30 years of experience at a single institution. J Neurosurg [Internet]. 2020;132(6):1675–82. Available from: https://thejns.org/view/journals/j-neurosurg/132/6/article-p1675.xml.
68. Zhao Z, Yuan X, Yuan J, Cai L, Jiang W, Xie Y, et al. Treatment strategy for Petroclival Meningiomas based on a proposed classification in a study of 168 cases. Sci Rep [Internet]. 2020;10(1):4655. Available from: http://www.nature.com/articles/s41598-020-61497-y.
69. Bernard F, Troude L, Isnard S, Lemée J-M, Terrier LM, François P, et al. Long term surgical results of 154 petroclival meningiomas: a retrospective multicenter study. Neurochirurgie [Internet]. 2019;65(2–3):55–62. Available from: https://linkinghub.elsevier.com/retrieve/pii/S002837701930027X.
70. Misra B. Management of petroclival meningioma: the role of excision and radiosurgery. In: Al-Mefty O, editor. Controversies in neurosurgery II. New York: Thieme Publishers; 2014. p. 30–6.

Chapter 10
Parasagittal Meningiomas: Prognostic Factors for Recurrence

Apio Antunes and Rafael Winter

10.1 Introduction

Meningioma is the most common benign intracranial neoplasm, accounting for about 30% of all primary brain tumors. Its incidence increases with age, and it is more prevalent in females, with a male-to-female ratio of 2:111 [1, 2].

The brain and spinal cord are covered by layers of connective tissue and fibroblasts known as the meninges. These layers are subdivided into three: the dura mater, the pia mater, and the arachnoid. It is in the latter that the cellular origin of meningiomas lies [3].

There are three grades of meningioma, based on histological classification, with 90% being benign and the rest subdivided into atypical and anaplastic.

Often diagnosed incidentally during neuroimaging (computed tomography or magnetic resonance imaging) performed for other purposes, meningiomas are characterized by marked contrast uptake and by their extra-axial location.

Not all diagnosed patients require treatment. A decision must be made taking into account the patient's clinical status and symptoms, tumor characteristics (topography, appearance on imaging), tumor biology, and the risk/benefit ratio of

A. Antunes
Neurosurgical Department, University Hospital, Porto Alegre, Brazil

Porto Alegre Medical School, UFRGS, Porto Alegre, Brazil
e-mail: aantunes@hcpa.edu.br

R. Winter (✉)
University Hospital, Porto Alegre, Brazil

Neurosurgery Department, Hospital de Clínicas de Porto Alegre, Porto Alegre, Brazil
e-mail: rwinter@hcpa.edu.br

C. Di Rocco (ed.), *Advances and Technical Standards in Neurosurgery*,
Advances and Technical Standards in Neurosurgery 48,
https://doi.org/10.1007/978-3-031-36785-4_10

any potential intervention. Surgical management is always the first choice for the treatment of meningioma.

Other therapeutic modalities, such as radiosurgery, radiotherapy, proton therapy, anti-hormonal therapy, antiangiogenic therapy, and, more recently, gene therapy, are available—sometimes as first-line treatment, sometimes as an adjunct to surgical resection.

10.2 Classification

Parasagittal meningiomas can be classified on the basis of their relationship to the sagittal sinus:

- Anterior third (from the crista galli to the coronal suture).
- Middle third (from the coronal suture to the lambdoid suture).
- Posterior third (from the lambdoid suture to the confluence of sinuses).

The prevalence of meningioma ranges from 14% to 33% in the anterior third, 44% to 70% in the middle third, and 9% to 29% in the posterior third.

Bonnal and Brotchi [4], in a 1978 article describing their operative technique for reconstruction of the superior sagittal sinus in an attempt to obtain a Simpson grade I resection [5], found six types of parasagittal meningiomas, classified according to their relationship with the superior sagittal sinus (Fig. 10.1):

- Type I: Tumor invading only the external layer of the SSS wall.
- Type II: Tumor involving the entire wall of the SSS, without invading it.
- Type III: Tumor invades only the lateral recess of the SSS.
- Type IV: Tumor invades the wall and SSS unilaterally.
- Type V: Tumor invades two walls of the SSS but does not obstruct it.
- Type VI: Tumor invades two walls of the SSS, without obstructing it, extending to the contralateral side.
- Type VII: Tumor invades two walls of the SSS, obstructing it.
- Type VIII: Tumor invades all three walls of the SSS, obstructing it.

In the 2000s, a new classification deemed more useful for deciding on surgical treatment was suggested by Sindou et al. [6], considering the type of tumor invasion of the SSS and the patency of venous blood flow within it (Fig. 10.2):

- Type I: Tumor invading only the external layer of the SSS wall.
- Type II: Tumor invades only the lateral recess of the SSS.
- Type III: Tumor invades the ipsilateral wall of the SSS.
- Type IV: Tumor invades the ipsilateral wall and roof of the SSS, without obstructing it.
- Type V: Tumor invades the ipsilateral wall and roof, completely obstructing the SSS.

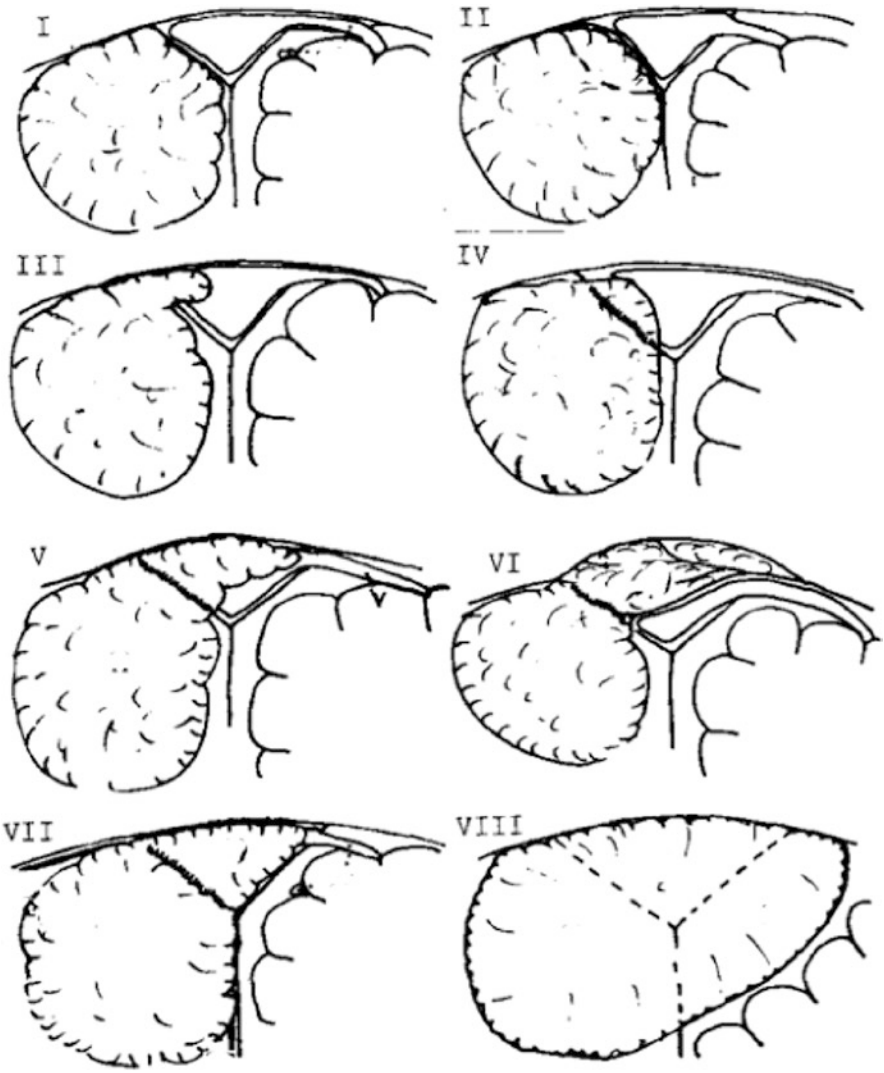

Fig. 10.1 Parasagittal meningiomas, classified according to their relationship with the superior sagittal sinus [4]

- Type VI: Tumor invades two walls and the roof of the SSS, completely obstructing it.

As described above, the term parasagittal meningioma applies to those tumors that are associated with the superior sagittal sinus, originating from the dura in close relation to the parasagittal wall or angle. However, a 1989 case report by Steiger et al. [7] described the radical resection of a meningioma located within the sinus

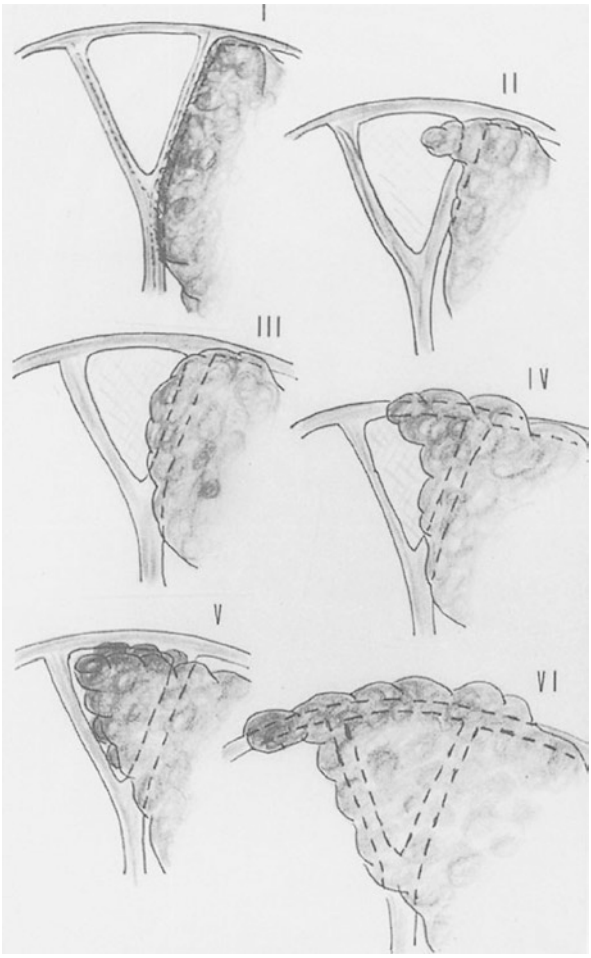

Fig. 10.2 Type of tumor invasion of the SSS. (From 28, with permission)

without, however, invading its lateral wall. This did not meet the criteria used at the time to describe parasagittal meningiomas.

In this regard, in a 2020 letter to the editor, Yin et al. [8] reported on growing evidence of tumors originating within the superior sagittal sinus, suggesting that these tumors did not originate from the arachnoid cells located in the parasagittal angle but rather from the arachnoid cells present in arachnoid granulations within the sagittal sinus; they named this type of tumor *superior sagittal sinus meningioma*. Taking these aspects into account, they suggested a new classification, which still requires support from additional studies:

Type I: Tumors arising from the lateral angle of the SSS wall.

Ia: Tumor invades only the lateral recess or the outer surface of the SSS wall.
Ib: Tumor invades one or two inner wall surfaces, with or without displacement or constriction of the SSS.

Ic: Complete occlusion of the SSS, with or without one of its walls free.

Type II: Tumors arising within the SSS.

IIa: Tumor invades only the lateral recess or the inner surface of the SSS wall.
IIb: Tumor invades the medial surface of two walls, with bilateral enlargement of the SSS.
IIc: Tumor invades all medial surfaces of the SSS walls, with complete occlusion with or without subdural space invasion.

10.3 Histology

The histological classification of parasagittal meningiomas is identical to that of meningiomas located elsewhere, based on the 2016 WHO criteria. This classification divides meningiomas into three grades:

Grade 1: Benign meningiomas (85% to 90% of cases), which includes meningothelial, fibrous (fibroblastic), transitional, psammomatous, angiomatous, microcystic, secretory, lymphoplasmocyte-rich, and metaplastic meningiomas.

Grade 2: More aggressive meningiomas (5–10% of cases), which include clear-cell, choroidal, and atypical meningiomas.

Grade 3: Malignant meningiomas, which account for 3–5% of cases and include papillary, rhabdoid, and anaplastic meningiomas.

10.4 Clinical Presentation and Diagnosis

Meningiomas originating from the anterior third tend to have a more insidious course, often reaching quite large dimensions before a diagnosis is established. Due to their topography, symptoms may include behavior and personality changes, dementia, or apathy. Generalized seizures are unusual, with headache being the most common symptom. For tumors originating in the middle third of the SSS, focal, motor, or sensory seizures are more frequent, as is a progressive motor deficit, with onset usually occurring in the lower limbs. Tumors originating in the posterior third can manifest as visual symptoms, most commonly visual field defects, but headache is still more prevalent.

The diagnosis is established through imaging. Due to the increasingly frequent use of neuroimaging in current medical practice, many parasagittal meningiomas are diagnosed incidentally in asymptomatic patients.

The general appearance is that of an extra-axial, rounded, or lobulated mass with well-demarcated boundaries, adherent to the dura of the outer surface of the SSS wall, usually growing from its lateral recess, either space-occupying or displacing adjacent neurovascular structures (Fig. 10.3). Invasion of the cerebral parenchyma

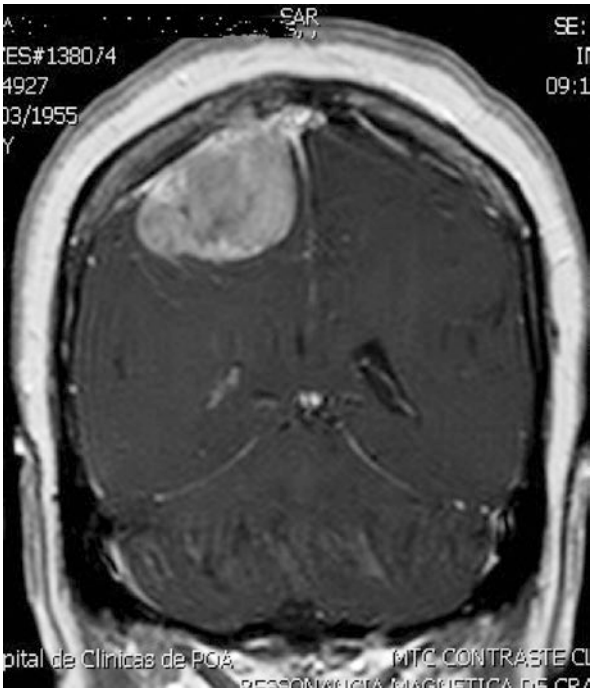

Fig. 10.3 Parassagital meningioma displacing or invading sinus sagittal

is uncommon and, when present, is indicative of greater histological aggressiveness. As discussed above, intrusion into the SSS may or may not be present (Fig. 10.4).

- Head CT:
  - Hyperdense (75%) or isodense (25%).
  - Necrosis or hemorrhage is rare.
  - 25% are calcified.
  - Hypodense adjacent parenchyma (suggesting peritumoral vasogenic edema) in up to 60% of cases.
  - Hyperostosis (often denoting bone invasion) is not associated with worse histological prognosis.
  - Contrast enhancement is usually uniform.
- Brain MRI:
  - Isointense (or slightly hypointense) on T1, hyperintense on T2.
  - Hypointense on T2/FLAIR (very hypointense tumors tend to be quite hard and may appear extremely calcified on head CT).
  - Can vary from iso- to hyperintense on FLAIR. Useful for diagnosing cerebral edema, suggesting tumor nutrition through the pial vessels and expression of vascular growth factors; neither, however, correlates with histological grade.

Fig. 10.4 Magnetic resonance venography showing the sinus sagittal filling defect caused by tumor invasion

- Essentially all meningiomas, even extremely calcified ones, present some degree of contrast enhancement. A total of 95% exhibit even and consistent uptake.
- Most meningiomas do not restrict diffusion.
- Increased perfusion suggests greater aggressiveness, being more commonly present in grade II and III meningiomas.

A common feature is the "dural tail." This refers to a focus of dural thickening and enhancement, which is adjacent to but extends beyond the tumor boundaries and represents a benign, non-pathognomonic reaction of the dura.

10.5 Treatment

Surgical treatment of meningiomas involving the superior sagittal sinus always presents a challenge.

In 1957, Simpson [3] described the association between tumor recurrence and grade of tumor resection, creating the five-grade classification, which now bears his name:

Simpson I: Macroscopically complete removal (i.e., gross total resection) of the tumor, with excision of its dural attachment and of any abnormal bone (if pres-

ent). In the case of the superior sagittal sinus, this entails resecting the lateral wall of the SSS.

Simpson II: Macroscopically complete removal of the tumor with thermal coagulation of its dural attachment.

Simpson III: Macroscopically complete removal of the tumor without thermal coagulation or resection of its dural attachment or, alternatively, of its extradural extensions.

Simpson IV: Subtotal tumor resection.

Simpson V: Tumor decompression alone, with or without biopsy.

The recurrence rate associated with each Simpson grade of resection is 6% for grade I, 16% for grade II, 29% for grade III, and 44% for grade IV, clearly demonstrating the importance of the extent of resection for prognosis.

In 2021, Spille et al. [9] used postoperative MRI with the aim of eliminating the subjective factor inherent to the Simpson scale and found residual tumor in 8% of patients previously described has having a Simpson grade I-III resection. They concluded that residual tumor volume on postoperative MRI had a higher predictive value for recurrence compared to Simpson grade of resection. Interestingly, these meningiomas erroneously classified as Simpson I–III were either situated at the base of the skull or infiltrating the SSS.

Considering this association, the dilemma of surgical treatment of parasagittal meningioma is whether to leave residual tumor behind or attempt total resection, which places cerebral venous drainage at risk, with an obvious increase in morbidity and mortality. Although radiosurgery is considered effective in controlling growth of residual tumors [10–13], gross total resection of the tumor and its dural attachment (Simpson I) is still superior when disease-free survival is used as the primary outcome [12].

The surgical technique used in the resection of parasagittal meningiomas, and whether SSS reconstruction is necessary, depends on the type of SSS invasion and is divided into three main strategies [14]:

1. Resection of the outer surface of the SSS wall and coagulation of its inner surface.
2. Resection of the entire tumor-invaded SSS wall and subsequent reconstruction using one of three methods:
   (a) Resection of the intraluminal tumor portion and suture of the parasagittal recess edges.
   (b) Resection of the invaded SSS wall followed by repair with an autologous graft (fascia lata, temporal fascia, pericranium, or dura).
   (c) Resection of the tumor-invaded SSS wall and restoration of venous drainage through an autologous (saphenous vein or jugular vein) or heterologous bypass graft.
3. Resection of the invaded SSS wall or coagulation of the residual fragment with no subsequent restoration of venous drainage (Fig. 10.5).

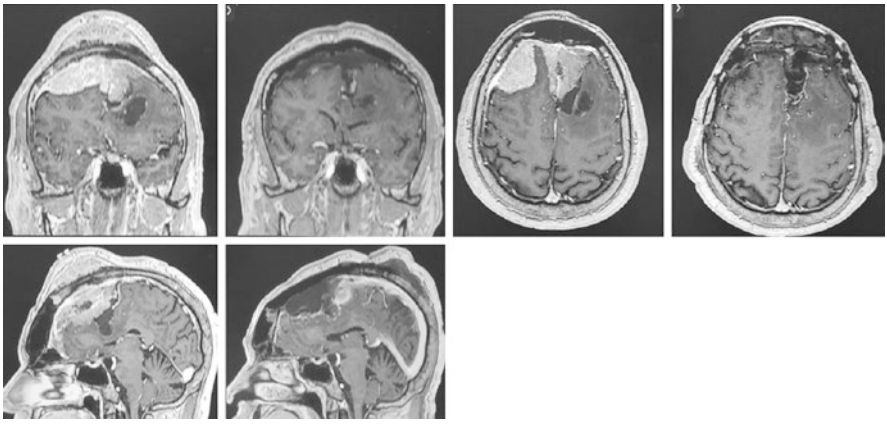

Fig. 10.5 Complete resection of an extensive meningioma invading superior sagittal sinus and skull with no subsequent needing for restoration of venous drainage

Whether complete tumor resection with restoration of venous drainage is necessary or subtotal resection with subsequent radiosurgery/Gamma Knife treatment of the residual lesion is preferred has been hotly debated, with the scales tipped in favor of the latter concept. Some authors suggest resection of the extraluminal portion of meningiomas, which invade the SSS (types III and IV) followed by yearly control MRI, with stereotactic radiotherapy in case growth of any residual tumor is observed. Total resection of the tumor and SSS would be indicated in type V meningiomas with complete occlusion of the SSS and proof of collateral venous drainage [15]. The prognostic value of Simpson grade of resection remains a key factor in therapeutic decision-making and is strongly correlated with disease-free survival. Ossama Al-Mefty, in a 1993 article and, more recently, in a 2022 video, described the concept of "grade-zero" (Simpson) resection, demonstrating the importance of resecting 2–3 cm of dura beyond the tumor attachment [16–18]. When Simpson grade I resection is not possible, the use of adjuvant radiosurgery results in a similar prognosis for Simpson II, III, or IV cases [12], with no increase in morbidity and mortality [11, 19, 20]. As Sindou stated in 2016: "When considering [superior sagittal] sinus surgery, the benefits must be carefully weighed against the risks" [6].

10.6 Radiomics in Meningioma

The concept of radiomics—using imaging to obtain the greatest amount of objective data possible for subsequent computer-aided analysis—has found several tumor characteristics to be closely related to the behavior and biology of meningiomas.

Regarding tumor shape, studies have shown a correlation between histological grade and sphericity, or, more specifically, the extent to which a meningioma is spherically disproportionate. High-grade meningiomas (grades 2 and 3) tend to be

less spherical than low-grade meningiomas (grade 1). This characteristic is also associated with a higher rate of local recurrence and a less favorable prognosis [21–25].

One of the leading factors related to longer disease-free survival is total tumor resection. In parasagittal and skull-base meningiomas, as well as meningiomas with a harder consistency in general, this surgical goal is less likely to be achieved. The former, because they are closely related to vascular structures or cranial nerves; the latter, because they make the procedure more technically challenging without increasing postoperative morbidity and mortality. According to Cepeda et al., tumor consistency can be determined preoperatively—thus facilitating surgical planning—by analyzing radiomic characteristics extracted from MRI (T2W, contrast-enhanced T1W, and ADC map), with 94% accuracy [26].

Another important characteristic that, if determined preoperatively, modifies the objective of surgical resection—as it is closely related to meningioma behavior—is Ki-67 expression. This can be predicted with high accuracy and sensitivity by analyzing certain radiomic features [27].

Other aspects such as the lack of uniformity in the level/intensity of gray, heterogeneity of contrast uptake by the tumor, and poorly defined tumor borders are associated with histological subtype [28, 29], tumor recurrence [24], and invasion of the brain parenchyma [30] and can be useful for differential diagnosis [31], as reported in the literature. As it is a relatively new concept, multicenter prospective studies are still needed to further develop the massive potential of radiomics, which has already been demonstrated in single-center pilot or retrospective studies.

10.7 Molecular Biology in Meningioma

The concept that meningiomas share molecular characteristics with other tumors of the central nervous system and that these are closely related to tumor biological behavior, location, and histology has been increasingly appreciated in recent studies.

Sahm et al. [32] identified six distinct, clinically relevant DNA methylation classes that are more accurate than the WHO histological classification for identifying patients with grade 1 meningiomas at high risk of tumor progression and patients with grade 2 tumors at lower risk of recurrence.

As of 2021, the WHO classification of meningiomas began to include molecular markers for certain histological subtypes. Secretory meningiomas can be diagnosed by simple detection of KLF4/TRAF7 mutations. Likewise, any meningioma with the TERT promoter molecular mutation and/or CDKN2A/B homozygous deletion will be classified as grade 3; these also serve as markers for high risk of tumor recurrence [33].

The most frequent molecular abnormalities in meningiomas are deletions and mutations in chromosome 22q. These molecular changes are additive and are progressively associated with an increase in tumor grade or aggressiveness, with deletion of the short arm of chromosome 1 (1p deletion) and chromosome 10 being the

first events and homozygous deletion CDKN2A/B indicating the most aggressive behavior [33].

More precisely, these genomic features are related to tumor aggressiveness, survival, and disease-free survival, regardless of the grade of initial surgical resection.

Discovery of genetic mutations allowing an advance in the understanding of the molecular biology of meningioma is necessary for the development of new, targeted pharmacotherapies—especially adjuvant or neoadjuvant immunotherapies—for those tumors displaying more aggressive behavior, recurrent tumors, and those in which the therapy of choice, surgery, is associated with high morbidity and mortality [34–37].

Despite advances in the understanding of the radiomics or genomics of meningioma and the potential of these methods to support new drug treatments, the great heterogeneity and mutability of these tumors—even after adjuvant radiotherapy, which is widely indicated and employed in the neurosurgical arsenal—mean that maximal surgical resection is still the mainstay of meningioma treatment and the extent of resection, the only modifiable prognostic factor.

Conflicts of Interest There are no conflicts of interest.

References

1. Central brain tumor registry of the United States. In: Hinsdale 2006;IL:12–26.
2. Cushing H. Meningiomas: their classification, regional behaviour, life history, and surgeical and results. Hafner; 1938.
3. Denizot Y, De Armas R, Caire F, Moreau JJ, Pommepuy I, Truffinet V, Labrousse F. The quantitative analysis of bFGF and VEGF by ELISA in human meningiomas. Mediat Inflamm. 2006 Jan;1:2006.
4. Bonnal J, Brotchi J. Surgery of the superior sagittal sinus in parasagittal meningiomas. J Neurosurg. 1978;48(6):935–45.
5. Simpson D. The recurrence of intracranial meningiomas after surgical treatment. J Neurol Neurosurg Psychiatry. 1957;20(1):22.
6. Sindou M, Auque J. The intracranial venous system as a neurosurgeon's perspective. Adv Tech Stand Neurosurg. 2000:131–216.
7. Steiger HJ, Reulen HJ, Huber P, Boll J. Radical resection of superior sagittal sinus meningioma with venous interposition graft and reimplantation of the rolandic veins. Acta Neurochir. 1989;100(3):108–11.
8. Yin T, Lin K, Wang J, Zhang L, Wang S. Advances in the understanding of Meningiomas involving the superior sagittal sinuses. Neurosurgery. 2020;87(1):E74–6.
9. Spille DC, Hess K, Bormann E, Sauerland C, Brokinkel C, Warneke N, Mawrin C, Paulus W, Stummer W, Brokinkel B. Risk of tumor recurrence in intracranial meningiomas: comparative analyses of the predictive value of the postoperative tumor volume and the Simpson classification. J Neurosurg. 2020;134(6):1764–71.
10. Bowden G, Faramand A, Mallella A, Wei Z, Patel K, Niranjan A, Lunsford LD. Does the timing of radiosurgery after grade 1 meningioma resection affect long-term outcomes? Stereotact Funct Neurosurg. 2021;99(6):506–11.
11. Lv P, Wang JJ, Xiong NX, Liu XM, Yao DX, Jiang XB, Zhao HY, Zhang FC, Fu P. Long-term outcome in meningiomas involving the major dural sinuses with combined therapy

of subtotal resection and early postoperative gamma knife radiosurgery. Acta Neurochir. 2021;163(6):1677–85.
12. Przybylowski CJ, Hendricks BK, Frisoli FA, Zhao X, Cavallo C, Moreira LB, Gandhi S, Sanai N, Almefty KK, Lawton MT, Little AS. Prognostic value of the Simpson grading scale in modern meningioma surgery: Barrow Neurological Institute experience. J Neurosurg. 2020;1(aop):1–9.
13. Sheehan J, Pikis S, Islim AI, Chen CJ, Bunevicius A, Peker S, Samanci Y, Nabeel AM, Reda WA, Tawadros SR, El-Shehaby AM. An international multicenter matched cohort analysis of incidental meningioma progression during active surveillance or after stereotactic radiosurgery: the IMPASSE study. Neuro-Oncology. 2022;24(1):116–24.
14. Sindou MP, Alvernia JE. Results of attempted radical tumor removal and venous repair in 100 consecutive meningiomas involving the major dural sinuses. J Neurosurg. 2006;105(4):514–25.
15. Hancq S, Baleriaux D, Brotchi J. Surgical treatment of parasagittal meningiomas. In: Seminars in neurosurgery, vol. 14, no. 3. New York, NY: Thieme Medical Publishers, Inc.; 2003. p. 203–210.
16. Emerson SN, Rassi MS, Al-Mefty O. Grade zero removal of a Pterional meningioma: 2-dimensional operative video. Operat Neurosurg. 2022;22(2):e80.
17. Kinjo T, Al-Mefty O, Kanaan I. Grade zero removal of supratentorial convexity meningiomas. Neurosurgery. 1993;33(3):394–9.
18. Mooney MA, Abolfotoh M, Bi WL, Tavanaiepour D, Almefty RO, Bassiouni H, Pravdenkova S, Dunn IF, Al-Mefty O. Is falcine meningioma a diffuse disease of the falx? Case series and analysis of a "grade zero" resection. Neurosurgery. 2020;87(5):900–9.
19. Fatima N, Meola A, Ding VY, Pollom E, Soltys SG, Chuang CF, Shahsavari N, Hancock SL, Gibbs IC, Adler JR, Chang SD. The Stanford stereotactic radiosurgery experience on 7000 patients over 2 decades (1999–2018): looking far beyond the scalpel. Journal of Neurosurgery. 2021;1(aop):1–7.
20. Karaaslan B, Celtikci E, Bulduk EB, Borcek AO, Kurt G, Kaymaz M, Aykol S, Emmez H. Stereotactic radiosurgery after subtotal resection of critically-located grade I meningioma: a single-center experience and review of literature. Turk Neurosurg. 2021;31(4):519–29.
21. Coroller TP, Bi WL, Huynh E, Abedalthagafi M, Aizer AA, Greenwald NF, Parmar C, Narayan V, Wu WW, Miranda de Moura S, Gupta S. Radiographic prediction of meningioma grade by semantic and radiomic features. PLoS One. 2017;12(11):e0187908.
22. Morin O, Chen WC, Nassiri F, Susko M, Magill ST, Vasudevan HN, Wu A, Vallières M, Gennatas ED, Valdes G, Pekmezci M. Integrated models incorporating radiologic and radiomic features predict meningioma grade, local failure, and overall survival. Neuro-oncol Adv. 2019;1(1):vdz011.
23. Ward M, Doran J, Paskhover B, Mammis A. The 50 most cited articles in invasive neuromodulation. World Neurosurg. 2018;114:e240–6.
24. Zhang Y, Chen JH, Chen TY, Lim SW, Wu TC, Kuo YT, Ko CC, Su MY. Radiomics approach for prediction of recurrence in skull base meningiomas. Neuroradiology. 2019;61(12):1355–64.
25. Zhu Y, Man C, Gong L, Dong D, Yu X, Wang S, Fang M, Wang S, Fang X, Chen X, Tian J. A deep learning radiomics model for preoperative grading in meningioma. Eur J Radiol. 2019;116:128–34.
26. Cepeda S, Arrese I, García-García S, Velasco-Casares M, Escudero-Caro T, Zamora T, Sarabia R. Meningioma consistency can be defined by combining the radiomic features of magnetic resonance imaging and ultrasound elastography. A pilot study using machine learning classifiers. World Neurosurg. 2021;146:e1147–59.
27. Khanna O, Fathi Kazerooni A, Farrell CJ, Baldassari MP, Alexander TD, Karsy M, Greenberger BA, Garcia JA, Sako C, Evans JJ, Judy KD. Machine learning using multiparametric magnetic resonance imaging Radiomic feature analysis to predict Ki-67 in World Health Organization Grade I meningiomas. Neurosurgery. 2021;89(5):928–36.

28. Li X, Lu Y, Xiong J, Wang D, She D, Kuai X, Geng D, Yin B. Presurgical differentiation between malignant haemangiopericytoma and angiomatous meningioma by a radiomics approach based on texture analysis. J Neuroradiol. 2019;46(5):281–7.
29. Niu L, Zhou X, Duan C, Zhao J, Sui Q, Liu X, Zhang X. Differentiation researches on the meningioma subtypes by radiomics from contrast-enhanced magnetic resonance imaging: a preliminary study. World Neurosurg. 2019;126:e646–52.
30. Zhang J, Yao K, Liu P, Liu Z, Han T, Zhao Z, Cao Y, Zhang G, Zhang J, Tian J, Zhou J. A radiomics model for preoperative prediction of brain invasion in meningioma non-invasively based on MRI: a multicentre study. EBioMedicine. 2020;58:102933.
31. Tian Z, Chen C, Zhang Y, Fan Y, Feng R, Xu J. Radiomic analysis of Craniopharyngioma and meningioma in the Sellar/Parasellar area with MR images features and texture features: a feasible study. Contrast Media Mol Imaging. 2020;2020:4837156.
32. Sahm F, Schrimpf D, Stichel D, Jones DT, Hielscher T, Schefzyk S, Okonechnikov K, Koelsche C, Reuss DE, Capper D, Sturm D. DNA methylation-based classification and grading system for meningioma: a multicentre, retrospective analysis. Lancet Oncol. 2017;18(5):682–94.
33. Goldbrunner R, Stavrinou P, Jenkinson MD, Sahm F, Mawrin C, Weber DC, Preusser M, Minniti G, Lund-Johansen M, Lefranc F, Houdart E. EANO guideline on the diagnosis and management of meningiomas. Neuro-Oncology. 2021;23(11):1821–34.
34. Bi WL, Dunn IF. Current and emerging principles in surgery for meningioma. Chin Clin Oncol. 2017;6(Suppl 1):S7.
35. Bi WL, Prabhu VC, Dunn IF. High-grade meningiomas: biology and implications. Neurosurg Focus. 2018;44(4):E2.
36. Gupta S, Bi WL, Dunn IF. Medical management of meningioma in the era of precision medicine. Neurosurg Focus. 2018;44(4):E3.
37. Winter RC, Antunes AC, de Oliveira FH. The relationship between vascular endothelial growth factor and histological grade in intracranial meningioma. Surgical. Neurol Int. 2020;11:328.

Chapter 11
Pediatric Pineal Region Tumors: Special Reference to Posterior Interhemispheric Trans-Tentorial Approach

Tadanori Tomita

11.1 Introduction

11.1.1 Anatomy and Physiology

The pineal region is bordered by the cerebrospinal fluid (CSF) space, the third ventricle anteriorly, and the quadrigeminal cistern posteriorly around the pineal gland. The brain structures that surround the pineal gland are inferiorly the tecum (quadrigeminal plate), the superior medullary velum (SMV) and the superior cerebellar peduncles and posteriorly the cerebellar vermis posteriorly, and superiorly the splenium of the corpus callosum. Anterolaterally to the pineal gland are the posterior thalami, and anteroinferiorly is the posterior commissure and the tegmentum of the midbrain, which composes the posterior floor of the third ventricle. Laterally across the cistern, there is the isthmus of the cingulate gyrus at the medial temporooccipital lobe junction (Fig. 11.1).

The tela choroidea and fornix form the roof of the third ventricle. The tela choroidea, a pial infolding, extends through the transverse fissure below the splenium of the corpus callosum. Posteriorly, the superior layer of the tela choroidea is continuous with the pia of the splenium of the corpus callosum, and the inferior layer of the tela choroidea is continuous with the pia covering the midbrain and the sheath for the pineal gland. The tela choroidea passes between the fornix and the roof of the third ventricle. The tela choroidea narrows anteriorly and ends in an apex at the

T. Tomita (✉)
Division of Pediatric Neurosurgery, Ann & Robert Lurie Children's Hospital of Chicago, Chicago, IL, USA

Neurological Surgery, Northwestern University Feinberg School of Medicine, Chicago, IL, USA
e-mail: ttomita@luriechildrens.org; ttomita@northwestern.edu

C. Di Rocco (ed.), *Advances and Technical Standards in Neurosurgery*, Advances and Technical Standards in Neurosurgery 48,
https://doi.org/10.1007/978-3-031-36785-4_11

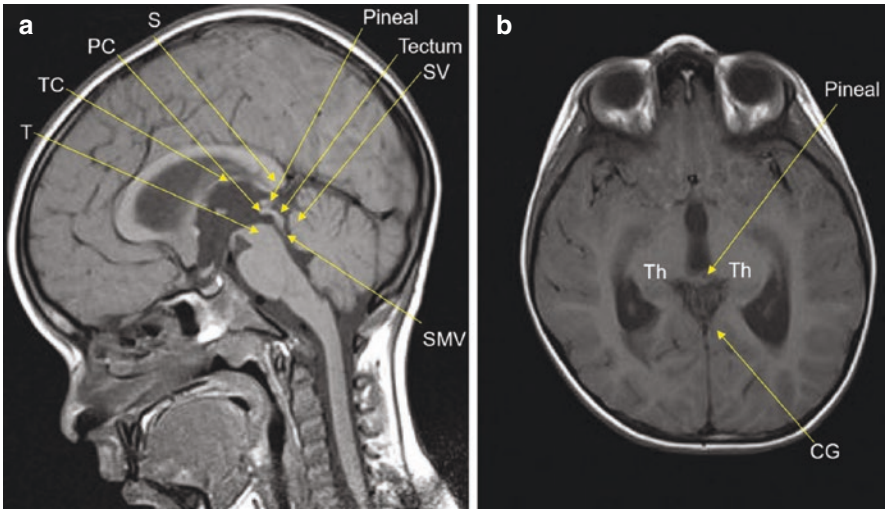

Fig. 11.1 Pineal region anatomy (CG, isthmus of cingulate gyrus; PC, posterior commissure; S, splenim of corpus callosum; SMV, superior medullary velum; SV, superior vermis; T, tectum; TC, tela choroidea; Th, thalamus)

foramen of Monro. This pial infolding of tela choroidea contains the internal cerebral veins and posterior choroidal arteries. The choroid plexus of the third ventricle attaches to the tela choroidea.

Deep venous structures surround the pineal gland. The internal cerebral vein of each side receives venous blood from the corresponding subependymal veins (thalamostriate vein and septal vein) and anterior choroidal veins from the choroid plexus of the lateral and third ventricles. The internal cerebral veins run parallel in the tela choroidea in the roof of the third ventricle and unite to form the vein of Galen. At the quadrigeminal cistern, the vein of Galen also receives the tributaries from the basal veins of Rosenthal, which originate at the anterior perforating substance of each side and runs posteriorly around the midbrain. The vein of Galen is located under the splenium and above the pineal gland and enters the straight sinus. At that point, it receives the precentral vein. Also the internal occipital vein drains into the vein of Galen through the calcarine fissure from the calcarine cortex of the occipital lobe. The pineal gland is surrounded by the vein of Galen and its tributaries.

The normal pineal gland measures only 5–10 mm. The principal cells in the pineal gland are pinealocytes, and the gland is composed of pinealocytes (95%) and glial cells (5%). Pinealocyte, a specialized form of neuronal cells, functions as a neuroendocrine transducer. In lower mammals, these cells exhibit structural characteristics of photoreceptor cells. In primitive animals such as fish and amphibians, the pineal gland is a neurosensory photoreceptor organ. In mammals, it has a

neurotransmitter secretory function. In higher vertebrates, the pineal gland has two functions, sensing light and melatonin production. While the pineal gland remains the main site of melatonin production, the light information sensed by the retina travels through a complex route involving the suprachiasmatic nucleus and the superior cervical ganglia, ultimately modulating pineal activity [1]. Secretory function, specifically melatonin and serotonin synthesis and release from the pinealocytes, has been studied extensively [2]. The pineal gland has the highest concentration of serotonin in the brain. Melatonin release in animals follows a circadian rhythm with high serum levels during the night and low levels during the daytime. Melatonin also has an inhibitory gonadal effect on the hypothalamic-pituitary axis and also at the gonadal level [3]. In humans, melatonin levels are highest between the ages of 1 and 5 years and then decrease until the end of puberty [4].

11.1.2 Pathology

In the pineal region between the infratentorial and supratentorial locations, a variety of tumor histological types can occur. Pineal region tumors are located predominantly in the third ventricle or in the quadrigeminal cistern/the cerebellomedullary fissure (CMF) or extending to both spaces (Fig. 11.2). Pineal region tumors derive from either the pineal gland (pineal) or para-pineal structures. Tumors of pineal and para-pineal origin differ in histological type. Those of pineal origin are germ cell tumors and pineal parenchymal cell tumors. Para-pineal tumors arise from the surrounding neural structure of the midbrain, the thalamus, the SMV, the cerebellar peduncles, and cerebellum. They are likely benign gliomas, and some are embryonal tumors.

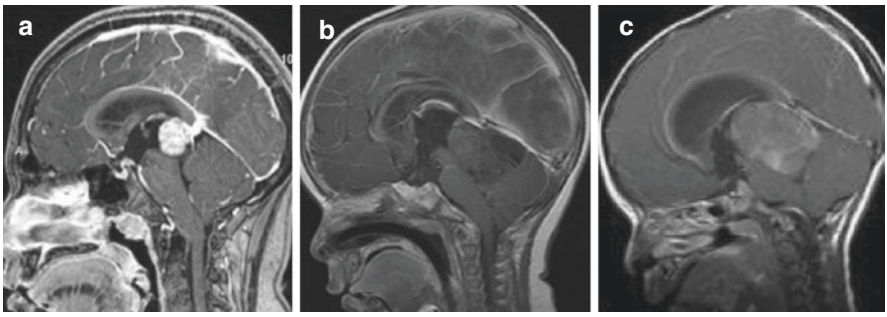

Fig. 11.2 Postcontrast sagittal MR of pineal region tumors. The tumor is predominantly located in the third ventricle (**a**), in the quadrigeminal/cerebellomedullary fissure (**b**) or extending to both spaces (**c**)

11.1.2.1 Germ Cell Tumors

Germ cell tumors (GCTs) are classified as germinomas, embryonal carcinomas, yolk sac tumors, choriocarcinomas, mature and immature teratomas, teratomas with somatic-type malignancy, and mixed germ cell tumors [5]. Germinomas, which are the most common among germ cell tumors (GCTs), compose 60% of intracranial GCTs. Others are non-germinomatous germ cell tumors (NGGCT). Embryonal carcinomas are considered to be tumors of pluripotential cells. They further give rise to either embryonal tumors consisting of all three germ layers (i.e., mature teratomas and immature teratomas) or tumors of extra-embryonal origin. The latter include choriocarcinomas through trophoblastic differentiations or yolk sac tumors through yolk sac formation. Among all GCTs, only teratoma is considered to be benign. Immature teratomas are usually noted within mature teratomas. They comprise incompletely differentiated or embryonal components, which resemble fetal tissue, most commonly primitive neuroectodermal elements and embryonic mesenchyme. Elements of germinoma and/or NGGCT often coexist in a single tumor, which is categorized mixed GCT.

The histogenesis of GCTs remains debatable. It has been considered they derive from primordial germ cells (PGCs) and span a wide range of differentiation and malignant characteristics. The PGCs appear in the yolk sac wall early in the gestational week and migrate via the dorsal mesentery of the hindgut into the genital ridges in the sixth gestational week. Ectopic PGCs that migrate and disseminate further usually undergo apoptosis. Aberrant PGCs that did not undergo apoptosis continue migration in the extragonadal location but often remain in two midline sites: the mediastinum and around the third ventricle. This "germ cell theory" explains as to why extragonadal GCT frequently develop in the thymus and in the pineal and hypothalamic regions. However, the PGCs are not found in the normal human brain. Sano theorized that misplaced embryonic tissues incorrectly enfolded at the time of neural tube formation become the source of intracranial GCTs [6]. Another theory is "stem cell theory," which explains the histogenesis of GCTs from native pluripotent neural stem cells through transformation of PGCs or from embryonic stem cells. Despite their early migration, these germ cells tend to develop neoplastic transformation in a much later stage of life, around puberty. One assumes that gonadotropins or gonadotropin-releasing hormones secreted by the hypothalamus at puberty may have a carcinogenic effect [7].

11.1.2.2 Pineal Parenchymal Tumors

Pineal parenchymal tumors are derived from pinealocytes. Pineal parenchymal tumors are classified into pineoblastoma, pineal parenchymal tumor of intermediate differentiation, and pineocytoma, depending on the cellular differentiations. The 2021 WHO Classification of Tumors of the CNS added two other tumors to "pineal tumors": papillary tumor of the pineal region and desmoplastic myxoid tumor of the pineal region, SMARCB1-mutant [5].

Pineoblastomas are poorly differentiating malignant embryonal tumors, and pineocytomas, on the other hand, are differentiated and clinically benign. Recently, based on DNA methylation profiling, pineoblastomas are classified into five molecular subgroups (Group 1, 2, 3, RB and MYC), which are analyzed for copy number, whole exome and targeted sequencing, and miRNA expression [8]. Groups 1 and 2, which affect older children, exhibit recurrent miRNA biogenesis gene defects; Group 3, which affects adolescents and adults, exhibit few alterations, and RB and MYC sub-groups occurring in infants age <18 months harbor RB1 and MYC alterations. Liu et al. classified pineoblastomas into four groups based on DNA methylation array, whole-exome sequencing, and RNA sequencing. They found a good outcome among older children with average-risk pineoblastoma treated with reduced-dose CSI [9]. Papillary tumor of pineal region is considered to be derived from specialized ependymal cells of the subcommissural organ. It is a benign tumor but tends to recur if not resected totally. Desmoplastic myxoid tumors affect adults and are relatively benign [10].

11.1.2.3 Tumors of Glial and Miscellaneous Cell Origin

Glial cell tumors can occur in the pineal gland because astrocytes are scantly present there, but pure pineal gland glioma is exceedingly uncommon [11]. Nearly all glial tumors arise from the glial tissue elements of brain tissue intimately surrounding the pineal gland and extend to the pineal region. They are considered to be parapineal tumors. The most common pathological type in childhood is juvenile pilocytic astrocytoma (JPA), which often originate in the midbrain, the cerebellar peduncle, the cerebellum, or the thalamus. Embryonal tumors may take origin from the cerebellum, and/or SMV, and rostrally extend to the pineal location mimicking a pineal tumor. Others are from the medial occipital lobe or the splenium of the corpus callosum. Tumors of other histological types also occur. Among tumors of mesenchymal origin, meningioma and hemangioma may occur in the pineal region but are rare in pediatric population.

11.1.2.4 Non-neoplastic Mass Lesion

Pineal cysts are relatively common and are identified on approximately 0.5–5% of brain MRI and 20% of autopsies [12]. Pineal cysts result from focal degeneration of the pineal gland and contain gelatinous material. The cyst wall consist of three layers: an outer fibrous layer, a middle layer of pineal parenchymal cells with variable calcification, and an inner layer of hypocellular glial tissue [13]. Other developmental cysts include epidermoid and dermoid cysts. They may occur as a component of GCTs. Other cystic lesions are arachnoid cysts and cavum velum interpositum. These cystic lesions may have a similar appearance on neuroimages. Vascular malformation such as cavernous angioma or arteriovenous malformation can be localized in the pineal region.

11.2 Epidemiology

Pineal tumors are uncommon tumors, and they are predominantly childhood malignancies representing 3–11% of all pediatric brain tumors compared to <1% of brain tumors in adults [14]. Intracranial GCTs (iGCTs) account for 0.5–3.2% of primary intracranial tumors in adults and 11.8% in children. Germinomas are the most common variety among them, constituting from 35% to 65% of pineal tumors [15, 16]. GCTs of pineal region almost exclusively occur among males. However, among suprasellar germ cell tumors, the sexual distribution is about equal between male and female, or female may be predominant [17, 18]. About 65% of pineal GCTs occur between the ages of 10 and 21 years, and only 11% occur before the age of 9 years.

Most of these NGGCTs affect males in the first two decades of life. Choriocarcinomas tend to occur at a younger age (mean age, 8 years) than do embryonal carcinomas and yolk sac tumors (mean age, 14 and 17 years, respectively). Of choriocarcinomas, 35% occur before the age of 9 years, whereas only 10–12% of embryonal carcinomas and endodermal sinus tumors occur before the age of 9 years.

Teratomas and immature teratomas in the pineal region also affect males. They are usually identified within the first two decades of life but often occur in much younger children than other GCT. Most teratomas occur in children younger than 9 years; however, 20% occur between the ages of 16 and 18 years.

The rate of mixed GCTs diagnosis has increased due to a recent trend of aggressive tumor biopsy and the availability of tumor marker studies. In a study by Matsutani et al., 49 of 153 intracranial germ cell tumors were of mixed type [15]. The common components frequently present in mixed GCTs are germinoma and teratoma. In Matsutani's series, none of the mixed tumors were a combination of germinoma and choriocarcinoma. In the whole group of mixed GCTs, germinoma components were found in 79%, teratoma components in 63%, yolk sac tumor components in 33.3%, and embryonal carcinoma components in 15.8% [6]. The correct identification of mixed GCT and NGGCT components requires adequate tumor sampling, tumor markers, and proper preparation of the tissue for immunohistochemical examination.

Pineal parenchymal tumors occur at variable ages. Pineoblastomas occur in infancy and childhood, whereas pineocytomas occur in older children and young adults. There are strong correlation of age and sexual preponderance with molecular base classifications among pineoblastomas [8, 9]. Li et al. reported that Groups 1–3 occur in older children (median ages 5.2–14.0 years), while Group RB and MYC PB patients are much younger (median age 1.3–1.4 years) [8].

In Japan, GCTs are much more common than pineoblastomas, which consist of only 5.1% of pineal region tumors [19]. Lin et al. reviewed pineal region tumors and found the most common entities are pineal parenchymal tumors (25.3%), glial neoplasms (18.6%), and GCTs (17.6%) though their data was based on predominantly in adult patients [20]. Katyal et al. reported about 60% of pineal region tumors are

of pineal gland origin, and the rest are derived from para-pineal structures [21]. Awa et al. reviewed image data of 93 pineal region tumors and noted four main groups: germinoma in 33, nongerminomatous germ cell tumor (NGGCT) including teratoma in 30, pineal parenchymal tumor (PPT) in 20, and miscellaneous tumor in ten patients [22]. Qi et al. reported 148 histologically verified pineal tumors of all age group excluding germinomas [23]. In their report, NGGCTs were most common (56) followed by neuroepithelial tumors (41) and pineal parenchymal tumors (21). Of NGGCTs, 29 were teratomas, and 19 were mixed GCTs.

11.2.1 Symptomatology

The common signs and symptoms of pineal region tumors are primarily related to obstructive hydrocephalus at the aqueduct of Sylvius. Headaches are the most common presentation and usually occur intermittently initially but become more frequent and intense. They are worse in the morning and often awaken the patient during sleep. Nausea and emesis are common signs in association with headaches. Double vision may be due to either tectal compression by the tumor mass or abducens nerve palsy due to increased ICP. Occasional blurred vision could be due to the tectal compression but could also be related to visual obscuration secondary to papilledema. In the later stage of hydrocephalus, patients experience ataxic gait and altered mental status. Papilledema is a frequent sign of hydrocephalus secondary to pineal region tumors.

Parinaud syndrome is well known to be a pathognomonic sign for pineal region tumors. Qi et al. reported 39.9% of patients with NGGCT had Parinaud sign at presentation [23]. Parinaud sign is due to compression or structural damage on the posterior commissure. The signs of Parinaud's syndrome include upward gaze palsy with impaired convergence. Pupils are dilated and poorly respond to light, while they may respond to accommodation. Also, spasms of convergence or retraction nystagmus are often present. This inability of upward gaze in Parinaud's syndrome differs from the sunsetting phenomenon due to hydrocephalus in which spontaneous intermittent downward deviation of the eyes is the primary sign.

Synchronous germinomas in the pineal and suprasellar regions (bifocal tumor) often cause diabetes insipidus and other hormonal dysfunctions and visual impairment [18, 24]. Pineoblastomas and less commonly germinomas may show dissemination at the time of diagnosis, which can cause various signs such as spinal cord compression and optic nerve compression [25, 26]. Although precocious puberty is historically considered to be a common sign of pineal region tumors, its occurrence is rare [27, 28]. Precocious puberty observed in boys with choriocarcinomas or germinomas with syncytiotrophoblastic cells is due to the luteinizing hormone-like effect of β-HCG, which secondarily stimulates androgen secretion by the Leydig cells of the testes [29]. Teratomas and mixed tumor, however, can also cause precocious puberty [15].

11.2.2 Diagnostic Studies

11.2.2.1 Neuroimaging

Both computed tomography (CT) and magnetic resonance (MR) imaging are helpful for diagnosis. Associated abnormalities, such as hemorrhage or calcifications, may be better appreciated with CT. MR imaging, however, is extremely useful for identification of detailed tumor location and extension. MR imaging often enables the determination of the pineal or extrapineal origin of the tumor because the uninvolved pineal gland may be appreciated by a careful interpretation of the MR image. The involvement of the midbrain, the thalamus, or other surrounding structures is often determined. The MR image may also depict tumor multiplicity or dissemination in the ventricular or subarachnoid spaces.

Calcifications often occur in the pineal gland. Calcifications are laid around corpora arenacea, which are made due to membrane remains or byproducts of pineal neuronal and glial polypeptide exocytosis [2]. A calcification in the pineal gland on CT scans normally start to occur 61/2 years and is noted in 40% by the age of 17 years [30]. The presence of calcification in children younger than 6 years is abnormal and needs to be investigated for a potential neoplastic process.

CT Images

On CT scans, germinomas show soft tissue masses of hyper-density relative to the surrounding brain tissue. Pineal calcification of GCTs occurs in 70% of cases and tends to be localized centrally or displaced peripherally in the tumor mass. Hyperdensity of pineoblastomas, if present, is dispersed in the tumor but often inconclusive as to if they represent calcifications or microhemorrhages. Calcifications can occur either centrally or peripherally, but occurrence of calcification is less common among pineoblastomas [31, 32]. NGGCTs tend to have similar homogeneous soft tissue density and are also similarly calcified as germinomas. The most common character of choriocarcinomas is intratumoral hemorrhagic foci. On the other hand, the appearance of teratomas is more distinct and often heterogeneous with a variable degree of soft tissues, calcifications, and cyst formation. Pineoblastomas are relatively homogeneous and hyperdense on precontrast CT scans. No characteristic CT features could be found to differentiate pineal germ cell tumors other than teratomas and pineal parenchymal tumors [33].

Benign astrocytomas are often hypodense relative to the surrounding brain tissues on precontrast CT scans. Calcification may occur but is uncommon. Dermoid and epidermoid tumors tend to be hypodense and show little or no enhancement after infusion of contrast material. Some epidermoid tumors may have density equal to that of CSF, and their appearance may mimic that of an arachnoid cyst or pineal cyst.

MR Imaging

Although CT complements MR, MRI is the diagnostic method of choice because of the ability to obtain high-resolution images and multidimensional views providing information of tumor location and extension. Spine MR provides the evidence of spinal subarachnoid dissemination. Detailed anatomic information on MR imaging, on sagittal images in particular, delineate the relationship between the pineal gland, the quadrigeminal plate, and other structures.

Obstructive hydrocephalus is common, occurring in more than 90% of pineal region tumors. Acute onset of hydrocephalus is accompanied by peri-ependymal lucency due to transependymal edema. The disseminated disease in the ventricles and subarachnoid space may be detected on head and spine MR images. The suprasellar region in particular should be carefully evaluated for potential bifocal GCTs. From a surgical viewpoint, sagittal MR images provide surgeons with sufficient information about the floor of the third ventricle for third ventriculostomy, the relationship between the tumor and deep venous structures, and the angle of the tentorium for the selection of surgical approaches to the pineal region.

Teratomas are often heterogeneous with the presence of multi-cyst formation. Germinomas show low signal intensity to isointensity on T1-weighted images. They show high signal intensity or are isointense on T2-weighted images [34]. After infusion of contrast material, germinomas show intense enhancement. Multiplicity of lesion is restricted to GCTs, germinomas in particular. Thick peritumoral edema was more frequent in germinoma than in NGGCT, and bi-thalamic extension of tumor was seen in 78.8% of germinomas (Fig. 11.3) [22]. High proliferative indices and low collagen development may contribute to invasive growth of pineal

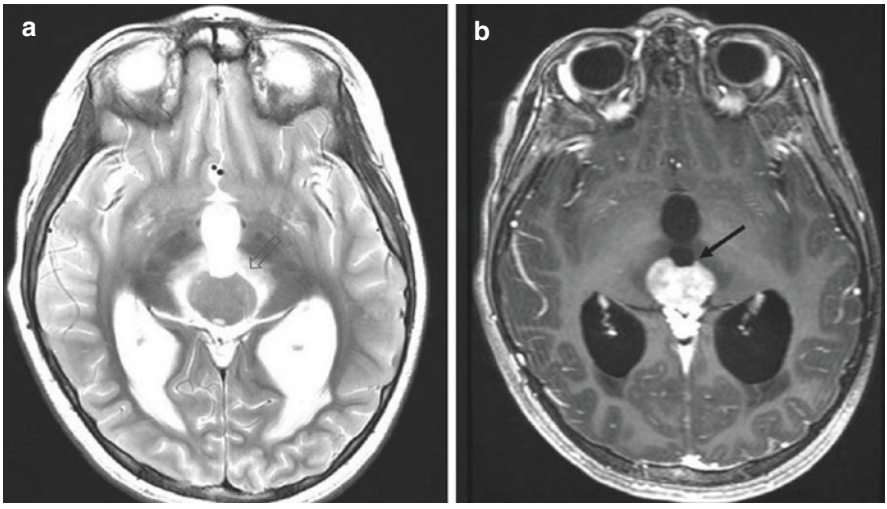

Fig. 11.3 Axial MR of a pineal germinoma. T-2 weighted (**a**) showing a bi-thalamic edema (*open arrow*) and postcontrast MR (**b**) showing subependymal bi-thalamic extension (*arrow*)

germinoma into the thalami [22]. These bi-thalamic extensions of germinomas present a butterfly- or heart-shaped appearance [22, 35]. The concurrent enhancing lesions in both the anterior and posterior third ventricle strongly suggest bifrocal GCT, which are noted in 39.4% of germinoma and in 10.0% of NGGCTs [18, 22]. The frequency of this multiplicity has increased with the use of more sensitive neurodiagnostic methods. For instance, Sugiyama et al. reported the frequency of bifocal GCTs increased from 4.2% before to 17.4% after the introduction of MR imaging [29]. Similarly, Esfahani et al. reported that 16 (19%) of 84 intracranial GCTs had bifocal lesions [18]. When pineal region tumors present with diabetes insipidus, the pituitary stalk and the tuber cinereum should be carefully looked at in order to detect the multiplicity of the lesions because 75% of bifocal lesions present with DI [18].

Pineoblastomas are hypo- or isointense on T1-weighted images, and variable degrees of enhancement are noted. In general, MR signal characteristics are usually nonspecific, and correlation with the patient's age, sex, and other associated factors needs to be analyzed for diagnostic purposes [36, 37].

Midbrain tumors are localized in the tectum or extending to the tegmentum and often further toward the thalamus. Most of midbrain tumors are JPA and enhance after contrast infusion. Primary midbrain malignant gliomas are rare unlike pontine gliomas. JPA of the posterior thalamus can extend into the third ventricle medially or posteriorly to the cistern. Tumors of the cerebellar vermis or the superior cerebellar peduncle can extend to the quadrigeminal cistern mimicking a pineal tumor. Tumors of the SMV extend superiorly to the quadrigeminal cistern and inferiorly to the fourth ventricle. They displace the superior vermis and the fastigium of the fourth ventricle backward and the tectal plate dorsally [38].

Pineal cysts, which are present in 2.4% of the normal population, are rarely symptomatic and usually remain stable in size [39]. They have a contrast-enhancing cyst wall and subtle hyperintencity of the cyst content. Mostly, they are a singular cyst, while occasionally multicystic changes can occur. Pineal cysts often show radiographic evidence of tectal compression in spite of the absence of hydrocephalus or signs of tectal compression. The occurrence of hydrocephalus is very rare, while Fain reported that of 20 patients with symptomatic pineal cyst, eight were noted to be hydrocephalic [13]. A pineal cyst rarely causes symptoms without hydrocephalus [40].

The non-enhancing tectal lesions presenting with obstructive hydrocephalus are often dormant and rarely require surgical biopsy or oncological treatment [41]. They are often hamartoma or low-grade glioma, and contrast enhancement may vary during follow-up. Some may show an exophytic nature beyond the quadrigeminal plate and/or contrast enhancement in which case one should differentiate them from active astrocytomas.

11.3 Laboratory Tests

Certain GCTs secrete tumor markers that are identified in the serum and the CSF [42]. This noninvasive laboratory test is important not only for diagnostic purposes but also for monitoring responses to treatment and detecting relapses. Alpha-fetoprotein (AFP), a glycoprotein, is normally produced by the yolk sac endoderm, the fetal liver, and embryonic intestinal epithelium, but its production ceases by the time of birth, and the value drops to the adult level by 1 year of life. An AFP value less than 5 ng/mL in both serum and CSF is considered to be normal [43]. In the CNS, yolk sac tumors show the greatest expression of AFP. Embryonal carcinomas and immature teratomas produce AFP to a lesser extent.

Beta-HCG is another glycoprotein that is normally secreted by syncytiotrophoblastic giant cells of placental trophoblastic tissue. Therefore, the presence of β-HCG strongly indicates GCTs. The normal value in the serum and CSF is less than 5 mIU/mL [43]. Marked elevation of β-HCG greater than 2000 ng/mL is noted in choriocarcinomas, but mild elevations (<100 ng/mL) can occur among germinomas and embryonal carcinomas. The biological half-life is about 5 days for AFP, whereas it is less than 24 h for β-HCG. The titers of β-HCG and AFP reflect the number of cells secreting these glycoproteins; this is useful for differentiating tumors with predominantly choriocarcinoma or yolk sac tumor, but not confirmative for histological diagnosis [15]. Abnormal concentrations of AFP and/or β-HCG in the serum or CSF are generally regarded to NGGCTs.

Of malignant GCTs, 39–70% showed positive tumor markers for either β-HCG or AFP or both [15, 34]. The results of positivity for these tumor markers are variable-dependent on cellular composition within the tumor. However, β-HCG value tends be higher in the CSF than the serum [44]. Thus, it is important to obtain the values of tumor titers from both serum and CSF.

Other tumor markers are placental alkaline phosphatase (PLAP) and soluble C-kit. PLAP was reported as a specific marker for primary intracranial germinomas. Serum or CSF PLAP levels are measured with an enzyme-linked immunosorbent assay, but their sensitivity and specificity need further investigation. C-kit is a tyrosine kinase receptor for stem cell factors and diffusely expressed on primordial germ cell (PGC). Both PLAL and C-kit have a half-life of 6 days and are an indicator for germinomas. The soluble C-kit receptor is significantly high in concentration in the CSF among the patients with germinomas [45].

Melatonin secretion by the pineal gland follows 24-h nyctohemeral rhythm. When the pineal gland is disturbed by invasive tumors such as GCT, the melatonin rhythm is dramatically reduced. However, clinical diagnostic value of melatonin profiles is limited for pineal region tumors [46].

11.4 CSF Cytology

The CSF, whenever available either by means of lumbar puncture or from the ventricle at CSF diversion, should be submitted for cytological studies together with tumor markers for pineal region tumors. The frequency of CSF disseminations among malignant GCTs is low [47]. On the other hand, pineoblastomas disseminate along the CSF pathway with a frequency higher than 50% at diagnosis and almost 100% at the terminal stage [48, 49].

11.5 Hydrocephalus

Hydrocephalus occurs in more than 90% of pineal tumor cases, and it is the primary cause of presenting symptoms. Hydrocephalus is controlled with either tumor mass reduction and/or a CSF diversion procedure. Germinomas and most of malignant NGGCTs can be considerably reduced in size in a short time following chemotherapy or radiotherapy (RT), and hydrocephalus is often resolved without surgery. Germinoma contains a significant amount of T cell lymphocytes, as such, its volume can be reduced following a short course of steroid therapy (Fig. 11.4).

Due to its obstructive nature, the treatment of choice for the hydrocephalus is endoscopic third ventriculostomy (ETV). ETV is often successful to control hydrocephalus, and its success rate is reported at 80–90% of patients with pineal region tumor [50, 51]. Ventriculoperitoneal (VP) shunt leads to shunt dependency and development of slit-like ventricle. Also, shunt-related intraperitoneal metastases of germinoma and pineoblastoma are a remote concern [52–54]. Presence of mass at

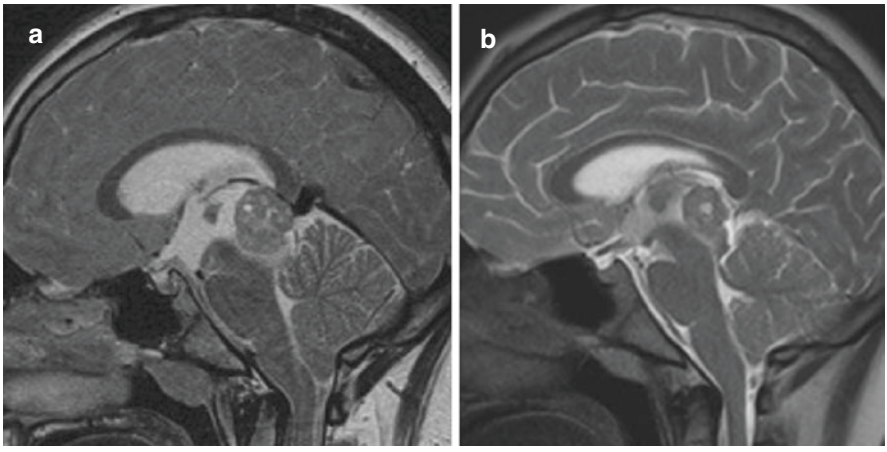

Fig. 11.4 Sagittal T2-weighted MR of pineal germinoma before (**a**) and after (**b**) a 3-day use of dexamethasone therapy. There is a marked reduction of the tumor mass together with decreased hydrocephalus and degree of tonsillar ectopia

the floor of the third ventricle typically in the case of bifocal germinoma hinders ETV. In the case of bifocal germinoma, a short course of steroid therapy with a placement of EVD or a ventricular access devise such as Ommaya reservoir followed by early initiation of chemotherapy may alleviate the need of the shunting because of the rapid response to the chemotherapy. Another alternative for ETV is a ventriculocisternostomy through the lamina terminalis to the cistern when the ventricular anatomy does not allow access to the floor of the third ventricle [55].

The risks related to ETV include hemorrhage and hypothalamic damage, particularly diabetes insipidus. The small opening at the floor of the third ventricle created by the ETV may be closed by blood clots induced with subsequent tumor biopsy or resection, or may be closed much later by an adhesive arachnoiditis. An Ommaya reservoir is connected to the ventriculostomy catheter following the ETV is helpful for subsequent ventricular access [56].

11.6 Biopsy

Histological verification on the basis of tumor markers and/or biopsy leads to appropriate treatment selection. The information of patient's age and sex, neuroimaging findings, and tumor markers add to accuracy of tentative diagnosis of certain GCTs. Neoadjuvant chemotherapy without tissue biopsy has been widely practiced as a therapeutic modality in pineal GCTs on the basis of neuroimaging findings and positive tumor markers [22, 57–59].

11.6.1 Stereotactic Biopsy

Most of recent pineal region tumor biopsies are done with neuroendoscopy when in the presence of enlarged ventricles. When the ventricles are small or the tumor is located in the extra-ventricular location such as the thalamus and midbrain, stereotaxic biopsy is indicated. There is a potential concern that stereotactic procedures result in hemorrhagic complication because pineal region tumors are surrounded by veins of the Galenic system. Most reports concerning stereotactic biopsy for pineal region tumors indicate that the risks of surgical intervention are minimal and diagnostic accuracy is high [60, 61].

11.6.2 Neuroendoscopic Biopsy

Neuroendoscopic biopsy of the third ventricle tumor has been widely practiced. Endoscopic biopsies are performed at the same time as third ventriculostomy [50, 51, 62, 63]. The pineal region tumor is often difficult to visualize in the posterior

third ventricle through the trajectory used for the ETV. In order to overcome this difficulty, some use a 30-degree angle rigid scope [51], perform an additional burr hole that is placed further anteriorly to the hairline [62], or place the exact midpoint between both entry points [50]. A flexible endoscope provides access to both locations through a single burr hole (Fig. 11.5). Endoscopic inspection may detect unexpected tumor seeding at the ventricular floor or wall, which is not apparent on neuroimaging detections (Fig. 11.6). Minor hemostasis can be achieved with a bipolar cautery. However, controlling a major hemorrhage is often difficult because of the limited surgical field for ventriculoscopic instrumentation compounded with poor visibility through hemorrhagic CSF. Almost always the intraoperative hemorrhage stops after copious intraventricular irrigation. If significant hemorrhage occurs, it is prudent to keep external ventricular drainage. Postoperative tumoral hemorrhage can occur after endoscopic biopsy for pineal tumors due to loose tumor tissue, hypervascularity in the tumor, and/or abrupt reduction in the ICP to zero during endoscopic procedures [64].

The tumor samples obtained with either a stereotactic procedure or ventriculoscopy are small. Diagnostic accuracy rate of biopsy is as high as 96% [50], and histological diagnosis can be determined from these small tumor samples for most tumors. For mixed GCT, however, heterogeneous components are likely overlooked, and a small sample obtained with these methods may not indicate the true nature of these tumors.

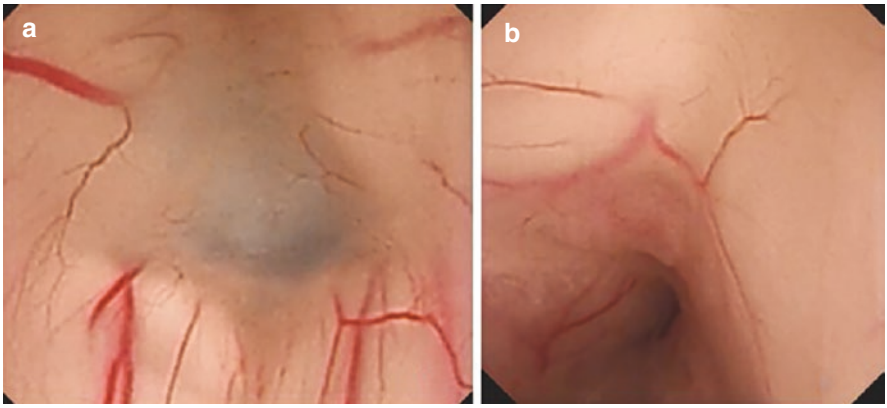

Fig. 11.5 Surgical views through a flexible neuroendoscope. The view of thin anterior floor of the third ventricle for an endoscopic third ventriclostomy (**a**) and the posterior floor of the periaqueductal location for tumor biopsy (**b**). Note germinoma is infiltrating the around the aqueduct of Silvius

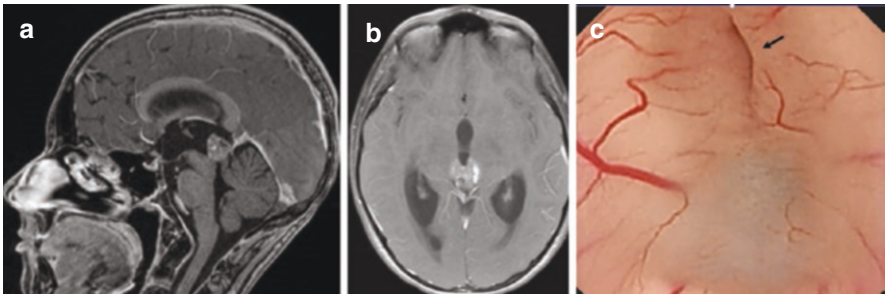

Fig. 11.6 Contrast enhanced MR, mid-sagittal (**a**) and axial (**b**) images showing pineal germinoma. An endoscopic inspection (**c**) shows a second lesion in the tuber cinereum (*arrow*), which was not shown on MR. Tumor biopsy showed germinoma

11.7 Treatment

11.7.1 Craniotomy

The purposes of craniotomy for pineal region tumors are histological verification, maximum cytoreduction, and restoration of the CSF pathway. Much larger tissue samples can be obtained by open biopsy, which leads to more accurate histological diagnosis. Among GCTs, teratomas (mature or immature), either pure or as a component of mixed GCT, are resistant to both radiation and chemotherapy; thus, cure is only achieved with surgical extirpation. The extent of resection of childhood malignant tumors such as pineoblastoma and ATRT seems to influence patient prognosis if they are localized [65]. Also, total resection of JPA, pineocytoma and papillary tumor of pineal region can lead to a patient's cure.

Initial experiences of direct surgical resection were quite discouraging due to high morbidity and mortality rates. Cushing made the statement in 1932 that he had "never succeeded in exposing a pineal tumor sufficiently well to justify an attempt to remove it" [66]. Dandy in 1936, in reviewing his experiences with ten cases of pineal tumor, reported seven consecutive deaths during the period from 1921 to 1931 and stated that this "seemed almost to indicate the futility of further efforts" [67].

Pineal region tumor resections have become more successful because of the surgical microscope, microsurgical instrumentation, and advanced neuroimaging studies. Several surgical approaches to deep-seated location of these tumors have been advocated and practiced. Dandy reported on an interhemispheric transcallosal approach in 1921 [68]. Later, Horrax in 1937 [69] and subsequently Poppen in 1966 [70] developed an occipital transtentorial approach through a supratentorial craniotomy. It was later modified by Jamieson in 1971 [71]. The infratentorial route is primarily approached along the superior surface of the cerebellum and the inferior surface of the tentorium. This infratentorial supracerebellar approach was first described by Krause in 1926 [72] and was popularized by Stein in 1971 [73].

Each approach has advantages and disadvantages and should be chosen on the basis of anatomical information provided from neurodiagnostic images, along with the surgeon's familiarity, comfort, and confidence with the approach. Tumor location and extension, the deep venous system, and affected neural structures need to be taken in consideration for a planned surgical approach. Also, other factors should be in consideration for selecting the optimal approach. They are patients age, presence or absence of hydrocephalus, angle of the tentorium, and purpose of surgery (biopsy vs. total resection) and operating surgeon's comfort. Other important factors are what neural and vascular structures need to be dealt when approaching the lesion and where blind spots are at the tumor resection. Ideally, none of the neural and vascular structures are sacrificed, and one should be familiar with the blind spots for each approach. The current most common approaches are infratentorial supracerebellar (ITSC) approach and OT approach.

11.7.1.1 Infratentorial Supracerebellar Approach

The advantages of ITSC approach are the midline approach to the midline lesion approaching the center of the tumor between the cerebellum and tentorial opening. It provides a better orientation and the view of the vein of Galen by displacing the superior cerebellar vermis caudally. The exposed surgical view includes the tectum, upper part of CMF up to the tentorial incisura and below the Galenic venous system. The pineal tumor is seen under the vein of Galen and its tributaries; thus, during the dissection, these veins are not transgressed. This approach has been carried out with the patient in a sitting position; thus, the gravity allows the cerebellum to fall, and the tumor is readily separated from the vein of Galen. Also, these veins are less distended due to enhanced venous return and less vulnerable to mechanical manipulation. The surgical field is dry because of decreased pooling of the blood and CSF, which are drained out by the gravity.

However, there are disadvantages to the ITSC approach. The sitting position places the patient at risk for air embolism and hypotension. The surgeon's neck needs to be extended because the targeted pineal region is above the surgeon's eye level; thus, his/her arms and hands need to be elevated and outstretched to reach long focal distance. This awkward positioning results in the surgeon experiencing discomfort and fatigue. A Concorde position has been advocated with the patient in prone position with head elevated, but it still causes discomfort to the surgeon due to cramped unnatural position [74]. In infants or young children, the posterior fossa is small, and the distance from the foramen magnum to the torcular Herophili is only about 4.0 cm; thus, the entry space through the posterior fossa is restricted. Even older children or adults may have a low-set torcular Herophili, which needs to be evaluated on preoperative MR imaging. The surgical field through a posterior fossa craniotomy is often restricted because of small posterior fossa when the tentorium and straight sinus are vertically positioned. Retracting the cerebellum and sectioning the superior vermian veins and the precentral vein by the ITSC approach can result in postoperative cerebellar swelling. In addition, the surgical opening is too

small to have second surgeon assist effectively in the pineal region. The width of the surgical field at the depth is limited by the tentorial opening.

The blind spots during the ITSC approach are as follows: It is difficult to remove tumors located above the deep venous system or located laterally beyond the tentorial opening and those extending into the lateral ventricle. In the posterior fossa, the portion of the tumor located in the CMF between the superior vermis and the inferior colliculi or extending into the fourth ventricle are hard to reach and resect unless the vermis is split. It has been advocated to use endoscope assisted resection of pineal lesions through the ITSC approach [74, 75]. More recently, Cai et al. reported endoscope-assisted microsurgical resection through the ITSC approach in pediatric pineal region tumors provided expanding visualization of the blind corners of the microscope [76]. All these patients had the endoscope-assisted ITSC in the sitting position. However, Shirane et al. used a modified Concorde position with the patient's head in a neutral position [77]. The benefits of the endoscope assistance are surgeon's comfort and the capability to inspect blind spots by adjusting ranging and angulation of the endoscope to maximize view lines. Further improvements of instrumentation and techniques provide better assessment and accuracy at the removal of pineal region tumors through a key hole approach.

11.7.1.2 Occipital Transtentorial Approach

Poppen described an occipital craniotomy and suboccipital approach by elevating the occipital lobe from the tentorium. Through the suboccipital approach, a wedge of tentorium was removed and exposed the underlying cerebellar hemisphere [70]. Jamieson described in 1971 approach through a more medially placed occipital craniotomy and mobilizing the occipital pole upward and laterally after exposing the sagittal, ipsilateral transverse sinus, and torcular Herophili. The tentorium is divided from a point anterior to the transverse sinus forward to the free edge [71].

These two approaches, suboccipital approach and posterior interhemispheric approach, through occipital craniotomy have become the foundation of current OT approach to the pineal region. The suboccipital approach is performed by elevating the occipital lobe from the tentorial surface and the posterior interhemispheric approach by retracting the occipital lobe laterally away from the falx. The tentorial edge is sectioned in both approaches.

For the suboccipital approach, the craniotomy is placed more laterally from the midline exposing the ipsilateral transverse sinus. This approach provides a relatively lower trajectory angle to the posterior third ventricle. The elevation of the occipital lobe off the tentorium can be done safely due to the lack of draining veins in the posteromedial surface of the occipital lobe [78]. The suboccipital approach allows "a wider angle for maneuverability in the lateral to medial direction," which improves the accessibility to the contralateral side [78, 79]. The suboccipital approach provides a shorter anatomical route and a good view of both the floor of the third ventricle and of the lateral wall of the contralateral side. Also, a direct compression of the visual cortex is avoided at the occipital lobe retraction. However,

the access to ipsilateral wall may be limited [80]. It limits the vertical angle to access the splenium superiorly and the CMF inferiorly.

The posterior interhemispheric approach provides a wider exposure of the vertical sagittal angle from the corpus callosum to the upper posterior fossa. It provides upper posterior fossa access to the tumor in the CMF, the SMV, and the upper fourth ventricle ventral to the superior cerebellar vermis [81]. The trajectory angle is adjusted according to the target along the sagittal plane (Fig. 11.7).

The most posterior cortical bridging vein entering the superior sagittal sinus is usually 2–3 cm anteriorly to the lambda. This lack of the parasagittal bridging veins in the posterior interhemispheric fissure allows for easy access to the interhemispheric fissure along the falx. The interhemispheric parasagittal surgical entry is 8–10 cm in length, and its corridor is gradually widened to adjust the surgical trajectory angles. The surgical anatomical orientation is attained by identifying the splenium of the corpus callosum, the tentorium, and the vein of Galen. Through the opening of the tentorium, the upper posterior fossa structures of the ipsilateral side are under direct vision, ranging from the tectum to the superior vermis. Surgical trajectories can be adjusted from vertical to horizontal angle aiming to the posterior surface and the superior and inferior surface of the tumor, respectively. Another advantage of the inter-hemispheric approach is access to the splenium of the corpus callosum. If the space between the vein of Galen and the corpus callosum is not adequate enough to the third ventricle, the trans-splenial or infra-splenial approach can be performed [82, 83] (Fig. 11.8).

Disadvantages of the OT approach are potential concerns of postoperative hemianopia due to retraction of the occipital lobe, diagonal angles to the vein of Galen and its tributaries, and blind spots in the contralateral structures.

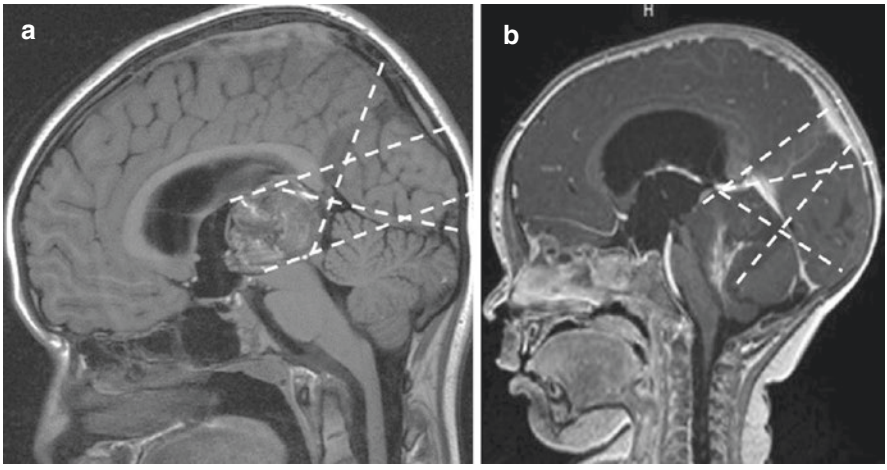

Fig. 11.7 Sagittal postcontrast MR images of pineal region tumor, a posterior III ventricle NGGCT (left) and a ATRT of the superior medullary velum extending from the quadrigeminal cistern to the IV ventricle and cisterna magna (right). Dotted lines show sagittal surgical trajectories to the superior and inferior aspects of the tumor through occipital transtentorial approach

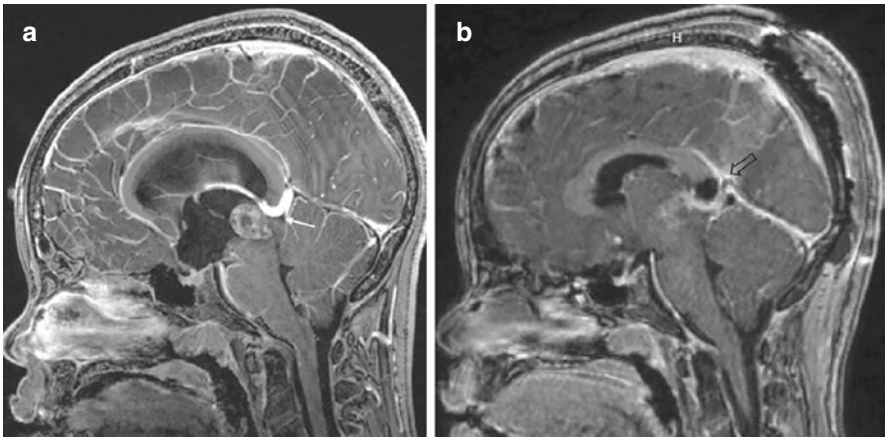

Fig. 11.8 Postcontrast sagittal MR (**a**) showing a tight space (*arrow*) between the splenium of the corpus callosum and the vein of Galen. (**b**) The posterior third ventricle tumor removed through a transcallosal approach (*open arrow*) shown on postoperative sagittal MR

The stria cortex, the primary visual cortex, is located along the superior and inferior sides of the calcarine fissure of the medial occipital lobe. The cuneus above the calcarine fissure controls visual processing and the lingua below visual memory [84]. Not only the striate cortex but also the extra-striate visual associate cortex also plays a role in visual perception [85]. Thus, forcible retraction upon the medial occipital lobe may cause hemianopia of the contralateral side. It is a frequent occurrence postoperatively after OT approach, but a rapid resolution of the symptom is the rule. Qi et al. reported 16.1% had postoperative hemianopia following the interhemispheric OT approach in a three quarter position. However, the hemianopia was resolved rapidly, and only 3.5% had permanent hemianopia [23]. In another series of adult patients reported by Yoshimoto et al., 11 of 14 patients had hemianopia after the interhemispheric OT approach in the prone position with head turning to the craniotomy site. Their symptoms rapidly diminished, and all resolved in less than 3 days [85]. However, the objective Goldman perimetry test showed inferior quadrant or homonymous hemianopia with macular sparing 4–37 days postoperative. Only three patients had prolonged visual field deficits affecting the inferior quadrant or more than 1 year [85].

The importance of brain relaxation and surgical position need to be stressed to avoid excessive retraction of the occipital lobe at the OT approach. For brain relaxation, hydrocephalus needs to be controlled either with ETV, EVD, or shunting. A controlled drainage of the CSF via intraoperative ventriculostomy provides the most effective method to attain the brain relaxation. Also helpful is draining the CSF from the pericallosal and quadrigeminal cisterns. Gravity-assisted occipital lobe retraction is often used, which include the three quarter-prone position [78] or ipsilateral recumbent position [86] with surgical side down, which allow the brain to fall away from the falx by the gravity. However, in children with a prone position, it

is usually sufficient to turn the head about 15–20° to contralaterally. If necessary, the operating table is turned further ipsilaterally to gain more gravity-assisted retraction.

The vein of Galen and its ipsilateral tributaries are present dorsally to the tumor in the interhemispheric approach (Fig. 11.9). Tributaries include the ICV dorsally, the basal veins of Rosenthal laterally, the internal occipital vein posterolaterally, and the precentral cerebellar and the superior vermian veins at the posterior midline. The vein of Galen and its tributaries are under direct vision. Approaching to the pineal tumor is primarily between the basal vein of Rosenthal and the precentral vein. The arachnoid covering over the pineal region surrounds not only the vein of Galen and its tributaries but also the suprapineal recess and the pineal gland. The vein of Galen and its tributaries, as well as the pineal body and the suprapineal recess, are typically wrapped by a thickened arachnoid membrane over the pineal region. The internal cerebral veins are within the tela choroidea at the roof of the third ventricle. However, there is no intervening arachnoid layer between the pineal gland and the internal cerebral vein. Therefore, tumors arising from the pineal gland are more prone to adhere with the internal cerebral vein, causing a potential risk of venous injury during dissection [87]. For those tumors of pineal gland origin located within the arachnoid barrier, the arachnoid barrier needs to be dissected prior to tumor removal to minimize the retraction or injury of the deep veins. However, for paraspinal tumors arising outside the arachnoid barrier, the barrier should be preserved to protect deep veins during tumor removal [23].

These deep veins need to be protected throughout. At the entry of the interhemispheric fissure, the vein of Galen is not necessarily in the surgical view initially because it is located just posteroventral to the splenium at the most proximal end of the straight sinus. The internal occipital and posterior calcarine veins, which drain the striate cortex, course along the medial surface of the occipital lobe to enter the vein of Galen. Excess retraction of the occipital lobe can cause damage to these veins. Occlusion of these veins may cause a postoperative visual field defect due to venous congestion [84].

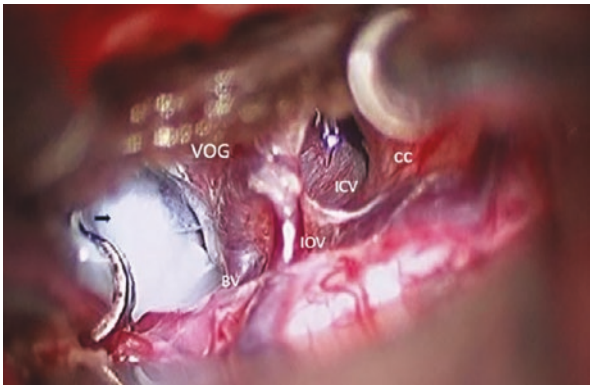

Fig. 11.9 Surgical view of the Galenic system through the tentorial opening. Note a thick arachnoid membrane of the quadrigeminal cistern (*arrow*) (VOG, vein of Galen; ICV, internal cerebral vein; BV, basal vein of Rosenthal; IOV, internal occipital vein; CC, corpus callosum)

There is extensive collateral circulation in the vein of Galen and its tributaries. The incidence of venous infarcts in the thalamus and the basal ganglia following occlusion of the vein of Galen or its tributaries is not known. The consequences to surgical occlusion of the Galenic system may have been exaggerated [88], but one should try to preserve these deep veins. Intraoperative hemorrhage from the Galenic system is usually controlled by an application of hemostatic agents and gentle compression with a cottonoid pledget.

Blind spots at posterior interhemispheric transtentorial approach are due to limited visibility and access to the third ventricle, the tecum, and posterior fossa structures of the contralateral side. Also, lesions deep in the ipsilateral wall require further lateral occipital lobe retraction. The suboccipital approach expands the access to the contralateral side with little lateral retraction of the medial occipital lobe [81]. There is a report in the literature of a thalamic tumor, which was resected through a contralateral occipital craniotomy crossing the midline through the section of the falx and tentorium after a ligation of the inferior sagittal sinus [89]. Intraoperative use of endoscope is helpful to expose this area of tumor and enhance the resectability [90–92]. A combined technique with suboccipital and inter hemispheric approaches as originally used by Jamieson [71] provides wider exposure of the pineal region tumor [80]. However, further superior lateral retraction of the occipital lobe needs further brain relaxation.

The OT approach is preferable to ITSC approach because childhood pineal region tumors tend to be large and extend in various directions and also because of the relatively narrow posterior fossa space in infants and young children. The OT approach provides wide ranges of surgical trajectory angles through a large interhemispheric avenue. The comfort of the surgeon and assistant surgeon is owing to their head and arms being in thew downward position with the patient in a prone position compared with the ITSC approach.

11.8 Surgical Technique for Posterior Interhemispheric Approach

11.8.1 Surgical Position and Craniotomy

The prone position is used routine. The patient is placed in a prone position with the head turned slightly (about 15–20°) away from the surgical side for patients who are old enough to receive head pins in a head holder. If needed, the operating table is further turned to gain the gravity assistance needed for occipital lobe retraction. The side of craniotomy is usually on the right, unless the tumor extension is more toward the left side. If the patient is young or has thin skull due to chronic hydrocephalus, head pins are avoided. The head is secured on the well-padded, horse-shoe head holder without turning of the head. Intraoperative ventriculostomy and ventricular drainage are routinely used at the interhemispheric approach particularly when

hydrocephalus is present. Retraction of the occipital and parietal lobes is more restricted for patients with slit ventricles due to an existing shunt. In such case, the brain should be relaxed with administration of mannitol, or sometimes by externalizing the existing shunt intraoperatively.

Scalp incision is made in a hockey stick fashion with the midline incision from the inion to 4–5 cm anteriorly to the lambda from there a curvilinear incision extending laterally toward the base of the mastoid process. For the craniotomy, three burr holes are made in the sagittal plane: one just above the torcular Herophili, the second at the lambda, and the third 4–5 cm anteriorly to the lambda. Another burr hole is made on the lambdoid suture about 5 cm from the midline (Fig. 11.10). A parieto-occipital craniotomy is performed crossing the midline about 1 cm, and the bone flap is lifted after dissecting the suture lines from the inner table of the bone flap. It is not necessary to expose the lateral sinus in the surgical field unless suboccipital route is considered.

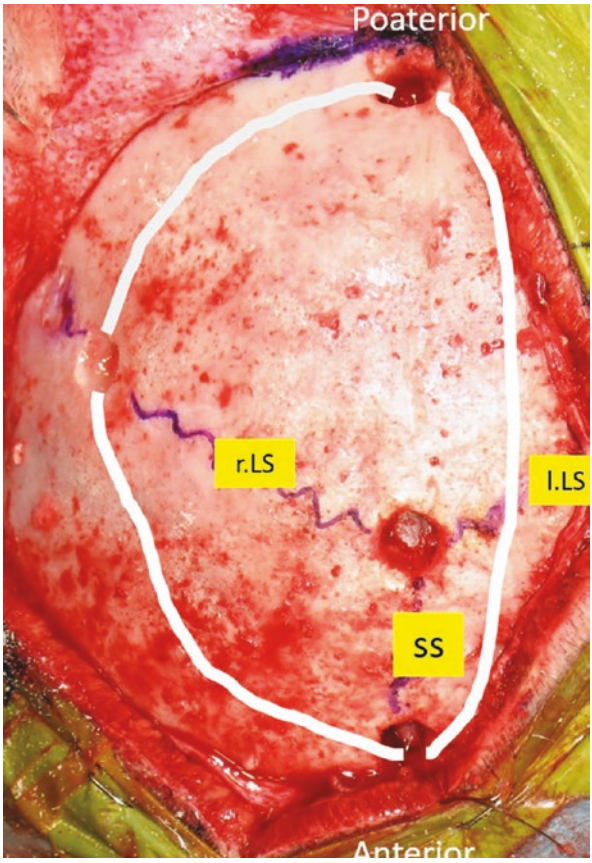

Fig. 11.10 Surgical picture of a right parieto-occipital craniotomy for interhemispheric OT approach. White lines indicate the craniotomy site connecting the burr holes (r.RS, right lambdoid suture; l.RS, left lambdoid suture; SS, sagittal suture)

Dural opening is done in a X- or C-shape, and the medial dural flap is turned over the superior sagittal sinus. At the dural opening, the last cortical vein is traced anteriorly at the anteromedial corner to the point of the entry to the sinus.

The interhemispheric fissure is entered over the precuneus gyrus, while the CSF is drained through the EVD, and the operating table is further turned downward ipsilaterally in order to gain brain relaxation. The interhemispheric fissure is entered along the falx, and then, at the depth the corpus callosum anteriorly, the straight sinus posteriorly and the tentorium laterally are identified. The pericallosal fissure is opened, and the CSF is drained for further brain. The most posterior cortical vein, which runs rostrally before entering the superior sagittal sinus, is confirmed and protected with a cottonoid (Fig. 11.11).

The ipsilateral tentorium is sectioned approximately 1 cm lateral to the straight sinus in a length of 2–3 cm exposing the underlying superior vermis. The tentorium is thick and often vascular in some due to venous lake. The tentorium section is extended from the tentorial incisura, and both edges are reduced by coagulation to widen the tentorial opening. The posterior extension of the tentorial opening is carried out when further posterior fossa exposure is needed just anteriorly to the torcular Herophili. The microscope trajectory needs to be adjusted in a more horizontal angle from near the occipital pole, and the dorsal surface of the tumor is separated from the vein of Galen to further visualize deep into the third ventricle. When the microscope trajectory is adjusted vertically, the posterior portion of the tumor and the superior vermis is visualized through the sectioned tentorium (Fig. 11.7). It allows access to the CMF or to the superior vermis and upper fourth ventricle. The veins are separated from the tumor surface under direct vision.

It is preferable to avoid sectioning of the splenium of the corpus callosum. However, at times, it may be necessary when resecting a massive tumor of the third ventricle, or when the space between the quadrigeminal plate and the vein of Galen is limited (Fig. 11.8). This parietooccipital craniotomy and posterior interhemispheric approach allows this option. If the tumor is originating from the posterior thalamus or growing into the atrium of the lateral ventricle, the retrosplenial

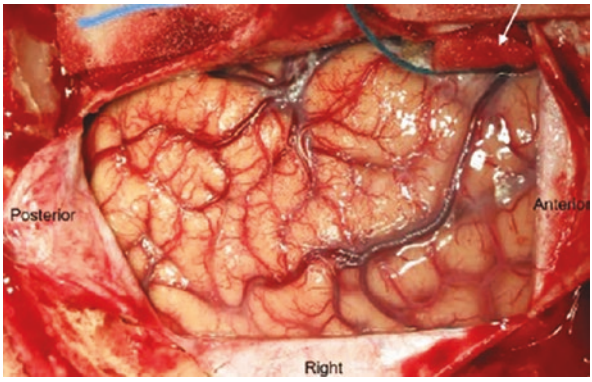

Fig. 11.11 Surgical photograph of exposed right parieto-occipital lobe. The last cortical bridging vein at the entry site to the superior sagittal sinus is protected with a cottonoid pledget (*arrow*)

parahippocampal gyrus is further laterally retracted. With or without sectioning of the splenium, the lateral ventricle is entered.

11.9 Tumor Exposure and Resection

The quadrigeminal cistern has a thick arachnoid membrane. Once the arachnoid membrane is opened, and after the tectal plate is identified, the pineal tumor is exposed in the quadrigeminal cistern under the vein of Galen. However, there is no or little exposure of the tumor when it is confined in the posterior third ventricle. The lesion of contralateral side beyond the falx and the lesion deep in the ipsilateral thalamus become blind spots within the third ventricle or the CMF, which require further occipital lobe retraction. In these cases, a size reduction of the mass volume by internal decompression of the tumor helps to bring the lateral wall into the surgical view (Fig. 11.12).

Teratomas, which are the most common surgical candidate among GCTs, are well encapsulated and contain multiple cysts. The inner content of most teratomas are firm and often are too fibrous and rubbery to aspirate even with an ultrasonic aspirator. A tedious piece meal resection is needed to debulk the tumor capsule. Pineal germinomas are encapsulated, granular, and fibrous. They do not need aggressive resection once frozen section confirms the pathology. Choriocarcinomas, yolk sac tumors, and embryonal carcinomas are vascular and yet encapsulated. Choriocarcinoma is often extremely vascular, and one may need to terminate further

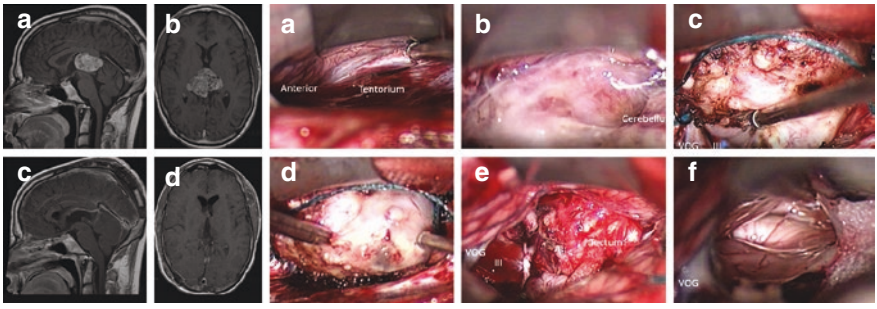

Fig. 11.12 An 18-year-old male with double vision with deconjugated eyes and increasing headaches. Postcontrast MR, sagittal (**a**) and axial (**b**) showing a large heterogeneous enhancing tumor. The serum AFP was elevated (184 ng/mL) and was initially treated with chemotherapy, but the tumor size and serum AFP increased. He had a right parietooccipital craniotomy in a prone position. Through a right interhemispheric approach, the right tentorial opening is coagulated (**e**), and the tumor was uncovered under the arachnoid membrane through the tentorial opening (**f**). The tumor was firm and rubbery; thus, internal decompression was done and the mobilize the tumor separating the capsule from the third ventricle walls and floor (**g**). Following tumor isolation, the rest of the tumor was removed en bloc (**h**). The tectal plate is identified (**i**), and the column of the fornices is observed at the anterior end of the third ventricle (**j**). Postoperative postcontrast MR (**c**, **d**) showing resolution of the pineal NGGCT (VOG, vein of Galen; III, third ventricle)

surgical resection. The use of neoadjuvant chemotherapy for these malignant GCTs reduces not only the tumor size but also its vascularity. Pineoblastoma and ATRT are mostly soft and necrotic. They can often be suctioned away, but they can be vascular due to tumor neo-vascularization. Pineocytomas, however, are well demarcated and less vascular.

Glial tumors are mainly from the midbrain or thalamus. A grayish pineal gland may be present in the vicinity of the tumor. JPAs of the tectum, the tegmentum, and/or the posterior thalamus are also resectable when there is exophytic extension into the quadrigeminal cistern with or without a pia or thin cortical tissue covering. Unilateral section of the inferior colliculus is well tolerated because of reciprocal connection with contralateral side [93]. Although uni- or bilateral superior colliculi ablations reportedly do not lead to a permanent deficit in oculomotor function [93], the posterior commissure next to the superior colliculi needs to be protected. Cavalheiro et al. enter the brain stem for peri-collicular route through transverse incision either just above the superior colliculi or between the inferior colliculi and the fourth nerve [94]. Another safe zone is the lateral mesencephalic sulcus, which is located between the peduncular and tegmental segments of the midbrain and has a concave shape extending from the medial geniculate body to the ponto-mesencephalic sulcus [95]. However, the sulcus and other landmarks are often obscured due to the underlying mass in the midbrain. If anatomical landmark is not recognizable, going through the thinnest covering over the tumor is the best entry site to uncover the subjacent tumor. Once the underlying tumor is identified, it is removed in piece meal fashion (Fig. 11.13). An ultrasonic aspirator is helpful. Because most JPA are soft and grayish, distinct from the surrounding neural tissues, it is of paramount importance to identify the tumor-brain interface and never go beyond it.

For tumors of the superior medullary velum and superior vermis, a longer tentorial section provides a much wider view of the posterior fossa structures. These tumors are directly under the tentorium and are exposed in the subarachnoid space once the tentorial section is done. The tentorium is sectioned parallel to the straight sinus till normal cerebellar structure is identified. Tumors of the SMV involve both the quadrigeminal cistern and the fourth ventricle (Fig. 11.14). The OT approach allows access to the deep region without intersecting any normal neural or vascular structures [38]. Once the portion of the fourth ventricle is removed, the aqueduct and displaced tectal plate come into the surgical view.

11.10 Management Protocols

Neuroimaging studies, both CT and MR imaging, should be carefully reviewed and their findings correlated with patients age, sex, presenting symptoms, and tumor markers. The presence and absence of hydrocephalus should be determined. If hydrocephalus is the presenting sign, immediate medical attention is needed. Placement of a ventriculoperitoneal shunt is avoided if possible because of concerns

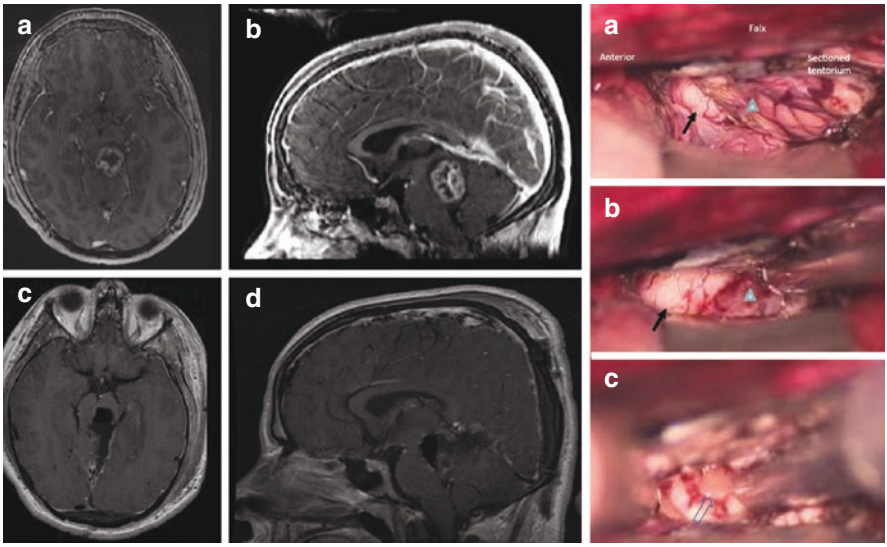

Fig. 11.13 A 17-year-old male with neurofibromatosis 1 presented with increasing headaches and ataxic gait. He was initially placed a VP shunt for hydrocephalus prior to transfer. Contrast-enhanced MR, axial (**a**) and sagittal (**b**) images showed a heterogeneously enhancing exophytic tumor at the tectum to the tegmentum. Surgical photograph (**e**) after the tentorial opening showing the tectal mass (*arrow*) visualized, which is overlapped by the cerebellum (*arrow head*). Following retraction of the cerebellum (**f**), the tumor, which is covered by thin neural tissue (*arrow*), is uncovered. Through a small incision over the thinnest neural tissue (*open arrow*), a piece meal tumor resection was done. Immediate postoperative contrast-enhanced MR, axial (**c**) and sagittal (**d**), showed a gross total resection

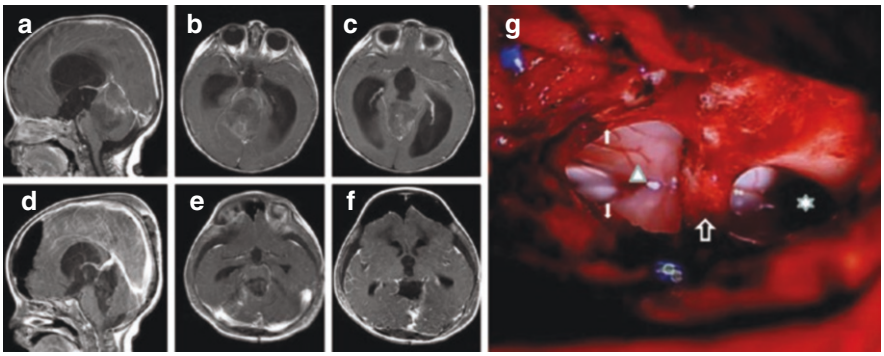

Fig. 11.14 Postcontrast MR sagittal (**a**) and axial (**b**, **c**) images of 9-month-old baby girl with ATRT of the superior medullary velum. The tumor was resected totally through a posterior interhemispheric approach on postoperative MR sagittal (**d**) and axial (**e**, **f**) images. Intraoperative photograph (**g**) after transtentorial resection showing the third ventricle (*triangle*) and the fourth ventricle (*star*). The posterior commissure (*open arrow*) is in the center over the aqueduct of Sylvius, and the tectum (*solid arrows*) is displaced rostrally

of developing shunt dependency, slit ventricles, and intraperitoneal metastases. The best option is an ETV combined with endoscopic tumor biopsy. At that time, CSF samples are collected for tumor markers and cytology. The other option is a craniotomy with tumor resection to restore the CSF pathway.

11.11 Tumors of the Pineal Gland

Children and adolescents with pineal region tumors should be evaluated with serum/CSF tumor markers for AFP and β-HCG to rule out NGGCT. For patients with negative tumor markers, surgical biopsy is indicated. Neuroimaging findings often enable differentiation of pineal teratomas (mature or immature) from other tumors because of their distinct characteristic appearance [22]. Germinoma is likely when there is mild elevation of β-HCG in the CSF, while NGGCT is the most likely diagnosis with elevated β-HCG and/or AFP. In such a case, neoadjuvant chemotherapy is recommended without surgical biopsy to attain reduction of the tumor size and tumor vascularity. These patients undergo a second-look operation if there is potential residual tumor and are often found to have teratoma (Fig. 11.15). When the tumor markers are normalized yet the tumor size is increasing during the chemotherapy, a growing teratoma is likely and needs to be resected. After initial chemotherapy, 61.7% of patients with localized NGGCT had either complete or partial responses, and with/without second look, surgery proceeded with limited field RT. Fangusaro et al. reported greater than 90% recurrence-free survival after 3 years of therapy [59]. A similar result was also reported by Calaminus et al. When localized malignant NGGCT attained complete response after initial chemotherapy, the 5 year progression survival rate was 85% when a complete response is attained, while it was 48% if residual tumor was present [96]. The pattern of relapse suggests inclusion of ventricles in the radiation field. Reduced-dose craniospinal radiation alone is effective in metastatic disease [59, 96]. Localized germinomas were treated with reduced dose CSI alone or with chemotherapy and reduced-field radiotherapy to the whole ventricle [97]. However, current protocols at Children's Oncology Group (COG ACNS1123) treat the localized germinomas with upfront chemotherapy followed by whole ventricle RT. Bifocal tumors in the third ventricle are very likely a malignant GCT and require chemotherapy, followed by radiation therapy. However, if bifocal tumor shows negative tumor markers, surgical biopsy is indicated.

Both pineoblastomas and ATRT, which are considered to be embryonal tumors, need aggressive tumor resection. Radical tumor resection shows a trend toward better survival rather than following partial resection [65]. However, the extent of tumor resection did not show statistical differences in patients' outcome [8, 48, 98]. Also, there are high CSF dissemination rates in both tumors. Molecular classifications correlate with the survival of patients with pineoblastoma. Li et al. reported Groups 1–3 arose in older children (median ages 5.2–14.0 years) and had intermediate to excellent survival (5-year survival of 68.0–100%), while Group RB and MYC PB patients were much younger (median age 1.3–1.4 years) with dismal survival (5-year survival 37.5% and 28.6%, respectively). They conclude age younger than

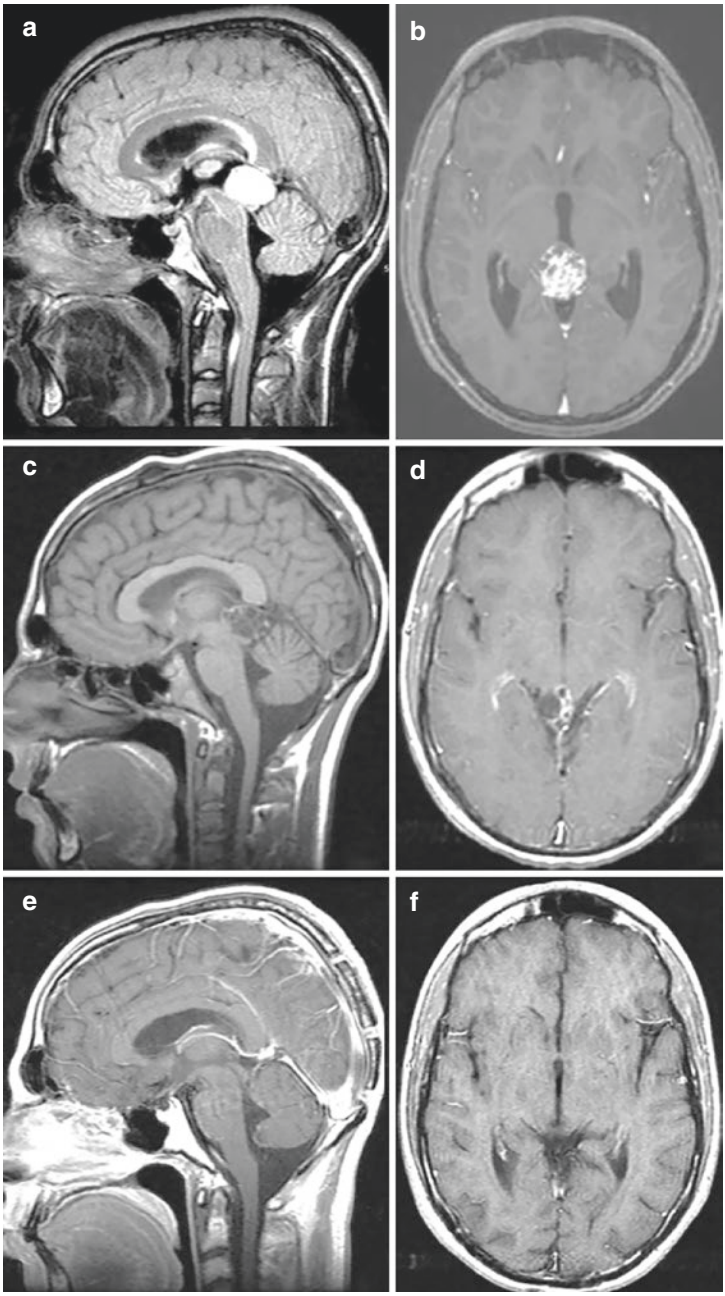

Fig. 11.15 Contrast-enhanced MR (**a**, **b**) showing a pineal tumor of a 17-year-old male. Serum AFP elevated serum AFP (62 ng/mL). He underwent an ETV followed by chemotherapy. His serum AFP was normalized, but post-chemotherapy MR (**c**, **d**) showed a reduced but persistent disease at the pineal location. At a subsequent second look surgery, a mature teratoma was resected (**e**, **f**)

3 years, at diagnosis, metastatic disease, omission of upfront radiation, and chromosome 16q loss as significant negative prognostic factors across all pineoblastomas [8]. Those who had only chemotherapy without RT among young children, the long-term survival was 5 out of 29, which is 17.2%.

11.12 Tumors of Midbrain or Posterior Thalamic Origin

Hydrocephalus, if present, is treated with ETV. If the lesion is non-enhancing, small, and intrinsic, they can be followed closely with MR imaging. However, if the lesion is progressive, large, contrast-enhancing, or largely cystic, a craniotomy is indicated, and histologic diagnosis needs to be confirmed. For benign astrocytomas, once adequate tumor resection is accomplished, follow-up without adjuvant therapy is recommended. However, unresectable, intrinsic astrocytomas are treated with chemotherapy and/or radiation therapy. JPA of the tectum and tegmentum can be amenable to surgical resection through the OT approach. Of paramount importance is choosing and securing neural entry and identifying the tumor-brain interface. Exophytic tumors extending to the cistern or third ventricle space can be excised following the exophytic portion of tumor deeper. However, an intrinsic tumor with a substantial neural structure has a higher risk of causing neurological deficits. It is prudent to treat these intrinsic benign tumors with chemotherapy upfront (Fig. 11.16).

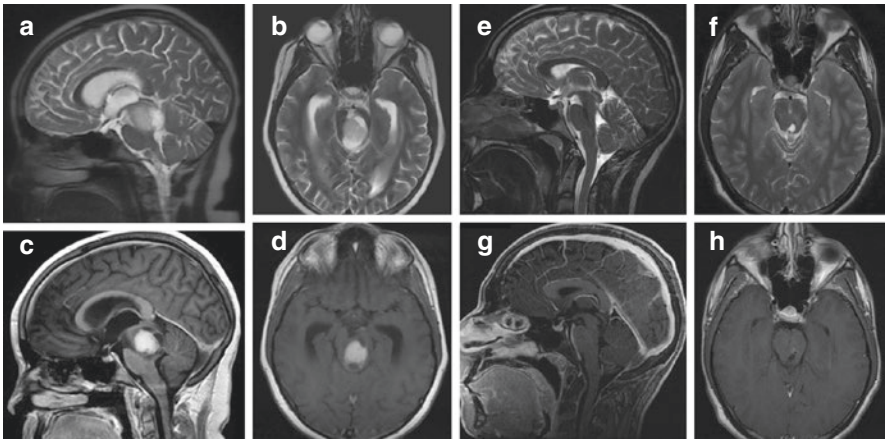

Fig. 11.16 A 9-year-old boy with increasing gait ataxia and mild right sided weakness. T-2 weighted MR sagittal (**a**) and axial (**b**), postcontrast MR sagittal (**c**), and axial (**d**) shows a mural tumor with surrounding cyst in the tegmentum of the midbrain and hydrocephalus. He had a stereotaxic tumor biopsy and then ETV from the left side pre-coronal burr holes. Histology showed JPA, and then he was treated with chemotherapy consisting of carboplatin and vincristine. Complete response was attained after the completion of chemotherapy with normal neurological findings. T-2 weighted MR sagittal (**e**) and axial (**f**), postcontrast MR sagittal (**g**), and axial (**h**) showed no signs of tumor recurrence without RT 11 years after diagnosis without RT

11.13 Conclusion and Future Direction

In the pineal region during childhood, GCTs and pineoblastoma from the pineal gland and JPA from the midbrain and thalamus are the most common histological types. Hydrocephalus is the most common cause of the presenting symptom and is ideally treated with ETV. Endoscopic tumor biopsy for intraventricular tumor in conjunction with ETV provides fairly accurate histological verification. A stereotaxic biopsy is recommended if the tumor is located extra-ventricularily. The serum and CSF tumor markers for GCTs are an important diagnostic method. When malignant GCT is suspected based on tumor markers and neuroimaging characteristics, it is often treated with neoadjuvant chemotherapy and may be completely resolved or at least reduced in size and vascularity. Patients with successfully resected teratomas, pineocytoma, and JPA do not need further oncological treatment.

Surgical resection of pineal region tumors remains challenging. Due to improved diagnostic and microsurgical methods, resection rates have risen with fewer complications. The OT and ITSC approaches have been commonly practiced, but each has advantages and disadvantages. When resecting these deep-seated tumors using either approach, surgical blind spots may hinder successful extirpation. The ITSC approach has blind spots at the CMF anteriorly to the cerebellar vermis and to the structures above the tentorium. For the OT approach, the structures opposite to the midline becomes the blind spot. Employing either ITSC or OT approaches, endoscope-assisted microneurosurgery provides a wider surgical view to the portion of the tumor in these blind spots by using an angled scope. Strictly endoscopic tumor resection has been documented in the recent literature [90, 99, 100]. The use of endoscopy will be popularized for pineal region tumor resection in the future once standard techniques are established. Midbrain or thalamic JPAs are amenable to resection if they are extrinsic or exophytic. However, these tumors, intrinsic tumors in particular, can also be treated with either chemotherapy or molecular target therapy.

References

1. Sapede D, Cau E. The pineal gland from development to function. Curr Top Dev Biol. 2013;106:172–215.
2. Patel S, Rahmania B, Jason Gandhia J, Seyama O, Joshic G, Reida I, Smithd NL, Waltzer WC, Khan SA. Revisiting the pineal gland: a review of calcification, masses, precocious puberty, and melatonin functions. Int J Neurosci. 2020;130:464–75.
3. Bojkowski CJ, Arendt J. Factors influencing urinary 6-sulphatoxymelatonin, major melatonin metabolite, in normal human subjects. Clin Endocrinol. 1990;33:435–44.
4. Garcia-Patterson A, Piig-Domingo M, Webb SM. Thirty years of human pineal research: do we know its clinical relevance? J Pineal Res. 1996;20:1–6.
5. Louis DN, Perry A, Wesseling P, Brat DJ, Cree IA, Figarella-Branger D, Hawkins C, Ng HK, Pfister SM, Reifenberger G, Soffietti R, von Deimling A, Ellison DW. The 2021 WHO

Classification of Tumors of the Central Nervous System: a summary. Neuro-Oncology. 2021;23(8):1231–51.
6. Sano K. Pathogenesis of intracranial germ cell tumors reconsidered. J Neurosurg. 1999;90:258–64.
7. Jennings MT, Gelman R, Hochberg F. Intracranial germ-cell tumors: natural history and pathogenesis. J Neurosurg. 1985;63:155–67.
8. Li BK, Vasiljevic A, Dufour C, Yao F, Ho BLB, Lu M, Hwang EI, Gururangan S, Hansford JR, Fouladi M, Nobusawa S, Laquerriere A, Delisle M-B, Fangusaro J, Forest F, Toledano H, Solano-Paez P, Leary S, Birks D, Hofman LM, Szathmari A, Faure-Conter C, Fan X, Catchpoole D, Zhou L, Schultz KAP, Ichimura K, Gauchotte G, Jabado N, Jones C, Loussouarn D, Mokhtari K, Rousseau A, Ziegler DS, Tanaka S, Pomeroy SL, Gajjar A, Ramaswamy V, Hawkins C, Grundy RG, Hill DA, Boufet E, Huang A, Jouvet A. Pineoblastoma segregates into molecular sub-groups with distinct clinico-pathologic features: a Rare Brain Tumor Consortium registry study Based on DNA-methylation analysis. Acta Neuropathol. 2020;139:223–41.
9. Liu APY, Gudenas B, Tong Lin T, Orr BA, Klimo P Jr, Kumar R, Boufet E, Gururangan S, Crawford JR, Kellie SJ, Chintagumpala M, Fisher MJ, Bowers DC, Hassall T, Indelicato DJ, Onar-Thomas A, Ellison DW, Boop FA, Merchant TE, Robinson GW, Northcott PA, Gajjar A. Risk-adapted therapy and biological heterogeneity in pineoblastoma: integrated clinicopathological analysis from the prospective, multi-center SJMB03 and SJYC07 trials. Acta Neuropathol. 2020;139:259–71.
10. Matsumura N, Goda N, Yashige K, Kitagawa M, Yamazaki T, Nobusawa S, Yokoo H. Desmoplastic myxoid tumor, SMARCB1-mutant: a new variant of SMARCB1-deficient tumor of the central nervous system preferentially arising in the pineal region. Virchows Arch. 2021;479(4):835–9.
11. Barnett DN, Olson JJ, Thomas WG, Hunter SB. Low-grade astrocytomas arising from the pineal gland. Surg Neurol. 1995;43:70–6.
12. Masina R, Ansaripour A, Beneš V, Berhouma M, Choque-Velasquez J, Eide PK, Fedorko S, Fleck S, Hernesniemi J, Koziarski A, Májovský M, Podgorski A, Schroeder H, Teo C, Unterberg AW, Yeung JT, Kolias A, Santarius T. Surgical treatment of symptomatic pineal cysts without hydrocephalus—meta-analysis of the published literature. Acta Neurochir. 2022;164:61–77.
13. Fain JS, Tomlinson FH, Scheithauer BW, et al. Symptomatic glial cyst of the pineal gland. J Neurosurg. 1994;80:454–60.
14. Favero G, Bonomini F, Rezzani R. Pineal gland tumors: a review. Cancers. 2021;13(7):1547.
15. Matsutani M, Sano K, Takakura K, Fujimaki T, Nakamura O, Funata N, Seto T. Primary intracranial germ cell tumors: a clinical analysis of 153 histologically verified cases. J Neurosurg. 1997;86:446–55.
16. Villano JL, Propp JM, Porter KR, Stewart AK, Valyi-Nagy T, Li X, Engelhard H, McCarthy BJ. Malignant pineal germ-cell tumors: an analysis of cases from three tumor registries. Neuro-Oncology. 2008;10:121–30.
17. Zhang H, Qi ST, Fan J, Fan LX, Qiu BH, Liu Y, Qiu XY. Bifocal germinomas in the pineal region and hypothalamo-neurohypophyseal axis: primary or metastasis? J Clin Neurosci. 2016;34:151–7.
18. Esfahani DR, Alden T, Dipatri A, Xi G, Goldman S, Tomita T. Pediatric suprasellar germ cell tumors: a clinical and radiographic review of solitary vs bifocal tumors and its therapeutic implications. Cancers. 2020;12(9):E2621.
19. The Committee of Brain Tumor Registry of Japan (BTRJ). Brain Tumor Registry of Japan (BTRJ 1969-1996) 11th ed. Neurol Med Chir. 2003;43(Suppl):29.
20. Lin C-C, Mansukhani MM, Bruce JN, Canoll P, Zanazzi G. Rosette-Forming glioneuronal tumor in the pineal region: a series of 6 cases and literature review. J Neuropathol Exp Neurol. 2021;80:933–43.

21. Katyal A, Anil Jadhav A, Katyal A, Jagetia A, Bodeliwala S, Singhal GD, Wajid Nazir W, Batra V, Kumar Srivastava AK, Daljit Singh D. Occipital transtentorial approach for pineal region lesions: addressing the controversies in conventional teaching. Surg Neurol Int. 2021;12:503.
22. Awa R, Campos F, Arita K, Sugiyama K, Tominaga A, Kurisu K, Yamasaki F, Karki P, Tokimura H, Fukukura Y, Fujii Y, Hanaya R, Oyoshi T, Hirano H. Neuroimaging diagnosis of pineal region tumors—quest for pathognomonic finding of germinoma. Neuroradiology. 2014;56:525–34.
23. Qi S, Fan J, Zhang X-A, Zhang H, Qiu B, Fang L. Radical resection of nongerminomatous pineal region tumors via the occipital transtentorial approach based on arachnoidal consideration: experience on series of 143 patients. Acta Neurochir. 2014;156:2253–62.
24. Sugiyama K, Uozumi T, Kiya K, et al. Intracranial germ-cell tumor with synchronous lesions in the pineal and suprasellar regions: report of six cases and review of the literature. Surg Neurol. 1992;38:114–20.
25. Manos RS, Bar-Ziv J, Tadmor R, Eisbruch A, Rechavi G. Pineal germinoma with unilateral blindness: seeding of germinoma cells in optic nerve sheath. J Clin Neuroophthalmol. 1990;10:239–43.
26. Hertle RN, Robb RM. Pinealoblastopma metastatic to the optic nerve. J Clin Neuroophthalmol. 1990;10:95–9.
27. Tomita T. Pineal tumor. In: Selden N, Baird L, editors. Pediatric neurosurgery. Oxford: Oxford University Press; 2019. p. 165–76.
28. Hammadur Rahaman SK, Khandelwal D, Khadgawat R, Devasenathipathy K, Sameer B. Peripheral precocious puberty caused by human chorionic gonadotropin producing pineal gland tumor. Indian Pediatr. 2018;55(3):254–6.
29. Mavridis IN, Pyrgelis E-S, Eleni Agapiou E, Meliou M. Pineal region tumors: pathophysiological mechanisms of presenting symptoms. Am J Transl Res. 2021;13(6):5758–66.
30. Zimmerman RA, Bilaniuk LT. Age-related incidence of pineal calcification detected by computed tomography. Radiology. 1982;142:659–66.
31. Chiechi MV, Smirniotopoulos JG, Mena H. Pineal parenchymal tumors: CT and MR features. J Compt Assist Tomogr. 1995;19:509–17.
32. Sugiyama K, Tominaga A, Kurisu K, Yamasaki F, Karki P, Tokimura H, Fukukura Y, Fujii Y, Hanaya R, Oyoshi T, Hirano H. Neuroimaging diagnosis of pineal region tumors—quest for pathognomonic finding of germinoma. Neuroradiology. 2014;56(7):525–34.
33. Chang T, Teng MM, Gou WY, et al. CT of pineal tumors and intracranial germ-cell tumors. AJNR. 1989;10:1039–44.
34. Sumida M, Uozumi T, Kiya K, et al. MRI of intracranial germ cell tumours. Neuroradiology. 1995;37:32–7.
35. Konovalov AN, Pitskhelauri DI. Principles of treatment of the pineal region tumors. Surg Neurol. 2003;59:250–68.
36. Tien RD, Barkovich AJ, Edwards MSB. MR imaging of pineal tumors. Am J Neuroradiol. 1990;11:557–65.
37. Nakamura M, Saeki N, Iwadate Y, et al. Neuroradiological characteristics of pineocytoma and pineoblastoma. Neuroradiology. 2000;42:509–14.
38. Tomita T, Frassanito P. Tumors of the superior medullary velum in infancy and childhood: report of 6 cases. J Neurosurg Pediatr. 2013;11:52–9.
39. Golzarian J, Baleriaux D, Bank WO, Matos C, Flament-Durand J. Pineal cyst: normal or pathological? Neuroradiology. 1993;35:251–3.
40. Masina R, Ansaripour A, Beneš V, Berhouma M, Choque-Velasquez J, Eide PK, Fedorko S, Fleck S, Hernesniemi J, Koziarski A, Májovský M, Podgorski A, Schroeder H, Charles Teo C, Unterberg AW, Yeung JT, Kolias A, Santarius T. Surgical treatment of symptomatic pineal cysts without hydrocephalus—meta-analysis of the published literature. Acta Neurochir. 2022;164:61–77.

41. Igboechi C, Vaddiparti A, Sorenson EP, Rozzelle CJ, Tubbs S, Loukas M. Tectal plate gliomas: a review. Childs Nerv Syst. 2013;29:1827–33.
42. Takami H, Graffeo CS, Perry A, Giannini C, Nakazato Y, Saito N, Matsutani M, Nishikawa R, Ichimura K, Daniels DJ. Roles of tumor markers in central nervous system germ cell tumors revisited with histopathology-proven cases in a large international cohort. Cancers. 2022;14:979.
43. Balmaceda C, Heller G, Rosenblum M, et al. Chemotherapy without irradiation: a novel approach for newly diagnosed CNS germ cell tumors: results of an international cooperative trial. J Clin Oncol. 1996;15:2908–15.
44. Qaddoumi I, Sane M, Li S, Kocak M, Pai-Panandiker A, Harreld J, et al. Diagnostic utility and correlation of tumor markers in the serum and cerebrospinal fluid of children with intracranial germ cell tumors. Childs Nerv Syst. 2012;28:1017–24.
45. Kamakura Y, Hasegawa M, Minamoto T, Tamashita J, Fujisawa H. C-kit gene mutation: common and widely distributed in intracranial germinomas. J Neurosurg. 2006;104:173–80.
46. Leston J, Mottolese D, Champier J, Jouvet A, Brun J, Sindou M, Chazot G, Claustrat B, Fevre-Montange M. Contribution of the daily melatonin profile to diagnosis of tumors of the pineal region. J Neuro-Oncol. 2009;93:387–94.
47. Wolden SL, Wara WM, Larson DA, et al. Radiation therapy for primary intracranial germcell tumors. Int J Radiat Oncol Biol Phys. 1995;32:943–7.
48. Gutierrez FA, Tomita T, Leestma J, et al. Pineoblastomas in children. Concepts. Pediatr Neurosurg. 1990;10:118–28.
49. Duffner PK, Cohen ME, Sanford RA, et al. Lack of efficacy of postoperative chemotherapy and delayed radiation in very young children with pineoblastoma. Med Pediatr Oncol. 1995;25:38–44.
50. Schulz M, Afshar-Bakshloo M, Koch A, Capper D, Driever PH, Tietze A, Grün A, Thomale U-W. Management of pineal region tumors in a pediatric case series. Neurosurg Rev. 2021;44:1417–14271.
51. Wong T-T, Chen H-H, Liang M-L, Yen Y-S, Chang F-C. Neuroendoscopy in the management of pineal tumors. Childs Nerv Syst. 2011;27(6):949–59.
52. Gururangan S, Heideman RL, Kovner EH, et al. Peritoneal metastases in two patients with pineoblastoma and ventriculo-peritoneal shunts. Med Pediatr Oncol. 1994;22:417–20.
53. Ung AO, Triscott JA, Leditschke JF, et al. Metastasis of pineal germinoma via ventriculoperitoneal shunt. Aust NZ J Surg. 1993;63:409–12.
54. Pallini R, Bozzini V, Scerrati M, et al. Bone metastases associated with shunt-related peritoneal deposits from a pineal germinoma: case report and review of literature. Acta Neurochir. 1991;109:78–83.
55. Giussani C, Guida L, Trezza A, Sganzerla EP. Effectiveness of intraventricular endoscopic lamina terminalis fenestration in comparison with standard ETV: systematic review of literature. World Neurosurg. 2017;103:257–64.
56. Navarro R, Gil-Parra R, Reitman AJ, Olavarria G, Grant JA, Tomita T. Endoscopic third ventriculostomy: early and late complications and their avoidance. Childs Nerv Syst. 2005;22:506–13.
57. Choi JU, Kim DS, Chung SS, et al. Treatment of germ cell tumors in the pineal region. Childs Nerv Syst. 1998;14:41–8.
58. Kanamori M, Kumabe T, Tominaga T. Is histological diagnosis necessary to start treatment for germ cell tumours in the pineal region? J Neurol Sci. 2008;15:978–87.
59. Fangusaro J, Wu S, MacDonald S, Murphy E, Shaw D, Bartels U, Soumen Khatua S, Souweidane M, Lu H-M, Morris D, Panigrahy A, Onar-Thomas A, Fouladi M, Gajjar A, Dhall G. Phase II trial of response-based radiation therapy for patients with localized CNS nongerminomatous germ cell tumors: a children's oncology group study. J Clin Oncol. 2019;37:3283–90.
60. Dempsey PK, Kondziolka D, Lunsford LD. Stereotactic diagnosis and treatment of pineal region tumours and vascular malformations. Acta Neurochir. 1992;116:14–22.

61. Zacharia BE, Bruce JN. Stereotactic biopsy considerations for pineal tumors. Neurosurg Clin N Am. 2011;22:359–66.
62. Oi S, Shibata M, Tominaga J, Shinoda M, Takei F, Tsugane R, Matsuzawa K, Sato O. Efficacy of neuroendoscopic procedures in minimally invasive preferential management of pineal region tumors: a prospective study. J Neurosurg. 2000;93:245–53.
63. Pople IK, Athanasiou TC, Sandeman DR, et al. The role of endoscopic biopsy and third ventriculostomy in the management of pineal region tumours. Br J Neurosurg. 2001;15:305–11.
64. Wong T-T, Yen S-H, Ho DM, Chang FC, Chang KP. Pineal Germinoma with intratumoral hemorrhage after neuroendoscopic tumor biopsy. Childs Nerv Syst. 2003;19:769–72.
65. Parikh KA, Venable GT, Orr BA, Choudhri AF, Boop FA, Gajjar AJ, Klimo P Jr. Pineoblastoma—the experience at St. Jude Children's Research Hospital. Neurosurgery. 2017;81:120–8.
66. Cushing H. Intracranial tumors: notes upon a series of two thousand verified cases with surgical mortality pertaining thereto. Springfield, IL: Charles C Thomas; 1932. p. 64.
67. Dandy WE. Operative experiences in cases of pineal tumor. Arch Surg. 1936;33:19.
68. Dandy WE. An operation for the removal of pineal tumors. Surg Gynecol Obstet. 1921;33:113–9.
69. Horrax G. Extirpation of a huge pinealoma from a patient with pubertas praecox. Arch Neurol Psychiatr. 1937;37:385–97.
70. Poppen JL. The right occipital approach to a pinealoma. J Neurosurg. 1966;25:706–10.
71. Jamieson KG. Excision of pineal tumors. J Neurosurg. 1971;35:550–3.
72. Krause F. Operative Frielegung der Vierhugel, nebst Beobachtungen uber Hirndruck und Dekompression. Zentrabl Chir. 1926;53:2812–9.
73. Stein BM. The infratentorial supracerebellar approach to pineal lesions. J Neurosurg. 1971;35:197–202.
74. Mamelak AN, Drazin D, Shirzadi A, Black KL, Berci G. Infratentorial supracerebellar resection of a pineal tumor using a high definition video exoscope (VITOM). J Clin Neurosci. 2012;19:306–9.
75. Uschold T, Abla AA, Fusco D, Bristol RE, Nakaji P. Supracerebellar infratentorial endoscopically controlled resection of pineal lesions: case series and operative technique. J Neurosur (Pediatr). 2011;8:554–64.
76. Cai Y, Xiong Z, Xin C, Chen J, Kui Liu K. Endoscope-assisted microsurgery in pediatric cases with pineal region tumors: a study of 18 cases series. Front Surg. 2021;8:641196.
77. Shirane R, Shamoto H, Umezawa K, et al. Surgical treatment of pineal region tumours through the occipital transtentorial approach: evaluation of the effectiveness of intra-operative microendoscopy combined with neuronavigation. Acta Neurochir. 1999;141:801–9.
78. Ausman JI, Malik GM, Dujovny M, Mann R. Three-quarter prone approach to the pineal-tentorial region. Surg Neurol. 1988;29:298–306.
79. Azab WA, Nasim K, Salaheddin W. An overview of the current surgical options for pineal region tumors. Surg Neurol Int. 2014;5:39.
80. Mottolese C, Szathmari A, Ricci-Franchi AC, Beuriat PA, Grassiot B. The sub-occipital transtentorial approach revisited base on our own experience. Neurochirurgie. 2015;61:168–75.
81. Moshel YA, Parker EC, Kelly PJ. Occipital transtentorial approach to the precentral cerebellar fissure and posterior incisural space. Neurosurgery. 2009;65:554–64.
82. Tanaka R, Washiyama K. Occipital transtentorial approach to pineal region tumors. Oper Tech Neurosurg. 2003;6:215–21.
83. Fukui M, Natori Y, Matsushima T, Nishio S, Ikezaki K. Operative approaches to the pineal region tumors. Childs Nerv Syst. 1998;14:49–52.
84. Matsuo S, Baydin S, Gungor A, Middlebrooks EH, Komune N, Iihara K, Thoton AL. Prevention of postoperative visual field defects after the occipital transtentorial approach: anatomical study. J Neurosurg. 2018;129:188–97.

85. Yoshimoto K, Araki Y, Amanoa T, Matsumoto K, Nakamizo A, Sasaki T. Clinical features and pathophysiological mechanism of the hemianoptic complication after the occipital transtentorial approach. Clin Neurol Neurosurg. 2013;115:1250–6.
86. Davidson L, Krieger DK, McCombs JG. Posterior interhemispheric retrocallosal approach to pineal region and posterior fossa lesions in a pediatric population. J Neurosurg Pediatr. 2011;7:527–33.
87. Zhang XA, Qi S, Fan J, Huang G, Peng J, Xu J. The distribution of arachnoid membrane within the velum interpositum. Acta Neurochir. 2012;154:1711–5.
88. McComb JG. Is there risk to occlusion of the deep veins when removing pineal location tumors? Concepts. Pediatr Neurosurg. 1987;7:72–80.
89. Iwami K, Fujii M, Saito K. Occipital transtentorial/falcine approach, a "cross-court" trajectory to accessing contralateral posterior thalamic lesions: case report. J Neurosurg. 2017;127:165–70.
90. Tanikawa M, Sakata T, Yamada H, Kawase-Kamikokura H, Ohashi K, Ueki T, Mase M. Endoscopic high occipital interhemispheric transtentorial approach for lesions in the anterosuperior cerebellum, upper fourth ventricle, and upper dorsal brain stem. World Neurosurg. 2022;159:e260–6.
91. Ma Y, Qing Lan Q. An anatomic study of the occipital transtentorial keyhole approach. World Neurosurg. 2013;80(1–2):183–9.
92. Liu JK. Endoscopic-assisted interhemispheric parieto-occipital transtentorial approach for microsurgical resection of a pineal region tumor: operative video and technical nuances. Neurosurg Focus. 2016;40(Suppl 1):V13.
93. Kaku Y, Yonekawa Y, Taub E. Transcollicular approach to intrinsic tectal lesions. Neurosurgery. 1999;44:338–43.
94. Cavalheiro S, Yagmurlu K, da Costa MDS, Nicácio JM, Rodrigues TP, Chaddad-Neto F, Rhoton AL. Surgical approaches for brainstem tumors in pediatric patients. Childs Nerv Syst. 2015;31:1815–40.
95. Cavalcanti DD, Morais BA, Figueiredo EG, Spetzler EF, Preul MC. Surgical approaches for the lateral mesencephalic sulcus. J Neurosurg. 2020;132:1653–8.
96. Calaminus G, Frappaz D, Kortmann RD, et al. Outcome of patients with intracranial non-germinomatous germ cell tumors-lessons from the SIOP-CNS-GCT-96 trial. Neuro-Oncology. 2017;19(12):1661–72.
97. Calaminus G, Kortmann R, Worch J, et al. SIOP CNS GCT 96: final report of outcome of a prospective, multinational nonrandomized trial for children and adults with intracranial germinoma, comparing craniospinal irradiation alone with chemotherapy followed by focal primary site irradiation for patients with localized disease. Neuro-Oncology. 2013;15(6):788–96.
98. Reddy AT, Janss AJ, Phillips PC, Weiss HL, Packer RJ. Outcome for children with supratentorial primitive neuroectodermal tumors treated with surgery, radiation and chemotherapy. Cancers. 2000;88:2189–93.
99. Gu Y, Zhou Q, Zhu W, Wu Q, Xie T, Wu S, Hu F, Yu Y, Sun C, Li C, Zhang B, Zhan L, Zhang X. The purely endoscopic supracerebellar infratentorial approach for resecting pineal region tumors with preservation of cerebellomesencephalic vein: technical note and preliminary clinical outcomes. World Neurosurg. 2019;128:e334–9.
100. Tanikawa M, Yamada H, Sakata T, Hayashi Y, Sasagawa Y, Watanabe T, Nagatani T, Mase M. Exclusive endoscopic occipital transtentorial approach for pineal region tumors. World Neurosurg. 2019;131:167–73.

Chapter 12
Clinical and Surgical Approach for Cerebral Cortical Dysplasia

Marcelo Volpon Santos, Camila Araujo Bernardino Garcia, Ana Paula Andrade Hamad, Ursula Thome Costa, Americo Ceiki Sakamoto, Antonio Carlos dos Santos, and Helio Rubens Machado

12.1 Introduction

Epilepsy, or the state of recurrent seizures, encompasses a wide spectrum of pathological substrates and syndromes, with different clinical semiology, onset, and etiology, which can be both acquired and/or genetic [1]. Broadly speaking, primary epilepsies might be divided into three main categories: (1) genetic generalized epilepsy (formerly known as idiopathic generalized epilepsy), (2) focal epilepsy, and (3) epileptic encephalopathy [2, 3]. Epilepsy could also be the main clinical manifestation of various cerebral abnormalities and lesions, such as traumatic injury, tumors, infections, vascular malformations, and so forth.

Fortunately, there are many available therapies for epilepsy, especially from a pharmacological standpoint (antiepileptic drugs, AEDs), which provide seizure control in about 60–70% of patients [4]. Surgical treatment can be offered for patients who do not respond well to clinical therapy, when they can be diagnosed with refractory epilepsy. Epilepsy surgery has already been proven to have sturdy and favorable results, allowing seizure freedom in 50–70% of patients overall [5].

M. V. Santos (✉)
Center for Pediatric Epilepsy Surgery (CIREP), Ribeirão Preto Medical School, University Hospital, University of São Paulo, São Paulo, SP, Brazil

Department of Surgery and Anantomy, Ribeirão Preto Medical School, University of São Paulo, São Paulo, SP, Brazil
e-mail: marcelovolpon@usp.br

C. A. B. Garcia · A. P. A. Hamad · U. T. Costa · A. C. Sakamoto · A. C. dos Santos · H. R. Machado
Center for Pediatric Epilepsy Surgery (CIREP), Ribeirão Preto Medical School, University Hospital, University of São Paulo, São Paulo, SP, Brazil
e-mail: anahamad@fmrp.usp.br; ursulathome@hcrp.usp.br; sakamoto@hcrp.usp.br; acsantos@hcrp.usp.br; hrmachad@fmrp.usp.br

C. Di Rocco (ed.), *Advances and Technical Standards in Neurosurgery*, Advances and Technical Standards in Neurosurgery 48,
https://doi.org/10.1007/978-3-031-36785-4_12

Nevertheless, preventive treatments or therapeutic alternatives that could mitigate the deleterial progression of this pathology (the so-called disease-modifying agents) have not been developed [6].

Historically, the basic pathophysiological mechanisms of epilepsy have been described with an emphasis on histological features; more recently, the study of genetic alterations in epileptic patients has gained widespread acceptance. This "genetic era" of epilepsy started decades ago, with reports of familial monogenic epilepsy syndromes, and has evolved to modern genomics, due to large-scale studies of molecular sequencing that led to the identification of an extensive number of genes associated with this disease [7].

Mutations in genes that change the spatial and functional structures of ionic channels of the plasmatic membrane (channelopathies) have been known for quite some time, as well as genetic mutations that affect other pathways, including partial idiopathic epilepsy, progressive myoclonic epilepsy, and X-chromosome-liked epilepsy [8]. In upcoming years, these developments will be even more vigorous, since DNA mutations responsible for messenger RNA and protein synthesis have been implicated in the deposition of metabolites and aberrant neuronal excitability, which will ultimately wind up as clinical seizures [9]. However, most epileptic syndromes have complex genetic mechanisms that still need further clarification.

12.2 Malformations of Cortical Development (MCD)

Abnormal development of the cerebral cortex during embryogenesis is a frequent cause of cognitive deficits and epilepsy, resulting from a broad group of pathological entities named malformations of cortical development [10, 11]. Their exact incidence is unknown; however, MCDs have been seen much more frequently in recent years ever since advanced diagnostic techniques, particularly high-resolution magnetic resonance imaging (MRI), are being used for clinical investigation of patients with congenital neurological defects, epilepsy, and neurodevelopmental delay [12, 13]. Approximately 25–40% of intractable or pharmacoresistant epilepsies in childhood are attributable to MDCs, and at least 75% of patients with such malformations will present with seizures during their lifetime [13, 14].

The classification of MDCs is based on three fundamental embryological events of cortical formation: (1) cell proliferation into the germinal matrix, (2) cell migration within the developing cortex, and (3) horizontal and vertical organization of cortical neural cells with the generation of axonal and dendritic ramifications [15, 16]. Therefore, they can be categorized according to their primary neurodevelopmental defect into three subgroups: (1) MCDs secondary to abnormal cell proliferation and/or apoptosis, (2) MCDs related to abnormal cell migration, and (3) MCDs associated with aberrant post-migrational development [10].

Moreover, MCDs are further subdivided in [17]:

- Group I (abnormal neuronal/glial cell proliferation/apoptosis): reduced proliferation or expedited apoptosis: microcephaly; augmented proliferation or diminished apoptosis: megalencephaly; and abnormal proliferation: cortical dysplasias, focal or diffuse.
- Group II (abnormal cell migration): neuroependymal malformations (early migration), including periventricular heterotopia, generalized migrational abnormalities such as lissencephaly, transmantle dysplastic heterotopia, and subcortical band heterotopia.
- Group III (post-migrational malformations): polymicrogyria, schizencephaly, focal cortical dysplasias, and post-migrational microcephaly (Table 12.1).

Although environmental factors are certainly involved in the pathogenesis of cortical development malformations, several research studies have established a variety of genes that have an important role in cell proliferation and differentiation, as well as neuronal migration and final stages of cortical organization [8, 19], many of which have been implicated as specific causes of MCDs. Classifying MCD based on molecular biology was determinant for the description of multiple genes associated with the abovementioned disorders, which have different phenotypes resulting from mutation of different genes, so important for the adequate understanding of the mechanisms of certain diseases and genetic counselling [20]. For instance, recessive mutations of the human gene WDR62 have been identified in MCD patients, using whole genome sequencing techniques [21]. Other examples of recent genetic discoveries, which are related to MCDs, include mutations in five distinct genes (*LIS1, DCX, 14–3-3 e RELN,* e *ARX*) causing lissencephaly; mutations in genes *SPRX2, KIAA1279, GPR56, PAX6, TBR2, COL18A1, RABG3GAP1, and TUB2B* in the cases of polymicrogyria; copy number variants and mutations have been described in genes *FLNA1, ARFGEF2, and LRP2* in patients with periventricular nodular heterotopia; cases with subcortical band heterotopia have been shown to have mutation in genes *DCX* and *LIS1*; and mutations in gene EMX2 were found in patients with schizencephaly [9].

As far as it comes to epilepsy specifically, many mutated genes have been deemed causative of this disease, such as *CNKSR2, KCNQ2, SCN1A, CDKL5, STXBP1, CHD2, SCN3A, SCN9A, TSC2, MBD5, POLG, EFHC1 MYH1*, and e *CLCN6*, among others. Most of these genes regulate ionic channel subunits, which modulate neural electric activity, and thus induce seizures through mechanisms that either promote excitatory stimuli or hinder inhibitory pathways [22–24].

The prominent role of the *Mammalian Target of Rapamycin* (MTOR) pathway, among all genetic pathways involved in cell signaling and expression, must be highlighted; it centrally regulates important physiological functions, such as cell proliferation and growth, metabolism, autophagia, and apoptosis, and has been related to the development of cardiovascular diseases, obesity, and diabetes [25, 26]. It also generates a rapamycin protein whose excessive signaling represents a primary pathogenic event of cortical dysplasias and tuberous sclerosis, working as a catalyst within two distinct complexes, which differ in sensibility to rapamycin and cell targets. mTORC1 is sensitive to rapamycin and modulates protein synthesis directly,

Table 12.1 Classification of malformations of cortical development

I. Malformations due to abnormal neuronal and glial proliferation or apoptosis
A. Decreased proliferation/increased apoptosis or increased proliferation/decreased apoptosis—Abnormalities of brain size
1. Microcephaly with normal to thin cortex
2. Microlissencephaly (extreme microcephaly with thick cortex)
3. Microcephaly with extensive polymicrogyria
4. Macrocephalies
B. Abnormal proliferation (abnormal cell types)
1. Nonneoplastic
(a) Cortical hamartomas of tuberous sclerosis
(b) Cortical dysplasia with balloon cells
(c) Hemimegalencephaly
2. Neoplastic (associated with disordered cortex)
(a) Dysembryoplastic neuroepithelial tumor
(b) Ganglioglioma
(c) Gangliocytoma
II. Malformations due to abnormal neuronal migration
A. Lissencephaly/subcortical band heterotopia spectrum
B. Cobblestone complex/congenital muscular dystrophy syndromes
C. Heterotopia
1. Subependymal (periventricular)
2. Subcortical (other than band heterotopia)
3. Marginal glioneuronal
III. Malformations due to abnormal cortical organization (including late neuronal migration)
A. Polymicrogyria and schizencephaly
1. Bilateral polymicrogyria syndromes
2. Schizencephaly (polymicrogyria with clefts)
3. Polymicrogyria or schizencephaly as part of multiple congenital anomaly/mental retardation syndromes
B. Cortical dysplasia without balloon cells
C. Microdysgenesis
IV. Malformations of cortical development, not otherwise classified
A. Malformations secondary to inborn errors of metabolism
1. Mitochondrial and pyruvate metabolic disorders
2. Peroxisomal disorders
B. Other unclassified malformations
1. Sublobar dysplasia
2. Others

(Adapted from Barkovich et al. 2005 [18])

through ribosome kinase S6 and eukaryotic protein factor 4E-1 (4E-BP1) [27]. mTORC2 activates several other kinases, such as AKT and protein kinase C, as well as cytoskeleton regulators. They can both be stimulated or inhibited by many

environmental and metabolic demands, including insulin/phosphatidylinositol 3-kinase (PI3K)/AKT and AMP-activated protein kinase (AMPK) [28]. The mTOR pathway has already been described in relation with histopathological alterations found in MCDs and refractory epilepsies, and it seems reasonable to correlate abnormal cellular counts and phenotypes with mTOR mutations, as seen in focal cortical dysplasia.

12.3 Epilepsy Related to Malformations of Cortical Malformation: Pathological, Clinical, and Surgical Aspects

Within the very diverse group of MCDs, the role of focal cortical dysplasias needs to be emphasized, due to their higher epidemiological frequency and specific pathological and epileptogenic features. Nevertheless, prior to reviewing FCDs, it is also important to discuss certain aspects, from a surgical standpoint, of other relevant types of MCD, with their own particularities. As a general rule, the location of functional cortex in patients with MCDs can be different than normal controls, especially in those with MCDs due to abnormal neuronal proliferation, which have been shown to have marked reorganization of the functional cortex [29], whereas in patients with FCD, language and motor function, as defined by electrical stimulation, are often preserved in the dysplastic and highly epileptogenic cortex surrounding the actual abnormality [30].

The definitive diagnosis of MCD is based on neuropathological findings; however, for most practical purposes, diagnosis begins with the neuroimaging features, associated clinical phenotyping, and genetic findings [31]. Therefore, it is of great importance to become familiar with the changes in imaging appearance of MCD associated with the age of the patient and the type of magnetic resonance sequences that are best suited to detect these anomalies (Fig. 12.1) [32, 33]. Moreover, these malformations seem to share common signaling pathways, and MCD-related genes can be involved at multiple developmental stages, so proliferation, migration, and post-migrational organization are genetically and functionally interdependent [29]. As the boundaries between disorders of neuronal migration, cortical organization, and proliferation are vanishing, it is expected that future classifications of MCDs will rely on the precise knowledge of those biological pathways.

12.3.1 Gray Matter Heterotopia

Gray matter (or nodular) heterotopia (GMH) is characterized by irregular clusters of gray matter along the ventricle (PNH) or within the white matter (SNH) [34]. They can be identified on MRI T1-sequences as conglomerates of gray matter in various

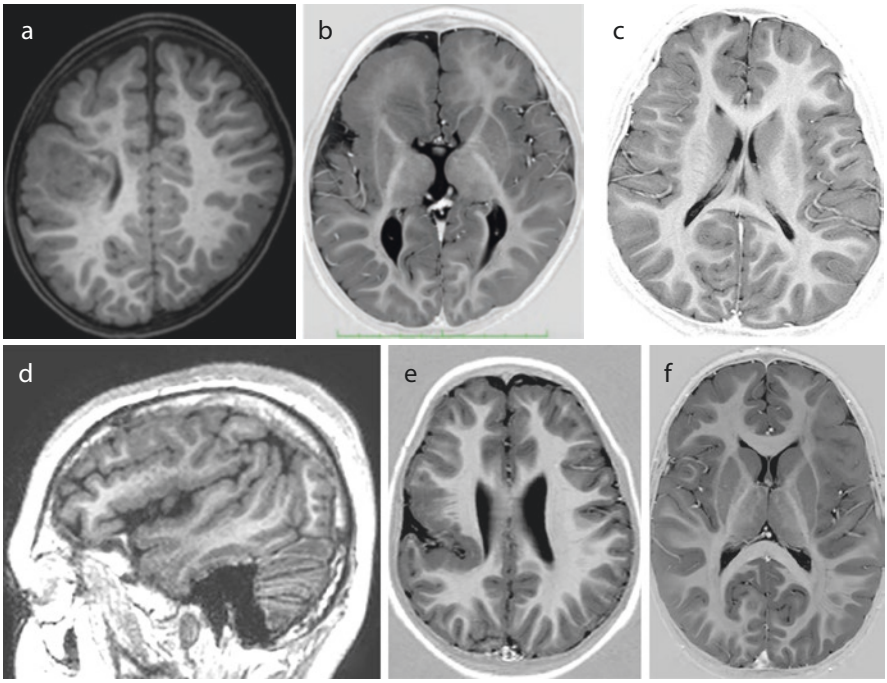

Fig. 12.1 Complex malformations of cortical development (submitted to surgical treatment): (**a**) large gray matter heterotopia in the right parietal region, (**b**) large right frontal polimicrogyria, (**c**) right frontal polymicrogyria, (**d**) extensive perisylvian polymicrogyria, (**e**) right perisylvian transmantle polymicrogyria, and (**f**) left sided "crown of gyrus" cortical dysplasia type IIb

locations; the most common one is periventricular nodular heterotopia (previously designated subependymal heterotopia), consisting of nodules of gray matter lining the ventricular wall. They must not be confused with the subependymal nodules of tuberous sclerosis, which are not isointense with gray matter and have other distinct radiological characteristics [35]. The other frequent type of GMH is subcortical heterotopia, which refers to collections of neurons dispersed in the white matter of the cerebral hemispheres [35]. They can be seen anywhere not only from the ventricle wall to the overlying cortex but also in deep white matter locations [36]. Cases in which the heterotopic tissue extends from the ventricular surface to the overlying cortex, which is usually dysplastic, have an arrangement called transmantle heterotopia, with a columnar morphology and a bulkier appearance [35, 36]. While the role of periventricular heterotopic nodules is still unclear and seems to require resection mainly in the context of dual pathology (most often with hippocampal sclerosis), subcortical nodules have intrinsic epileptogenicity, so resection of the nodular tissue and the surrounding dysplastic cortex has been proven beneficial to such patients [37].

12.3.2 Schizencephaly

Described many decades ago, schizencephaly is defined as a cleft lined by abnormal gray matter and/or heterotopia extending across the full thickness of the cerebral hemispheres from the ventricular surface (ependyma) to the periphery (pial surface) of the brain, probably the result of an early prenatal focal injury to the germinal matrix or, possibly, in infarct in very immature cerebrum with consequent liquefaction of injured tissue [29, 38–40]. They can be open, when the cleft extends through all cortical-subcortical layers and is filled with cerebrospinal fluid (CSF), or closed, if it is completely enclosed by cortical margins [29]. Surgery for schizencephaly associated with epilepsy is usually not indicated, mostly due to the wide extension and bilateral location (in up to 50% of cases) of the clefts, as well as proximity to eloquent areas. Resection of the cleft and its boundaries, guided by intraoperative electrocorticography, is feasible, yet very few results of this procedures have been published [41].

12.3.3 Polymicrogyria

The definition of polymicrogyria (PMG) is the presence of abnormally small gyri with focal, multifocal, or generalized location [42]. Embryologically, polymicrogyria is thought to ensure a premature folding of the neuronal band along with abnormal fusion of adjacent gyri and laminar necrosis of the developing cortex, giving it a typical delicate and bumpy appearance, like palisades of cortex [43]. Likely causes are both genetic and acquired, the first including chromosomal abnormalities (such as 22q11 deletions and 1p36 monosomy) and single gene mutations (such as COL4A1/COL4A2, OCLN, RTTN, and GRIN1 mutations) and the latter in utero infections, trauma, exposure to teratogens, arterial ischemic infarcts, and twin-to-twin transfusion syndrome [42].

Patients with PMG frequently present with epilepsy (around 80%), two thirds of which are pharmacoresistant [44]. Analysis of the PMG cortex, using nuclear medicine techniques, revealed intense hyperperfusion in the polymicrogyric lesion during epileptic seizures, suggesting its early involvement in seizure generation and propagation [45]. Albeit it constitutes the primary pathology only in about 5% of surgical candidates, satisfactory results can be achieved, and seizure-freedom has been reported in up to 50% of patients [46, 47]. Just like for other types of MCDs, epilepsy surgery in PMG raises specific issues, such as the extent of the malformation (often bilateral or multifocal), co-existence of epileptogenic and eloquent cortex, and the potentially favorable prognosis of some PMG-associated epilepsy syndromes, thus not requiring surgical treatment [46, 48].

A large multicentric study of 58 cases of PMG-related drug-resistant epilepsy patients undergoing surgical treatment revealed that the epileptogenic zone entangled only part of the PMG in 60% of cases, with the additional involvement of

remote cortical areas in 18% [49]. These observations underline the need for a different strategy in PMG-related drug-resistant epilepsy compared to other MCDs, namely, one that is not predominantly anatomo-radiological but rather electrophysiology-oriented [46]. Nevertheless, even these patients in whom the epileptogenic zone may involve only a portion of the malformation may still be good candidates for surgery, with about 50% of seizure freedom following surgery. Obviously, intracranial ECoG or stereoelectroencephalography (SEEG) is paramount to provide additional localizing information and guide resection of epileptogenic foci [49, 50].

12.3.4 Lissencephaly

Unlike polymicrogyria, with its overfolded and pseudo-thickened cortex, lissencephaly (literally "flat, smooth head") refers to a gyral abnormality that ranges from agyria (absent gyration) to oligogyria (reduced gyration)—pachygyria (thick gyri), according to the degree of the malformation of the cerebral convolutions [51]. It is usually caused by impaired neuronal migration, but genetic etiologies have been found in many individuals, such as deletions or single nucleotide mutations in **the platelet-activating factor acetyl hydrolase IB** enzyme (PAFAH1B1) or larger deletions in chromosome 17p13.3, as well as mutations in tubulin-encoding genes [52, 53]. The majority of lissencephaly cases have therapy-resistant epilepsy, yet very few of these patients have undergone surgery; the best therapeutic response to seizure control is given by ketogenic diet, vigabatrin, and valproate [53].

Table 12.2 Historical distribution of pathological substrates of operated patients at our hospital (Pediatric Epilepsy Surgery Center, University Hospital, Ribeirão Preto Medical School, University of São Paulo, Brazil)

Pathology	
Cortical dysplasia	31.8%
Gliosis	15.1%
Epileptogenic tumors (LEATs)	14.4%
Mesial temporal sclerosis	11.7%
Rasmussen encephalitis	6.8%
Porencephaly	4.6%
Tuberous sclerosis	4.6%
Sturge-Weber syndrome	2.2%
Others	8.3%

12.4 Focal Cortical Dysplasias (FCD)

In the pediatric age group, focal cortical dysplasias constitute the most common etiology of refractory epilepsy and thus have a particular importance for the epilepsy surgeon (Table 12.2) [54, 55].

Cortical dysplasias (CD) were initially described by Taylor and collaborators, in 1971, as a disorder of cortical architecture with large atypical neurons [56], but subsequent studies have characterized CDs more precisely, within the broader definition of alterations in cerebral cortical microarchitecture, together or not with abnormal cells, such as dysmorphic neurons (gigantic, dysplastic) and balloon cells [57].

Furthermore, the Commission for Classification and Terminology of the International League Against Epilepsy (ILAE), in recent years, has adequately redefined several conceptual and structural terms related to cortical dysplasias and epilepsy. Currently, CDs are subdivided into three main groups, described below in detail. This classification has been proven to be very useful, albeit inefficient in cases of isolated fCD type I versus those associated with other primary entities [58, 59]. It is also important to have in mind that these histopathological classifications are dynamic and constantly amended as we advance toward a better understanding of such entities. This has been mostly achieved through genetic and molecular studies; for instance, DNA methylation patterns have been found to provide an integrated and more precise diagnostic classification scheme for epilepsy-associated MCD, since the genomic DNA methylation in bulk epileptic brain tissue has been highly specific to the seizure phenotype across species and model systems, irrespective of cellular composition and appeared further specific for etiology and histopathology [60]. Nevertheless, the categories described below are still the mainstay to guide clinical management of patients throughout most epilepsy surgery centers.

12.4.1 Focal Cortical Dysplasia Type I

This specific type of cortical dysplasia is now considered as an isolated form and characterized by abnormal cortical layering affecting one or multiple lobes and including three subtypes, as follows [61]:

1. fCD type Ia: Abnormal radial cortical organization, the most frequent subtype,
2. fCD type Ib: Abnormal tangential cortical lamination,
3. fCD type Ic: Abnormal radial and tangential cortical organization.

Tassi et al. studied a series of 215 patients and those with the isolated form showed more frequent seizures; MRI was negative in 33%, and only 46% of these cases were seizure-free after surgery, upholding some of the difficulties in dealing with these cases [59].

12.4.2 Focal Cortical Dysplasia Type II

In this category, there is disruption of cortical lamination and specific cytological abnormalities, defining types IIa and IIb as follows:

1. fCD type IIa: Dysmorphic neurons (enlarged cell body and nucleus, abnormally distributed intracellular Nissl substance and cytoplasmic accumulation of neurofilament proteins). No discrimination of individual cortical layers (cortical dyslamination). Blurred gray/white matter junction.
2. fCD type IIb: Dysmorphic neurons and balloon cells (similar lesions are observed in cortical tubers and hemimegalencephaly).

From a neuroimaging perspective, the transmantle sign, described by Barkovich et al. in 1994, is considered a hallmark of fCD type II b. Other signs are not exclusively seen in typical fCD type II as blurring of white and gray matter junction or increased subcortical white matter signal in T2-weighted and FLAIR images. Abnormal cortical gyration and sulcation are considered frequent findings in fCD type II b. There are specific findings in electrophysiological recordings (subdural or intracerebral) typical of fCD such as repetitive high amplitude slow waves, interspersed with flat periods, that can be correlated with surgical outcome [62].

12.4.3 Focal Cortical Dysplasia Type III

Focal cortical dysplasia type III refers to cortical lamination abnormalities (similar to type I) associated to or affecting the same cortical area/lobe as certain other pathologies, characterized as follows:

1. fCD type IIIa: Cortical lamination abnormalities in the temporal lobe associated with hippocampal sclerosis,
2. fCD type IIIb: Cortical lamination abnormalities adjacent to a glial or glioneuronal tumor (Fig. 12.2).
3. fCD type IIIc: Cortical lamination abnormalities adjacent to a vascular malformation (cavernoma, AVM, leptomeningeal vascular malformation, telangiectasia, and meningioangiomatosis),
4. fCD type IIId: Cortical lamination abnormalities adjacent to any other lesion acquired during early life, for example, trauma, ischemic injury, limbic encephalitis/bacterial or viral infection, and Rasmussen encephalitis, glial scarring after prenatal or perinatal ischemic injury or bleeding.

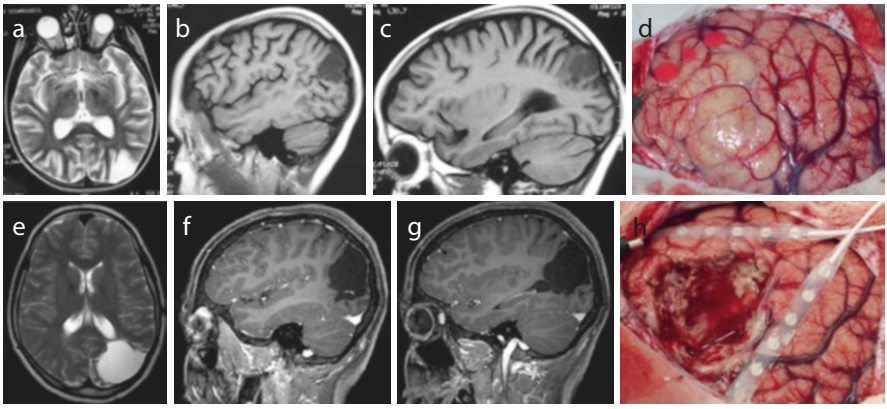

Fig. 12.2 Case of a 7-year-old boy with daily seizures since the age of 1 year and 6 months, characterized by oculocephalic version to the right followed by right hemiclonies, loss of consciousness, and manual automatisms. (**a**–**d**), preoperative MRI scans and tumor at surgery, respectively. (**e**–**h**), respectively, postoperative MRI scans and tumor site after resection. Pathology: dysembrioplastic neuroepithelial tumor (DNET) and cortical dysplasia type III b

12.4.4 Dual Pathology

Dual pathology refers only to patients with hippocampal sclerosis who have a second principal lesion affecting the brain and which may be located outside the ipsilateral temporal lobe, such as tumors (the most frequent ones are DNET and ganglioglioma), vascular malformations, glial scars, limbic and Rasmussen encephalitis, and MCD (including fCD type II a/II b) [63–65].

If architectural abnormalities are found in the temporal lobe associated with hippocampal sclerosis, one should not categorize it as fCD type I or dual pathology but as fCD type III a. Clear identification of this situation is of utmost importance because removal of both the lesion and the atrophic hippocampus is the best surgical approach and should be considered whenever possible. Complete resection of epileptogenic area, as well as the hippocampus, along with the presence of dysmorphic neurons or balloon cells on histopathology, are positive predictive factors of favorable surgical outcome [63, 64].

12.4.5 Mild Malformation of Cortical Development with Oligodendroglial Hyperplasia (MOGHE)

Despite the many recent advances in immunohistochemical and molecular diagnosis, 2–26% of epilepsy surgery specimens remain classified as nonlesional [66]. Blümcke et al. studied a series 1381 en bloc resected epilepsy surgery brain specimens, of which 52 could not be histopathologically classified and were considered

nonlesional (3.7%). Twenty-two cases (42%) displayed an increase of Olig2- and PDGFR-alpha-immunoreactiveoligodendroglia in white matter and deep cortical layers, as well as increased proliferation activity and heterotopic neurons in white matter [66].

Since all these cases shared a characteristic histopathology pattern and their MRI was suggestive of focal cortical dysplasia (FCD), these authors coined the term mild malformation of cortical development with oligodendroglial hyperplasia (MOGHE) to further classify these specimens. It is mostly distinctive of frontal lobe epilepsy, but some histopathological features and the natural history of this disease still need further clarification. Some recent insights into specific mechanisms of MOGHE have helped help to bridge the diagnostic gap in children and young adults with difficult-to-treat epilepsy though. Histopathologically, MOGHE is characterized by clusters of increased oligodendroglial cell densities, patchy zones of hypomyelination, and heterotopic neurons in the white matter [66]. Another recent finding is that mosaic SLC35A2 variants, which encode the major Golgi localized UDP galactose transporter required for protein and sphingolipid glycosylation and likely occur in a neuroglial progenitor cell during brain development, are a genetic marker for MOGHE [67].

The outcome of surgical therapy for MOGHE has been variable and is currently restricted, with many case reports only. In a case series of 22 operated patients, seizures recurred in 61%, whereas 33% were free of disabling seizures [66]. Conversely, a more recent study showed more favorable results, with Engel Class I and II outcomes in 16–25 (64%) patients, although with short follow-up periods [68]. Garganis et al. and Seetharam et al. described two MOGHE patients each, two of which were rendered seizure-free, while the other two had poorer outcomes (Engel class IV and III, respectively) [69, 70].

12.4.6 Bottom-of-Sulcus Dysplasia

Continuous improvement in magnetic field strength for MRI diagnosis and the application of advanced post-processing analyses has significantly enhanced clinical identification of FCD subtypes in vivo, in particular, of deep seated FCD type II [71, 72], which constitute the so-called “bottom-of-sulcus dysplasia (BOS FCD)” (Fig. 12.3). This is not a separate pathological group, but patients with BOS FCD have been found to present with a similar clinical syndrome, comprised of stereotyped seizures of frontal localization, due to small and localized lesions at the bottom of a sulcus on MRI, usually without the transmantle sign, and with intrinsic epileptogenicity. These are exclusively FCD type II lesions with immunohistochemical and/or genetic evidence for activation of the mTOR pathway, with favorable postsurgical seizure outcome following complete resection of the epileptic region, and as such have been managed accordingly. Future progress in precision medicine is still necessary to develop a targeted drug treatment for specific mTOR

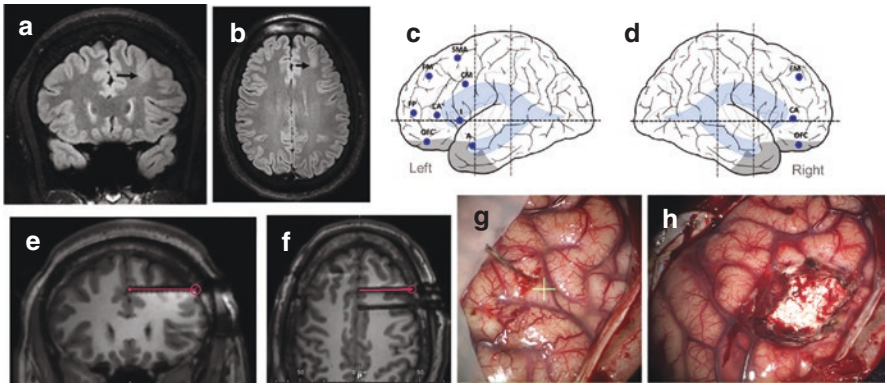

Fig. 12.3 Clinical case of a 17-year-old boy, with seizures since 5 years of age, refractory to AED. Video-EEG was compatible with a frontal localization but failed to lateralize. (**a** and **b**) MRI scans showing mild blurring in the middle frontal gyrus, typical of "bottom of sulcus" dysplasia. A decision to explore with SEEG was made, using nine electrodes (**c**) on the left side and 3 (**d**) on the right side. (**e** and **f**) MRI scan showing the location of the electrodes related to the epileptogenic zone (EZ). (**g** and **h**) intraoperative images showing the electrodes in place (yellow arrow) and excision of the EZ. Pathology: cortical dysplasia type II b

signaling molecules, but it is important to have BOS FCD in mind when assessing a given patient with difficult-to-localize epilepsy [73].

12.5 Radiological Pitfalls

Since the last ILAE proposal for protocol standardization [74], data acquisition with volumetric images has been gradually improving and became an essential part of the MRI protocol for epilepsy assessment (Fig. 12.4).

In addition to the MPRAGE 3DT1 sequences, used since the 1990s, and mandatory in any study, more recently 3D-FLAIR images have prevailed over high-resolution two-dimensional FLAIR images acquired in the axial and coronal planes. The advantages of 3D imaging not only to include the ability to acquire 1 mm slice-thickness data but also to obtain information about the whole brain tissue. With this dataset, the expert can visually study any portion of the brain, in multiple planes and different angles, with concomitant T1- and T2-weighting visualization of any suspected lesion. This dataset can be exhaustively studied qualitatively or be computed by different algorithms [75]. More recently, 3D-DIR (Double Inversion Recovery) volumetric images have also become available, with a 1-mm resolution, adding essential information about delicate nuances of FCD, including cortical enhancement and the underlying white matter [76].

Thus, multiparametric whole brain imaging data is essential to show subtle lesions like focal cortical dysplasia. The qualitative analysis of image data is quite sufficient to identify FCD 2B, with its frequent features of cortical thickening,

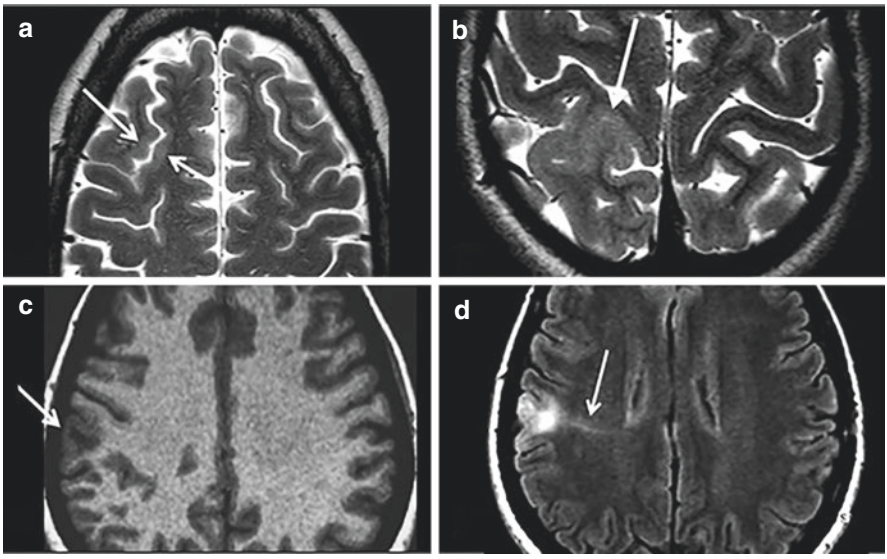

Fig. 12.4 (**a** and **b**) axial high-resolution T2-weighted TSE axial imaging. (**a**) Arrow pointing areas of cortical thickening with isointense subcortical white matter, and (**b**) hyperintense white and grey matter without clear boundaries. (**c**) 3DT1 MPRAGE slice showing hipointense white matter with sharp demarcation of the cortex. (**d**) FCD type IIb with the transmantle sign is pointed out on an axial FLAIR slice

blurring of gray/white matter junction, hyperintensity of both cortex and subcortical tissue, and the transmantle sign of deep white matter [77, 78]. On the other hand, identification of FCD type 1 and type 2A is more challenging. The very subtle blurring of neocortex/underlying WM junction and the minimal subcortical WM volume reduction are the only clues to pinpoint FCD type I. Additionally, poor boundaries are responsible for persistent postsurgical seizures despite detailed multidisciplinary evaluation.

Again, volumetric data acquisition is crucial for surgical planning of lobar or multilobar resection, based on high-quality structural 3DT1 MPRAGE, 3D-FLAIR, and 3D-DIR data, plus high-resolution axial and coronal T2-weighted TSE imaging. However, supplemental multidirectional diffusion transfer imaging (DTI) tractography is essential for mapping the subcortical location of clinically significant tracts, such as the corticospinal tract and the arcuate fasciculus. Lastly, functional blood oxygenation level-dependent (BOLD) MRI allows for a minimal and safe cortical resection, which is oftentimes sufficient for seizure control.

12.6 Selection of Patients for Surgery

Although the initial concepts of epilepsy surgery have been extrapolated from adults, it is now absolutely accepted that children are unique and peculiar, and somewhat different techniques for selecting cases for surgery should be applied. For example, after thorough history and clinical examination, the definition of pharmacoresistance should be made as quick as possible, sometimes after only weeks of treatment because in children, catastrophic epilepsy is the rule—and one of the main causes of this severe progression of epilepsy is cortical dysplasia [79, 80].

Criteria for selection of children for surgery have been recently revised by a panel of experts of the Pediatric Epilepsy Task Force of the ILAE [81], defining resources that are mandatory and required for all epilepsy surgical centers, including scalp EEG, video EEG, and magnetic resonance imaging (with specific protocols for epilepsy), and tests that are highly recommended for cortical dysplasia, such as electrocorticography (ECoG) and invasive monitoring. It is important to recognize the value of each test depending on the availability for each center, including fMRI, EEG source imaging, PET, and SPECT.

Surgical treatment is considered for patients with refractory epilepsy whose brain scans show lesions suspected of cortical dysplasia [54]. The goal of a complete presurgical workup is to identify the cerebral area responsible for generation of seizures (epileptogenic zone) so that it can be removed without causing additional unacceptable deficits [54]. Completeness of resection seems to be a key factor for a successful surgery. However, there is no simple test to outline the epileptogenic zone, and this is often a toilsome task requiring many comprehensive clinical, radiological, and electrophysiological examinations.

Mapping of the anatomo-electro-clinical network functional status of the epileptic region is achieved with multiple investigations [82]. Scalp EEG not only confirms the diagnosis of refractory epilepsy but also identifies cortical structures involved in seizure generation and progression, even though EEG may show generalized alterations even in focal lesions. The association of scalp EEG and videorecording of the patient's seizures (telemetry) allows for a careful evaluation of the clinical manifestations of epilepsy.

12.6.1 Invasive Monitoring

The use of invasive techniques, such as subdural grids and stereoelectroencephalography (SEEG), has been developed to overcome the challenges and limitations of noninvasive ones. Generally, invasive monitoring is indicated when preoperative data are inconclusive, when more information is required to localize the epileptogenic zone, or when there is involvement of eloquent cortex, and a functional cortical map is necessary to avoid additional deficits [82]. However, it must be remembered that these techniques pose some risks, albeit infrequently, due to

violation of anatomical structures. Therefore, they should be carefully considered only for children who are possible candidates for epilepsy surgery [83]. For instance, in children with suspected multifocal or bilateral epilepsy, who do not meet the requisites for resective surgical treatment, the intrinsic risks of an invasive evaluation should be avoided [82, 83]. Likewise, patients with hemispheric pathologies can be usually referred for hemispherotomy without presurgical invasive assessments.

Situations in which invasive monitoring should be considered include MRI-negative cases, that is, patients in whom there is no identifiable lesion on high-resolution scans; also, for cases in which there is no concordance between the MRI scan alterations and electro-clinical-functional findings; deeply seated brain lesions such as nodular heterotopia; when scalp EEG recordings show interictal spikes that range in their distribution from lobar to lateralized, making them difficult to localize or diffuse; presence of two or more anatomical lesions, and it remains unclear which one is epileptic (or both); and whenever the epileptogenic zone and thus the resection area involve eloquent cortex [82] (Fig. 12.5).

Subdural grids and strips can be used either acutely, during the surgical procedure itself, to help delineate the dysplastic area to be resected, or extraoperatively, when the patient is monitored in the ward for a few days (chronic monitoring). Acute electrocorticography (ECoG) requires decisions to be taken during the surgical procedure usually based on interictal discharges, since recording of seizures is rare, even in children with daily seizures. Therefore, if further information is required, chronic monitoring is warranted. Conversely, acute ECoG avoids the complications, such as infection and cerebrospinal fluid (CSF) leaks, of having foreign materials in the subdural space for a longer period. Moreover, in acute intraoperative ECoG, it is possible to change the position of the electrodes during recording, allowing for the evaluation of more extensive areas, and avoiding a common mistake that consists of discharges at the extremities of the grid [62]. Also, it involves only one anesthesia and one craniotomy, lowering costs and risks to the patient. However, it has a few disadvantages: anesthetic agents can significantly modify the distribution and frequency of discharges; very prolonged seizures may have a long-lasting postictal change of electrographic pattern that considerably increases operating times; there is also the possibility of absence of electroencephalographic changes during surgery rendering ECoG ineffective.

However, subdural electrodes provide only electrophysiological data of seizures arising from the surface of the cerebral cortex, but it is well known that the anatomo-electro-clinical networks that lead to generation of epilepsy usually follow a three-dimensional pattern, whose spatial-temporal organization is located within both cortical and subcortical brain structures. In such cases, stereoelectroencephalography (SEEG) must be chosen and consists in the insertion of deep electrodes inside the brain parenchyma of predefined regions, to gather data from electrodes in contact with gray and white matter and to correlate these data with seizure semiology avoided [82, 83]. The implantation strategy is individualized with electrode placement based on a preimplantation hypothesis that takes into consideration the primary organization of the epileptiform activity and the hypothetical functional

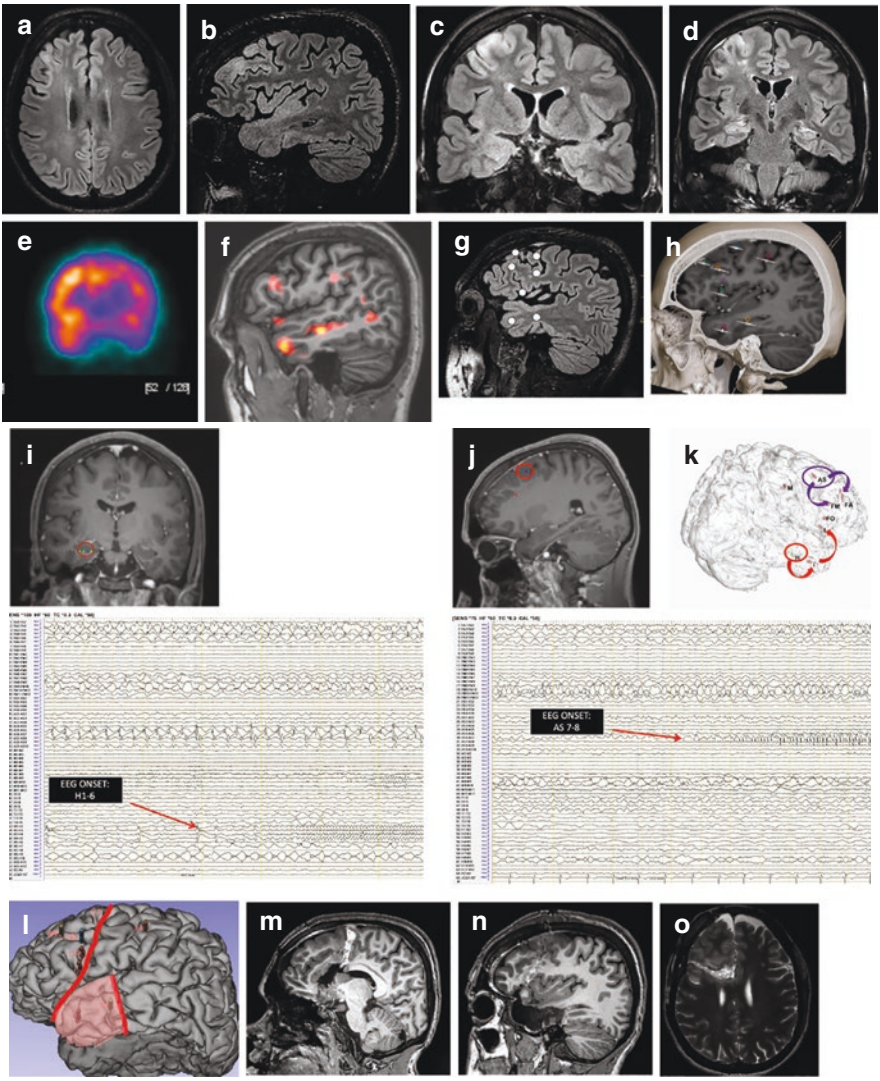

Fig. 12.5 A 16 years old with a focal motor epilepsy refractory to ASD, started at the age of 8. VEEG showing signs of involvement of the right hemisphere and right temporal lobe. (**a**–**d**) Preoperative FLAIR-weighted MRI scans showing hyperintense abnormalities over the frontal and temporal lobes; (**e**) ICTAL SPECT depicting hyperflow in the fronto-temporal region; (**f**) SISCOM showing hyperflow in the fronto-temporal region. (**g** and **h**) SEEG planning with the insertion of electrodes in the suspected frontal and temporal regions and (**h**) post implantation MR confirming the exact location of the electrodes. (**i** and **j**) MRI scans showing the exact location of seizure onset as depicted in EEG registration (lower images) in the temporal and frontal regions; (**k**) spreading of seizures in the temporal and frontal region. (**l**–**o**) planned and performed frontal lobe disconnection and temporo-mesial resection. Pathology: cortical dysplasia type 1

epileptic network that may be involved in the propagation of seizures avoided [82, 83].

In the context of cortical dysplasias, SEEG is usually indicated when other types of invasive monitoring are deemed ineffective, such as deep-seated lesions who are not amenable to cortical monitoring (e.g., dysplasias within the mesial temporal lobe, opercular areas, posterior orbitofrontal area, depths of sulci, insula, cingulate gyrus, and interhemispheric regions) [84]. Also, SEEG is particularly useful in cases requiring extensive bihemispheric evaluations and those with normal MRI scans in which the noninvasive investigations suggest a deep functional network. Lastly, SEEG can provide additional information whether subdural grids have failed to delineate the epileptogenic zone (due to deep white matter involvement).

12.7 Surgical Approaches to Cortical Dysplasia

The surgical treatment of cortical dysplasia in children basically follows the same patterns used in pediatric epilepsy surgery. A thorough presurgical workup is essential to come up with a strict operative plan that will be adapted to the patient's requirements. Obviously, the patient's family must be fully aware of the risks and benefits of surgery and seizure control rates. Whenever the family is not willing to accept possible transient or permanent deficits or the perspective of repeat procedures, surgical therapy should not be offered. Nevertheless, they should be reminded that a negative decision at this stage is always counterbalanced by the burden of the persistence of seizures and a lifelong worry of cognitive decline.

In general, the operative management of CD encompasses a wide range of technical options, from focal resections (lesionectomies) on one side to large hemispheric approaches. Limited resections have the advantages of reducing the risk of neurological deficits and those associated with longer operating times; however, in the long term, extended resections show better seizure outcomes than focal ones, due to higher rates of complete excision of the dysplasia. Moreover, lesionectomies are more often used in cases of type II and III CD, since the limits of type I CD tend to be more blurred [85].

Many epilepsy centers are currently favoring disconnective procedures, seeking to completely isolate the epileptogenic zones and eliminate seizure propagation while avoiding complications related to large intracranial cavities, particularly hydrocephalus [86]. Disconnections are mostly useful for patients with widespread lesions, including MCDs, since complete disconnection of the epileptogenic cortex from the surrounding brain tissue and downstream midbrain is sufficient for controlling seizures, even if the pathological substrate is left in situ [87].

FCDs, otherwise, are not infrequently prone to be managed with localized or focal resections with or without the aid of intraoperative ECoG or invasive monitoring with brain mapping [88]. Nevertheless, some FCS patients will require more extensive procedures, particularly those with the so-called sublobar dysplasia, which consists of a focal dysplastic segment of a cerebral lobe, well demarcated and

separated or cleaved from the remaining normal hemisphere by a deep cerebral sulcus ("lobe within a lobe"), ergo, sublobar (partial lobar) resections are indicated [89].

A major difficulty involved in children's refractory epilepsy is that CDs frequently span eloquent areas, so it can be quite challenging to avoid permanent disability while preserving brain function. However, these patients have recurring seizures, which are severe enough to jeopardize their immature and incompletely myelinated brain, resulting in epileptic encephalopathies with dire prognosis. Therefore, since withdrawing or postponing surgery can have devasting consequences, the neurosurgeon must take into consideration that neuroplasticity is acting in favor of the patient, and precocity of the insult and slow progression of the deficit are contributing factors. Full recovery might be expected due to reallocation of eloquent functions in brain areas close to the lesion. Neuronavigation and complete cortical mapping by direct stimulation may further help the surgeon decide the exact configuration of the resection area preserving not only functional areas but also important arteries and veins crossing the region or limiting the boundaries of the area to be excised.

12.8 Outcome

Certain intriguing peculiarities should be taken into consideration when analyzing the outcome of the surgical treatment of CD. Moosa and Gupta drew attention to some of these specificities: (1) subtle lesion or nonlesional MRI or the fact that CD is still the most frequent pathology even in cases of normal MRI; (2) "tip of the iceberg phenomenon" or the need to go beyond the limits of the apparent lesion; (3) frequent need for invasive monitoring, both to localize the epileptogenic lesion and limits of eloquent areas; (4) determination of completeness of resection is difficult if based only on preoperative MRI; (5) pathological diagnosis sometimes is difficult and with large interobserver variability (even among neuropathologists); (6) atypical electroclinical phenotype typically observed in young children showing that even in generalized epilepsy, we may find pathological substrates; and (7) the fact that some CD are in reality related to genetic disorders and hence not suitable surgical candidates [90].

CD has a worse seizure outcome than other brain lesions causing epilepsy, like low-grade epilepsy-associated neuroepithelial tumors (LEAT), vascular malformations, and hippocampal sclerosis. The overall seizure-free rates are approximately 50–70% after at least 5 years of postoperative follow-up [91]. The worst seizure outcomes in these patients are seen in focal cortical dysplasia type I or malformations of cortical development (only 50% become free from disabling seizures) [92]. The latter has been related to the poorest outcome of all types of CD. Veersema et al. reported that 32% of MCD patients reached steady seizure freedom (Engel class 1A) at the latest median follow-up of 8 years, as compared to 59% in FCD [93].

Aside from etiology, completeness of resection in children with FCD is a significant predictor of seizure freedom. Oluigbo et al. (2015) described that satisfactory seizure control among those who underwent complete resection was about six times higher than in partial resection cases [94]. Different reports have described other predictors of good seizure outcome in patients with CD: focal seizures, temporal lobe location, and positive unifocal findings on MRI [95–97]. Conversely, multiple seizure types, type I FCD, and immediate postoperative seizures were predictors of seizure persistence after surgery [98].

Concerning results of surgery in early childhood, Dorfmüller et al. have shown good results in 84% of children under 5 years of age explored by SEEG and operated on [99]. Many children with CD present with early-onset and severe epilepsy. Due to intense brain plasticity at this particular age, early surgical intervention for epilepsy has a marked positive impact not only on seizure control but also on cognitive function and quality of life [100].

Thirty-three to 54% of patients will continue to have seizures after a first surgical procedure due to incomplete resection of the lesion, or the epileptogenic zone, or secondary epileptogenesis. Reoperation is beneficial in the majority of these patients, especially in those with residual dysplasia and concordant intraoperative ECoG and MRI localization [101, 102].

Even though the primary endpoint of the surgical treatment pharmacoresistant epilepsy is to provide seizure freedom, improvement in the quality of life (QOL) and neurodevelopment should be considered just as important. Since its recognition as a critical measurement for evaluating treatment efficacy by the International League Against Epilepsy (ILAE) Epidemiology Commission, health-related quality of life (HRQL) has been increasingly included as an essential patient-reported outcome in studies examining the impact of epilepsy surgery [103].

Developmental delay, worsening of pre-existing familial stressors, intellectual or neurological deficits, and the burden of anti-seizure medication (ASM) were suggested as determinant factors on the impact of QOL related to pediatric epilepsy [104]. The clinical and therapeutic impact of epilepsy extends the domains of QOL, constituted by physical, social, behavioral, and cognitive aspects; thus, it is essential to improve and understand the reality of patients and their caregivers [105].

A meta-analysis that reviewed studies about QOL and epilepsy surgery in children showed that patients who obtained complete seizure freedom after surgery had considerable improvement in QOL, whereas patients with residual seizures did not substantially improve postoperatively, validating that Engel I is the most desirable outcome of epilepsy surgery [106]. Nevertheless, objective QOL studies in children and adolescents who underwent epilepsy surgery are limited, especially those analyzing a single pathology like FCD within a uniform cohort of patients. A recent study assessed QOL in 52 children and adult patients with FCD who underwent resective surgery and found a highly significant improvement in QOL (final QOLIE-89 with an absolute improvement of 49.03%; $P < 0.001$). The authors evaluated all 17 health domains measured by this questionnaire. The parameters that improved significantly were seizure worry, role limitation due to emotional factors, overall quality of life, role limitation due to physical factors, emotional well-being,

and medication effects. Type II FCD and younger age at surgery were some of the significant positive predictors of favorable seizure outcome [107].

Likewise, cognition and behavior are also relevant factors that must be considered when analyzing the outcomes of pediatric epilepsy surgery. It is well known that patients with pharmacoresistant epilepsies are at risk for various levels of intellectual disability, mostly moderate or severe. There are numerous risk factors for the cognitive decline seen in children with epilepsy as per reported in the medical literature: the occurrence of the seizure itself, seizure-related variables such as frequency and/or severity, duration of epilepsy, underlying pathology, and anti-seizure medications (ASMs). The cognitive and developmental outcomes in postoperative patients have demonstrated neither cognitive decline nor improvement, so abilities remain mostly unchanged. This could be considered a good result for encephalopathies [108, 109].

Children with more severe cognitive or adaptive disabilities achieved similar improvements in QOL after epilepsy surgery compared to those with normal or borderline intelligence [110]. Nevertheless, this intellectual impairment could play a role in the caregiver's burden [105]. In the abovementioned series of patients with FCD who underwent surgical treatment, the authors have also evaluated preoperative and found normal intellectual function in seven patients (13.5%), neuropsychological deficits limited to one cerebral hemisphere in 13 (25%), and deficits distributed bilaterally in 32 (61.5%). The absence of intellectual impairment on the preoperative intelligence quotient assessment was the only neuropsychological factor associated significantly with a favorable seizure outcome [107].

Chen et al., in 2014, also studied cognition, neuropsychological development, and QOL in 30 children who underwent resective surgery for FCD. FCDs were located in the frontal lobe in 18 cases, temporal lobe in 7, parietal lobe in 2, bilobar frontoparietal in 2, and parieto-occipital in 1. The histopathological types of FCDs were type Ia in 1, type Ib in 7, type IIa in 7, type IIb in 12, and type III in 3 patients. FCDs were completely resected in 20 patients. Eleven patients (50%) had developmental delay preoperatively. Normal cognitive function was associated with best outcomes regarding seizure control and QOL. They concluded that delay in cognitive development and poor QOL are common in children treated for FCDs and that early surgical intervention and complete resection of the lesion could help achieve better seizure control, cognitive function, and QOL [100].

Overall, published studies have shown improvement in developmental or cognitive abilities and QOL during 1 or 2 years of follow-up. Thus, long-term follow-up assessments are still required to analyze many postoperative clinical features, especially those that are complex and interconnected [105, 110, 111].

Obviously, the efficacy of the surgical treatment of epilepsy influences the decision of withdrawing ASM. Especially in the pediatric population, there is no agreement on the best moment for weaning off and discontinuing ASM. Reports based on literature data show that the meantime of ASM withdrawal was 28.8 months, with mean weaning off starting at 12.5 months after surgery [112]. Still, even in well-structured referral centers, there is no consensus or guidelines on this matter [113, 114].

In 25 patients (50%) surgically treated for epilepsy with FCD studied by Chatuverdi et al., 2018, ASMs were either reduced in dosage or numbers, or in both at the last follow-up. In 15 patients (30%), the numbers or dosages of ASMs were unchanged at their last follow-up [107].

ASM reduction during follow-up is also an acceptable criterion for the effectiveness of surgical therapy and may be started within 6 months and continued over time. Hence, the importance of ASM withdrawal in the pediatric population must be emphasized, since it is not only capable of optimizing cognitive function through neuroplasticity but also avoid deleterious pharmacological side effects.

References

1. Otsuki T, Honda R, Takahashi A. Surgical management of cortical dysplasia in infancy and early childhood. Brain Dev. 2013;35(8):802–9.
2. Jamuar SS, Walsh CA. Genomic variants and variations in malformations of cortical development. Pediatr Clin N Am. 2015;62(3):571–85.
3. Myers CT, Mefford HC. Advancing epilepsy genetics in the genomic era. Genome Med. 2015;7(1):91.
4. Pasquier B, Péoc'H M, Fabre-Bocquentin B, Bensaadi L, Pasquier D, Hoffmann D, Kahane P, Tassi L, Le Bas JF, Benabid AL. Surgical pathology of drug-resistant partial epilepsy. A 10-year-experience with a series of 327 consecutive resections. Epileptic Disord. 2002;4(2):99–119.
5. Fauser S, Essang C, Altenmüller DM. Long-term seizure outcome in 211 patients with focal cortical dysplasia. Epilepsia. 2015;56(1):66–76.
6. Mrelashvili A, Witte RJ, Wirrell EC, Nickels KC, Wong-Kisiel LC. Seizure freedom in children with pathology-confirmed focal cortical dysplasia. Pediatr Neurol. 2015;53(6):513–8.
7. Helbig I, Heinzen EL, Mefford HC, Genetics ILAE, Commission. Primer part 1-the building blocks of epilepsy genetics. Epilepsia. 2016;57(6):861–8.
8. Parrini E, Conti V, Dobyns WB, Guerrini R. Genetic basis of brain malformations. Mol Syndromol. 2016;7(4):220–33.
9. Marin-Valencia I, Guerrini R, Gleeson JG. Pathogenetic mechanisms of focal cortical dysplasia. Epilepsia. 2014;55(7):970–8.
10. Desikan RS, Barkovich AJ. Malformations of cortical development. Ann Neurol. 2016;80(6):797–810.
11. Squier W, Jansen A. Abnormal development of the human cerebral cortex. J Anat. 2010;217(4):312–23.
12. Guerrini R, Dobyns WB. Malformations of cortical development: clinical features and genetic causes. Lancet Neurol. 2014;13(7):710–26.
13. Leventer RJ, Guerrini R, Dobyns WB. Malformations of cortical development and epilepsy. Dialogues Clin Neurosci. 2008;10(1):47–62.
14. Abdijadid S, Mathern GW, Levine MS, Cepeda C. Basic mechanisms of epileptogenesis in pediatric cortical dysplasia. CNS Neurosci Ther. 2015;21(2):92–103.
15. Barkovich AJ, Kuzniecky RI, Dobyns WB, Jackson GD, Becker LE, Evrard P. A classification scheme for malformations of cortical development. Neuropediatrics. 1996;27:59–63.
16. Jiang X, Nardelli J. Cellular and molecular introduction to brain development. Neurobiol Dis. 2016;92(Pt A):3–17.
17. Guerrini R, Duchowny M, Jayakar P. Diagnostic methods and treatment options for focal cortical dysplasia. Epilepsia. 2015;56(11):1669–86.

18. Barkovich AJ, Kuzniecky RI, Jackson GD, Guerrini R, Dobyns WB. A developmental and genetic classification for malformations of cortical development. Neurology. 2005;65(12):1873–87.
19. Rubenstein JL. Annual research review: development of the cerebral cortex: implications for neurodevelopmental disorders. J Child Psychol Psychiatry. 2011;52(4):339–55.
20. Barkovich AJ, Guerrini R, Kuzniecky RI, Jackson GD, Dobyns WB. A developmental and genetic classification for malformations of cortical development: update 2012. Brain. 2012;135:1348–69.
21. Bilgüvar K, Oztürk AK, Louvi A. Whole-exome sequencing identifies recessive WDR62 mutations in severe brain malformations. Nature. 2010;467(7312):207–10.
22. Damiano JA, Do H, Ozturk E. Sensitive quantitative detection of somatic mosaic mutation in "double cortex" syndrome. Epileptic Disord. 2017;19(4):450–5.
23. Veeramah KR, Johnstone L, Karafet TM. Exome sequencing reveals new causal mutations in children with epileptic encephalopathies. Epilepsia. 2013;54(7):1270–81.
24. Wang Y, Du X, Bin R. Genetic variants identified from epilepsy of unknown etiology in Chinese children by targeted exome sequencing [published correction appears in Sci Rep. 2017 May 04;7:46520]. Sci Rep. 2017;7:40319.
25. Sarbassov DD, Ali SM, Sabatini DM. Growing roles for the mTOR pathway. Curr Opin Cell Biol. 2005;17(6):596–603.
26. Crino PB. Focal brain malformations: a spectrum of disorders along the mTOR cascade. Novartis Found Symp. 2007;288:260–81.
27. Chodraui FI, Garcia CAB, Mendes ND, Santos MV, Beggiora PS, Silva SC, Teixeira TL, da Silva LL, Saggioro FP, Neder L, Machado HR. Phosphorylation of S6 protein as a potential biomarker in surgically treated refractory epilepsy. Dev Neurosci. 2020;42(5–6):230–6.
28. Düvel K, Yecies JL, Menon S. Activation of a metabolic gene regulatory network downstream of mTOR complex 1. Mol Cell. 2010;39(2):171–83.
29. Burneo JG, Kuzniecky RI, Bebin M, Knowlton RC. Cortical reorganization in malformations of cortical development: a magnetoencephalographic study. Neurology. 2004;63:1818–24.
30. Lüders H, Schuele SU. Epilepsy surgery in patients with malformations of cortical development. Curr Opin Neurol. 2006;19(2):169–74.
31. Severino M, Geraldo AF, Utz N, Tortora D, Pogledic I, Klonowski W, Triulzi F, Arrigoni F, Mankad K, Leventer RJ, Mancini GMS, Barkovich JA, Lequin MH, Rossi A. Definitions and classification of malformations of cortical development: practical guidelines. Brain. 2020;143(10):2874–94; Erratum in: Brain 2020 Dec 1;143(12):e108.
32. Eltze CM, Chong WK, Bhate S, Harding B, Neville BGR, Cross JH. Taylor-type focal cortical dysplasia in infants: some MRI lesions almost disappear with maturation of myelination. Epilepsia. 2005;46:1988–92.
33. Martinez-Rios C, McAndrews MP, Logan W, Krings T, Lee D, Widjaja E. MRI in the evaluation of localization-related epilepsy. J Magn Reson Imaging. 2016;44:12–22.
34. Raymond AA, Fish DR, Stevens JM. Subependymal heterotopia: a distinct neuronal migration disorder associated with epilepsy. J Neurol Neurosurg Psychiatry. 1994;57:1195–202.
35. Barkovich AJ, Kuzniecky RI. Gray matter heterotopia. Neurology. 2000;55:1603–8.
36. Raybaud C, Widjaja E. Development and dysgenesis of the cerebral cortex: malformations of cortical development. Neuroimaging Clin N Am. 2011;21:483–543.
37. Tassi L, Colombo N, Cossu M. Electroclinical, MRI and neuropathological study of 10 patients with nodular heterotopia, with surgical outcomes. Brain. 2005;128:321–37.
38. Yakovlev P, Wadsworth RC. Schizencephalies: a study of the congenital clefts in the cerebral mantle, I: clefts with fused lips. J Neuropathol Exp Neurol. 1946;5:116–30.
39. Yakovlev P, Wadsworth RC. Schizencephalies: a study of the congenital clefts in the cerebral mantle, II: clefts with hydrocephalus and lips separated. J Neuropathol Exp Neurol. 1946;5:169–206.

40. Byrd SE, Osborn RE, Bohan TP, Naidich TP. The CT and MR evaluation of migrational disorders of the brain. Part II. Schizencephaly, heterotopia and polymicrogyria. Pediatr Radiol. 1989;19:219–22.
41. Zhang J, Yang Z, Yang Z, He X, Hou Y, Wang Y. Successful surgery for refractory seizures associated with bilateral schizencephaly: two case reports and literature review. Neurol Sci. 2016;37(7):1079–88.
42. Stutterd CA, Leventer RJ. Polymicrogyria: a common and heterogeneous malformation of cortical development. Am J Med Genet C Semin Med Genet. 2014;166C:227–39.
43. Barkovich AJ. MRI analysis of sulcation morphology in polymicrogyria. Epilepsia. 2010;51:17–22.
44. Cossu M, Pelliccia V, Gozzo F, Casaceli G, Francione S, Nobili L, Mai R, Castana L, Sartori I, Cardinale F, Lo Russo G, Tassi L. Surgical treatment of polymicrogyria-related epilepsy. Epilepsia. 2016;57(12):2001–10.
45. Wichert-Ana L, de Azevedo-Marques PM, Oliveira LF, Fernandes RM, Velasco TR, Santos AC, Araújo D, Kato M, Bianchin MM, Sakamoto AC. Ictal technetium-99 m ethyl cysteinate dimer single-photon emission tomographic findings in epileptic patients with polymicrogyria syndromes: a subtraction of ictal-interictal SPECT coregistered to MRI study. Eur J Nucl Med Mol Imaging. 2008;35(6):1159–70.
46. Maillard L, Ramantani G. Epilepsy surgery for polymicrogyria: a challenge to be undertaken. Epileptic Disord. 2018;20(5):319–38.
47. Jalloh I, Cho N, Nga VDW, Whitney R, Jain P, Al-Mehmadi S, Yau I, Okura H, Widjaja E, Otsubo H, Ochi A, Donner E, McCoy B, Drake J, Go C, Rutka JT. The role of surgery in refractory epilepsy secondary to polymicrogyria in the pediatric population. Epilepsia. 2018;59(10):1982–96.
48. Shain C, Ramgopal S, Fallil Z, et al. Polymicrogyria associated epilepsy: a multicenter phenotypic study from the epilepsy phenome/genome project. Epilepsia. 2013;54:1368–75.
49. Wang DD, Knox R, Rolston JD, Englot DJ, Barkovich AJ, Tihan T, Auguste KI, Knowlton RC, Cornes SB, Chang EF. Surgical management of medically refractory epilepsy in patients with polymicrogyria. Epilepsia. 2016;57(1):151–61.
50. Maillard LG, Tassi L, Bartolomei F, Catenoix H, Dubeau F, Szurhaj W, Kahane P, Nica A, Marusic P, Mindruta I, Chassoux F, Ramantani G. Stereoelectroencephalography and surgical outcome in polymicrogyria-related epilepsy: a multicentric study. Ann Neurol. 2017;82(5):781–94.
51. Dobyns WB. The clinical patterns and molecular genetics of lissencephaly and subcortical band heterotopia. Epilepsia. 2010;51(Suppl 1):5–9.
52. Di Donato N, Chiari S, Mirzaa GM, Aldinger K, Parrini E, Olds C, et al. Lissencephaly: expanded imaging and clinical classification. Am J Med Genet A. 2017;173:1473–88.
53. Kolbjer S, Martin DA, Pettersson M, Dahlin M, Anderlid BM. Lissencephaly in an epilepsy cohort: molecular, radiological and clinical aspects. Eur J Paediatr Neurol. 2021;30:71–81.
54. Sisodiya SM. Surgery for focal cortical dysplasia. Brain. 2004;127(Pt 11):2383–4.
55. Yao K, Duan Z, Zhou J, Li L, Zhai F, Dong Y, Wang X, Ma Z, Bian Y, Qi X, Li L. Clinical and immunohistochemical characteristics of type II and type I focal cortical dysplasia. Oncotarget. 2016;7(47):76415–22.
56. Taylor DC, Falconer MA, Bruton CJ, Corsellis JA. Focal dysplasia of the cerebral cortex in epilepsy. J Neurol Neurosurg Psychiatry. 1971;34(4):369–87.
57. Kabat J, Król P. Focal cortical dysplasia—review. Pol J Radiol. 2012;77(2):35–43.
58. Spreafico R, Blümcke I. Focal cortical Dysplasias: clinical implication of neuropathological classification systems. Acta Neuropathol. 2010;120(3):359–67.
59. Tassi L, Garbelli R, Colombo N, Bramerio M, Lo Russo G, Deleo F, Milesi G, Spreafico R. Type I focal cortical dysplasia: surgical outcome is related to histopathology. Epileptic Disord. 2010;12(3):181–91.
60. Jabari S, Kobow K, Pieper T, Hartlieb T, Kudernatsch M, Polster T, Bien CG, Kalbhenn T, Simon M, Hamer H, Rössler K, Feucht M, Mühlebner A, Najm I, Peixoto-Santos JE, Gil-

Nagel A, Delgado RT, Aledo-Serrano A, Hou Y, Coras R, von Deimling A, Blümcke I. DNA methylation-based classification of malformations of cortical development in the human brain. Acta Neuropathol. 2022;143(1):93–104.
61. Blümcke I, Thom M, Aronica E, Armstrong DD, Vinters HV, Palmini A, Jacques TS, Avanzini G, Barkovich AJ, Battaglia G, Becker A, Cepeda C, Cendes F, Colombo N, Crino P, Cross JH, Delalande O, Dubeau F, Duncan J, Guerrini R, Kahane P, Mathern G, Najm I, Ozkara C, Raybaud C, Represa A, Roper SN, Salamon N, Schulze-Bonhage A, Tassi L, Vezzani A, Spreafico R. The clinicopathologic spectrum of focal cortical dysplasias: a consensus classification proposed by an ad hoc task force of the ILAE diagnostic methods commission. Epilepsia. 2011;52(1):158–74.
62. Widdess-Walsh P, Jeha L, Nair D, Kotagal P, Bingaman W, Najm I. Subdural electrode analysis in focal cortical dysplasia: predictors of surgical outcome. Neurology. 2007;69(7):660–7.
63. Cendes F, Cook MJ, Watson C, Andermann F, Fish DR, Shorvon SD, Bergin P, Free S, Dubeau F, Arnold DL. Frequency and characteristics of dual pathology in patients with lesional epilepsy. Neurology. 1995;45(11):2058–64.
64. Kim DW, Lee SK, Nam H, Chu K, Chung CK, Lee SY, Choe G, Kim HK. Epilepsy with dual pathology: surgical treatment of cortical dysplasia accompanied by hippocampal sclerosis. Epilepsia. 2010;51(8):1429–35.
65. Li LM, Cendes F, Andermann F, Watson C, Fish DR, Cook MJ, Dubeau F, Duncan JS, Shorvon SD, Berkovic SF, Free S, Olivier A, Harkness W, Arnold DL. Surgical outcome in patients with epilepsy and dual pathology. Brain. 1999;122(Pt 5):799–805.
66. Schurr J, Coras R, Rössler K, Pieper T, Kudernatsch M, Holthausen H, Winkler P, Woermann F, Bien CG, Polster T, Schulz R, Kalbhenn T, Urbach H, Becker A, Grunwald T, Huppertz HJ, Gil-Nagel A, Toledano R, Feucht M, Mühlebner A, Czech T, Blümcke I. Mild malformation of cortical development with Oligodendroglial hyperplasia in frontal lobe epilepsy: a new clinico-pathological entity. Brain Pathol. 2017;27(1):26–35.
67. Bonduelle T, Hartlieb T, Baldassari S, Sim NS, Kim SH, Kang HC, Kobow K, Coras R, Chipaux M, Dorfmüller G, Adle-Biassette H, Aronica E, Lee JH, Blumcke I, Baulac S. Frequent SLC35A2 brain mosaicism in mild malformation of cortical development with oligodendroglial hyperplasia in epilepsy (MOGHE). Acta Neuropathol Commun. 2021;9(1):3.
68. Hartlieb T, Winkler P, Coras R, Pieper T, Holthausen H, Blümcke I, Staudt M, Kudernatsch M. Age-related MR characteristics in mild malformation of cortical development with oligodendroglial hyperplasia and epilepsy (MOGHE). Epilepsy Behav. 2019;91:68–74.
69. Garganis K, Kokkinos V, Zountsas B, Dinopoulos A, Coras R, Blümcke I. Temporal lobe "plus" epilepsy associated with oligodendroglial hyperplasia (MOGHE). Acta Neurol Scand. 2019;140(4):296–300.
70. Seetharam R, Nooraine J, Mhatre R, Ramachandran J, Iyer RB, Mahadevan A. Mild malformation of cortical development with oligodendroglial hyperplasia and epilepsy (MOGHE): a widespread disease with an apparently focal epilepsy. Epileptic Disord. 2021;23(2):407–11.
71. Wagner J, Weber B, Urbach H, Elger CE, Huppertz HJ. Morphometric MRI analysis improves detection of focal cortical dysplasia type II. Brain. 2011;134:2844–54.
72. Wang ZI, Alexopoulos AV, Jones SE, Najm IM, Ristic A, Wong C, Prayson R, Schneider F, Kakisaka Y, Wang S, Bingaman W, Gonzalez-Martinez JA, Burgess RC. Linking MRI postprocessing with magnetic source imaging in MRI-negative epilepsy. Ann Neurol. 2014;75(5):759–70.
73. Ying Z, Wang I, Blümcke I, Bulacio J, Alexopoulos A, Jehi L, Bingaman W, Gonzalez-Martinez J, Kobow K, Niestroj LM, Lal D, Koelble K, Najm I. A comprehensive clinicopathological and genetic evaluation of bottom-of-sulcus focal cortical dysplasia in patients with difficult-to-localize focal epilepsy. Epileptic Disord. 2019;21(1):65–77.
74. Wellmer J, Quesada CM, Rothe L, Elger CE, Bien CG, Urbach H. Proposal for a magnetic resonance imaging protocol for the detection of epileptogenic lesions at early outpatient stages. Epilepsia. 2013;54(11):1977–87.

75. Urbach H, Kellner E, Kremers N, Blümcke I, Demerath T. MRI of focal cortical dysplasia. Neuroradiology. 2022;64(3):443–52.
76. Soares BP, Porter SG, Saindane AM, Dehkharghani S, Desai NK. Utility of double inversion recovery MRI in paediatric epilepsy. Br J Radiol. 2016;89(1057):20150325.
77. Colombo N, Salamon N, Raybaud C, Ozkara C, Barkovich AJ. Imaging of malformations of cortical development. Epileptic Disord. 2009;11(3):194–205.
78. Barkovich AJ, Kuzniecky RI, Bollen AW, Grant PE. Focal transmantle dysplasia: a specific malformation of cortical development. Neurology. 1997;49(4):1148–52.
79. Hirsch E, Arzimanoglou A. Les épilepsies partielles pharmaco-résistantes Quels sont les critères d'éligibilité à un traitement chirurgical chez l'enfant? [Children with drug-resistant partial epilepsy: criteria for the identification of surgical candidates]. Rev Neurol (Paris). 2004;160:5S210–9.
80. Pestana Knight EM, Gonzalez-Martinez J, Gupta A. Pre-operative evaluation in pediatric patients with cortical dysplasia. Childs Nerv Syst. 2015;31(12):2225–33.
81. Jayakar P, Gaillard WD, Tripathi M, Libenson MH, Mathern GW, Cross JH, Task force for Paediatric Epilepsy Surgery, Commission for Paediatrics, and the Diagnostic Commission of the International League Against Epilepsy. Diagnostic test utilization in evaluation for resective epilepsy surgery in children. Epilepsia. 2014;55(4):507–18.
82. Gonzalez-Martinez J, Najm IM. Indications and selection criteria for invasive monitoring in children with cortical dysplasia. Childs Nerv Syst. 2014;30(11):1823–9.
83. Cossu M, Cardinale F, Castana L, Nobili L, Sartori I, Lo RG. Stereo-EEG in children. Childs Nerv Syst. 2006;22(8):766–78. https://doi.org/10.1007/s00381-006-0127-2; Epub 2006 Jun 20.
84. Gonzalez-Martinez J, Mullin J, Vadera S, Bulacio J, Hughes G, Jones S, Enatsu R, Najm I. Stereotactic placement of depth electrodes in medically intractable epilepsy. J Neurosurg. 2014;120(3):639–44.
85. Mühlebner A, Gröppel G, Dressler A, Reiter-Fink E, Kasprian G, Prayer D, Dorfer C, Czech T, Hainfellner JA, Coras R, Blümcke I, Feucht M. Epilepsy surgery in children and adolescents with malformations of cortical development—outcome and impact of the new ILAE classification on focal cortical dysplasia. Epilepsy Res. 2014;108(9):1652–61.
86. Kawai K. Epilepsy surgery: current status and ongoing challenges. Neurol Med Chir (Tokyo). 2015;55(5):357–66.
87. De Ribaupierre S, Delalande O. Hemispherotomy and other disconnective techniques. Neurosurg Focus. 2008;25(3):E14.
88. Santos AC, Escorsi-Rosset S, Simao GN, Terra VC, Velasco T, Neder L, Sakamoto AC, Machado HR. Hemispheric dysplasia and hemimegalencephaly: imaging definitions. Childs Nerv Syst. 2014;30(11):1813–21.
89. Tuxhorn I, Woermann FG, Pannek HW, Hans VH. Sublobar dysplasia—a clinicopathologic report after successful epilepsy surgery. Epilepsia. 2009;50(12):2652–7.
90. Moosa AN, Gupta A. Outcome after epilepsy surgery for cortical dysplasia in children. Childs Nerv Syst. 2014;30(11):1905–11.
91. Lamberink HJ, Otte WM, Blümcke I, Braun KPJ, European epilepsy brain Bank writing group; study group; European reference network EpiCARE. Seizure outcome and use of antiepileptic drugs after epilepsy surgery according to histopathological diagnosis: a retrospective multicentre cohort study. Lancet Neurol. 2020;19(9):748–57.
92. Jehi L, Braun K. Does etiology really matter for epilepsy surgery outcome? Brain Pathol. 2021;31(4):e12965.
93. Veersema TJ, Swampillai B, Ferrier CH, van Eijsden P, Gosselaar PH, van Rijen PC, Spliet WGM, Mühlebner A, Aronica E, Braun KPJ. Long-term seizure outcome after epilepsy surgery in patients with mild malformation of cortical development and focal cortical dysplasia. Epilepsia Open. 2018;4(1):170–5.
94. Oluigbo CO, Wang J, Whitehead MT, Magge S, Myseros JS, Yaun A, Depositario-Cabacar D, Gaillard WD, Keating R. The influence of lesion volume, perilesion resection volume, and

completeness of resection on seizure outcome after resective epilepsy surgery for cortical dysplasia in children. J Neurosurg Pediatr. 2015;15(6):644–50.
95. Krsek P, Maton B, Jayakar P, Dean P, Korman B, Rey G, Dunoyer C, Pacheco-Jacome E, Morrison G, Ragheb J, Vinters HV, Resnick T, Duchowny M. Incomplete resection of focal cortical dysplasia is the main predictor of poor postsurgical outcome. Neurology. 2009;72(3):217–23.
96. Chern JJ, Patel AJ, Jea A, Curry DJ, Comair YG. Surgical outcome for focal cortical dysplasia: an analysis of recent surgical series. J Neurosurg Pediatr. 2010;6(5):452–8.
97. Rowland NC, Englot DJ, Cage TA, Sughrue ME, Barbaro NM, Chang EF. A meta-analysis of predictors of seizure freedom in the surgical management of focal cortical dysplasia. J Neurosurg. 2012;116(5):1035–41.
98. Jayalakshmi S, Vooturi S, Vadapalli R, Madigubba S, Panigrahi M. Predictors of surgical outcome in focal cortical dysplasia and its subtypes. J Neurosurg. 2021;136(2):512–22.
99. Dorfmüller G, Ferrand-Sorbets S, Fohlen M, Bulteau C, Archambaud F, Delalande O, Chipaux M, Taussig D. Outcome of surgery in children with focal cortical dysplasia younger than 5 years explored by stereo-electroencephalography. Childs Nerv Syst. 2014;30(11):1875–83. https://doi.org/10.1007/s00381-014-2464-x.
100. Chen HH, Chen C, Hung SC, Liang SY, Lin SC, Hsu TR, Yeh TC, Yu HY, Lin CF, Hsu SP, Liang ML, Yang TF, Chu LS, Lin YY, Chang KP, Kwan SY, Ho DM, Wong TT, Shih YH. Cognitive and epilepsy outcomes after epilepsy surgery caused by focal cortical dysplasia in children: early intervention maybe better. Childs Nerv Syst. 2014;30(11):1885–95. https://doi.org/10.1007/s00381-014-2463-y; Epub 2014 Oct 9.
101. Sacino MF, Ho CY, Whitehead MT, Kao A, Depositario-Cabacar D, Myseros JS, Magge SN, Keating RF, Gaillard WD, Oluigbo CO. Repeat surgery for focal cortical dysplasias in children: indications and outcomes. J Neurosurg Pediatr. 2017;19(2):174–81.
102. Muthaffar O, Puka K, Rubinger L, Go C, Snead OC 3rd, Rutka JT, Widjaja E. Reoperation after failed resective epilepsy surgery in children. J Neurosurg Pediatr. 2017;20(2):134–40.
103. Thurman DJ, Beghi E, Begley CE, Berg AT, Buchhalter JR, Ding D, Hesdorffer DC, Hauser WA, Kazis L, Kobau R, Kroner B, Labiner D, Liow K, Logroscino G, Medina MT, Newton CR, Parko K, Paschal A, Preux PM, Sander JW, Selassie A, Theodore W, Tomson T, Wiebe S, ILAE Commission on Epidemiology. Standards for epidemiologic studies and surveillance of epilepsy. Epilepsia. 2011;52(Suppl 7):2–26.
104. Miller V, Palermo TM, Grewe SD. Quality of life in pediatric epilepsy: demographic and disease-related predictors and comparison with healthy controls. Epilepsy Behav. 2003;4(1):36–42.
105. Leal STF, Santos MV, Thomé U, Machado HR, Escorsi-Rosset S, Dos Santos AC, Wichert-Ana L, Leite JP, Fernandes RMF, Sakamoto AC, Hamad APA. Impact of epilepsy surgery on quality of life and burden of caregivers in children and adolescents. Epilepsy Behav. 2020;106:106961.
106. Maragkos GA, Geropoulos G, Kechagias K, Ziogas IA, Mylonas KS. Quality of life after epilepsy surgery in children: a systematic review and meta-analysis. Neurosurgery. 2019;85(6):741–9.
107. Chaturvedi J, Rao MB, Arivazhagan A, Sinha S, Mahadevan A, Chowdary MR, Raghavendra K, Shreedhara AS, Pruthi N, Saini J, Bharath RD, Rajeswaran J, Satishchandra P. Epilepsy surgery for focal cortical dysplasia: seizure and quality of life (QOLIE-89) outcomes. Neurol India. 2018;66(6):1655–66.
108. Battaglia D, Chieffo D, Lettori D, Perrino F, Di Rocco C, Guzzetta F. Cognitive assessment in epilepsy surgery of children. Childs Nerv Syst. 2006;22(8):744–59.
109. Korkman M, Granström ML, Kantola-Sorsa E, Gaily E, Paetau R, Liukkonen E, Boman PA, Blomstedt G. Two-year follow-up of intelligence after pediatric epilepsy surgery. Pediatr Neurol. 2005;33(3):173–8.
110. Conway L, Widjaja E, Smith ML. Impact of resective epilepsy surgery on health-related quality of life in children with and without low intellectual ability. Epilepsy Behav. 2018;83:131–6.

111. van Empelen R, Jennekens-Schinkel A, van Rijen PC, Helders PJ, van Nieuwenhuizen O. Health-related quality of life and self-perceived competence of children assessed before and up to two years after epilepsy surgery. Epilepsia. 2005;46(2):258–71.
112. Boshuisen K, Arzimanoglou A, Cross JH, Uiterwaal CS, Polster T, van Nieuwenhuizen O, Braun KP, TimeToStop study group. Timing of antiepileptic drug withdrawal and long-term seizure outcome after paediatric epilepsy surgery (TimeToStop): a retrospective observational study. Lancet Neurol. 2012;11(9):784–91.
113. Berg AT, Langfitt JT, Spencer SS, Vickrey BG. Stopping antiepileptic drugs after epilepsy surgery: a survey of U.S. epilepsy center neurologists. Epilepsy Behav. 2007;10(2):219–22.
114. Lamberink HJ, Geleijns K, Otte WM, Arzimanoglou A, Helen Cross J, Korff CM, Ramantani G, Braun KPJ. Why the TimeToStop trial failed to recruit: a survey on antiepileptic drug withdrawal after paediatric epilepsy surgery. Epileptic Disord. 2018;20(5):374–85.

Chapter 13
Corpus Callosotomy Is a Safe and Effective Procedure for Medically Resistant Epilepsy

Andrew T. Hale, Ariana S. Barkley, and Jeffrey P. Blount

13.1 Introduction

In this chapter, we outline the historical context of corpus callosotomy (CC), provide an anatomic basis for the procedure, review indications and relative contraindications to assist with preoperative decision-making, and summarize some of the evolving techniques in CC including endoscopic and LITT ablation. Given the favorable safety profile, efficacy of the procedure, evolving success of minimally invasive approaches, and potential as a low-cost procedure in resource limited environments, we advocate for CC to be in the armamentarium of all pediatric neurosurgeons worldwide.

13.1.1 Historical Context

The first reported corpus callosotomy (CC) in humans was performed by Dandy in 1936 in patients undergoing pineal region tumor resection [1]. Posterior callosotomy performed during these procedures reportedly resulted in no appreciable deficits prompting conclusions that it was well tolerated. Corpus callosotomy as a surgical treatment for epilepsy, however, was pursued only after primate experiments by Erickson in 1940 demonstrated that discharges were detected after stimulation of the contralateral cortex [2], thereby suggesting that the corpus callosum affords a pathway for spread of epileptogenic discharges as well as to establish bilateral synchroneity.

A. T. Hale · A. S. Barkley · J. P. Blount (✉)
Division of Pediatric Neurosurgery, Children's of Alabama, Birmingham, AL, USA
e-mail: Jeffrey.blount@childrensal.org

C. Di Rocco (ed.), *Advances and Technical Standards in Neurosurgery*, Advances and Technical Standards in Neurosurgery 48,
https://doi.org/10.1007/978-3-031-36785-4_13

Extrapolating these conclusions to humans, in 1940, Van Wagenen and Herren performed CC coupled with anterior and hippocampal commissure divisions in ten patients with epilepsy [3]. Six-week follow-up demonstrated mixed seizure control, but tolerance of the procedure was deemed favorable [3]. This led to subsequent case series by Gazzaniga et al. in 1962 [4], Bogen and Vogel in 1965 [5], Lussenhop in 1970 [6], and Wilson in 1975 [7, 8]. However, concerns surrounding the procedure were highlighted after one series reported one mortality within two weeks postoperatively in addition to complications affiliated with hydrocephalus and aseptic meningitis [6]. To minimize these complications, less extensive resections were proposed including two stage operations allowing recovery between resections as well as partial callosotomy with reports of 56–100% having greater than 50% seizure reduction up to 6 years postoperatively [9]. Continued encouraging results have solidified this technique as a useful tool in treating severe medically intractable generalized epilepsy.

13.2 Relevant Anatomy

Several commissural pathways interconnect the two hemispheres including the supraoptic, anterior, posterior, habenular, dorsal hippocampal commissures, the massa intermedia, and the corpus callosum [10]. The three main interconnections demonstrated through topographical studies, however, are the anterior, dorsal hippocampal, and the corpus callosum, the latter of which is the largest pathway.

The corpus callosum contains over 200 million predominantly myelinated axons and connects approximately 70–80% of the cortex [11]. It is divided into the rostrum, the genu with inferior, superior and posterior divisions, the body with anterior, middle and posterior subdivisions, the isthmus, and the splenium [10]. The corpus callosum connects both homotopic and heterotopic sites contralaterally with a modality-specific bias. The rostrum extends to the superior portion of the lamina terminalis and connects bilateral orbitofrontal regions, which in turn are implicated in emotion, memory, and higher cognitive decision-making given its sensory and limbic system connections. The genu is contiguous with the forceps minor, which connect the medial and lateral prefrontal as well as to supplementary and premotor areas. The genu to anterior body connects the premotor and motor areas, the posterior body connects the somatosensory and posterior parietal areas, the isthmus connects the posterior parietal and superior temporal areas, and the splenium connects the occipital and inferior temporal areas [10].

The vascular supply of the corpus callosum arises from both the anterior and posterior circulation [12]. The anterior blood supply consists of the median callosal artery, which commonly arises from the anterior communicating artery, and the pericallosal arteries, which are terminal anterior cerebral artery branches. The posterior pericallosal-or splenial-artery supplies the splenium and most commonly arises from the parieto-occipital terminal branch of the posterior cerebral artery [13]. The callosal and calloso-cingulate veins in turn drain into the internal cerebral

veins via septal and atrial branches [13]. When performing CC, the surgeon must be mindful and exercise caution to avoid essential vascular supplies.

13.3 Patient Selection

13.3.1 Open Corpus Callosotomy

CC candidacy includes medical intractability (i.e., failure on multiple anti-seizure medications), injuries from drop attacks, significant impairment of seizure burden on patient/family life, and absence of a focal target for surgical resection. Thus, selection of candidacy is based on clinical and EEG findings, without the need for invasive workup and mobilization of significant resources. Candidacy for CC has focused on attenuating drop attacks where rapid-onset bihemispheric synchrony causes rapid-onset hypertonia or hypotonia, resulting in tonic or atonic events, respectively [14–17]. Patients with Lennox-Gastaut syndrome, characterized by diffuse slow spike and slow wave (<2.5 Hz activity) and progressive, profound multisemiology seizure burden, are often candidates for CC [18]. In addition, patients with bifrontal epilepsy and generalized MRE may be candidates as well [18]. An illustrative preoperative EEG (Fig. 13.1a), preoperative MRI (Fig. 13.1b), and postoperative EEG (Fig. 13.1c) are shown to demonstrate the effectiveness of CC (in this case, anterior two-third). Patients with lissencephaly and diffuse cortical dysplasia often do not respond to CC [19]; these diagnoses are considered relevant contraindications to CC.

13.3.2 Endoscopic Approaches

Endoscopic approaches to performing CC have recently been introduced to the surgical armamentarium [20–29]. In addition to the previously described selection criteria for CC, endoscopic CC is typically offered for patients who have not undergone a previous craniotomy, have preserved falx, and sufficiently disparate medial hemisphere anatomy since the endoscope requires some degree of fixation to surrounding structures for stabilization. Use of the endoscope also minimizes blood loss since a large craniotomy is avoided. Vascular imaging is also an important determinant of patient selection and trajectory planning as endoscopic approaches make it potentially more difficult to control bleeding from the bridging veins if encountered. Not surprisingly, selection of candidates is also highly dependent on surgeon experience and comfort with endoscopy.

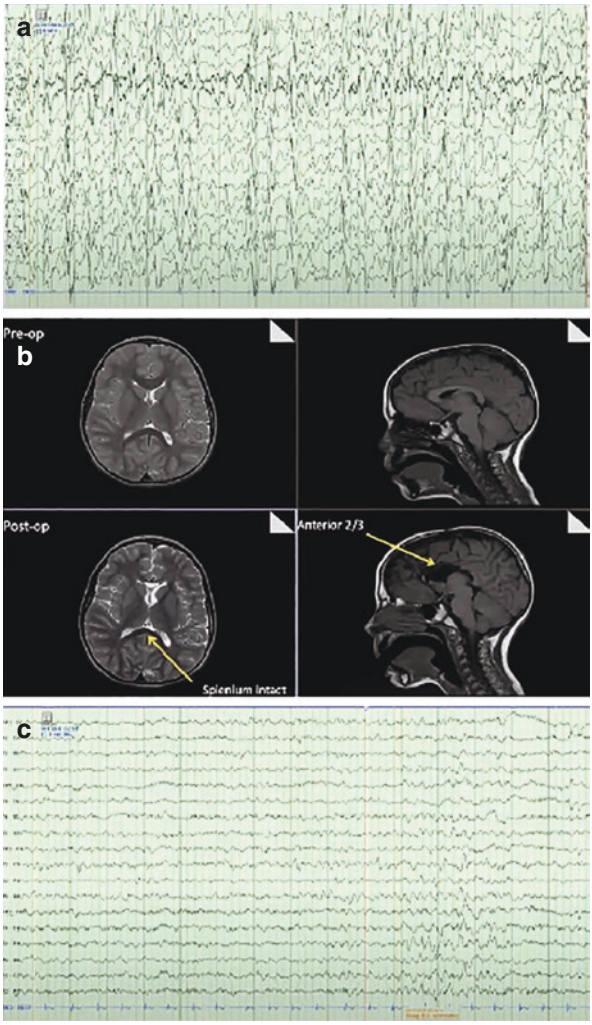

Fig. 13.1 Illustrative preoperative electroencephalography (EEG, **a**) magnetic resonance imaging (**b**), and postoperative EEG (**c**) findings of patient undergoing anterior two-thirds corpus callosotomy

13.3.3 Laser Interstitial Thermal Therapy (LITT)

The introduction of MRI-guided laser interstitial thermal therapy (LITT) initially gained popularity as a technique for ablation of focal lesions prior to its use to perform CC [30–39]. Like endoscopic approaches, MRI-guided LITT for CC were initially performed in patients who had not undergone a prior craniotomy. In addition, patients who were determined to be candidates for CC through multidisciplinary epilepsy conference were considered candidates for MRI guided LITT for CC if they had favorable anatomy including a robust and flat body of the corpus callosum, no prior implant that would prevent fiber placement and could safely undergo an MRI under general anesthesia [38]. High-volume LITT centers have

also been the first adopters of this approach for CC but do acknowledge the necessity of clinical equipoise between endorsing one approach over another.

The first case series using MRI-guided LITT for CC included five patients without any reported immediate or delayed surgical complications and with similar clinical efficacy to open approaches [37]. These patients also underwent diffusion tensor imaging, resting state functional connectivity, and functional MRI postoperatively to demonstrate disconnection [37]. A larger series of ten patients underwent 11 CC via MRI-guided LITT, where five patients underwent anterior CC and one patient required an additional LITT operation due to incomplete callosotomy [38]. Functional and seizure freedom outcomes were similar to CC performed using open approaches [38]. Another series of six patients underwent LITT CC where two-third adults achieved Engel I or II, whereas pediatric patient outcomes were modest [34].

13.4 Technical Considerations

Several techniques and approaches have been used to perform CC. These include open anterior interhemispheric approaches, endoscopic approaches, and MRI-guided LITT [26]. Radiosurgery approaches [33, 36, 40–48], with similar seizure-freedom and functional outcomes to open approaches, have also been reported, and our center has not used this approach. CC has also been used as an adjunctive procedure that allows further localization of epileptic foci as well as in patients who already have a vagus nerve stimulator (VNS) to augment seizure control [49].

13.4.1 Open Approaches

Open craniotomy with microsurgical dissection may facilitate complete disconnection of the corpus callosum through a single incision. The highly somatotopic organization of the corpus callosotomy has led to clinical hypotheses that selective CC would lead to generalized seizure attenuation through blocking propagation through specific somatotopic distributions. This has led to some advocating for anterior callosotomy in isolation versus staged callosotomy disconnecting the anterior 2/3 followed by the posterior 1/3 of the corpus callosum during a second procedure to minimize morbidity of conducting an open total corpus callosotomy in one procedure.

The patient is positioned supine with head flexed approximately 15–20°. A bicoronal incision eccentric to the right side stopping above the superior temporal line and anterior to the coronal suture is performed to enable an interhemispheric approach with lateral retraction of the hemisphere. An approximately 6 cm long by 5 cm wide craniotomy is planned with 2/3 in front and 1/3 behind the coronal suture 3/5 and 2/5 to the right and left of midline, respectively (Fig. 13.2a). The dura is reflected with the base towards the sagittal sinus (Fig. 13.2b).

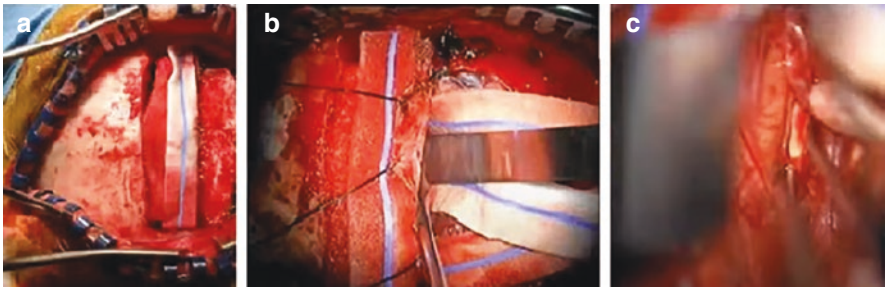

Fig. 13.2 Illustrative case demonstrating the open approach to performing CC. (**a**) 6 cm long by 5 cm wide craniotomy is planned with 2/3 in front and 1/3 behind the coronal suture 3/5 and 2/5 to the right and left of midline, respectively. The dura is reflected with the base toward the sagittal sinus (**b**). Under microscopic visualization dissection is performed parallel to the falx with care taken to identify the transition from medial frontal to cingulate gyrus to facilitate protection of the callosomarginal and pericallosal arteries which run superior and inferior, respectively, to the cingulate gyrus (**c**)

Under microscopic visualization dissection is performed parallel to the falx with care taken to identify the transition from medial frontal to cingulate gyrus to facilitate protection of the callosomarginal and pericallosal arteries, which run superior and inferior, respectively, to the cingulate gyrus (Fig. 13.2c). The corpus callosum will appear as a white structure beneath the commonly paired pericallosal arteries [26]. Cottonoids are used to protect the superficial medial structures. Callosotomy can then be performed utilizing bipolar, suction, and/or ultrasonic aspiration until the ventricular ependyma is encountered with care taken to avoid transgression.

Maxwell et al. in the 1980s described a two-staged approach to CC consisting of (1) anterior 2/3 sectioning of the corpus callosum using a frontal interhemispheric approach and followed by (2) posterior parietal craniotomy for posterior disconnection [50]. Of note, both the anterior 2/3 and complete CC approach are effective, but single stage complete CC is most effective toward a broader spectrum of seizure types compared to anterior or staged approach [50].

During anterior CC, dissection follows the curve of the genu to the rostrum commonly using the anterior cerebral arteries as a guide until the anterior commissure near the level of the Foramen of Monroe is encountered. Posterior CC is accomplished by following ventricular ependyma until encountering the inferior turn of the splenium. The arachnoid plane protecting the underlying Vein of Galen serves as a marker that complete splenial disconnection has been achieved.

13.4.2 Endoscopic Approaches

Endoscopic approaches may provide decreased operative morbidity, and a wide variety of approaches have been described with similar efficacy to the open technique [20–29]. Here, we describe our preferred approach. Patient positioning and

incision placement are like open approaches as described above. An ~3 × 2 cm wide craniotomy is planned eccentric to the patient's right with "C"-shaped dural opening oriented, so the base is toward the superior sagittal sinus. A 4 mm rigid endoscope is introduced for visualization with some authors advocating for using a coupling clamp to mount the endoscopic cannula on a ten French suction [28], having the endoscope free hand and held by an assistant versus mounting it on a rigid stand. For complete CC, some authors advocate for starting from the splenial dissection and progressing anteriorly following the curve of the genu until the bilateral A2 divisions are encountered with further rostral progression ensuring anterior commissure division as well. If desired, the hippocampal commissure will be encountered immediately beneath the posterior body/isthmus/splenium of the corpus callosum and divided until the third ventricle is encountered [21, 22].

13.4.3 MRI-Guided Laser Interstitial Thermal Therapy for Corpus Callosotomy

LITT was most widely adopted in neurosurgery for thermal ablation of tumors [51]. This was followed by application to mesial temporal lobe epilepsy specifically [52], and more recently, epileptic foci localized elsewhere [53]. Positioning for completion of a 2/3 or complete callosotomy is dependent on planned trajectories with lateral fixation if posterior entry points are required. The patient is positioned with either a Leksell or Mayfield head holder affixed to the ROSA robotic system [54] after bone fiducials and an O arm spin for stereotactic co-registration is performed. The ROSA is used to mark the trajectory and entry point with a 3.4 mm guide tube utilized to direct a 3.2 mm handheld drill. A bone anchor is subsequently placed, and the ROSA utilized to measure the distance to the prespecified target. The laser fiber is subsequently passed, and the process repeated at all planned trajectories to complete the desired CC. The patient is then transferred to the MRI suite where MRI thermometry is conducted using standard LITT technique ensuring that each treatment ablation area has some overlap with the prior ablated segment. An illustrative case from our center demonstrating ablation zone after using laser interstitial thermal therapy (LITT) in the sagittal (Fig. 13.3a) and coronal (Fig. 13.3b) planes. After ablation, some authors advocate for DWI followed by T1-MPRAGE to verify extent of ablation [38].

13.4.4 Corpus Callosotomy as a Diagnostic Procedure

CC may also be useful in determining lateralization and identification of lesions amenable to focal resection. Clarke et al. observed a subset of patients who underwent CC developed lateralized findings where invasive monitoring approaches and

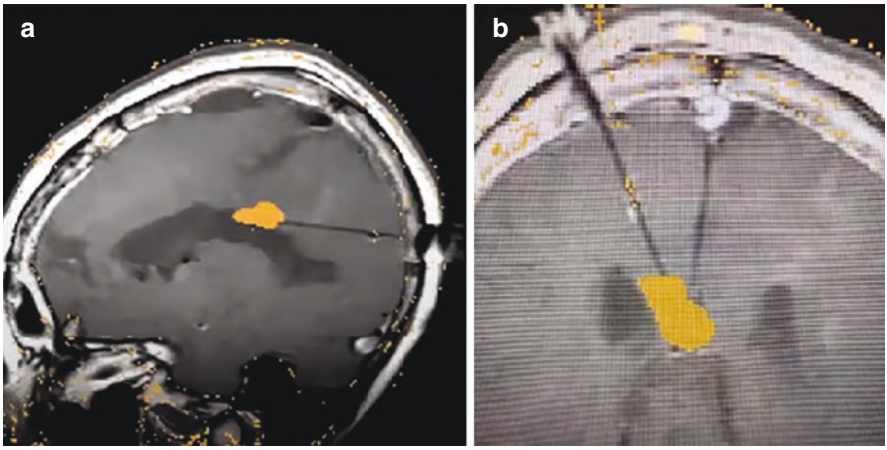

Fig. 13.3 Illustrative case demonstrating ablation zone after using laser interstitial thermal therapy (LITT) in the sagittal (**a**) and coronal (**b**) planes

identification of focal lesions that could be safely resected [55]. Lin et al. describe the Milwaukee Children's Hospital experience of 21 patients undergoing CC where 18/21 patients underwent placement of grid electrodes at the same time as CC [56]. Interestingly, 12 of these patients ultimately underwent focal resection and all achieved Engel class I or II outcomes (mean follow-up of ~3 years) [56]. Thus, CC should be thought of as both a treatment for seizure reduction and as a diagnostic procedure that can be used to identify frontal foci that may be removed through classic focal resection approaches.

13.4.5 Corpus Callosotomy and Vagus Nerve Stimulator (VNS) Therapy

While much of the literature has been focused on identifying which procedure (CC vs. VNS) is most effective [57–60], others have proposed that CC is highly effective in combination with VNS [49]. This is based on the observation that effectiveness of CC tends to diminish over time, whereas the opposite is observed with VNS. In a series of ten patients with Lennox-Gastaut syndrome (LGS) where patients initially underwent CC but later received VNS therapy, two patients achieved Engel I after VNS, but more significantly, VNS was effective against residual seizure semiologies and even nonresponders to CC demonstrated improvement after VNS therapy [49]. Hong et al. also reported a series of ten patients who underwent VNS placement followed by CC (with 53 months mean follow-up) where nine out of ten patients are Engel III, but half of their cohort demonstrated >50% reduction in seizure frequency [33]. An additional series with patients receiving either CC or VNS as the index therapy demonstrated similar efficacy with five out of six patients

demonstrating seizure reduction [33]. Thus, while most patients are not achieving "successful" Engel scores, their reduction in seizure freedom is still quite appreciable and impactful on quality of life.

13.5 Outcomes and Complications

Most of the reported outcomes for CC have been reported based on case series where the open approach was the preferred technique [61–64]. Arrest or cessation of drop attacks have been observed in approximately 90% of patients undergoing complete CC and approximately two-third of patients undergoing partial CC. The largest drop in atonic events is observed in patients less than 16 years of age at surgery. While less than 10% are expected to achieve seizure freedom after CC, there is still significant benefit in reducing drop attack frequency and morbidity of MRE. CC often results in a 10–15% better response but can require a second operation. Overall, reduction in clonic and tonic-clonic seizures is most typically observed, and pediatric patients tend to have better outcomes compared to adults [65]. Over time, however, there appears to be a lower percentage (~35%) of patients that are drop attack free at 5 years after CC. Non-seizure-related improvements in hyperactivity (93%), behavioral attentiveness (75%), daily functional activities (62%), emotional well-being (42%), social interaction (36%), and speech (21%) are also observed [66]. Electroencephalography readings after CC often demonstrates better organization (90%) and loss of bihemispheric synchrony (85%) [64]. However, it should be noted that the retrospective nature of these studies may overestimate the effectiveness of CC.

The safety of CC has been established over nearly 8 decades since its inception. CC has traditionally been thought of as a palliative operation, but the role of palliative intervention has been greatly expanded and is no longer a pejorative concept. Most patients (> 90%) undergoing CC will not achieve seizure freedom, but there is still a significant degree of benefit to be achieved by reducing drop attack frequency and improvements in neurocognitive outcomes, largely in agreement with several patients undergoing resective surgery [67]. Finally, while complete CC may achieve greater seizure reduction than anterior approaches alone, the risk of surgical complications may be greater [61].

13.5.1 Corpus Callosotomy Does Not Require Expensive Evaluation

CC is also highly cost-effective [68]. Along with lesional resection, hemispherectomy (especially in peri-natal strokes), and anterior temporal lobectomy, CC can be a highly effective operation where candidacy can be determined without the use of

invasive monitoring [69, 70]. The utility, safety, and efficacy of CC and epilepsy surgery have been demonstrated in many resource-limited settings [15, 69–74]. In close collaboration with colleagues in Vietnam, we have developed a CC and epilepsy surgery program [70, 71]. Eleven complete and five anterior CC were performed with 38% of the cohort achieving >75% seizure reduction and > 50% achieving >50% seizure reduction without any long-term morbidity, mortality, or complications from surgery (12–44 months follow-up) [71]. Thus, similar clinical outcomes can be achieved in developing nations.

Adverse responses or complications related to CC are seldom observed [36]. Specifically, disconnection syndromes (the most severe complication) are very rare and usually only occur with complete CC [75]. Disconnection syndrome is characterized by objected being present that cannot be described, nondominant hand with variable response to verbal directive, and the "alien hand" where the patient perceives alienation from and loss of control of hand function where they may reach for and/or manipulate objects unknowingly [75, 76]. However, many CC candidates are profoundly disadvantaged, and these subtle clinical findings cannot be detected [77]. In addition, patients may experience akinetic symptoms, which are typically transient (~1–2 weeks in duration) and are also more likely to be observed in patients who undergo complete CC [78]. Approximately 27% of adults and 6% of children undergoing CC report overall decrease in daily function but are quick to resolve [66]. Finally, retraction-related hemiparesis occurs in ~10–20% of patients and are also transient [66]. In sum, virtually all adverse reactions are transient, and the overall rate of serious long-term complications is <3% [66]. Appraisal of complication rates between open, minimally invasive, LITT, and radiosurgery approaches have not been performed. Since patient selection for each approach is varied and surgeon experience with each modality is highly variable, direct comparison of complication rates is not valid.

13.6 Conclusions

Corpus callosotomy (CC) can be a highly beneficial treatment for children with medically resistant generalized experiencing drop attacks and other bifrontal seizure semiologies. Here, we outline technical considerations for performing CC using a variety of approaches. CC is a safe procedure, and the role of minimally invasive approaches including endoscopic and MRI-guided LITT is being increasingly performed. Preliminary data suggests that minimally invasive CC is effective and safe, but additional investigation is needed. CC is an inexpensive procedure relying largely on clinical diagnosis and EEG findings that should be in the armamentarium of all pediatric epilepsy surgeons. Since the costs of performing CC are relatively low, this may be an ideal operation to perform in LMICs where invasive monitoring and comprehensive epilepsy services are unavailable.Conflict of InterestNone.

Disclosure of Funding No funding sources were used to generate the data presented herein.

References

1. Dandy WE. Operative experience in cases of pineal tumor. Arch Surg. 1936;33(1):19–46.
2. Erickson TC. Spread of the epileptic discharge: an experimental study of the after-discharge induced by electrical stimulation of the cerebral cortex. Arch Neurol Psychiatr. 1940;43(3):429–52.
3. Van Wagenen WP, Herren RY. Surgical division of commissural pathways in the corpus callosum: relation to spread of an epileptic attack. Arch Neurol Psychiatr. 1940;44(4):740–59.
4. Gazzaniga MS, Bogen JE, Sperry RW. Some functional effects of sectioning the cerebral commissures in man. Proc Natl Acad Sci. 1962;48(10):1765–9.
5. Bogen JE, Fisher E, Vogel P. Cerebral commissurotomy: a second case report. JAMA. 1965;194(12):1328–9.
6. Luessenhop AJ, dela Cruz TC, Fenichel GM. Surgical disconnection of the cerebral hemispheres for intractable seizures: results in infancy and childhood. JAMA. 1970;213(10):1630–6.
7. Gazzaniga M, Risse G, Springer S, Clark E, Wilson D. Psychologic and neurologic consequences of partial and complete cerebral commissurotomy. Neurology. 1975;25(1):10.
8. Wilson DH, Culver C, Waddington M, Gazzaniga M. Disconnection of the cerebral hemispheres: an alternative to hemispherectomy for the control of intractable seizures. Neurology. 1975;25(12):1149.
9. Wilson DH, Reeves AG, Gazzaniga MS. "Central" commissurotomy for intractable generalized epilepsy: series two. Neurology. 1982;32(7):687.
10. Raybaud C. The corpus callosum, the other great forebrain commissures, and the septum pellucidum: anatomy, development, and malformation. Neuroradiology. 2010;52(6):447–77. https://doi.org/10.1007/s00234-010-0696-3. Epub 2010/04/28. PubMed PMID: 20422408.
11. de Lacoste MC, Kirkpatrick JB, Ross ED. Topography of the human corpus callosum. J Neuropathol Exp Neurol. 1985;44(6):578–91.
12. Türe U, Yaşargil MG, Krisht AF. The arteries of the corpus callosum: a microsurgical anatomic study. Neurosurgery. 1996;39(6):1075–84.
13. Rhoton AL Jr. Rhoton's cranial anatomy and surgical approaches. Oxford: Oxford University Press; 2019.
14. Maehara T, Shimizu H. Surgical outcome of corpus callosotomy in patients with drop attacks. Epilepsia. 2001;42(1):67–71. https://doi.org/10.1046/j.1528-1157.2001.081422.x. Epub 2001/02/24. PubMed PMID: 11207787.
15. Rathore C, Abraham M, Rao RM, George A, Sankara Sarma P, Radhakrishnan K. Outcome after corpus callosotomy in children with injurious drop attacks and severe mental retardation. Brain Dev. 2007;29(9):577–85. https://doi.org/10.1016/j.braindev.2007.03.008. Epub 2007/05/18. PubMed PMID: 17507193.
16. Sorenson JM, Wheless JW, Baumgartner JE, Thomas AB, Brookshire BL, Clifton GL, et al. Corpus callosotomy for medically intractable seizures. Pediatr Neurosurg. 1997;27(5):260–7. https://doi.org/10.1159/000121264. Epub 1998/06/10. PubMed PMID: 9620004.
17. Turanli G, Yalnizoğlu D, Genç-Açikgöz D, Akalan N, Topçu M. Outcome and long term follow-up after corpus callosotomy in childhood onset intractable epilepsy. Childs Nerv Syst. 2006;22(10):1322–7. https://doi.org/10.1007/s00381-006-0045-3. Epub 2006/03/23 PubMed PMID: 16552568.
18. Asadi-Pooya AA, Malekmohamadi Z, Kamgarpour A, Rakei SM, Taghipour M, Ashjazadeh N, et al. Corpus callosotomy is a valuable therapeutic option for patients with Lennox-Gastaut

syndrome and medically refractory seizures. Epilepsy Behav. 2013;29(2):285–8. https://doi.org/10.1016/j.yebeh.2013.08.011. Epub 2013/09/10. PubMed PMID: 24012506.
19. Kawai K, Shimizu H, Yagishita A, Maehara T, Tamagawa K. Clinical outcomes after corpus callosotomy in patients with bihemispheric malformations of cortical development. J Neurosurg Pediatr. 2004;101(2):7–15.
20. Bahuleyan B, Vogel TW, Robinson S, Cohen AR. Endoscopic total corpus callosotomy: cadaveric demonstration of a new approach. Pediatr Neurosurg. 2011;47(6):455–60. https://doi.org/10.1159/000338984. Epub 2012/07/11. PubMed PMID: 22777273.
21. Chandra PS, Kurwale N, Garg A, Dwivedi R, Malviya SV, Tripathi M. Endoscopy-assisted interhemispheric transcallosal hemispherotomy: preliminary description of a novel technique. Neurosurgery. 2015;76(4):485–94. https://doi.org/10.1227/neu.0000000000000675. discussion 94-5. Epub 2015/02/25.PubMed PMID: 25710106.
22. Chandra SP, Kurwale NS, Chibber SS, Banerji J, Dwivedi R, Garg A, et al. Endoscopic-assisted (through a mini craniotomy) corpus callosotomy combined with anterior, hippocampal, and posterior commissurotomy in Lennox-Gastaut syndrome: a pilot study to establish its safety and efficacy. Neurosurgery. 2016;78(5):743–51. https://doi.org/10.1227/neu.0000000000001060. Epub 2015/10/17. PubMed PMID: 26474092.
23. Chandra SP, Tripathi M. Endoscopic epilepsy surgery: emergence of a new procedure. Neurol India. 2015;63(4):571–82. https://doi.org/10.4103/0028-3886.162056. Epub 2015/08/05. PubMed PMID: 26238894.
24. Doddamani R, Kota RC, Ahemad N, Chandra SP, Tripathi M. Endoscopic Total corpus Callosotomy and pan Commissurotomy for Lennox-Gastaut syndrome. Neurol India. 2022;70(1):63–7. https://doi.org/10.4103/0028-3886.338654. Epub 2022/03/11. PubMed PMID: 35263855.
25. LoPresti MA, Wagner K, Lam S. Endoscope-assisted posterior quadrant disconnection plus corpus callosotomy: case report. J Neurosurg Pediatr. 2021;27(4):406–10. https://doi.org/10.3171/2020.8.Peds20432. Epub 2021/01/16. PubMed PMID: 33450733.
26. Smyth MD, Vellimana AK, Asano E, Sood S. Corpus callosotomy-open and endoscopic surgical techniques. Epilepsia. 2017;58(Suppl 1):73–9. https://doi.org/10.1111/epi.13681. Epub 2017/04/08. PubMed PMID: 28386923.
27. Sood S, Asano E, Altinok D, Luat A. Endoscopic posterior interhemispheric complete corpus callosotomy. J Neurosurg Pediatr. 2016;25(6):689–92. https://doi.org/10.3171/2016.6.Peds16131. Epub 2016/09/10. PubMed PMID: 27611896.
28. Sood S, Marupudi NI, Asano E, Haridas A, Ham SD. Endoscopic corpus callosotomy and hemispherotomy. J Neurosurg Pediatr. 2015;16(6):681–6. Epub 2015/09/26. PubMed PMID: 26407094. https://doi.org/10.3171/2015.5.Peds1531.
29. Tubbs RS, Smyth MD, Salter G, Doughty K, Blount JP. Eyebrow incision with supraorbital trephination for endoscopic corpus callosotomy: a feasibility study. Childs Nerv Syst. 2004;20(3):188–91. https://doi.org/10.1007/s00381-003-0894-y. Epub 2004/01/28. PubMed PMID: 14745578.
30. Badger CA, Lopez AJ, Heuer G, Kennedy BC. Systematic review of corpus callosotomy utilizing MRI guided laser interstitial thermal therapy. J Clin Neurosci. 2020;76:67–73. Epub 2020/04/20. PubMed PMID: 32305273. https://doi.org/10.1016/j.jocn.2020.04.046.
31. Consales A, Cognolato E, Pacetti M, Mancardi MM, Tortora D, Di Perna G, et al. Magnetic resonance-guided laser interstitial thermal therapy (MR-gLiTT) in pediatric epilepsy surgery: state of the art and presentation of Giannina Gaslini Children's Hospital (Genoa, Italy) series. Front Neurol. 2021;12:739034. Epub 2021/11/13. PubMed PMID: 34764929; PubMed Central PMCID: PMCPMC8577648. https://doi.org/10.3389/fneur.2021.739034.
32. Hect JL, Alattar AA, Harford EE, Reecher H, Fernandes DT, Esplin N, et al. Stereotactic laser interstitial thermal therapy for the treatment of pediatric drug-resistant epilepsy: indications, techniques, and safety. Childs Nerv Syst. 2022;38(5):961–70. https://doi.org/10.1007/s00381-022-05491-x. Epub 2022/03/12. PubMed PMID: 35274185.

33. Hong J, Desai A, Thadani VM, Roberts DW. Efficacy and safety of corpus callosotomy after vagal nerve stimulation in patients with drug-resistant epilepsy. J Neurosurg. 2018;128(1):277–86. https://doi.org/10.3171/2016.10.Jns161841. Epub 2017/03/17. PubMed PMID: 28298036.
34. Huang Y, Yecies D, Bruckert L, Parker JJ, Ho AL, Kim LH, et al. Stereotactic laser ablation for completion corpus callosotomy. J Neurosurg Pediatr. 2019;24:1–9. https://doi.org/10.3171/2019.5.Peds19117. Epub 2019/08/03. PubMed PMID: 31374542.
35. Mallela AN, Hect JL, Abou-Al-Shaar H, Akwayena E, Abel TJ. Stereotactic laser interstitial thermal therapy corpus callosotomy for the treatment of pediatric drug-resistant epilepsy. Epilepsia Open. 2022;7(1):75–84. https://doi.org/10.1002/epi4.12559. Epub 2021/11/11. PubMed PMID: 34758204; PubMed Central PMCID: PMCPMC8886067.
36. Markosian C, Patel S, Kosach S, Goodman RR, Tomycz LD. Corpus Callosotomy in the modern era: origins, efficacy, technical variations, complications, and indications. World Neurosurg. 2022;159:146–55. https://doi.org/10.1016/j.wneu.2022.01.037. Epub 2022/01/17. PubMed PMID: 35033693.
37. Palma AE, Wicks RT, Popli G, Couture DE. Corpus callosotomy via laser interstitial thermal therapy: a case series. J Neurosurg Pediatr. 2018;23(3):303–7. https://doi.org/10.3171/2018.10.Peds18368. Epub 2018/12/24. PubMed PMID: 30579267.
38. Roland JL, Akbari SHA, Salehi A, Smyth MD. Corpus callosotomy performed with laser interstitial thermal therapy. J Neurosurg. 2019;134:1–9. https://doi.org/10.3171/2019.9.Jns191769. Epub 2019/12/14. PubMed PMID: 31835250
39. Tao JX, Satzer D, Issa NP, Collins J, Wu S, Rose S, et al. Stereotactic laser anterior corpus callosotomy for Lennox-Gastaut syndrome. Epilepsia. 2020;61(6):1190–200. https://doi.org/10.1111/epi.16535. Epub 2020/05/14. PubMed PMID: 32401350.
40. Bodaghabadi M, Bitaraf MA, Aran S, Alikhani M, Ashrafian H, Zahiri A, et al. Corpus callosotomy with gamma knife radiosurgery for a case of intractable generalised epilepsy. Epileptic Disord. 2011;13(2):202–8. https://doi.org/10.1684/epd.2011.0436. Epub 2011/06/02. PubMed PMID: 21628134.
41. Celis MA, Moreno-Jiménez S, Lárraga-Gutiérrez JM, Alonso-Vanegas MA, García-Garduño OA, Martínez-Juárez IE, et al. Corpus callosotomy using conformal stereotactic radiosurgery. Childs Nerv Syst. 2007;23(8):917–20. https://doi.org/10.1007/s00381-007-0356-z. Epub 2007/04/24. PubMed PMID: 17450365.
42. Eder HG, Feichtinger M, Pieper T, Kurschel S, Schroettner O. Gamma knife radiosurgery for callosotomy in children with drug-resistant epilepsy. Childs Nerv Syst. 2006;22(8):1012–7. https://doi.org/10.1007/s00381-006-0138-z. Epub 2006/06/14. PubMed PMID: 16770617.
43. Feichtinger M, Schröttner O, Eder H, Holthausen H, Pieper T, Unger F, et al. Efficacy and safety of radiosurgical callosotomy: a retrospective analysis. Epilepsia. 2006;47(7):1184–91. https://doi.org/10.1111/j.1528-1167.2006.00592.x. Epub 2006/08/05. PubMed PMID: 16886982.
44. Hamdi H, Boissonneau S, Hadidane S, Guenot M, Bartolomei F, Regis J. Effective posterior extension of callosotomy by gamma knife surgery. Epileptic Disord. 2020;22(3):342–8. https://doi.org/10.1684/epd.2020.1170. Epub 2020/06/20. PubMed PMID: 32554339.
45. Pendl G, Eder HG, Schroettner O, Leber KA. Corpus callosotomy with radiosurgery. Neurosurgery. 1999;45(2):303–7. https://doi.org/10.1097/00006123-199908000-00021. discussion 7-8. Epub 1999/08/17. PubMed PMID: 10449075.
46. Sachdev S, Sita TL, Shlobin NA, Gopalakrishnan M, Sucholeiki R, Régis J, et al. Completion corpus callosotomy with stereotactic radiosurgery for drug-resistant, intractable epilepsy. World Neurosurg. 2020;143:440–4. https://doi.org/10.1016/j.wneu.2020.08.102. Epub 2020/08/23. PubMed PMID: 32827745.
47. Smyth MD, Klein EE, Dodson WE, Mansur DB. Radiosurgical posterior corpus callosotomy in a child with Lennox-Gastaut syndrome. Case report. J Neurosurg. 2007;106(4 Suppl):312–5. https://doi.org/10.3171/ped.2007.106.4.312. Epub 2007/05/01. PubMed PMID: 17465368.

48. Tripathi M, Maskara P, Rangan VS, Mohindra S, De Salles AAF, Kumar N. Radiosurgical corpus Callosotomy: a review of literature. World Neurosurg. 2021;145:323–33. https://doi.org/10.1016/j.wneu.2020.08.205. Epub 2020/09/07. PubMed PMID: 32891831.
49. Guillamón E, Miró J, Gutiérrez A, Conde R, Falip M, Jaraba S, et al. Combination of corpus callosotomy and vagus nerve stimulation in the treatment of refractory epilepsy. Eur Neurol. 2014;71(1–2):65–74. https://doi.org/10.1159/000353979. Epub 2013/12/18. PubMed PMID: 24334999.
50. Maxwell R, Gates J, Gumnit R. Corpus callosotomy at the University of Minnesota. Surgical Treatment of the Epilepsies New York: Raven; 1987. p. 659–66.
51. Missios S, Bekelis K, Barnett GH. Renaissance of laser interstitial thermal ablation. Neurosurg Focus. 2015;38(3):E13.
52. Kang JY, Wu C, Tracy J, Lorenzo M, Evans J, Nei M, et al. Laser interstitial thermal therapy for medically intractable mesial temporal lobe epilepsy. Epilepsia. 2016;57(2):325–34.
53. Prince E, Hakimian S, Ko AL, Ojemann JG, Kim MS, Miller JW. Laser interstitial thermal therapy for epilepsy. Curr Neurol Neurosci Rep. 2017;17(9):1–9.
54. Gonzalez-Martinez J, Vadera S, Mullin J, Enatsu R, Alexopoulos AV, Patwardhan R, et al. Robot-assisted stereotactic laser ablation in medically intractable epilepsy: operative technique. Oper Neurosurg. 2014;10(2):167–73.
55. Clarke DF, Wheless JW, Chacon MM, Breier J, Koenig MK, McManis M, et al. Corpus callosotomy: a palliative therapeutic technique may help identify resectable epileptogenic foci. Seizure. 2007;16(6):545–53. https://doi.org/10.1016/j.seizure.2007.04.004. Epub 2007/05/25. PubMed PMID: 17521926.
56. Lin JS, Lew SM, Marcuccilli CJ, Mueller WM, Matthews AE, Koop JI, et al. Corpus callosotomy in multistage epilepsy surgery in the pediatric population. J Neurosurg Pediatr. 2011;7(2):189–200. https://doi.org/10.3171/2010.11.Peds10334. Epub 2011/02/03. PubMed PMID: 21284466.
57. Lancman G, Virk M, Shao H, Mazumdar M, Greenfield JP, Weinstein S, et al. Vagus nerve stimulation vs. corpus callosotomy in the treatment of Lennox-Gastaut syndrome: a meta-analysis. Seizure. 2013;22(1):3–8. https://doi.org/10.1016/j.seizure.2012.09.014. Epub 2012/10/17. PubMed PMID: 23068970; PubMed Central PMCID: PMCPMC3655762.
58. Rolston JD, Englot DJ, Wang DD, Garcia PA, Chang EF. Corpus callosotomy versus vagus nerve stimulation for atonic seizures and drop attacks: A systematic review. Epilepsy Behav. 2015;51:13–7. https://doi.org/10.1016/j.yebeh.2015.06.001. Epub 2015/08/08. PubMed PMID: 26247311; PubMed Central PMCID: PMCPMC5261864.
59. Ye VC, Mansouri A, Warsi NM, Ibrahim GM. Atonic seizures in children: a meta-analysis comparing corpus callosotomy to vagus nerve stimulation. Childs Nerv Syst. 2021;37(1):259–67. https://doi.org/10.1007/s00381-020-04698-0. Epub 2020/06/13. PubMed PMID: 32529546.
60. You SJ, Kang HC, Ko TS, Kim HD, Yum MS, Hwang YS, et al. Comparison of corpus callosotomy and vagus nerve stimulation in children with Lennox-Gastaut syndrome. Brain Dev. 2008;30(3):195–9. https://doi.org/10.1016/j.braindev.2007.07.013. Epub 2007/09/11. PubMed PMID: 17825516.
61. Chan AY, Rolston JD, Lee B, Vadera S, Englot DJ. Rates and predictors of seizure outcome after corpus callosotomy for drug-resistant epilepsy: a meta-analysis. J Neurosurg. 2018;130:1–10. https://doi.org/10.3171/2017.12.Jns172331. Epub 2018/07/13. PubMed PMID: 29999448; PubMed Central PMCID: PMCPMC6274594.
62. Cukiert A, Cukiert CM, Burattini JA, Lima AM, Forster CR, Baise C, et al. Long-term outcome after callosotomy or vagus nerve stimulation in consecutive prospective cohorts of children with Lennox-Gastaut or Lennox-like syndrome and non-specific MRI findings. Seizure. 2013;22(5):396–400. https://doi.org/10.1016/j.seizure.2013.02.009. Epub 2013/03/16. PubMed PMID: 23490456.
63. Stigsdotter-Broman L, Olsson I, Flink R, Rydenhag B, Malmgren K. Long-term follow-up after callosotomy—a prospective, population based, observational study. Epilepsia.

2014;55(2):316–21. https://doi.org/10.1111/epi.12488. Epub 2014/01/01. PubMed PMID: 24372273; PubMed Central PMCID: PMCPMC4165268.
64. Téllez-Zenteno JF, Dhar R, Wiebe S. Long-term seizure outcomes following epilepsy surgery: a systematic review and meta-analysis. Brain. 2005;128(Pt 5):1188–98. https://doi.org/10.1093/brain/awh449. Epub 2005/03/11. PubMed PMID: 15758038.
65. Graham D, Tisdall MM, Gill D. Corpus callosotomy outcomes in pediatric patients: a systematic review. Epilepsia. 2016;57(7):1053–68. https://doi.org/10.1111/epi.13408. Epub 2016/05/31. PubMed PMID: 27237542.
66. Asadi-Pooya AA, Sharan A, Nei M, Sperling MR. Corpus callosotomy. Epilepsy Behav. 2008;13(2):271–8. https://doi.org/10.1016/j.yebeh.2008.04.020. Epub 2008/06/10. PubMed PMID: 18539083.
67. Bulacio JC, Jehi L, Wong C, Gonzalez-Martinez J, Kotagal P, Nair D, et al. Long-term seizure outcome after resective surgery in patients evaluated with intracranial electrodes. Epilepsia. 2012;53(10):1722–30. https://doi.org/10.1111/j.1528-1167.2012.03633.x. Epub 2012/08/22. PubMed PMID: 22905787.
68. Abel TJ, Remick M, Welch WC, Smith KJ. One-year cost-effectiveness of callosotomy vs vagus nerve stimulation for drug-resistant seizures in Lennox-Gastaut Syndrome: a decision analytic model. Epilepsia Open. 2022;7(1):124–30. https://doi.org/10.1002/epi4.12570. Epub 2021/12/11. PubMed PMID: 34890113; PubMed Central PMCID: PMCPMC8886071.
69. Fandiño-Franky J, Torres M, Nariño D, Fandiño J. Corpus callosotomy in Colombia and some reflections on care and research among the poor in developing countries. Epilepsia. 2000;41(Suppl 4):S22–7. https://doi.org/10.1111/j.1528-1157.2000.tb01541.x. Epub 2000/08/30. PubMed PMID: 10963473.
70. Rocque BG, Davis MC, McClugage SG, Tuan DA, King DT, Huong NT, et al. Surgical treatment of epilepsy in Vietnam: program development and international collaboration. Neurosurg Focus. 2018;45(4):E3. https://doi.org/10.3171/2018.7.Focus18254. Epub 2018/10/03. PubMed PMID: 30269583.
71. Duc Lien N, Tuan DA, Vu Hung C, Lepard JR, Rocque BG. Corpus callosotomy for treatment of drug-resistant epilepsy: a review of 16 pediatric cases in northern Vietnam. J Neurosurg Pediatr. 2020;25:1–6. https://doi.org/10.3171/2019.12.Peds19638. Epub 2020/02/29. PubMed PMID: 32109876
72. Mikati MA, Ataya N, El-Ferezli J, Shamseddine A, Rahi A, Herlopian A, et al. Epilepsy surgery in a developing country (Lebanon): ten years experience and predictors of outcome. Epileptic Disord. 2012;14(3):267–74. https://doi.org/10.1684/epd.2012.0522. Epub 2012/09/07. PubMed PMID: 22951375.
73. Romach MK, Rutka JT. Building healthcare capacity in pediatric neurosurgery and psychiatry in a post-soviet system: Ukraine. World Neurosurg. 2018;111:166–74. https://doi.org/10.1016/j.wneu.2017.11.178. Epub 2017/12/13. PubMed PMID: 29229346.
74. Watila MM, Xiao F, Keezer MR, Miserocchi A, Winkler AS, McEvoy AW, et al. Epilepsy surgery in low—and middle-income countries: a scoping review. Epilepsy Behav. 2019;92:311–26. https://doi.org/10.1016/j.yebeh.2019.01.001. Epub 2019/02/10. PubMed PMID: 30738248.
75. Jea A, Vachhrajani S, Widjaja E, Nilsson D, Raybaud C, Shroff M, et al. Corpus callosotomy in children and the disconnection syndromes: a review. Childs Nerv Syst. 2008;24(6):685–92. https://doi.org/10.1007/s00381-008-0626-4. Epub 2008/04/01. PubMed PMID: 18373102.
76. Seymour SE, Reuter-Lorenz PA, Gazzaniga MS. The disconnection syndrome. Basic findings reaffirmed. Brain. 1994;117(Pt 1):105–15. https://doi.org/10.1093/brain/117.1.105. Epub 1994/02/01. PubMed PMID: 8149205.
77. Berlucchi G. Frontal callosal disconnection syndromes. Cortex. 2012;48(1):36–45. https://doi.org/10.1016/j.cortex.2011.04.008. Epub 2011/06/15. PubMed PMID: 21663900.
78. Fuiks KS, Wyler AR, Hermann BP, Somes G. Seizure outcome from anterior and complete corpus callosotomy. J Neurosurg. 1991;74(4):573–8. https://doi.org/10.3171/jns.1991.74.4.0573. Epub 1991/04/01. PubMed PMID: 2002370.

Chapter 14
Blood Blister-Like Aneurysms of the Internal Carotid Artery

Eduardo Vieira, Arlindo U. Netto, Auricelio B. Cezar Jr, Igor Faquini, Nivaldo S. Almeida, and Hildo R. C. Azevedo-Filho

14.1 Introduction

Intracranial aneurysms are abnormal dilations of the intracranial arteries, in which the layers of the vessel wall are affected by degenerative changes, leading to vascular dilation. This dilation can be focal (saccular aneurysms) or generalized (fusiform aneurysms). Eventually, probably due to inflammatory factors, there is a progressive weakening in a certain site of the aneurysm wall, leading to rupture and intracranial bleeding. Saccular aneurysms occur at branch points of intracranial arteries, usually on a curve of the artery, and its dome points in the direction that blood flow would go if there were no such curve.

Conventional intracranial aneurysms maintain a somewhat preserved histological structure. Although disorganized, the intima, media, and adventitial layers are present in most of the aneurysm, with the exception of the internal elastic lamina, which is characteristically ruptured. Such histological features are maintained, especially in the aneurysm neck, although inflammatory changes can lead to the disappearance of the layer organization and rupture at the aneurysm dome.

Some aneurysms, however, do not maintain this histological pattern, originating from non-branching sites, through gaps in the wall of an intracranial artery, without a defined neck [1, 2]. Such lesions do not maintain the characteristic layered histological organization of saccular aneurysms. Sometimes, the aneurysm lumen is separated from the subarachnoid space only by the adventitial layer. As expected, such aneurysms are very likely to cause intracranial hemorrhage due to the fragility of their walls. In addition, they constitute a real therapeutic challenge, since their thin walls can rupture during manipulation, whether exo or endovascular. Such

E. Vieira · A. U. Netto · A. B. CezarJr · I. Faquini · N. S. Almeida
H. R. C. Azevedo-Filho (✉)
Department of Neurological Surgery, Hospital Da Restauração, Recife, Brazil

C. Di Rocco (ed.), *Advances and Technical Standards in Neurosurgery*, Advances and Technical Standards in Neurosurgery 48,
https://doi.org/10.1007/978-3-031-36785-4_14

lesions can occur in several intracranial arteries, such as the anterior communicating artery, the middle cerebral artery or the vertebral artery [3–5], but they are more frequent in the internal carotid artery (ICA) and this will be the objective of our review.

14.2 Nomenclature

Histologically fragile aneurysms that occur in the ICA have been named in different ways: dorsal wall aneurysms, ventral wall aneurysms, superior wall aneurysms, dissecting aneurysms, blister-like aneurysms, among other terms. Although different nomenclatures have been used, they all refer to small, fragile, broad-based aneurysms without an identifiable neck, occurring at non-branching sites of the ICA. Such aneurysms can occur throughout the circumference of the ICA and it makes no sense to name them according to their location in the vessel wall

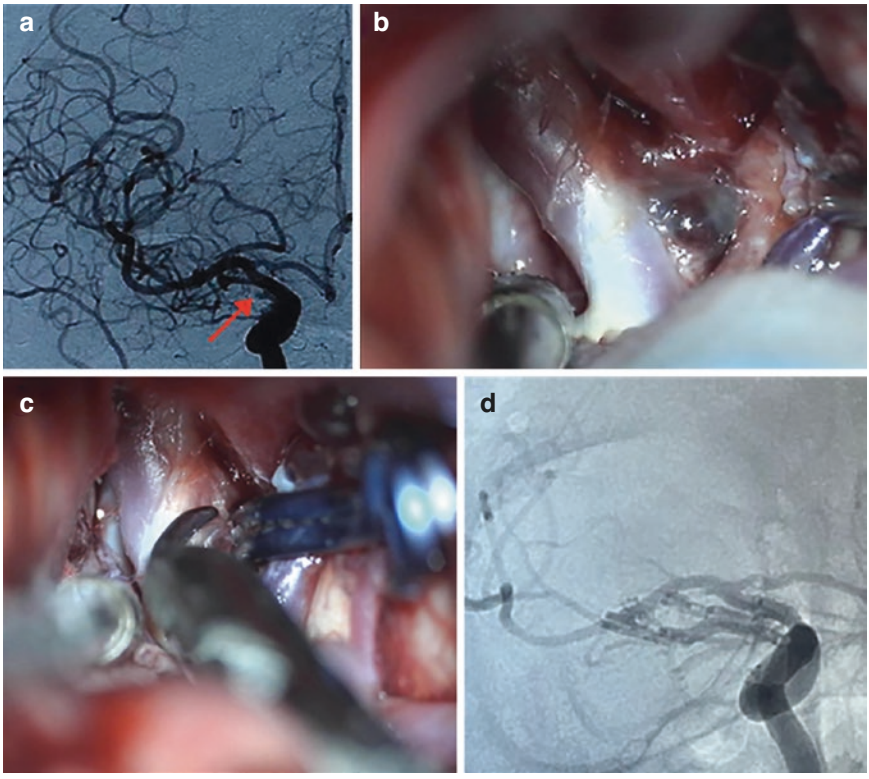

Fig. 14.1 (**a**) BBA arising from the lateral wall of the ICA (red arrow). (**b**) Intraoperative finding of a typical BBA. (**c**) The aneurysm was clipped incorporating a healthy portion of the artery wall in order to prevent IOR. (**d**) Post-operative DSA showing complete obliteration of the BBA

Table 14.1 Characteristics of BBA

Characteristics of blood blister-like aneurysms
Small
Broad-based
No identifiable neck
Non-branching site
Fragile and friable
High propensity for rebleeding and IOR

(Fig. 14.1). Therefore, we will refer to these lesions as blood blister-like aneurysms (BBA) of the ICA (Table 14.1).

14.3 Epidemiology

BBA are rare lesions. They represent 0.3–1% of all intracranial aneurysms, 0.5–2% of all ruptured intracranial aneurysms, and 0.9–6.5% of all ruptured ICA aneurysms. Given the low frequency of BBAs, it is impossible to know prevalence data. Studies suggest that these aneurysms occur in a younger population with a predilection to affect women [6–8].

14.4 Pathology

The intracranial arteries have three well-defined layers: intima, media, and adventitia. Separating the intima from the media is the internal elastic lamina. Histopathological analysis of BBAs reveal that such aneurysms arise from a rupture in the intima and media layers. The only layer separating the arterial lumen from the subarachnoid space is the adventitia [9]. When the aneurysm ruptures, which occurs in the vast majority of cases, the "dome" of the aneurysm is composed only of fibrin and fragments of the adventitia. Inflammatory infiltrates commonly observed in the wall of ruptured saccular aneurysms are not seen in BBAs. Likewise, dissection of the vessel wall leading to the formation of a false lumen is also not observed [10].

14.5 Pathogenesis

The pathogenesis of BBAs is still controversial. There appears to be a progressive rupture of the intima and media layers determined by hemodynamic stress in the carotid siphon, which can be facilitated by the presence of atherosclerotic lesions. The defect in the inner layers progresses until the arterial lumen reaches the adventitia (Fig. 14.2). At this stage, rapid rupture of the outermost layer can occur, leading

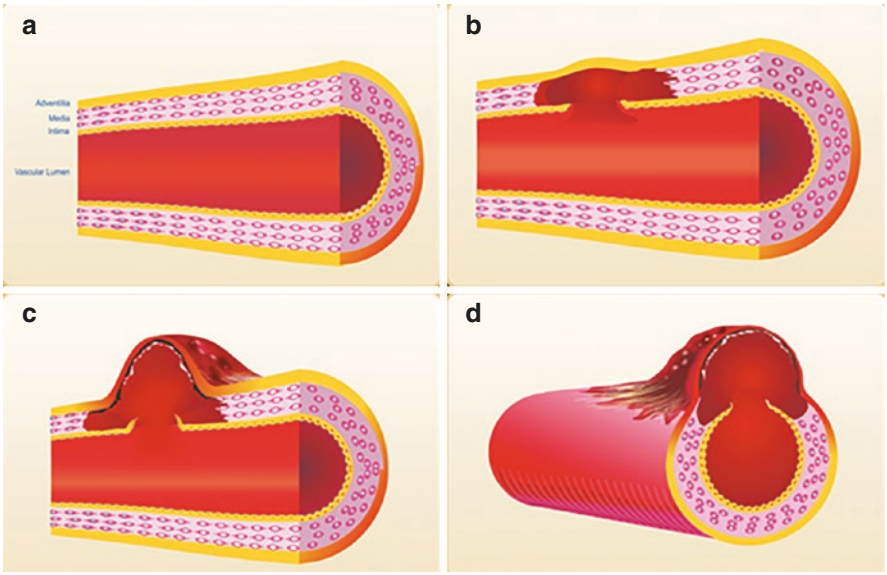

Fig. 14.2 (**a**) The normal arterial wall has three well-defined layers: intima, media, and adventitia. (**b**) BBA forms from a progressive rupture in the intima and media layers. (**c**, **d**) The arterial lumen reaches the adventitia which is the only structure

to subarachnoid hemorrhage (SAH). In such cases, initial digital subtraction angiography (DSA) may be negative. The defect in the ICA wall is tamponade by fibrin and adventitial fragments and if no new rupture and bleeding occurs, the lesion may grow until an equilibrium is reached. At this point, a second DSA might finally reveal the BBA. In some cases, however, there is no immediate rupture of the aneurysm and, during the formation process, the lesion can be diagnosed before rupture, usually incidentally during imaging studies performed for other reasons [10, 11].

The pathogenesis of BBAs may be associated with atherosclerotic disease in ICA and this may have therapeutic implications. When microsurgical treatment of BBAs is performed, the clipping of the BBA wall, composed basically of fibrin and adventitia, may lead to intraoperative rupture (IOR), with potentially catastrophic consequences, thus a healthy portion of the ICA wall must be incorporated into the clip blades (Fig. 14.3). In younger patients with healthy ICA, free from atherosclerosis, this can be achieved relatively easily. On the other hand, in older patients with atherosclerotic disease, clipping can lead to prohibitive ICA stenosis or, in some cases, precipitates IOR of the aneurysm and enlargement of the defect in the vessel wall. In these patients, aneurysms trapping and cerebral revascularization may be necessary [11].

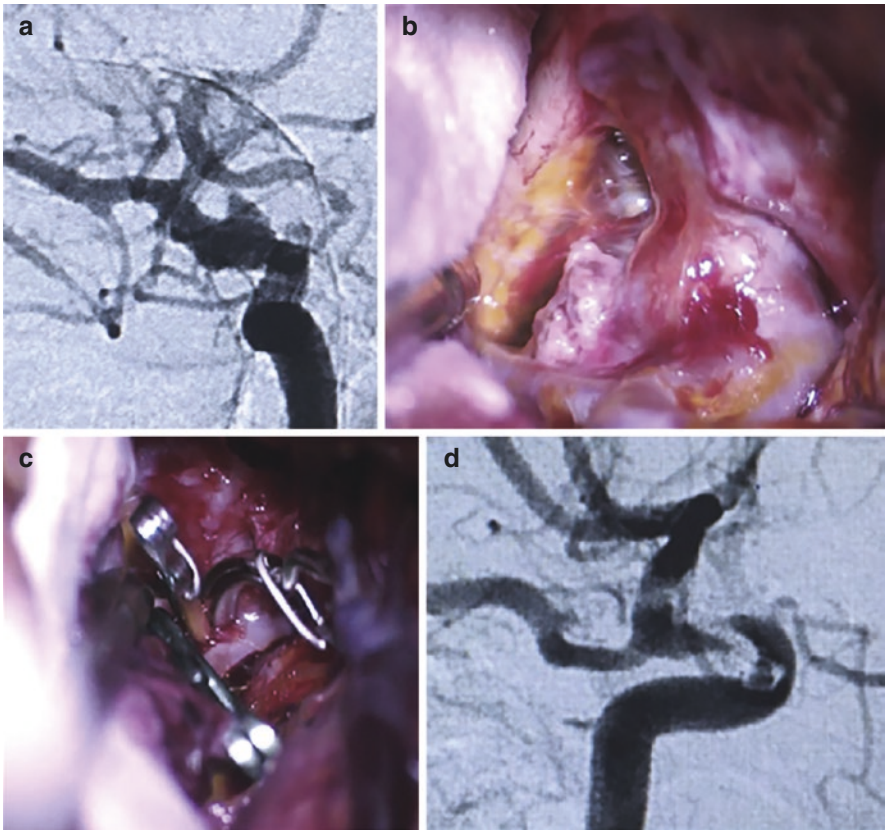

Fig. 14.3 This 34-years-old male patient presented with sudden onset headache and drowsiness due to SAH. (**a**) Preoperative DSA revealed a broad-based, non-branching site ICA dorsal wall aneurysm. (**b**) Intraoperatively, a typical BBA was visualized. Note the aneurysm "dome" is mainly composed of fibrin. (**c**) Multiples stacked clips were needed to reconstruct the ICA. (**d**) Postoperative DSA confirms complete occlusion of the BBA

14.6 Clinical Presentation

Most patients will present with SAH, with the typical symptom of sudden onset headache, associated or not with altered level of consciousness. BBAs are rarely diagnosed incidentally in imaging tests performed to investigate other diseases.

14.7 Diagnosis

Head computed tomography (CT) scan is performed to diagnose SAH and any associated conditions such as intracerebral hematomas or hydrocephalus. Unfortunately, CT brain angiography is of little use in diagnosing BBAs, due to its low sensitivity for diagnosing small aneurysms.

The gold-standard imaging study for the diagnosis of BBAs is the DSA, which reveals a small aneurysm with a broad base and no identifiable neck, originating from non-branching sites of the ICA trunk. It is important to emphasize that, due to the above-mentioned characteristics, BBAs are dynamic lesions, thus there may be a change in the radiological characteristics of the aneurysm between two DSAs (if a second exam is needed). A recent study has shown that aneurysms arising from non-branching sites of the ICA tend to be saccular when the ophthalmic artery (OA) has an anomalous origin. When the OA originates from its usual position, the diagnosis of a BBA is presumed [12]. It is important to emphasize that, in many cases, the definitive diagnosis of a BBA can only be established intraoperatively.

When a BBA is diagnosed, it is important to perform a balloon occlusion test (BOT) of the affected ICA. Once arterial occlusion may be necessary, the collateral circulation must be evaluated to define the need for an eventual cerebral revascularization procedure.

14.8 Treatment

The treatment of BBAs is a therapeutic challenge for both, neurosurgeons and neurointerventionists. Regardless of the method used to occlude the aneurysm, first of all it is important to stabilize the patient clinically. He or she must be admitted to the intensive care unit (ICU), adequate airway and hemodynamic support must be provided when necessary. In cases of hydrocephalus, an external ventricular drainage (EVD) should be installed, ideally associated with intracranial pressure monitoring system. Once the patient is stable, he should then be referred to the diagnostic center for DSA.

14.8.1 Endovascular Treatment

Since the early 2000s, several case series have been published describing the endovascular treatment of BBAs. Several techniques have been described, including: parent vessel occlusion, conventional embolization, balloon-assisted embolization, stent-assisted embolization, and flow diverter stenting (with or without embolization). Parent vessel occlusion with endovascular aneurysm trapping is a low-morbidity alternative in cases in which the patient has adequate collateral circulation

and tolerates ICA occlusion. Conventional embolization of BBAs is difficult not only because of the absence of a well-defined neck, but also because of the fragility of the aneurysmal dome. The simple introduction of coils into the aneurysm can precipitate its rupture.

In order to deal with the absence of a well-defined neck, strategies such as balloon-assisted or stent-assisted embolization can be used, but it is still necessary to place coils inside the aneurysm, which can lead to its rupture. When stents are used, antiplatelet medications are necessary, greatly increasing the chance of hemorrhagic complications in the acute phase after SAH. Currently, the most used endovascular method in the treatment of BBAs is flow diverter stenting, with better results when compared to other endovascular techniques. Even so, it is not a risk-free procedure and major complication rates (with neurological morbidity or mortality) have been described in up to 27% of cases. In addition, the necessity of antiplatelet therapy after flow diverter stenting may be a source of complications in aneurysms treated during the acute phase after SAH [13–15].

14.8.2 Microsurgical Treatment

Microsurgery is still the gold-standard treatment for BBAs [16]. As with endovascular treatment, several techniques have been described, such as: clipping, wrapping, clip-wrapping, direct suture, trapping without bypass, and trapping with bypass. Direct clipping is the most studied and used method. The ICA is reconstructed with clips applied to the base of the aneurysm, incorporating a small portion of the healthy ICA wall. In some cases, aneurysms are so small that clips cannot be applied. In addition, the application of clips to a healthy portion of the artery wall may lead to prohibitive stenosis of ICA. In such cases, the wrapping or clip-wrapping strategy can be used. Several materials can be used for this purpose, including: cotton, muscle, gauze, Teflon, fibrin glue, among others [17]. Such agents can be placed over the aneurysm (wrapping) or around and involving the ICA and kept in place by an aneurysm clip (clip-wrapping). The presence of exogenous material produces an inflammatory response followed by fibrosis and protects against rebleeding, although in a lesser magnitude when compared to conventional clipping [18]. In cases in which the wrapping or clip-wrapping technique is performed, the treatment should be complemented with flow diverter stenting 60–90 days after SAH [19]. Direct suturing of the ICA wall defect is one of the techniques described for the treatment of BBAs. It can be used for small defects in surgically accessible portions of the circumference of the ICA, as long as there is no significant atherosclerosis. Apart from these conditions, it is not a viable surgical technique.

BBA trapping can be performed as long as the origin of the anterior choroidal artery is not included between the clips. Likewise, in patients with a fetal posterior cerebral artery, the origin of the posterior communicating artery cannot be included in the trapped segment of the ICA. It is essential to perform an ICA BOT

preoperatively, in order to determine whether a cerebral revascularization procedure will be necessary or not. Trapping with bypass has been identified as the procedure with the best clinical results among all described microsurgical techniques for BBAs. It is essential that the surgeon is prepared to perform this procedure, regardless of the microsurgical technique initially planned. In case of any complication that requires trapping of the aneurysm and occlusion of the ICA, the revascularization procedure can, then, be performed.

14.9 Experience of the Hospital da Restauração

Between 2014 and 2021, 20 patients with BBAs underwent microsurgical treatment at the Hospital da Restauração (Recife/BRA). The mean age was 45.1 years, slightly below the age group at which there is a peak in the incidence of SAH due to saccular aneurysms (50–55 years-old), supporting literature data that indicate that BBA occurs in younger patients. Most patients were women and only one patient did not present with SAH. Among the patients who had SAH, the vast majority (90%) had favorable Hunt-Hess grade (< 3) and 90% had Fisher grade 3 or 4 SAH on admission CT. Most patients (85%) were treated in the acute phase after SAH (< 14 days

Table 14.2 Characteristics and outcomes of patients treated at the Hospital da Restauração over an 8-year period

Number	Age	Sex	Fisher	Hunt-Hess	Treatment	Complication	Outcome (mRS)
1	50	F	3	2	Clipping	–	2
2	61	M	3	1	Clipping	–	2
3	43	F	3	2	Clipping	–	2
4	51	F	3	3	Clipping	–	2
5	47	F	3	3	Clipping	–	1
6	54	M	3	3	Clip-wrap.	–	4
7	42	F	1	2	Clipping	–	2
8	38	M	3	1	Clipping	–	0
9	33	F	1	3	Clipping	Reop CR	2
10	48	F	3	2	Clipping	–	1
11	34	M	4	4	Clipping	–	3
12	40	F	4	2	Clipping	IOR	1
13	47	F	3	4	Clipping	–	4
14	24	M	4	2	Clipping	–	2
15	46	M	2	2	Clipping	–	1
16	67	F	4	3	Clipping	IOR	6
17	56	F	3	1	Clipping	Infection	1
18	31	F	3	3	Clipping	–	2
19	58	F	3	2	Clipping	–	1
20	32	F	0	0	Clipping	–	0

after bleeding). All patients underwent preoperative DSA for diagnosis of BBA (Table 14.2).

14.9.1 Microsurgical Technique

Most patients are approached through a pterional or lateral supraorbital craniotomy, depending on the patient's grade. Based on the characteristics and topography of the aneurysm, exposure of the cervical ICA through a cervicotomy is performed to obtain proximal control. After introducing the surgical microscope, a wide and meticulous dissection of the Sylvian fissure is performed. Fixed cerebral retractors are not used in our department. Instead, dynamic retraction using the suction cannula is our preferred method of brain retraction and is performed cautiously, especially when treating BBAs. It is extremely important to avoid frontal lobe retraction, which can precipitate IOR, due to the fact that BBAs in the dorsal wall of the ICA can be tamponade by the orbital gyri.

Once the Sylvian fissure is dissected, the aneurysm can be visualized and the diagnosis of BBA is confirmed by visual inspection. It is extremely important to obtain proximal and distal control. Distal control is relatively easy to obtain once ICA bifurcation is visualized. In order to obtain proximal control, removal of the anterior clinoid process or exposure of the cervical ICA may be necessary. We are very liberal regarding anterior clinoidectomy, a surgical maneuver that provides proximal control, space and maneuverability for applying clips to the aneurysm. Once vascular control is obtained, the aneurysm neck is gently and sharply dissected with microscissors, in order to prevent traction on the structures surrounding the aneurysm, which can precipitate IOR. After proper dissection of the neck, the clip is applied. It is important that the clipping is performed under temporary ICA occlusion, which makes the ICA walls more flaccid and reduces the risk of IOR. The clip must be applied longitudinally and it is extremely important to include a healthy portion of the ICA wall in the clip blades, which usually leads to a discrete and hemodynamically insignificant stenosis of the vessel. Once the aneurysm has been clipped, the flow in the ICA is checked with intraoperative micro-Doppler and closure is carried out. The patient is admitted to a dedicated ICU and a postoperative DSA is always performed to confirm aneurysm occlusion (Fig. 14.4).

Occasionally, the ICA wall defect can be large and conventional clipping may not be possible without prohibitive arterial stenosis. In these cases, the clip-wrapping technique can be performed, in which the ICA is circumferentially wrapped with cotton or gauze and a clip is applied parallel to the artery with discreet counterpressure to keep the wrap in place (Fig. 14.5). Another option in such cases is trapping the aneurysm with or without bypass, depending on preoperative BOT result.

The most feared complication in microsurgery for BBAs is IOR. In general, it can be prevented by avoiding cerebral retraction, clipping the aneurysm longitudinally, under temporary ICA occlusion and including a healthy portion of the artery wall in the blades of the clip. If despite these maneuvers an IOR happens, the

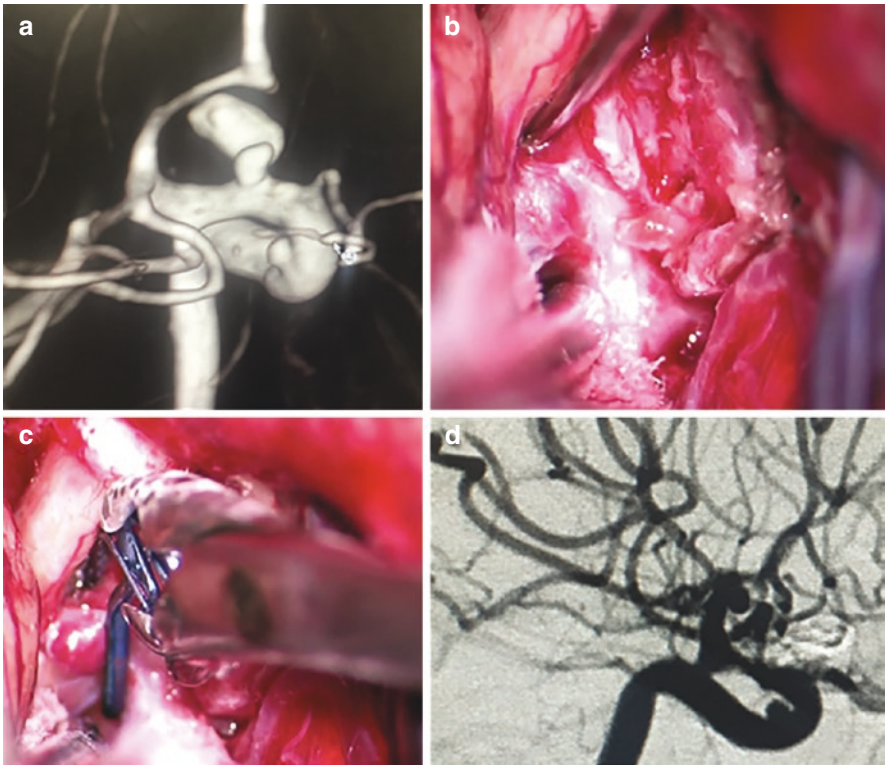

Fig. 14.4 This 48-years-old male patient presented with sudden onset headache and a Fisher grade 3 SAH. (**a**) Preoperative DSA revealed a typical BBA projecting superiorly. (**b** and **c**) The aneurysm is dissected and a side-angled clip is applied longitudinally, incorporating a small healthy portion of the ICA wall. (**d**) Postoperative DSA confirms complete occlusion of the BBA and a small, non-significant, ICA stenosis is observed

aneurysm should then be trapped and an attempt can be made to reconstruct the ICA wall with clips. If direct clipping is not possible, the BBA should be definitively trapped and a revascularization procedure performed. In patients with significant ICA atherosclerosis, it may be difficult to reconstruct the artery without leading to IOR. In fact, the probability of a revascularization procedure is high in such cases. In the microsurgical treatment of BBAs, one must always be ready to perform a bypass.

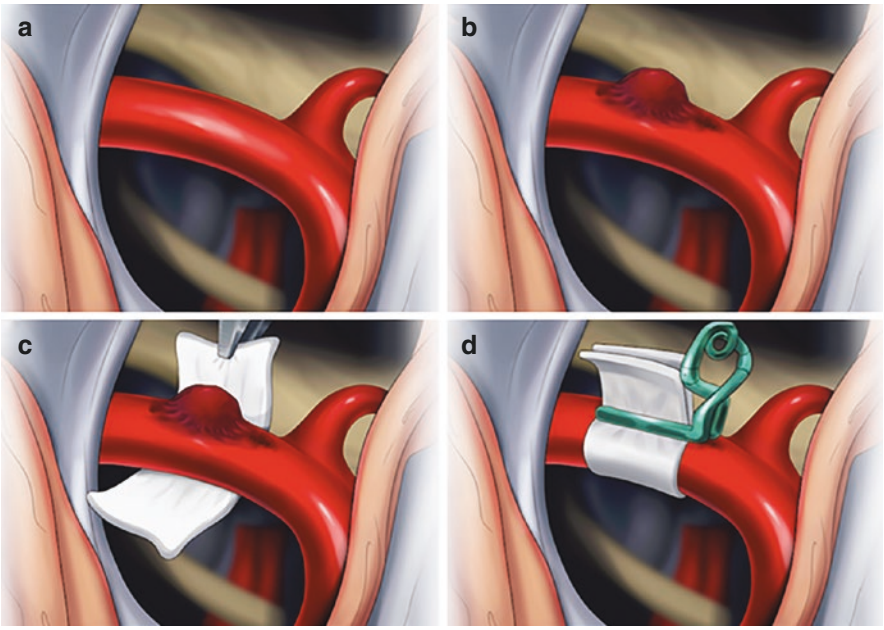

Fig. 14.5 The clip-wrapping technique. (**a**) Normal ICA. (**b**) BBA in the dorsal wall of ICA. (**c**) The ICA is circumferentially wrapped with cotton or gauze and (**d**) a clip is applied parallel to the artery with discreet counter-pressure to keep the wrap in place

Table 14.3 Summary of preoperative characteristics and post-operative clinical and radiological outcomes

Variable	Results
Age (mean)	45,1 years-old
Female sex	14 (70%)
Good grade (HH grade 1–3)	18 (90%)
Complications	4 (20%)
Major complications	1 (5%)
Good outcome (mRS 0–2)	17 (85%)
Mortality	1 (5%)
Complete occlusion	19 (95%)

14.9.2 Results

Direct clipping was performed in all cases, except in one patient, in which the clip-wrapping maneuver was performed. Overall, complications occurred in four cases (20%): IOR in two cases (10%), surgical wound infection in one case (5%) and reoperation for clip repositioning in one case (5%). In only one case, the complication resulted in permanent morbidity or mortality (major complications rate = 5%). Overall, 85% of patients had a favorable clinical outcome (mRS 0–2) and the mortality rate was 5% (1 patient). Postoperative DSA demonstrated complete occlusion

in 95% of cases and only one patient had a residual neck and required treatment complement with flow diverter stenting 60 days after SAH (Table 14.3).

14.10 Conclusion

BBAs are challenging lesions for both microsurgical and endovascular treatment. They are caused by acquired defects in the intima and media layers of the ICA, probably due to hemodynamic stress in the carotid siphon. Since the "dome" of the aneurysm is formed only by fragments of adventitia and fibrin, they are extremely friable lesions with great propensity for rebleeding and IOR. Diagnosis requires performing DSA and small aneurysms originating from non-branching points of the ICA should be considered BBAs until proven otherwise. Although challenging, microsurgical treatment is feasible provided it is performed with a meticulous technique (avoid brain retraction, apply the clip under temporary ICA occlusion, in the longitudinal axis of the artery and incorporating a small healthy portion of the artery wall in the clip blades). In our experience, it is possible to obtain good clinical results and high occlusion rates with direct clipping.

References

1. Nakagawa F, Kobayashi S, Takemae T, Sugita K. Aneurysms protruding from the dorsal wall of the internal carotid artery. J Neurosurg. 1986;65:303–8.
2. Sundt TM Jr. Murphey F: clip-grafts for aneurysm and small vessel surgery. Clinical experience in intracranial internal carotid artery aneurysms. J Neurosurg. 1969;31:59–71.
3. Andaluz N, Zuccarello M. Blister-like aneurysms of the anterior communicating artery: a retrospective review of diagnosis and treatment in five patients. Neurosurgery. 2008;62:807–11.; discussion 811,.
4. Peschillo S, Miscusi M, Caporlingua A, Cannizzaro D, Santoro A, Delfini R, et al. Blister-like aneurysms in atypical locations: a single-center experience and comprehensive literature review. World Neurosurg. 2015;84:1070–9.
5. Peschillo S, Missori P, Piano M, Cannizzaro D, Guidetti G, Santoro A, et al. Blister-like aneurysms of middle cerebral artery: a multicenter retrospective review of diagnosis and treatment in three patients. Neurosurg Rev. 2015;38:197–202. discussion 202–193.
6. Abe M, Tabuchi K, Yokoyama H, Uchino A. Blood blisterlike aneurysms of the internal carotid artery. J Neurosurg. 1998;89:419–24.
7. Meling TR, Sorteberg A, Bakke SJ, Slettebo H, Hernesniemi J, Sorteberg W. Blood blister-like aneurysms of the internal carotid artery trunk causing subarachnoid hemorrhage: treatment and outcome. J Neurosurg. 2008;108:662–71.
8. Ogawa A, Suzuki M, Ogasawara K. Aneurysms at nonbranching sites in the surpaclinoid portion of the internal carotid artery: internal carotid artery trunk aneurysms. Neurosurgery. 2000;47:578–83. discussion 583–576.
9. Ishikawa T, Nakamura N, Houkin K, Nomura M. Pathological consideration of a "blister-like" aneurysm at the superior wall of the internal carotid artery: case report. Neurosurgery. 1997;40:403–5. discussion 405–406.

10. Chen S, Chen X, Ning B, Cao Y, Wang S. Supraclinoid internal carotid artery blister-like aneurysms: hypothesized pathogenesis and microsurgical clipping outcomes. Chin Neurosurg J. 2021;7:10.
11. Zhai XD, Hu P, He C, Feng YS, Li GL, Zhang HQ. Current knowledge of and perspectives about the pathogenesis of blood blister-like aneurysms of the internal carotid artery: a review of the literature. Int J Med Sci. 2021;18:2017–22.
12. Indo M, Oya S, Tanaka M, Matsui T. High incidence of ICA anterior wall aneurysms in patients with an anomalous origin of the ophthalmic artery: possible relevance to the pathogenesis of aneurysm formation. J Neurosurg. 2014;120:93–8.
13. Rouchaud A, Brinjikji W, Cloft HJ, Kallmes DF. Endovascular treatment of ruptured blister-like aneurysms: a systematic review and meta-analysis with focus on deconstructive versus reconstructive and flow-diverter treatments. AJNR Am J Neuroradiol. 2015;36:2331–9.
14. Yoon JW, Siddiqui AH, Dumont TM, Levy EI, Hopkins LN, Lanzino G, et al. Feasibility and safety of pipeline embolization device in patients with ruptured carotid blister aneurysms. Neurosurgery. 2014;75:419–29. discussion 429.
15. Zhu D, Yan Y, Zhao P, Duan G, Zhao R, Liu J, et al. Safety and efficacy of flow diverter treatment for blood blister-like aneurysm: a systematic review and meta-analysis. World Neurosurg. 2018;118:e79–86.
16. Cezar-Junior AB, Viturino U. Vieira de Carvalho EJ, Faquini IV, Almeida NS, Azevedo-Filho HRC: blister aneurysms of the internal carotid artery: surgical treatment and management outcome from a single center experience. Clin Neurol Neurosurg. 2019;182:136–41.
17. Figueiredo EG, Foroni L, Monaco BA, Gomes MQ, Sterman Neto H, Teixeira MJ. The clip-wrap technique in the treatment of intracranial unclippable aneurysms. Arq Neuropsiquiatr. 2010;68:115–8.
18. Herrera O, Kawamura S, Yasui N, Yoshida Y. Histological changes in the rat common carotid artery induced by aneurysmal wrapping and coating materials. Neurol Med Chir (Tokyo). 1999;39:134–9. discussion 139–140.
19. Kalani MY, Zabramski JM, Kim LJ, Chowdhry SA, Mendes GA, Nakaji P, et al. Long-term follow-up of blister aneurysms of the internal carotid artery. Neurosurgery. 1033;73:1026. discussion 1033, 2013.

Chapter 15
Vascular Malformations of the Spinal Cord in Children

Feng Ling, Gao Zeng, and Yutong Liu

15.1 Spinal Cord Vascular Anatomy

Understanding vascular malformations of the spine and spinal cord, as well as the associated intravascular and surgical treatment, is inextricably linked to vascular anatomy. Also, the discussion of vascular anatomy has to start from embryonic development; otherwise, it will be clueless. The anatomy of blood vessels in this chapter is based on the hierarchy of vascular supply (i.e., "vascular trees") and the traces left by these vessels during the embryonic period.

The embryo forms more than 30 pairs of somatic segments between the fourth and fifth weeks, 31 pairs of which eventually develop into the spinal cord, and 31 pairs of segmental arteries branching from the dorsal aorta to supply the various levels of tissue of the corresponding somite. The development of all body organs is closely related to the body segments. All subsequent blood vessels that supply the spinal cord and the spine are derived from these pairs of arteries. The blood vessels derived later are named after the corresponding tissue. The traces they leave behind during the developmental evolution process are significantly vital for interventional therapy.

We will discuss the blood vessels supplying the spinal cord and spine from the outer to the inner layers of the trunk, adding contents of embryonic generation to help the reader better understand the anatomy of the blood vessels.

F. Ling · G. Zeng (✉) · Y. Liu
Department of Neurosurgery, Xuanwu Hospital Capital Medical University, Beijing, China

China International Neuroscience Institute (China-INI), Beijing, China

Di Rocco Center of Pediatric Neurosurgery, Department of Neurosurgery, Xuanwu Hospital Capital Medical University, Beijing, China

C. Di Rocco (ed.), *Advances and Technical Standards in Neurosurgery*, Advances and Technical Standards in Neurosurgery 48,
https://doi.org/10.1007/978-3-031-36785-4_15

15.1.1 Segmental Arteries

During the embryonic period, all 31 pairs of segmental arteries supply tissues of the corresponding segments uniformly and symmetrically. These tissues include skin, muscle, bone, meninges, nerve roots, and the spinal cord. The intervertebral foramen is where the branches originate from segmental arteries, supplying the structures within the spinal canal. Segmental arteries are vascular units of tissues found throughout the segment of the vertebral body (Fig. 15.1).

However, as embryonic structures differentiate, the arterial supply of tissues in different parts of the segment has been remodeled or degenerated with different emphases. Some mainly branched into the anterior and posterior spinal arteries, and some only supply structures such as the vertebral body, nerve roots, and dura mater. Under normal circumstances, these arteries are difficult to see in angiography. However, in some spinal cord vascular malformations or some neoplastic lesions with rich blood supply, these rarely seen branches are unusually prominent. For example, when there is a vertebral hemangioma, the branches from the segmental artery supplying the vertebral body become very pronounced, and segmental arteries feeding spinal arteriovenous malformations may emit large anterior or posterior spinal arteries.

After these segmental arteries mature, they are named after the new tissue they supply, and the tissues may all be related to the spinal cord. The blood vessels highlighted with orange in Fig. 15.1 are the key arteries that supply the spinal cord, and their path and morphology must be recognized during angiography to avoid injury.

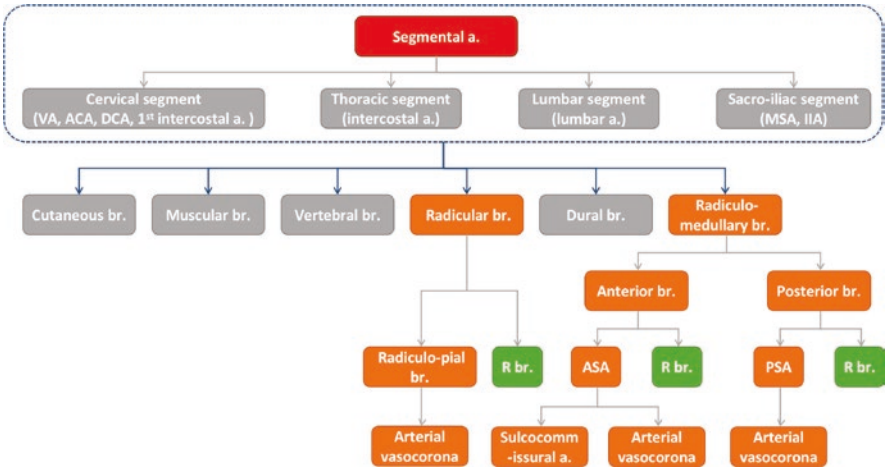

Fig. 15.1 Branches of the segmental artery. Arteries highlighted with orange are key arteries that supply the spinal cord. *a* artery, *ACA* ascending cervical artery, *ASA* anterior spinal artery, *br* branch, *DCA* deep cervical artery, *IIA* internal iliac artery, *MSA* median sacral artery, *PSA* posterior spinal artery, *R* root, *VA* vertebral artery

Based on the names given to the blood vessels after maturation, this section will divide those arteries into three groups and describe them from rostral to caudal.

The first group is the cervical segment (Fig.15.2). It consists of the vertebral artery, ascending cervical artery (branch of the thyrocervical trunk), deep cervical artery, and the first intercostal artery (branch of the costocervical trunk).

From the anatomical point of view, these blood vessels all originate from the subclavian artery (SCA). The left SCA branched directly from the aortic arch and is slightly longer than the right SCA, which is the branch of the innominate artery. The main branches of SCA from medial to lateral are the vertebral artery, internal thoracic artery, thyrocervical trunk, costocervical trunk, etc. All participate in the blood supply of the spinal cord except the internal thoracic artery. The vertebral artery, thyrocervical trunk, and costocervical trunk should not be overlooked when performing spinal vascular angiography.

The second group is the thoracic and lumbar segments. It mainly includes intercostal arteries and lumbar arteries.

The thoracic aorta gives rise to approximately 7–11 pairs of intercostal arteries. When compared to the right intercostal artery, which arises from the posterolateral wall of aorta, the left intercostal artery primarily emerges from the midline of the aorta's posterior wall. Since the aortic arch is at the fourth thoracic (T4) vertebral body level, the T2–4 intercostal arteries can be superselected at the T5 vertebral body level during selective angiography. Because of the proximity, multiple or double vessels are frequently visible simultaneously. The supreme intercostal artery can arise from the aortic arch. Bronchial, esophageal, and diaphragm arteries are frequently injected during intercostal artery angiography. When doing interventional treatment for lesions at the thoracic segment, it is sometimes necessary to obtain a

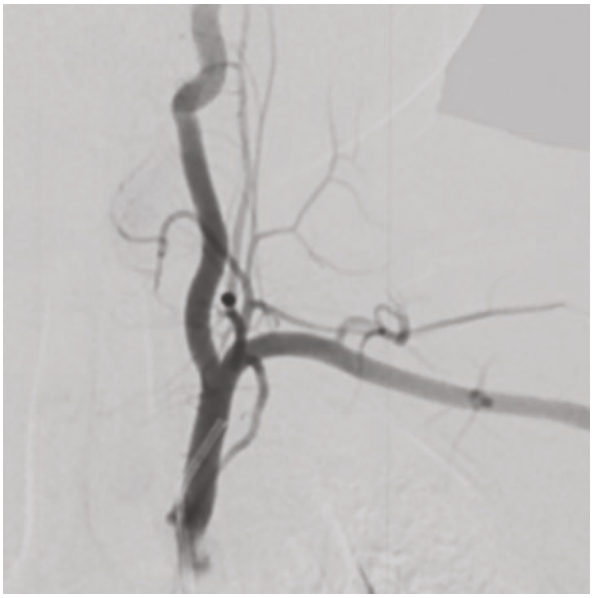

Fig. 15.2 Subclavian artery angiography of a 3-year-old girl (antero-posterior projection). The position of the vertebral artery, thyrocervical trunk, and costocervical is shown

better view by general anesthesia and temporarily turn off the ventilator. Figure 15.3 shows the results of the intercostal artery angiography.

Mostly there are 4 pairs of lumbar arteries. The left ones begin at the posterolateral and posterior median walls of the abdominal aorta, while the right ones begin at the right posterolateral wall. The two lumbar arteries that run parallel to each other are about one vertebral body apart.

The third group includes the middle sacral artery, the iliolumbar artery, and the lateral sacral artery from the internal iliac artery.

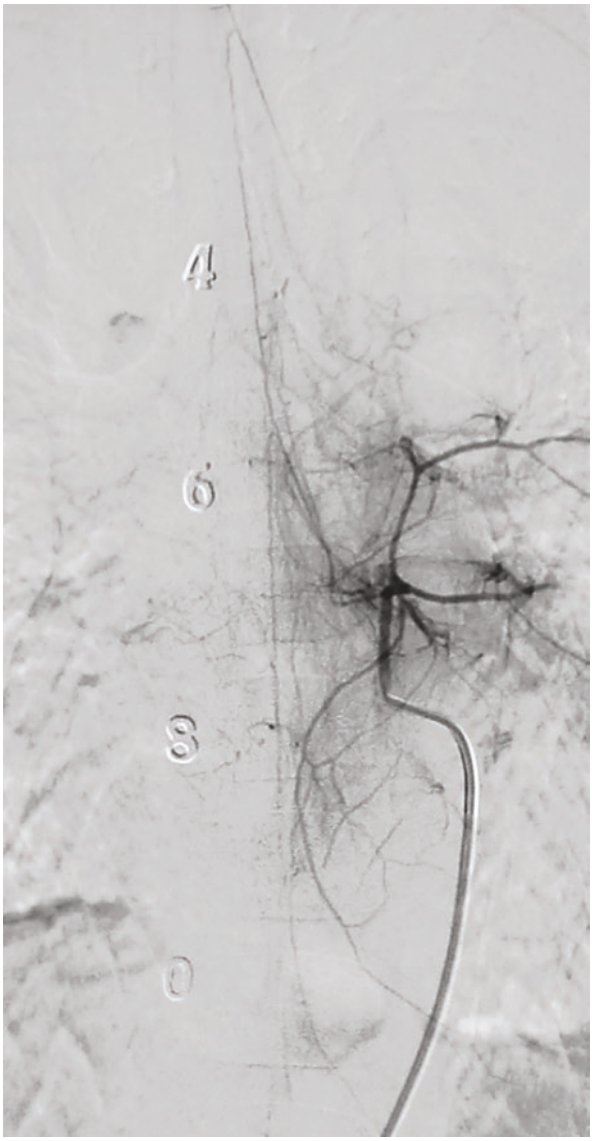

Fig. 15.3 Thoracic intercostal artery angiography of a 15-year-old boy (antero-posterior projection). ASA main trunk is on display. By antegrade or retrograde contrast agent flow, it is demonstrated that numerous radiculomedullary arteries join the main trunk of the ASA. The vertebral body and paravertebral tissues in normal dye are also displayed. *ASA*, anterior spinal artery

After the maturation of all these segmental blood vessels, most of the arteries that supply the spinal cord degenerate. Only 6–8 anterior radiculomedullary arteries and 10–23 posterior radiculomedullary arteries remain. The originating place is extensive and non-constant.

Special note: All segmental arteries must be superselected during diagnostic spinal angiography. Especially for lesions of the cervical, upper thoracic segment, and cone, do not forget the injection of the subclavian artery and internal iliac artery.

15.1.2 Spinal Dural Artery

Every segment artery gives rise to the dural artery, which forms an antero-posterior anastomosis along the nerve root cuff at the intervertebral foramen. The anastomosis of the dural arteries is extremely abundant (Fig. 15.4). In clinical work, the dural artery of any segment may become the feeding artery of spinal dural arteriovenous fistula (SDAVF), and if the glue N-butyl cyanoacrylate (NBCA) does not reach the proximal end of the draining vein through the fistula, the dural artery will soon resupply the fistula through this rich anastomosis and lead to the recurrence of SDAVF.

Special note: The spinal dural artery has a very rich vascular anastomosis, which is the anatomical basis for the recurrence of the spinal dural arteriovenous fistula.

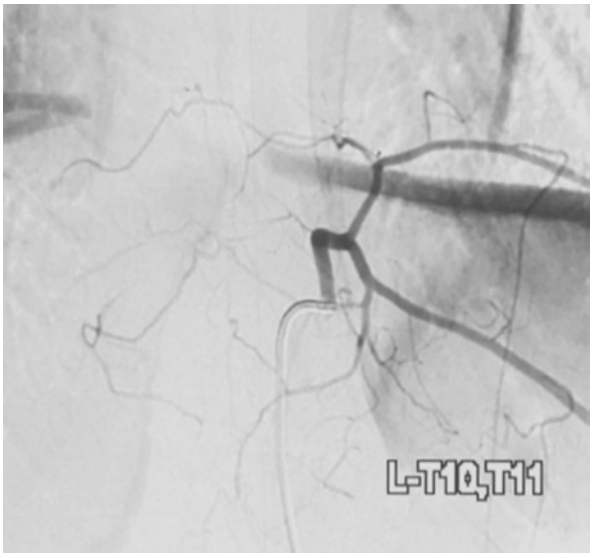

Fig. 15.4 Thoracic spinal angiography of a 12-year-old girl (antero-posterior projection). Note the characteristic "hexagonal" spinal dural arterial anastomosis

15.1.3 Nerve Root Arteries

Each segmental artery from the embryonic stage has branches that supply nerve roots (except that C1 roots are supplied by the occipital artery or the meningeal branch of the extracranial segment of a vertebral artery). However, they are very small and difficult to detect on angiography. The ASA also has small branches that laterally lead from the spinal cord to the nerve roots. The typical "hairpin-like" structure can only be seen during angiography when the radiculomedullary artery is produced concurrently (Fig. 15.3).

Special note: Nerve roots receive multiple blood supplies including root arteries, radiculo-pial arteries, radiculomedullary arteries, and spinal arteries.

15.1.4 Radiculo-pial Artery

The radiculo-pial artery is important for interventional therapy. These vessels travel along the nerve roots to the surface of the spinal cord, where they supply the pial mater's coronary vessel network but do not penetrate deep into the spinal cord to anastomose the anterior median vessel axis of the spinal cord. These arteries are the feeding arteries for many spinal arteriovenous malformations. Embolization via these arteries by superselection is much safer than via ASA. Radiculo-pial artery is mainly involved in the formation of bilateral posterolateral axes. It is also known as the posterior radiculomedullary artery when there is a distinct "hairpin-like" structure.

Special note: The most ideal path for embolization of spinal arteriovenous malformations is the radiculo-pial artery.

15.1.5 Radiculomedullary Artery

The radiculomedullary artery is the main vessel that supplies the spinal cord. After maturation, most of the 31 pairs of radiculomedullary branches degenerate, leaving only 6–8 anterior radiculomedullary arteries and 10–23 posterior radiculomedullary arteries.

The radiculomedullary artery appears as a typical "hairpin-like" pattern on angiography film, with the radiculomedullary section ascending obliquely, and the subsequent branches that turn upwards and downwards are known as anterior spinal arteries (ASA) or the anterior median axis of the spinal cord (Figs. 15.3 and 15.5). From the starting point of radiculomedullary arteries to the injection point toward ASA/PSA, the radiculomedullary arteries give small branches to supply the corresponding nerve roots and sometimes participate in the blood supply of the coronary vessel network of the pial mater. The radiculomedullary arteries that supply the

Fig. 15.5 Selective angiography of right T8 intercostal artery of a 12-year-old boy with Cobb's syndrome. The right anterior and posterior radiculomedullary arteries originate from the T8 intercostal artery and join the ASA and PSA main axes. Note the medial-lateral position of ASA and PSA. A white arrow marks the "basket-like" anastomosis at conus medullaris

cervical and lumbar enlargement of the spinal cord are particularly important. The latter ones are also known as the Adamkiewicz artery (AKA).

Special note: The obliquely ascending section of the "hairpin-like" vessel is called the radiculomedullary artery, and the subsequent branches that turn upwards and downwards are called anterior/posterior spinal arteries or the anterior median axis of the spinal cord.

15.1.6 Spinal Cord Arteries

Blood supply to the spinal cord comes from three consecutive longitudinal axes: one anterior to the spinal cord is the anterior median axis (or ASA), the latter two are the posterior lateral axis (or PSA), and several transverse axes (also known as coronary anastomosis). Blood of the top of the anterior median axis comes from the branches of the bilateral vertebral arteries before merging into the basal artery (Fig. 15.6). The branches converge to form a Y-shape structure and run downwards within the anterior median fissure all through the entire length of the spinal cord to the cone. It is joined in turn by each ascending branch of the ASA originating from the anterior radiculomedullary artery at each segment.

Angiography could reveal a typical "hairpin-like" structure. The upward slope angle of the anterior radiculomedullary artery is larger than that of the posterior radiculomedullary artery (Fig. 15.5). The descending branch of the ASA is larger than the rising branch, located in the middle of the spinal canal. It is generally straight, except for the slightly corrugated morphology at the cervical and lumbar enlargement. The lateral projection film shows that ASA is located against the posterior edge of the vertebral body, with a gap of less than 2 mm. The narrowest section of the anterior longitudinal axis is in the mid-thoracic segment, and sometimes

Fig. 15.6 Normal selective angiography of right VA of a 7-year-old girl. ASA originates from the VA. *VA*, vertebral artery

it seems that the axis is not continuous on the film. As long as the longitudinal axis remains intact, even if one of the anterior radiculomedullary arteries is cut or ligated, it will not affect the function of the spinal cord.

The PSAs originate from bilateral vertebral arteries and travel down in the left and right posterolateral sulcus of the spinal cord. They are joined by the ascending and descending branches from the radiculomedullary arteries of different segments and are also anastomosed to the coronary vascular network. The PSAs can form two posterolateral longitudinal axes but are less complete than the anterior median axis. There can also be a "hairpin-like" structure, but its angle is very small, and even the two sides can be close to each other. The lateral projection shows that there is a distance of about 10–13 mm between PSAs and the posterior edge of the vertebral body.

Special note: Although the anterior median axis receives blood from different segments, its longitudinal axis can have a full-length continuous arterial supply to the spinal cord. As long as the longitudinal axis remains intact, even if one of the anterior radiculomedullary arteries is cut or ligated, it will not affect the function of the spinal cord.

15.1.7 Arterial Anastomosis of the Spinal Cord

Humans create good compensatory and reserve functions for themselves during development. In addition to the three main longitudinal axes to supply the spinal cord, there is also an axial vascular network to build good up–down and left–right connections. The arterial anastomosis between the PSAs is relatively large, and it is also common to see the arterial bridges connect the double trunk of ASA in the cervical region.

The radiculomedullary branches, spinal arteries, and radiculo-pial arteries are all involved in the blood supply of the coronary vessel network. This multi-source, multi-anastomosis mesh structure can help us identify safe routes for interventional treatment and predict future spinal cord functional recovery when performing diagnostic angiography (Fig. 15.7).

There are some important branches or anastomosis that need to be kept in mind:

15.1.7.1 Lateral Spinal Artery

The lateral spinal artery is a branch of the vertebral artery or posterior inferior cerebellar artery (PICA) with low origination. It crosses the dura mater at the first cervical (C1) level to supply the posterolateral side of the spinal cord [1]. The artery may also be the starting point of the posterolateral axis of the spinal cord. All arteries supplying this area could be the feeding artery of arteriovenous fistulas in the occipital foramen area, including the spinal artery, lateral spinal artery, radiculo-pial

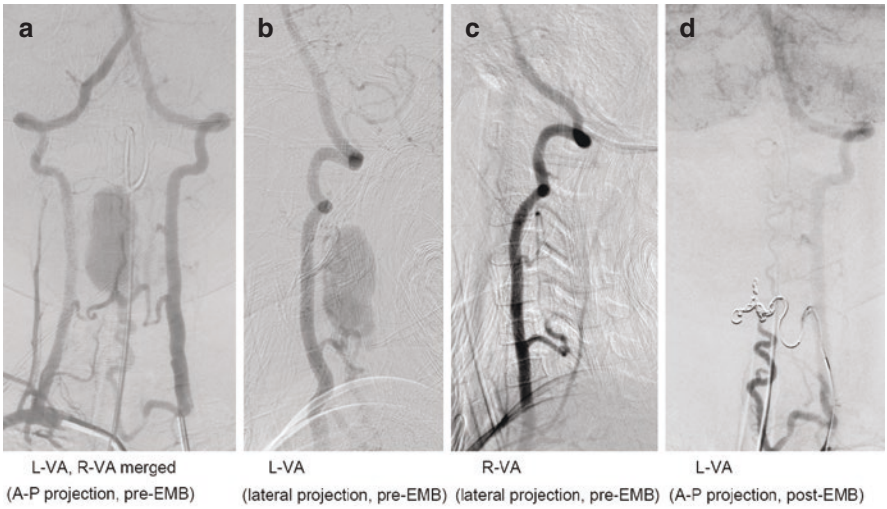

Fig. 15.7 Cervical perimedullary arteriovenous fistula of a 2-year-old girl. (**a**, **b**, **c**) The double trunk of ASA (black arrow) could be viewed. The orifice of the fistula is located at the lower edge of the venous pouch. (**d**) Selective injection of left VA after embolization by coils. The right trunk of ASA is embolized, and the main trunk and left trunk of ASA are intact. After 8-year's follow-up, the modified Ashworth Scale of the girl is 0, meaning that there is no spinal cord-related symptom. *A-P* anterior-posterior, *EMB* embolization, *L* left, *R* right

artery, or even the dural branch of an external carotid artery supplying the posterior fossa. It is important to distinguish the various blood vessels during angiography to choose a safe path for interventional treatment.

15.1.7.2 Basket Anastomosis

The three longitudinal axes of the spinal cord form a basket-like anastomosis net at 1.5 cm below the conus medullaris. It is most easily visualized during ASA injection (Fig. 15.5).

15.1.8 Regional Blood Supply and Compensatory Circulation of the Spinal Cord

According to the characteristics of the blood supply to the spinal cord, it can be divided into three areas.

15.1.8.1 Cervical Area

This area includes the full-length cervical spinal cord and the upper two thoracic segments. It is fed by about 2–4 branches of anterior radiculomedullary arteries: the first branch originates from the vertebral artery and accompanies the C3 nerve root; there is a commonly appeared branch from the deep cervical artery called artery of cervical enlargement, which accompanies the C6 nerve root; the first intercostal artery often originates a branch that accompanies the C8 nerve root. When these radiculomedullary arteries pass through the dura mater at the intervertebral foramen, they travel a short distance and a small slope, with an angle of about 60–80 degrees to the ASA. The spinal cord of these areas is also fed by 3–4 branches of the posterior radiculomedullary arteries.

Therefore, the cervical spinal cord possesses the most abundant blood supply. If the subclavian artery or vertebral artery is occluded, the upper third of cervical spinal cord can be inversely fed by the atlantoaxial anastomosis, which is formed by muscular branch of vertebral artery, the muscular branch of deep cervical artery, the ascending cervical artery, the occipital artery, and PICA. The blood supply of the lower third comes from the superior and inferior thyroid arteries, deep cervical artery, and internal thoracic artery.

15.1.8.2 Middle Thoracic Area

It includes the spinal cord of the upper 7 thoracic segments. There is only one anterior radiculomedullary artery in this segment, which accompanies any one of the thoracic nerve roots among T4–T7. However, the length of the thoracic spinal cord is twice as much as the cervical and lumbar segments, so this area is the worst in blood supply, and sometimes the anterior longitudinal axis of the spinal cord can even be discontinuous. This area is called the “danger zone.”

15.1.8.3 Thoracolumbar Area

It includes the spinal cord from T8 to conus medullaris. The Adamkiewicz artery is the main artery supplying the ASA. There are several posterior radiculomedullary arteries as well. The terminal filament is always accompanied by 1–2 radiculomedullary branches from lumbar arteries, iliolumbar arteries, or lateral sacral arteries. Once the Adamkiewicz artery is occluded, the “basket-like” anastomosis could connect the anterior and posterior axes of the spinal cord to compensate for the blood deficiency (Fig. 15.5).

Special note: The cervical and lumbar enlargement region possess the most abundant blood supply of the spinal cord, while the middle thoracic area has the worst.

15.1.9 Intra-spinal Cord Blood Supply

The distribution of the intramedullary arteries is relatively constant. It is divided into two sections: central and peripheral. The central branches are sulcal commissural arteries that originate from ASA at the anterior median fissure. The sulcal commissural arteries either penetrate the pial mater and enter the spinal cord directly or enter the spinal cord after ascending a little way. Central branches supply the anterior two-thirds of the spinal cord, mainly including the anterior horn and the middle part of the gray matter, and the reticular structure around the gray matter. The peripheral branches are located around the spinal cord. They are the centripetal branches that arise from the coronary arterial plexus formed by ASA, PSAs, and other arteries. These branches supply the white matter and posterior horn of the spinal cord.

The intramedullary arteries are terminal arteries with anastomosis only at the capillary level. There is an overlap of the blood supply region between sulcal commissural arteries and between peripheral branches and central branches. Blood vessels in the spinal cord anastomose not only antero-posteriorly but also longitudinally. Anastomosis is abundant, especially in the thoracic segments.

ASA is the artery that directly supplies the spinal cord. The occlusion of this artery can lead to ischemic necrosis of the anterior horn cells of the spinal cord. The patient would present complete flaccid paralysis of bilateral lower extremities, that is, anterior spinal artery syndrome. It can occur in both adults and children, especially common in children. The reason is still unknown. The diameter of the sulcal commissural artery is between 50 and 250 μm. If the surgeon chooses to embolize through ASA with particles, the diameter of the particles should not be less than 250 μm; otherwise, the particles will directly enter the sulcal commissural arteries through ASA, resulting in occlusion of most of the sulcal commissural arteries. The patient will present similar anterior spinal artery syndrome, which is extremely serious. Angiography will show that the ASA is patent at this time, but the patient's paralysis of bilateral lower limbs will be difficult to recover.

The table below shows the number and diameter of arteries in the spinal cord (Table 15.1)

15.1.10 Venous Drainage of the Spinal Cord

The anatomical study of the spinal venous system has received more and more attention in the past 50 years. People became very interested in the spinal venous system after Kendall [2] and Merland [3] discovered the phenomenon of spinal dural arteriovenous fistula (SDAVF) draining to the surface of the spinal cord, which corrected the diagnosis of the so-called extramedullary vascular malformations. In clinical work, it has also been found that many patients' symptoms are related to intravenous drainage. For example, if the drainage of the lesion is poor, or the lesion

Table 15.1 Arterial supply of spinal cord

	Cervical segment	Upper two-third of thoracic segment	Lower one-third of thoracic segment	Lumbosacral segment
Sulcal commissural artery (total 200–240 branches)	60–80 branches, 100–200 μm in diameter, 3–10 branches per cm	70–100 branches, 80–200 μm in diameter for ascending branches at sulcus, 1–3 branches per cm, supplying 15–20% of parenchyma		80–100 branches, 250 μm in diameter, 6–8 branches/cm, supplying 30–50% of parenchyma
Peripheral branches of coronary network	50 μm in diameter of perforating branches	(1) Perforating branches (2) Longitudinal anastomosis	–	Diameter 60 μm for perforating branches
Intra-spinal cord branches	Horizontal	Ascending and descending	–	Horizontal

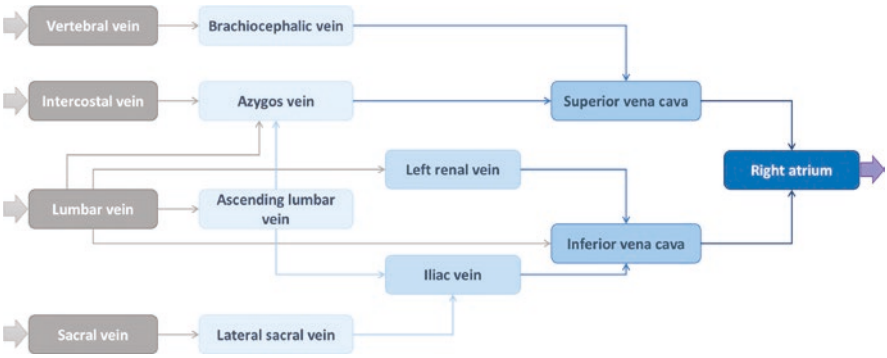

Fig. 15.8 Extra-spinal canal venous draining routes [1]

causes venous hypertension of the normal spinal cord, the patient would present spinal cord-related symptoms. Acute thrombosis of draining veins can also cause acute exacerbation of patients' symptoms. MRI provides us with a platform to study spinal veins. However, it is difficult for the veins to present well on spinal angiography. As a result, it is critical to learn the anatomical knowledge of predecessors to strengthen one's understanding of the venous system.

The drainage routes of the veins are intramedullary capillaries → intramedullary veins→ perimedullary veins → radicular veins → intra-spinal canal venous plexus → extra-spinal canal venous plexuses.

The extra-spinal canal venous plexus drains in different directions in different segments (Fig. 15.8).

15.2 Classification of Pediatric Spinal Vascular Malformations

Correct and full understanding of the etiology, anatomy, and pathophysiology of the disease is the premise of standardizing scientific disease classification. Because of their rarity and complexity, spinal vascular malformations have been the subject of extensive research.

The earliest classification of spinal vascular malformations was in the 1940s, and it divided the disease into venous type (description similar to spinal cavernous hemangioma) and arteriovenous type (description similar to SAVM and PMAVF). Since the end of the 1960s, due to the application of selective spinal angiography technology, people have deepened their understanding of spinal vascular malformations and have continuously tried to classify this disease from the aspects of vascular construction, disease course, and clinical manifestations. In 1977–1980, a team of Kendall and Logue [2] and Merland [3] classified the lesions according to the relative location to the spinal dura mater. In 1987, Rosenblum [4] separated fistula from malformation. In 1992, two major taxonomic factions emerged: the Merland [5] and the team of Berenstein and Lasjaunias's [6] classification focused on spinal vascular imaging and endovascular treatment, while Anson and Spetzler's [7] classification focused on the surgical approach. Merland's classification divided the disease into simple and complex categories. According to regional anatomy, the former was further divided into intramedullary, perimedullary, dural, vertebral, and paravertebral conditions. The latter included metameric disease. Berenstein and Lasjaunias's classification divided the spinal vascular malformations into two categories: the spine, including paravertebral, epidural, and dural lesions, and the spinal cord, including all subdural lesions and metameric lesions. Anson and Spetzler proposed a four-class taxonomy that focused on surgical treatment (Table 15.2). Although many academics still use this taxonomy in their publications, it has a lot of flaws. For example, it only covered dural and subdural lesions and ignored the substantial differences in the nature and location of lesions between different diseases. Since then, Spetzler's team [8] and the Lasjaunia's team [9] have proposed new classifications based on their former ones, focusing on surgical treatment and disease occurrence, respectively. However, these classifications have not been widely used, and the practicality has not been looked into.

In 1997, our center has proposed to classify spinal vascular malformations into intramedullary AVMS, intradural AVFs, dural AVFs, paravertebral AVMs, and Cobb's syndrome [10]. Our clinical experience has shown that this classification,

Table 15.2 Anson-Spetzler classification of spinal vascular malformation

Type I	Dural (intradural or extradural) AVF
Type II	Glomus AVMs
Type III	Juvenile AVMs
Type IV	Direct spinal AVF

which assigns AVM to intramedullary lesions and AVF to paravertebral lesions, is deficient. Therefore, based on the previous classification and literature, after 36 years of clinical work on more than 3000 patients with spinal vascular malformations of various ages, our center proposes a new classification of spinal vascular malformations:

I. Subdural lesions
    1. Cavernous malformation (CM)
    2. Telangiectasia
    3. Spinal arteriovenous malformation (SAVM)
       (i) Perimedullary, (ii) intramedullary, (iii) peri- and intramedullary
    4. Spinal arteriovenous fistula (SAVF)
       (i) Perimedullary, (ii) filum terminalis, (iii) nerve root
    5. Aneurysm
II. Spinal dural arteriovenous fistula (SDAVF)
III. Intrathecal epidural lesions
    1. Cavernous malformation
    2. Arteriovenous malformation
IV. Extrathecal
    1. Paravertebral arteriovenous malformation (PVAVM)
    2. Paravertebral arteriovenous fistula (PVAVF)
V. Vertebral angioma
VI. Metameric angiomatosis

The overall incidence of pediatric spinal vascular malformations is low. The proportion of pediatric patients of all ages varies greatly between different reports, which may be related to the diagnosis and age distribution of the cohort. Our center has 10% of its cases from children under the age of 18.

The incidence of each subtype of spinal vascular malformations in children is quite different from that in adults. For example, SDAVF, which accounts for 40% of the overall population, is extremely rare in children. In some reports, the child was diagnosed with SDAVF; however, after reviewing the angiography with multiple experienced doctors in our center, it was determined that the orifice of the fistula is not at the dura mater, and the diagnosis should be paravertebral fistula or perimedullary fistula. Another example is the spinal metameric AVM. It only accounts for less than 10% of the adult cases but exceeds 30% of the pediatric cases in our center. Figure 15.9 shows the proportion of pediatric patients of various spinal vascular malformation subtypes at our center till the end of 2019.

Intradural spinal arteriovenous shunts include arteriovenous malformation and arteriovenous fistula. The core of the spinal arteriovenous malformation, the so-called malformed vascular lesion, can be located anywhere in the spinal cord. There is usually a connective tissue boundary between the lesion and the spinal cord tissue. The mass pushes and squeezes the surrounding spinal cord. The feeding arteries and draining veins can run on the spinal cord's surface or penetrate and pass through the medulla. In a few cases, lesions are scattered and intertwined with

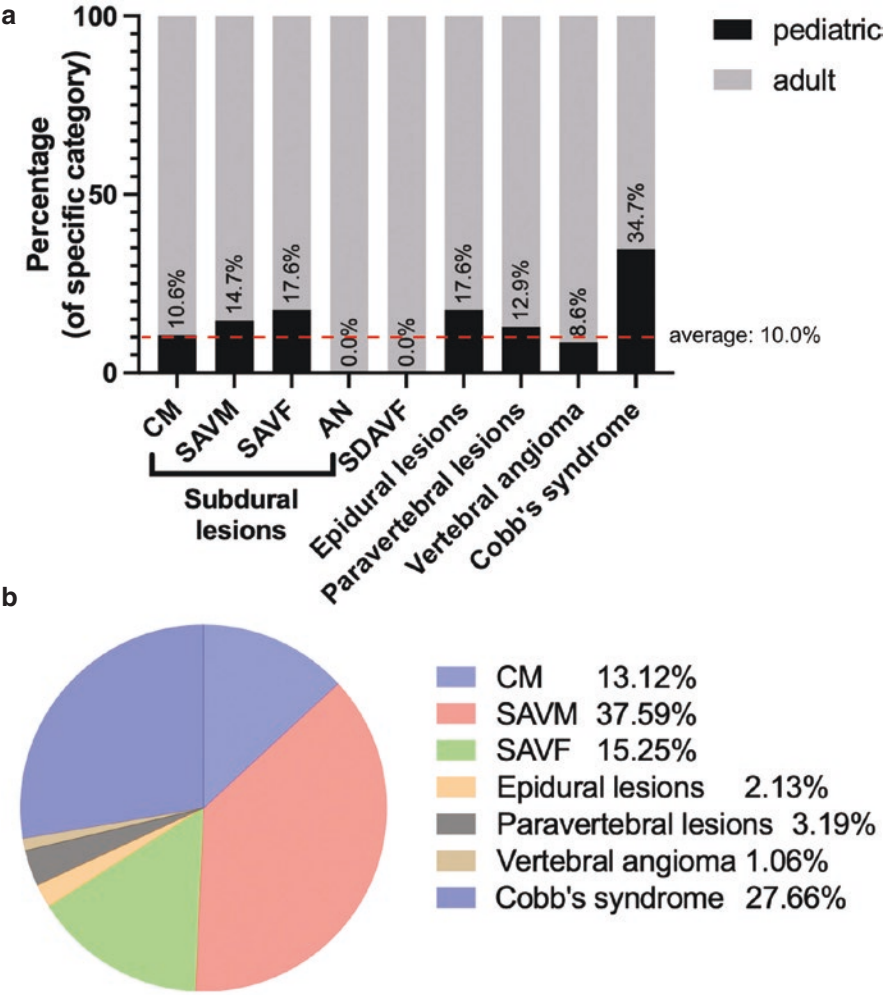

Fig. 15.9 The proportion of spinal vascular malformation subtypes is based on the data from our center till 2019. (**a**) The percentage of pediatric patients for different subtypes. In our center, 10% of the cases are under the age of 18. Cobb's syndrome is the subtype that exceeds the average percentage the most. (**b**) Percentage of different subtypes in pediatric cases. The most common subtype is SAVM, followed by Cobb's syndrome, SAVF, and CM. *AN* aneurysm, *CM* cavernous malformation, *SAVF* spinal arteriovenous fistula, *SAVM* spinal arteriovenous malformation, *SDAVF* spinal dural arteriovenous fistula

spinal cord tissue. When the lesion is located completely under the spinal pial mater, it is called the "intramedullary type"; if the lesion is located partially under and partially outside the pial mater, it would be called the "intramedullary-perimedullary type"; and if the mass is located completely outside the pial mater, it is called

"perimedullary type." The lesion could be large or small, ranging from one that involves several segments of the spinal cord to a single small fistula.

The essence of the vascular construction of arteriovenous shunt is the abnormal direct communication between arteries and veins due to the absence of a capillary network. Lesions presented as irregular "mass" is commonly seen in clinical work, that is, there is a "**nidus"** existing between the feeding arteries and the draining veins. The basis of such lesions is the multiple arteriovenous fistulas between the arteries and veins. When the wall of the direct feeders and drainers of the fistula is thickened and expanded under the stimulation of high-pressure blood flow, the abnormally dilated blood vessels are coiled and wound in a limited space to form the macroscopic mass of vascular malformation. The other type of shunt is the "**fistulous"** type, in which the orifice of fistulas is limited in number but large in diameter. In digital subtraction angiography (DSA), doctors can always recognize the full length of the lesion from the feeding artery to the orifice and the draining vein. According to most previous classification criteria, this "fistulous" lesion is always classified as an independent subtype called "perimedullary fistula," which was thought to include only the perimedullary region.

The arteriovenous shunt can involve the spinal cord, nerve roots, terminal filament, dura, surrounding vertebrae, muscles, and other structures. If a lesion affects at least one type of tissue in the same body segment other than the spinal cord, it is called a spinal metameric arteriovenous malformation (SMAVM). From the perspective of embryology, if there is a mutation in the gene *KRAS* or *BRAF* during the period when the primary vascular network forms relatively independent developmental units accompanying the development of somites, it will eventually form multiple arteriovenous malformations involving the same somatic segment.

Spinal cavernous hemangioma is the most common angiography-negative vascular malformation of the spinal cord. Magnetic resonance imaging (MRI) is the main diagnostic modality of spinal CM (see below: Diagnostic imaging of spinal vascular malformations in children). This chapter does not focus on this disease.

15.3 Pathophysiology of Pediatric Spinal Vascular Malformations

The pathophysiology of spinal cord dysfunction caused by spinal arteriovenous malformations includes bleeding, blood stealing, congestion (venous hypertension), and space-occupying effect. Sometimes it is a single factor that works, and sometimes multiple factors work together or at different stages of the course of the disease, which is more complex.

15.3.1 Bleeding

Bleeding is the most common cause of symptoms in subdural spinal arteriovenous malformations. In some patients, rupture of the vascular malformation may be induced by trauma, specific movements of the spine, or sudden change in blood pressure (e.g., strenuous exercise, constipation, etc.).

Patients with bleeding typically present sudden pain in the corresponding area, with limb movement dysfunction, sensory disturbances, and/or urination and defecation disorders below the corresponding spinal segment occur in a short period or at the same time. Some patients may gradually worsen over hours or days. Patients with lesions located in the high cervical segment may experience breathing disturbances and even cardiac arrest.

Rupture of perimedullary lesions or the rupture of aneurysm-like structures located at feeding arteries or draining veins can cause subarachnoid hemorrhage (SAH). Because the subarachnoid space surrounding the spinal cord is narrow and long, bleeding could spread upwards and downwards, even into the intracranial subarachnoid space and ventricles. As a result, it is critical to check for spinal vascular malformations in children with SAH, particularly SAH with fourth ventricular hemorrhage.

In clinical practice, some children are misdiagnosed due to atypical onset symptoms, resulting in a delay in diagnosis and treatment. For example, a child may be misdiagnosed with a thoracic and abdominal problem such as appendicitis due to pain radiating to the abdominal region, and there was a child in our center that had received an appendectomy in a local hospital because of this condition. Doctors may miss the correct diagnosis in children with SAH due to negative intracranial angiography results.

The prognosis of bleeding due to spinal vascular malformations in children, based on our clinical experience, is generally better than that in adults in terms of faster functional recovery and better functional results.

15.3.2 Blood stealing

In lesions containing large or multiple arteriovenous fistulas, excessive arterial blood leaks directly into the veins, resulting in inadequate perfusion of the normal spinal cord, which can cause chronic ischemia of the spinal cord. The patient would present slow-progressing limb muscle atrophy and motor dysfunction.

15.3.3 Congestion

That is spinal cord venous hypertension. It is the pathophysiology for spinal vascular malformations, especially fistulous type lesions.

Vascular malformations cause the high-flow arterial blood to enter the venous system directly without passing through the capillary network, resulting in increased venous pressure, which could further lead to edema of the spinal cord. The patient would present progressive spinal cord dysfunction. During angiography, doctors could find delicate draining veins with tortuous shape, retained flow of contrast agent, and lack of access to exit the spinal canal.

15.3.4 Space Occupying Effect

Subdural perimedullary arteriovenous fistula-type 3 and epidural and paravertebral arteriovenous malformations are more likely to have the mass effect. It is caused by the direct compression of the spinal cord, dural sac, or nerve roots by AVM nidus or dilated venous pouch. When formulating a treatment plan for such children, it is necessary to consider not only the dangerous structure and blood flow but also the compressive effect of the lesion itself on the spinal cord, which is often overlooked by interventional neurosurgeons.

If paravertebral lesions or draining veins compress the nerve roots, there may be radicular pain due to direct compression and pulsatile stimulation, or abnormal sensations such as itching in the area innervated by the nerves. However, it is difficult for children to describe such symptoms accurately.

15.4 Clinical Features of Pediatric Spinal Vascular Malformations

Due to the low incidence of spinal vascular malformations in children, except for the previously reported case series of children AV shunt, PMAVF, and CM by our center, the remaining reports are mostly individual case reports or small case series, or they are based on a population with multiple subtypes of spinal vascular malformations. Thus, it is difficult to have a comprehensive picture of the natural history of each subtype.

As early as 1982, Riche et al. [11] reported the clinical manifestations and treatment results of 38 cases of pediatric SAVM. However, at that time, MRI was not yet widespread, not to mention angiography. Some children only received diagnostic aortography. Thus, the evaluation and treatment of the disease were quite underdeveloped compared with the current level. In 2019, Consoli et al. [12] reported the natural history and treatment outcomes of 36 cases of spinal vascular malformations in children, including 20 cases of SAVM (with or without fistula) and 16 cases of SAVF, and this case series did not distinguish the 18 cases of metameric malformations from the others. This case series is a relatively large one in terms of the pediatric population. The average age of onset was 9.22 years. In 72% of cases, the first

symptom was related to bleeding. Before treatment, 75% of patients' symptoms were completely or partially relieved. Most lesions were located at the cervical and thoracic segments. 17% of patients had scoliosis.

In 2006, professor Lasjaunias' team [13] focused on extremely young patients with spinal arteriovenous shunt, 10 of which were AVF cases, suggesting that age of onset might be lower in patients with fistulous lesions compared with nidus type. 6 patients had the comorbidity of HHT, and 2 were metameric cases. This discovery suggested that somatic mutations and germline mutations might be associated with a more severe natural history. Of the 13 children younger than 2 years of age, only 3 presented bleeding-related symptoms, which may be related to the pathophysiology of fistulous lesions.

In this section, we analyze the clinical features of patients who have been diagnosed with SAVM, PMAVF, or Cobb's syndrome and admitted to the pediatric neurosurgery center of Xuanwu Hospital of Capital Medical University from 2007 to 2021. All patients were under 18 years of age. The study included 104 cases with complete data, of which 23 (22%) were SAVM, 47 (45%) were PMAVF, and 34 (33%) were Cobb's syndrome.

The three types of diseases show different distribution patterns in terms of the segments (Fig. 15.10), which are different from some previous literature.

SAVM are mostly distributed at the middle cervical segments, the cervicothoracic junction, and the conus medullaris, but bias might exist due to the relatively small sample size. The orifice of the fistula in PMAVF cases tends to be located at the conus medullaris. Cobb's syndrome tends to involve the lower thoracic segments and the conus medullaris, which is consistent with previous literature.

The male-to-female ratio of pediatric spinal vascular malformation is 3:2. The average onset of age is 7.7 years, and age distribution varies between diseases (Fig. 15.11). The onset age of PMAVF is significantly earlier than that of SAVM and Cobb's syndrome. The PMAVF patients can be found to have decreased lower limb movement, no response to heat, and abnormal bowel movements and urination in early infants. However, in literature of the whole-age group, the average age of onset of SAVM is lower than that of PMAVF [14–16], suggesting that there may be a difference in the natural history of spinal vascular malformations in childhood and adulthood, which needs to be further explored.

The onset pattern of vascular malformations in children can be divided into two broad categories (Fig. 15.12).

The first category is acute onset, accounting for 85.6% of the total cases, which is higher than the report of adult cases in our center [16]. Among them, 12.4% had relevant predisposing factors including exercise, trauma, defecation, etc. The child presents with sudden pain in the trunk or limbs of the corresponding segment (back, head and neck, anterior chest, abdomen, etc.) followed by movement disorders, sensory disturbances, and/or urinary and stool disturbances below the corresponding segments. In most cases, the pathophysiology behind this onset pattern is bleeding. Symptoms can start to resolve after 10 days and gradually resolve to normal or with mild sequela in several weeks or months. In conditions where the predisposing factor is serious trauma, and the patient has a severe vertebral fracture, the spinal

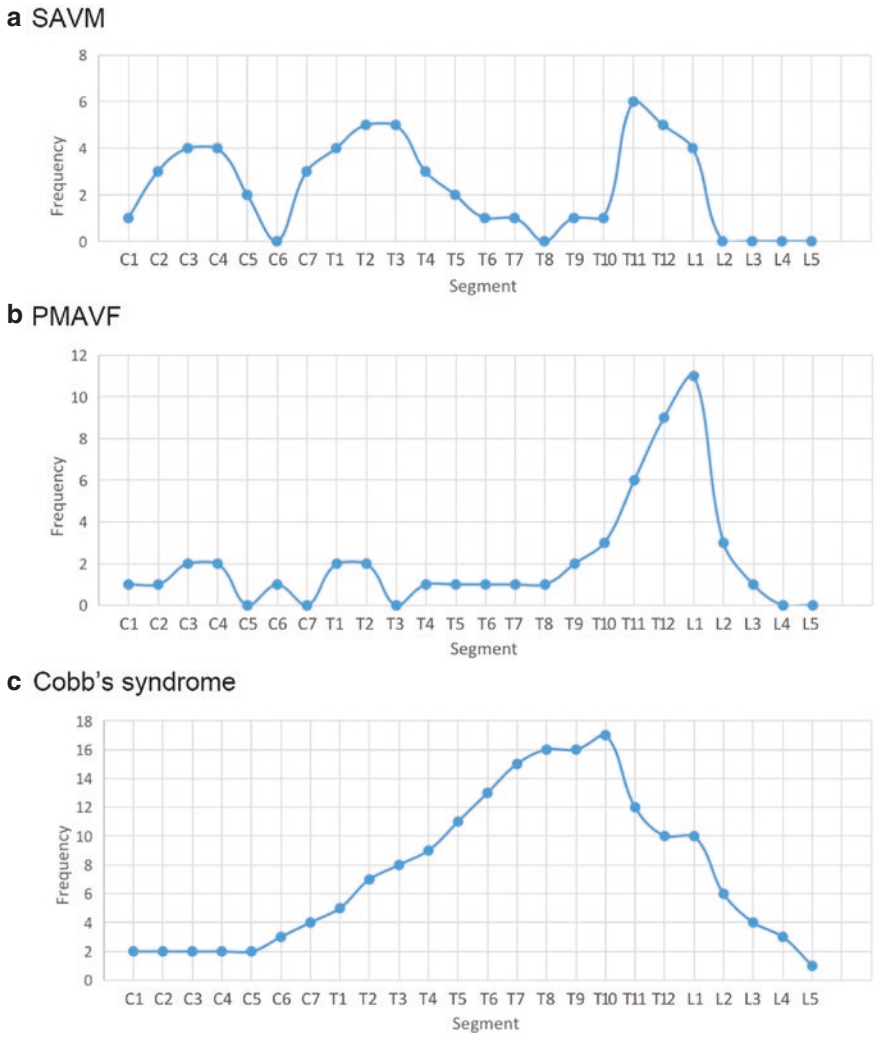

Fig. 15.10 Segment distribution of different types of pediatric spinal vascular malformations, including **(a)** SAVM, **(b)** PAMVF and **(c)** Cobb's syndrome. *PMAVF* perimedullary arteriovenous fistula, *SAVM* spinal arteriovenous malformation

cord injury is often more serious and the functional injury is not easy to alleviate. Because pain is the most common initial symptom of children in this category, and other symptoms appear gradually after that, it is often difficult for parents and caregivers to notice other symptoms such as decreased lower limb movements, sensation disturbance, and urination or defecation difficulty if the child is bedridden due to pain. As a result, it is frequently misdiagnosed as other illnesses like acute abdominal disease, especially in cases of thoracolumbar arteriovenous malformations. Some children in our center even underwent an emergency appendectomy in the local hospital.

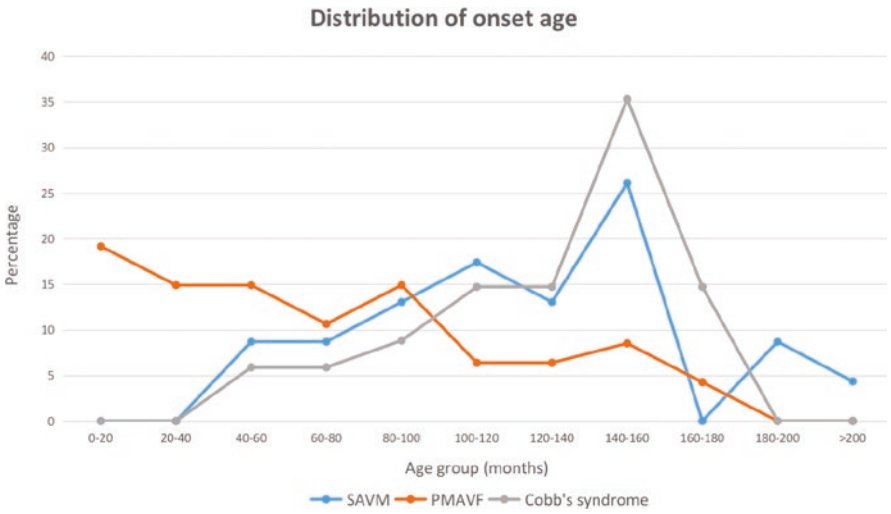

Fig. 15.11 Onset age distribution of SAVM, PMAVF, and Cobb's syndrome. *PMAVF* perimedullary arteriovenous fistula, *SAVM* spinal arteriovenous malformation

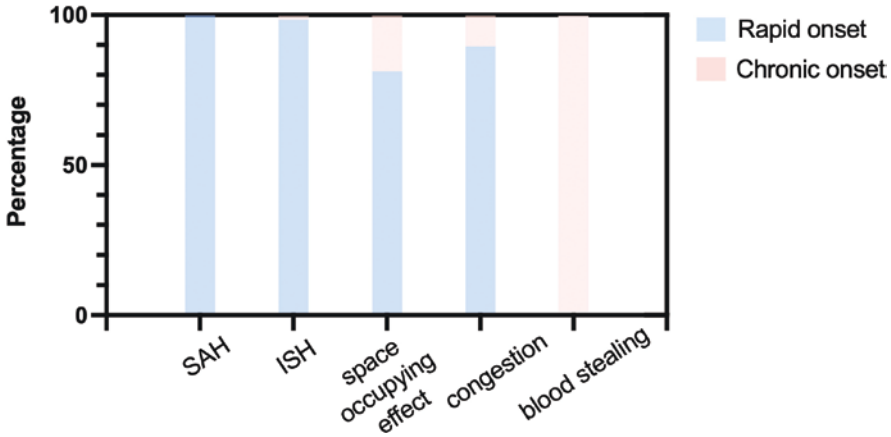

Fig. 15.12 The onset pattern and pathophysiology of pediatric spinal vascular malformation. The pathophysiology of each case was decided based on the clinical presentations and changes in images. *ISH* intra-spinal hemorrhage, *SAH* subarachnoid hemorrhage

The second category is cases with a chronic course of the disease, accounting for less than 15%, of which more than 70% are PMAVF. Children may develop progressive lower limb movement disorders, postural abnormalities, sensory impairments, and urination or defecation disorders in the early postnatal period, which are difficult to resolve spontaneously. This category is often more insidious and tends to be confused with growth retardation or congenital diseases if occurs in young children. Flett et al. [17] reported a child with spinal vascular malformation manifested

Table 15.3 Baseline characteristics of pediatric spinal vascular malformation in our center

	SAVM ($n = 23$)	PMAVF ($n = 47$)	Cobb's syndrome ($n = 34$)	Total ($n = 104$)	p value*
Male, *n* (%)	15 (65.2)	32 (68.1)	19 (55.9)	66 (63.5)	$p = 0.520$
Age of onset (months), *mean ± SD*	114.7 ± 41.3	62.1 ± 49.3	117.5 ± 34.6	91.8 ± 50.7	$p < 0.001$
Acute onset, *n* (%)	21 (91.3)	36 (76.6)	32 (94.1)	89 (85.6)	$p = 0.058$
SAH onset, *n* (%)	5 (21.7)	2 (4.3)	7 (20.6)	14 (13.5)	$p = 0.027$
Intra-spinal cord bleeding onset, *n* (%)	17 (73.9)	25 (53.2)	25 (73.53)	67 (64.42)	$p = 0.094$
Space occupying effect, *n* (%)	4 (17.4)	34 (72.3)	10 (29.4)	48 (46.2)	$p < 0.001$
Venous hypertension, *n* (%)	8 (34.8)	14 (29.8)	16 (47.1)	38 (36.5)	$p = 0.276$
Arterial steal, *n* (%)	0 (0)	3 (6.4)	1 (2.9)	4 (3.8)	$p = 0.552$
Spine deformity, *n* (%)	3 (13)	2 (4.3)	21 (61.8)	26 (25)	$p < 0.001$
mALS score before treatment, *median [IQR]*	2 [0–6]	3 [1–6]	3 [1–6]	3 [1–6]	$p = 0.364$

ANOVA analysis of variance, *IQR* interquartile range, *mALS* modified Aminoff and Logue scale, *PMAVF* perimedullary arteriovenous fistula, *SAH* subarachnoid hemorrhage, *SAVM* spinal arteriovenous malformation, *SD* standard deviation

*p value is calculated by comparison between SAVM, PMAVF, and Cobb's syndrome. Variables were compared using the ANOVA test, rank-sum test, or chi-square test according to their variable type and normality

as spastic monoparesis and had received botulinum toxin treatment for a long time due to misdiagnosis. 7 out of 10 cases of pediatric spinal arteriovenous shunts were incorrectly diagnosed as growing pains, foot deformities, cerebral palsy, cerebellar dysplasia, and even psychosis, according to the report by Seung-Ki Kim et al. [18]. In our case series, the average course from initial presentation of symptoms to a definitive diagnosis is 3.5 months for patients with acute onset and 22.9 months for patients with chronic disease. The main cause of this chronic disease course is arterial stealing, though mass effect and venous hypertension also contribute in some measure. These three pathogeneses are also the most important and characteristic pathophysiological basis of PMAVF.

Table 15.3 shows the baseline characteristics of our case series.

68% of children have objective evidence of bleeding at the initial presentation (computed tomography [CT], MRI, lumbar puncture suggesting SAH, and/or ISH). The proportion of bleeding in PMAVF is lower than that of the other two diseases, but there is no significant difference. The proportion of SAH in SAVM and Cobb's syndromes is significantly higher than that of PMAVF, which is associated with the vasculature of the lesion and its pathological mechanisms. In this case series, the annual bleeding rate of SAVM in its natural history is 8.3%, PMAVF is 10.7%, and Cobb's syndrome is 11.0%. Although the percentage of bleeding in PMAVF is low,

Table 15.4 Modified Aminoff and Logue Scale score of disability

Classification of gait disturbance (G)
Grade 0: normal gait and activity
Grade 1: leg weakness or abnormal gait, no restricted activity
Grade 2: grade I with restricted activity
Grade 3: requires cane or similar support for walking
Grade 4: requires walker or crutches for walking
Grade 5: unable to stand, confined to bed or wheelchair
Classification of micturition (U)
Grade 0: normal
Grade 1: hesitance, urgency, or frequency
Grade 2: occasional urinary incontinence or retention
Grade 3: total urinary incontinence or retention
Classification of defecation (F)
Grade 0: normal
Grade 1: slight constipation, react to laxation
Grade 2: occasional incontinence or severe constipation
Grade 3: total incontinence

the annual bleeding rate is high since the age of onset of PMAVF patients is low. The annual bleeding rates of these diseases are higher than that of all-age group patients in previous reports (2.1% for SAVM and 4% for spinal metameric syndrome) but are comparable to the results of the all-age group of our center. Thus, whether children with spinal vascular malformations are more likely to bleed and whether there are natural history differences between different races still need further research. In cases with bleeding events, the annual re-bleeding rate was higher than the overall annual bleeding rate, with SAVM rising to 10.7%, PMAVF to 36.0%, and Cobb's syndrome to 39.2%. This finding suggests that in cases of bleeding, a proactive attitude toward treatment is necessary to prevent the spinal cord from suffering irreparable harm from persistent bleeding.

Modified Aminoff and Logue Scale (mALS) is a commonly used spinal cord dysfunction score (Table 15.4). The score of about 20% of children is 0 before treatment, that is, children have no spinal cord-related symptoms. Movement disorders are more common than stool disorders, and the percentage and severity of associated symptoms are higher in Cobb's syndrome than that in SAVM and PMAVF (Fig. 15.13).

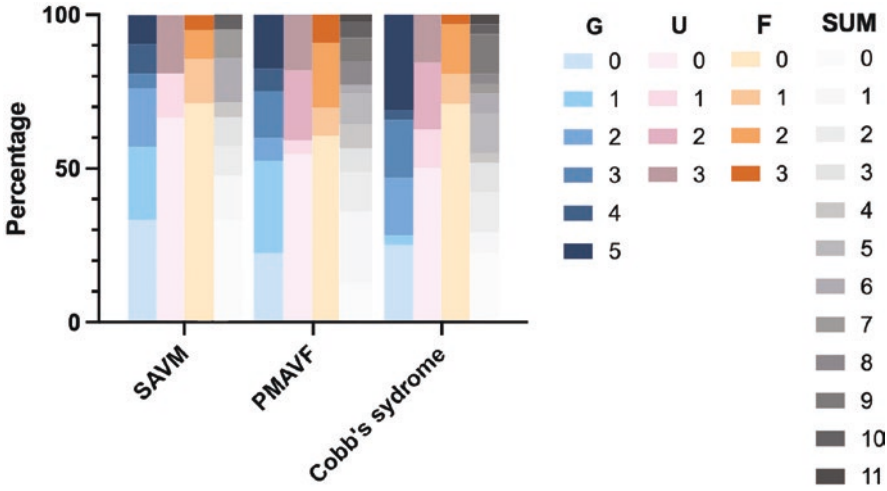

Fig. 15.13 mALS score of pediatric spinal vascular malformation patients of our center before treatment. The overall functional condition of Cobb's syndrome is worse than that of SAVM and PMAVF. "G" for gait disturbance, "U" for micturition, "F" for defecation. *mALS* Modified Aminoff and Logue Scale, *PMAVF* perimedullary arteriovenous fistula, *SAVM* spinal arteriovenous malformation

15.5 Diagnostic Imaging of Vascular Malformations of the Spinal Cord in Children

15.5.1 Computed Tomography (CT)

A spinal cord CT scan can identify potential segments of vascular malformation and quickly identify bleeding of spinal vascular malformation as a quick and easy imaging diagnosis method. CT scan showed abnormalities of the vertebral body and spinal canals, such as spina bifida, bony diastematomyelia, scoliosis, and bone destruction of the vertebral body in Cobb's syndrome (Fig. 15.14).

15.5.2 Computed Tomographic Angiography (CTA)

CTA is a non-invasive vascular imaging technology. Especially in recent years, the rapid development of multi-slice spiral computed tomography (MSCT) allows a qualitative leap in both temporal resolution and spatial resolution. CTA can show arteries and veins separately and scan a large area in a short period. The great improvement in spatial resolution makes it possible to display blood vessels with a

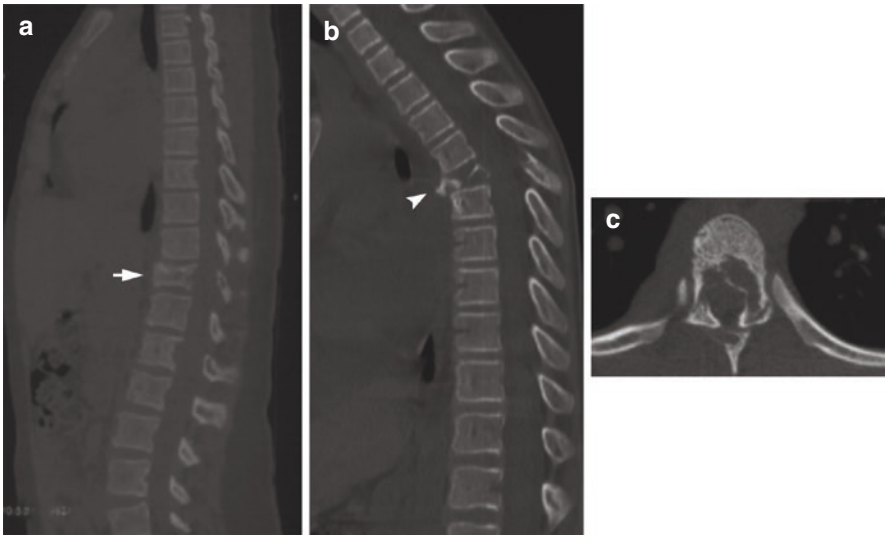

Fig. 15.14 Plain CT scans of the spine suggest vertebral bone abnormalities in three cases of pediatric Cobb's syndrome. (**a**) Vertebral compression fracture (arrow). (**b**) Severe pathological bone fracture of the vertebral body and spinal deformity (arrowhead). (**c**) Extensive destruction of the vertebral body, pedicles, lamina, and spinous process

diameter under 1 mm. By applying a variety of postprocessing reconstruction techniques, doctors can obtain high-quality vascular images with CTA. As a result, it is becoming increasingly common in the examination of the vascular system.

CTA has high accuracy in displaying the structure of spinal vascular malformation. Most previous studies have focused on SDAVF, possibly because the structure of SDAVF is relatively simple, and the dilated vessels are easy to show, while there are fewer studies on other lesions such as PMAVF and SAVM. Even though CTA is very clear for displaying spinal vascular malformations, with the current popularity of spinal cord MRI and the rapid development of spinal cord MR angiography (MRA) technology, CTA is gradually being used less for the diagnosis and follow-up of spinal vascular malformations in children due to radiation issues. However, for children who are not eligible for MRI and digital subtraction angiography (DSA) of the spinal cord, CTA is still a good method for diagnosis and follow-up (Fig. 15.15). Recent studies have shown that intra-arterial computed tomography angiography (IA-CTA) can more accurately show lesions, but IA-CTA also needs a transarterial puncture procedure, which limits its application as a primary diagnostic method. Its practical value in pediatric spinal vascular malformations remains to be explored, such as whether it can help quickly determine the lesion structure or guide a more targeted superselection DSA.

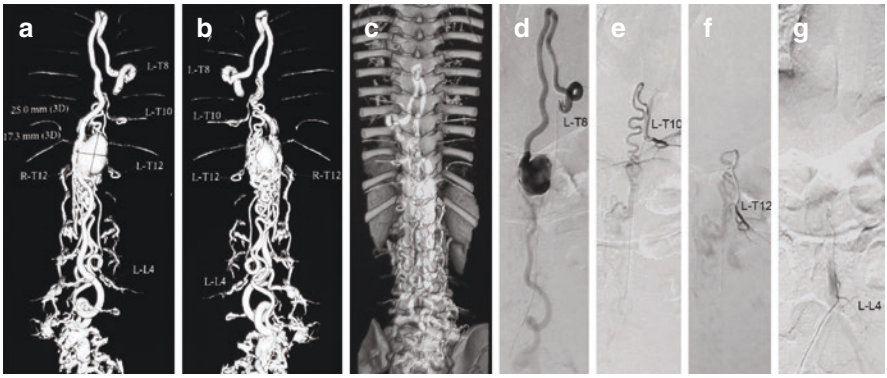

Fig. 15.15 A case of pediatric perimedullary arteriovenous fistula (3-year-old boy). (**a**–**c**) Lesion structure shown by CTA is consistent with (**d**–**g**) the result of superselective DSA in terms of feeding arteries, location of fistula, and the diameter of venous pouch

15.5.3 Plain Magnetic Resonance Imaging (MRI) and MRI with Contrast

Since spinal vascular malformations are relatively rare and lack characteristic clinical manifestations, it is prone to be misdiagnosed in clinical practice. The diagnosis of spinal vascular malformations is largely dependent on imaging findings. Spinal DSA is the "gold standard" for diagnosing spinal vascular malformations, which can accurately display the feeding arteries, nidus, fistulas, and draining veins through superselective angiography. However, spinal DSA is an invasive examination with high technical requirements. It is expensive and has radiation problem. Moreover, serious complications related to angiography may occur. These feedbacks limit its use to a certain extent. In addition, DSA cannot show the parenchyma of the spinal cord.

MRI is the main imaging modality for the initial detection and diagnosis of spinal vascular malformations. It is an effective and non-invasive examination for observing spinal cord lesions, which can clearly show spinal cord abnormalities, such as congestion, edema, infarction, and the presence of bleeding. These advantages are irreplaceable by DSA and other test methods. Due to the high-density resolution of MRI, doctors can evaluate the injury to the spinal cord and the abnormal blood vessels, which significantly improves the detection rate of spinal vascular malformations. T2 weighted images (WI) and enhanced MRI can show blood vessels more clearly and have become the first choice to evaluate spinal vascular malformations.

15.5.3.1 Spinal Arteriovenous Shunts

On an MRI, a spinal arteriovenous shunt typically shows up as a clustered intramedullary or perimedullary flow void with apparently dilated draining veins. Signals such as venous stasis and bleeding can also be seen. It can involve both intramedullary and perimedullary regions, and full-thickness of the spine, including spinal cord, nerve roots, dura mater, bony structures, paravertebral muscles, and soft tissues of the same somatic segment (Fig. 15.16). In particular, in cases with large paravertebral lesions, DSA images may be disturbed or obscured by the flow of paravertebral lesions so that the intramedullary lesion may not be clearly displayed. In this case, MRI can be used as a means to help determine intramedullary abnormalities.

15.5.3.2 Cavernous Malformation

CM is a low-flow vascular malformation, lacking mature vascular structure and is embedded in the parenchyma of the spinal cord. It can be dormant, but it can also grow, bleed, or resolve. Patients can manifest neurological dysfunction when acute bleeding occurs. MRI is the primary imaging test and the diagnostic modality of CM. Features on T1 WI and T2 WI of MRI include a mix of ultra-low and low signal with a mesh structure, with characteristic low-signal edges in T2 WI or gradient echo sequence. Enhanced MRI helps to detect developmental venous abnormalities

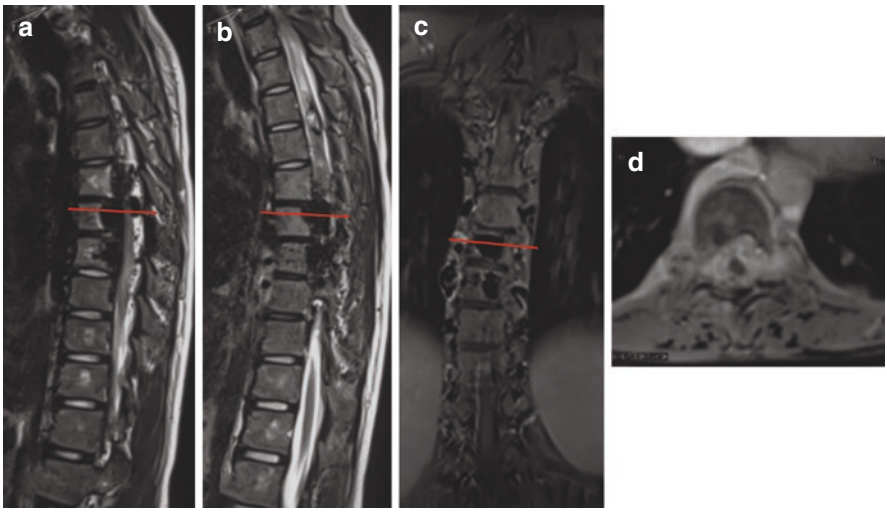

Fig. 15.16 A case of pediatric Cobb's syndrome (12-year-old girl). (**a–c**) Note the intramedullary abnormal flow void at the T4–5 segment, venous dilation dorsal to the spinal cord, spinal cord edema and extensive flow void in the vertebral bodies, and paravertebral soft tissue. (**d**) corresponds to the level of the red line in **a–c**

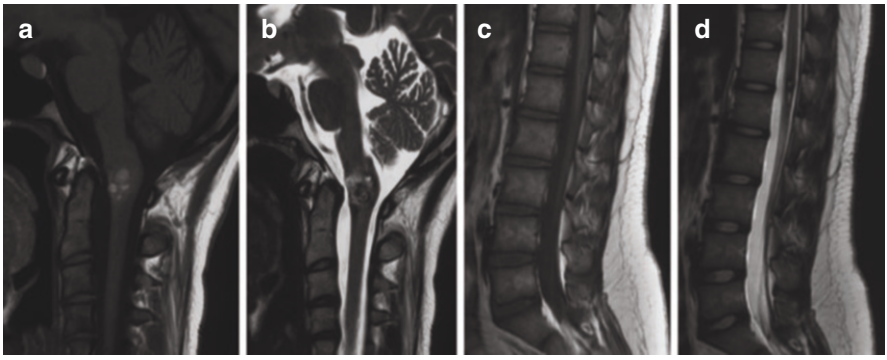

Fig. 15.17 Two cases of pediatric spinal CM. (**a**, **b**) A 17-year-old girl with CM at the craniocervical junction and extensive intramedullary bleeding. (**c**, **d**) A 14-year-old girl with CM at conus medullaris. Characteristic presentation of hemosiderin edge can be seen

associated with sporadic CM and may further support the diagnosis of CM. Spinal CM can be extradural, intradural, extramedullary, or intramedullary (Fig. 15.17).

15.5.4 Magnetic Resonance Angiography (MRA)

MRA is vascular imaging modality with the advantages of non-invasive, non-radiation, and no iodine-containing contrast agents. It has broad clinical application prospects (Fig. 15.18).

The improvements in k-space sampling have improved the spatial resolution and signal-noise ratio of MRI. The time-resolved contrast-enhanced MRA (TR-CE-MRA) was created to better provide information on the vascular lesion by using the MRA sequence after contrast injection and multiple phase acquisition. MRA can help localize the lesion, determine the feeding arteries and draining veins, analyze the architecture of the lesion, and evaluate the kinetics of the blood flow. It can even reveal a normal artery of Adamkiewicz [19]. However, the resolution of MRA was still limited compared with DSA, and the different compartments of the nidus cannot be "superselected" under MRA [20].

15.5.5 Signs on MRI Prone to be Confused with Spinal Vascular Malformations

15.5.5.1 Spinal Angioblastoma

Because spinal angioblastoma can cause vein dilation, it must be distinguished from spinal arteriovenous malformations. Angioblastoma is a kind of neoplastic disease rich in blood supply. It is homogeneously enhanced in enhanced MRI, whereas the

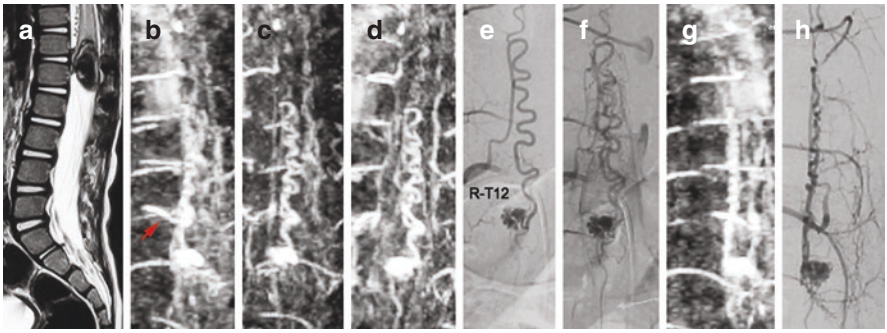

Fig. 15.18 A case of pediatric PMAVF (3-year-old boy). (**a**) Plain T2 WI MRI image (sagittal view), indicating ball-like vessel dilation with space-occupying effect at T12–L1 vertebral body level. (**b**–**f**) MRA indicates that the feeding artery is located at one segment above the dilated vascular ball. The location and morphology of the feeding artery are consistent with that in the DSA image. (**g**–**h**) MRI and DSA (lateral view) show that the feeding artery is ventral to the spinal cord. *DSA* digital subtraction angiography, *MRA* magnetic resonance angiography, *PMAVF* perimedullary arteriovenous fistula, *WI* weighted image

enhancement pattern of AVM nidus is unhomogeneous. The edge of spinal angioblastoma is clear, and the lesion is often accompanied by syringomyelia, while intramedullary vascular malformation has no clear boundary, and the incidence of syringomyelia is low (even if present, the cavities are smaller in diameter) (Fig. 15.19).

15.5.5.2 Cerebral Spinal Fluid (CSF) Flow Artifacts

Since normal CSF artifacts look similar to flow voids, they are often mistaken for spinal vascular malformations (Fig. 15.20). In most cases, the signal of the artifacts is the same as the CSF on the T1 WI image. Artifacts have no mass effect, with unfixed location, and without enhancement. Care should be taken in children with tethered cord syndrome. The spinal cord is stretched and straightened in this condition, which can be mistaken for a mass effect.

15.5.5.3 Differential Diagnosis Between Spinal Vascular Malformations

Small AVMs may also be confused with CMs, which requires spinal DSA to distinguish between them.

PMAVF may be confused with SDAVF in MRI, but with spinal DSA, one can easily distinguish between the two. In addition, since SDAVF is extremely rare in children, care should be taken when diagnosing a child with SDAVF.

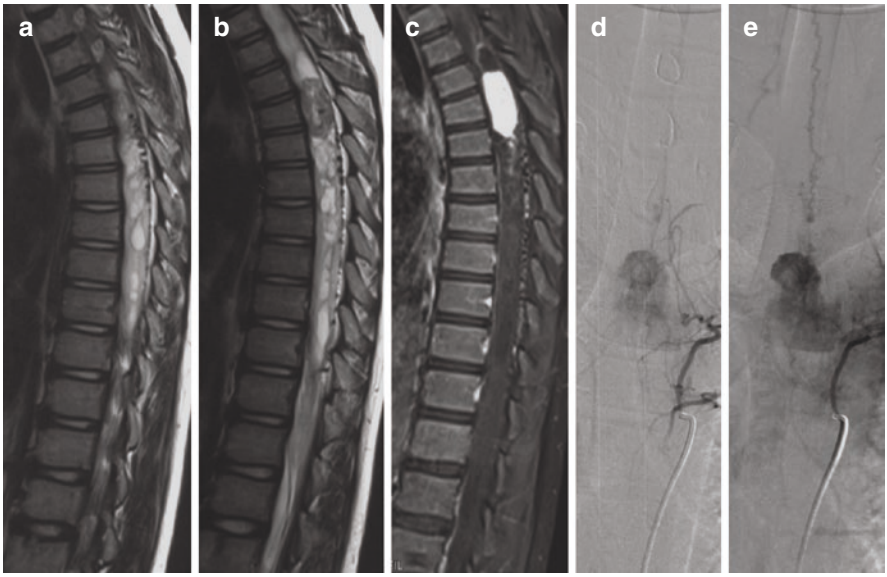

Fig. 15.19 A case of pediatric spinal angioblastoma (10-year-old boy). (**a**, **b**) MRI T2 WI indicates an intramedullary occupying lesion with syringomyelia. Note the dilated blood vessels posterior to the spinal cord. (**c**) Enhanced T1 WI shows that the lesion is homogeneously enhanced. (**d**) The late arterial phase of DSA clearly shows the tumor's arterial supply as well as the dye of the lesion itself. (**e**) Draining veins of the tumor appear

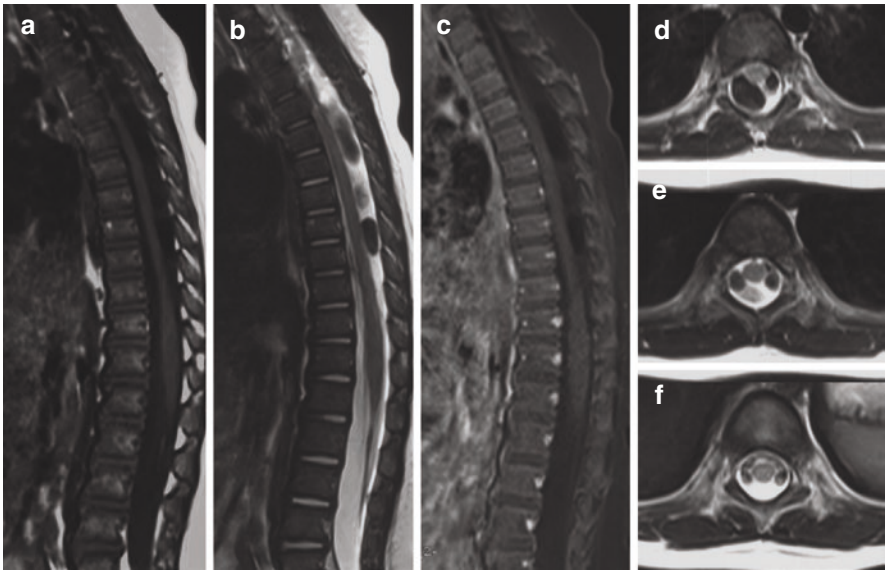

Fig. 15.20 Tethered cord syndrome with CSF artifacts (17-month-old boy). Enhanced MRI and intra-operative exploration verified that they were artifacts. (**a**) T1 WI. (**b**) T2 WI. (**c**) Enhanced T1 WI. (**d**–**f**) Axial view of different layers on T2 WI. *CSF* cerebral spinal fluid, *WI* weighted image

15.5.6 Digital Subtraction Angiography (DSA)

DSA is the gold standard for diagnosing all spinal vascular malformations. The DSA can clearly show some of the normal blood vessels and the structure of vascular malformations, including feeding arteries, draining veins, the internal structure of the nidus, and whether there are dangerous structures. These characteristics directly determine the treatment strategy.

When reading DSA images of spinal arteriovenous malformations, the following information should be obtained: (1) The source of the feeding arteries, that is, the radiculomedullary arteries that supply the ASA and PSA axes. (2) All branches from ASA, PSAs, and radiculo-pial arteries that directly feed the nidus. The diameter, length, and curvature of feeding arteries, and whether there is an aneurysm-like structure. (3) Structure of the lesion, including density, size, relative position of fistula, and whether there is an aneurysm-like structure, etc. (4) The structure of the draining veins, including the diameter, curvature, the location to exit the spinal canal, the flow rate of contrast agent, and whether there is a narrowing or an aneurysm-like dilation.

We conducted a detailed analysis of the characteristics of DSA in the 104 patients with SAVM, PMAVF, or Cobb's syndrome.

15.5.6.1 SAVM

There are 23 SAVM cases. The nidus tends to locate in three sections (Fig. 15.10). Feeding artery of nearly 70% (16/23) is from both ASA and PSA, the other 4 from ASA alone, and 3 from PSA alone. 65% (15/23) have aneurysm-like structures, and 48% (11/23) have poor venous drainage. Taking these two conditions into consideration, nearly 80% (18/23) had bleeding-related risk factors (aneurysm-like structure and/or poor venous drainage). 89% of them have initial presentations related to bleeding.

15.5.6.2 PMAVF

A total of 47 children with PMAVF are in this series, one of whom was a bi-local fistula. Thus, there are 48 lesions in total. PMAVF tends to occur in the conus medullaris (Fig. 15.10). 66% (31/48) have multiple feeding arteries, among which most (20/31) have multiple feeders converging into a single fistula. A total of 18

cases have a single feeder, 14 of which are supplied by branches of ASA. Such lesions require special care to protect the patency of the trunk of the feeding artery during embolism. Since arteriovenous fistula is the direct communication between artery and vein, it is common that the draining vein is dilated under the impact of blood flow. 71% (34/48) have globoid dilation at the beginning of the draining vein, and the fistula is directly located on the venous pouch; 23% (11/48) have simply dilated draining veins; 6% (3/48) have no obvious drainer dilation. Four cases have lesions containing aneurysm-like structures. The multivariate analysis does not show a correlation between bleeding events and factors including drainage, aneurysms, number of fistulas, and number of feeding arteries. However, among children with delicate or simple dilated draining veins, 2/3 have hemorrhagic onset, while only 1/2 of cases of venous globoid dilation have such condition. Only half of the cases without an aneurysm-like structure experience bleeding, compared to 3/4 of cases with such structure. Therefore, we can identify trends of bleeding-related factors, and this finding needs to be further verified.

15.5.6.3 Cobb's Syndrome

A total of 34 children with Cobb's syndrome are included. Lesions tend to occur in the lower thoracic segment and cone and are rare in the cervical region (Fig. 15.10). Most of the lesions of different tissue levels are located in the same somatic segment, and only one case presents with bi-focal intramedullary lesions involving both cervical segment and cone. Lesions can affect two or more layers of tissue, including the skin, paravertebral soft tissue, vertebral body, and spinal cord parenchyma. Most (23/34) cases predominantly involve the spinal cord. Only 4 cases do not have obvious intramedullary involvement (Fig. 15.21). The aneurysm-like structure is common in Cobb's syndrome (23/34), which may be located either intramedullary or paravertebrally.

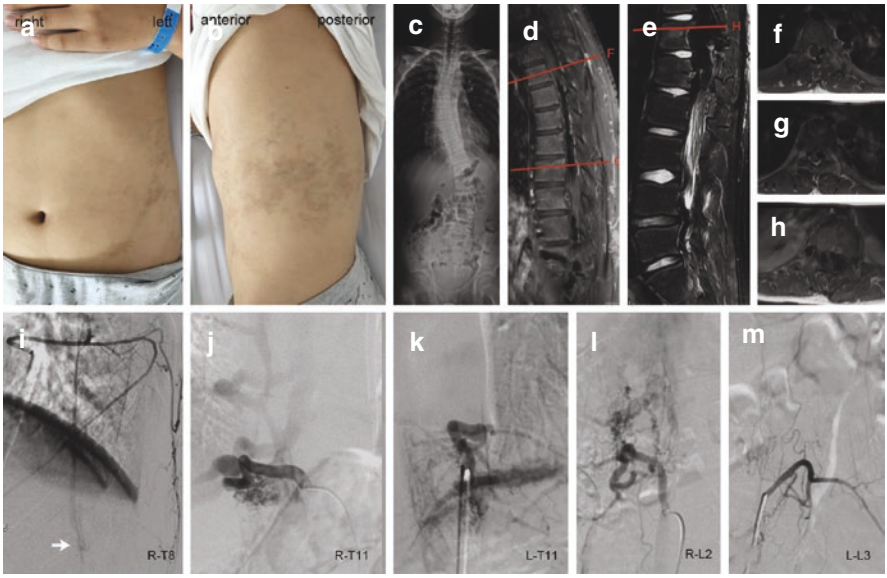

Fig. 15.21 A case of pediatric Cobb's syndrome (12-year-old boy) with predominantly paravertebral arteriovenous malformations. The child initially presented with low back pain and weakness of bilateral lower limbs, and the symptoms worsened in 9 months before admission. (**a**, **b**) Rash on lateral chest and abdomen. (**c**) Full-length spine plain film showing scoliosis deformity at the time of onset. (**d**–**h**) MRI T1 WI enhancement sequence and T2 WI sequence suggest abnormally dilated flow void at paravertebral and subcutaneous regions (red line shows the section location of **f**–**h**). **(i)** Lateral view of right T8 intercostal artery injection. The arrow indicates the intramedullary vascular malformation at the conus medullaris. (**j**–**m**) The results of the superselective intercostal and lumbar artery injection, suggesting to paravertebral arteriovenous malformations with medium-flow fistulas in the lesions. *T* thoracic, *WI* weighted image

15.6 Treatment of Vascular Malformations of the Spinal Cord in Children

15.6.1 Overview

The lesion structure of spinal arteriovenous shunts is complex. The close anatomical relationship between lesions and the spinal cord greatly increases the difficulty of surgical treatment of such diseases. In previous literatures on the treatment of subdural spinal arteriovenous shunts, the cure rate for a relatively large case-cohort is often less than 40%, and the incidence of treatment-related permanent spinal cord dysfunction could be as high as 25%. As a result, subdural spinal arteriovenous

shunts are now one of the most challenging diseases to treat in neuro-intervention and neurosurgery. For most lesions, the complex vascular structure and close anatomical relationship with the spinal cord (especially the lesions located ventrally to the spinal cord) greatly limit the role of microsurgery. In addition, the invasive nature of microsurgery makes operation safety an unavoidable issue [21]. Patients who meet the indication for microsurgery have a higher chance of cure, but interventional embolism has an advantage in terms of therapeutic safety. A few literatures report the role of radiation therapy in the treatment of spinal vascular malformations in adults [22, 23], but this method is still very immature compared with interventional and microsurgery, and the decision should be more careful with pediatric patients.

For spinal metameric arteriovenous malformation, the lesions that are mainly responsible for spinal cord injuries are the subdural lesions. As a result, subdural arteriovenous malformations are the focus of treatment of metameric disease, and their treatment methods and strategies are generally the same as those of non-metameric spinal arteriovenous malformations.

Doppman and other surgeons carried out the interventional therapy for such disease for the first time in the 1960s by performing endovascular embolization procedure for spinal arteriovenous shunts. In recent years, the development of selective spinal DSA techniques and interventional device has significantly contributed to the diagnosis and management of spinal cord vascular malformations. In addition, interventional therapy can maintain the stability of the child's spine and decrease the probability of spinal deformities in the future. Neuro-interventional techniques have become the absolute first choice of treatment for some kinds of spinal arteriovenous malformations, especially in children. At present, endovascular therapy is the first-line treatment for children with spinal vascular malformations in our center, and for children with no interventional treatment chance, doctors will assess whether the children can receive microsurgery. This principle is consistent with most literature [21, 24, 25].

Among the 104 children with a spinal vascular malformation in our center, 4 (3.8%) had no surgical or interventional treatment chances since the lesion has diffused structure or the microcatheters cannot reach a proper site. 3 cases (2.9%) received only surgical treatment, 84 cases (80.8%) only interventional treatment, and 13 cases (12.5%) received both interventional and surgical treatment. The proportion of microsurgery is lowest in the group of PMAVF, followed by Cobb's syndrome, and is highest in the SAVM group. The percentage of children who have received microsurgery is lower than the statistical results of our previous report [26]. This ratio differs from center to center, and from time to time [27, 28], which is inseparable from the change in treatment concepts brought about by the advancement of interventional technology and is also related to the clinical experience of different centers and different doctors.

15.6.2 Key Points of Interventional Treatment for Spinal Vascular Malformations in Children

15.6.2.1 Instruction for DSA and Related Cautions

Selective DSA of spinal arteriovenous malformations has several points that doctors should pay attention to: (1) First to find all blood supply arteries. For lesions at cervical segments, do not forget the subclavian artery; for lesions at conus medullaris, perform both lumbar arteries and internal iliac artery injection. (2) The dose and rate of contrast agent should be determined according to the lesion structure and blood flow. (3) The scope and area of fluoroscopy should be focused on and determined based on the location of the lesion, the source of feeding arteries, and the outlet of draining veins. (4) Anterior–posterior injection and lateral injection should be performed. If necessary, an appropriate operating angle should be selected according to individualized conditions. (5) Sometimes transient apnea by stopping the ventilator could help obtain a clearer image. (6) In cases of Cobb's syndrome, the intramedullary lesion might be shielded by large paravertebral lesions. As a result, in addition to combining MRI results for judgment, the working angle should be selected with flexibility during angiography. If necessary, a superselection of the radiculomedullary artery should be performed to show the intramedullary lesion.

Specific to the group of children, several points need additional attention: (1) Children's femoral arteries and femoral veins are slender, and the vascular wall is smooth, so vascular puncture is difficult. What's more, children's blood vessels are easy to spasm. Thus, 2–3 times of punctuation may lead to vasospasm. Ultrasound can be used actively to help with difficult vascular puncture procedures. (2) There is a radiation concern with DSA, so children's spinal DSA needs to be performed by an experienced physician to ensure a certain speed and efficiency of operation. It is also important to consider the radiation dose and the amount of contrast agent used during the procedure. The width of the grating should be adjusted according to lesion location and characteristics to avoid excess radiation. Important gonads and endocrine glands should be protected with lead. (3) Aortic angiography with a pigtail catheter can be performed at the start of the DSA procedure to more efficiently locate the lesion and feeding arteries, reducing unnecessary radiation and contrast agent use (Fig. 15.22). (4) Pay attention to identifying children's normal muscle and vertebral body stains, and abnormal paravertebral and vertebral vascular malformations. (5) To observe the changes of spinal cord function, surgeons often choose to perform intravascular treatment under local anesthesia in adults with spinal vascular malformation, which is difficult to realize in children. Children are always under general anesthesia since they cannot endure the pain and keep unmoved on the operation table, and the provocative test is unable to be carried out in this condition. As a result, the interventional treatment of children's spinal vascular malformations may tend to be conservative. For high-risk cases, intra-operative electrophysiological monitoring can be used for safety concerns.

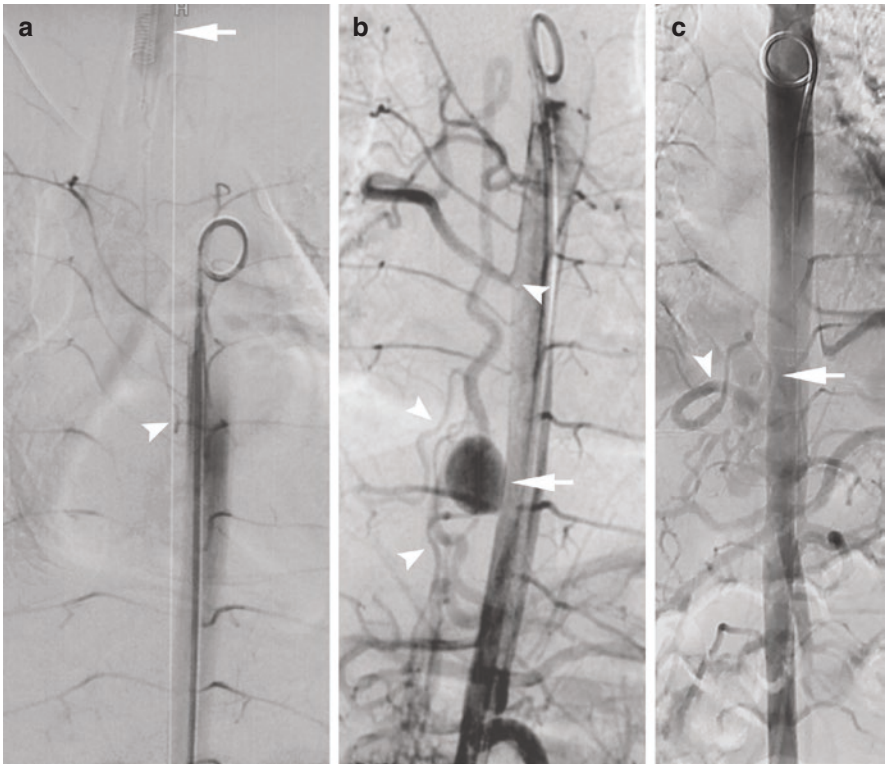

Fig. 15.22 Three cases of pediatric PMAVF. Aortic angiography is performed using pigtail catheter. The venous pouch (arrows) and feeding arteries (arrow heads) can be identified quickly. (**a**) A 7-year-old girl. (**b**) A 1-year-old boy. (**c**) A 6-year-old girl

15.6.2.2 Indication and Technical Essentials for the Embolization of Subdural Spinal Vascular Malformations

The general principle of treatment is to completely occlude arteriovenous fistulas and malformations while preserving the patency of normal arteries and veins. The following is an introduction to the treatment experience of our center.

The treatment principle of spinal arteriovenous malformation is to cure the bleeding-related factors and to eliminate the malformation as completely as possible under the premise of protecting the function of the spinal cord. Whether it is the ASA or PSA, it is necessary to maintain the integrity of the main trunk and important branches. An ideal embolization is a permanent embolization with a liquid agent (N-butyl cyanoacrylate [NBCA] or Glubran), but it requires surgeons to have good skills to control the glue injection and have experience in judging hemodynamic change. There are usually coronary branches from the ASA feeding the nidus. The key point of using liquid embolizing agents is to superselectively inject the microcatheter into the nidus while ensuring that there are no collateral branches

distal to the tip of the microcatheter. During operation, the surgeon should select a thin and soft microcatheter and micro guide wire. Using micro guide wire to guide the microcatheter or using a blood flow guide microcatheter with the tip bent into a short right angle, let the microcatheter inject into the nidus superselectively. Carefully inject the mixture of NBCA and iodized oil. The concentration of NBCA should be determined according to the speed of blood flow and the size of fistula. The concentration should not be too low to avoid prolonged setting time. If the time is too long, the glue will float to the end of the draining vein, resulting in undesired occlusion of the vein. Proper and precise injection of a small amount of glue can achieve the purpose of occlusion.

If an aneurysm or pseudoaneurysm is discovered in a lesion with a history of bleeding, it should be the primary target of embolization. If the aneurysm located in the main trunk of the feeding artery associated with the abnormal blood flow is the cause of bleeding, a controllable coil should be used for embolization, because the embolism should not only ensure the immediate patency of the parent artery but also prevent the delayed occlusion of the parent artery due to vascular retraction after the occlusion of the nidus.

In some cases of spinal arteriovenous malformation, multiple branches from ASA feed the nidus, some of which are difficult to both be reached by microcatheter and be exposed by microsurgery since they are located anteriorly or anterolaterally to the spinal cord. In these circumstances, doctors can choose spherical particles for embolization since they can enter the nidus with blood flow. The feedback of embolization with particles is that it is uncontrollable with a higher recurrence rate, so basically it is only used as preoperative embolism now. There are multiple fistulas with different diameters within an AVM nidus. For a single fistula, the diameter of the blood vessel from the feeding artery to the draining vein is mostly gradually enlarged, so the target of embolization with particles is blocking the distal end of the feeding artery with one or more particles with comparative or larger diameter compared with that of the artery. Many particles will enter the veins. Thus, if there is a narrowing in the venous outlet, it will affect the normal venous drainage, causing spinal cord dysfunction. In previous adult case series in our center, patients may have developed delayed spinal cord dysfunction after complete occlusion of malformations with particles. The diameter of the particles used for embolization in ASA must be greater than 100 μm to avoid them entering the normal anterior sulcal commissural artery, and particles with a diameter of 300–500 μm are the most commonly used ones.

The principle of treatment of fistula structure is the elimination of the fistula orifice. Some have a large arteriovenous fistula, whose feeding arteries are unusually enlarged and have a very fast blood flow rate. This type of AVF requires a balloon or coils to occlude the fistula. However, if the condition is permitted, embolization with glue should be carried out as much as possible, which is the same as spinal AVM. Anticoagulation therapy may be required following embolization or surgery if the draining veins are long and tortuous to prevent thrombogenesis, which would otherwise obstruct the normal spinal veins.

15.6.2.3 Treatment Results of Spinal Vascular Malformation in Children

The treatment of spinal vascular malformation itself is difficult. For children, on the basis of avoiding treatment-related spinal cord function injury, the treatment of pediatric spinal vascular malformation is often conservative. As a result, the overall cure rate of spinal vascular malformations in children is relatively low within the limited follow-up period. In a review published in 2020 by Zhang et al. [21], a total of 143 children of spinal vascular malformation with prognostic information were reported in the literature, and only 23.8% of the children had complete recovery of preoperative symptoms and 44.8% had significant improvement in their symptoms.

Due to the low incidence of vascular malformation in children, most literature put various types of spinal vascular malformation together to analyze the treatment and prognosis. However, the treatment strategies, treatment difficulties, and functional prognosis of different types of the disease are different.

After an average of 64 months of follow-up in our center, PMAVF is the type with the highest cure rate among the three major types (SAVM, PMAVF, and Cobb's syndrome) of spinal vascular malformation. Except for one case that is ineligible for treatment, the remaining 87.0% of PMAVF cases are treated endovascularly alone, with 6 cases requiring hybrid resection or interventional embolization combined with microsurgery. The total cure rate is 78.7%. Most of the cases could be cured at the first or second treatment. Because the treatment goal of fistula-type lesions is to eliminate the fistula, in principle, complete healing is most difficult to achieve in lesions with multiple fistulas, and the cure rate of this type in our center is only 63.6%; lesions with multiple feeders converging into a single fistula are easier to embolize than lesions with a single feeder because there are more potential embolization routes. However, in clinical practice, it is important to examine each case's treatment difficulty individually. In cases with feeding arteries from ASA or PSA alone, patients with PSA feeders have a higher possibility to be completely cured since PSA has a double axis structure and is located dorsally to the spinal cord, which is safer for endovascular treatment and is easier in terms of microsurgery accessibility. In our center, the cure rate for lesions fed by PSA alone is 92.3%, while lesions by ASA are 82.4%. From the functional perspective, 54.5% of children with PMAVF have an mALS score of 0 at the last follow-up, which means they do not have symptoms related to spinal cord injury. Nearly 80% of PMAVF patients only have mild symptoms (mALS score less than or equal to 3 points). Except for 2 young children, nearly 90% of the children can take care of themselves completely. To stratify children with PMAVF by disease course, we can find that the functional prognosis of children with the chronic progressive course was statistically significantly worse than that of children with acute onset. Only 25% of children with chronic progressive course have mALS score equal to 0, and 62.5% have mALS less than or equal to 3 points, whereas for children with acute onset, 64% have mALS equal to 0, and more than 80% have mALS less than or equal to 3. This result suggests that the pathological mechanisms behind different natural histories may be related to the recoverability of spinal cord functional impairment. When stratifying patients according to the pathophysiological mechanism, we can find that the

function prognosis of children with hemorrhagic onset was significantly better than that of children with non-hemorrhagic onset. Children with presumed pathological mechanisms of blood stealing have the worst prognosis.

As shown in Table 15.5, the cure rate for AVM is only 8.7%, and only more than 60% of cases have a 50% decrease in nidus volume. Although the cure rate was lower than that of PMAVF, at the time of the last follow-up, 90% of the children have mALS scores below 3, and 90% can take care of themselves even if the lesion is not cured. This finding indicates that after embolizing dangerous structures and lesions as much as possible, the children could still obtain a good functional outcome despite coexisting with the lesions.

Since Cobb's syndrome is a metameric disease, it is impossible to achieve a complete cure. The treatment goal should be the intramedullary lesions, dangerous structures, and high-flow fistulas associated with spinal edema and bleeding. Children with Cobb's syndrome have the worst functional outcome at follow-up, with only 67.9% of children able to take care of themselves.

Although spinal vascular malformations are extremely difficult to cure, neurosurgeons can still improve patients' spinal function. Maintaining spinal cord function is always the starting point of treatment. Only when we care about the functional outcome more than the cure rate our patients can obtain a better quality of life.

Table 15.5 Follow-up analysis of cases in our center*

	SAVM (n = 23)	PMAVF (n = 47)	Cobb's syndrome (n = 34)	Total (n = 104)	p value#
Cure rate, n (%)	2 (8.7)	26 (78.7)	0 (0)	39 (37.5)	$p < 0.001$
Lesion volume decreased over 50%, n (%)	14 (60.9)	NA	7 (20.6)	–	$p = 0.002$
	SAVM (n = 20)	PMAVF (n = 33)	Cobb's syndrome (n = 29)	Total (n = 82)	p value#
Follow-up mALS score,* *median [IQR]*	1 [0–1.75]	0 [0–2]	1 [0–5]	1 [0–2]	$p = 0.335$
Follow-up mALS = 0,* n (%)	36.8%	54.5%	35.7%	43.8%	$p = 0.264$
Follow-up mALS <= 3,* n (%)	90.0%	78.8%	67.9%	77.8%	$p = 0.188$
Basic living skills,* n (%)	90.0%	81.8%	67.9%	79.0%	$p = 0.156$

ANOVA analysis of variance, *IQR* interquartile range, *mALS* modified Aminoff and Logue scale, *PMAVF* perimedullary arteriovenous fistula, *SAVM* spinal arteriovenous malformation, *SD* standard deviation

*Functional analysis was done based on 82 cases with follow-up functional outcomes

#p value is calculated by comparison between SAVM, PMAVF, and Cobb's syndrome. Variables were compared using the ANOVA test, rank-sum test, or chi-square test according to their variable type and normality

Acknowledgement We would thank all surgeons in our department for performing interventional surgery to patients in this manuscript and thank all patients and their parents for giving their trust to our team.

Compliance with Ethical Standards The authors disclose no conflict of interest. No funding sources for this manuscript. All patients included in the observational study in this manuscript have signed informed consent to receive surgery and follow-up. Clinical practice and the observational study adhere to corresponding ethical requirements.

References

1. Lasjaunias P, ter Brugge KG, Berenstein A. Surgical neuroangiography. 2nd ed. Heidelberg: Springer; 2006.
2. Kendall BE, Logue V. Spinal epidural angiomatous malformations draining into intrathecal veins. Neuroradiology. 1977;13(4):181–9.
3. Merland JJ, Riche MC, Chiras J. Intraspinal extramedullary arteriovenous fistulae draining into the medullary veins. J Neuroradiol. 1980;7(4):271–320.
4. Rosenblum B, Oldfield EH, Doppman JL, Di Chiro G. Spinal arteriovenous malformations: a comparison of dural arteriovenous fistulas and intradural AVM's in 81 patients. J Neurosurg. 1987;67(6):795–802.
5. Merland JJ, Riche D, Laurent A. Embolization of spinal cord vascular lesions. In: Vinuela F, Halbach VV, Dion JE, editors. Interventional neuroradiology: endovascular therapy of the central nervous system. New York: Raven Press; 1992.
6. Berenstein A, Lasjaunias P. Endovascular treatment of spinal and spinal cord lesions. In: Surgical neuroangiography. 1st ed. Berlin, Heidelberg: Springer; 1992.
7. Anson JA, Spetzler RF. Classification of spinal arteriovenous malformations and implications for treatment. BNI Quarterly. 1992;8:2–8.
8. Spetzler RF, Detwiler PW, Riina HA, Porter RW. Modified classification of spinal cord vascular lesions. J Neurosurg. 2002;96(2 Suppl):145–56.
9. Rodesch G, Hurth M, Alvarez H, Tadie M, Lasjaunias P. Classification of spinal cord arteriovenous shunts: proposal for a reappraisal—the Bicetre experience with 155 consecutive patients treated between 1981 and 1999. Neurosurgery. 2002;51(2):374–9. discussion 379–380
10. Bao YH, Ling F. Classification and therapeutic modalities of spinal vascular malformations in 80 patients. Neurosurgery. 1997;40(1):75–81.
11. Riche MC, Modenesi-Freitas J, Djindjian M, Merland JJ. Arteriovenous malformations (AVM) of the spinal cord in children. A review of 38 cases. Neuroradiology. 1982;22(4):171–80.
12. Consoli A, Smajda S, Trenkler J, Soderman M, Rodesch G. Intradural spinal cord arteriovenous shunts in the pediatric population: natural history, endovascular management, and follow-up. Childs Nerv Syst. 2019;35(6):945–55.
13. Cullen S, Alvarez H, Rodesch G, Lasjaunias P. Spinal arteriovenous shunts presenting before 2 years of age: analysis of 13 cases. Childs Nerv Syst. 2006;22(9):1103–10.
14. Cho WS, Kim KJ, Kwon OK, Kim CH, Kim J, Han MH, Chung CK. Clinical features and treatment outcomes of the spinal arteriovenous fistulas and malformation: clinical article. J Neurosurg Spine. 2013;19(2):207–16.
15. Jing L, Su W, Guo Y, Sun Z, Wang J, Wang G. Microsurgical treatment and outcomes of spinal arteriovenous lesions: learned from consecutive series of 105 lesions. J Clin Neurosci. 2017;46:141–7.
16. Yu JX, Hong T, Krings T, He C, Ye M, Sun LY, Zhai XD, Xiang SS, Ma YJ, Bian LS, et al. Natural history of spinal cord arteriovenous shunts: an observational study. Brain. 2019;142(8):2265–75.

17. Flett PJ, Baulderstone D, Russo R, Davies RP. Spinal arteriovenous malformation presenting as spastic monoplegic cerebral palsy in a child. J Paediatr Child Health. 2012;48(1):71–4.
18. Cho WS, Wang KC, Phi JH, Lee JY, Chong S, Kang HS, Han MH, Kim SK. Pediatric spinal arteriovenous malformations and fistulas: a single institute's experience. Childs Nerv Syst. 2016;32(5):811–8.
19. Nijenhuis RJ, Mull M, Wilmink JT, Thron AK, Backes WH. MR angiography of the great anterior radiculomedullary artery (Adamkiewicz artery) validated by digital subtraction angiography. AJNR Am J Neuroradiol. 2006;27(7):1565–72.
20. Condette-Auliac S, Boulin A, Roccatagliata L, Coskun O, Guieu S, Guedin P, Rodesch G. MRI and MRA of spinal cord arteriovenous shunts. J Magn Reson Imaging. 2014;40(6):1253–66.
21. Zhang HJ, Silva N, Solli E, Ayala AC, Tomycz L, Christie C, Mazzola CA. Treatment options and long-term outcomes in pediatric spinal cord vascular malformations: a case report and review of the literature. Childs Nerv Syst. 2020;36(12):3147–52.
22. Rashad S, Endo T, Ogawa Y, Sato K, Endo H, Matsumoto Y, Takahashi A, Tominaga T. Stereotactic radiosurgery as a feasible treatment for intramedullary spinal arteriovenous malformations: a single-center observation. Neurosurg Rev. 2017;40(2):259–66.
23. Kalani MA, Choudhri O, Gibbs IC, Soltys SG, Adler JR, Thompson PA, Tayag AT, Samos CH, Chang SD. Stereotactic radiosurgery for intramedullary spinal arteriovenous malformations. J Clin Neurosci. 2016;29:162–7.
24. Jermakowicz WJ, Weil AG, Vlasenko A, Bhatia S, Niazi TN. Cognard Type V intracranial dural arteriovenous fistula presenting in a pediatric patient with rapid, progressive myelopathy. J Neurosurg Pediatr. 2017;20(2):158–63.
25. Lorenzoni PJ, Scola RH, Kay CS, Queiroz E, Cardoso J, Leite Neto MP, Grisotto KP, Grande CV, Bruck I, Werneck LC. Spinal cord arteriovenous malformation: a pediatric presentation. Arq Neuropsiquiatr. 2009;67(2B):527–9.
26. Du J, Ling F, Chen M, Zhang H. Clinical characteristic of spinal vascular malformation in pediatric patients. Childs Nerv Syst. 2009;25(4):473–8.
27. Cullen S, Krings T, Ozanne A, Alvarez H, Rodesch G, Lasjaunias P. Diagnosis and endovascular treatment of pediatric spinal arteriovenous shunts. Neuroimaging Clin N Am. 2007;17(2):207–21.
28. Nikova A, Ganchev D, Birbilis T. Pediatric dilemma: endovascular versus surgical intervention for spinal vascular malformations. Pediatr Neurosurg. 2018;53(5):291–8.